WATER RESOURCE SYSTEMS RESEARCH LABORATORY

DEPARTMENT OF CIVIL ENGINEERING
UNIVERSITY OF NEWCASTLE UPON TYNE

The Impacts of Climatic Change and Variability on Water Resources in Yorkshire

By

Hayley Jane Fowler *MA Cantab. MSc.*

NEWCASTLE UNIVERSITY LIBRARY
200 13086 2
Thesis L6790

Submitted in partial fulfilment of the requirements for the degree of Doctor of Philosophy

November 2000

" In the light of the 1995-96 drought, a reappraisal of the water demand/resources balance in the North West and elsewhere across the country is needed in order to ascertain whether long-term water resources plans are adequate and resilient"

Walker (1998)

Abstract

Observational evidence and future climate change scenarios suggest an amplification of climatic contrasts across the UK. This is seen most prominently in the marked increase in notable flood events and drought episodes and may profoundly affect water resource systems in vulnerable areas, as exemplified by the 1995 Yorkshire drought. The 1995-96 drought resulted in severe stress to the Yorkshire water supply, necessitating the emergency measure of tanking in water from outside the region, and was caused by an unusual pattern of weather and precipitation. This research is an investigation into both natural climatic variability and possible future climate change in Yorkshire aiming to quantify the risk of future occurrence of severe drought events, such as that of 1995.

Historical drought characteristics and spatial-temporal precipitation variability in Yorkshire are examined and linked to synoptic weather patterns. A multi-site stochastic rainfall model is then developed using conditioning by synoptic weather types. The model can account for spatial variability and allows the concurrent simulation of precipitation time-series for very different climatological sub-regions within the same water resource area. This model is used to investigate the impact of natural climatic variability and possible future climate change upon water resource reliability, resilience and vulnerability in Yorkshire.

The structure of the stochastic rainfall model enables the impact of variations in weather type persistence or frequency to be investigated. In addition, rainfall model statistics can be altered to simulate instances of increased precipitation intensity or proportion dry days for example, for individual weather groups. The UKCIP98 Medium-High climate change scenarios for 2021-2050 and 2051-2080 are investigated using modifications to weather type frequency, precipitation and potential evapotranspiration.

Results indicate that water resources in Yorkshire are likely to become more reliable on average under the examined climate change scenarios due to increased winter precipitation. However, model simulations also suggest a reduction in resource resilience and increased vulnerability to drought. Severe droughts comparable to that of 1995 show only a slight increase in frequency by 2080. However, there will be a significant increase in both magnitude and duration of severe drought, as a consequence of summer precipitation reductions and increased climatic variability.

This methodology of simulating the impacts of potential atmospheric circulation change on precipitation regimes can provide a basis for the future planning and management of water resource systems.

Acknowledgements

This work was funded by an Engineering and Physical Sciences Research Council (EPSRC) CASE studentship in conjunction with the Environment Agency (Leeds regional office). Many people have put a lot of time and effort into this thesis. Special thanks must be directed to my supervisor, Chris Kilsby, who has provided a huge amount of helpful advice and support throughout the last three years, not to mention feeding me his children's Easter eggs. I am also grateful to my other supervisor, Prof. P. Enda O'Connell, who originally put together the proposal for the project and gave invaluable advice. Another special mention goes to Aidan Burton whose coding expertise was vital to the successful completion of the project. He adapted the GNSRP modelling package, RainSim, to perform precipitation simulation according to the modelling process described within this thesis (and in amazingly quick time!).

I am also indebted to all those people who supplied me with data. In particular, Mike Stokes at the York Environment Agency has always been very helpful and expedient. Data was also taken from British Atmospheric Data Centre and some long-term records compiled by Tim Burt at Durham University. The subjective and objective Lamb Weather Type data was supplied by Phil Jones (CRU, UEA).

Support from the Environment Agency has been excellent. I would especially like to thank John Jepps for advice and help setting up the Yorkshire Grid water resources model. Other support has been gratefully received from both Stuart Homann and Mark Sitton.

Finally, I would like to thank all those people who have kept me sane these last few months, particularly Clare for the squash matches and Sean.

Common Abbreviations

ADM	A Distributed Model
BLRP	Bartlett-Lewis Rectangular Pulses
CCIRG	Climate Change Impacts Review Group
CET	Central England Temperature
CRU	Climate Research Unit, University of East Anglia
DSI	Drought Severity Index
EA	Environment Agency
ENSO	El Niño Southern Oscillation
GCM	General Circulation Model
GNSRP	Generalised Neyman-Scott Rectangular Pulses
IPCC	Intergovernmental Panel on Climate Change
LAM	Limited Area Model
LWT	Lamb Weather Type
MORECS	Meteorological Office Rainfall and Evaporation Calculation System
MSE	Mean Squared Error
MSLP	Mean Sea Level Pressure
MWD	Mean Wet Day
NAO	North Atlantic Oscillation
NSRP	Neyman-Scott Rectangular Pulses
OFWAT	Office of Water Services
OWT	Objective Lamb Weather Type
PD	Proportion Dry Days
PE	Potential Evapotranspiration
SA	Summer Anticyclonic
SN	Summer Northerly
SST	Sea Surface Temperature
SW	Summer Westerly
SWG	Stochastic Weather Generator
UK	United Kingdom
UKCIP	UK Climate Impacts Programme
UKWIR	UK Water Industry Research Limited
US	United States
WA	Winter Anticyclonic
WN	Winter Northerly
WRAP	Water Resources and Planning
WRINCLE	Water Resources: the INfluence of CLimate change in Europe
WRPM	Water Resources Planning Model
WW	Winter Westerly
YWS	Yorkshire Water Services

Table of Contents

List of Figures

List of Tables

Chapter 1: Introduction

"...the possibility that there may be significant changes in the water resources of the UK – with increased risk of regional and seasonal water shortages – should cause planners to check carefully the long-term viability of present and planned schemes."

Arnell (1992*a*)

1.1 Background to the project

1.1.1 The water resource situation of the UK in relation to droughts

The 1988-1992 drought underlined the sensitivity of water resources in the UK to climatic variations (Marsh and MacRuairi, 1993). The years 1988, 1989 and 1990 were, taken together, the warmest 3 years on record since 1659 (Brugge, 1992). The drought also showed exaggerated hydrologic seasonality and was highly regionalised with northwest Scotland being very wet (Marsh and Monkhouse, 1993), whereas parts of eastern England showed the most extreme runoff deficits for 150 years (Bryant *et al.*, 1994). The juxtaposition of wetter winters and drier summers continued from the 1980s into the 1990s, culminating in the serious drought of 1995, which affected mainly the north and west of the country. An extension of these climatic variations and trends will have serious implications for water resource systems in the 21st Century.

In order to assess the water resource situation of the UK in terms of both demand and the effects of drought it is appropriate to draw a line from Teeside, down the east of the Pennines, south to Dorset. The area to the southeast is densely populated with low effective precipitation but a high demand for water that is met mainly through groundwater abstraction. The area to the northwest is characterised by lower population densities and higher effective precipitation, but is mainly reliant on surface water resources.

There have been many attempts to define drought. The UK meteorological definition is a period of 15 or more days without measurable precipitation but this is of little relevance in the assessment of water resources. A more practical definition however, would be that drought is "*a prolonged period with a significant reduction in effective precipitation*" (Price, 1998). Water resource indicators should be the most meaningful, but have an inability to express drought unambiguously. They are unable to distinguish between absolute drought and drought unjustified in hydrological or meteorological terms, but developed due to imprudent management of the water resource system. Meteorological and hydrological indicators therefore provide a method that is easy to measure and compare. However, a major problem is that there

are no generally accepted drought indicators or measures of severity in the UK. A solution to this has been developed for the US, the National Electronic Drought Atlas (NEDA) (Wallis and Guttman, 1997). This uses L-moments (Hosking, 1990) and regional frequency analysis (Hosking and Wallis, 1997) to group annual precipitation data into clusters that respond to the same physical controlling processes.

UK water-supply droughts have been defined by Mawdsley *et al.* (1994). A *moderate* drought event is defined when demand restrictions are necessary to reduce the total consumption by the public by approximately 10 percent. This corresponds to a level of service defined by OFWAT (Office of Water Services) that should only be imposed on consumers once every 8 to 10 years on average. A *serious/severe* drought is when there is a risk of standpipes being imposed in the near future. A *serious* drought event occurs when the risk is greater than 20 percent, and a *severe* drought when it is more than 50 percent. In the first case, it is expected that Drought Orders will have been sought or in place and in the second case Drought Orders should already be in place. The 1995 Yorkshire drought would be defined as *severe* using this classification method.

Within the UK, two main types of drought have been defined by Price (1998). The first type (I) is characterised by a steepening of the precipitation gradient between the northwest and southeast of the UK. Precipitation in the south and east is reduced but in the north and west precipitation may increase, reduce slightly or remain average. The second type of drought (II) is characterised by a notable reduction in effective precipitation across the whole of the UK (Price, 1998).

The 1988-1992 drought can be classed as a type I drought. This type of drought affects mainly the south and east of the country which may be better able to deal with precipitation deficits due to large groundwater reserves and having to cope with lower average precipitation totals. The drought will only become significant if it lasts for more than about two years, due to the reduction, or lack, of normal winter recharge to the aquifer (Price, 1998). A type II drought may severely affect surface water resources but have little impact upon groundwater levels. Until 1995, type II droughts have been of short duration, lasting less than a year, and usually occurring in the summer (Price, 1998). An example of this type of drought would be the 1975/76 drought that severely affected water resources in both southern and northern England. However, the 1995 drought raised concerns that the spatial and temporal variations in precipitation that may occur under changed climatic conditions may exaggerate the present gradient of water storage.

Future climate change scenarios suggest that changes to the spatial and temporal distribution of precipitation across the UK may be part of an enhanced hydrological cycle (Hulme and Jenkins, 1998). An exaggeration of the northwest to southeast precipitation gradient has resulted in substantial increases to runoff in winter in the northwest (e.g. Black and Bennet, 1995) but decreases in summer precipitation across the UK (e.g. Mayes, 1998). However, there are concerns that increased precipitation intensity may decrease the hydrological effectiveness of this increased winter runoff in northern and western regions due to lower infiltration rates (Marsh, 1996). This, coupled with the summer precipitation decreases, may increase the occurrence of type II droughts, so raising the frequency of drought in the north and west of the country which is the area most vulnerable to short-term precipitation deficiency (Price, 1998).

Prior to the 1995 drought, the southeast of the UK was generally regarded as most vulnerable to drought because of lower average precipitation totals and research concentrated on quantifying the effects of changes in the intensity, duration and frequency of winter precipitation upon groundwater recharge. For example, Arnell (1992*a*) noted that although the winter of 1989-90 was considerably milder than average and had below average precipitation, the precipitation was concentrated into a very short period and tended to produce floods rather than replenish groundwater storage. Bryant *et al.* (1994) have also expressed concern that winter precipitation following dry summers will have reduced hydrological effectiveness as the period of groundwater recharge is shortened by the necessary replenishment of soil moisture deficits. This may be borne out by evidence from the persistent drought of 1988-1992 where groundwater deficits continued even through the wet winter of 1989-90 (Marsh *et al.*, 1994). It has also been determined that relatively small changes in potential evapotranspiration (PE) rates may lead to large differences in estimated change in resources (e.g. Arnell, 1992*a*).

The number of studies investigating water shortages in areas dependent upon surface water systems is limited, as until 1995 any droughts occurring in such regions were thought to be short-lived. However, water shortages can develop rapidly in areas dependent upon small reservoir systems, especially where large differences in precipitation between adjacent seasons is observed (Burt, 1992). An example of one such study is that of Cole *et al.* (1991). Runoff sequences were generated for different areas of England and Wales based on estimations of precipitation in 2030 and it was predicted that annual runoff would decline by eight percent in the southeast and four percent in the northwest. This translated to a 4 to 25 percent loss of storage in direct supply reservoirs in the north, and an 8 to 15 percent loss in the south. However, even where evidence pointed to the contrary, it was still assumed that climate change impacts would be felt more severely in the south and east of the UK.

The number of water resource studies looking at climate variability rather than mean changes is also inadequate. For an impact assessment of climate change on water resources the potential changes in variability, the magnitude of the fluctuations about an average condition, are at least as important as changes in mean conditions (Buishand and Beersma, 1996). The frequency of extreme events will be much more sensitive to changes in the variability than the mean (Katz and Brown, 1992). Statistical tests have been derived by some researchers to compare variances of observed and simulated multivariate data on a monthly (Wigley and Santer, 1990) and daily (Buishand and Beersma, 1996) time-step. However, more sophisticated methodologies must be developed to facilitate the assessment of water resource systems under changed climatic conditions.

Clearly, climatic change within the UK may severely affect water resource systems. For example, a return to the highly anticyclonic-westerly winters of the late 1980s and early 1990s would provide diminished precipitation receipt over the groundwater dependent east of England and have highly detrimental effects on water resources in such regions. This was an important effect of the 1988-92 drought and contributed to slow recovery times for aquifers after the wet winter of 1989-90 (Marsh and Bryant, 1991).

The recent autumn 2000 floods in the south and east of the UK, as well as Yorkshire, illustrate the very serious implications of climatic change. In terms of water resources, if the underlying trend from the 1970s towards a higher North Atlantic Oscillation (NAO) with associated higher winter temperatures and a steeper northwest to southeast precipitation gradient continues then there may be serious drought concerns. The north and west of the country may receive greater winter rainfalls, with associated flood control implications, whereas the south and east may suffer winter precipitation deficits (Mayes, 1996). Lowland areas dependent on major aquifers are particularly vulnerable to precipitation deficiencies that extend over several dry and mild winters. If the summer half-year is dry too, and soil moisture deficits are high, aquifer recharge may be restricted to a period of weeks as occurred in 1989/90 and 1990/91 for Eastern Britain (Marsh *et al.,* 1994). The north and west of the country will also receive reduced summer precipitation, and the reliance upon single-season resources may increase the risk of drought in these areas.

It has been shown in this discussion that regional and seasonal resources may change, with an increasing concentration of available water in winter and in northern and western areas. An increased risk of flooding in such areas is already being observed under both the highly positive NAO of the early 1990s when Scotland was affected, and under the present reduction in NAO where southern and north-eastern England were affected. However, with increased climatic

variability the reverse may also be true. If a hot, dry summer such as that of 1995 is followed by a relatively dry winter then this would have serious implications for water resources in surface-water reliant regions as well as groundwater resources. The recent observed downward trend in summer precipitation might increase the occurrence of short-term water shortages in the north and west of the UK (Marsh, 1996). These shortages may be exacerbated by a rising demand for water. If current trends are assumed, peak domestic demands in a warm summer month may be 25 percent higher than in a winter month, and agricultural demand may increase. Sustained spatial and temporal changes to the precipitation regime of the British Isles arising from a strongly positive NAO may therefore be the "*most hydrologically inconvenient change possible, given the geography of Britain's water resources and the issue of effective flood management*" (Mayes, 1995).

1.1.2 The 1995 drought in Yorkshire

The water resources outlook throughout the UK was very healthy in the late winter of 1994-95. The protracted drought of 1988-92 had been immediately followed by the wettest 32-month sequence this century. Reservoirs were at capacity and groundwater levels were close to seasonal maxima. However, for much of the spring and summer of 1995, a northward extension of the Azores high-pressure belt deflected rain-bearing frontal systems and precipitation deficiencies built up rapidly (Marsh, 1996). Precipitation totals from April to August in 1995 were at 42 percent of the long-term average from 1872-1996 in Yorkshire (Marsh, 1996; Table 1-1). This gave an estimated rainfall return period for this sequence of over 200 years. The deficiency in precipitation was more acute in the west of the region than elsewhere, a reversal of the normal pattern. Most precipitation across the UK during this period resulted from patchy showers or localised thunderstorms. However, some areas, including west Yorkshire, experienced intense drought conditions. Hot, sunny conditions also increased average evaporative demands by up to 20 percent (Marsh, 1996).

By May, unprecedented demands began to reveal weaknesses in water supply distribution networks and there were calls for voluntary restraint on water use. By the end of June 1995, reservoir supplies serving the Bradford and Calderdale areas were already under stress. From mid-July to late August, there was a notable decline in reservoir levels, especially in west Yorkshire and the Pennines, to below 20 percent of capacity. Precipitation for September roughly translated to the long-term average. However, this was a temporary respite as in October precipitation was once again below 50 percent of the long-term average, remaining below the long-term average for the rest of 1995 and into January 1996 (see Table 1-1). After

February 1996 reservoir levels improved but by the independent inquiry in March 1996 (Uff, 1996), the accumulated precipitation deficit had amounted to some 400 mm.

1995	Apr	May	Jun	Jul	Aug	Sep	Oct	Nov	Dec
Precipitation amount (mm)	26	44	22	29	13	96	29	65	70
% of long-term average	44	73	37	49	18	141	40	91	84

1996	Jan	Feb	Mar	Apr	May	Jun	Jul	Aug	Sep
Precipitation amount (mm)	46	78	31	41	52	35	41	80	31
% of long-term average	58	134	46	69	87	58	69	107	45

Table 1-1: Comparison of observed precipitation and long-term areal averages (1872-1996) for Yorkshire during the 1995-96 drought.

The 1995-96 drought lies outside all previously recorded events in the region over 124 years of record and constituted a reversal of the normal precipitation pattern, having a more severe impact in the west than the east. In terms of severity, the return period has been estimated to be in the range of 1 in 50 years to 1 in 200 years, but a severe impact was felt due to the unusual nature of the drought. During other dry years, normal precipitation patterns have re-established themselves in the autumn. However, this was not the case in 1995 (Uff, 1996).

The timing of the drought and type of resources involved meant that the 1995-96 drought had a much more severe impact upon northern England than the southeast. The southeastern half of the country tends to be reliant on groundwater resources for water supply. With the protracted wet period from 1992-95, these aquifers were near their maxima, and since the main recharge occurs in winter months, the summer drought had little impact upon aquifer levels. However, the north of England is reliant on surface water resources. Much of Yorkshire, in particular, is dependent upon a large number of single-season upland reservoirs in the Pennine hills. These fill during winter months and are drawn-down in summer months, with relatively little carry-over from one year to the next. If low precipitation totals persist into autumn and winter these resources become increasingly vulnerable (Marsh, 1996).

Many emergency measures were taken by Yorkshire Water Services (YWS) during the 1995-96 drought. For example, the number of drought orders implemented is shown in Table 1-2 (Uff, 1996). Towards the end of June 1995 YWS implemented a publicity campaign aimed at reducing consumption, by which time reservoir supplies were already depleted. On July 7th, the first hosepipe ban took effect, covering the West Yorkshire area. This was quickly followed by

the first applications for Drought Orders to reduce reservoir compensation flows, increase river abstraction and impose restrictions on the non-essential use of water on 26th July (Uff, 1996).

The erection of standpipes began in Bradford on 8th August, and was followed by Calderdale later that month. However, it was decided that rota-cuts were the preferred option. Tankering water by road began on the 7th September, after the Chairman of Yorkshire Water was summoned to a meeting with the Secretary of State for the Environment on the 4th September 1995. YWS then made it a policy to adopt all possible means, regardless of cost, to avoid rota cuts. The number of tankers needed in order to implement this policy rose to over 700 tankers daily, at a cost of over £47 million (Uff, 1996).

Type of Drought Order	Number of Drought Orders
Increased abstraction	6
Increased river abstraction	10
Reduced compensation flows	8
Restriction of use	4
Total	**28**

Table 1-2: Number of drought orders implemented by YWS in 1995-96 (after Uff (1996))

On the 18th September 1995, Yorkshire Water announced the first phase of emergency measures, designed to improve the operation of the grid system, and costing £50 million. The second phase was announced on the 25th of October at similar cost. The objective was to have the scheme in place by April 1996 to avoid a repeat of measures taken to alleviate the 1995 drought. One of the major proposals was the creation of a direct grid link into west Yorkshire. Previously there had only been the capability to transfer water from the west of Yorkshire to the east. However, had this direct link been available in 1995 it would have obviated the need for tankering from east to west Yorkshire (Uff, 1996).

The road tankering ceased on the 12th January 1996 and, despite the continuing low precipitation totals throughout the spring months of 1996, YWS were able to maintain supplies without the need for further restrictions (Uff, 1996).

Yorkshire Water was severely criticised at the independent inquiry (Uff, 1996) held in March 1996 for its lack of drought contingency plans. It is clear that if YWS had taken precautionary measures earlier then many of the desperate actions would have been avoided later. They were also criticised for their use of the WRAP model for managing existing resources with its main

objective being the minimisation of operating costs. No provisions were available within the model for dealing with drought severities outside the design standard. In fact, the objective function of the WRAP model contributed to the problems by drawing down the cheapest sources of water (i.e. reservoirs in western Yorkshire) when they were at their most vulnerable, rather than using the more expensive river and groundwater sources in eastern Yorkshire. The independent enquiry in March 1996 (Uff, 1996) suggested that a better objective function would have been to maximise resource value.

"*What appears to have been overlooked is the old axiom that resources should be held as near to the top of the system as possible rather than vice versa*", the Independent Inquiry report (Uff, 1996).

1.1.3 Actions from the 1995 drought

Largely as a result of the 1995 drought, water resources management in the UK has received considerable attention. In 1996, the Department of the Environment published an Agenda for Action (DoE, 1996) and the House of Commons Environment Select Committee conducted hearings and published recommendations (Environment Select Committee, 1996). Both reports acknowledged climate change as high on the agenda and recommended that the potential implications of climate change for water resources in the UK should be examined. The Director General of OFWAT announced in 1997 that in 1999 there would be a periodic review of water company investment proposals. For these, companies would be required to consider the effects of climate change in the assessment of future resources, demands and investments. Although there have been several studies into the possible effects of climate change on hydrological regimes in the UK, few have considered the implications for water resources. Those that have include Hewett *et al.* (1993) and Wardlaw *et al.* (1996). Therefore, a project was commissioned jointly by UKWIR (UK Water Industry Research Limited) and the EA (Environment Agency) to examine the effects of climate change on river flows and groundwater recharge and produce guidelines for resource assessment.

The results were presented in 1997 (UKWIR/EA 1997) and consist of a series of regional factors that can be applied to observed monthly streamflow or annual groundwater recharge data to represent the consequences, by 2020, of four of the Hadley Centre's future climate change scenarios. The effects of climate change on yields can then be examined by comparing yields determined using the original data and the perturbed data. This approach was applied by the UK

water companies to investigate the likely effect of future climate change upon long-term yields, and results were included in the 1999 OFWAT assessment.

The Yorkshire Water draft Water Resources Plan was published in 1998 (YWSL, 1998) and details Yorkshire Water's long-term planning strategy up to 2024/25, including future climate change. It compares forecasts of customer demand for water with the water available from the supply system, with a margin (target headroom) of nine percent between demand and supply to allow for uncertainties. Demand forecasts were calculated in line with national standards and show a fall in total water delivered of about six percent over the period to 2024/25. The dry year average annual demand is predicted to rise from 1365Ml d^{-1} in 1998/99 to 1376Ml d^{-1} in 2024/25. These will be achieved mainly by larger licensed abstractions from the Rivers Ouse, Wharfe and Ure, and leakage reductions beyond the OFWAT target for 1999/2000 of 329Ml d^{-1}.

However, the 'factor' approach has shortcomings, namely:

- The methodology allows no change to occur to temporal and spatial patterns of precipitation. There is no evidence that observed temporal (wet and dry transition probabilities) and spatial patterns will still occur in a future perturbed climate.
- There is also no scope for changing the temporal variability of the precipitation time series, for example, changing the frequency of occurrence of extreme events or prolonged dry periods.
- Biases may be introduced by keeping a fixed proportion of dry days with a changed mean precipitation amount.
- No examination can be made of long precipitation time series to determine return periods of extreme events such as droughts. The precipitation time series is fixed at the observed length, usually at a maximum of 100 years.

A more serious limitation of the 'factor' approach detailed above may be that it is difficult to quantify the risk of failure of the whole or part of a water resource system under future climate change as no spatial or temporal change to precipitation patterns have been made. A more useful approach, and the one taken by this thesis, is to construct a stochastic precipitation model capable of producing long data series with the same characteristics as the observed data. The model parameters are then perturbed to simulate future climate change scenarios and produce long synthetic data series. This will provide a method of changing both temporal and spatial

precipitation patterns, and all precipitation statistics. In this way, the likelihood of failure may be quantified, using a return-period type approach or other more sophisticated tools.

1.2 Principal research aims

This project was funded by an Engineering and Physical Sciences Research Council CASE studentship in conjunction with the northeast Environment Agency (Leeds regional office).

The 1995 Yorkshire drought has raised concerns for both the Environment Agency and Yorkshire Water. This thesis aims to examine whether the 1995 Yorkshire drought was a chance occurrence or whether this type of event is expected to occur with increasing regularity. The research will be carried out in four main stages. Firstly, an analysis will be made of both the spatial and temporal historical climatic variability within Yorkshire and attempt to link this to large-scale atmospheric circulation processes. Secondly, an examination will be made of historical drought events in Yorkshire using a drought index approach based on precipitation deficits. These will then be linked to weather type occurrence patterns. Thirdly, a spatial stochastic rainfall model will be developed to reproduce historical precipitation variability in Yorkshire, developed using a baseline scenario for 1961-1990. This will be validated using historical data. Fourthly, a risk analysis of the Yorkshire water supply grid will be undertaken using future climate change scenario data from the Hadley Centre in conjunction with the stochastic rainfall model.

The principal research aims of this thesis are therefore as follows:

1. Examination of historical climate records

- To examine long climatic records in Yorkshire, UK, for signs of climatic instability, variability and change. In particular, this should include an analysis of changes to mean precipitation receipts, as well as to extreme event occurrence. The implications of both spatial and temporal change should be considered.
- To attempt to link any climatic change discovered to large-scale atmospheric circulation indices, on both an annual and monthly basis.
- To determine changes in the large-scale atmospheric circulation indices, and whether this has an effect upon local-scale climatic variables within Yorkshire.

2. Examination of historical drought events

- To examine the spatial and temporal extent of historical drought events within the Yorkshire region using observed precipitation records, and a precipitation deficit index.
- To relate these drought events to large-scale atmospheric circulation structures to attempt to explain the processes involved in both drought initiation and persistence.
- To determine critical drought duration and temporal sequencing within the Yorkshire region.

3. Development of a spatial-temporal stochastic rainfall model for Yorkshire

- To delineate Yorkshire into climatically similar sub-regions based upon the prior analysis of both local-scale climatic variables and large-scale atmospheric circulation.
- To develop a spatial precipitation model for each sub-region, incorporating information from large-scale atmospheric circulation processes.
- The model should be capable of reproducing inter-annual variability, as well as important drought events, and be an improvement upon unconditioned stochastic models that are currently available.
- The correct spatial correlations should be preserved between sites within a sub-regional model, and between sub-regional models.
- The model should be capable of producing long daily precipitation series at sites where inflows are required for the Yorkshire grid model.

4. Risk analysis of the Yorkshire water supply grid

- Rainfall-runoff models should be calibrated using historical data series and used as input to the Yorkshire grid model.
- The precipitation model sensitivity to natural climatic variability should be examined.
- Future climate change scenario information should be used within both the precipitation model and the rainfall-runoff model (in terms of potential evapotranspiration changes) and used to determine areas of potential vulnerability in the Yorkshire water supply grid.

- The risk posed by such climatic change to water supply reliability, resilience and vulnerability should also be quantified.

1.3 Structure of thesis

The thesis is split into eight chapters. Chapter 1 provides an introduction, and sets out the aims and objectives of the thesis. Chapter 2 then shows how this research relates to past literature. Chapters 3 and 4 examine historical evidence of natural climatic variability and droughts to attempt to provide a context for the 1995 drought event. Chapter 5 details the construction of a stochastic spatial precipitation model conditioned by large-scale atmospheric circulation. Chapter 6 describes the calibration of rainfall-runoff models for Yorkshire. Chapter 7 then uses both the stochastic rainfall models and rainfall-runoff models to investigate the impacts of natural climatic variability and change on the reliability, resilience and vulnerability of water resources in Yorkshire. Finally, Chapter 8 presents the conclusions of the research and suggests future work.

Chapter 2: Literature Review

"Is there a climate? Obviously the average weather over the last 12,000 years is different than the average weather over the previous 12,000 years when most of North America was covered by ice. Is it possible that a system like the weather may never converge to an average?"

Edward Lorentz, the climatologist pioneer of chaos theory, quoted by Gleick (1987*b*)

2A.1 Recent climate change in the UK

There have been significant changes in the temporal and spatial distribution of precipitation across the UK since the 1960s, with an enhancement of partitioning between winter and summer precipitation and an exaggeration of the northwest to southeast precipitation gradient being particularly prominent characteristics (Mayes, 1995). This has resulted in substantial increases in runoff in parts of upland Scotland (Smith, 1995). Over the past 20 years summer precipitation has been more than 20 percent below and temperatures 0.6 °C above the preceding average (Marsh, 1996). In addition, much of the recent past has been exceptionally mild and encouraged very high rates of evaporation (Marsh, 1996). There has also been a marked increase in notable flood events (Black and Bennet, 1995) and drought episodes (Marsh *et al.*, 1994). This may restrict aquifer recharge to a period of weeks, as occurred in 1989/90 and 1990/91 for Eastern Britain (Marsh *et al.,* 1994), and soil moisture deficits may persist well into the autumn months (Marsh, 1996).

There is no historical parallel to the recovery of water resources after the 1988-92 drought when the driest 28-month sequence since the 1850s was immediately followed by the wettest 32-month sequence of the last 100 years (Wilby *et al.*, 1997). The winter of 1994/95 was one of the wettest in Britain since 1869 but was followed by the driest 5-month sequence for 200 years, bringing groundwater levels to an all time low. In addition, 1995 was not only, according to the Central England Temperature (CET) record, the hottest summer on record over England and Wales, but also the driest.

The direction, frequency and vigour of Atlantic frontal systems, together with the concentration of high relief in Britain, and associated rain-shadow effects, are important determinants of UK precipitation patterns. Many of the observed changes in climate in the UK are consistent with changing frequencies of regional weather types (such as Lamb (1972)) which show an increased influence of the westerlies over western Europe (Bardossy and Caspary, 1990) and increasing anticyclonic and cyclonic airflows, manifested by more northerly paths for the preferred tracks

of Atlantic frontal systems (Sweeney and O'Hare, 1992; Wilby, 1997). Significant change has occurred in the three most common atmospheric circulation patterns since records began in 1861 (Lamb, 1972). Most notably a marked rise in southerly days and/or a decline in northerly days since the 1970s causing increased meridional flow over the British Isles. No significant correlations have been found between these and decadal CETs (Sowden and Parker, 1981). However, a study of monthly CET anomalies in very warm years (Murray, 1992) showed an increase in meridional airflows, and more frequent blocking in July and August, accompanied by decreased precipitation over England (Mayes, 1998). The decline in summer precipitation totals in coastal areas of southeast England since 1980 has also been linked to recent changes in the frequency of regional weather types (Mayes, 1991*b*; 1995).

In recent years, there has been an amplification of the seasonal pattern of precipitation, exemplified by many examples within the literature. Mayes (1996) suggests that the increased proportion of annual precipitation in the UK in the winter half-year between 1941-1970 and 1961-1990 is a consequence of an enhanced seasonal cycle in the vigour of the mid-latitude westerly circulation, originating in enhanced baroclinicity over the North Atlantic. A possible cause of this would be a contrast in weather patterns between an anticyclonic pattern over England and Wales and a westerly flow across northern Scotland (Mayes, 1998). Evidence for this has been demonstrated in both studies of the Northern Hemisphere zonal circulation (Kozuchowski, 1993) and from British Isles airflow type frequencies, although this is better shown by a regional airflow catalogue (Mayes, 1994). Enhanced baroclinicity can usually be identified by stronger than average latitudinal gradients between sea-surface and air temperature between 30 and 60 °N. Evidence of temperature anomalies in the 1980s (Folland *et al.*, 1990) and 1990s have confirmed this pattern. Cooling has been focussed near Greenland and a large part of the North Atlantic whereas warming has occurred over most of terrestrial western Europe (Walsh, 1993). This is comparable to many climate change scenarios produced for Europe (Gates *et al.*, 1992). An amplification of climatic contrasts across the UK is evident in some of the recent scenarios of future climatic change to the mid-twenty-first century (e.g. CCIRG, 1996) and the climate of the British Isles during the last decade has been notable for its enhanced variability (Wilby *et al.*, 1997).

Many researchers have linked recent changes in spatial and temporal precipitation patterns across the UK to large-scale atmospheric circulation. For example, Wilby *et al.* (1994) demonstrated a clear correlation between a simple synoptic weather index and annual precipitation totals since 1861 and Wilby (1993*a*) showed that the frequencies of floods and droughts depend upon the prevalence of dominant synoptic weather types. Similarly, Wilby (1997) determined that pronounced shifts in dominant storm tracks and associated synoptic eddy

activity affecting the transport and convergence of atmospheric moisture were also significantly correlated with regional precipitation. An investigation has also been made into the correlation between UK regional precipitation and other climatic variables in relation to decadal variations in the atmospheric circulation during winter over the North Atlantic (Wilby *et al.*, 1997). The North Atlantic Oscillation (NAO) is a measure of pressure gradient between Gibraltar and Iceland and exerts an important control over spatial precipitation receipts within the UK. Years with a high mean NAO index experience above average temperatures, more frequent westerly circulation types, greater airflow strengths, and higher precipitation totals in northwest England and Scotland, with lower runoff totals in other parts of England and Wales. Since the 1980s, the index has been strongly positive with an underlying trend towards a higher NAO with associated higher winter temperatures and a steeper northwest to southeast precipitation gradient. However, the present annual trend is towards a reduction in the NAO. The presently more negative NAO tends to push weather systems further south, producing increased winter precipitation receipts in the south and east but reducing those of the north and west relative to that of a highly positive NAO.

Important feedbacks between the North Atlantic thermohaline circulation and freshwater input from terrestrial hydrology could also lead to temperature changes of a few degrees within periods of only a few years (Rahmstorf, 1995). An example of this effect is provided by the Younger Dryas event of 10,000 BP (Manabe and Stouffer, 1995) that was caused by meltwater. However, recent work by Cubasch *et al.* (2000) suggests that although precipitation changes in a climate change environment are sufficient in some instances to decrease the thermohaline circulation noticeably, the amount of freshwater needed to bring the circulation to a halt is magnitudes larger than the anticipated change in precipitation due to anthropogenic activities.

2A.2 General Circulation Models (GCMs)

General Circulation Models (GCMs) are used to provide information on how the climate may evolve or change under certain conditions, and produce climate change scenarios. They are three-dimensional climate models, either atmospheric with a crude 'slab' ocean or coupled ocean-atmosphere with a three-dimensional ocean. The equations that govern GCM operation describe changes in momentum, temperature and moisture and subdivide the atmosphere vertically into discrete layers. The typical horizontal resolution of a GCM is between 300 and 1000 km and there are usually between two and 19 vertical levels. Many atmospheric processes occur at smaller scales than these and tend to be represented collectively by parameterisation schemes. Parameterisation introduces two main problems. Firstly, empirical statistical elements must be used and thus bias may be included. Secondly, model validation becomes more difficult

as comparisons cannot be truly independent since empirical evidence is used in model construction (Airey and Hulme, 1995).

GCMs generally simulate precipitation as two types, stratiform and convective. The simplest kinds assume that stratiform precipitation will fall when relative humidity exceeds 80 percent. Schemes either assume that all condensed moisture will fall instantly to the ground (e.g. Shultz *et al.*, 1992) or take account of evaporative processes within the atmosphere (e.g. Smith, 1990). Convective precipitation is harder to model as it occurs due to instability within the atmospheric column, generally at the sub-grid scale. The major problem with the modelling of convective precipitation has been finding suitable relationships between the microphysics of individual clouds and the average precipitation occurring over a grid-box. This has been noted as a critical issue by many researchers (e.g. Senior and Mitchell, 1993). Even when a GCM model has been run there are problems with the evaluation of the precipitation component due to the lack of a reliable observed global data set with which to compare the simulated field.

Historically, GCM simulations have been equilibrium experiments, providing a scenario for a point in the future where the climate system has reached a balance with a given increase in concentration of greenhouse gases. However, transient simulations of the climate system, with gradually changing levels of greenhouse gases, are now commonplace. The first GCMs were run to simply simulate a change in carbon dioxide concentration. However, recently there has been increasing evidence that the response of climate to an increasing array of greenhouse gases may be modified by the effect of sulphate aerosols (e.g. Mitchell *et al.*, 1995*a*). Sulphate aerosols scatter sunlight in the atmosphere and so tend to cool climate. They can also have a more indirect effect, increasing the concentration of condensation nuclei in the atmosphere, so producing brighter cloud. However, they have lifetimes of only 1-2 weeks, in contrast to greenhouse gases with 10-150 year residence times, and so tend to concentrate downwind of industrial areas. Estimates have been made of the geographical distribution of sulphate loading (e.g. Taylor and Penner, 1994) and climate models have estimated the effects upon global warming. These show markedly different patterns of future change from greenhouse gas only integrations. It appears likely that northern mid-latitudes will be radiatively cooled, and in winter high-latitudes concentrations will increase due to feedbacks between sea ice and temperature. It must be remembered though that in the long-term sulphate aerosol loading may diminish, whereas carbon dioxide has a lifetime of more than a century.

The 'new' GCMs incorporating both greenhouse gas and sulphate aerosol forcing give a better representation of the observed pattern of temperature change in recent decades, both at surface and in the free atmosphere (Santer *et al.*, 1994; 1995; Santer, 1996; Mitchell *et al.*, 1995*b*; Johns

et al., 1997). Mitchell and Johns (1997) used a GCM to simulate global greenhouse gas plus sulphate aerosol forcing. Results showed that the response to a gradual increase in CO_2 concentrations would be drying in northern mid-latitudes in summer and the intensification of the Asian summer monsoon. However, the addition of sulphate aerosols reduced the warming, especially in northern mid-latitudes. Summer precipitation and soil moisture levels were found to decrease over South East Asia, but conversely, increase over southern Europe and Asia.

McGuffie *et al.* (1999) compared the ability of five different GCMs to accurately simulate temperature and precipitation variability. Results showed that although there was reasonable agreement on the global scale, there were significant differences regionally. Regional climate change prediction is regarded as a "cascade of uncertainty" (Mitchell and Hulme, 1999) by many researchers and, as such, using model estimates of variability changes must be carefully justified. Additionally, precipitation change predictions for the UK are hindered by the fact that mixed ocean/land grid squares are used (Beven, 1993).

Although, GCM experiments provide the basis for climate impact applications it is important that these studies are not constrained by the relatively narrow sampling of future climate scenarios explored by GCM experiments (Hulme, 1999). Whereas most GCMs have looked at an increase of one percent per annum of greenhouse gas concentrations, the real figure may be somewhere between 0.5 and 1.1 percent. Different climate scenario construction methods have been proposed that take account of these greater uncertainties by rescaling GCM predictions (e.g. Hulme and Brown, 1998; Hulme and Jenkins, 1998). A GCM pattern scaling method first proposed by Santer *et al.* (1994) has now been extended by Hennessey *et al.* (1998). By adopting a Monte-Carlo approach, this uncertainty can now be more fully explored, thus improving risk assessments of climate change impacts.

2A.3 IPCC, CCIRG and UKCIP research and current projections

The first Intergovernmental Panel on Climate Change (IPCC) estimation of global warming, under the business-as-usual emissions scenario, was given in 1990 (IPCC, 1990). This projected an average rate of global warming of about 0.3 °C per decade. In 1992, the IPCC supplementary report (IPCC, 1992) also recognised that there may be changes in variability and that occasional extreme events may have a larger impact than changes in mean climate (Katz and Brown, 1992). The ability of GCMs to accurately model changes in precipitation variability due to a doubling of CO_2 concentrations has been questioned by many researchers (e.g. Cess *et al.*, 1990), especially in the inference of changes in inter-annual and regional events. However, there

is a general pattern of increased variability under a rising mean precipitation, and vice versa (Wilson and Mitchell, 1987; Rind *et al.,* 1989). There is also evidence that a warmer climate would produce an increased frequency of convective rainstorms, and thus less events of more persistent, gentler precipitation (Noda and Tokioka, 1989; Gordon *et al.,* 1992).

The IPCC second report (IPCC, 1996) concludes with the statement that, "*the balance of evidence suggests a discernible human influence on global climate.*" It is estimated that there will be an increase in mean surface air temperature relative to 1990 of about 2°C by 2100 (using the mid-range scenario IS92*a*). This is a third lower than the 1990 projection. As part of this report the effects of climate change on hydrological regimes were also considered. Conclusions were that:

(a) GCMs predict an increase in global mean precipitation of 3 to 15 percent for a temperature increase of 1.5 to 4.5 °C, with higher-latitude regions expected to experience more precipitation, particularly in winter.
(b) Case studies have shown increased annual and monthly flows due to increased precipitation in high-latitudes, although dry areas were more sensitive than wet areas to climate variations.
(c) There will be changes to precipitation characteristics.

The CCIRG (Climate Change Impacts Review Group) produced its first report considering the potential impacts of climate change in the UK in 1991 (CCIRG, 1991). This was updated in the second report (CCIRG, 1996). The second report uses the best estimate scenario at the time (IPCC IS92*a*) (Leggett *et al.*, 1992) to provide predictions. More recently, four new climate change scenarios have been considered by UKCIP (UK Climate Impacts Programme) using the Hadley Centre's HadCM2 model (Hulme and Jenkins, 1998). These are called the UKCIP98 climate scenarios and are labelled as Low, Medium-Low, Medium-High and High, spanning a range of emissions scenarios and different climate sensitivities. For further information on the Hadley Centre models, see Hulme *et al.* (1999). The CCIRG UK patterns of precipitation changes are broadly similar to UKCIP98, although the newer UKCIP98 model projects a more uniform winter wetting than CCIRG. The UKCIP98 projections are as follows:

(a) Temperatures across the UK are expected to rise at a similar rate to the global mean, at slightly less than 0.15 °C per decade, with a pattern of larger increases in the southeast of the country than in the northwest.
(b) Changes in mean annual precipitation are modest, with increases by 2080 of between 0 and 10 percent over England and Wales, and between 5 and 20 percent over Scotland.

(c) Winter and autumn precipitation will increase across the whole of the UK, but in spring, and especially summer, the southeast of the country becomes drier whereas the northwest becomes wetter.
(d) Year-to-year variability in precipitation increases almost everywhere, even in seasons and regions where drier conditions are experienced.
(e) The number of raindays will increase slightly over much of the county in winter, but only over the northern UK in summer.
(f) Intense daily precipitation events will become more common in all seasons, but especially winter.

However, the use of model derived estimates of change must be very carefully justified as there are huge differences between models on a regional scale (McGuffie *et al.*, 1999). Until improvements are made to GCMs, regional climate change prediction can still be regarded as a "*cascade of uncertainty*" (Mitchell and Hulme, 1999; p57).

2A.4 Evidence of climatic change and variability

Evidence of climatic change and variability has been found in both temperature and precipitation records across the globe. Observed trends have been delineated from natural variability, but there are many problems with this type of approach. Modelled changes have also been derived.

2A.4.1 Difficulties in trend detection

Many difficulties are apparent in detecting trends in environmental time series (Kite, 1993). Firstly, the components of a time series may change with time; what appears to be a trend now may turn out to be part of a periodic cycle when looked at over a longer time period. Secondly, jumps in the data must be accounted for since otherwise any trend analysis can be misleading. Thirdly, most current research uses averaged data from hundreds or thousands of climate stations and it is possible that using average rather than individual time series may hide underlying patterns in the data or opposing trends (Matalas, 1997) Finally, without reliable statistical inference any climatic trend discovered could be as easily attributed to chance or the variation of natural fluctuations rather than a true climatic change.

It is therefore very difficult to separate any global warming signal from the considerable year-to-year variability in climate, as the signal-to-noise ratio is very low. The 'fingerprint' approach is a method of detection that is now frequently used. The greenhouse effect will have a particular fingerprint, which will differ from the effects of natural climate variability, for example an increase in global temperature at the Earth's surface with a concurrent decrease in temperature higher in the atmosphere. A fingerprint method applied by Karoly *et al.* (1994) however acknowledges that not only the greenhouse effect will have a bearing upon stratospheric temperature data. The depletion of stratospheric ozone has contributed to stratospheric cooling, more frequent and stronger ENSO events during the 1980s have contributed a warmer troposphere, and a global increase in sea surface temperatures during the 1980s may have other explanations.

Karl (1994) suggests that improvements must therefore be made in the ability to distinguish anthropogenically-derived change from natural variability and to link variables affected by climate change and variables that affect life on the planet. Recent work by Radziejewski *et al.* (1998) has attempted to determine the best methodology for trend detection within discharge time series. A method was devised to compare different test results, which allows, to a certain extent, the differentiation between trends and natural fluctuations.

2A.4.2 Temperature data

2A.4.2.1 Sources of error

A number of independent sources of error in temperature trends have been identified by the IPCC (1990), including urban heat island bias, changes in observing times, changes in instrumentation, station relocations and inadequate spatial and temporal sampling. Karl *et al.* (1993) examined errors in estimates of temperature trends due to inadequate temporal and spatial sampling. Results indicate that errors in century-scale trends are probably minimal compared to the actual warming trend. However, on a decadal time-scale errors are large and observed trends unreliable. It is suggested that analyses could show immediate improvement by addressing the over-sampling of the Northern Hemisphere relative to the rest of the globe.

2A.4.2.2 Observed and modelled changes

Stouffer *et al.* (1994) developed a mathematical model to reproduce low frequency natural climatic variability and found that 'naturally' a temperature change as large as 0.5 °C per

century will not be sustained for more than a few decades. However, in an analysis of land and marine records over the past century a 0.5 °C warming was observed (Jones and Wigley, 1990). Hulme and Jones (1994) also revealed a global-mean warming of 0.4 ± 0.15 °C in a comparison of 140 years of historical data. This is analogous to the magnitude of cooling that caused the 'Little Ice Age'. Although records indicate that global temperature has increased over the last few decades, the extreme west of Europe and north-east Atlantic have only slightly warmed, or even cooled, suggesting that change will be spatially non-uniform (IPCC, 1996).

Possible changes to day-to-day temperature variability in the Northern Hemisphere were examined by Karl *et al.* (1995). It is proposed that the day-to-day variability of maximum and minimum temperatures has decreased, but on larger temporal scales such as inter-annual, it is concluded that variability has increased in recent decades (Parker *et al.*, 1994).

Results from a transient GCM experiment in western Europe where carbon dioxide concentrations were increased by one percent per year over 75 years (Rowntree *et al.*, 1993) suggest that warming will be at a minimum near the Atlantic coast and a maximum in eastern Europe. The temperature increase from 1990 to 2030 appears to range from 0.75 °C in the west to about 1 °C in the east of the UK and 1.5 °C in eastern Europe. The model also suggests more extreme warm anomalies in winter. In the UK, the largest changes are expected to be in the east, mitigating cold spells in the winter and enhancing warm spells in the summer. A decrease in frost occurrence is also likely; a 1 °C rise in temperature may induce a 25 percent reduction (Rowntree, 1990). Gregory and Mitchell (1995), using the UKMO model under an equilibrium scenario, found a reduction in temperature variability due to a decrease in the land-sea temperature difference in winter, but increased variability in summer temperatures.

The Central England Temperature record compiled by Manley (1974) provides the most comprehensive record of temperature changes in the UK since 1659. This record was partially reworked by Parker *et al.* (1992) before being analysed by Hulme and Jenkins (1998). Three main points were highlighted by this study:

(a) There has been a warming of 0.7 °C of UK climate since the 17th century and 0.5°C during the 20th century.
(b) The warming is greater in winter (1.1 °C) than in summer (0.2°C).
(c) The last decade 1988-1997 is the warmest in the entire series, with four of the five warmest years since 1659 occurring in a short period.

This evidence backs up claims that temperatures throughout the UK have shown an increasing trend in recent years. The CET temperature record confirms that the post-1986 decade is the warmest on record and four of the eight warmest years this century cluster in the 1986-1995 period (Marsh and Sanderson, 1997). However, Willmott (1996) noted that the recent summer warming has been restricted to the months of July and August and that the frequency of cool Junes has increased since the early twentieth century.

Such studies assess mean changes only but changes in daily temperature extremes were examined by Hulme and Jenkins (1998). There has been a marked reduction in the frequency of 'cold' days (mean temperature below 0°C) since the eighteenth century. There has also been a rise in the number of 'hot' days (mean temperature above 20°C) in recent years. The 1990s have seen the highest frequency of 'hot' days within a decade in the entire record since 1772; at 7.5 days a year nearly twice the long-term average.

Long-term temperature records are available for many locations in the UK but these are generally restricted to lowland areas. There are little available upland temperature records prior to the last 100 years. However, it cannot be assumed that temperature changes will be uniform across upland and lowland areas. One such study of trends in temperature data in an upland record is that of Garnett *et al.* (1997); they found no warming trend.

2A.4.3 Precipitation data

2A.4.3.1 Sources of error

Precipitation measurements that have been taken at approximately the same location for more than 200 years are fairly common in Europe (Tabony, 1981) and there are about 100,000 precipitation gauges worldwide (Groisman and Legates, 1995). However, many biases exist in precipitation measurements and this makes analyses of trends problematic.

The spatial distribution of terrestrial precipitation gauges is not uniform but instead biased towards coastal and urban locations, and long-term data is available for only a small sub-set of stations (Groisman and Legates, 1995). Gauge densities are high in the USA and Europe, but some areas are poorly represented, especially mountainous areas (Airey and Hulme, 1995). Many mountain gauges are located in the valleys despite the recognised increase in precipitation with altitude (Barros and Lettenmaier, 1993) and thus provide inadequate readings. Oceanic precipitation data exists for only a small number of atoll and island stations, and ship-based

gauges which are subject to many biases (Quayle, 1974). Techniques have been developed to estimate oceanic precipitation from atmospheric synoptic circulation patterns (e.g. Dorman and Bourke, 1981) or nearby terrestrial measurements (e.g. Reed, 1980). However, these suffer many limitations and have now been superseded by radar or satellite measurements (e.g. Arkin and Xie, 1994). Global fields have been produced since 1986 (e.g. Hulme, 1992).

Biases in precipitation gauge measurements can be substantial. Systematic biases can be attributed to seven major sources: the effect of the wind, wetting losses, evaporation from the gauge, splashing effects, blowing and drifting snow, the treatment of trace precipitation events, and the impact of automatic recording (Folland, 1988). The effect of wind upon gauge catch is thought to provide the largest bias and accounts for an undercatch in annually averaged global precipitation climatology of about eight percent (Legates, 1987). Air is forced to blow around the gauge and wind speed increases over the gauge orifice, causing a gauge undercatch. This error increases with both altitude and latitude and can have particular emphasis on snowfall measurements. National standard precipitation gauges vary in size, shape and design, as well as elevation of the orifice above ground level, and thus the effect of the wind is gauge dependent. Wetting can contribute a further two percent loss and the evaporation of precipitation stored in the gauge can lead to another one percent loss.

For example, Essery and Wilcock (1991) examined the precipitation catch between 1976 and 1988 from three standard MKII Meteorological Office gauges; one exposed, one surrounded by a turf wall and the other mounted at ground level. The annual difference in catch of the turf wall and ground level gauges, relative to the standard exposed gauge, were found to be increases of two and five percent respectively. Correction equations were produced, and found to be very similar to those of a similar study based in Nigeria (Olaniran, 1982).

Inconsistencies have also been found in precipitation time series caused by gauge relocation, recording practices or changes in instrumentation (Karl *et al.*, 1993). The adoption of new gauges has produced marked discontinuities in precipitation records in many countries, especially if the height or location of the gauge is changed. Instantaneous changes can be spotted in the record but gradual changes may be difficult to detect.

A significant amount of precipitation variability occurs on the micro-scale and gauges located only 100m apart can differ in total precipitation by a factor of two for a single storm (Golubev, 1975). These biases can make the detection of precipitation 'trends' problematic. For small networks, Willmott and Legates (1991) found that precipitation is generally overestimated, while as sample size increases, the network bias decreases, i.e. the choice of station distribution

has less effect. The overestimation of precipitation for small networks occurs due to the bias in location towards urban centres. However, sparse gauge networks may also cause underestimation by overlooking individual storm events, especially in dry climates where convective rainstorms are a more important component (Kay and Kutiel, 1994).

Climate change may itself affect gauge biases in an indeterminate way. Wind speed, precipitation type and air temperature changes may mask or enhance changes in precipitation measurement, even where actual changes are minimal. Urbanisation may also increase precipitation gauge measurements. However, this bias can be reduced by using a large number of stations and by the careful pre-processing of data. Experience with climate change studies shows that large scale changes in annual precipitation over land areas can be documented when data from several thousand stations are used (Hulme, 1995).

Despite these difficulties a number of global precipitation records have now been constructed, for example LEG-COR (Legates and Willmott, 1990) and CRU0092 (Hulme, 1994). In LEG-COR, gauge measurements are adjusted using the methodology of Sevruk (1982) and accounting for wind, wetting loss, evaporation, splashing, blowing snow and random errors. The highest spatial coverage would occur if all gauges were used irrespective of the time-period over which a record was available. This is used in the LEG-COR record, using 24,000 gauges, and assumes that climate is constant on this timescale. Conversely, if a fixed period is used for analysis, for example 1961-90, then spatial coverage is lost, but temporal coherence is increased. Airey and Hulme (1995) suggest that this area warrants further research.

2A.4.3.2 Observed and modelled changes

Most current GCMs predict a prominent change of precipitation occurring in the high latitudes (Manabe *et al.*, 1991, 1992; Murphy and Mitchell, 1995). This is also supported by palaeoclimatic reconstructions, and by the analyses of precipitation trends (Bradley *et al.*, 1987; Diaz *et al.*, 1989; Groisman and Easterling, 1994). Studies of the high latitude Northern Hemisphere suggest a trend towards increased precipitation (Hulme, 1994; Groisman *et al.*, 1999) and enhanced variability (Matyasovszky *et al.*, 1993; Karl *et al.* 1993; Groisman and Easterling, 1994; Easterling *et al.*, 2000). The proportion of precipitation contributed by extreme, one-day events has also increased significantly in the both the Northern and Southern Hemisphere. Significant positive trends in intensity have been observed in the US (Karl *et al.*, 1995; Karl and Knight, 1998), Japan (Iwashima and Yamamoto, 1993), Italy (Brunetti *et al.*, 2000), China (Zhai *et al.*, 1999) and Australia (Suppiah and Hennessey, 1996). However, within

the tropical latitudes of the Northern Hemisphere there has been notable drying in recent decades (Hulme, 1994).

Results from 75-year transient GCM experiment over Europe with carbon dioxide increasing at one percent per annum were compared with equilibrium experiments by Rowntree *et al.* (1993). Conclusions were that precipitation over the UK would show an annual increase, with the largest changes in winter. However, in summer, precipitation totals would decrease except in the north, and winter snowfall totals may decrease. Equilibrium results tend to suggest that over western Europe precipitation will increase in the north and decrease in the south, with the line of zero change further north in the summer (southern Britain) than in the winter (the Alps). Maximum changes in both directions could approach 40 percent. An analysis across Europe based upon the Palmer drought severity index (Briffa *et al.*, 1994) supports this evidence, identifying a statistically significant increase in moisture supply and a notable increase in extreme wet/dry moisture conditions from 1892-1991.

Within the UK, an early monthly England and Wales precipitation series extending back to 1727 was produced by Nicholas and Glasspoole (1931) but lacked long-term homogeneity (Jones *et al.*, 1997*a*). A more recent series back to 1766 was developed by Wigley *et al.* (1984) and has been variously updated (Wigley and Jones, 1987; Gregory *et al.*, 1991; Jones and Conway, 1997). National time series for the period 1931-1989 (Gregory *et al.*, 1991) showed no obvious long-term trend in precipitation, although Wigley and Jones (1987) noted a tendency towards wetter springs and drier summers. However, many researchers have noted a recent amplification of the UK seasonal precipitation regime (e.g. Wilby 1995).

The decrease in UK summer precipitation from the late 1960s has been widely cited as an indicator of climatic instability. For example, Morris and Marsh (1985) found a clear reduction in summer precipitation since the 1970s but no trends in other seasons. Folland *et al.* (1984) acknowledged that four of the driest summers since 1766 in England and Wales have occurred between 1976 and 1984. Similarly, Wood (1989) found that six out of the ten driest summers in London occurred between 1972 and 1984. The largest decreases in summer precipitation across the UK have been observed in the southeast (Mayes, 1991*a*). Marsh and Monkhouse (1991) have shown that the ratio of winter to summer half-year precipitation for England and Wales increased to about 1.3 in the 1980s as compared to close to 1.0 in the last century. However, since about 1980, summer precipitation has increased in the northwest region, reversing previous decreases and contributing to a sharp contrast between northwest increases and southeast decreases (Mayes, 1991*a*).

This contrast may be explained by an increase in westerly airflow types in summer (Briffa *et al.,* 1990) acting in conjunction with an anticyclonic influence in southern Britain to displace storm tracks northwards. Mayes (1996) determined that the primary change from 1941-1970 to 1961-1990 was a reduced influence of the westerlies from April to June but an increased influence in the winter half year. This is thought to contribute to precipitation increases between April and June in eastern districts but decreases in the west. Osborn *et al.* (2000), in an investigation into trends in wetday frequencies and wetday amounts, also noted an increase in winter precipitation over the 1961-1995 period, especially in western and more mountainous regions. This is manifested in the west by a combination of an increase in wet days and an increase in the wet day amount, whereas in the east it is entirely driven by the latter. They found that there has been a weak increase in the mean wet day amount over eastern England in spring, coincident with a decline in the number of wet days which offsets the former effect in amount. In summer there has been a widespread decline in the number of wet days over the 1961-1995 period, occurring at 99 out of 110 stations across the UK and peaking in northern England. In the autumn, there has also been a weak decrease in wet day frequency, but an increase in wet day amount at the majority of stations, which yields enhanced precipitation amounts. Whatever the reasons it is apparent that there is a growing amplification of the seasonal precipitation regime, with the run of very dry summers and wet winters since the early 1980s reinforcing this fact (Mayes, 1996). However, although recent spatial and temporal variations in precipitation across Britain have been unusual (Marsh and Sanderson, 1997), few convincing trends away from the long-term average are discernible.

Osborn *et al.* (2000), developing the work of Karl and Knight (1998), conducted a study into changes to the intensity distribution of daily precipitation amounts in the United Kingdom over the period from 1961-1995. Results of an analysis of 110 UK sites indicate that, on average, daily precipitation is becoming more intense in winter and less intense in summer. They also used 11 stations where longer time series were available from 1908-1995 and the regional means for 1931-1997 (as Wigley *et al.,* 1984). This is further supported by Gregory and Mitchell (1995) who found that precipitation in all seasons shows a tendency towards increased dry days and heavier events due to an increase in convective activity.

The frequency of extreme events can be altered either by changes in the distribution of precipitation intensities or a change in the proportion of wet days, or both. Karl *et al.* (1995) and Karl and Knight (1998) demonstrated a methodology for the US that factors out the influence of changes in the frequency of wet days. However, there are differences between this approach and that of Osborn *et al.* (2000). Karl and Knight (1998) categorised all daily precipitation amounts into twenty classes, each with 5 percent of precipitation events in them, whereas Osborn *et al.*

(2000) delineated ten classes, each containing 10 percent of the total precipitation for the month. Although this varies with both month and season, approximately 50 percent of the lightest events contribute 10 percent of the total precipitation, and 0.5 to 1.5 percent of the heaviest events are sufficient to contribute the final 10 percent of the total. The use of amount quantiles rather than frequency quantiles is thought to improve the approach as each quantile can exhibit large contribution trends.

Results from this analysis suggest that in eastern Yorkshire there has been an increase in heavy precipitation in autumn months but, conversely, a decrease in precipitation intensity in the Pennines. In winter there is an increase in intensity of precipitation across the region, and evidence that the 1990s have had an anomalously low contribution of light events to winter precipitation. Longer records support this as a genuine change. A correlation between this and a coincident increase in the occurrence of thunder over the period 1961-1995 leads to the tentative suggestion of an increase in convective precipitation, associated with vigorous cold fronts, even in winter. In spring and summer, significant trends indicate a transfer in the source of precipitation from heavy to lighter events. However, this may be a return to the longer-term average from an anomalous period in the 1960s rather than a movement towards anomalous conditions.

Some of the most recent global climate model (GCM) integrations, e.g. HadCM2 (Johns *et al.*, 1997), also support these observed trends in the intensity distribution of precipitation. In future scenarios, there is an increased frequency of extreme precipitation events over the UK in winter, with a decrease over northern UK in summer (Hulme and Jenkins, 1998).

2A.5 Studies of the impacts of climate change

Many studies have also been made of the impacts of changes in temperature and precipitation regimes upon hydrological systems, for example, evapotranspiration changes, impacts upon soil properties and groundwater systems. These have generally assumed two forms; empirical studies looking for evidence of the impacts of climate change in historical data series, and modelling studies that examine the changing inputs of precipitation and temperature upon hydrological regimes.

2A.5.1 Impacts upon groundwater

The susceptibility of groundwater systems to climate change or variability has been little studied compared to that of surface water systems. Simple water balance studies have been applied at specific locations to assess the effect of climate change scenarios upon water resource systems (e.g. Bultot *et al.*, 1988; Ayers *et al.*, 1990) but attention has not been specifically focussed on groundwater resources, although Thomsen (1990) considered groundwater recharge in Denmark.

Wilkinson and Cooper (1993) provided the first study of the effect of changes in climate specifically on aquifer storage and river recharge, using a simple model of an idealised aquifer-river system. Using the most likely estimates of climate change for the UK, with an increase of eight percent in winter precipitation, it would be expected that winter recharge to groundwater would increase. However, this will depend upon the antecedent conditions of the soil and aquifer system, the length of the recharge period, the type of aquifer under consideration and the relationship between infiltration rates and precipitation intensity. Transient behaviour was explored and it was determined that slow response aquifer systems, such as Triassic sandstones, are more robust to future climate change. Therefore, time would be available to develop and adjust water resource planning to meet any adverse effects as they may take 15 to 20 years to establish a new equilibrium. However, fast response systems, such as chalk, may take only one to three years. It is also likely that any delay in the onset of recharge in autumn may have a marked effect on those rivers supported by baseflow from rapid response aquifers. Similarly, rapid response aquifers may show a reduction in baseflow to rivers if the recharge period is reduced, even if the volume of recharge is increased, whereas slow response aquifers will show a converse reaction.

Cooper *et al.* (1995) extended this study by introducing the extra variable of changed potential evapotranspiration (PE); one climate change scenario showing a low percentage increase and the other a high percentage increase in PE. Conclusions were that the low PE increase scenario produced little change in the slow response system, but a small change in the fast response aquifers. However, the high PE increase scenario produced a significant reduction in recharge in both aquifers. This translated to a reduction in simulated baseflow of 40 and 15 percent in the fast and slow response aquifers respectively, especially in autumn months. This may have serious implications for water resources.

Recent studies of the impacts of climatic change on groundwater have been conducted under the auspices of the GRACE (Groundwater Resources And Climate Change Effects) project (EC Framework III Project RTD EV5V-CT94-0471). This concentrated on the impacts of climate

change on water resources in a carbonate aquifer. Results suggested that the annual spring discharge will not differ much for the next fifty years under the IS92a scenario (Sauter and Liedl, 1998). However, it is expected that with increasing temperatures over the next 100 to 200 years both aquifer recharge and spring discharge will be adversely affected (Sauter and Liedl, 1998).

A study was also made of the future sustainability of the East Yorkshire Chalk aquifer by Elliot *et al.* (1998). Long established pumping wells only abstract seven percent of the total recharge of the aquifer. However, the aquifer has displayed all-time low piezometric levels during recent droughts (Elliot *et al.*, 1998) due to the high transmissivity and and low storage of the aquifer. The aquifer is affected by the ingress of saline water and diffuse pollution sources. The long-term management of the aquifer must take account of the fact that the aquifer contains a complex mix of modern recharge, modern seawaters and ancient seawaters.

2A.5.2 Impacts upon streamflow

2A.5.2.1 Observed changes

There have been several attempts to identify trends in streamflow data using a variety of statistical techniques (Schadler, 1987; Kite, 1989; 1993; Chiew and McMahon, 1993; Burn, 1994; Lettenmaier, *et al.* 1994; Lins and Michaels, 1994; Mitosek, 1995; Marengo, 1995), most of which have failed to find significant trends. However, an analysis of the stability of flow regimes in Norway (Krasovskaia and Gottschalk, 1992) showed that moderate fluctuations in the mean annual temperature and precipitation can cause changes in both the timing and magnitude of high and low flows. Flood events are shown to have an increased intensity (by 10 to 15 percent on average) during 'warm' years and vice versa during 'cold' years (Krasovskaia and Gottschalk, 1993). Similarly, Lettenmaier *et al.* (1994) found clear increases in November to April river-flow across much of the US over the period from 1948 to 1988. Lins and Michaels (1994) linked these increases to global warming using a longer period of record and Burn (1994) determined that in west-central Canada a greater number of rivers displayed earlier spring runoff than could be attributed to chance, thus consistent with global warming. Additionally, in a global study, Mitosek (1995) analysed 176 worldwide long discharge time-series, with respect to climate variability and change and found annual trends in 42 and 9.1 percent of cases for the mean value and variance respectively, and some monthly trends.

Within the UK, hydrological variability has been notable over much of the past decade (Marsh *et al.*, 1994; Black and Bennet, 1995; Marsh, 1996; Marsh and Sanderson, 1997). In particular, the variation in flow rates captured during the period 1993-1997 is much wider than would be expected over a 4-year period (Law *et al.*, 1997; Fox and Johnson, 1997). Arnell *et al.* (1990) also conducted a comprehensive analysis of daily flow records held in the UK Surface Water Archive. They concluded that there had not been an unusually high number of extreme events in the 1980s, but that 'notable' events had a tendency to cluster in time. However, detecting trends in hydrological data is highly problematic, not least due to the paucity of records over 40 years in length.

2A.5.2.2 Case-studies of hydrological change

Hydrological regimes are by varying degrees, sensitive to precipitation variability and climate change. This view is supported by recent empirical evidence of extreme flows (e.g. Marsh and Lees, 1985; Marsh and Monkhouse, 1991), detailed modelling experiments (e.g. Arnell, 1992*b*), and by the reconstruction of long riverflow records (e.g. Rumsby and Macklin, 1994). To date, however, relatively few studies have concentrated on variability in river water quality (e.g. Wilby, 1993*a*), instead concentrating on the river water quantity implications of climate change.

One of the first studies of the impacts of climate change on the hydrological regime, was that of Nemec and Schaake (1982). They used hypothetical climate change scenarios to drive hydrologic models of both an arid and a humid catchment and assess the effects of climatic variations on runoff. Significant changes of runoff resulted from only moderate changes in temperature and precipitation, especially in the humid basin. For example, a decrease in precipitation of 10 percent coupled with an increase in temperature of 1°C reduced average annual runoff by 25 percent in the arid catchment and by 50 percent in the humid catchment. The climatic changes were found to have a major impact upon the design and operation of reservoir storage. Other early studies include Idso and Brazel (1984) who estimated changes in streamflow in Arizona, varying from a decrease of 30 to 60 percent for a 10 percent decrease in precipitation, and Wigley and Jones (1985) who theoretically showed that changes in precipitation always have an amplified effect on runoff.

A growing awareness of the possible effects of climate change and variability has led to a large number of hydrological impact studies. These can be broadly split into two groups; those concerned with the changes in discharges (I) caused by perturbations of precipitation and temperature, varying widely with climate change scenario and catchment type adopted (e.g. Gleick, 1987*a,b*; Karl and Riebsame, 1989; Lettenmaier and Gan, 1990; Panagoulia, 1992); and

those interested in the effect of catchment type (II) upon the impacts of climate change (e.g. Bultot *et al.*, 1988; Gellens, 1991; Arnell, 1992*b*; Cooper *et al.*, 1995; Van der Wateren-de Hoog, 1995). The latter studies tend to stress the importance of storage capacity and geology using various methods.

2A.5.2.2.1 Hydrological studies concerned with change in discharge (I)

The most common methodology used to study the effect of climate change on the hydrological response of a catchment is the calibration of a rainfall-runoff model against observed precipitation and flow data. This is then used to simulate flows and derive a hydrological index. The input data are then perturbed using the climate scenarios to represent future climatic conditions, and the model is re-run. The two results are then compared (e.g. Gleick, 1986; Bultot *et al.*, 1988; Nash and Gleick, 1991; McCabe and Hay, 1995; Chiew *et al.*, 1995). However, many studies note the uncertainties within this methodology and do not claim to produce definitive results (e.g. Arnell, 1992*b*; Whetton *et al.*, 1993; Chiew *et al.*, 1995), as any feedbacks that may occur under the changed climatic regime and, more importantly, changes in climatic variability are ignored.

Therefore, some studies have investigated climate change effects on runoff using sensitivity tests (e.g. Nemec and Schaake, 1982; Skiles and Hanson, 1994; McCabe and Hay, 1995) rather than the 'climate scenario' output from GCMs, but many studies use both (e.g. Nash and Gleick, 1991). If GCM results are used, it is suggested that results from a number of GCMs should be considered in assessing climate change as they do not even necessarily agree on the direction of change (e.g. Sefton and Boorman, 1997). Research has generally focussed on annual and seasonal changes, but some studies have been done at a monthly (e.g. Cohen, 1986; Gleick, 1987*b*; Arnell, 1992*b*) or daily (e.g. Skiles and Hanson, 1994; McCabe and Hay, 1995) timestep. Similarly, most studies concentrate on changes in mean flows and relatively few look at effects on extreme high or low flows. A few UK studies that have looked at extreme events are Arnell (1992*b*), Arnell and Reynard (1993) and Wilby *et al.* (1994).

Hydrological assessments have tended to concentrate upon simple water-balance regression methods with the assumption that land-use remains constant and that the hydrology responds in a linear way to the imposed conditions (as Gleick, 1986; 1987*a,b*). For example, Bryant *et al.* (1992) stated that a 20 percent reduction in precipitation would result in a halving of runoff owing to a concurrent increase in evapotranspiration. Rotmans *et al.* (1994) show runoff decreases clearly focussed on southeast England by the year 2050.

Within the UK, Arnell (1992*a*) demonstrated that with unchanged potential evaporation (PE), a 10 percent increase in annual precipitation would produce an increase in runoff of 28 percent in southeast England, but only 12 percent in the more humid north and west. However, when changes in PE were included, the net effect was shown to be increased runoff in the northern and western UK due to higher autumn-to-spring precipitation, but decreased runoff in southern and eastern catchments due to higher summer evapotranspiration. However, the current summer water balance and catchment geology are the most important determinants of the sensitivity of flow regimes to a given climate change scenario.

Similarly, Arnell and Reynard (1996) examined 21 catchments in Great Britain using a daily rainfall-runoff model and both equilibrium and transient climate change scenarios. It is predicted that by 2050 runoff will have increased and decreased annually by 20 percent in the wettest and driest scenarios respectively. Under all scenarios considered there was a greater concentration of winter precipitation and less snowfall, and hence snowmelt, was virtually eliminated.

A recent study by Pilling and Jones (1999) improves upon past analyses of the effects of future climate change in the UK. The HYSIM model was used to produce flows for 10 by 10 km grid cell across the UK, for baseline and futures climate change scenarios. Climate change scenarios were constructed using a transient and equilibrium GCM experiment for 2050. Results from both show an increasing gradient in runoff between a wetter northern Britain and a drier southern and eastern UK. Changes in effective runoff show an increased seasonality under both scenarios.

One of the most common conclusions from all hydrological impact studies is to note that changes in precipitation produce greater effects on streamflow. Karl and Riebsame (1989) suggest that the 'amplification factor' between precipitation and runoff may be as high as 4.5 (i.e. a 10 percent change in precipitation results in a 45 percent change in runoff). A study by Wilby (1993*a*) utilised the LWT register in conjunction with observed 24h precipitation totals in order to determine the daily precipitation event probabilities and magnitudes associated with eight dominant synoptic classes. The generated stochastic precipitation time series were used to drive a hydrological model of a catchment in the East Midlands, UK. Interestingly, model results suggested that the frequencies of flood and drought are dependent upon the synoptic scenario, and especially the historical prevalence of anticyclonic and cyclonic circulation patterns.

2A.5.2.2.2 Hydrological studies concerned with catchment type effects (II)

Other studies have concentrated on the effect of catchment type on the impacts of climate change. Bultot *et al.* (1988), for example, demonstrated using three catchments in Belgium that, where geology allows rapid infiltration, increased groundwater storage, baseflow and total flow would result from a warmer and wetter climate. In surface water dominated catchments however, increased winter flood risk, and reduced summer runoff and groundwater recharge are anticipated. Gellens (1991) extended this study by examining the impact of a doubling of CO_2 upon river flow variability. It was found that in catchments with prevailing surface flow the considered change in climate could induce an increase in both frequency and magnitude of floods in winter, a decreased summer streamflow, and possible shortages in groundwater sources in summer. In catchments with a strong groundwater component, it is suggested that an increase in groundwater storage may induce increased baseflow and higher risk of flooding in the winter, but less low flow events in the summer and a possible increase in water availability from aquifers.

Van der Wateren-de Hoog (1995) studied catchment sensitivity to climate change using flow duration curves from small catchments in the Upper Loire region, France. It was concluded that the effects of climate variability, or prolonged wet and dry periods, depend upon the gradient of the flow duration curve. In catchments with a high gradient, discharge variability was found to be high and storage capacity low, and vice versa in low gradient catchments. In high gradient catchments, storage capacity is regularly exceeded during high precipitation events but at other times precipitation is stored, whereas in the low gradient catchments any precipitation excess is easily stored due to the large available storage capacity. This implies that catchment sensitivity to climate variability depends upon available catchment storage capacity and the potential maximum reservoir storage. This was extended by Van der Wateren-de Hoog (1998) who proposed an empirical regional model that quantifies catchment sensitivity as the ratio of present maximum reservoir storage to catchment storage capacity. Average annual present conditions were used to test the model using data from 15 catchments in the Upper Loire region, France. The model was found to easily identify both flood and drought prone catchments as well as a catchment's sensitivity to a catchment-type transition.

In the UK, Arnell (1992*b*) used a monthly water balance model to examine factors controlling the effects of climate change on 15 catchments with a range of climatic and geological conditions. It was concluded that the effect of climate change on annual runoff depends upon the current ratio of average annual runoff to average annual precipitation, with the greatest sensitivity shown in the driest catchments. Thus, upland, responsive catchments may show a very large percentage change in summer runoff. In groundwater dominated catchments, higher

winter and spring rainfalls could mitigate drier summer conditions and actually maintain minimum flows (Arnell and Reynard, 1989). The uncertainty in both the prediction of future climates and the runoff response means that confidence intervals around forecasts of future flows are wide. However, the 1988-1992 drought has lent support to the scenarios of Arnell *et al.* (1994).

The importance and influence of the choice of catchment and data, rainfall-runoff model, climate scenario and flow index on the assessment of climate change impacts on flow regime was assessed by Boorman and Sefton (1997). They used three UK catchments, two rainfall-runoff models and ten sets of climatic conditions. It was shown that it is necessary to examine more than one index of flow response to assess the probable impact of climate change as there may be no change in mean flow but, for example, reduced low flows. Indices must be more sophisticated and appropriate to a particular investigation (Sefton and Boorman, 1997). Climate change is also observed to vary significantly between catchments, and thus care must be taken with the extrapolation of results. Contrasting results were obtained for different climate change scenarios. However, broadly speaking, the results showed severe reductions in low flows in catchments in central and eastern England, but increased flooding in the north and west (Sefton and Boorman, 1997).

Finally, an interesting investigation by Wilby and Vitkovic (1993) looked at the relative sensitivity of daily flows in two East Anglian rivers that had been subjected to land-use change, groundwater abstraction and climatic variability. They concluded that low flows were most sensitive to groundwater abstractions, median flows to the effects of land-use change. Climate change effects assumed only secondary importance.

2A.5.3 Impacts upon evapotranspiration rates

Numerous studies have investigated the effect of increased atmospheric CO_2 concentrations on evapotranspiration rates that can be affected by temperature, humidity, wind speed and net radiation as well as plant physiology. The sensitivity of potential evapotranspiration to changes in the environmental controls appears to depend upon their initial magnitude (Martin *et al.*, 1989). However, there is also growing evidence of the effects of climate change on plant physiology (Drake, 1992; Kimball *et al.*, 1993; Tyree and Alexander, 1993). These use controlled laboratory experiments and, increasingly, field experiments (Hendry *et al.*, 1993).

Aston (1984) showed that a doubling of CO_2 could raise plant stomatal resistance, reducing evapotranspiration and increasing streamflow by 40 to 90 percent. Certainly, higher stomatal resistance can reduce evapotranspiration rates by up to one third (Idso and Brazel, 1984). However, Bultot *et al.* (1988) suggested that the physiological response of plants would be more sensitive to fluctuations of temperature and precipitation than to a CO_2-enriched atmosphere, and it is likely that higher CO_2 levels would result in more luxuriant plant growth. In any case, the increase in CO_2 and raised stomatal resistance could be offset by an increased air temperature, which has been shown to decrease plant stomatal resistance (Lockwood, 1993). Gifford (1988) observed that plants maintain a balance between stomatal resistance and leaf area in order to maintain a particular water usage and speculated that regional evapotranspiration rates would not be significantly affected by changes in plant physiology.

It is likely that the exact response will also depend upon the initial conditions. Rabbinge *et al.* (1993) state that typically, under a doubling of CO_2, evapotranspiration will be reduced by between 10 and 25 percent depending upon vegetation type. However, at temperatures below about 10°C the increase in potential evapotranspiration (PE) associated with the rise in temperature may be large enough to fully account for the suppression of transpiration associated with CO_2. In contrast, at air temperatures above 25°C, the increase of PE with temperature is very small and PE could be reduced by increases in atmospheric CO_2.

Lockwood (1993) investigated the differences in response between a grassland pasture and a coniferous forest. The results showed that evapotranspiration from grass pasture does not vary widely with temperature, but is dominated by the surface radiation balance, whereas the coniferous forest shows significant variations and canopy controls are of significant importance. An interesting point made by Lockwood (1994) is that the most significant increases in British PE values with global warming will probably be observed in the autumn and spring, since the daily change in PE is most marked for days with afternoon temperatures around 10°C or below.

Plants can be classified into two groups; C_3 and C_4, depending upon the photosynthetic pathway used by the plant (Lockwood, 1995). Most UK plants fall into the C_3 group, which are the most sensitive to increased CO_2 concentrations (Arnell, 1996), although most trees are in the C_4 group (Lockwood, 1995). It is, however, very difficult to extrapolate results obtained under laboratory conditions to the catchment. Plant response to elevated CO_2 concentrations may be strongly affected by the presence of adequate nutrients or by changes in temperature or precipitation regime. It is also possible that plants may 'acclimatise' to higher CO_2 concentrations (Arnell, 1996) or soil moisture conditions (Lindroth, 1996).

However, in the UK during the 1990s potential evapotranspiration rates have been 10 to 15 percent greater than the long term average and 20 to 25 percent greater than the PE that characterised the 1960s (Marsh and Sanderson, 1997).

2A.5.4 Impacts upon soil properties

Rowntree *et al.* (1993) suggest that in Europe, using a transient GCM experiment with an annual increase of carbon dioxide of one percent, soil moisture levels will decrease, except in winter. Valdes *et al.* (1994) determined that under all climate change scenarios examined there was a net decrease in annual mean levels of soil moisture concentration in Texas, as well as changes in variability around the mean. However, the bi-modal probability distribution of soil moisture concentration, with a wet and dry mode, at large length scales noted by Rodriguez-Iturbe *et al.* (1991*a*, *b*) was not apparent.

It is likely that changes in vegetation cover induced by a change in climate could also change the infiltration properties of a soil (Arnell, 1992*a*). Drier summers, for example, could result in reduced infiltration rates, but, conversely, infiltration rates would increase if this led to greater soil cracking. Changes in soil structure and dynamics could also lead to changes in runoff-contributing zones and thus runoff generation (Arnell, 1992*a*). Increased precipitation could also lead to gleying, which would inhibit downward infiltration.

2A.6 Approaches linking atmospheric circulation to local weather elements (downscaling GCM predictions)

Although GCMs are used to generate future climate change scenarios, these scenarios are provided at a scale that is too large for regional analysis. Therefore, a method of 'downscaling' must be used to relate these climate change predictions on the large-scale, to local scale variables. Large-scale atmospheric circulation is an important driving force of surface climate and there have been many attempts to relate atmospheric circulation to local weather elements. In general there are two stages to this process; firstly, the classification of the atmospheric circulation and, secondly, an assessment of the relationship between categories of the atmospheric circulation classification and regional weather elements (Buishand and Brandsma, 1997). Two major procedures have been developed; manual and automated classification, and the emphasis of this discussion will be on those schemes that refer to the UK.

2A.6.1 Modification of observed precipitation time-series

The modification of observed precipitation time series is a frequently used methodology for relating GCM output to the local-scale (e.g. Arnell, 1992*a*). In this approach, a factor is derived from the ratio of the GCM control and perturbed simulation mean output (Kilsby *et al.*, 1998*b*) and observed annual or monthly average records are altered accordingly.

However, this methodology has major limitations. Firstly, there is no evidence that the observed temporal (wet and dry transition probabilities) and spatial patterns will still occur in a future perturbed climate. Biases may be introduced by keeping a fixed proportion of dry days with a changed mean precipitation amount (Kilsby *et al.*, 1998*b*). There is no scope for changing the temporal variability of the precipitation time series, for example, changing the frequency of occurrence of extreme events or prolonged dry periods. Finally, there are serious known deficiencies in GCM predictions, although this is a problem common to all current uses of GCM data (Kilsby *et al.*, 1998*b*).

2A.6.2 'Downscaling' methods

'Downscaling' approaches have emerged as a means of interpolating regional-scale atmospheric predictor variables (such as vorticity or mean sea level pressure (MLSP)) to local site-specific meteorological statistics (such as mean precipitation amount or proportion of dry days) (Wilby and Wigley, 1997) and rely on the principle that there is a close relationship between atmospheric circulation patterns and climatic variables. The development of such techniques has become necessary as, although it is generally recognised that Global Circulation Models (GCMs) provide the best source of currently available information on global climate change, the present generation of such models are restricted in their usefulness for many sub-grid applications due to their coarse spatial and temporal scales (Wigley *et al.*, 1990; Carter *et al.*, 1994). While current GCMs perform reasonably in simulating the present climate with respect to seasonal or monthly averages over large areas (typical grid size of 300 km^2), they are considerably less reliable in depicting the smaller-scale features relevant to impact questions (Grotch and MacCracken, 1991).

GCMs are primarily concerned with meso-scale fluid dynamics and parameterise higher resolution, sub-grid scale processes (Wilby *et al.*, 1998*b*). Conversely, hydrological models are most realistic at the hillslope or catchment scale, occurring on much smaller scales than those

resolved in GCMs, and must parameterise regional processes (Hostetler, 1994). According to Kite *et al.* (1994) the most serious problem, from a hydrological viewpoint, is that most GCMs contain no lateral transfers within the land phase and thus water 'excess' generated at a grid point is simply discarded, not exchanged with an adjacent cell, and can have important bearings upon the timing and magnitude of the annual runoff regime (e.g. Kuhl and Miller, 1992). These mismatches and scale-related sensitivities are further exacerbated as they generally involve the least well-understood components of climate models such as water vapour and cloud feedback effects (Rind *et al.*, 1992). Fundamental to the 'downscaling' approach are the assumptions that the local-scale parameter is dominantly a function of synoptic forcing, that the GCM circulation used to drive the derived relationship is valid at the synoptic scale, that stable empirical relationships can be identified between atmospheric process variables at disparate temporal or spatial scales, and that these will remain valid under climate change.

Since the 1990s, in particular, many such relationships have been identified. For example, meso-scale weather patterns have been used to determine correlations between various meteorological parameters, such as precipitation occurrence in Washington State (Hughes and Guttorp, 1994), space-time daily precipitation occurrence in eastern Nebraska (Matyasovszky *et al.*, 1993) and the Ruhr catchment (Bardossy and Plate, 1992), low frequency precipitation events in the UK (Wilby, 1998), extreme precipitation events and drought conditions (Hay *et al.*, 1991), and winter precipitation in Iberia (von Storch *et al.*, 1993). Relationships have also been determined between atmospheric circulation variables and environmental time-series (Wilby and Wigley, 1997).

Numerous 'downscaling' methodologies have also been established, including empirical regression methods (e.g. von Storch *et al.*, 1993), artificial neural networks (e.g. Hewitson and Crane, 1996), weather type classification methods (e.g. Bardossy and Plate, 1992), air flow indices or atmospheric circulation patterns (e.g. Conway *et al.*, 1996), stochastic weather generators (e.g. Wilks, 1992) and Limited Area models (LAMs) nested within GCMs (e.g. Giorgi *et al.*, 1994). These techniques can be split into two types: empirical/stochastic downscaling (e.g. using weather types and continuous atmospheric variables) and dynamical downscaling (e.g. LAMs or regional climate models). These will be discussed further.

2A.6.2.1 Weather Type Analysis

In 'weather type' downscaling, a statistical relationship is established between an objectively or subjectively derived weather type classification system and corresponding historic precipitation characteristics at individual sites. It is assumed that these relationships will stay constant under

climate change (Wilby, 1994). Objective weather classification procedures can include neural networks (Bardossy *et al.,* 1994), principal components analysis (White *et al.,* 1991; Briffa *et al.,* 1990), fuzzy rules (Bardossy *et al.,* 1995), canonical correlation analyses (Zorita *et al.,* 1992), compositing (Moses *et al.,* 1987) and analogue based techniques (Martin *et al.,* 1997). Subjectively derived circulation typing is generally used however, and examples include the British Isles Lamb Weather Types (LWTs) (Lamb, 1972; Jones *et al.,* 1993), the European Grosswetterlagen (Hess and Brezowsky, 1977), and daily weather types for the Delaware basin (Hay *et al.* 1991; Hay and McCabe, 1992). Conditional probability distributions are then obtained for observed data associated with given circulation patterns and meteorological time series are generated stochastically by applying input sequences of daily weather types to observed probability distribution functions, typically using a Monte Carlo technique (Wilby, 1994).

This type of approach is appealing as it is founded on sensible physical linkages between climate at the large scale and weather on a local scale. It provides high resolution sub-grid scale meteorological time series and also considerable potential as a means of validating the internal consistency of GCM control runs or as a procedure for removing the synoptic climate signal from environmental data sets (Wilby and Wigley, 1997).

There are limitations with this approach however and these can be roughly split into four fundamental problems pertaining to issues of classification, scale and stability (Wilby, 1997). Firstly, as atmospheric circulation is essentially dynamic then the identification of distinct 'weather' types is arbitrary, even when very clearly defined criteria are applied (El-Kadi and Smithson, 1992). Even objective classification techniques contain a certain amount of subjectivity as the results are sensitive to internal parameters such as grid size or number of different classes used (Yarnal *et al.,* 1988). Secondly, the replication of any analysis is currently very difficult as there is no universal classification system, all current approaches being highly subjective and parochial in nature (Wilby, 1994). Thirdly, downscaling approaches seldom capture spatial and temporal climatic variability at all scales, and there can be interdependence between variables. For example, Conway *et al.* (1996) compared two downscaling approaches and found that daily characteristics were generally well preserved but interannual variability was poorly reproduced. In addition, Hay and McCabe (1992) conclude that in mountainous regions there is a need to include orogenic influence in weather type predictions.

Finally, and perhaps the most serious hindrance to future confident downscaling approaches (Wilby, 1997), is that in many cases the relationship between weather type and its associated meteorological properties is constantly changing and, even assuming stability, the simulated

precipitation regime is highly dependent upon the period chosen for model calibration. Wilby *et al.* (1995) attribute this intra-weather class variability to subtle changes in the dominant precipitation mechanism (whether stratiform or convective), whereas Sweeney and O'Hare (1992) have suggested changes in the intensity of circulation development or depression trajectories as contributing factors.

In the UK, this approach has been followed by a few researchers. Wilby (1997) analysed historical atmospheric circulation and precipitation records for Durham (northeast England) and Kempford (Cotswolds) from 1881-1990. Trends in the precipitation data implied that the non-stationarity in mean precipitation amounts is more sensitive to local topographic and geographic factors than wet-day probabilities. There was also evidence of non-stationarity within airflow indices themselves, and changing seasonality and persistence of dominant circulation patterns. Pronounced shifts in the dominant storm tracks and associated eddy activity, affecting the transport and convergence of atmospheric moisture, were significantly correlated with regional precipitation. The El Niño Southern Oscillation (ENSO) was also advocated as a possible cause of change in relationships between circulation variables and precipitation under a changed climate. This appears an especially pertinent conclusion given the strongest ENSO ever recorded in 1997 and the subsequent breaking of various climatic records over the UK in 1998.

The calibrated model should not therefore be used to extrapolate future precipitation patterns from GCM output without acknowledging the non-stationary relationships that exist between historic precipitation and circulation patterns (Wilby, 1994). This has contributed to the development of downscaling approaches that employ continuous, independent circulation variables (such as vorticity and flow strength and direction) rather than discrete weather types (Wilby and Wigley, 1997).

2A.6.2.2 Air Flow Indices

Airflow indices are continuous and so preferable to weather type downscaling as they do not impose restrictive boundaries (Wilby, 1997). A number of studies have been performed that relate atmospheric circulation indices to precipitation statistics (e.g. Bardossy and Plate, 1991; Conway and Jones, 1998; Wilby, 1997; Kilsby *et al.*, 1998*a*; Wilby *et al.*, 1998*a*). For example, von Storch *et al.* (1993) determined a statistical relationship between North Atlantic MSLP and Iberian precipitation yields. Wigley *et al.* (1990) determined regression relationships between the site variables of temperature and precipitation, and spatial area averages of temperature, precipitation, MSLP, and circulation predictor variables, whereas Karl *et al.* (1990) used local

free-atmosphere parameters. Topography and distance from the nearest coast were found to have a strong influence on model performance.

This research has been extended by Kilsby *et al.* (1998*a*) where regression models were developed to predict point precipitation statistics in England and Wales using atmospheric circulation indices from GCM output for future climates. The models can be used to predict mean daily precipitation amount and proportion dry days (PD) for each calendar month at a site, using altitude, easting, northing, distance from nearest coast, and mean values of air flow indices derived from MSLP grids as explanatory variables. This approach allows the prediction of precipitation statistics at any site in England and Wales, and is therefore applicable where data is limited or unavailable. The methodology is validated using the 1961-1990 climatology of Barrow *et al.* (1993) and a reasonable agreement is noted. Temperature is not used as an explanatory variable but it is suggested that in other climates, and for future impact studies, it should be included, as a rise in temperature may be the major observed signal of climate change. A similar study has been undertaken in Nagano prefecture, Japan by Wilby *et al.* (1998*a*), building upon the previous research of Conway *et al.* (1996), Conway and Jones, (1996; 1998) and Wilby *et al.* (1996*a,b*). Here, the air flow indices (vorticity, flow strength and angular direction of air flow) were calculated using daily grid-point SLP data for two periods indicative of present and future greenhouse gas plus aerosol forcing and related to site characteristics of precipitation, air temperature, wind speeds, cloud cover, humidity, solar radiation and evaporation. Previously, airflow indices have only been considered with respect to daily precipitation. The analysis also extended the use of airflow indices to a mountainous environment.

The statistical regression-based approach is technically simple, can be applied to economic or ecological parameters as well as physical parameters, and shows a degree of consistency with observations (von Storch *et al.,* 1993). However, it can only be applied where a strong relationship between an atmospheric circulation variable and a site characteristic has been identified and is not necessarily valid beyond the range of data used to fit the model. It may also prove difficult to successfully validate a pre-supposed relationship between an atmospheric variable and site statistic using a split-record approach as such empirical relationships can show considerable interannual variability (Wilby, 1997). The present use of rather coarse resolution circulation data also means that some important climatic effects may be ignored (e.g. Mayes, 1991*b*). It may be possible to incorporate additional explanatory variables such as upper air circulation, humidity and atmospheric stability (Kilsby *et al.,* 1998*a*).

Wilby *et al.* (1998*b*) suggest that improvements in this type of downscaling method in the future will require the incorporation of other predictor variables as well as vorticity, such as airflow strength and direction, and divergence, as it is only one of a number of driver mechanisms for determining changes in the character of precipitation variability. By establishing empirical relationships between model parameters and local factors such as topography, it may also be possible to improve current downscaling methods (such as Kilsby *et al.*, 1998*a*; Daly *et al.*, 1994). It is also suggested that by relating temporal changes in model parameters to large scale atmospheric circulation anomalies such as the ENSO or NAO the low-frequency performance of downscaling methods may be improved (Wilby, 1993*b*; Wilby *et al.*, 1997).

2A.6.2.3 Stochastic Weather Generators

Stochastic weather generators (SWGs) provide another method of linking large-scale atmospheric processes to the local scale using the output from GCMs. They were originally developed to provide a means of simulating synthetic weather time series with certain statistical properties that could be used in impact assessments, and to allow an extension to unobserved locations. SWGs can be site-specific or used to generate time series for a number of sites (e.g. Hutchinson, 1995). The most commonly used SWG is WGEN (Richardson, 1981). This is based upon first- or multiple-order Markov renewal processes in which, for each successive day, the precipitation occurrence is governed by the outcome on the previous day, rather than being conditioned by circulation patterns. SWGs have been adapted and used in a variety of climate change and impact studies. For example, Wilks (1992) adapted the WGEN model to sequentially generate daily series of precipitation amount, maximum and minimum temperatures and solar radiation for a future climate. This was extended to simulate precipitation at multiple sites by Wilks (1998), and downscaling of climatic variables used by Wilks (1999). Similarly, Mearns *et al.* (1996) used WGEN to investigate the effect of changes in daily and interannual variability in temperature on crop yields in the central Great Plains.

Another common SWG is LARS-WG, which was developed by Racsko *et al.* (1991). This differs from WGEN as the simulation of precipitation occurrence is based on distributions of the length of continuous sequences of wet or dry days rather than the 'Markovian' approach of alternating sequences of wet and dry days. The Markov chain has a limited memory of rare events and can thus fail to accurately simulate long duration wet or dry sequences. This has been used in impact studies by Semenov and Porter (1994), and Semenov and Barrow (1997).

SWGs have also been developed by Hutchinson (1995) and Bardossy and Plate (1991; 1992) who developed a multi-dimensional stochastic model for the space-time distribution of daily

precipitation and applied it to the river Ruhr using data from 1977-1990. Precipitation was linked to atmospheric circulation indices using conditional spatial covariance functions and distributions. Matyasovszky *et al.* (1993) used the model developed by Bardossy and Plate (1992) in an eastern Nebraska, US, case study to estimate the space-time distribution of precipitation under climate change, and a very variable response was observed.

One of the most important issues regarding the use of stochastic weather generators to simulate future climates has been the development of a methodology of adjusting the model parameters in a physically realistic and internally consistent way (Wilby and Wigley, 1997). Katz (1996) has demonstrated by using daily observations at Denver, Colorado, that change in model parameters can produce unanticipated effects that may be unrealistic. For example, modifying the probability of dry days changed not only the mean daily temperature, but also its variance and autocorrelation, although this effect may be mitigated by adopting the approach of Wilby *et al.* (1998*a*) and modelling all variables unconditional on precipitation occurrence, in contrast to Wilks (1992). However, for WGEN-type models this kind of approach also raises the question of parameter sequencing, for example, whether cloud cover should be modelled before or after precipitation (Wilby *et al.*, 1998*a*).

However, a significant advantage of using weather generators is that it is possible to synthesise daily sequences of precipitation at a point or catchment scale with an observed frequency distribution, wet and dry-spell frequencies and seasonalities using GCM surface pressure data and historic datasets. It is then possible to undertake detailed impact assessments via catchment models. This was attempted for the UK by Wardlaw *et al.* (1996), who used this approach to generate precipitation scenarios in the Anglian region.

2A.6.3 Limited Area (LAMs) or 'Nested' Models

LAMs provide one of the most promising alternatives to statistical downscaling and are often referred to as dynamical downscaling. This is where a higher-resolution model is embedded within a coarse resolution GCM, using the GCM to define the boundary conditions for the LAM over an area of interest (e.g. Giorgi, 1990). Circulation from the LAM does not feed back into the GCM. LAMs can produce climatologies on a 10-20 km grid spacing and 100-1000 m vertical resolution and at temporal scales of hours or less. However, the present generation of LAMs lacks sufficient computational power to simulate large regions and, more importantly, are completely dependent upon the validity of the GCM grid-point boundary conditions that are used to drive the 'nested' model. Major improvements in parameterisations, especially for clouds, and spatial resolution are also needed (Kilsby *et al.*, 1998*b*). Recent work on the

validation of a LAM by Mearns *et al.* (1995*a,b*) has also shown that there may still be large differences between model output and observed weather statistics, especially in the case of climate variability. This means that the construction of local climate scenarios from LAMs may be as problematic as using GCM predictions.

Although these limitations are presently hindering the general use of LAMs they may ultimately provide the best means of simulating atmospheric data for impact assessment that will reflect the natural heterogeneity of climate at the regional scale (Hostetler, 1994). It has been demonstrated that the high heterogeneity of local-scale atmospheric processes affects regional climates and can provide important feedbacks to the global climate (Pielke *et al.*, 1991).

2A.6.4 Limitations of Downscaling.

The limitations of downscaling are well described in the literature (e.g. Grotch and MacCracken, 1991; Kattenberg *et al.*, 1996; von Storch *et al.*, 1993; Wilby, 1994; 1997; Wilby and Wigley, 1997). A major limitation is related to scale. It is difficult to accurately simulate all precipitation characteristics across a range of temporal and spatial scales when using downscaling approaches, and there can be interdependency between variables. The representation of extreme meteorological conditions has also been found to be problematic (Wilby, 1998).

To date, most downscaling studies have been conducted using daily or monthly precipitation time series at low elevation sites in a temperate, mid-latitude Northern Hemisphere location. The topographic bias has led to a preoccupation with downscaling liquid, as opposed to frozen, precipitation (Wilby and Wigley, 1997). Current downscaling methods also presuppose that anthropogenically-derived climate change *will* cause a significant change in the downscaling predictor variables. However, recent research has shown that circulation changes within GCMs predictions may be small (e.g. Wilby *et al.*, 1998*a,b*) and within the limits of interannual variability. The addition of temperature as a predictor variable is also found to have little effect (e.g. Kilsby *et al.*, 1998*a,b*). It is thus suggested that future downscaling approaches must include the effect on precipitation of changes in atmospheric moisture content unrelated to changes in circulation (e.g. Pilling *et al.*, 1998).

A major obstruction to the successful downscaling of future GCM predictions is that in many instances the relationship between atmospheric indices or weather patterns and associated meteorological properties are not constant in time (Wilby, 1997). It is suggested that non-stationarity should be ignored during model calibration if it is insignificant when compared to

other uncertainties (Wilby, 1997) However, this will cause an incorrect reproduction of trends in precipitation. It may be better to incorporate non-stationarity stochastically using conditional statistics from a gamma distribution or using isolated empirical relationships (Wilby *et al.*, 1995). Hewitson and Crane (1996) also offer a means of overcoming the problem of temporal and spatial non-stationarity through the use of ANN's and the development of multivariate downscaling schemes which incorporate a wider range of continuous atmospheric variables including temperature and humidity. Wilby *et al.* (1995) have additionally suggested that the incorporation of a weather front sub-model to increase the variability of interannual conditional precipitation probabilities may partly offset the problem. The inclusion of weather fronts was found to significantly improve the estimation of extreme precipitation events at a number of sites in the UK (Wilby, 1997).

Similarly, downscaling methods are currently unable to produce precipitation behaviour not observed in the present climate. 'New' weather types are a distinct possibility under a changed climate and cannot be discounted. A major improvement must be made in current statistical downscaling methods to include a sufficient physical basis to allow new weather types to be successfully modelled (Kilsby *et al.*, 1998*b*). Present downscaling studies also presuppose the veracity of GCM output, which has been questioned in many areas. An alternative approach may be to stochastically generate predictor variables based on observed changes in their statistics (Wilby *et al.*, 1998*b*).

However, the Department of the Environment (DOE, 1996) has suggested that the most urgent concerns regarding downscaling have been the need for the intercomparison of different methodologies and a quantification of their relative accuracy. A number of recent studies have made considerable progress in this respect by applying a number of downscaling methods to a common data set and assessing their relative merits (e.g. Wilby *et al.*, 1996*a*,*b*; Wilby and Wigley, 1997; Wilby *et al.*, 1998*b*).

Wilby *et al.* (1998*b*) calibrated a range of different statistical downscaling models using observed and GCM-generated precipitation time series. The downscaling methods compared were different weather generator techniques, two methods using grid-point vorticity data as an atmospheric predictor variable, and two variations of an artificial neural network (ANN) transfer function technique using circulation data as predictor variables. It was concluded that the ANN methods performed poorly due to an inadequate representation of wet-day transition probabilities. A major limitation of both the circulation-based and weather generation approaches was their marked failure to realistically reproduce the standard deviation of monthly precipitation totals. In most cases, the downscaling methods underestimated the low-frequency

variability, behaviour typical of many stochastic weather generators. The weather generation techniques however yielded the smallest differences between observed and simulated daily precipitation and were able to fit a number of daily precipitation statistics exactly.

2A.7 Large-scale atmospheric circulation indicators used in UK climate change analysis

Many researchers have linked precipitation measurements and other local-scale variables to indices of large-scale atmospheric circulation. In the main, these have been either the North Atlantic Oscillation (NAO) or a weather-type classification system, although continuous atmospheric variables have also been used.

2A.7.1 The North Atlantic Oscillation (NAO)

The North Atlantic Oscillation (NAO) index is a measure of pressure between the Azores and Iceland. For winter, a useful index of the strength of the NAO is the difference between the normalised sea level pressure over Gibraltar and the normalised sea level pressure over southwest Iceland. Jones *et al.* (1997*b*) used early instrumental data to extend this series back to 1823. A useful winter season is the December to March average of these values (Jones *et al.*, 1993). The NAO is driven in part by changes in North Atlantic storms (Hurrell and van Loon, 1997) and shifts may have a profound effect on temperature and precipitation in northern Europe (Hurrell, 1995).

There have been four main phases of the NAO during the observed historical record. Prior to the turn of the century, the index was close to zero. From 1900-1930 there were strong positive anomalies, followed by a low index from 1930 to the 1960s and since then the index has been strongly positive until recently (Wilby *et al.*, 1997). The upward trend in the NAO from the 1960s to the early 1990s has been coincident with the winter warming of Northern Hemisphere landmasses. However, there is considerable year-to-year variability and the NAO index was strongly negative from 1996-97. Although it again increased in 1997-98, it was to much lower values than the early 1990s (see Figure 2-1). Hurrell (1996) suggests that the NAO explains 31 percent of the variance of mean winter temperature in the extratropical Northern Hemisphere over the time-period studied. Variations in the strength of the NAO have been particularly associated with changes in the frequency and magnitude of surface westerlies across northern

Europe (Rogers, 1985). Hurrell (1995) found, for example, that during a high NAO winter the surface westerlies over Europe are 8 m s^{-1} stronger than during weak NAO winters.

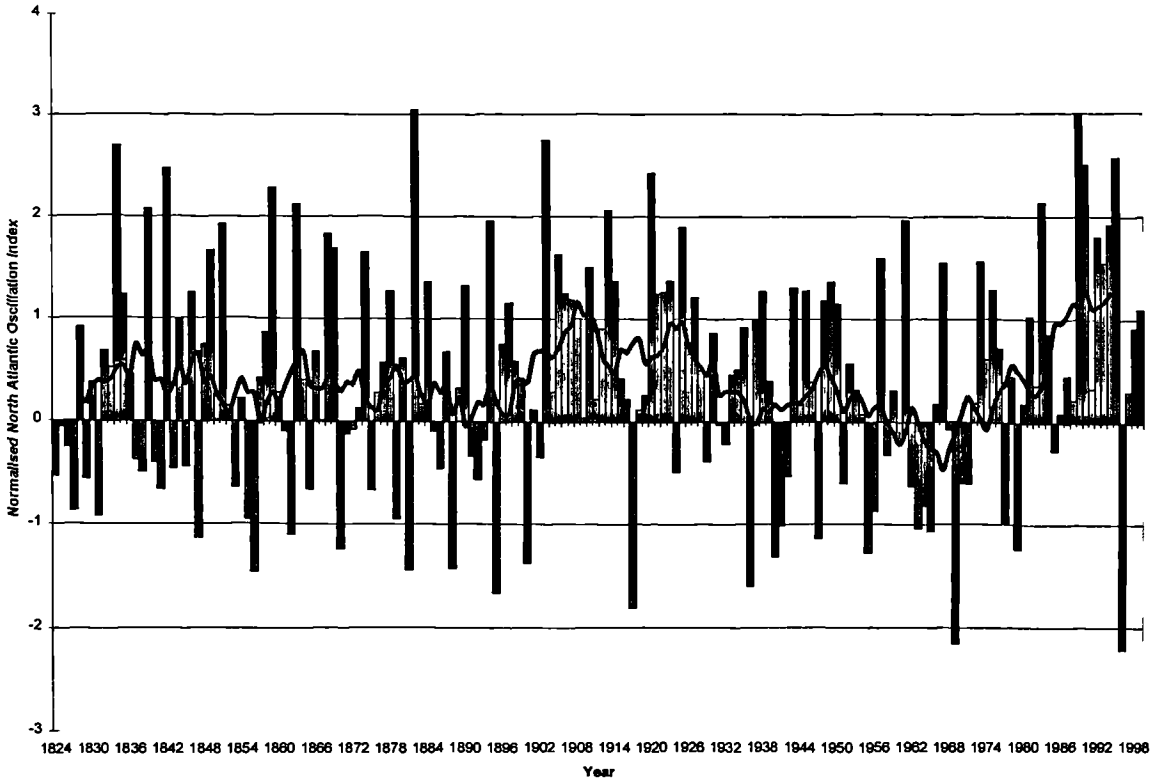

Figure 2-1: The North Atlantic Oscillation (NAO) index for winter (DJFM) as Jones et al. (1997b). Imposed upon the yearly values is an 11-yr centred moving average that shows the recent increase in the index.

Mitchell *et al.* (1999) performed two ensembles with HadCM2, each with 4 integrations, covering the period from 1860-2099. The first ensemble used historic estimates and an estimate of future greenhouse gases for forcing, whereas the second ensemble additionally included a representation of the effects of sulphate aerosols. Both ensembles indicate a long-term weakening of the NAO in the next century. However, before this occurs there is a weak peak in the NAO, occurring some time between 1987 and 1996. Trend analysis was also applied to these ensembles and 30-yr trends over the 1950-2000 period were found to be skewed towards positive values, but still not as positive as observed trends. Osborn*et al.* (1999) compared 30-yr observed trends in the winter NAO to a 1400-yr control integration of HadCM2. This indicated that the recent positive trend was highly unusual, and suggest that the observed changes have been externally forced if the climate model variability can be considered realistic.

Because of its dominant impact on the weather and climate of Europe, there is a growing interest in quantifying the possible limits of seasonal and interannual predictability of the NAO. Both Deser and Blackmon (1993) and Kushnir (1994) have studied decadal variability in atmospheric circulation over the Northern Hemisphere winter. Deser and Blackmon (1993) found two modes of variability in surface climate. One has an irregular periodicity between 9 and 12-yr, while the other represents a longer time-scale fluctuation. A simple fractionally integrated noise model can be used to make one-year ahead forecasts that have a small yet significant correlation (r = 0.17) with the observed NAO index for the period 1864-1998 (Stephenson *et al.*, 2000). However, Rodwell *et al.* (1999) obtained a higher correlation of r = 0.41 for the ensemble mean NAO simulated using the HadAM2b global climate model. This work has taken the further step of linking much of the multiannual to multidecadal variability of the winter NAO over the past 50 years to North Atlantic sea-surface temperatures (SSTs). GCM modelling by Delworth and Mann (2000) has further demonstrated that for both the model and observations, SST appears to be the primary carrier of the multidecadal signal.

It is argued that the winter NAO may be reconstructed from these SSTs as they are intimately connected through the processes of evaporation, precipitation and atmosphere-heating processes. It has also recently been proposed that North Atlantic SST patterns show significant multi-annual predictability (Sutton and Allen, 1997), and it is therefore possible that in the future European winter climate may be predicted several years in advance. However, Watanabe and Nitta (1999) have suggested that 1989 marks a distinct discontinuity on the decadal time-scale and that snow anomalies across Eurasia may play the role of an amplifier in atmospheric shifts and are as important for the atmospheric changes as changes in SSTs. It should also be noted that the research of Rodwell *et al.* (1999) does not provide useful forecasts alone, since it relies upon knowing *a priori* the sea surface temperatures, and fit only long-term variations. Since more than 75 percent of the variance of the NAO is found below the decadal time-scale, the difficulty will be to predict the shorter-term variations.

Investigations into correlations between British Isles regional precipitation and other climatic variables in relation to decadal fluctuations in the atmospheric circulation in winter months, explained by way of the NAO, have been conducted by Wilby *et al.* (1997). In the study Yorkshire is located mainly within the region of 'northeast England', although parts can be found in both the 'central' and 'northwest England' regions. Results indicate that the Central England Temperature (CET) series is significantly correlated with the NAO in all seasons, excepting summer, with the strongest correlation occurring in winter; high NAO values corresponding to positive temperature anomalies. The NAO is also highly positively correlated with the Lamb westerly weather type, and negatively correlated with the winter occurrence of

cyclonic types. As would be expected, given the strong westerly influence, positive correlations between a high winter NAO and regional precipitation amounts occurred in northwest England, whereas significant negative correlations were observed in central (83 percent anomaly) and northeast England (86 percent anomaly). A negative winter NAO, for example 1995/96, will, however, cause depressions to take a more southerly trajectory across Europe and may contribute to a reduction in precipitation across the UK.

2A.7.2 UK atmospheric classification schemes

2A.7.2.1 The Lamb Weather Types

2A.7.2.1.1 Subjective classification scheme

The Lamb weather types are the definitive classification of daily weather types for the British Isles, published by Lamb (1972). The classification is based on surface synoptic charts and also charts at the 500 hPa level, and is characterised by a number of 'pure' circulation types which may be combined to form 'hybrids'. It is an entirely subjective classification scheme, although an automated procedure has now been developed (Jenkinson and Collinson, 1977; Jones *et al.*, 1993).

The Lamb scheme contains eight directional types; north (N), northeast (NE), east (E), southeast (SE), south (S), southwest (SW), west (W), and northwest (NW), and three non-directional types; anticyclonic (A), cyclonic (C) and unclassifiable (U). The directional and non-directional types can also be combined to define more complex circulation types as 'hybrid' types, for example the cyclonic westerly (CW). However, the seven circulation types considered by Lamb (1972) to be the most important are the anticyclonic, cyclonic, westerly, northwesterly, northerly, easterly and southerly types. The average annual and seasonal frequencies of the Lamb weather types over the period from 1861-1990 can be found in Table 2-1 (after Kelly *et al.*, 1997).

Several investigators have linked the Lamb weather types to precipitation. A principal component analysis was applied to the Lamb classification data to find relationships between different weather types (Jones and Kelly, 1982; Briffa *et al.*, 1990). The results of this exercise highlighted that the dominant relationship was between the frequency of westerly and anticyclonic types. Over the last century, the frequency of westerlies has been accompanied by an inverse trend in the frequency of anticyclonic blocking conditions. Other important relationships are that when the combined frequency of westerly and anticyclonic types is low

then there is a rise in the frequency of cyclonic days, and vice versa (Wigley and Jones, 1987). It was determined that the first two principal components of the annual frequencies of weather types for the period 1861-1980 were significantly correlated at the 95 percent level with the England and Wales annual precipitation series.

Type	*Annual Days*	*(%)*	*Winter Days*	*(%)*	*Spring Days*	*(%)*	*Summer Days*	*(%)*	*Autumn Days*	*(%)*
U	14.3	(3.9)	3.4	(3.7)	3.9	(4.2)	3.5	(3.8)	3.5	(3.9)
A	66.3	(18.2)	14.4	(16.1)	17.3	(18.8)	17.3	(18.8)	17.2	(18.9)
ANE	5.0	(1.4)	0.8	(0.8)	1.7	(1.8)	1.4	(1.5)	1.2	(1.3)
AE	8.9	(2.4)	1.7	(1.9)	3.2	(3.5)	2.1	(2.3)	1.8	(2.0)
ASE	3.4	(0.9)	0.8	(0.9)	0.9	(1.0)	0.7	(0.7)	1.0	(1.1)
AS	4.0	(1.1)	1.2	(1.3)	0.8	(0.9)	0.8	(0.9)	1.1	(1.2)
ASW	3.1	(0.9)	1.0	(1.1)	0.6	(0.6)	0.7	(0.7)	0.8	(0.9)
AW	17.0	(4.7)	4.2	(4.7)	3.4	(3.7)	5.1	(5.6)	4.2	(4.6)
ANW	5.4	(1.5)	1.1	(1.2)	1.3	(1.4)	1.8	(2.0)	1.1	(1.2)
AN	7.4	(2.0)	1.4	(1.6)	2.4	(2.6)	2.1	(2.3)	1.5	(1.7)
NE	3.4	(0.9)	0.6	(0.7)	1.3	(1.4)	0.8	(0.9)	0.6	(0.7)
E	12.8	(3.5)	3.0	(3.3)	5.4	(5.9)	1.8	(2.0)	2.6	(2.9)
SE	6.3	(1.7)	2.1	(2.3)	1.9	(2.1)	1.7	(0.7)	1.6	(1.8)
S	15.4	(4.2)	4.9	(5.5)	4.0	(4.3)	2.3	(2.5)	4.3	(4.7)
SW	10.3	(2.8)	3.6	(4.0)	1.9	(2.1)	1.9	(2.1)	2.8	(3.0)
W	67.4	(18.4)	20.7	(23.0)	12.3	(13.3)	16.4	(17.9)	17.9	(19.7)
NW	13.8	(3.8)	3.4	(3.7)	3.1	(3.4)	4.2	(4.6)	3.1	(3.4)
N	17.0	(4.7)	3.3	(3.6)	5.2	(5.6)	4.4	(4.8)	4.2	(4.6)
C	47.5	(13.0)	9.6	(10.7)	12.0	(13.1)	14.8	(16.1)	11.0	(12.1)
CNE	1.4	(0.4)	0.3	(0.3)	0.5	(0.5)	0.2	(0.4)	0.3	(0.3)
CE	4.0	(1.1)	0.9	(1.0)	1.3	(1.4)	0.8	(0.9)	1.0	(1.1)
CSE	1.7	(0.5)	0.4	(0.4)	0.6	(0.7)	0.2	(0.2)	0.4	(0.5)
CS	4.6	(1.2)	1.2	(1.3)	1.3	(1.4)	0.9	(1.0)	1.2	(1.3)
CSW	2.4	(0.7)	0.7	(0.7)	0.4	(0.5)	0.6	(0.6)	0..7	(0.8)
CW	14.4	(3.9)	3.8	(4.3)	2.6	(2.9)	4.1	(4.5)	3.8	(4.2)
CNW	3.2	(0.9)	0.7	(0.7)	0.9	(1.0)	1.0	(1.1)	0.6	(0.7)
CN	4.8	(1.3)	1.0	(1.1)	1.5	(1.7)	1.2	(1.3)	1.1	(1.2)

Table 2-1: Average annual and seasonal frequencies of the Lamb weather types over the period from 1861-1990 (after Kelly et al., 1997)

The temporal frequency of the three main weather types, A, C, and W may be very important for the frequency of drought in the UK, and Yorkshire in particular. For the westerly type, there have been six main epochs (Lamb 1972, p11):

1861-1874	Westerly type very prevalent
1875-1899	Blocking prominent, westerly type less frequent
1903-1938	Main westerly epoch, westerly type predominant

1939-1954	Secondary peak of westerly type, moderately westerly period
1955-1972	Blocking prominent
1973-present	Continual decline in westerly type

There has been a decline in the westerly type over the last few decades, along with a decrease in the frequency of northerly and northwesterly types in the 1980s. This has been compensated for by an increase in anticyclonic and cyclonic types. Seasonally, a decrease in westerly types has been compensated for by other types, suggesting increased variability in atmospheric circulation (Briffa *et al.*, 1990). The frequencies of floods and droughts were found to depend upon the prevalence of dominant synoptic patterns (Wilby, 1993*a*) and cycles were observed within the model simulations. The westerlies have shown a recent decline in their 130-year cycle. The anti-cyclonic type showed a distinct cycle over 43.3 and 2 years. The cyclonic type showed a slightly less distinct cycle over 18.6 and 3 years, but their frequency has increased recently at the expense of the westerlies. A statistically significant linear reduction of the 10-year moving average since 1861 was also noted, which suggests a long-term trend towards a reduction in annual aridity.

Numerous studies have shown relationships between the Lamb weather types and various weather elements. An early study by Barry (1967) of the relationship between LWTs and precipitation in Southampton showed not only a clear seasonal cycle in the relative importance of the various weather types, but that most of the precipitation is associated with cyclonic and westerly types. Sweeney and O'Hare (1992) extended this type of analysis to determine the average precipitation amount (rain and snow) falling at a series of stations across the British Isles for a particular weather type. A cyclonic day, for example, produces 4.2 mm of precipitation on average across the British Isles, whereas an anticyclonic day will result in a mere 0.8 mm of precipitation on average. Wilby (1994) presented a stochastic precipitation model for regional climate change impact assessment using Lamb Weather Types. Wilby *et al.* (1994) also used the LWT-catalogue to predict present-day daily precipitation in the British Isles.

2A.7.2.1.2 Automated classification scheme

Jenkinson and Collinson (1977) developed an automated method based on LWTs and this has a large number of advantages for downscaling over the subjective method. It is based on the single, widely available, free atmosphere variable of daily-gridded MSLP and categorises surface flow by direction (with a resolution of 45°) and type, thus having a sound physical basis in climatology. The objective scheme classifies days using three indices of airflow: total shear

vorticity (a measure of the degree of vorticity); strength of the resultant flow; and overall direction of flow (Jones *et al.,* 1993). It is generally considered that free atmosphere variables are better simulated by GCMs than surface variables (Crane and Barry, 1988; Hewitson and Crane, 1992), and therefore provide better predictor variables (Palutikof *et al.,* 1997).

It has been tested by application to control-run GCM output for the British Isles (Hulme *et al.,* 1993) and the air flow indices have been used to predict present-day precipitation at two British sites (Conway and Jones, 1998). However, the objective scheme is based on the analysis of a single chart drawn at midnight, noon, or in the 'morning' (Jones *et al.,* 1993). The Lamb scheme is based for much of the 1861-1997 period on two, or possibly three, charts per day; hence avoiding the problem of a 'snapshot' single chart and giving an idea of the evolution of the weather during the day. Lamb's classification also makes use of the upper level winds, especially since the advent of 500 hPa charts in 1945.

An important advantage of the objective scheme is that it can be applied to other parts of Europe. It has been successfully used in both northern and southern Europe (Brandsma and Buishand, 1997*b*; Goodess and Palutikof, 1998). Brandsma and Buishand (1997*b*) compared the performance of the objective LWTs with that of other classification schemes such as the Grosswetterlagen and the objective P-27 scheme with respect to the prediction of daily temperature and the occurrence of raindays. For precipitation occurrence, the three schemes produce almost identical results, although the Lamb scheme is inferior in the prediction of temperatures.

2A.7.2.2 Discussion

The circulation-based approach to downscaling is a relatively new method. However, many studies have now used either weather types or continuous atmospheric circulation variables for downscaling. This kind of approach stresses the importance of physically based relationships between large-scale atmospheric circulation systems and weather at the local scale. Continuous atmospheric variables, such as vorticity, have significant advantages over weather types, not least because they continuously describe weather states rather than being discrete variables. They also show strong relationships to the probability of precipitation and the magnitude of precipitation events as well as giving information about the intensity of development of the weather system concerned. This makes it easier to simulate extreme events. However, all current techniques rely on air mass descriptions that use the source as definition. This may have a number of limitations such as a difficulty in relating precipitation yields to the air mass, a

variation in individual source regions and reliance upon surface temperature and humidity parameters (Musk 1988).

There are other major drawbacks to using weather types for downscaling, some of which have been previously described. The major problem affecting almost all weather typing classifications is that of assigning a 24-hr weather 'type' to a system that is in constant change (Phillips and McGregor, 1998). Sweeney and O'Hare (1992) cite an example of a strong westerly circulation on the 5th January 1991. The day is classified as westerly by Lamb, but if the 'snapshot' had been taken one hour later then the day would have been categorised as cyclonic or cyclonic southwesterly. To maximise data availability for accurate parameter estimation some of the weather classes must be clustered. However, this must be kept to a minimum to avoid the dilution of the unique attributes of minority classes.

Defining a weather type for the whole of the UK may also be problematic. The Lamb categories were originally considered to be representative of an area (50° –60°N and 10°W – 2°E) that includes the whole of the British Isles. On many days, however, a dual flow is apparent across the UK and thus it is often impossible to allocate a single Lamb weather type that is spatially representative of the whole country, even at one point in time. Regional weather types such as those produced by Mayes (1991*b*) may be more appropriate for a regional precipitation model but these are provided on a very short time-scale. As Smith (1995) remarks, Lamb's weather types have *"failed to reflect the recent regionally specific increase in westerly flows."* Mayes (1994) in a regional airflow catalogue for Scotland shows an increase starting as early as the 1970s and a country-wide increase throughout the 1980s (Mayes 1991*b*). Phillips and McGregor (1998) also cite an instance in the southwest of England where an anticyclonic weather type is assigned but the high precipitation totals over Devon and Cornwall clearly indicate that the regional type is not anticyclonic.

Weather conditions are likely to be very dependent upon features such as frontal systems (meso-scale) and katabatic airflow (micro-scale). The use of weather types for downscaling also relies upon the assumption that the relationships between weather type and local precipitation are stable and will not change in a perturbed climate. The use of GCM control integrations (e.g. Hulme *et al.,* 1993) show that the modelled frequencies of weather types differ from those observed and, additionally, that relationships between weather type and surface weather in GCMs differs from reality. This may not be a drawback however, as these differences may be hidden if complicated mathematical techniques such as canonical correlation analysis are used.

This also begs the question of whether GCMs actually have the ability to reproduce realistic sequences of daily airflow patterns at the regional scale. Hulme *et al.* (1993) attempted to answer this by using the results from two GCM experiments to assess their ability to produce real world weather. Although it was noted that the GCMs did not simulate either frequencies of weather types or their characteristics correctly, it is hoped that the more recent GCMs are more realistic. It may however be more useful to perform sensitivity analyses using current and projected climate trends in a Bayesian-type model than to use inaccurate GCM predictions.

Although there are many disadvantages, it is suggested that weather types provide a greater understanding of the problems involved in downscaling. Linkages are very apparent in a physical sense and strong relationships can be found between these and daily precipitation characteristics for the British Isles (Conway and Jones, 1998). Weather types offer an easy system of classification that also has dynamic and spatial elements, focussing on patterns which air mass analysis lacks. Weather types also provide a more simplistic model that can be easily understood by risk analysts in industry, with an invaluable daily time-span from the 1800s to the present day. Either subjective or objective types can be used. However, the objective scheme can be most easily applied to both observed and simulated MSLP fields (i.e. used in conjunction with GCMs for downscaling), and is applicable across Europe, providing a standard. The objective scheme also has the added advantage of being continually updated (from 1880 to present) whereas the subjective Lamb classification was discontinued in 1997, after his death.

Differences between the subjective and automated LWT schemes have been analysed by Jones *et al.* (1993) using data from the time-period 1881-1989. The frequencies of weather types in the two schemes were highly correlated, especially the anticyclonic and cyclonic types. However, the high year-to-year correlations mask what may be systematic differences between the two schemes, which are generally consistent from season to season. Northerlies, easterlies and westerlies are underestimated by the objective scheme compared with Lamb's, whereas northwesterlies, and southerlies in particular, are overestimated. The differences between the two schemes has diminished considerably since about 1960, with westerly days showing the same frequency in both schemes. A major difference between the two schemes is that the much-quoted decline in the westerlies since 1940 is less apparent in the objective scheme. There were also negligible differences between correlations of frequencies of weather types and regional precipitation.

Conway and Jones (1998) describe three methods of generating distributions of precipitation using the circulation-based approach to downscaling. The first two methods use the objective weather type classification (Jenkinson and Collinson, 1977; Jones *et al.,* 1993) and the third

uses subjective classifications derived from the differing magnitudes of the continuous atmospheric variables of vorticity, strength of flow and direction of flow. In the first method only the seven most common weather types (A, C, N, E, S, W, NW) and unclassified are used. In the second, all weather types are used, including the hybrids. This makes 27 types and means that some types have very low sample distribution sizes as they occur very infrequently. These methods were then used to simulate the mean monthly precipitation at a single site, Durham (UK), and results showed no significant differences between the three methods. This suggests that the objective weather types can be used with confidence for the generation of precipitation distributions.

2B. Rainfall and runoff modelling methodologies

2B.1 Generating temporal sequences of daily weather types

2B.1.1 Clustering Analysis

Although weather types can be used directly as circulation classifications (e.g. Bardossy and Plate, 1991) the infrequency of occurrence of certain types means that data scarcity will preclude their successful parameterisation for precipitation modelling. The clustering of similar weather types to provide weather 'clusters' will overcome this problem and allow a more simple precipitation generator to be provided. Many weather clustering procedures have been used successfully in the literature, the major ones being: k-means clustering, principal components analysis (PCA), a combination of the two (e.g. Corte-Real *et al.,* 1998), or a purely directional/synoptic clustering (e.g. Goodess and Palutikof, 1998), although Kalkstein *et al.* (1990) used an air mass-based clustering analysis to produce a spatial synoptic classification system for Yukon and Alaska. This was extended to the US by Kalkstein *et al.* (1998).

Wilson *et al.* (1992) compared four popular classification methods: *k*-means clustering, fuzzy *k*-means clustering, principal components analysis (PCA), and principal components combined with *k*-means clustering. Results showed that in distinguishing the circulation patterns responsible for precipitation events, all methods performed equally well. However, Gong and Richman (1992) showed that once the total number of clusters has been chosen that principal components analysis coupled with *k*-means clustering can provide the most separable system of clusters.

The *k*-means algorithm is based on Hartigan and Wong (1979) and its objective is to find group memberships that minimise the total within-cluster sum of squares over all *k* of the clusters. The objective function, ϕ, can be represented by (2-1) (Corte-Real *et al.,* 1998):

$$\phi = \sum_{k=1}^{K} \sum_{j=1}^{M} \sum_{i=1}^{N_k} (x_{ijk} - \overline{x}_{jk})^2 \qquad (2\text{-}1)$$

where K is the total number of classes, M is the number of variables used, N_k is the number of samples in the *k*-th cluster. A sample is assigned to a cluster by the minimisation of the Euclidean distance between the vector of observed values (variables) and the means of all the

variables within a cluster. The *k*-means algorithm regroups data until the optimal cluster membership combination is achieved and the samples no longer change clusters.

Corte-Real *et al.* (1998) used principal components analysis coupled with *k*-means clustering and an additional information measure, *Inf*, to determine the optimal number of clusters for southern Portugal, classified from daily SLP fields over the north-eastern Atlantic and western Europe. The information measure, *Inf*, was defined as (2-2):

$$Inf = \sum_{i=1}^{k} \left| n_{r_i} - p_r n_i \right| \qquad (2\text{-}2)$$

Where n_i and n_{r_i} are respectively, the number of days in a specific cluster *i* and the number of rainy days within that same cluster and p_r is the probability of occurrence of rain, for all observations. The optimal number of clusters, *k*, corresponds to the relatively highest score of Inf; the number of clusters that best differentiates between precipitation states.

In the UK, Wilby (1998) clustered the 27 Lamb weather types according to their relative wetness and the proportion of wet days, suggesting that three clusters adequately describe weather patterns: a low-yield/low wet day group (A, ANE, AE, ASE, AS, ASW, AW, ANW, AN), an intermediate group comprising the directionals and unclassified, and a high-yield/high wet day group (C, CNE, CE, CSE, CS, CSW, CW, CNW, CN). However, although grouping weather types has the advantage of increasing the size of the calibration data for low-frequency events, it conceals changes in the frequency of individual LWTs that are known to have occurred historically. This may have the detrimental effect of masking changes in more critical LWTs. Another complication was a consistent underestimation of wet and dry-spell persistence, as wet days were generated independently of whether the previous day had been wet or dry. Although there had been an assumption that persistence would be implicit to LWT day-to-day transitions, the results indicate that a persistence parameter, or some memory component, is required to increase autocorrelation.

2B.1.2 Weather-type generators

A typical feature of synoptic scale circulation is that the day-to-day variability is large during periods of high pressure, but typically small during periods of low pressure. Such state dependent behaviour cannot be reproduced using classical autoregressive (AR) processes. However, threshold AR models (TAR) have been used to reproduce time series of surface

pressure in the UK (Al-Awadhi and Jolliffe, 1998). These are very complex and generally univariate, in contrast to normal atmospheric classification schemes. Therefore, many methods have been developed to enable the generation of synoptic scale atmospheric circulation indices. Markov-chain models and resampling procedures, providing two of the simplest and most commonly used methodologies.

2B.1.2.1 Markov-chain processes

Several researchers have used Markovian-based approaches to generate synthetic weather type series for use in stochastic models of the precipitation process. The first of these may have been Maheras (1989) who used a weather classification technique that delineated 16 weather types to identify summer dry periods in Greece. Hay *et al.* (1991) used a Markovian-based model to generate temporal sequences of six daily weather types using the classification method of McCabe (1989) for the Delaware river basin. Wilson *et al.* (1991) used a semi-Markov transition matrix to characterise the daily weather structure in the Pacific northwest. However, in contrast to Hay *et al.* (1991), the classification scheme was based on a clustering algorithm that used large-scale meteorological variables rather than weather patterns based on point information. Bardossy and Plate (1991) also used a semi-Markov chain model to simulate atmospheric circulation patterns over Europe. Zucchini and Guttorp (1991) developed a model that is based on observed weather states and assumed to follow a Markov chain. It differs from the other approaches in that a purely Markovian approach is adopted, and that the probability of a weather class occurring is conditional upon the precipitation occurrence process. However, pure Markov methods do not give satisfactory results, especially over long durations (Bardossy and Plate, 1991).

In a pure Markov process, the transition from one weather type to the next depends upon the preceding weather type's probability distribution. A transition probability matrix is produced for daily transitions, for example, and a random number generator is used to predict the weather type of the next day. However, a semi-Markov chain process consists of two elements and has distinct advantages over a purely Markovian approach as it uses not only the transition probabilities between states, but also the distributions of durations of the different states. The semi-Markov process has a transition structure the same as that of a Markov process but, in addition, a probability distribution function is assigned to each state that prescribes its within-state length of stay. In general, a geometric distribution has been used to describe the duration of within-state residence (e.g. Hay *et al.*, 1991; Wilson *et al.*, 1992), although, in theory, other probability distributions may provide a better fit to observed persistence distributions.

The majority of models detailed above have concentrated on the reproduction of rainfall at a point, i.e. single-site models. The exceptions to this being the work of Zucchini and Guttorp (1991) and Wilson *et al.* (1992). However, as the weather states of Zucchini and Guttorp (1991) are based upon the precipitation process, described by a hidden Markov model, and are unobservable, then this model may not be used for climate change assessments. A recent development by Hughes and Guttorp (1994) presents a model for multi-station precipitation, conditioned on synoptic atmospheric patterns. The model is called the nonhomogeneous hidden Markov model (NHMM) and can be used to downscale large-scale space-time precipitation fields. It is unique as it determines the most distinct patterns in a multi-site, precipitation occurrence record rather than patterns in atmospheric fields. This has been applied with some success to southwest Western Australia by Bates *et al.* (1998), and Hughes and Guttorp (1999), and to Washington, US (Bellone *et al.* 2000). Other recent models that have reproduced precipitation statistics at multiple sites using weather type information include Wilks (1998; 1999). The difficulty with all schemes however, is how to perturb the results to simulate climate change.

2B.1.2.2 Resampling

Resampling techniques have also been used by many researchers to describe the precipitation process. In a general sense, resampling describes a procedure where a 'window' of time is defined and, within this window, a random sampling of data is taken. This may be conditional (i.e. dependent upon the previous day) and therefore providing an analogue for the historical record. Time dependence may also be important for the conservation of persistence properties, particularly for low pressure synoptic circulation and resampling may be performed on a weekly rather than a daily or hourly basis. However, in most cases, the resampling has been unconditional upon atmospheric circulation, and hence simply a method of producing new precipitation data series.

Researchers who have used this methodology to produce new time series of atmospheric circulation indices or weather types include Brandsma and Buishand (1997*a*; 1998; 1999). In 1996, Lall and Sharma showed that nearest-neighbour resampling is able to reproduce the non-linear behaviour of a TAR model. In nearest-neighbour resampling the weather type on day one is dependent upon the weather type of the previous day, or the previous two days, for example. This is defined within a state vector to find analogues in the historic record. An even better method may be to use non-parametric kernel estimates of the underlying probability density functions (Sharma *et al.*, 1997). This methodology is capable of generating values that differ from those in the historical series, in contrast to nearest-neighbour resampling.

2B.1.2.3 Discussion

Many different methods for the generation of weather-type series have been examined. The simplest and most commonly used approach is that of a clustering analysis followed by the use of a Markov-chain model for weather type generation. A clustering analysis is generally performed to decrease significantly the number of weather types being modelled, and thus the model complexity. A Markov-chain, or semi-Markov chain model, then appears the most simple, yet effective, model for the synthesis of weather-type time series to retain historical characteristics.

2B.2 Stochastic rainfall modelling

2B.2.1 Background

Traditional approaches to stochastic rainfall modelling have typically used Markov chains to simulate the occurrence of wet and dry days in the precipitation process (e.g. Gabriel and Neumann, 1962). Although these models acknowledge the event-based nature of the precipitation process, they are generally inadequate in the modelling of extremes and the phenomenon of persistence (e.g. Gregory *et al.*, 1992).

Attention has therefore, more recently, been focused on the development of event based precipitation models in continuous time. These have modelled the occurrence of precipitation events using a Poisson process, using attached, subsidiary intensity and duration parameters. Poisson cluster processes were originally developed in a spatial context by Neyman and Scott (1958). They were first applied to precipitation modelling by Le Cam (1961); one of their natural advantages being that they can be extended to a space-time model of precipitation (e.g. Gupta and Waymire, 1979). There are generally two approaches. In the first method, the precipitation occurrence process is described separately from the precipitation depth process and then superimposed to form an overall rainfall model. In the second approach, both the occurrence and depth processes are combined and parameter estimation is performed from hourly and integrated precipitation data. Recent developments in this field have been the Bartlett-Lewis rectangular pulses (BLRP) model and the Neyman-Scott rectangular pulses (NSRP) model (Rodriguez-Iturbe, 1987*a*) and the three-state continuous Markov process occurrence model of Hutchinson (1990) (Khaliq and Cunnane, 1996).

2B.2.2 Poisson based models

The simplest of the Poisson based models is the compound Poisson process (Fisher and Cornish, 1960) which attaches a single random instantaneous pulse to each occurrence. The resulting two-parameter model was found to simulate monthly precipitation totals well (Todorovic and Yevjevic, 1969), although the model parameters were sensitive to the level of aggregation of the data used to fit the model. The simplest of the Neyman-Scott models, known as the Neyman-Scott white noise model, was first introduced for representing precipitation by Kavvas and Delleur (1975). They derived expressions for the counting properties of rain cell occurrence and applied their results to daily precipitation sequences in Indiana. Rodriguez-Iturbe *et al.* (1984) found the second-order moments of the aggregated Neyman-Scott white noise model. This is desirable, as precipitation records only tend to be available as daily totals. Valdes *et al.* (1985) found that the Neyman-Scott white noise model performed better over time scales of 1 to 24 hours when compared with other current models, unfortunately being unable to preserve the statistics of extreme precipitation. Foufoula-Georgiou and Guttorp (1987) also found inadequacies in the Neyman-Scott white noise model, especially estimating the model's parameters.

Rodriguez-Iturbe *et al.* (1987*a*) thus developed the cluster-based NSRP and BLRP models, perhaps motivated by the inadequacies of the Neyman-Scott white noise model (Cowpertwait, 1991*a*). They suggested that if the marking process was extended to a random cluster of rectangular pulses with random intensities and durations then parameter estimates would be stable across different data aggregation levels. This sensitivity had been previously noted by Foufoula-Georgiou and Guttorp (1986), and hence the approach of attaching a time-duration to each pulse making up a cluster was adopted.

Both models do have significant limitations however, some of which have now been overcome. They are relatively intractable mathematically and the physical interpretation of each cluster of rectangular pulses as a series of showers is an approximation. The rectangular pulse Poisson process models analysed by Rodriguez-Iturbe *et al.* (1987*b*) also appeared to over-predict the frequency of occurrence of dry periods, although matching with accuracy the intensity statistics. Rodriguez-Iturbe *et al.* (1987*a*,*b*) found, however, that within these limitations the cluster-based rectangular pulse models adequately represented point precipitation processes through a wide range of aggregation levels.

To solve the problem of overestimation of the zero depth probability, Rodriguez-Iturbe *et al.* (1988) proposed a modified Bartlett-Lewis model by taking the mean duration of cells as a random variable between storms (Velghe *et al.*, 1994). Similarly, Entekhabi *et al.* (1989)

introduced modifications to the Neyman-Scott model, by allowing the cell duration to vary for each storm according to a gamma distribution. They found that the proportion of dry days given by the modified NSRP model compared favourably to the historical records (Cowpertwait, 1991*a*). The modified Neyman-Scott model was also applied to two Italian rain gauges where it was observed that the model performed poorly in preserving the historical zero depth probabilities. Burlando and Rosso (1991) also questioned the ability of the modified Bartlett-Lewis model to accurately reproduce the historic characteristics of precipitation in a criticism of Islam *et al.* (1990) who derived the second-order properties of the model. They concluded that the original Neyman-Scott model produced better results than both the original and modified Bartlett-Lewis models. However, Khaliq and Cunnane (1996) have reported a successful application of the model in Ireland. Additionally, Onof and Wheater (1993), in a UK study, found that when the Bartlett-Lewis model was extended to include a random cell duration there was a good reproduction of the proportions of dry periods at different durations.

Cowpertwait has directed most of the recent developments of the NSRP model. Additional properties of the NSRP model, such as the probability of an arbitrary interval of any chosen length being dry, were determined by Cowpertwait (1991*a*) and demonstrated in the context of 10 years of precipitation data from Blackpool, UK. A generalisation of the Neyman-Scott model, in which each rain cell is randomly classed as one of n types, was then formulated by Cowpertwait (1994). In this generalised model, the parameters of a rain cell depend upon the cell type, so that the intensity and duration of an arbitrary rain cell are correlated. Properties were derived and used to fit the model to precipitation data at a single site; further properties then being derived which enable the model to be fitted to multi-site precipitation data.

Cowpertwait (1995) then extended this spatially in the x-y plane, producing a spatial-temporal model of rainfall based on a clustered point process. In the x-y plane, rain cells were represented as discs, each disc having a random radius and the location of each disc centre being given by a two-dimensional Poisson process. Multi-site second-order properties were derived and used to fit the model to hourly precipitation data taken from six sites in the Thames Basin, UK. A two-cell model was used and a satisfactory fit suggested by a 75 percent explained variance.

In Cowpertwait *et al.* (1996*a*), a Neyman-Scott clustered point process model was developed that would be flexible in its model fitting procedure, involving the matching of a chosen set of historical precipitation statistics. In the second paper (Cowpertwait *et al.*, 1996*b*), the model was fitted to daily and hourly data taken from 112 sites scattered throughout the UK. The model was then regionalised by regressing estimates of model parameters on harmonic and site variables. This allows the application to catchments where data are either unavailable or limited.

Percentage errors were low, suggesting that the regionalised model could be used with reasonable confidence, except for reproduction of extreme values. A method of disaggregating hourly precipitation time series to 5-minute precipitation time series for urban applications was also developed and tested.

A modified single-site Neyman-Scott Poisson cluster model of rainfall was then fitted to the same 112 sites scattered throughout the UK (Cowpertwait and O'Connell, 1997). The modifications include the use of two different types of rain cells, convective and stratiform, within the model, and the use of harmonic variables to account for seasonality. The model was regionalised by regressing estimates of the harmonic variables on site dependent variables to enable the simulation of precipitation at any site in the UK. The regional variations of the parameter estimates were in agreement with meteorological knowledge and observation, and simulated 1-hr extreme rainfalls compared favourably with the historical records, although some disparity was shown at higher aggregation levels.

Recently, a method has been developed for the derivation of higher-order moments to obtain the third-order moment function for the NSRP model (Cowpertwait, 1998). This was used with second-order moments to fit the model to precipitation time-series from New Zealand. This is thought to improve the model fit to extreme values, by including the skew of the distribution in the parameter fitting. This may be very important for the reproduction of extreme precipitation events and hence for flood analysis.

2B.2.3 The Generalised Spatial-Temporal NSRP Model

Stochastic spatial-temporal rainfall models have been produced which are based upon the physical processes that have been observed in precipitation fields (e.g. Mellor, 1994). However, the fitting of such models is difficult and thus models that can be fitted using second-order properties taken from time-series records are likely to be of greater practical value in the simulation of long records of multi-site precipitation.

The Neyman-Scott Rectangular Pulses (NSRP) model is a clustered point process model. The model parameters broadly relate to underlying physical processes and the model is capable of preserving the statistical properties of a precipitation time series over a range of timescales. For mathematical convenience, some assumptions about the behaviour of raincells have been made. Namely, that rain cells are discs with a random radius and that the location of the disc centres are given by a spatial Poisson process.

The model considers a catchment of finite area, A, in the x-y plane. Storm origins occur in a Poisson process of rate λ, the arrival times being the same at any point on the x-y plane (Figure 2-2). The arrival of a storm origin at a catchment implies that the physical conditions necessary for precipitation have been met. However, rain only occurs at points covered by rain cells.

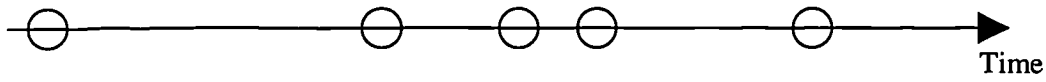

Figure 2-2: The storm origin arrival process.

Each storm origin generates a random number (C) of cell origins (Figure 2-3). The spatial positions of the disc centres are given by a Poisson process of rate ρ, so that the number of disc centres in a catchment of area A is a Poisson random variable with mean ρA. If t is the arrival time of the storm origin and s $(>t)$ is the starting time for a rain cell generated by the origin, then s-t (the waiting time for each cell origin after the storm origin) is taken to be an independent exponential random variable with parameter β, so that the arrival times of cells follows a Neyman-Scott process. No cell origin is located at the storm origin.

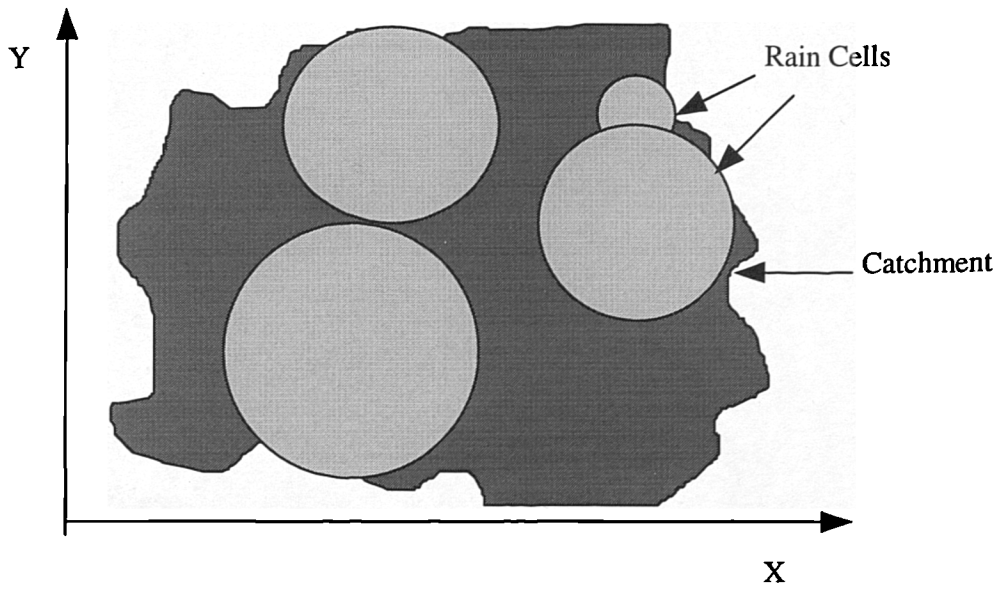

Figure 2-3: Graphical representation of the rain disks in the spatial-temporal model.

Each cell origin is classified as one of n types, where α_i is the probability that a cell origin is of type i (where $i = 1,...,n$). The radius R_i of a type i cell is an independent random variable with

parameter γ_i. A rectangular pulse is associated with each cell origin (Figure 2-4), depending upon the cell type defined previously. The duration of the pulse is an independent exponential random variable with parameter η, and the intensity of the pulse is an independent random variable X_i for type i cell origins, remaining constant over the lifetime of the cell and the area of the disc.

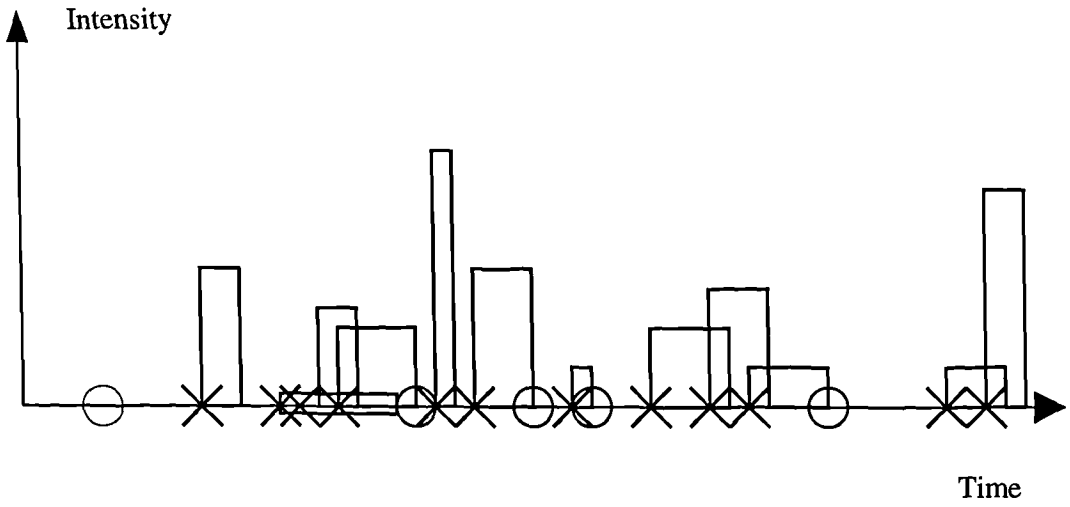

Figure 2-4: Graphical representation of precipitation pulses produced at raincells.

The total precipitation intensity at a time t and point m is then the sum of the intensities of all the active rain cells at time t that overlap point m (Figure 2-5). If $Y_i^{(m)}(t)$ is the total precipitation intensity at time t and point m given by the NSRP(n) model (sometimes called the Generalised NSRP model), and $X^{(i)}_{m,t}(u,s)$ is the precipitation intensity at time t and point m due to a type i cell with centre a distance u from m and starting time $t-s$, then (2-3):

$$Y_i^{(m)}(t) = \int_{u=0}^{\infty}\int_{s=0}^{\infty} X^{(i)}{}_{m,t}(u,s)\,dN^{(i)}(u;t-s), \quad \text{for } i=1,\ldots,n. \tag{2-3}$$

Where (2-4):

$$X^{(i)}{}_{m,t}(u,s)\begin{cases}\varphi_m X_i & \text{with probability } e^{-\gamma_i u}e^{-\eta_i s};\\ 0 & \text{otherwise}\end{cases} \tag{2-4}$$

The total intensity at time t and point m, $Y^{(m)}(t)$, is the sum of the intensities of all cells active at the time t and overlapping m, i.e. (2-5)

$$Y^{(m)}(t) = \sum_{i=1}^{n} Y_i^{(m)}(t) \qquad (2\text{-}5)$$

The mean number of cells per storm is denoted as μ_c and $E(X_i)$ as μ_i. The model is thus a generalised form of the Neyman-Scott Rectangular Pulses model with *n* cell types.

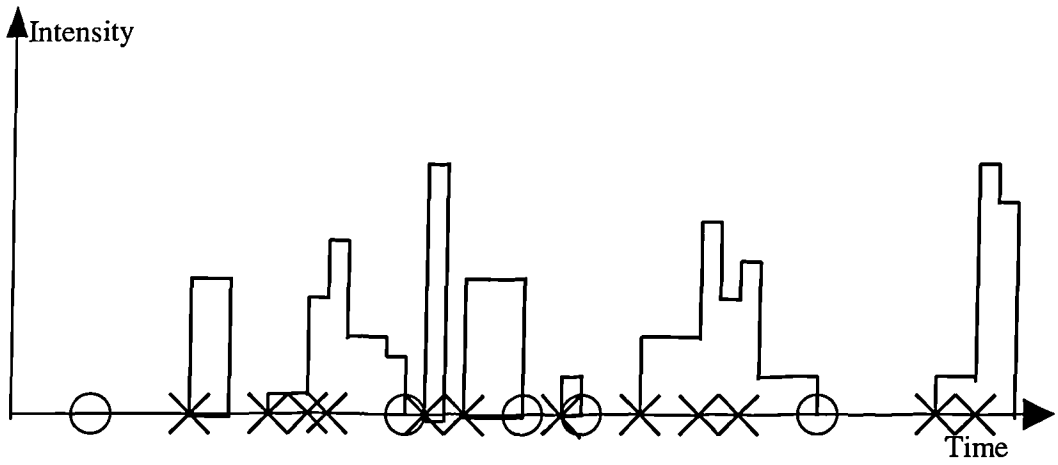

Figure 2-5: The calculation of the total precipitation intensity at a time t and point m.

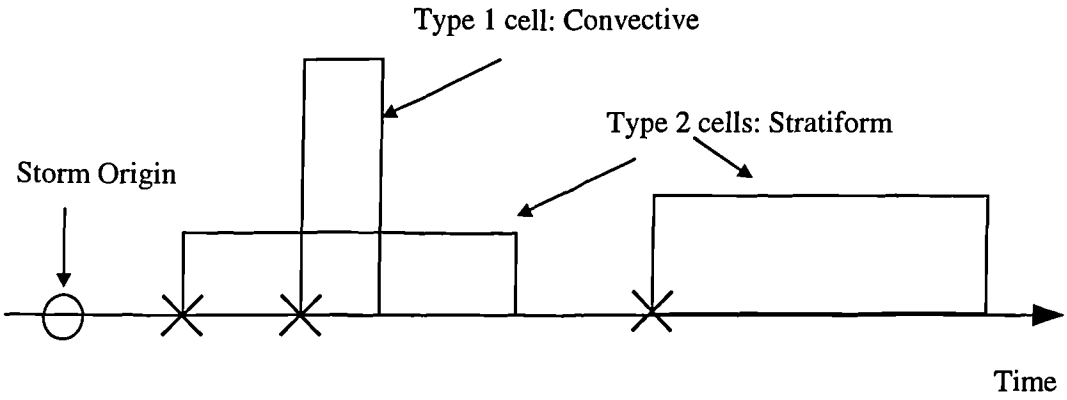

Figure 2-6: Different cell types represented by the model.

As with a single-site model, cells can be classified into different types. Cowpertwait and O'Connell (1997) suggest that the determination of the number of cell types to be included in the model can be guided by observing physical characteristics of the precipitation process. The simplest possible model uses only one cell type but the literature suggests that the precipitation field can be broadly classed into two types; convective and stratiform precipitation (Figure 2-6). The simplest model would contain only one cell type. However, in a two cell model type 1 cells

would be interpreted as 'heavy' short-duration convective cells and type 2 cells as 'light' long-duration stratiform cells, giving eight model parameters (see Table 2-2).

Parameter	Explanation
λ^{-1} (lambda)	the mean waiting time between adjacent storm origins
β_1^{-1} (beta)	the mean waiting time for cell origins after the storm origin
β_2^{-1} (beta)	the mean waiting time for cell origins after the storm origin
ν_1 (nu)	the mean number of type 1 rain cells associated with a storm origin.
ν_2 (nu)	the mean number of type 2 rain cells associated with a storm origin.
η_1^{-1} (eta)	the mean duration of a type 1 cell
η_2^{-1} (eta)	the mean duration of a type 2 cell
ξ_1^{-1} (xi)	the mean cell intensity for type 1 cells
ξ_2^{-1} (xi)	the mean cell intensity for type 2 cells
γ_1^{-1} (gamma)	the mean radius of a type 1 cell
γ_2^{-1} (gamma)	the mean radius of a type 2 cell

Table 2-2: The parameters of a two-cell GNSRP model.

This can be extended to include any number of cell types to give a better model fit. However, in practise it has been found that two cell types are almost universally sufficient for accurate simulation and increasing the number of cells above this simply increases the complexity of the model without greatly improving accuracy. Thus in the model fitting a maximum of two cell types will be used.

Other parameters also need to be specified within the model. In three-dimensional space, the intensity, ξ, at a point with co-ordinates (x, y, z) is scaled by a factor, φ_m, which can be a function of the altitude z of the point to make an allowance for the effects of orography, but is more commonly based on a scaling of the mean daily precipitation in a month at that site. However, for sites where this information is not available due to missing data or lack of a historical record, regression relationships are necessary to allow simulation at any site within the Yorkshire area under analysis. A survival probability can also be defined for each site, which gives the probability of a rain cell surviving to reach ground level as at low altitudes rain can evaporate before reaching ground level.

2B.2.4 Fitting using daily data

In fitting the model to daily data, estimates of the variances of sub-daily precipitation totals derived from regional regression relationships are used to ensure that sub-daily totals generated

by the fitted model exhibit the desired statistical properties (Cowpertwait *et al.*, 1996*a*). An assessment was made of the errors produced at the 1-hr aggregation level between historical and simulated sample values when the NSRP model is fitted using only properties at the 24-hr aggregation level. These ranged from between –38 and +36 percent, with underestimation of hourly variance being particularly severe over summer months. Higher aggregation levels are unlikely to contain enough information from which the properties of rain cells can be found as the parameters of the model generally relate to cells which have lifetimes of less than 1 hour.

It was suggested that an alternative approach was to estimate the sample hourly variance from the sample daily variance using a derived empirical relationship as it was found that the two sample moments are highly correlated. Hourly precipitation data from 27 stations across the UK were used to derive regression equations relating 1-hr, 3-hr, 6-hr, and 12-hr variances to 24-hr variance. Different regression equations are applicable for the south and north of Britain, north of a line running east-west through Berwick-upon-Tweed, whereas differences in the derived equations within regions could be reasonably be attributed to chance. This research is described in Cowpertwait and Cox (1992), Cowpertwait (1991*b*) and Cowpertwait *et al.* (1996a).

These equations (2-6–2-9) are reproduced below for region A, which contains the Yorkshire region:

$$\hat{\gamma}(1) = 0.03159 + 0.008597\hat{\gamma}(24) \qquad R^2 = 76\% \qquad (2\text{-}6)$$

$$\hat{\gamma}(3) = 0.1415 + 0.04931\hat{\gamma}(24) \qquad R^2 = 88\% \qquad (2\text{-}7)$$

$$\hat{\gamma}(6) = 0.2899 + 0.1426\hat{\gamma}(24) \qquad R^2 = 93\% \qquad (2\text{-}8)$$

$$\hat{\gamma}(12) = 0.4655 + 0.3874\hat{\gamma}(24) \qquad R^2 = 96\% \qquad (2\text{-}9)$$

It is suggested that for the fitting procedure firstly the mean 1-hr precipitation, $\mu(1)$, 24-hr variance, $\gamma(24)$, 24-hr dry-dry and wet-wet transition probabilities, and 24-hr dry period probability, $\phi(24)$ should be calculated from the historical daily precipitation time series. $\gamma(1)$, $\gamma(3)$, $\gamma(6)$, and $\gamma(12)$ should then be estimated using the above regression relationships for the appropriate region of the UK. These statistics should be used in minimising the sum of the squares function to estimate the NSRP model parameters. It is suggested that if this procedure is used then the fitted model can be used with reasonable confidence to generate hourly data when only daily data are available at the site in question. Calenda and Napolitano (1999) researched the role of data aggregation scale upon parameter estimation of the NSRP model. It is suggested

that if different aggregation levels are used then the optimisation procedure may fail if the selected scales are too close.

In the spatial model, $\mu(1)$ is used to estimate the scaling factor, φ_m, for each site m. This is equivalent to dividing each hourly series by the mean of an index site, i, to produce n transformed series. Each series then has the same mean and approximately the same variance (i.e. approximate stationarity in space). The model is then fitted to the transformed series using a simplex procedure. Parameters are estimated by minimising the following sum of squares (2-10):

$$\sum_{m=1}^{n} \sum_{f_m \in F} \omega(\hat{f}_m)\{1 - f_m / \hat{f}_m\}^2 \qquad (2\text{-}10)$$

subject to: $\lambda, \beta, \nu, \eta, \xi, \gamma > 0$, where $\hat{f}_m$ is a sample estimate taken from the hourly data for the mth site, and F denotes a set of aggregated single-site properties. The $\omega(\hat{f}_m)$ are weights that can be applied if some of the properties are to be fitted to a greater accuracy.

2B.3 Rainfall-Runoff modelling

2B.3.1 Background

A broad range of models have been created to study various different rainfall-runoff phenomena. The classification system proposed by Todini (1988) is the most convincing; where hydrological models are classified into four classes characterised by increasing degrees of *a priori* knowledge. A mathematical model is basically a combination of, firstly, the 'physical component' (Todini, 1988) which expresses all the prior information available on the process to be represented and, secondly, the 'stochastic component' (Todini, 1988) which expresses in statistical terms what cannot be explained by the 'physical component'. The level of this *a priori* knowledge is taken as the basis for model classification.

Todini (1988) thus defines four classes of models; purely stochastic, lumped integral, distributed integral, and distributed differential. This is graphically described in Figure 2-7. A purely stochastic model is simply a 'black-box model', where a cause and effect relationship between input and output variables is not even implied. These are generally avoided in rainfall-runoff modelling. A lumped integral, or lumped conceptual, model is a model where the system

dynamics are represented by considering the overall behaviour of the catchment as a whole. Parameters are generally estimated using statistical techniques and may have little or no physical meaning due to the aggregation. An attempt to overcome this problem is provided by distributed integral models. These are based upon the idea of representing all the phenomena at a sub-catchment scale and combining all the components by matching their boundary conditions. In this way, the model parameters are given physically meaningful values. However, these models (e.g. Stanford, Sacramento, ARNO) cannot provide a really distributed output unless the catchment is subdivided into many extremely small sub-units; generally impracticable due to the very large number of parameters involved (Todini, 1988). Instead of *a priori* measured values, effective values may have to be assumed for some of the parameters to give satisfactory results. These are generally assumed to take into account additional processes not described by the model, sub-grid effects and systematic errors (Kuchment *et al.*, 1996). These are commonly estimated by calibration with observed runoff and so, in practice, may differ little from the lumped conceptual models. Finally, distributed differential models, e.g. Systeme Hydrologique Europeen (SHE), represent catchment behaviour in terms of differential equations discretised in time and space. These models are difficult to integrate and require large amounts of data.

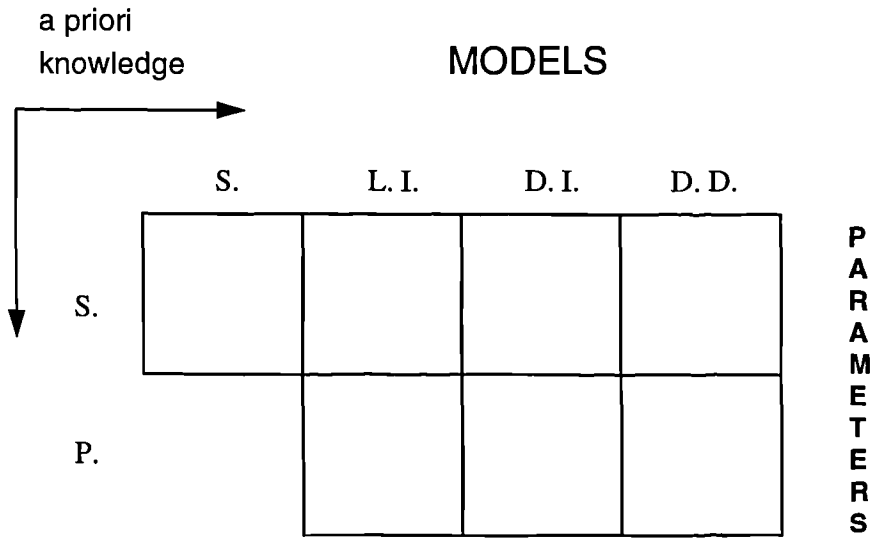

Figure 2-7: Hydrological model classification (after Todini, 1988). S=Stochastic component, P=Physical component. S=Statistical, L.I.=Lumped Integral, D.I.=Distributed Integral and D.D.=Distributed Differential.

As a simple model was required, a conceptual rainfall-runoff model was chosen. The ADM model ('A Distributed Model') is a simple version of the ARNO model with only six

parameters. The original ARNO model was developed at the Centro Idea, University of Bologna, and derives its name from its first application to the Arno river in Italy.

2B.3.2 The ARNO and ADM Rainfall-Runoff Models

The ARNO model is a semi-distributed conceptual rainfall-runoff model that is in widespread use operationally and in research. It is based on the schematic representation of catchment hydrology shown in Figure 2-8, and is characterised by two main components. The first component represents the soil moisture balance and the second describes the transfer of runoff to the outlet of the basin, mainly concentrating on the simulation of surface flows.

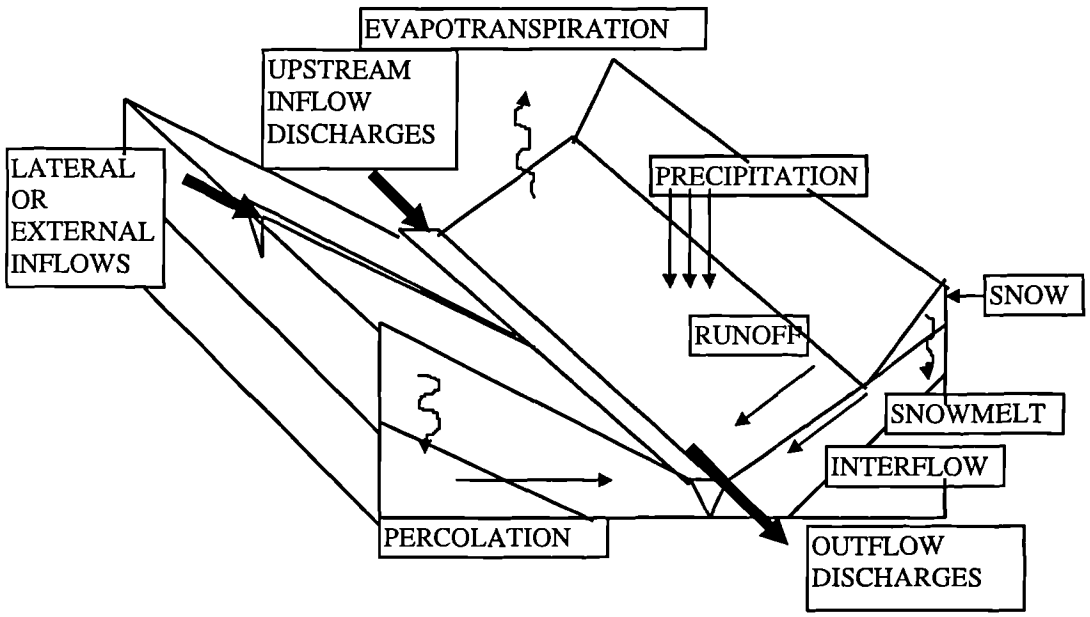

Figure 2-8: Schematic representation of processes within a catchment unit (after Todini, 1996).

Parameter	Variable Name	Description
W_m	WM	Maximum water storage capacity of the soil (mm).
b	B	Shape parameter of the water storage capacity curve (-)
D_1	D1	Maximum drainage rate (mm h^{-1})
D_2	D2	Shape parameter of the drainage curve (-)
Conv	CONV	Convectivity (m s^{-1})
Diff	DIFF	Diffusivity (m^2 s^{-1})

Table 2-3: Description of parameters in the ADM model.

The ADM model may be considered a combination of the ARNO model (Todini, 1996) and the XINANJIANG model (Zhao, 1977). It was developed by Franchini (1996), and Franchini and Galaeti (1997), requiring the calibration of only six parameters. These are detailed in Table 2-3.

In this version of the ADM model, the groundwater module of the ARNO model is omitted, and the drainage component simplified. The catchment can be divided into a series of sub-basins, to each of which the rainfall-runoff model is applied. For each sub-basin and for each time interval the model calculates the evapotranspiration and runoff production and its routing downstream using the following four modules within the model.

2B.3.2.1 Soil moisture balance module

The soil moisture balance component describes the non-linear mechanisms with which the soil moisture content and its distribution control the size and location of the saturated areas. These are responsible for a more or less direct conversion of rainfall to runoff. It is derived from the Xinanjiang model developed by Zhao (1977; 1984) who expressed the spatial distribution of the soil moisture capacity in the form of a probability distribution. Todini (1988) modified this original idea to allow more effectively for soil depletion owing to drainage.

Basic assumptions made in the soil moisture-balance module are that:

- precipitation input to the soil is considered uniform over the catchment area;
- all the precipitation will infiltrate into the soil unless the soil is either impervious or has reached its saturation limit;
- each catchment is divided into an infinite number of elementary areas which have different soil properties;
- the proportion of these areas that are saturated are described by a spatial distribution function which describes the dynamics of the contributing areas to surface runoff;
- the total runoff generated is the spatial integral of all the contributions;
- soil moisture storage is depleted by evapotranspiration as well as by drainage, both expressed by simple empirical expressions.

In the model, the total catchment area, S_T, is divided into a pervious area, S_P, and an impervious area, S_I, (2-11):

$$S_T = S_I + S_P \qquad (2\text{-}11)$$

If the entire pervious area, from equation (10), is $S_P = S_T - S_I$, and the generic surface area at saturation is denoted by $S - S_I$, then f/F will indicate the percentage of the pervious area at saturation (2-12):

$$\frac{f}{F} = \frac{S - S_I}{S_T - S_I} \tag{2-12}$$

Zhao (1977) showed that the following relationship is valid between the area at saturation and the local proportion of maximum soil moisture content w/w_m, where w is the elementary area soil moisture at saturation and w_m is the maximum possible soil moisture in any elementary area of the catchment (2-13):

$$\frac{f}{F} = 1 - \left(1 - \frac{w}{w_m}\right)^b \tag{2-13}$$

where; f/F = Saturated fraction of the sub-catchment

w = elementary area soil moisture at saturation

w_m = maximum soil moisture content in an elementary area

b = curve shape parameter

In the ADM model, an interception component is not explicitly included. However, to allow for a larger evapotranspiration component when the canopies are wet the following rule is used; if the precipitation is larger than the potential evapotranspiration then the actual evapotranspiration is assumed to equal the potential.

The surface runoff, R, generated by the entire catchment is obtained as the sum of two terms. Firstly, the product of the effective meteorological input (i.e. precipitation minus any evapotranspiration) and the percentage of impervious area and, secondly, the average runoff produced by the pervious area which is obtained by integrating the soil moisture capacity curve. After integration the following two terms are produced, which give an average over the whole catchment, rather than an elementary area. These are W, the catchment average soil moisture content, and W_m, the catchment average soil moisture content at saturation.

The total runoff from the catchment however also includes the components of horizontal drainage (affected by the soil moisture levels) and vertical percolation to groundwater or baseflow. The non-linear response of the unsaturated soil to precipitation is strongly affected by the horizontal drainage and vertical percolation losses. The drainage loss affects the soil

moisture storage and controls the hydrograph recession. The drainage loss, D, from interflow is described by (2-14):

$$D = D_1 \frac{W_t}{W_m}^{D_2} \tag{2-14}$$

where; D = drainage (mm h^{-1})

D_1 = Maximum drainage rate (mm h^{-1})

D_2 = Exponent of drainage curve

The total runoff per unit area produced by the precipitation P is thus expressed as (2-15):

$$R_{tot} = R + D \tag{2-15}$$

2B.3.2.2 Evapotranspiration module

Evapotranspiration plays a major role in the rainfall-runoff process as it has a cumulative temporal effect upon soil moisture volume depletion. In the ADM model, the effects of wind speed and vapour pressure are ignored and the evapotranspiration is calculated using the same methodology as Doorembos *et al.* (1984). The potential evapotranspiration for the period under consideration is translated to actual evapotranspiration by the model. In the model, the ratio between actual evapotranspiration and potential evapotranspiration increases linearly as the ratio between W and W_m increases.

2B.3.2.3 Snowmelt module

The snowmelt module is driven by a radiation estimate based upon temperature inputs. This module controls whether precipitation is solid or liquid by dividing the catchment into a number of equi-elevation zones (snow bands) according to the thermal gradient, where snowfall occurs if the air temperature is below that required for snow formation. It also determines any snowmelt that may occur by comparison of the energy budget based upon the hypothesis of no snowmelt with the total energy available for snowmelt.

Radiation is estimated by re-converting the latent heat (the reference evapotranspiration) back into radiation, depending upon the ambient air temperature and the temperature at which snow

will form (a model parameter). In addition, to account for albedo, an efficiency factor is applied to the equation, depending upon whether the sky is clear or overcast. Given the lack of information concerning this as input to the model, it is assumed that the sky is clear when there is no precipitation and overcast if precipitation is being measured.

2B.3.2.4 Parabolic transfer module

Hillslope routing and channel routing of distributed inflows are both performed using a distributed inflow linear parabolic model, whereas the channel routing of upstream flows to a sub-basin is performed by means of a concentrated input parabolic model (Todini, 1996). A differential equation is used in both cases with the main parameters of each being *Conv* and *Diff*, the convectivity and diffusivity coefficients for each response function. These are related to the dimensions, slopes and lengths of the individual sub-basins. In general, *Diff* increases with the size of river and with the inverse of the bottom slope. *Conv* stays at around the same values throughout.

2B.4 Water Resources Planning Model (WRPM) model

The WRPM model was developed by a M.Sc. student in the Operational Research department at the University of Lancaster in 1988 (Blackwell, 1988). The model acts as a routing system that allows the flow of a material around a pre-defined route. It enables the construction of complex systems through the progressive addition of small sub-units. Four main elements are defined for the construction of a supply system:

- Source — Either a reservoir, river or borehole.
- Treatment Works — All water that leaves a source may pass through a treatment works before arriving at its demand destination.
- Demand — A demand can be defined for the destination of the water.
- Links — Join the components of the system together (water mains) and restrictions can be defined.

The utility of the WRPM was demonstrated by a M.Sc. project undertaken at Lancaster University for the NRA Yorkshire and Northumbria Region (Ewing, 1993). In this study, the subsystem containing Grimwith Reservoir was modelled and ways of improving yield were identified. A simplified model of the Yorkshire water supply grid was then produced by Ribas (1994). The model was further enhanced by the development of an 'interpreter system' by

Jenkins and Tong (1996). This allows use of the model as a decision support system for the conjunctive use of resources within Yorkshire. It allows the user to:

- Improve the total yield of the water supply system
- Reduce operational costs
- Conserve resources for dry periods
- Design new control systems for water supplies

The model can be used to look at shortages within the water supply grid under the current climate and the exacerbated risk to supply of future climate change scenarios, pinpointing areas of shortfall and increased vulnerability.

Figure 2-9 shows the Yorkshire Grid (YG97) model developed by the Environment Agency, based upon the previous work of Ribas (1994), and Jenkins and Tong (1996). The model contains 14 sources; 4 rivers and 10 reservoir groups. These include the rivers Ouse, Wharfe, Derwent and Hull, and the reservoir groups Grimwith, Washburn, Nidd/Barden, Worth Valley, Calderdale, Huddersfield, Winscar, Brownhill, Pennine and Booth/Ryburn. The Harrogate reservoir group is modelled as a constant inflow, or borehole source, as it only supplies the demand centre of Harrogate. Similarly, the inflow from the Ladybower reservoir group is modelled as a constant. In addition, five other groundwater inputs are modelled at Doncaster, Selby, Hull and Wolds, Nutwell, and Leeds. The demand centres, water treatment works and link capacities within the model can be seen in Figure 2-9.

For each source, basic information is required for modelling, as well as control rules for that particular source. All information required is provided within the YG97 model and has been formulated by the Environment Agency using data from Yorkshire Water. For a reservoir source, some general parameters required by the model are:

1. The output junction number of the source.
2. The capacity of the output link. (Ml day^{-1})
3. The top water level of the reservoir (m).
4. The maximum storage capacity of the reservoir (Ml)
5. Leakage and evaporation data can be optionally input.

For a river or borehole source, only parameters 1 and 2 are required.

Control rules are also used for the operation of water supply sources within the model. These safeguard the supply of water to the required level of service. Control rules are entered as a series of discrete values for specified time of the year. In the case of a reservoir source, a storage value is entered for a particular date. The compensation flows that can be released at storage levels above this amount, and the total amount of supply water available are then specified. This provides yearly reservoir control curves. For a river source, for a given date, a prescribed flow is entered. Below this level, no water can be extracted from the river. Above this level of flow, an abstraction rate is specified.

Each source also requires an input data file of inflows. These are daily values, but in the case of reservoirs are a daily average taken from a monthly inflow value. Historical daily inflows have been produced by Mott MacDonald (1996; 1997) for 1948-1996. Although the control rules of various sources can be changed within the model structure and link (water main) capacities can be expanded at critical locations within the grid to take account of bottlenecks in supply, these are outside the scope of this thesis. The structure of the YG97 model will be kept constant within the study, providing an 'as is' examination of the possible impacts of climate change upon the water supply network within Yorkshire. Areas of vulnerability and possible improvement will, however, be highlighted.

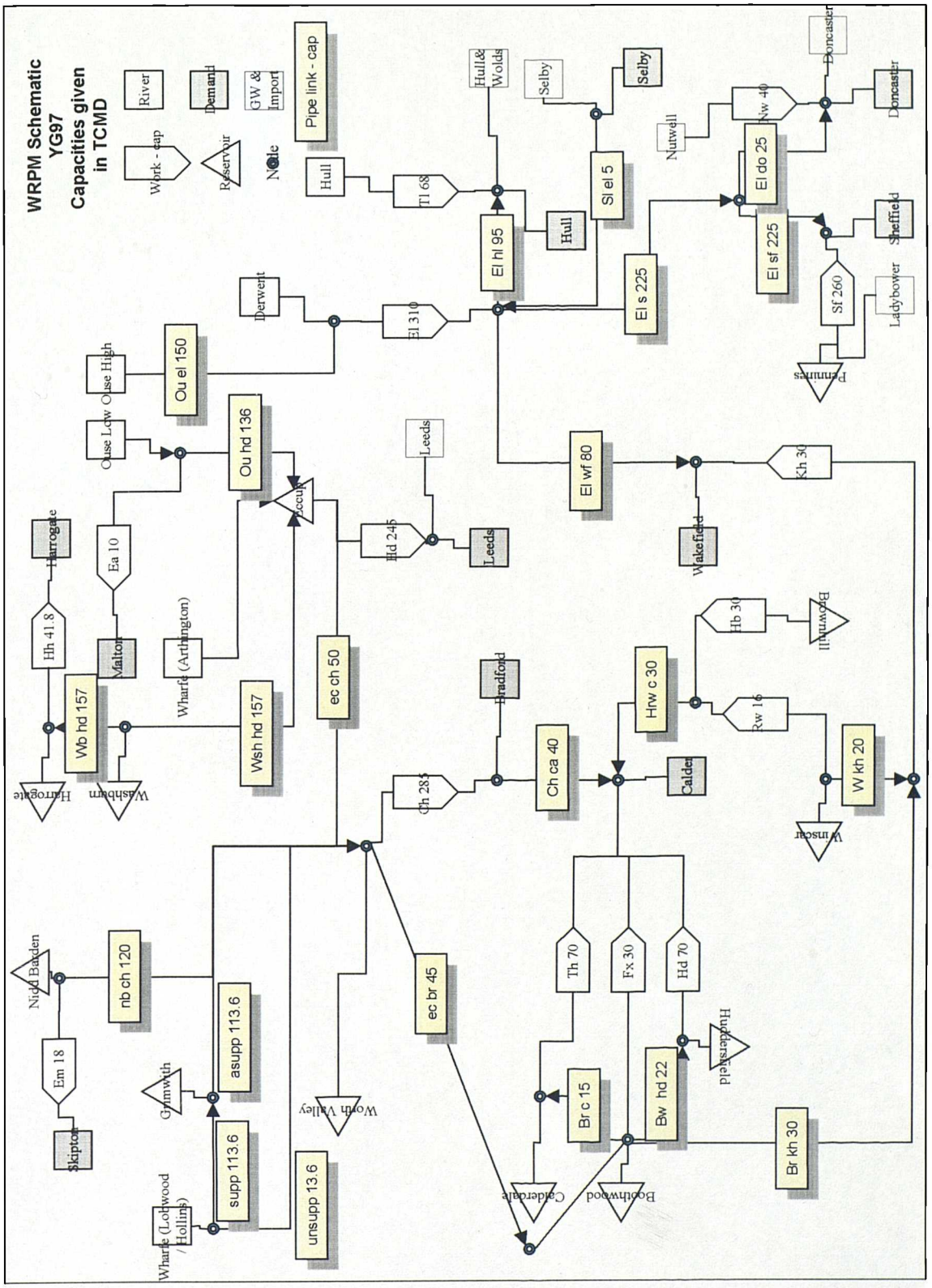

Figure 2-9: Schematic of the Yorkshire Grid (YG97) model showing sources, demands, water treatment works and links (water mains).

Chapter 3: Observed precipitation variability and links to large-scale atmospheric circulation

"We have to take a long-term view that things are changing in our weather. These incidents of weather extremities are occurring more frequently...it's a global problem and it needs a global solution."

UK Deputy Prime Minister, John Prescott, 2nd November 2000

It is important to set a context for future climate change. Therefore, the historical variability of precipitation in Yorkshire was examined and attempts were made to link this variability to large-scale atmospheric circulation.

3.1 Defining a dry day threshold

Previous research has used highly variable bounds for a dry day. It is important to have a non-zero threshold however, as, for example, a single day with precipitation less than 1 mm during a 20-day dry spell is of little significance (Jones *et al.*, 1997*a*). Wigley and Jones (1987), in their analysis of precipitation patterns throughout the UK, used a high threshold of 1 mm for wet days. Other researchers, such as Jones and Conway (1997), Jones *et al.* (1997*a*) etc., have also used 1 mm. For these researchers a very low threshold, say of 0.1–0.2 mm is considered prone to observer bias (Wigley and Jones, 1987). Recent work by both Wilby (1998) and Kilsby *et al.* (1998*a*) has used a dry day of > 0.1 mm and ≥ 0.2 mm respectively. These bounds are effectively the same since daily precipitation totals are measured to the nearest 0.1 mm. Work at the Water Resource Systems Research Laboratory at Newcastle University (A. Burton pers. comm.) has shown that the optimum dry bound to choose to avoid measurement errors, due to the change from imperial to metric measurement in the early 1970s, is ≥ 0.2 mm. Therefore, a dry bound of ≥ 0.2 mm will be used.

3.2 Observed Precipitation Variability in Yorkshire

The historical observed precipitation variability was examined at seven sites in Yorkshire where long daily records (50+ years) are digitally available (Table 3-1; Figure 3-1). The longest data set is from Lockwood Reservoir in the North York Moors and is complete from 1873 to 1998, excepting 1875. Data sets were validated using the Durham precipitation series, which is regarded as accurate. The northern sites, in particular, very closely match the Durham series.

Site	Location	Grid Ref.	Start Year	Altitude (m)	Missing and Suspect (%)	Mean Annual Precipitation (mm)	Mean Annual PD
28106	Hury Reservoir	NY 967193	1929	263	1.94	909	0.42
28408	Barnard Castle	NZ 056164	1926	171	1.94	765	0.48
29156	Raby Castle	NZ 128221	1929	140	8.61	812	0.45
34458	Lockwood Reservoir	NZ 668141	1873	193	1.70	803	0.45
37225	Scarborough, Manor Road	TA 031883	1911	52	0.00	660	0.52
47060	Moorland Cottage	SD 807923	1936	343	2.49	1939	0.41
87024	Kirk Bramwith	SE 618114	1891	7	4.18	593	0.58

Table 3-1: Sites in Yorkshire region where long daily precipitation records are available. Mean annual precipitation and PD given for the 1961-90 time-period.

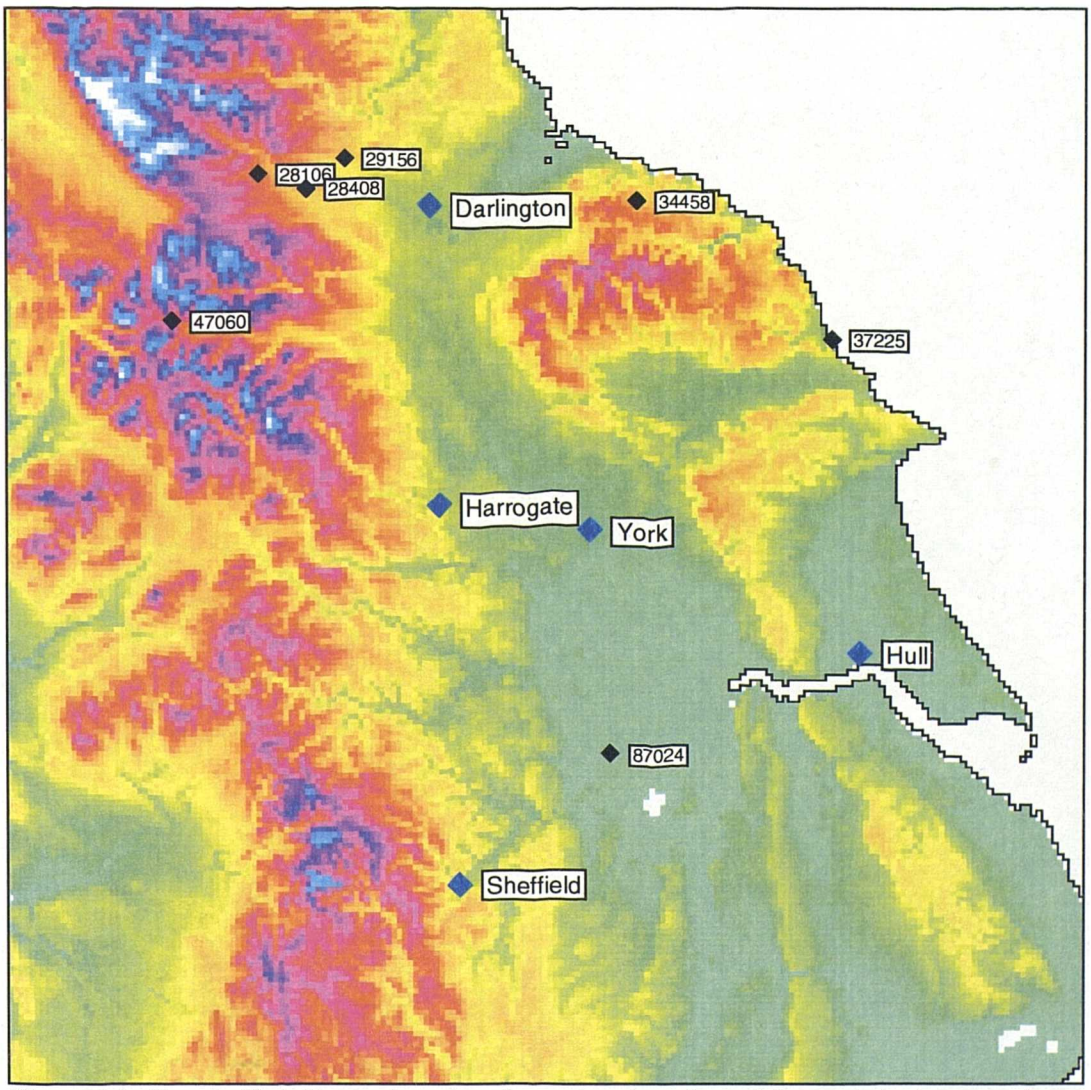

Figure 3-1: Sites in Yorkshire and surrounding area where long daily precipitation records are available.

3.2.1 Fluctuations in mean daily precipitation, PD and mean wetday

Seasonal variations in mean daily precipitation throughout the period from 1873-1998 show a decline in summer precipitation totals at all seven sites (see Figure 3-2), particularly since the 1930s.

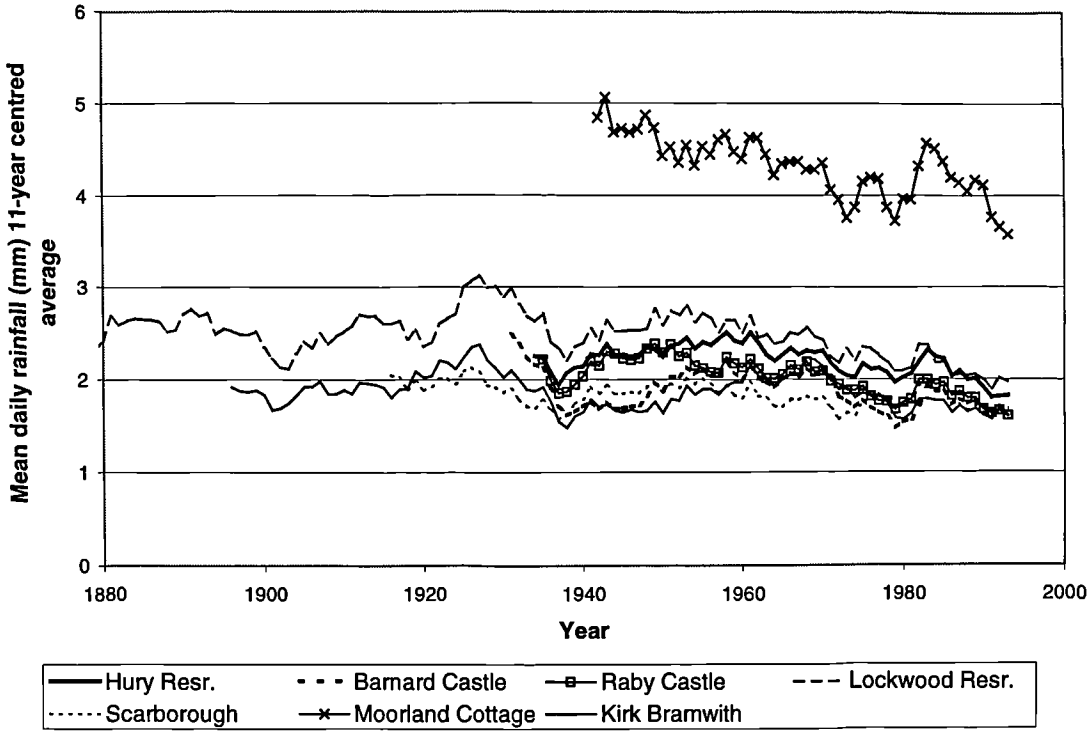

Figure 3-2: Mean summer daily precipitation (11-year centred moving average)

Westerly sites (i.e. Hury Reservoir, Barnard Castle and Moorland Cottage) show an increase in winter precipitation totals since the late 1970s which corresponds to the supposed increase in frequency and vigour of westerly circulation types (see Figure 3-3). This is especially noticeable at Moorland Cottage. The coastal site of Scarborough shows a rapid decline in spring precipitation since the late 1980s. Other sites show variations in autumn precipitation totals. For example, the Pennine site at Moorland Cottage notes increasing autumn precipitation until the late 1980s, when there is a rapid decline.

The mean wetday amount (MWD) shows a striking periodicity over the last 100 years. At both Lockwood Reservoir and Kirk Bramwith (see Figure 3-4), the mean annual rainday is very stable at low levels until approximately 1910. There is then a sudden increase to a peak in the 1920s/1930s and a slow decline back to prior levels until the 1960s. MWD then rises until the early 1980s and declines to present. Although this cyclicity corresponds well to variations in the

NAO, a correlation analysis finds no significant relationships on a year-to-year basis, although they may be there at low frequency.

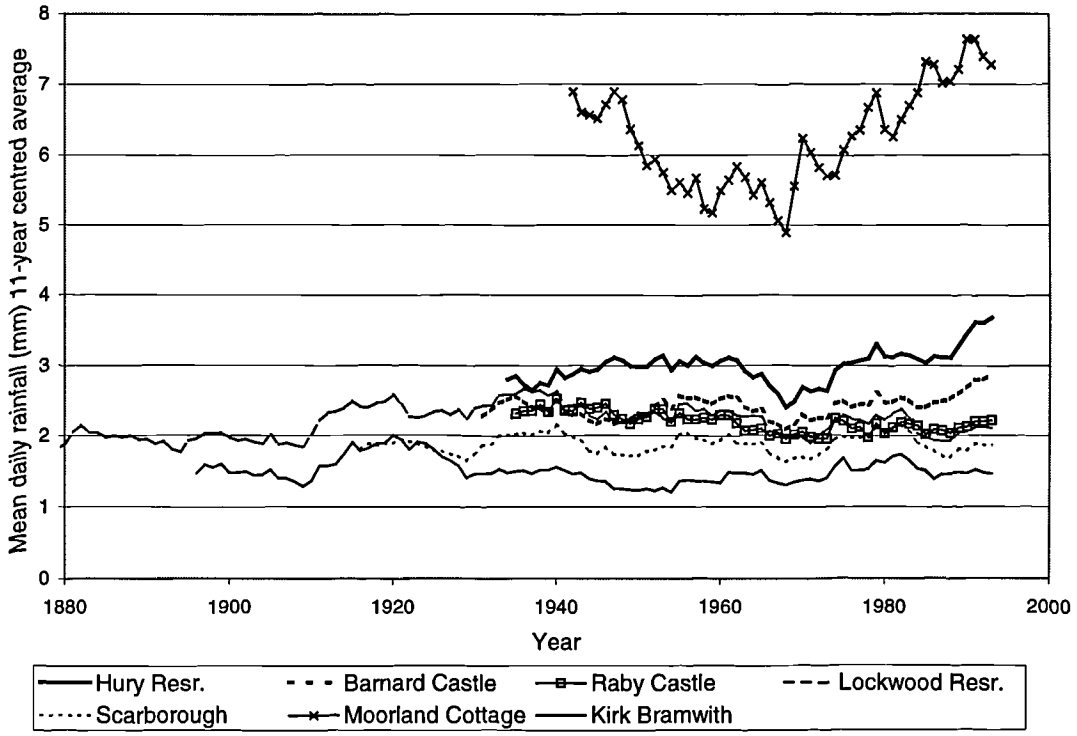

Figure 3-3: Mean winter daily precipitation (11-year centred moving average)

The eastern site of Scarborough records a noticeable decline in summer MWD since the start of historical record in 1911, from 5 to 4 mm on average. However, at this coastal site the MWD during other seasons remains stable. Both winter and summer MWD is stable at Pennine sites from the 1930s through to the 1970s. However, since the late 1970s there has been a dramatic increase in the winter MWD and a concurrent decline in the summer MWD. This may be a contributory factor to the recent change in the winter to summer precipitation ratio. Interestingly, data from Moorland Cottage indicates a decline in winter MWD over the Pennines since the late 1980s in sharp contrast to the other sites.

Regional trends in proportion dry days (PD) over the last 100 years have been increasing PD until the 1930s/1940s, a declining PD until the 1970s and a subsequent increase until the late 1980s in both summer and winter statistics. This corresponds well with the four stages of the NAO delineated by Wilby (1994). The Pennine sites at Moorland Cottage, Hury Reservoir and Barnard Castle show a declining winter PD since the late 1980s (see Figure 3-5). The North York Moors site of Lockwood Reservoir records a highly stable PD in all seasons from 1875 to 1915 (see Figure 3-6). After 1915 the range increases dramatically, with winter days in particular becoming more frequently wet.

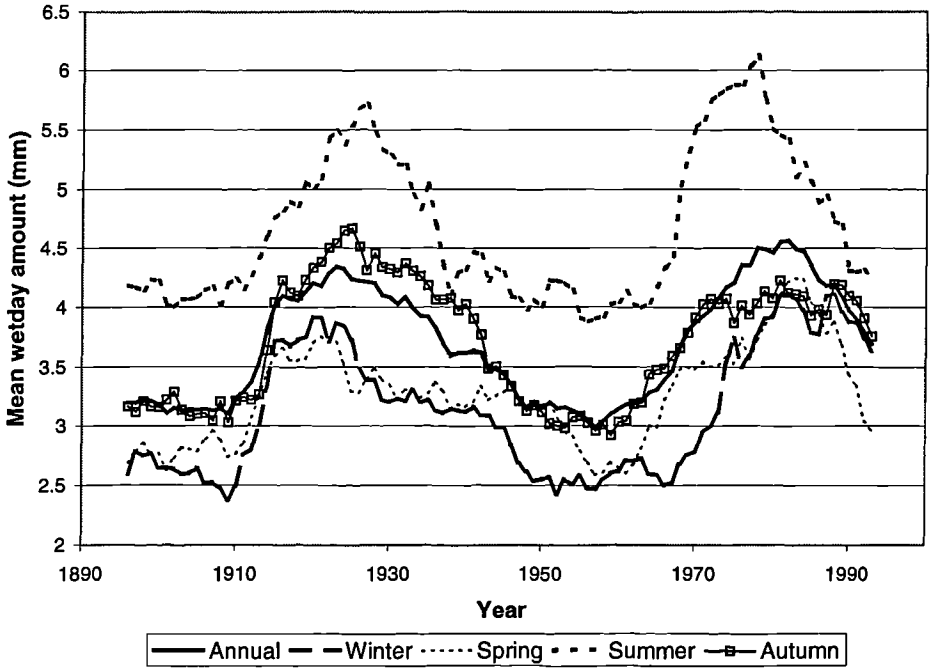

Figure 3-4: Mean wet day amount at Kirk Bramwith (11-yr centred moving average)

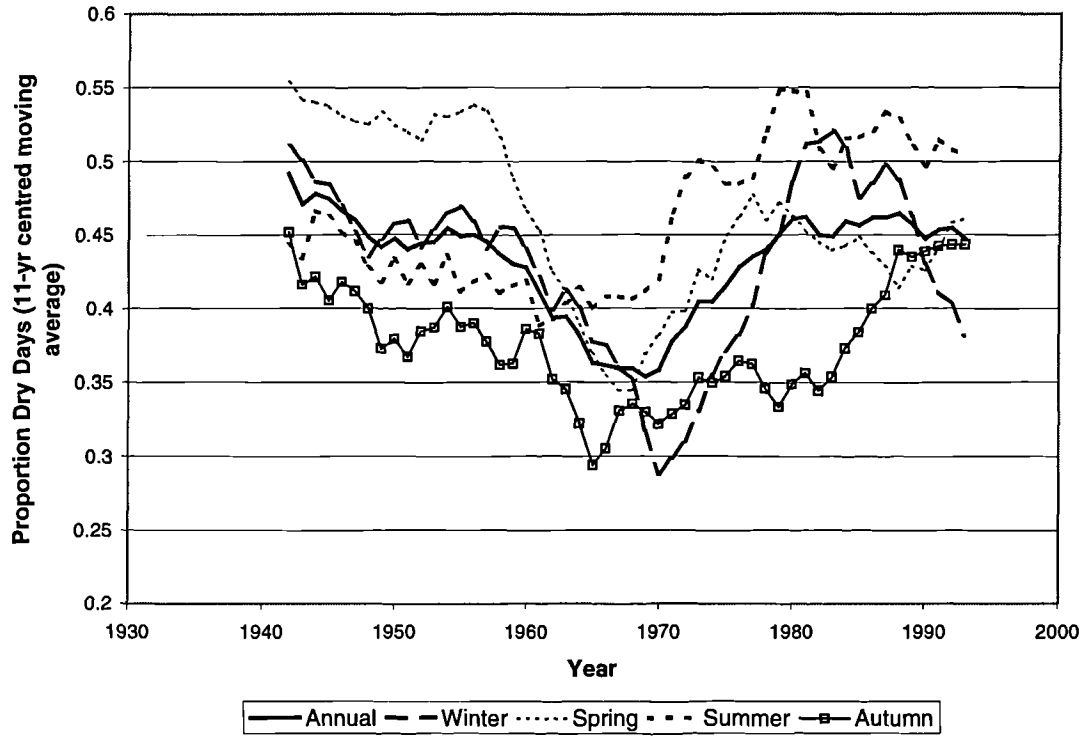

Figure 3-5: Mean proportion dry days at Moorland Cottage (11-yr centred moving average).

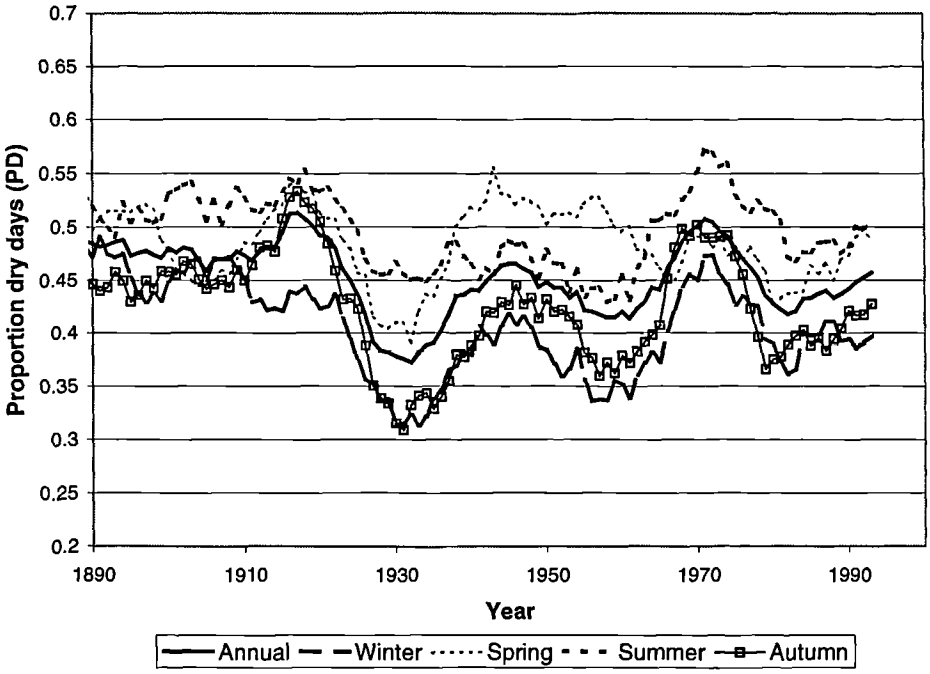

Figure 3-6: Mean proportion dry days at Lockwood Reservoir (11-yr centred moving average).

3.2.2 Analysis of space-time variability of 20-year means of observed precipitation within Yorkshire, expressed as percent anomalies from the 1937-1996 average at each site.

An examination was made of winter (DJF) and summer (JJA) precipitation totals and the average 24-hr PD (idea from New, 1999). For each of the seven sites, 20-year centred observed means for precipitation and PD in both summer and winter were computed. These means were expressed as percent anomalies from the 1937-1996 average at each site. The time-period from 1937-1996 constitutes a period common to all sites that is long enough to mask climatic anomalies.

In winter, all sites except Lockwood Reservoir show a positive precipitation anomaly at present, most between +10 and +20 percent of the 60-yr average (see Figure 3-7). However, large fluctuations are apparent in the series, especially in the longer records. Until approximately 1915, the precipitation anomaly was negative at both Kirk Bramwith and Lockwood Reservoir. After this time, however, the precipitation anomaly at Kirk Bramwith declines until the 1950s and then increases to present, showing large variations from –15 to +15 percent. At Lockwood Reservoir, there is simply a decline from 1930 to the present, suggesting that the North York Moors are becoming drier in the winter than they have been historically.

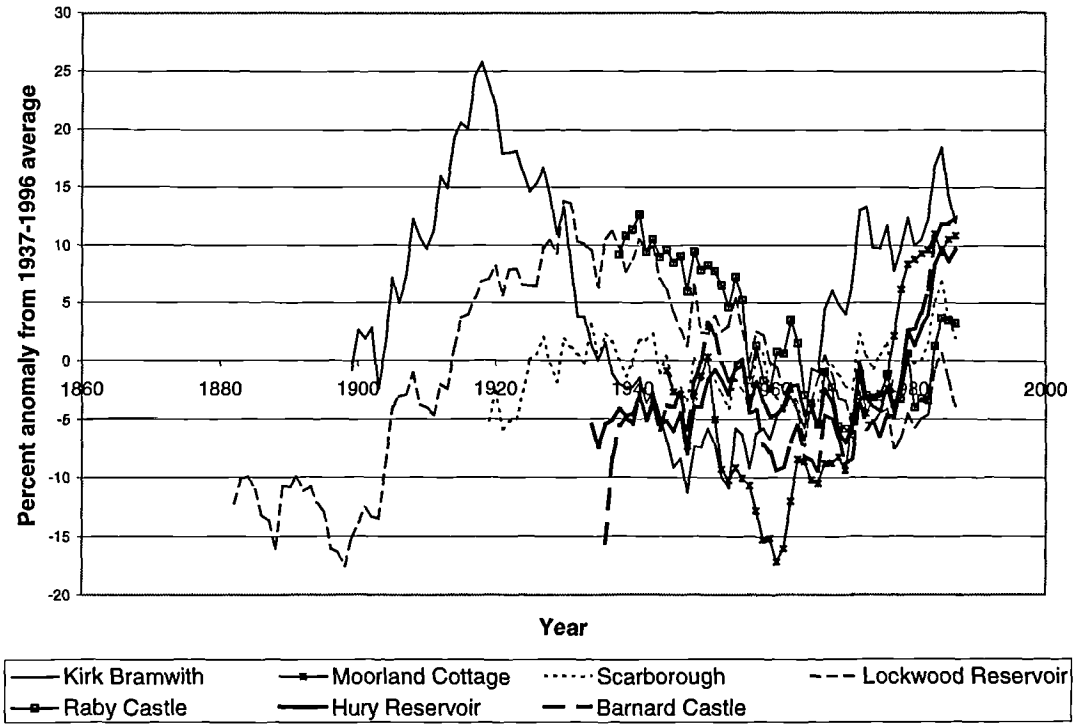

Figure 3-7: Winter anomalies in precipitation, expressed as percent from the 1937-1996 average.

Other sites record differing trends. Hury Reservoir, for example, documents a steady deficit of –5 percent until 1980 when the precipitation anomaly suddenly becomes highly positive (currently at +10 percent). Most other sites also show a recent positive anomaly starting in the 1980s.

In winter, there is also an increasing PD when compared to the 60-yr average from 1937-1996. Lockwood Reservoir records almost exactly opposite trends to Kirk Bramwith (Figure 3-8). Lockwood Reservoir shows a high positive anomaly from 1880 to 1910 of +20 percent, a rapid decline until 1930 to –10 percent, a steady increase until 1980 and then a decline so that presently the precipitation anomaly is just negative. The coastal site of Scarborough simply shows a steady increase with few fluctuations. The Pennine site at Moorland Cottage records a decline from 1940-1970 from +10 to –20 percent and then a rapid increase to the 1980s, with a recent slight decrease. The more northerly Pennine sites show slightly different trends with more positive precipitation anomalies.

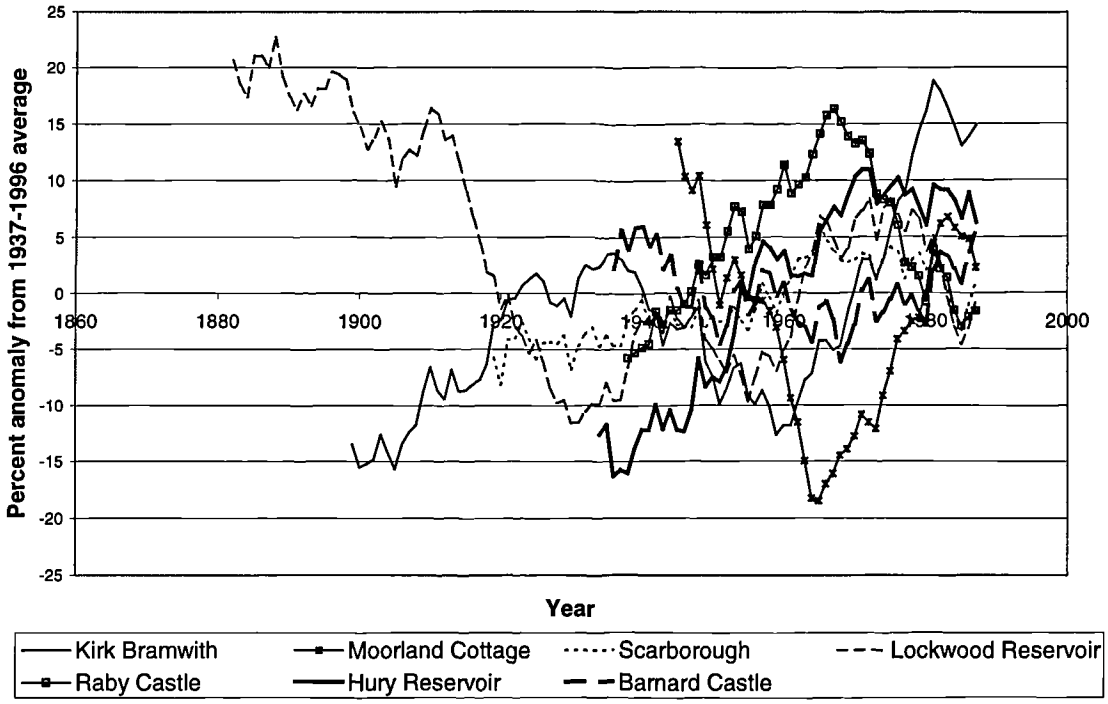

Figure 3-8: Winter anomalies in PD, expressed as percent from the 1937-1996 average.

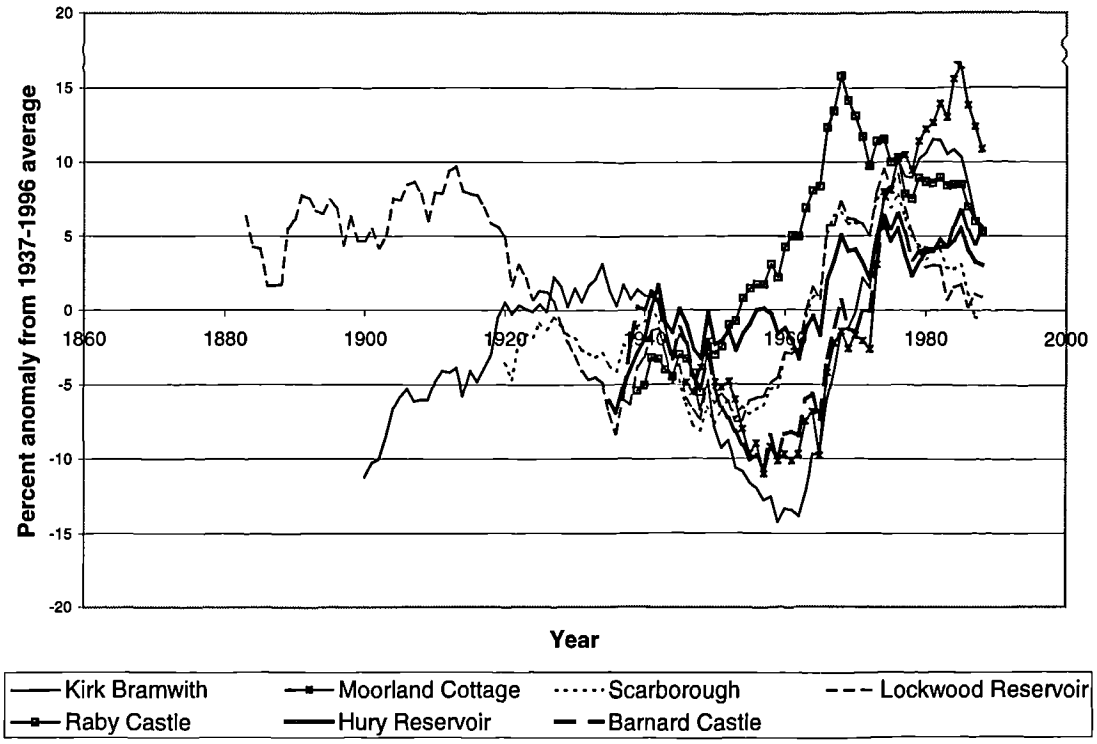

Figure 3-9: Summer anomalies in PD, expressed as percent from the 1937-1996 average.

In summer, trends in both precipitation and PD are more transparent. Most series show a recent increase in PD that is unprecedented historically (Figure 3-9). This is particularly apparent for the western sites such as Moorland Cottage and Raby Castle. The eastern sites document an opposite trend of recently declining PD. The increase in summer PD is even more striking if a dry bound of 1 mm is used.

However, trends in summer precipitation are the strongest of the four analyses. Figure 3-10 shows declining totals at all sites, although there has been a recent slight increase due to the wet summers of 1997 and 1998. The severity of the negative anomaly is, in most cases, unprecedented historically and ranges from –5 to –20 percent. All sites record a decline since the 1960s, imposed upon cyclic periodicities.

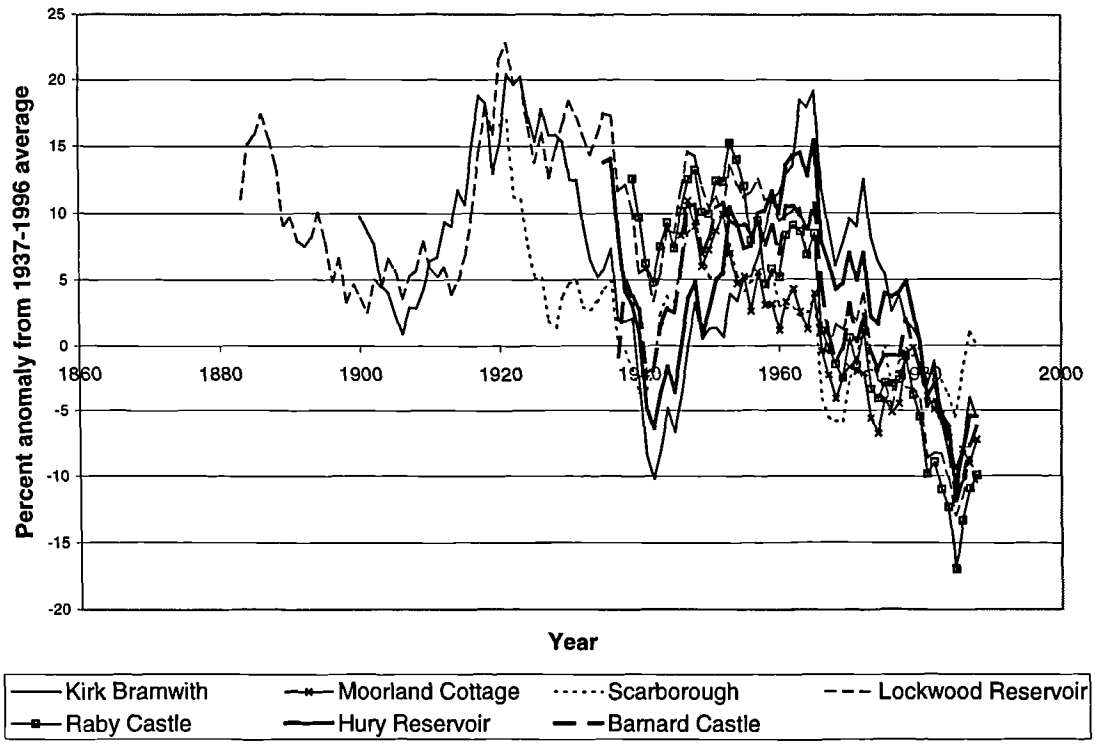

Figure 3-10: Summer anomalies in precipitation, expressed as percent from the 1937-1996 average.

Regression equations produced for two western sites, Moorland Cottage (Equation 3-1) and Raby Castle (Equation 3-2), show a particularly strong linear trend in summer precipitation and PD anomalies:

For site 47060:

$$Rain = -0.42y + 826 \qquad R^2 = 0.87$$
$$PD = 0.62y - 1213 \qquad R^2 = 0.72 \qquad (3\text{-}1)$$

For site 29156:

$$Rain = -0.52y + 1014 \qquad R^2 = 0.79$$
$$PD = 0.34y - 671 \qquad R^2 = 0.72 \qquad (3\text{-}2)$$

A comparison was made with other reliable historical records from Oxford, Durham and Moorhouse. Durham should show similar trends to the eastern sites of Scarborough or Lockwood Reservoir as it is located in north-east England and will be affected by the same northerly and easterly weather types, and less affected by westerly types. Moorhouse is located near to the northern Pennine sites at Hury Reservoir and Barnard Castle. Oxford may show very different changes as it is located far to the south of Yorkshire, and as such may be affected by very different weather systems.

Figure 3-11 shows that there has been a large increase in winter precipitation since the start of the Oxford record in 1780 when compared to the 1937-1996 average. The precipitation anomaly increases from a –25 percent deficit in 1780, fluctuating between –20 and 0 percent from 1780 to 1900. After 1900, there is a marked change to a positive anomaly of +10 percent, and thereafter the precipitation anomaly fluctuates from –5 to +5 percent. The Durham record documents a similar pattern, increasing from –30 percent in 1880 to reach 0 percent at about 1920, and then fluctuating between –5 and +5 percent until the present. The longer Yorkshire records also mimic this pattern.

For summer precipitation, the correlation between Durham and the longer Yorkshire series is good and suggests that results for Yorkshire are valid (see Figure 3-12). Both the Durham and Oxford series appear to show climatic cycles imposed upon a declining trend. Since 1850, the trend for Oxford has been downwards, except for a brief reversal from 1940 to 1970 when it again became positive, whereas Durham and the majority of Yorkshire sites are still declining. After 1970, however, all sites show a rapid reduction in precipitation. In Oxford's case, this reaches exceptional levels of –13 percent.

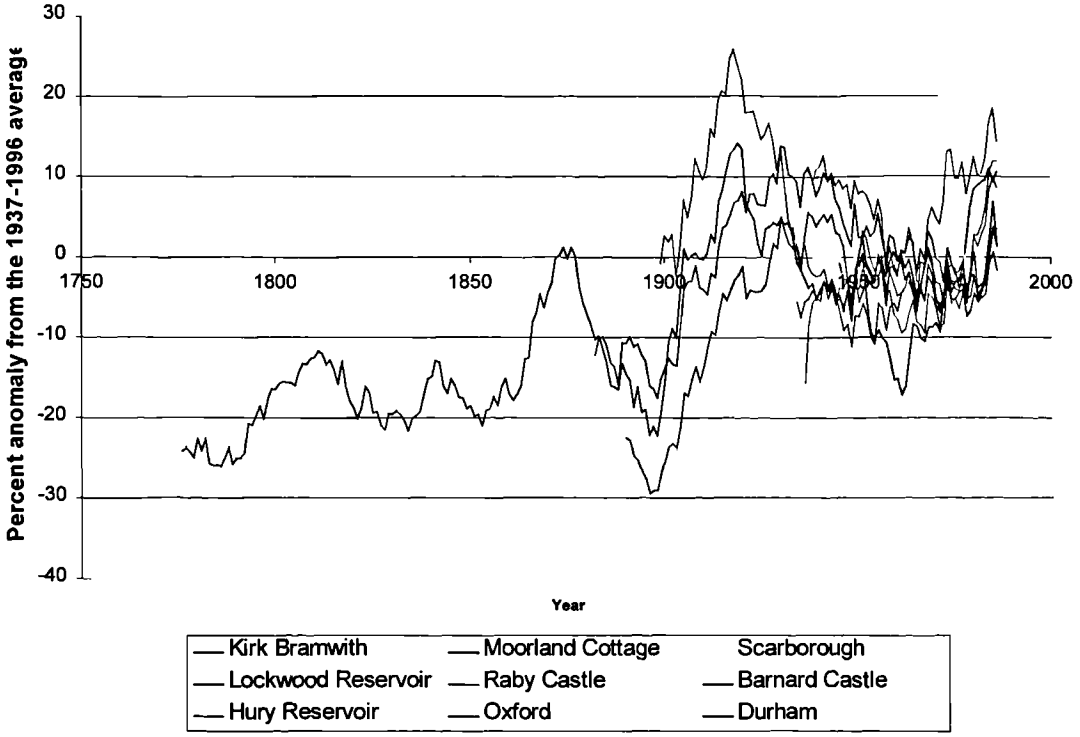

Figure 3-11: Winter anomalies in precipitation, expressed as percent from the 1937-1996 average. Comparison with Durham and Oxford.

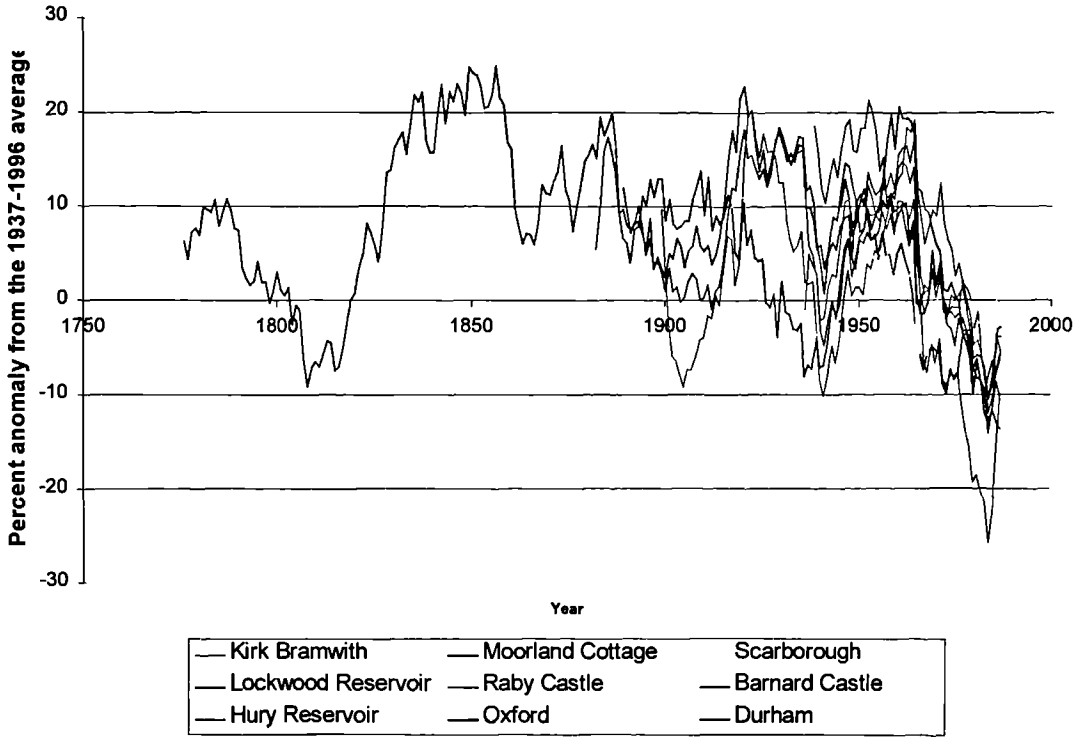

Figure 3-12: Summer anomalies in precipitation, expressed as percent from the 1937-1996 average. Comparison with Durham and Oxford.

Statistical tests were applied to examine differences in mean precipitation between the total time period from 1873-1998, and a latter period from 1960-1998 (which includes the normal climatological baseline period from 1961-1990). Observed summer precipitation totals were used rather than percent anomalies. The mean, median, minimum and maximum summer-precipitation totals for the two periods can be found in Tables 3-2 and 3-3 respectively. Confidence intervals are expressed at the 95 percent level for mean total-summer precipitation.

Site	Mean (mm)	Median (mm)	StDev	Min (mm)	Max (mm)	95.0 % C.I.
87024	171.96	169.15	60.00	51.50	348.50	(160.40, 183.52)
47060	394.70	388.30	123.30	168.40	666.80	(363.10, 426.30)
37225	170.01	173.40	56.05	25.20	283.90	(158.06, 181.96)
34458	227.55	229.90	77.20	44.50	469.40	(213.88, 241.22)
29156	187.41	180.45	63.35	35.90	360.10	(171.83, 202.99)
28408	179.96	173.15	65.96	29.80	339.50	(164.46, 195.46)
28106	201.79	201.15	64.41	40.50	345.00	(186.43, 217.15)

Table 3-2: Precipitation statistics for the period from 1873-1998 for the seven long records. All statistics are for total summer precipitation during the months of June, July and August. Confidence intervals are significant at the 95% level and were derived using Student's t-test.

The mean summer precipitation has reduced during the period from 1960 to 1998 when compared to the complete record; the lower 95 percent confidence interval decreasing at all sites. The median has also declined. With stability, the complete record would be expected to contain larger maximums and lower minimums. However, the period from 1960 to 1998 contains all the minimum values for summer precipitation totals for the entire period from 1873-1998. This suggests that the last 40 years have been drier than the long-term average.

Site	Mean (mm)	Median (mm)	StDev	Min (mm)	Max (mm)	95.0 % C.I.
87024	166.11	165.00	58.33	51.50	306.80	(147.20, 185.02)
47060	376.40	381.30	113.60	168.40	649.80	(339.10, 413.70)
37225	160.99	149.80	54.98	25.20	268.80	(143.17, 178.82)
34458	206.30	205.10	73.00	44.50	356.30	(182.70, 230.00)
29156	173.27	174.55	55.17	35.90	275.80	(154.60, 191.95)
28408	170.27	172.10	55.77	29.80	266.40	(151.94, 188.61)
28106	194.09	191.70	61.24	40.50	341.80	(174.24, 213.95)

Table 3-3: Precipitation statistics for the period from 1960-1998 for the seven long records. All statistics are for total summer precipitation during the months of June, July and August. Confidence intervals are significant at the 95% level and were derived using Student's t-test.

A confidence interval at the 95 percent level produced for the difference between mean summer precipitation totals during the period from 1873-1998 and the period from 1960-1998 shows a significant relationship. The difference shows a mean of 12.28 mm and the confidence interval is significantly positive at (6.94, 17.62). This suggests that there has been a decline in precipitation during the period from 1960-1998 when compared to the complete record.

Site	Mean (mm)	Median (mm)	StDev	Min (mm)	Max (mm)	95.0 % C.I.
87024	175.37	170.70	61.12	55.70	348.50	(160.45, 190.28)
47060	424.90	462.60	135.20	196.50	666.80	(366.40, 483.30)
37225	177.34	185.75	56.42	62.90	283.90	(160.95, 193.72)
34458	237.17	243.55	77.53	86.50	469.40	(220.55, 253.80)
29156	204.40	197.10	69.10	88.10	360.10	(178.60, 230.20)
28408	190.80	176.70	75.10	72.40	339.50	(164.60, 217.00)
28106	211.50	207.50	68.00	110.4	345.00	(186.50, 236.40)

Table 3-4: Precipitation statistics for the period from 1873-1959 for the 7 long records. All statistics are for total summer precipitation during the months of June, July and August. Confidence intervals are significant at the 95% level and were derived using Student's t-test.

An additional analysis of the change in summer precipitation totals and PD during the latter time-period of 1960-1998 when compared to the prior 1873-1959 period was made. Site statistics for the period from 1873 to 1959 can be found in Table 3-4.

A statistical measure for comparing the difference in means between two populations is described by Metcalfe (1994). It is assumed that the samples are independent and follow an approximately normal distribution, i.e. $\overline{X}_A \sim N(\mu_A, {\sigma_A}^2/n_A)$ and $\overline{X}_B \sim N(\mu_B, {\sigma_B}^2/n_B)$, where $\overline{X}_A$ and $\overline{X}_B$ represent the distribution of summer precipitation totals from 1960-1998 and 1873-1959 respectively. Since the samples are independent then the distribution for the difference between the two populations approximates to (3-3):

$$\overline{X}_A - \overline{X}_B \sim N\left(\mu_A - \mu_B, {\sigma_A}^2/n_A + {\sigma_B}^2/n_B\right) \tag{3-3}$$

The confidence interval for this difference is therefore (3-4):

$$\overline{X}_A - \overline{X}_B \pm z_{\alpha/2}\left({\sigma_A}^2/n_A + {\sigma_B}^2/n_B\right)^{1/2} \tag{3-4}$$

The variables for this analysis can be found in Table 3-5.

Site	μ_A	μ_B	σ_A	σ_B	n_A	n_B
87024	166.11	175.37	58.33	61.12	39	67
47060	376.40	424.90	113.60	135.20	38	23
37225	160.99	177.34	54.98	56.42	39	48
34458	206.30	237.17	73.00	77.53	39	86
29156	173.27	204.40	55.17	69.10	36	30
28408	170.27	190.80	55.77	75.10	38	34
28106	194.09	211.50	61.24	68.00	39	31

Table 3-5: Variables used in analysis of the difference between summer precipitation during the periods from 1873-1959 and 1960-1998.

Site	95% C. I.
87024	(-32.7, 14.2)
47060	(-114.5, 17.5)
37225	(-39.9, 7.2)
34458	(-59.5, -2.2)
29156	(-61.7, -0.5)
28408	(-51.3, 10.3)
28106	(-48.1, 13.3)

Table 3-6: Confidence Intervals at the 95 percent level for the difference between the two populations of 1873-1959 and 1960-1998 for summer (JJA) precipitation totals.

Confidence intervals at the 95 percent level were produced for the difference between summer precipitation totals during the two time-periods of 1873-1959 and 1960-1998 (Table 3-6). There is some evidence that there has been a decrease in summer precipitation at Lockwood Reservoir and Raby Castle during the period from 1960 to 1998, compared to the period prior to this. These are significant at the 95 percent level. It is also noticeable that, although the other sites do not show significant relationships, there is skewness towards negative values at all sites.

Site	μ_A	μ_B	σ_A	σ_B	n_A	n_B	95% C. I.
87024	0.61	0.58	0.129	0.106	39	67	(-0.009, 0.089)
47060	0.47	0.44	0.127	0.114	38	23	(-0.026, 0.100)
37225	0.60	0.56	0.105	0.093	39	48	(-0.009, 0.077)
34458	0.51	0.50	0.103	0.101	39	86	(-0.030, 0.050)
29156	0.60	0.52	0.103	0.105	36	30	(0.028, 0.130)
28408	0.56	0.52	0.092	0.116	38	34	(-0.010, 0.090)
28106	0.51	0.47	0.101	0.122	39	31	(-0.023, 0.085)

Table 3-7: Variables used in analysis of the difference between summer proportion dry days during the periods from 1873-1959 and 1960-1998 and results from the 95 percent confidence interval analysis.

The same analysis was repeated for PD, comparing the time-periods of 1873-1959 and 1960-1998. The variables used and confidence intervals produced can be found in Table 3-7. There is some evidence that PD has increased during the time-period from 1960-1998 when compared to 1873-1959. There is a significant relationship at Raby Castle only, although there is a positive skew at all sites. Unfortunately the relationships for winter precipitation and PD are not as strong and do not show significant trends.

3.2.3 Comparison of monthly precipitation statistics of PD and mean daily precipitation

Precipitation statistics for the post-1975 period were compared to those of the pre-1975 period for three sites, each of which is representative of a precipitation zone within Yorkshire (see Chapter 5). Moorland Cottage is representative of the Pennine sub-region, Lockwood Reservoir for the North York Moors (northeastern sub-region) and Kirk Bramwith for the southeastern lowlands.

Kiely (1999) noted that in Ireland a significant increase in precipitation has occurred on the western coast since about 1975 which is seen as increases in March and October precipitation. On the eastern coast there was almost no increase in annual precipitation but the same seasonal increases in March and October, with other months showing a slight decrease.

Figure 3-13 shows the mean daily-precipitation amounts for the pre- and post-1975 periods, in addition to the total period of record, for the sites of Moorland Cottage, Lockwood Reservoir and Kirk Bramwith. At Moorland Cottage, a similar pattern to that of Ireland emerges. Since 1975, an overall pattern of increasing winter precipitation and decreasing summer precipitation is apparent. There is a prominent increase in March precipitation that is also noted by Kiely (1999), but no similar increase in October totals. As a site predominantly affected by westerly weather patterns, Moorland Cottage would be expected to show the same, but weaker, precipitation trends as Ireland. However, no increase is apparent in October.

Both the eastern sites of Lockwood Reservoir and Kirk Bramwith show similar trends in the post-1975 period. Prior to 1975, the eastern sites exhibited two precipitation peaks, in August and November, and a low in March. The period since 1975 has seen a smoothing of these oscillations at Lockwood Reservoir. At both sites, the July/August peak has disappeared and, instead, a prominent precipitation trough occurs in July. Significantly, March precipitation totals also increase to the east of the region, whereas February totals show a decline.

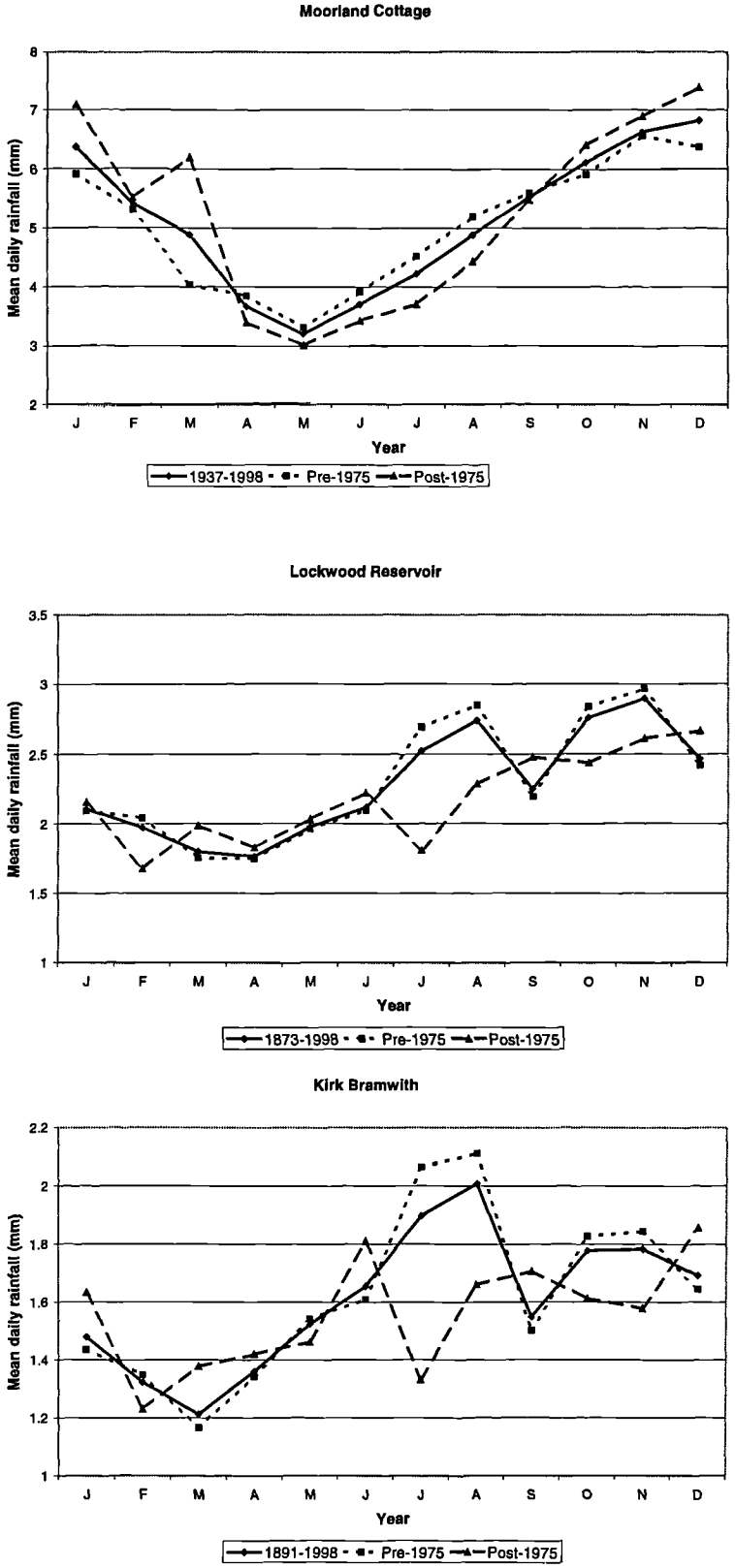

Figure 3-13: Mean daily precipitation (mm) for the pre- and post-1975 periods at Moorland Cottage, Lockwood Reservoir and Kirk Bramwith.

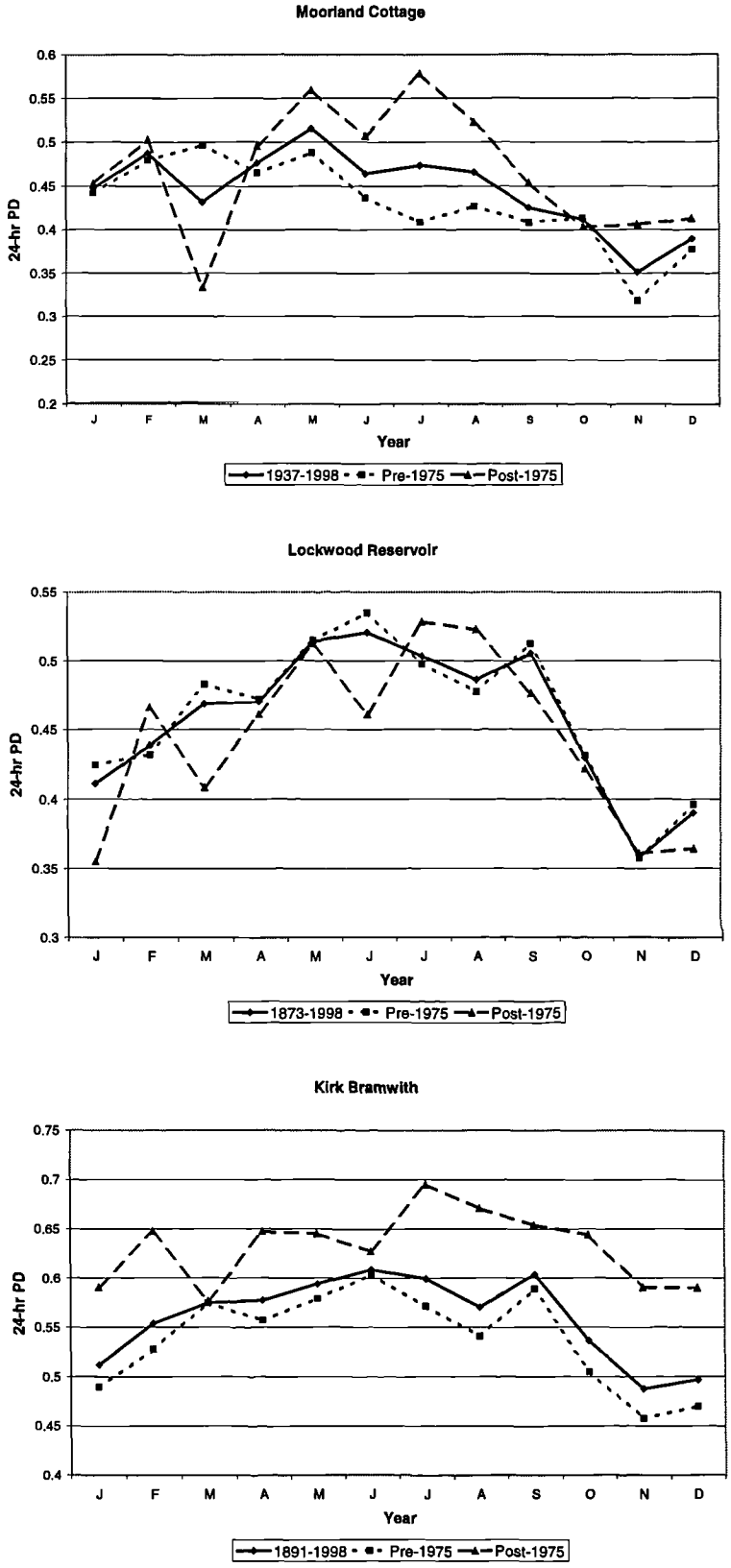

Figure 3-14: The 24-hr PD statistic for the pre- and post-1975 periods at Moorland Cottage, Lockwood Reservoir and Kirk Bramwith.

Change in the 24-hr PD statistic between the two time-periods is shown in Figure 3-14. At Moorland Cottage, a sharp decrease in the PD statistic in March accounts for the increased precipitation totals during this month. The increases in March precipitation being obtained from an increase in wet days rather than an increase in mean wetday amount. The PD statistic is significantly raised in the summer however, without a significant concurrent increase in precipitation totals. This may suggest an increase in mean wetday amount during the summer and be related to a rise in convective activity. Lockwood Reservoir shows an expected pattern of change in the PD statistic, given the previously discussed changes in monthly precipitation totals. There are increases in PD in the months of August and February, and decreases in March and June. At Kirk Bramwith, there is a significant increase in the PD statistic throughout the year, excepting the month of March. The reasons behind this are however, unclear.

3.2.4 Wet and dry spell lengths, and transition probabilities

There has been a recent increase in frequency of long dry spells during summer months. At Moorland Cottage prior to 1970, the longest dry spell length was 13 days. This statistic now surpasses 20 days. This is counterbalanced by a decreased frequency of short dry periods and is a noticeable trend at other northern Pennine sites. In spring, there has been an increase in very short-duration dry spells but a decrease in those lasting for longer than about 10 days. In the North York Moors (Lockwood Reservoir) there has been a shift towards longer duration winter wet spells in recent years. Since 1980, there has been a lower proportion of wet spells from 4-9 days in length, but an increase in 10-14 day events. Summer and spring dry spell lengths show no obvious pattern.

At western sites, and also prominent in the North York Moors, a decrease in the wet-wet transition probability and a concurrent increase in the dry-dry transition probability is observed in all seasons during the 1990s (Figures 3-15 and 3-16). The reverse is observed at Kirk Bramwith, and there is little or no change at the coastal site of Scarborough. The dry-dry and wet-wet transition probabilities can be shown to follow the PD time-series quite closely. However, results show that both wet-wet and dry-dry transition probabilities are highly variable interannually and seasonally.

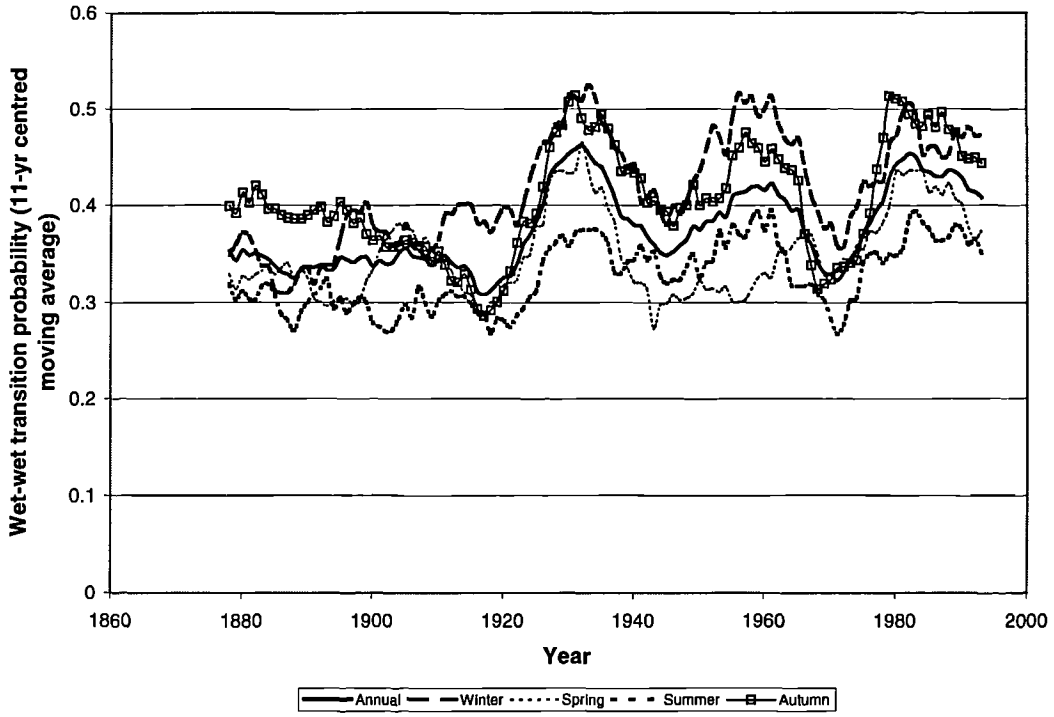

Figure 3-15: Wet-wet transition probability changes at Lockwood Reservoir from 1880-1998 (11-year centred moving average).

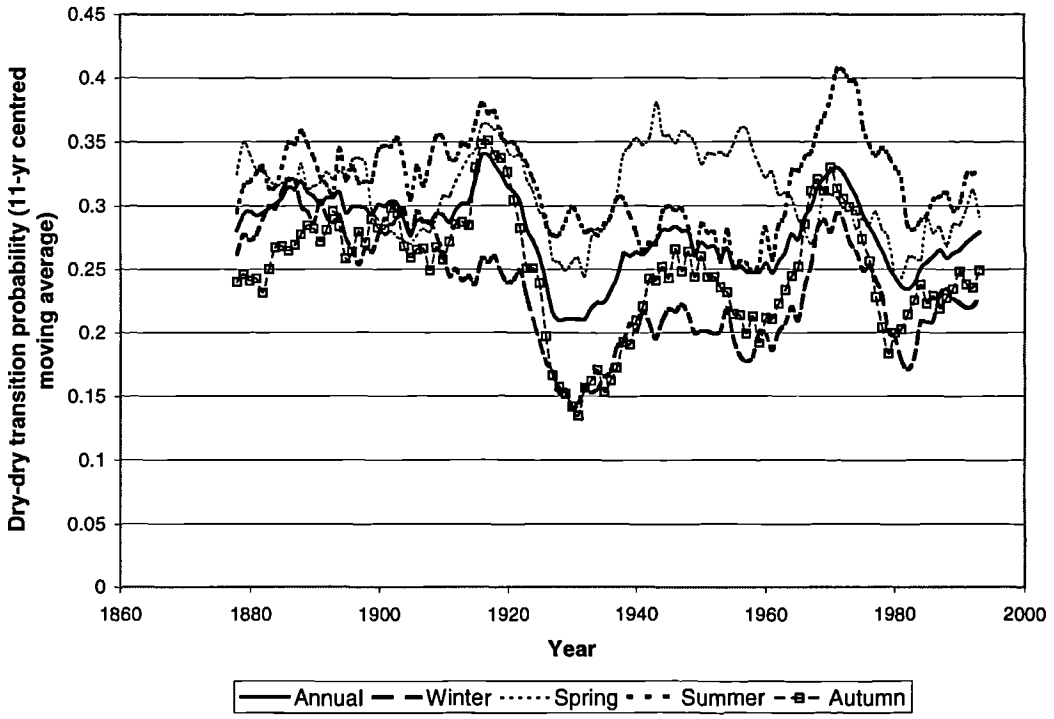

Figure 3-16: Dry-dry transition probability changes at Lockwood Reservoir from 1880-1998 (11-year centred moving average).

3.2.5 Interannual and interseasonal variability

To examine interannual and interseasonal variability at the seven sites, seasonal and annual precipitation totals and PD averages were calculated. These were then ranked to determine the driest and wettest years on record (after Burt *et al.*, 1998).

The regional average places the summer of 1899 as the driest on record, with 1913 placed second, thirdly the summer of 1989, and fourthly that of 1995. Six of seven years in the 1990s (1990-96) are found in the driest 23 summers, excepting 1993 which ranks 75th from 123 years. Summer months also show an increased proportion of dry days, with six out of seven years from 1990 to 1996 ranking in the top half of the table, excepting 1993. Annually though, the 1990s are not especially dry, mainly due to the high winter precipitation totals. Every winter from 1990 to 1996 is wetter than average. The winter of 1994-95 ranks as the wettest winter on record, with the winter of 1993-94 coming fifth. Interestingly, some years during the 1990s show a higher proportion of winter dry days than would be expected, given the high precipitation totals. The winters of 1991-92 and 1992-93 both have a high proportion of dry days but also high precipitation totals. This suggests that precipitation events were more infrequent but possibly more intense and that convective activity may be becoming more frequent in winter (see Osborn *et al.*, 2000).

Examination was also made of the winter/summer ratio of precipitation and produced results that accord with those of other researchers (e.g. Mayes, 1996). The DJF/JJA ratio was the highest of the 123-yr record in 1995, and at 4.04, almost double the second-placed 1994. The years of 1991, 1990, 1996 and 1992 are also ranked in the top 13. These results mirror those of Burt *et al.* (1998) for the sites of Moorhouse and Durham (northeast England). However, since 1996 the DJF/JJA ratio has dropped considerably as the summers of 1997 and 1998 were very wet, combined with a dry winter in 1996-97. Historical drought years are also highlighted by the DJF/JJA ratio. Historical hydrological droughts appear to be linked to hot and dry summers rather than dry winters, the conclusion reached by Burt (1999) for the southern Pennines. However, most of the sites are located in the east of Yorkshire and as such may not reflect drought characteristics of the Pennines where most of the Yorkshire water supplies are located.

Site specific analyses show important regional differences in the interannual and interseasonal variability of precipitation. In the northern Pennines at Hury Reservoir and Barnard Castle, the summers from 1990 to 1996 are ranked in the top 30 driest, whereas the 1980s were, on average, wet. The early 1990s also had very wet winters, seen prominently in the extreme DJF/JJA ratio at these two sites for 1995; in both cases more than four times the nearest year. A recent slight increase in annual precipitation in the northern Pennies is due to the increase in

winter precipitation. An annual increase in PD, combined with the annual increase in precipitation, suggests a possible increase in precipitation intensity. This may be backed up by the noticeable increase in flooding in the 1990s and continuing into the 21st century.

To the east of the region, the summer of 1976 supersedes that of 1995 as the driest summer on record. However, although Lockwood Reservoir in the North York Moors documents an increase in annual precipitation in the 1990s, the coastal site of Scarborough records a decrease. At both sites, the years of 1997 and 1998 are wet years on average but have a high proportion of dry days.

3.2.6 Extreme Events

Kiely (1999) noted that in Ireland the frequency of extreme value occurrence has increased since 1975. In a similar analysis, but using only 24-hr precipitation totals, the top 20 and top 100 extreme values in the observed record for the three sites of Moorland Cottage, Lockwood Reservoir and Kirk Bramwith were ranked according to severity. Table 3-8 shows the distribution of extreme events for the pre-1975 and post-1975 period.

	Top 20-ranked events		Top 100-ranked events	
	pre-1975	post-1975	pre-1975	post-1975
Moorland Cottage	13	7	58	42
Lockwood Reservoir	17	3	82	18
Kirk Bramwith	19	1	79	21

Table 3-8: Distribution of extreme events for the pre- and post-1975 period at Moorland Cottage, Lockwood Reservoir and Kirk Bramwith.

At all sites, the distribution of extreme events has undergone only slight change during the recent time-period. At Moorland Cottage, there is a similar relationship pre- and post-1975. However, at eastern sites there has been a reduction in extreme events since 1975 when compared to the historical past.

3.3 Linking precipitation measurements to large-scale atmospheric circulation

3.3.1 Links to the North Atlantic Oscillation (NAO) index

In a similar investigation to Wilby *et al.* (1997), mean daily precipitation and PD statistics were correlated with winter-NAO for the seven sites shown in Table 3-1. The increased NAO index since the 1960s (Figure 3-17) may be linked to the incidence of higher winter precipitation totals at western sites. However, the opposite trend of declining winter precipitation totals with an increasing NAO is noted at the eastern site of Lockwood reservoir. This evidence supports the conclusions of Wilby *et al.* (1997) of a negative correlation between winter precipitation and the NAO index in northeastern England, but a positive correlation in the west.

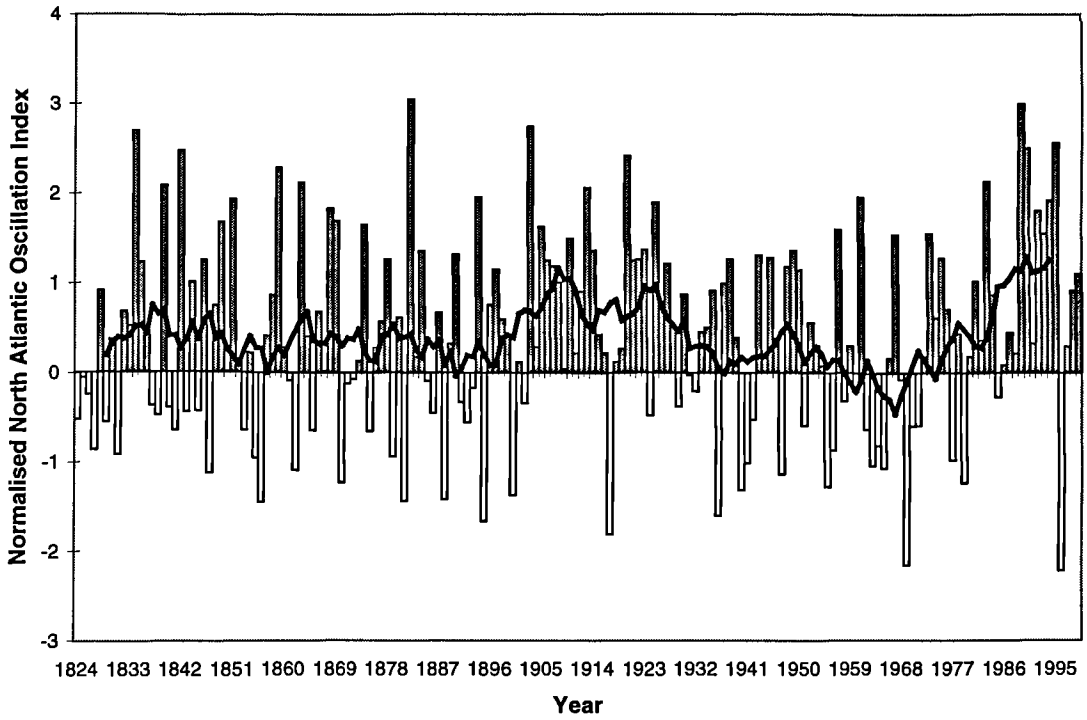

Figure 3-17: The North Atlantic Oscillation (NAO) index for winter (DJFM) after Jones et al. (1997b). Imposed upon the yearly values is an 11-yr centred moving average that shows the recent increase in the index.

Tables 3-9 and 3-10 show significant correlations at the 95 percent confidence level between the winter-NAO, and annual and seasonal mean daily precipitation and PD at the seven long-data sites within Yorkshire. Statistically significant correlations occur most frequently between winter precipitation or PD and the NAO. Significant positive correlations between mean winter daily precipitation and the NAO occur at western sites. This is especially true at Moorland Cottage, where the NAO appears to exert such a strong effect upon precipitation totals in winter

that the annual mean daily precipitation also shows a significantly positive correlation with the NAO. At eastern sites, the reverse is true; significant negative correlations occurring between the NAO and winter mean daily precipitation. This is consistent with the findings of Wilby *et al.* (1997).

Site	N	Ann-P	DJF-P	MAM-P	JJA-P	SON-P
28106	69		0.315			
28408	72					
29156	69					
34458	125		-0.243			
37225	87		-0.232			
47060	62	0.263	0.573			
87024	107					

Table 3-9: Significant seasonal correlations with the NAO (95 percent confidence level). P= Mean daily precipitation (mm), N= Number of years of data used.

Site	N	Ann-PD	DJF-PD	MAM-PD	JJA-PD	SON-PD
28106	69					
28408	72					
29156	69					
34458	125		0.182			
37225	87					
47060	62		-0.346			
87024	107				0.199	

Table 3-10: Significant seasonal correlations with the NAO (95 percent confidence level). PD= Mean proportion dry days, N= Number of years of data used.

Table 3-11 compares the mean annual precipitation arising from a positive and negative winter-NAO. Statistically significant correlations occur most frequently between winter precipitation or PD and the NAO. Winters with high NAO were wetter than average in the west of Yorkshire and drier than average in the east. Positive precipitation anomalies are greatest at the most western and highest altitude site of Moorland Cottage (112 percent of the long-term average and significant at the 95 percent level). The greatest negative precipitation anomalies are found at the easterly sites of Lockwood Reservoir and Scarborough (both 97 percent of the long-term average).

The positive winter precipitation anomaly during high NAO winters in the west of Yorkshire provides an increase in precipitation large enough to be noticeable in annual precipitation totals. At Moorland Cottage, this increase is significant at the 95 percent level. For low NAO winters, conversely, a positive anomaly can be found at eastern sites (107 and 106 percent respectively

for Lockwood Reservoir and Scarborough). Western sites, however, show negative precipitation anomalies. This reaches as low as a staggering 77 percent for Moorland Cottage.

Site	Ann-P		DJF-P		MAM-P		JJA-P		SON-P	
	+NAO	-NAO	+NAO	-NAO	+NAO	-NAO	+NAO	-NAO	+NAO	-NAO
28106	942	907	**289**	**246**	181	206	203	201	278	247
	(102)	(98)	**(107)**	**(91)**	(96)	(109)	(100)	(100)	(104)	(93)
28408	786	775	229	203	153	181	179	183	229	199
	(100)	(99)	(104)	(93)	(94)	(111)	(99)	(101)	(105)	(91)
29156	746	744	198	200	150	176	188	186	217	185
	(100)	(100)	(100)	(101)	(94)	(111)	(100)	(99)	(105)	(90)
34458	831	842	191	211	167	177	221	242	248	222
	(100)	(101)	(97)	(107)	(98)	(104)	(97)	(107)	(103)	(92)
37225	655	650	163	179	131	145	171	168	186	164
	(100)	(99)	(97)	(106)	(97)	(107)	(101)	(99)	(104)	(92)
47060	1959	1722	**636**	**442**	360	370	394	377	567	505
	(104)	(92)	**(112)**	**(77)**	(99)	(102)	(100)	(96)	(102)	(91)
87024	585	598	136	134	125	132	167	182	155	152
	(99)	(102)	(100)	(99)	(99)	(105)	(97)	(106)	(101)	(99)
Oxford	644	661	160	157	139	140	**160**	**185**	184	177
	(99)	(102)	(100)	(99)	(100)	(100)	**(96)**	**(110)**	(101)	(97)
Durham	640	651	147	157	134	147	174	184	184	167
	(100)	(101)	(98)	(105)	(97)	(106)	(98)	(104)	(103)	(94)

Table 3-11: Mean precipitation amounts, both annually and seasonally, associated with positive and negative winter-NAO. Numbers in parentheses indicate the percentage of the long-term average precipitation. Numbers both bold and italicised are from significantly different populations when positive and negative winter-NAO values are compared (95 percent confidence interval).

In autumn, a positive NAO will cause increased precipitation across Yorkshire, and a negative NAO causes a decrease. This is however scaled on both westerliness and altitude; sites in the west and at high altitude recording greater precipitation reductions than those further east and at lower altitude. The opposite effect occurs in spring with high NAO producing negative precipitation anomalies, and a low NAO producing high precipitation anomalies. The positive precipitation anomalies in spring can be as high as 111 percent and are greater in north Yorkshire. In summer, there are no obvious patterns except for an increased mean daily precipitation under a negative NAO at Durham and some of the eastern Yorkshire sites. The records from these sites stretch back into the last century, showing a trend to drier summers in

recent years under a highly positive NAO. This concurs with the claim of Mayes (1996) of an increased gradient between summer and winter precipitation since the 1960s, which was also shown by the inter-annual variability of precipitation in Yorkshire.

Site	Ann-PD		DJF-PD		MAM-PD		JJA-PD		SON-PD	
	+NAO	-NAO	+NAO	-NAO	+NAO	-NAO	+NAO	-NAO	+NAO	-NAO
28106	0.4 (101)	0.4 (97)	0.3 (97)	0.4 (103)	***0.5*** ***(104)***	***0.4*** ***(91)***	0.5 (101)	0.5 (98)	0.4 (99)	0.4 (102)
28408	0.5 (100)	0.5 (100)	0.4 (98)	0.4 (104)	***0.5*** ***(103)***	***0.5*** ***(94)***	0.5 (101)	0.5 (99)	0.4 (97)	0.5 (105)
29156	0.5 (101)	0.5 (99)	0.4 (98)	0.5 (104)	***0.6*** ***(104)***	***0.5*** ***(93)***	0.6 (101)	0.6 (99)	0.5 (98)	0.5 (104)
34458	0.5 (101)	0.4 (98)	0.4 (101)	0.4 (97)	0.5 (101)	0.5 (97)	0.5 (102)	0.5 (96)	0.4 (99)	0.4 (102)
37225	0.5 (100)	0.5 (99)	0.4 (101)	0.4 (97)	0.6 (102)	0.5 (96)	0.6 (101)	0.6 (98)	0.5 (98)	0.5 (105)
47060	0.4 (100)	0.4 (100)	***0.4*** ***(94)***	***0.5*** ***(113)***	0.5 (102)	0.4 (95)	0.5 (98)	0.5 (98)	0.4 (98)	0.4 (99)
87024	0.6 (101)	0.5 (98)	0.5 (99)	0.5 (100)	0.6 (101)	0.6 (98)	0.6 (102)	0.6 (96)	0.5 (101)	0.5 (100)

Table 3-12: Mean proportion dry days, both annually and seasonally, associated with positive and negative winter-NAO. Numbers in parentheses indicate the percentage of the long-term average precipitation. Numbers both bold and italicised are from significantly different populations when positive and negative winter-NAO values are compared (95 percent confidence interval).

Table 3-12 compares the mean proportion dry days occurring due to positive and negative winter-NAO. The most prominent PD anomaly is in winter at Moorland Cottage. A negative PD anomaly (113 percent of the long-term average and significant at the 95 percent level) is caused by a negative NAO, and vice versa. This decreased PD is also recorded at other westerly sites, whereas easterly sites record a positive PD anomaly during a negative winter-NAO. This suggests that there is an increase in winter wet days in the west during a positive phase of the NAO, as would be expected. However, there was no concurrent decrease in annual PD at Moorland Cottage, although there was an increase in annual mean daily precipitation. This may imply increased intensity of precipitation at western sites, particularly in winter, under a high NAO scenario.

A comparison of spring and autumn PD anomalies reveals a similar relationship to that of mean daily precipitation. A positive NAO causes an increased PD in spring, when compared to the long-term average, but a decreased PD in autumn months. The opposite relationship is recorded in a negative NAO. This relationship is especially prominent in northern Yorkshire during spring months where at all three sites of Hury Reservoir, Barnard Castle and Raby Castle a significant relationship at the 95 percent level is recorded.

The NAO and precipitation were also linked on a monthly time-scale, in a similar way to Kiely (1999). Significant correlations can be found in Table 3-13. It is notable that a high correlation is obtained between the monthly NAO and precipitation for winter months at Moorland Cottage, but a very low correlation in summer. Although, perhaps significantly, the March and October correlation statistics are low compared to other winter months. At the eastern sites of Lockwood Reservoir and Kirk Bramwith, high correlations are obtained only in July (positive) and October (negative). The declining NAO in July has contributed to reduced July precipitation totals at both sites.

	Moorland Cottage	Lockwood Reservoir	Kirk Bramwith
J	**0.719**	-0.140	0.072
F	**0.693**	**-0.292**	-0.060
M	**0.345**	**0.220**	**0.393**
A	**0.585**	**-0.492**	**-0.252**
M	0.256	**-0.206**	**0.230**
J	0.108	-0.122	**-0.506**
J	0.219	**0.672**	**0.561**
A	0.130	0.059	0.093
S	**0.523**	-0.177	**-0.319**
O	**0.467**	**-0.608**	**-0.525**
N	**0.525**	-0.196	-0.156
D	**0.707**	-0.044	**0.440**

*Table 3-13: Correlation coefficients between monthly precipitation and monthly-NAO at the three sites (**bold** indicates a significant correlation at the 95 percent level).*

It can be observed in Figures 3-18 to 3-21 that the NAO monthly index has increased dramatically in recent years during the months of January, February and March. This has led to increased precipitation during these months at western sites, such as Moorland Cottage. However, during autumn months, particularly September and October, there has been a decline in the monthly index since the mid-1980s. This has led to a declining receipt of precipitation in autumn at western sites.

The NAO controls the frequency of occurrence of different weather types across the UK. Therefore, a further step was made to link the monthly occurrence of the three weather states delineated in Section 5.3 to the monthly NAO index (Table 3-14). A positive relationship is found between the monthly NAO and the occurrence of the westerly weather-state in all months. The correlation is particularly strong in the month of March, at 0.932, and may account for the increased precipitation totals during March in Ireland discussed by Kiely (1999) and also found in Yorkshire (see Section 3.2.3). The anticyclonic and northerly weather states show a negative correlation for the majority of months. Again, a particularly high negative correlation is found during the month of March.

NAO	Weather State		
	A	N	W
J	**-0.204**	**-0.823**	**0.581**
F	**-0.337**	**-0.618**	**0.639**
M	**-0.847**	**-0.746**	**0.932**
A	0.021	**-0.762**	**0.708**
M	**-0.414**	**-0.649**	**0.705**
J	0.123	**-0.711**	**0.784**
J	**-0.710**	0.000	**0.632**
A	-0.330	**-0.378**	**0.403**
S	**-0.408**	**-0.308**	**0.497**
O	**-0.297**	**-0.633**	**0.584**
N	**-0.273**	**-0.540**	**0.556**
D	**0.197**	**-0.533**	**0.276**

*Table 3-14: Correlation coefficients between monthly-NAO and the occurrence of the three weather states: W = westerly, A = Anticyclonic, and N = Northerly (**bold** indicates a significant correlation at the 95 percent level) on interannual basis.*

This investigation shows that the relationship between seasonal indices of the NAO and the occurrence of different weather states is also strong at the monthly level. Kiely (1999) concluded that the increased precipitation totals in March and October seen in Ireland since 1975 were linked to increasing NAO (shown in Figures 3-18 and 3-21) and hence westerly weather types during these months. However, an investigation into the frequency of the three weather states in March and October (Figure 3-22) has shown otherwise.

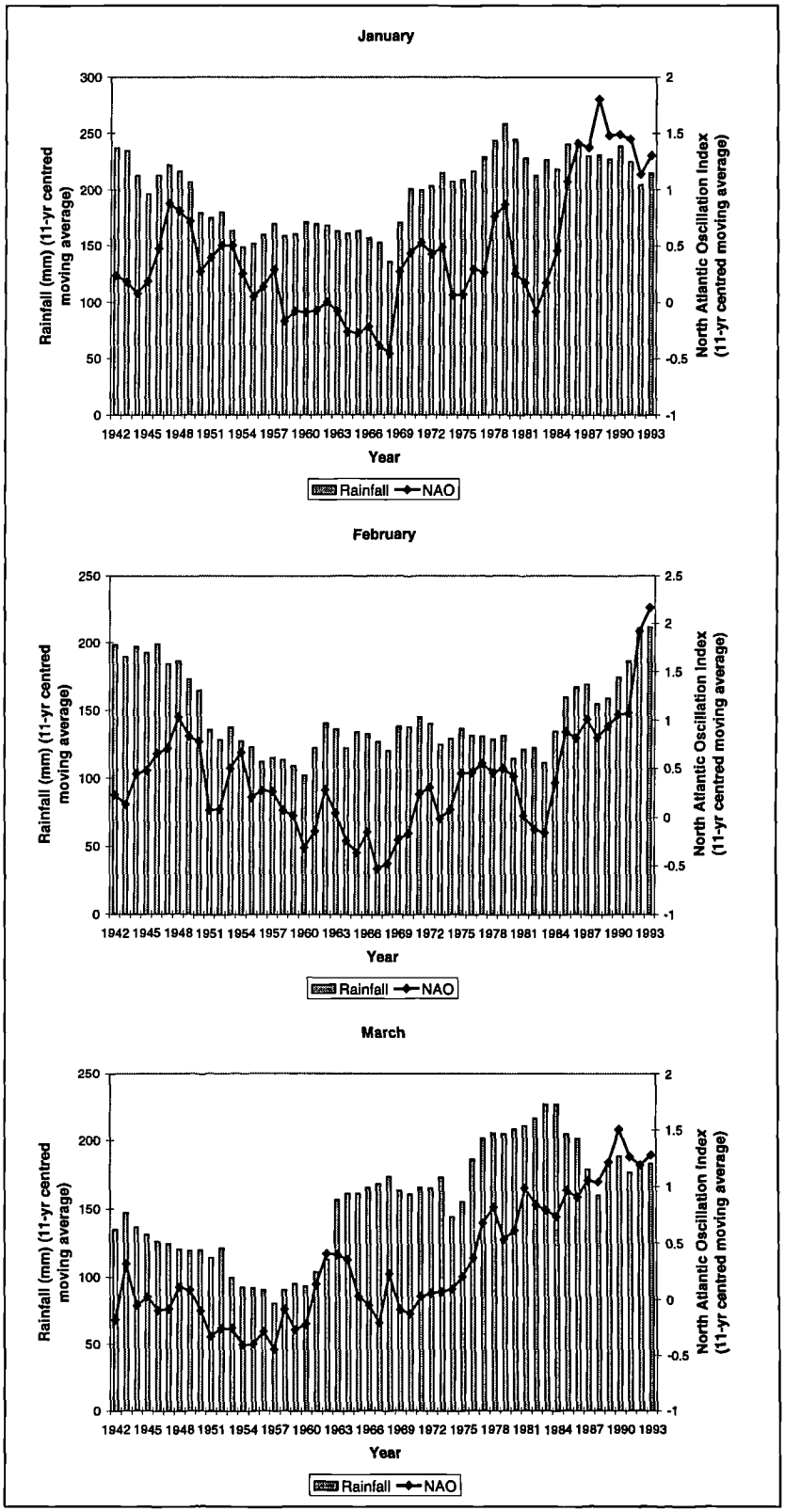

Figure 3-18: Monthly NAO and precipitation for Moorland Cottage, using data from 1937-1998 (11-yr centred moving average), for January, February and March.

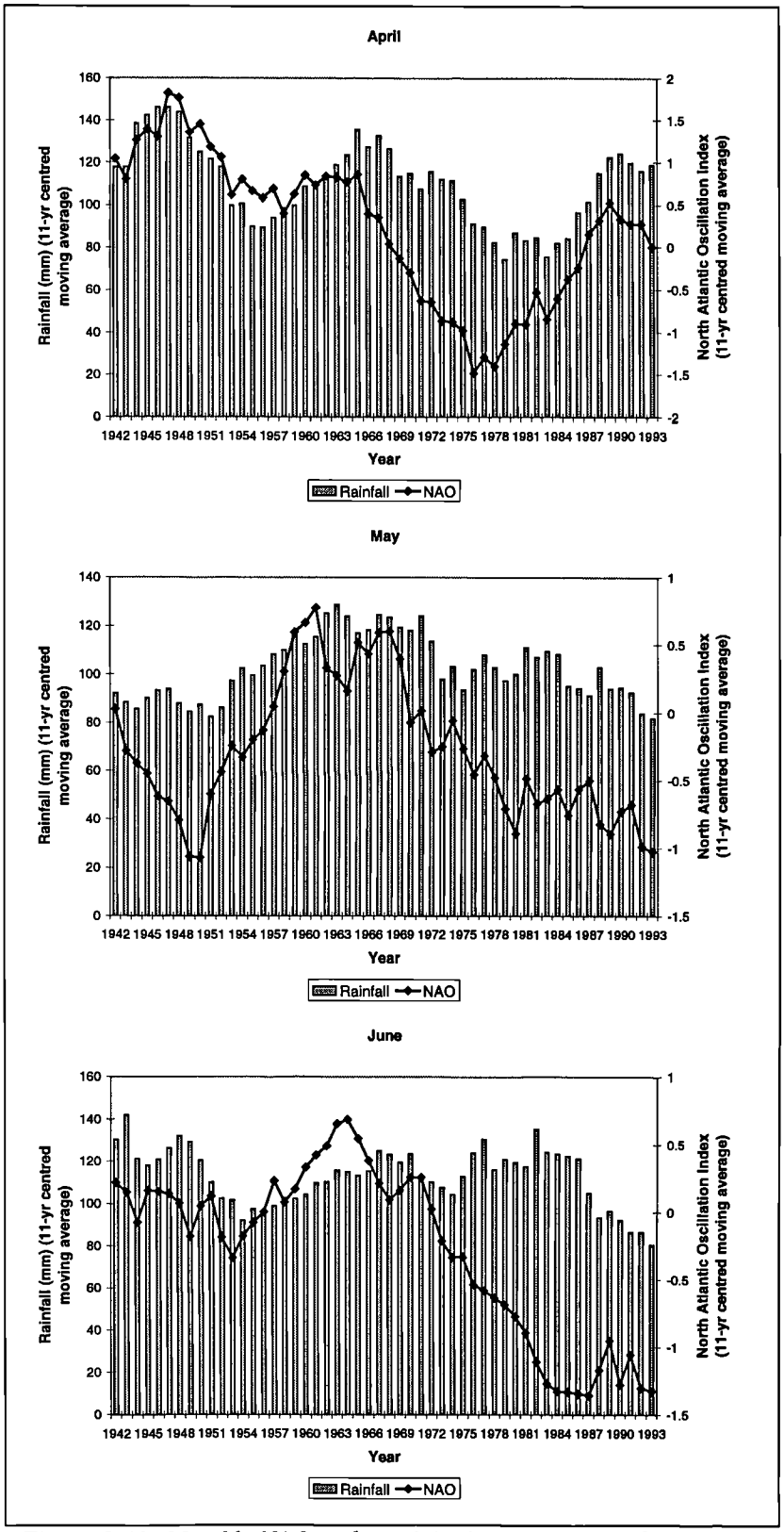

Figure 3-19: Monthly NAO and precipitation for Moorland Cottage, using data from 1937-1998 (11-yr centred moving average), for April, May and June.

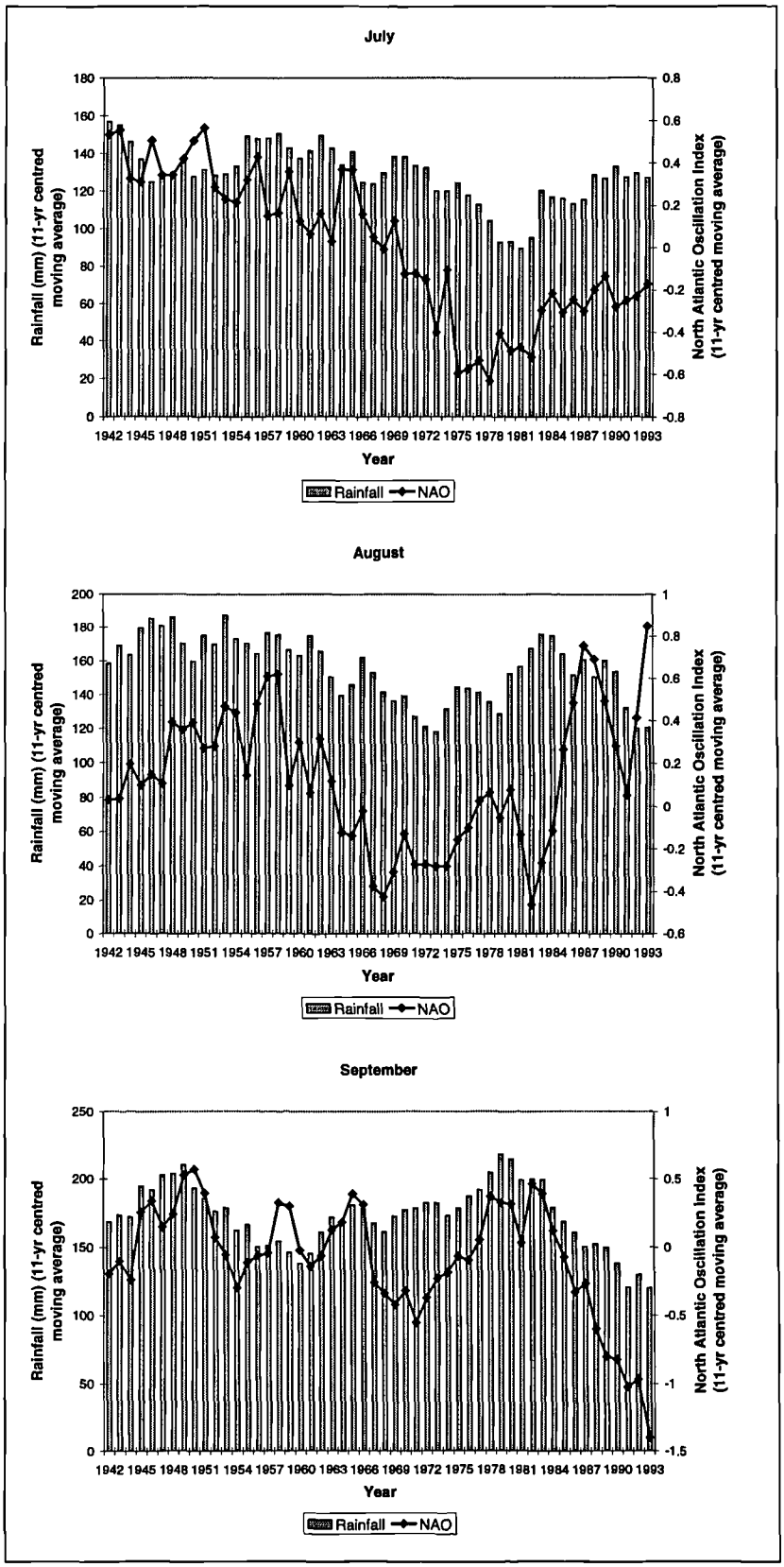

Figure 3-20: Monthly NAO and precipitation for Moorland Cottage, using data from 1937-1998 (11-yr centred moving average), for July, August and September.

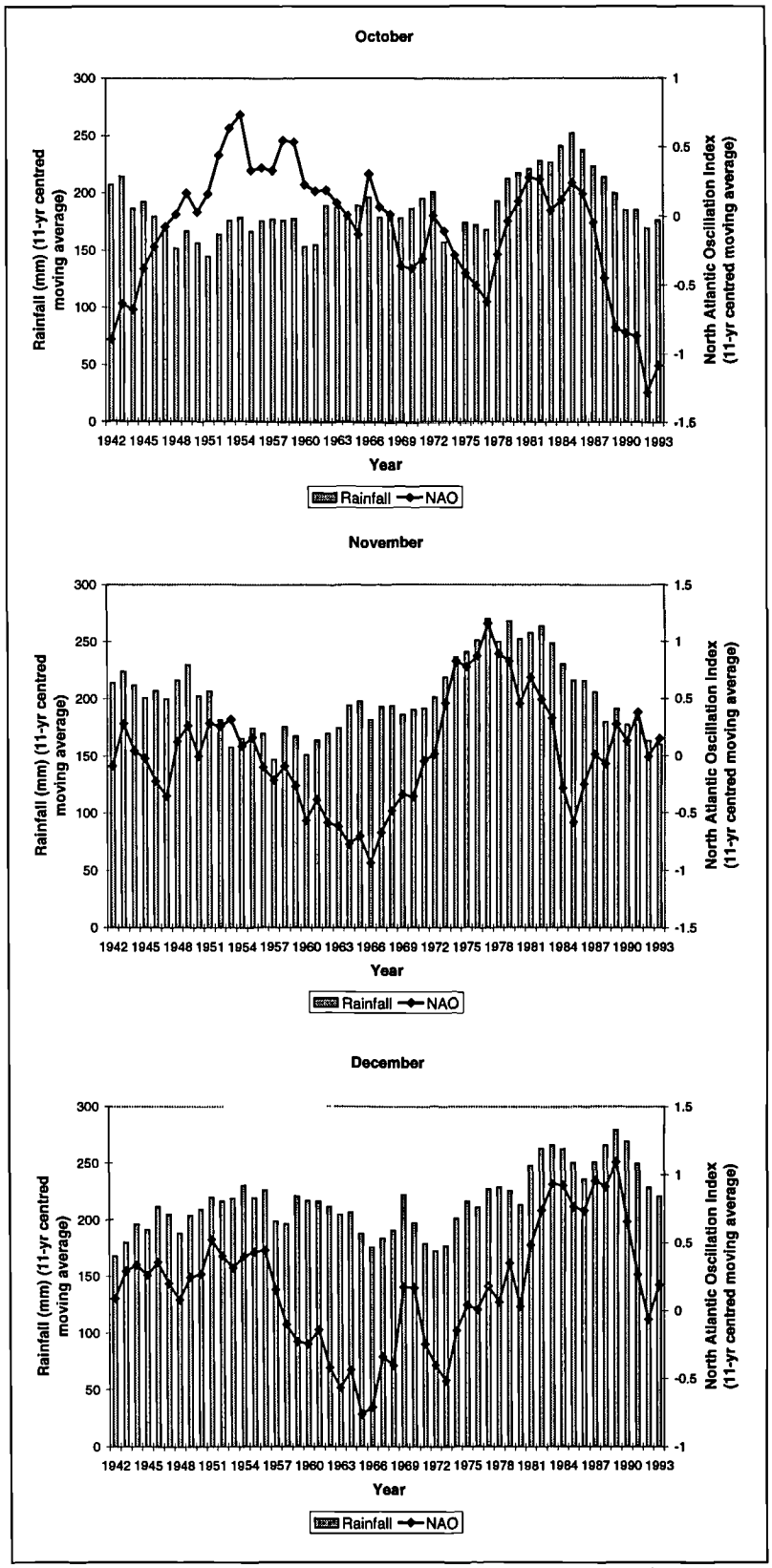

Figure 3-21: Monthly NAO and precipitation for Moorland Cottage, using data from 1937-1998 (11-yr centred moving average), for October, November and December.

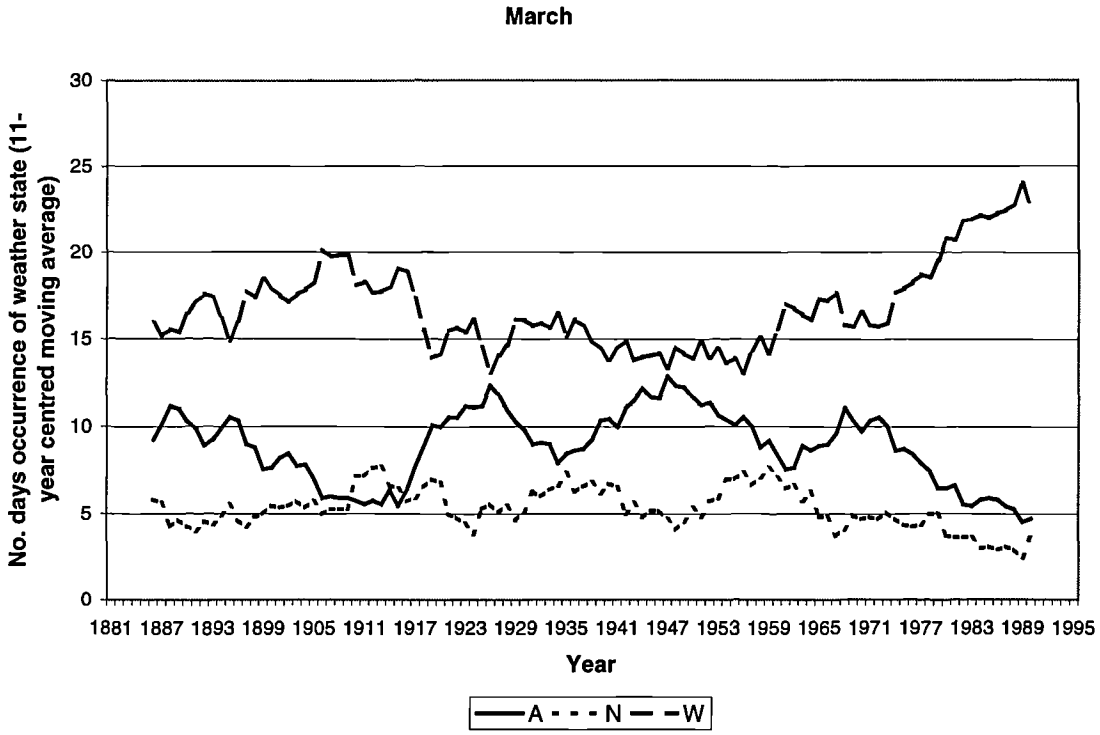

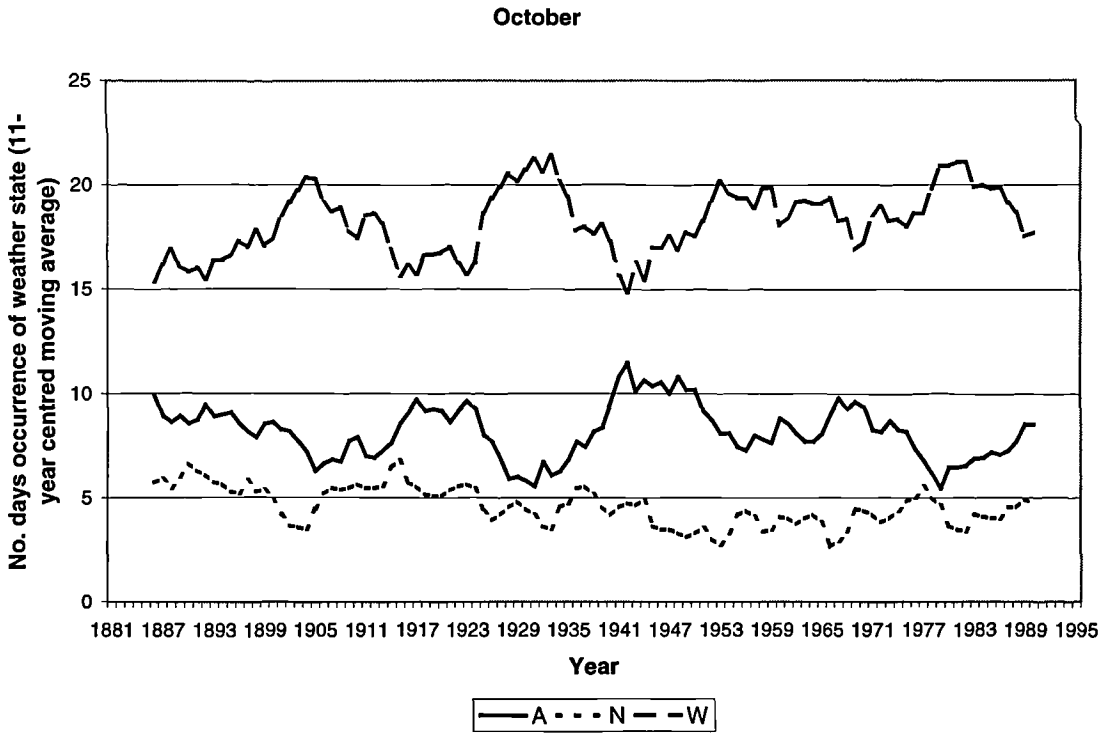

Figure 3-22: Frequency of occurrence of a weather state in March and October during the period from 1882-1998 (11-yr mean centred moving average).

In March, the westerly weather-state has increased in frequency from 16 to 24 days on average since 1975. In October, there has been an oscillation around a frequency of 19 days since the 1940s and, indeed, a recent decline since the mid-1980s to a current frequency of about 17 days. October increases may therefore be related to increased wetday amounts or an increase in convective activity. Indeed, a similar phenomenon noted at eastern sites in the months of September and October is related to increased convective precipitation totals arising from a maritime source. Importantly, however, all three weather-states display a close link to monthly-NAO. This has large implications for the prediction of monthly precipitation totals in regard to water resources and the prediction of droughts.

Since strong relationships were found between the monthly NAO and the three weather states, it is likely that similar links between weather states and monthly precipitation totals exist. These can be found in Table 3-15. A strong positive relationship exists between precipitation at Moorland Cottage and the frequency of the westerly weather-state, as would be expected. At the two eastern sites all significant correlations between precipitation and westerly weather state occurrence are positive.

	Moorland Cottage			Lockwood Reservoir			Kirk Bramwith		
	A	N	W	A	N	W	A	N	W
J	**-0.379**	**-0.553**	**0.548**	**-0.279**	**0.462**	-0.093	**-0.375**	**0.220**	0.121
F	**-0.313**	**-0.426**	**0.497**	**-0.435**	0.105	0.165	**-0.294**	**-0.285**	**0.348**
M	**-0.669**	**-0.749**	**0.803**	**-0.551**	**-0.296**	**0.595**	**-0.711**	**-0.370**	**0.763**
A	-0.141	-0.265	**0.361**	**-0.608**	**0.676**	-0.052	**-0.596**	**0.585**	0.019
M	**-0.701**	**-0.465**	**0.838**	**-0.222**	**0.322**	-0.006	**-0.607**	0.157	**0.457**
J	0.031	-0.255	**0.293**	-0.154	0.072	0.046	-0.180	**0.327**	-0.179
J	**-0.774**	0.073	**0.639**	**-0.488**	-0.064	**0.421**	**-0.317**	**0.256**	0.141
A	**-0.474**	0.171	**0.419**	**-0.499**	-0.018	**0.414**	**-0.564**	**-0.189**	**0.531**
S	-0.266	-0.238	**0.336**	**-0.363**	**-0.295**	**0.398**	**-0.240**	**-0.313**	**0.303**
O	**-0.469**	0.278	**0.331**	**-0.365**	**0.440**	0.066	**-0.383**	**0.460**	0.070
N	**-0.458**	-0.13	**0.469**	**-0.213**	**0.478**	-0.074	**-0.332**	**0.502**	0.033
D	-0.078	-0.145	0.223	**-0.607**	0.025	**0.581**	**-0.616**	0.032	**0.586**

*Table 3-15: Correlation coefficients between monthly precipitation and monthly occurrence of a weather-state at the three sites (**bold** indicates a significant correlation at the 95 percent level).*

Interestingly, positive correlations are also observed between the northerly weather state and precipitation totals at eastern sites during spring and autumn months. All sites exhibit a strong positive correlation between westerly weather state frequency and precipitation during the month of March.

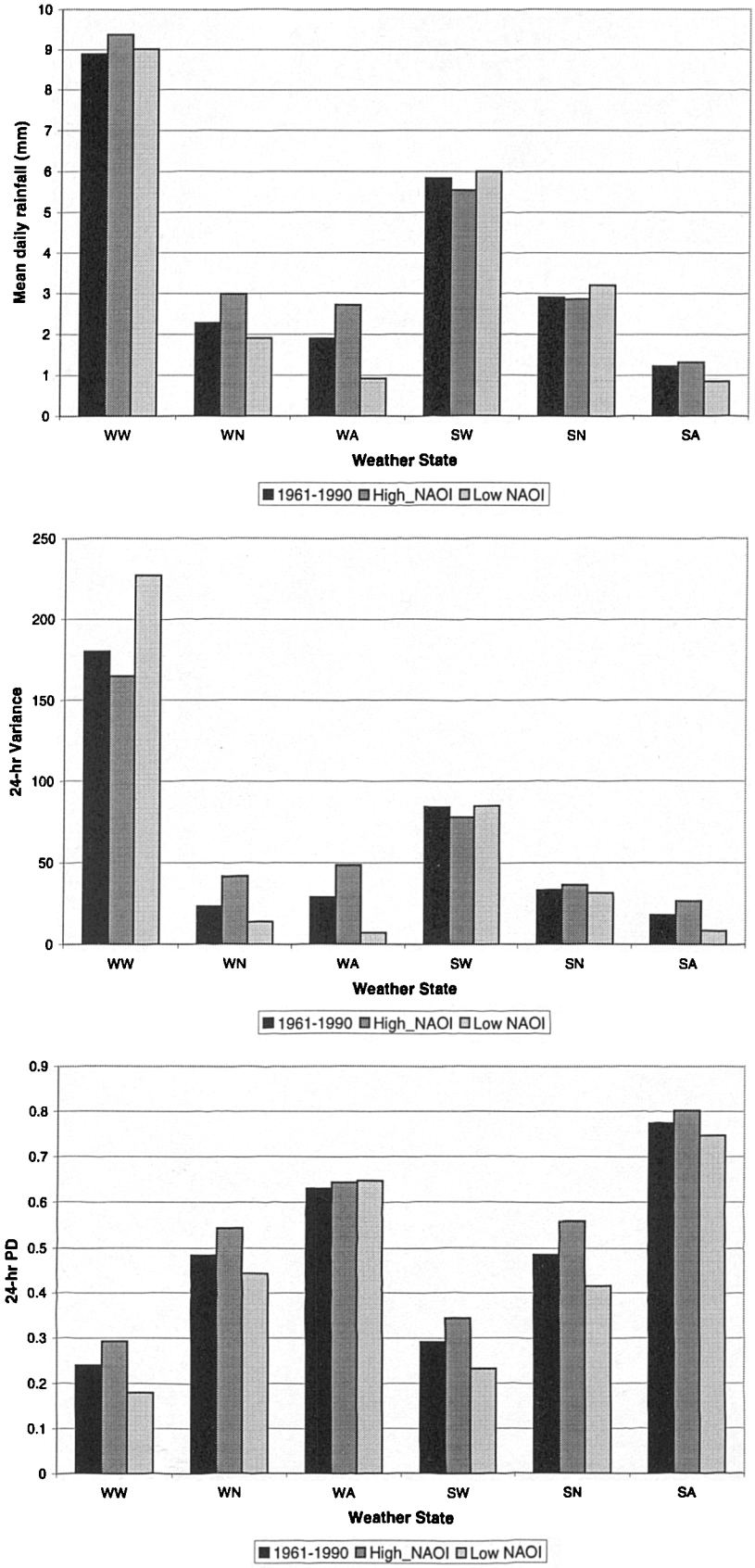

Figure 3-23: Effect of low and high winter-NAO phases upon mean daily precipitation, PD and variance statistics.

Investigation was made into the effect of high and low winter-NAO phases upon the mean daily precipitation, PD and variability of precipitation for the six weather states at Moorland Cottage (Figure 3-23). Mean daily precipitation for 'winter' weather states is increased during a high phase winter-NAO and is, conversely, decreased during a low phase. For summer weather states there is little change. The 24-hr PD is in general reduced during a low phase winter-NAO and increased during a high phase. Variability of summer and winter westerly weather state precipitation is noticeably enhanced during a low phase, but northerly and anticyclonic weather states show reduced variability. These relationships are reversed during a high phase.

Strong relationships are apparent between winter mean daily precipitation amounts and the NAO, especially in western Yorkshire where most surface water supplies are located. If these relationships can be successfully quantified and predictive abilities using SSTs are realised (as Sutton and Allen 1997 and Rodwell *et al.* 1999) then it is possible that the winter replenishment of many of the Pennine reservoirs will be capable of being estimated a few months or a year in advance.

3.3.2 Links to the objective Lamb weather types (OWTs)

3.3.2.1 Changes in the frequency of objective Lamb weather types

Many studies have been made of changes in the frequency of the subjective Lamb weather types. The most well known recent change has been the major decline in westerly days to 60 to 70 percent of their frequency during the 1930s and 1940s. This decline has been most pronounced in winter months, although it exists for all seasons (Briffa *et al.,* 1990). Sweeney and O'Hare (1992) suggested that a similar decline has also taken place in the cyclonic westerlies, whereas anticyclonic and cyclonic types have shown increases, particularly in the 1980s. Other significant changes identified by Briffa *et al.* (1990) using principal components analysis are that south-westerlies have doubled in frequency since the 1980s; northerlies have steadily declined since the 1950s; and north-westerlies have sharply declined in the 1980s.

This can be explained, in part, by changes in the North Atlantic Oscillation (NAO). Wilby *et al.* (1997) investigated the correlation between the winter NAO and the frequency of the three most common Lamb weather types. The westerly type was, on average, over 15 days more frequent for high than low NAO winters (see Section 2A.7 for more explanation). Years with high mean NAO also experience fewer easterly, northerly and hybrid circulation types.

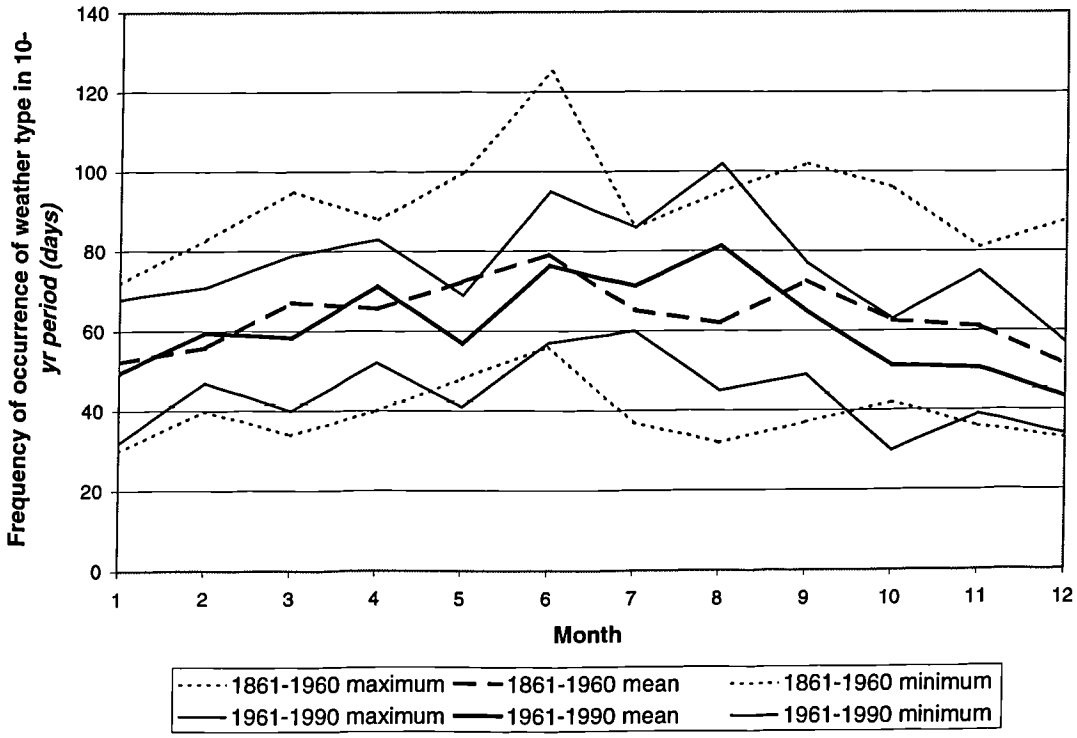

Figure 3-24: Comparison of the frequency of monthly occurrence of the anticyclonic (A) weather type in a 10-yr period during 1861-1996 and 1961-1990.

Although investigations have been made into changes in the frequency of the Lamb weather types, there has been little additional analysis of the objective Lamb weather types of Jones *et al.* (1993). It is useful to determine both the annual and seasonal magnitude of change for the most frequent weather types. An analysis was made of the monthly frequency of a weather type in a 10-year period (as Corte-Real *et al.*, 1998). Mean, maximum and minimum frequencies were obtained and the differences occurring in the time-period 1861-1960 and 1961-1990 compared.

It can be observed in Figure 3-24 that there has been no significant change in the frequency of anticyclonic weather types, although there has been a slight increase in the mean occurrence in July and August. The oft-quoted decline in the westerlies highlighted by Briffa *et al.* (1990) is not seen in the OWT record. Figure 3-25 shows an increasing occurrence of westerly weather types during the months of September to December. This may have been compensated for by a decrease in cyclonic weather types during these months with an increased incidence in spring. In Figure 3-26, it can be noted that the maximum incidence of cyclonic types in March is without precedent.

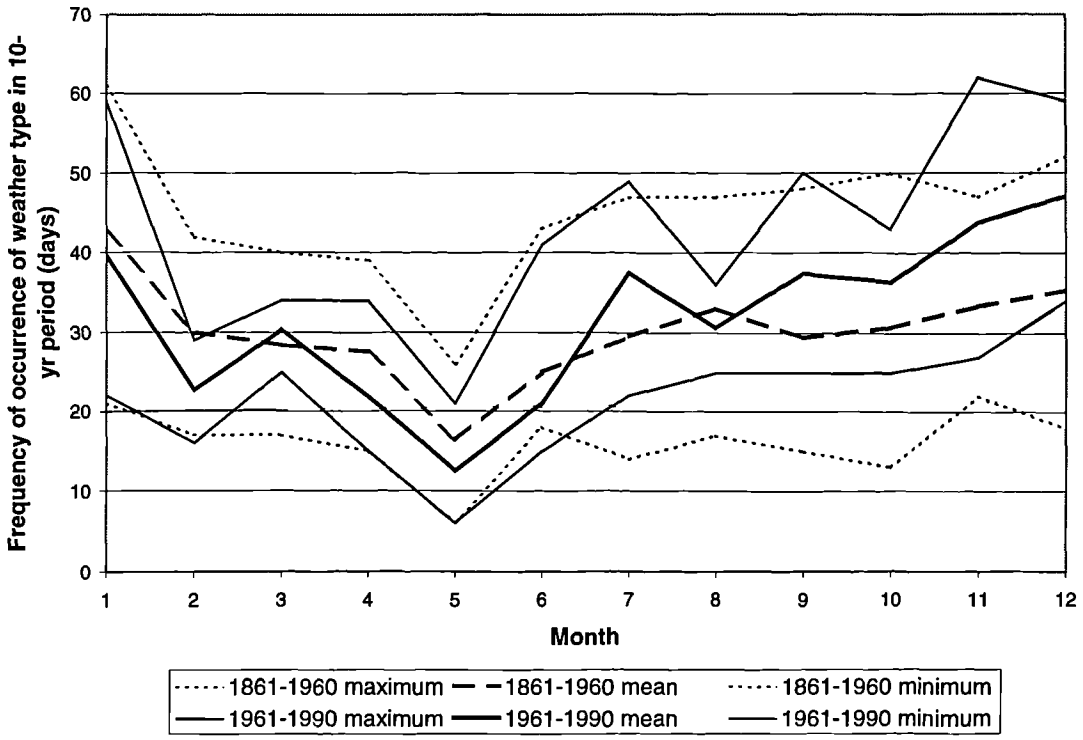

Figure 3-25: Comparison of the frequency of monthly occurrence of the westerly (W) weather type in a 10-yr period during 1861-1996 and 1961-1990.

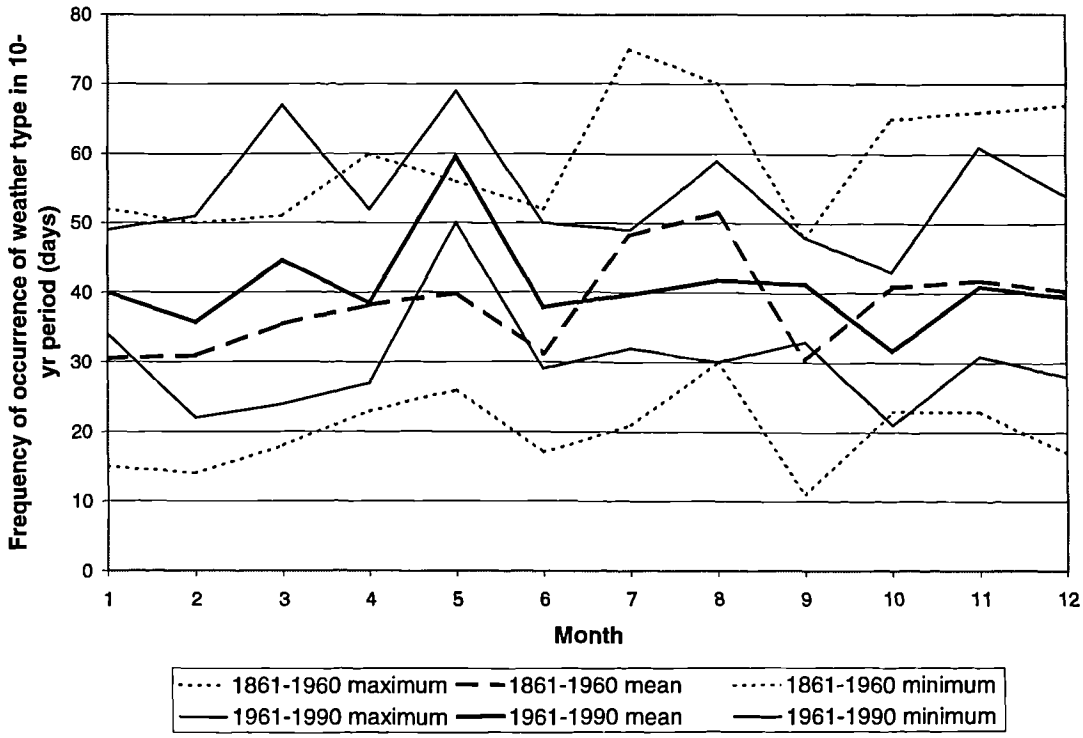

Figure 3-26: Comparison of the frequency of monthly occurrence of the cyclonic (C) weather type in a 10-yr period during 1861-1996 and 1961-1990.

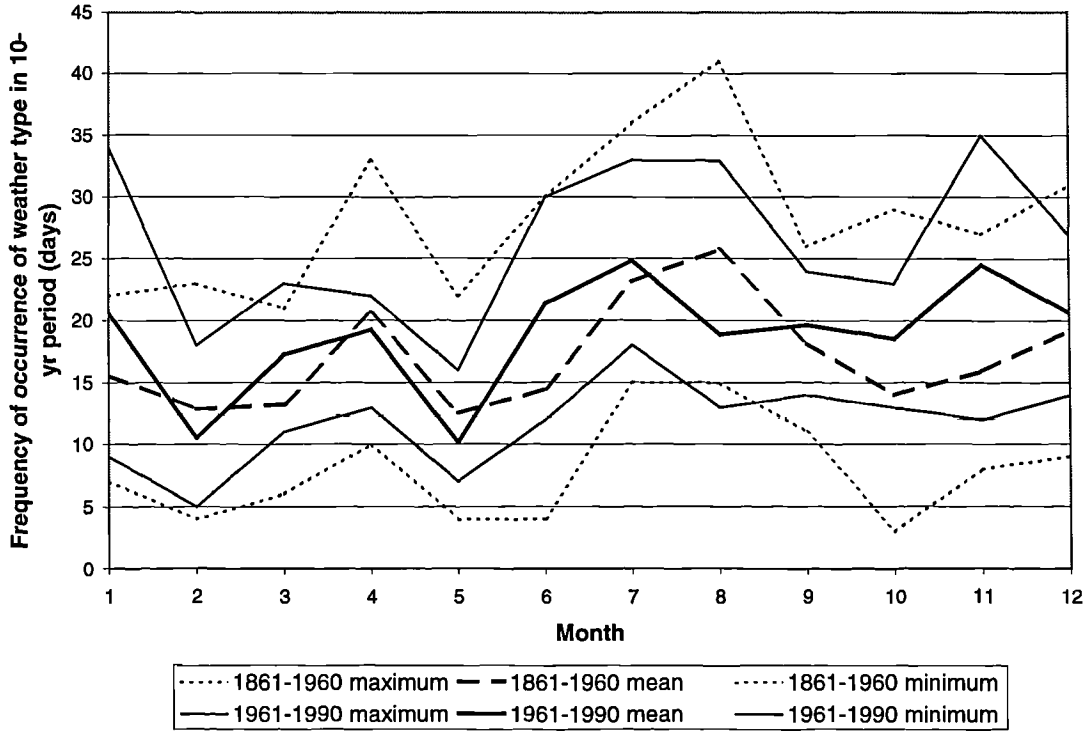

Figure 3-27: Comparison of the frequency of monthly occurrence of the north-westerly (NW) weather type in a 10-yr period during 1861-1996 and 1961-1990.

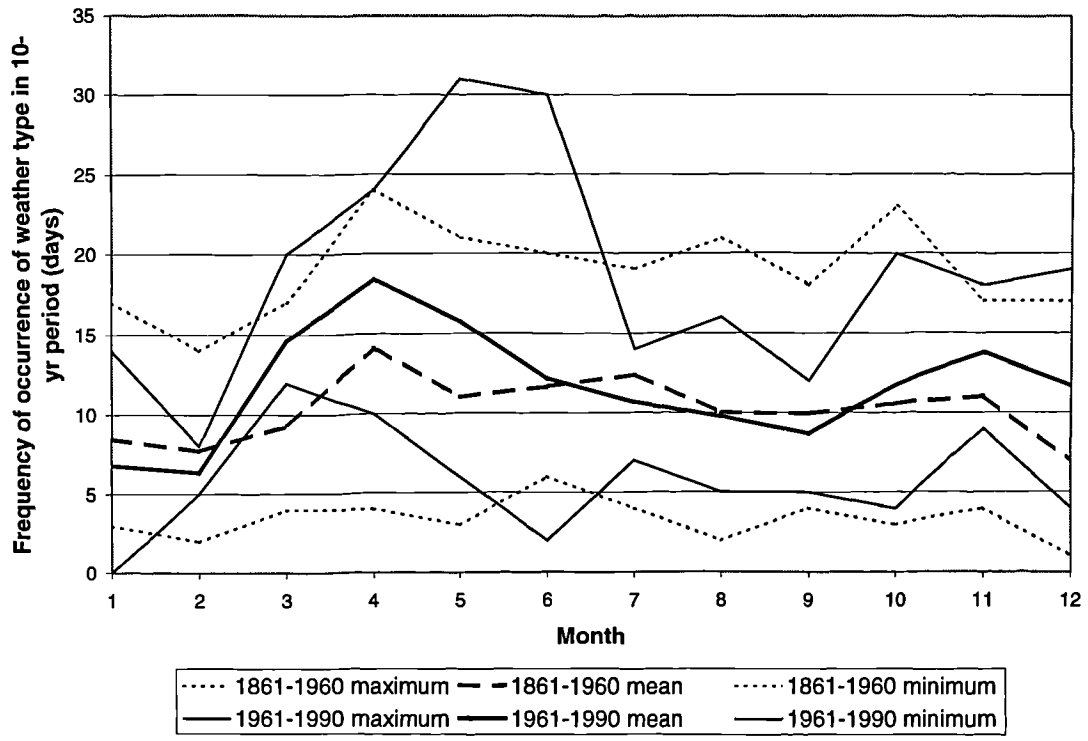

Figure 3-28: Comparison of the frequency of monthly occurrence of the northerly (N) weather type in a 10-yr period during 1861-1996 and 1961-1990.

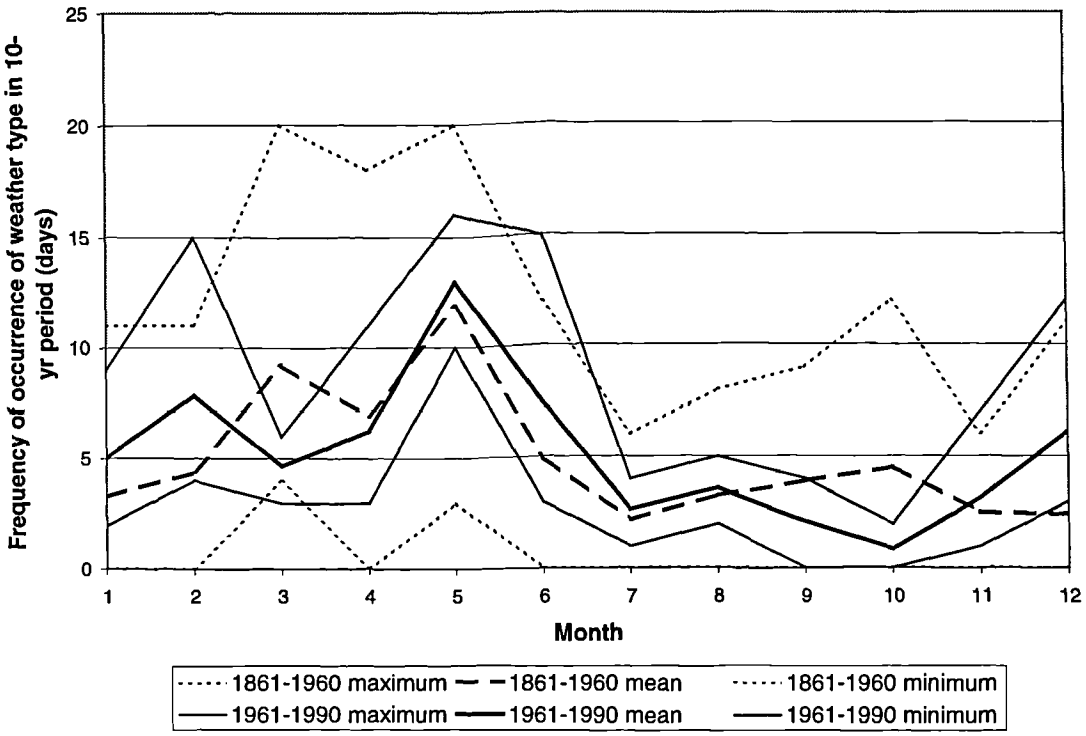

Figure 3-29: Comparison of the frequency of monthly occurrence of the easterly (E) weather type in a 10-yr period during 1861-1996 and 1961-1990.

Other weather types also show interesting patterns of change. The north-westerlies, for example, can be shown to have increased in frequency, on average, during the recent time period, but especially in winter months (see Figure 3-27). The northerly weather type has become more frequent in the spring but has declined in occurrence during January and February (see Figure 3-28). The easterly type shows no real change, but an interesting pattern of incidence. It can be observed in Figure 3-29 that the easterly type records a prominent peak in frequency during the spring months of March, April and May historically, but appear to have shifted one month later in the recent time period. This weather type occurs twice as often during these three months than during any other month of the year.

3.3.2.2 Non-stationarity in yield of objective Lamb weather types

The assumption that relationships between long-term precipitation statistics and the frequency of weather types stay constant is a major caveat of downscaling. Recent work by Conway and Jones (1998) found evidence that changes may have occurred to the relationship between weather types and precipitation over time. Conway *et al.* (1996) also suggested that the error in the number of modelled wet days at Kempsford (UK), using a rainfall model based on continuous atmospheric variables, may mean that a stationarity assumption is not always

accurate. The exact source of non-stationarity remains unclear, although there have been many suggestions, such as changes in the vigour of westerly circulation patterns (Bardossy and Caspary, 1990) or changes in the relative importance of frontal and convective precipitation (Osborn *et al.*, 2000). An interesting recent discussion by Jones *et al.* (1999*a*) also proposed that temperature changes could have an effect on the internal properties of weather types.

Sweeney and O'Hare (1992) calculated mean daily-precipitation amounts for each of the Lamb weather types for each of 65 lowland stations across the UK where 40-yr records were available. Additionally, 16 longer records extending back as far as 1875 were used. An analysis was made of whether significant variations in yield for the same airflow type had occurred over time. Twenty-year breakdowns were produced for the three most common circulation types, C, A and W, for the 16 longer records, which include York. Temporal variations are relatively minor although the period from 1901-1921 produced higher daily rainfalls for cyclonic and westerly circulation types in York than has been seen since. Anticyclonic precipitation is always low but has steadily decreased since the turn of the century in York.

Wilby (1997) found evidence of non-stationarity within circulation patterns in an investigation of the annual wet-day probabilities and mean wet-day amounts at Durham (northeast England) and Kempsford (central southern England). He defined a wet day as >1 mm day^{-1} of precipitation. A notable feature was a lack of correlation between the 10-yr running mean of the annual mean wet-day amounts at the two sites. Many weather types, particularly the cyclonic, southerly, anticyclonic, and westerly, have shown declining wet day probabilities in recent years, although all are within bounds of historical variability. The high correlation in wet-day probability between two sites separated by 400 km over a 110-yr record suggests that large-scale forcing mechanisms may be responsible. Additionally, the non-stationarity in mean precipitation amounts is more sensitive to local topographic controls than wet-day probabilities. The causes of non-stationarity were investigated using the daily CET record, British Isles daily weather-front frequencies and types (Wilby *et al.*, 1995), and the monthly NAO.

Wilby (1997) also suggests approaches that can be taken to incorporate non-stationarity into model calibration. Non-stationarity can be incorporated stochastically, i.e. by sampling the conditional statistics from a probability distribution such as the gamma or normal (Richardson 1981). However, for the less frequently occurring weather types, a major factor governing the distribution characteristics will be the limited wet-day sample size, and the approach may not capture the time series evolution. Therefore, it is proposed that incorporating non-stationarity empirically may be a more successful approach. This may be achieved by isolating significant relationships between conditional weather type precipitation statistics and other atmospheric

variables, such as the NAO. This information can then be used to adjust precipitation model parameters. It is also recognised that there may be scope for a hybrid approach where stochastic models are driven by airflow sequences.

An analysis was made of trends in the westerly and cyclonic weather type characteristics of mean daily precipitation, mean wetday and proportion dry days at the seven sites. This was performed on both an annual and seasonal basis using 0.2 mm as dry bound.

For the westerly weather type, at most sites, there has been a decline in mean daily precipitation since the mid-1980s. There are also fluctuations that may correspond to low frequency oscillations in synoptic climatology such as the NAO. The most interesting feature, however, is the step-like change in spring mean daily precipitation occurring between the 1960s and the mid-1980s (see Figure 3-30).

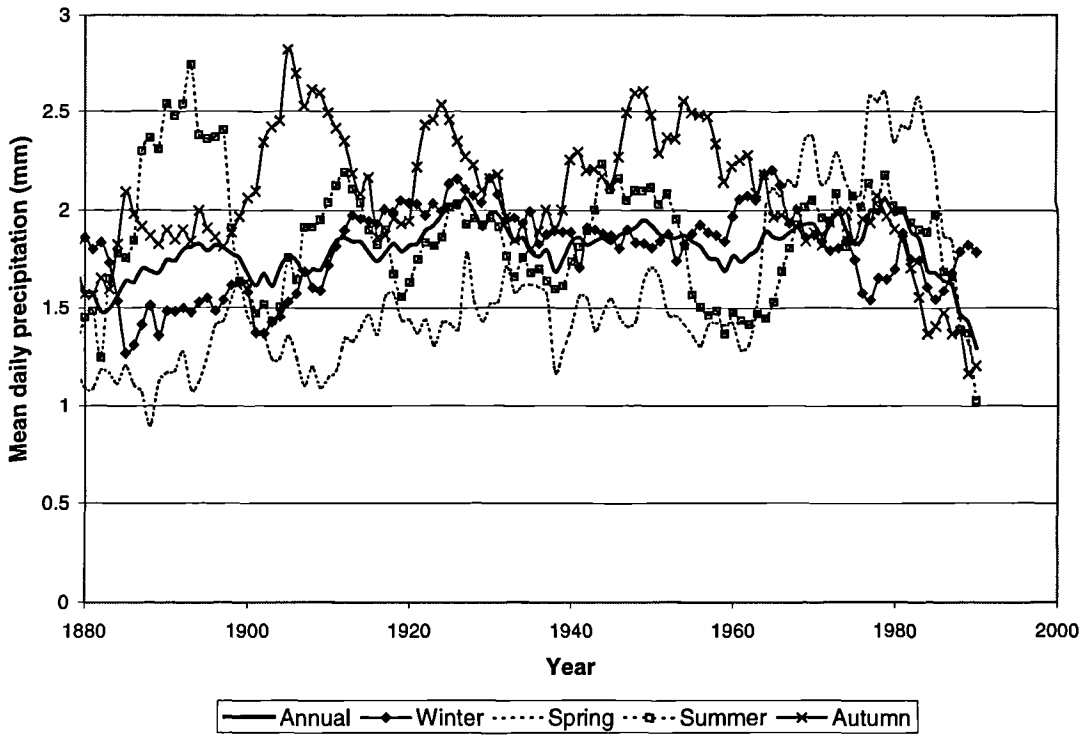

Figure 3-30: Mean daily precipitation at Lockwood Reservoir occurring due to a westerly weather type (11-year centred moving average).

This anomaly occurs at all sites, although it is more prominent in the east than the west, and coincides with the well-established increase in the westerlies and their subsequent decline since the 1980s to the present day. For many sites, the stepped increase in spring westerly type mean daily precipitation in the 1960s corresponds to a decline in winter precipitation and the

subsequent decrease in the mid-1980s coincides with a rise in winter precipitation. There has been a decline in autumn mean daily precipitation since the 1960s at all sites, until a recent stabilisation in the 1980s (see Figure 3-31). Indeed, at many sites this is at historically unprecedented levels. Most sites in the west show an increase in winter precipitation starting in the mid-1980s. However, in the east there has been a decline in westerly winter mean daily precipitation. Summer mean daily precipitation for the westerly type has decreased at all sites.

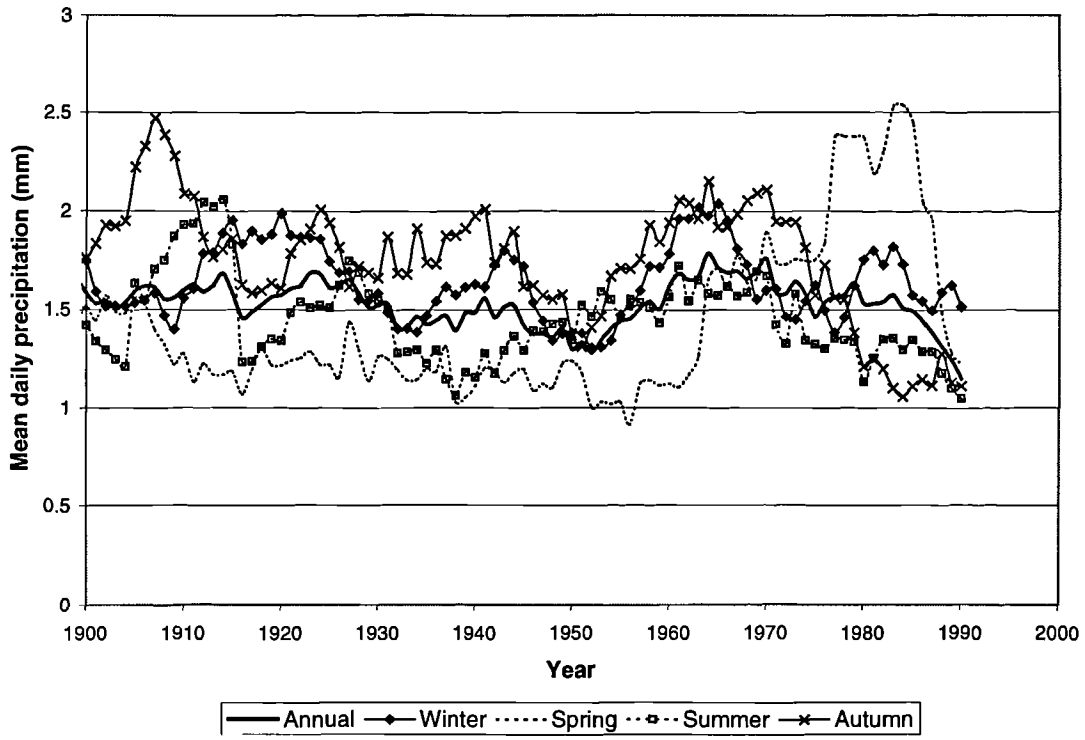

Figure 3-31: Mean daily precipitation at Kirk Bramwith occurring due to a westerly weather type (11-year centred moving average).

The mean wet day for the westerly weather type shows similar trends to the mean daily precipitation amount, which would be expected given that the majority of westerly days at most of the sites will be wet. Especially prominent is the same step change from 1960 to the mid-1980s in spring wet day that is seen in the mean daily precipitation. Apart from this anomaly, most sites show a decline in wet day for all seasons, possibly excepting winter. This is particularly noticeable in the eastern Yorkshire and northern Pennine sites (see Figure 3-32). For example, trend analysis at Hury Reservoir gives an R^2 of 0.8 ($Wetday = -0.0165y + 37.115$) and 0.85 ($Wetday = -0.043y + 89.431$) for the decline in annual and autumn wet day respectively, where y is year. All sites show a decrease in summer wet day, whereas only the eastern sites record a decline in winter wet day amounts, western sites documenting an increase.

The proportion dry days for the westerly weather type show a general downward trend in all seasons (see Figure 3-33). Significant regression relationships are found at many sites, e.g. for annual PD there are significant declines at Hury Reservoir ($PD = -0.0017y + 3.50$, R^2=0.8) and Lockwood Reservoir ($PD = -0.0013y + 3.01$, R^2=0.68).

Spring and summer PD record a decline until the 1980s but then show a rapid increase at most sites across the region. Winter PD shows a recent increase at westerly sites, but a decrease in the east.

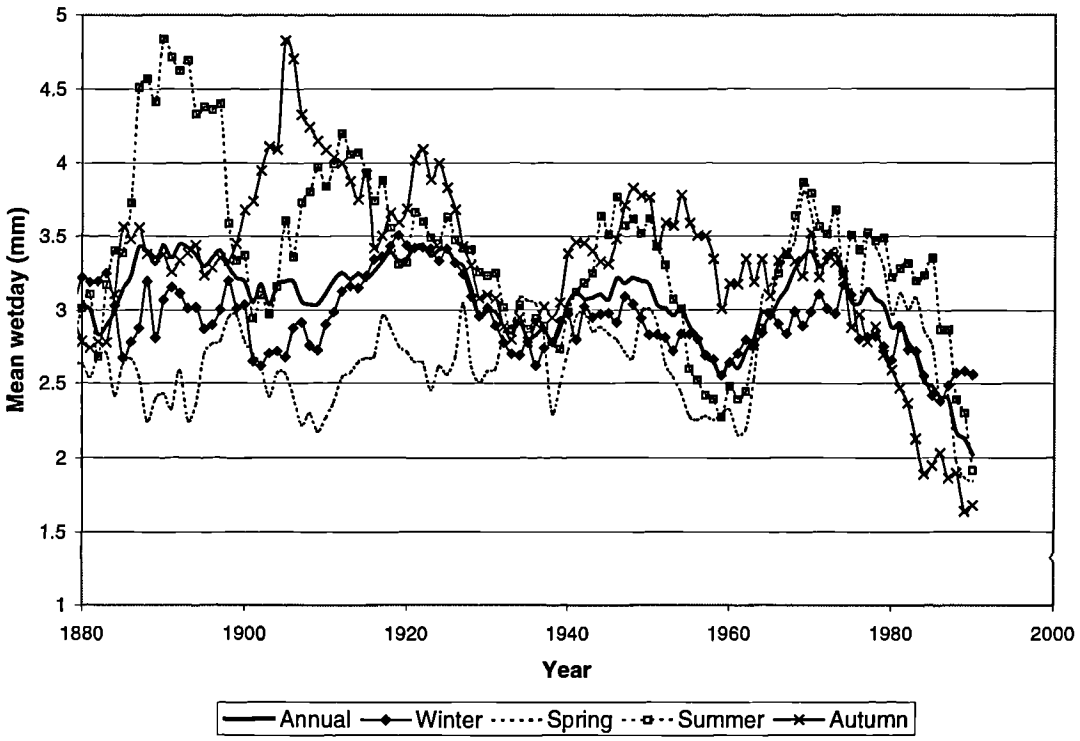

Figure 3-32: Mean wet day (in mm) at Lockwood Reservoir occurring due to a westerly weather type (11-year centred moving average).

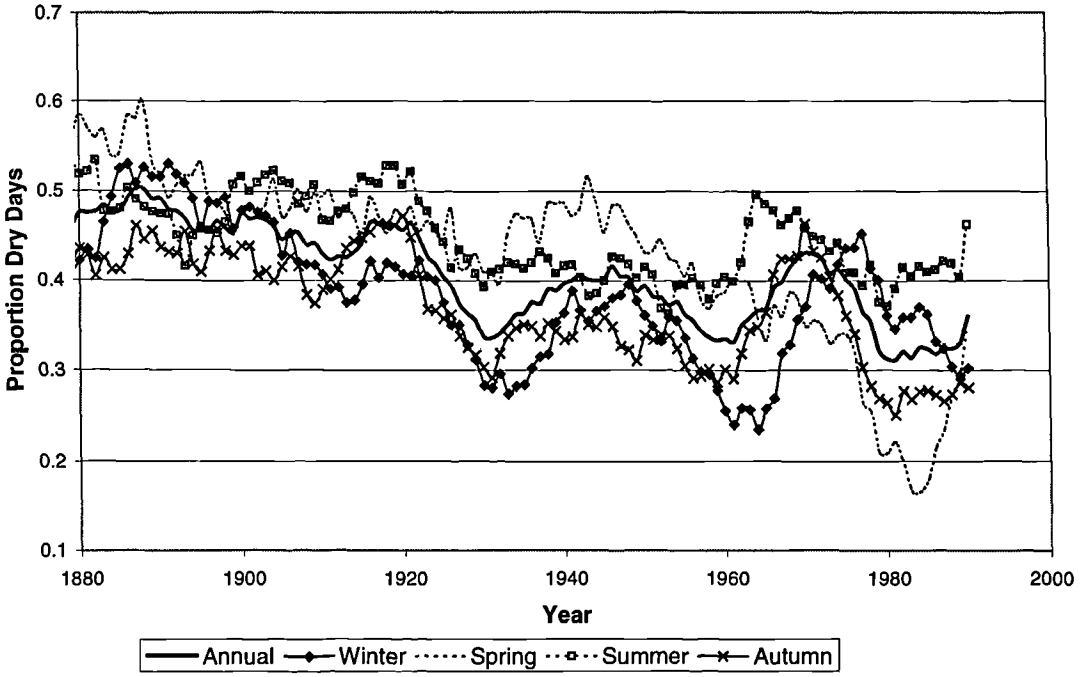

Figure 3-33: Mean proportion dry days at Lockwood Reservoir occurring due to a westerly weather type (11-year centred moving average).

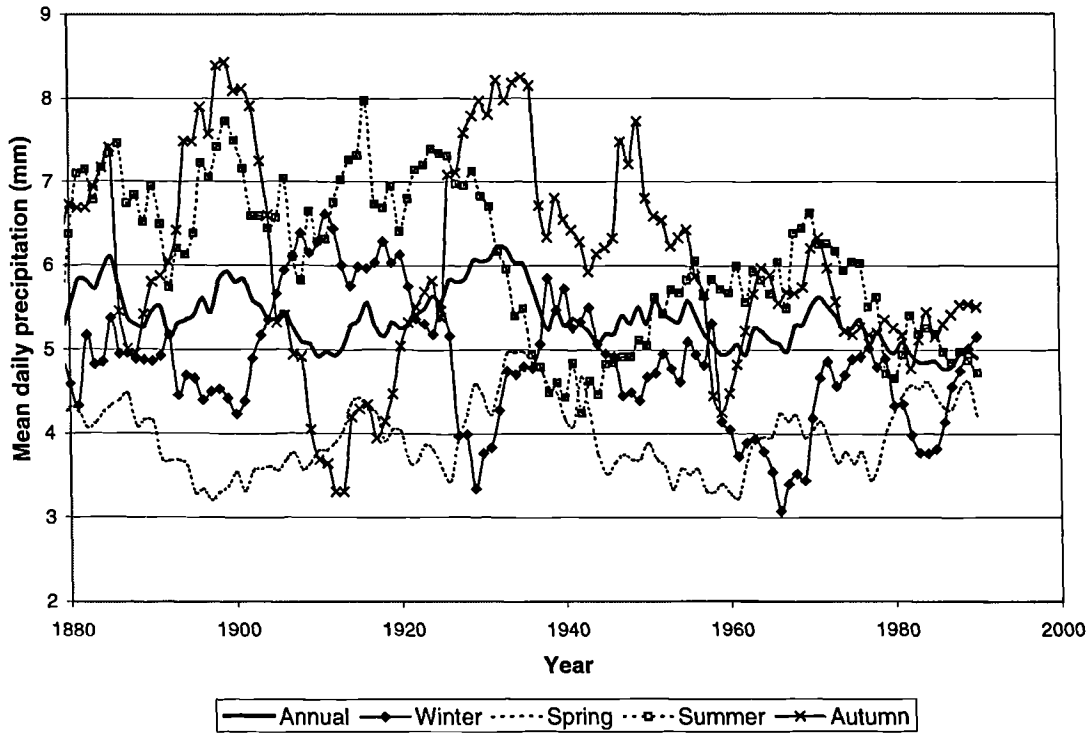

Figure 3-34: Mean daily precipitation at Lockwood Reservoir occurring due to a cyclonic weather type (11-year centred moving average).

The trends apparent for the cyclonic weather type are less transparent than those of the westerlies. A major observation is that the cyclonic type has a much higher mean daily

precipitation total at all sites than the westerly type. This is especially true for eastern sites, and suggests that cyclonic weather types equally affect eastern and western sites. Autumn mean daily precipitation shows a strong oscillatory trend at eastern sites that may be linked to synoptic circulation changes such as the NAO (see Figure 3-34). However, at Pennine sites there is a decline from 1930 to 1960 and then relative stability.

For the cyclonic weather type, there are no noticeable regional variations or trends in PD except for a decrease in spring PD since about 1980 in the east. There has also been a possible recent increase in winter PD in the east, coinciding with a decrease in the west. Other than these trends, the sites show highly different and varying patterns, even when 11-yr centred means are used.

3.3.2.3 Links between precipitation and the Lamb weather types

Many studies have examined the relationships between Lamb weather types and local climate. For example, Jones *et al.* (1993) showed that the weather types have the potential to explain 70 to 80 percent of the seasonal variability of precipitation in England and Wales. Relationships may be improved by using additional explanatory variables such as weather fronts (e.g. Wilby 1995; Wilby *et al.,* 1995) or by using the three indices of circulation that the objective scheme is based upon (e.g. Conway *et al.,* 1996).

Conway and Jones (1998) describe an approach for downscaling using an objective weather classification scheme. An analysis was made of observed relationships between the OWTs and counts of weather fronts, airflow indices, and local precipitation at a single site (Durham) and a regional area-average for the northeast of England. The probability of precipitation and the mean precipitation amount was determined for the seven most frequent weather types of A, C, E, N, W, S, and NW. It was established that at Durham the cyclonic weather type produces the greatest probability of precipitation, except for the eastern type in autumn, and the highest precipitation depth, except for the eastern type in the summer. Predictably, the anticyclonic type produces the lowest probability of precipitation and the lowest precipitation depth.

An analysis was undertaken to determine the precipitation characteristics of an OWT in Yorkshire. Daily precipitation amounts from 1970-90 recorded at each of 90 sites within Yorkshire and the surrounding area were related to the prevailing OWT (see Figure 3-35). Sites used contained less than 5 percent missing or suspect data during the period from 1970-1990. Mean site statistics for the period from 1970-1990 can be found in Appendix 1, Table A1-1.

Figure 3-36 shows the relationship between mean annual precipitation and maximum daily precipitation in Yorkshire. The annual precipitation ranges in magnitude from 500 to 1500 mm and the maximum daily precipitation amount varies from 45 to 125 mm. These figures are highly dependent upon the location and altitude of the site under consideration. No relationship can be seen between mean annual precipitation and maximum daily precipitation. However, at sites in the east of the region a low annual precipitation total may be combined with a high maximum daily precipitation amount due to the high incidence of convective summer storms.

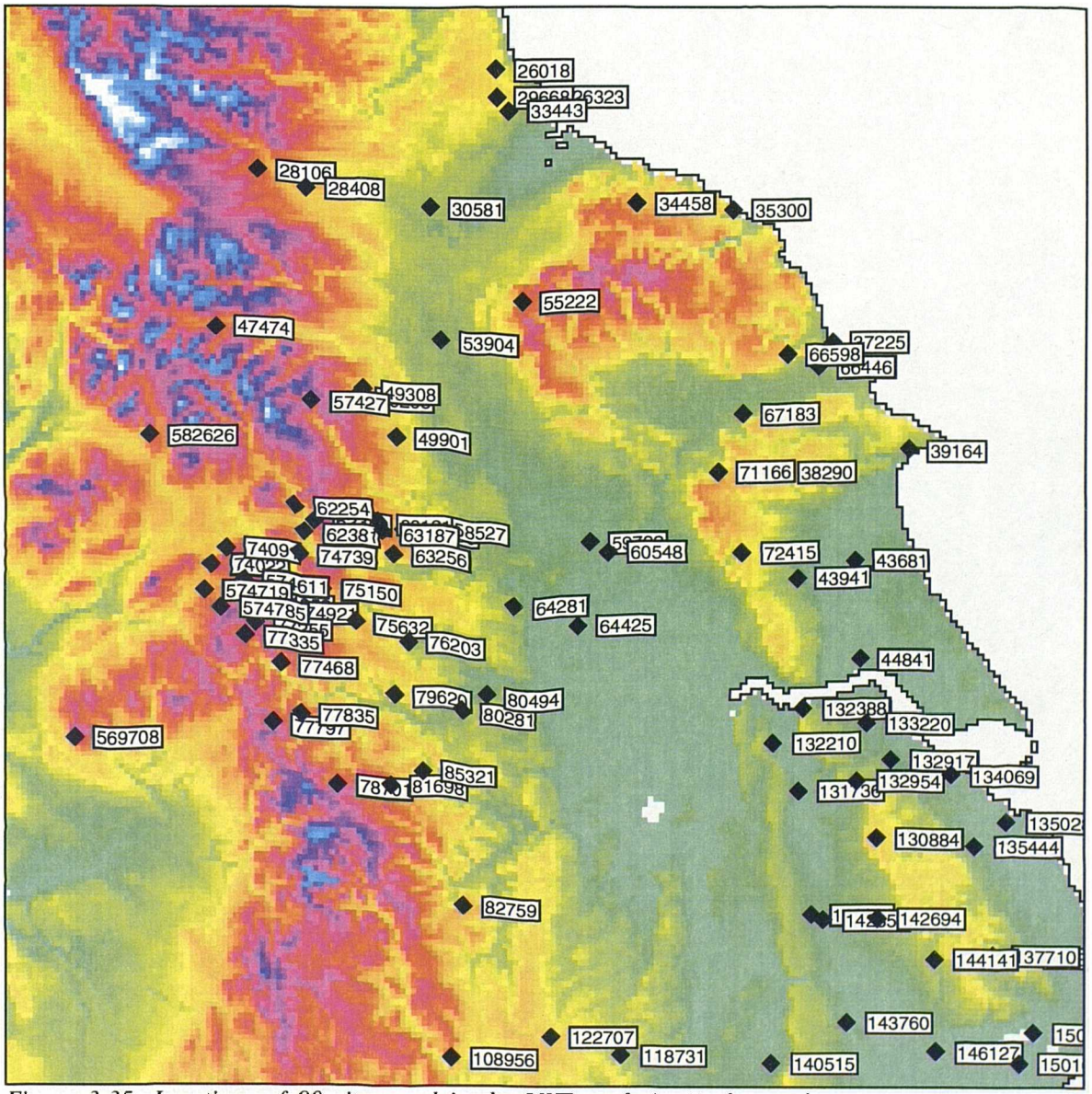

Figure 3-35: Locations of 90 sites used in the LWT analysis. Background raster map is of elevation with a scale of 1 km^2 per pixel.

Figure 3-37 shows the strong relationship between mean annual precipitation and mean annual rainday amounts in Yorkshire. A similar relationship, although negative, can also be found between PD and mean annual precipitation.

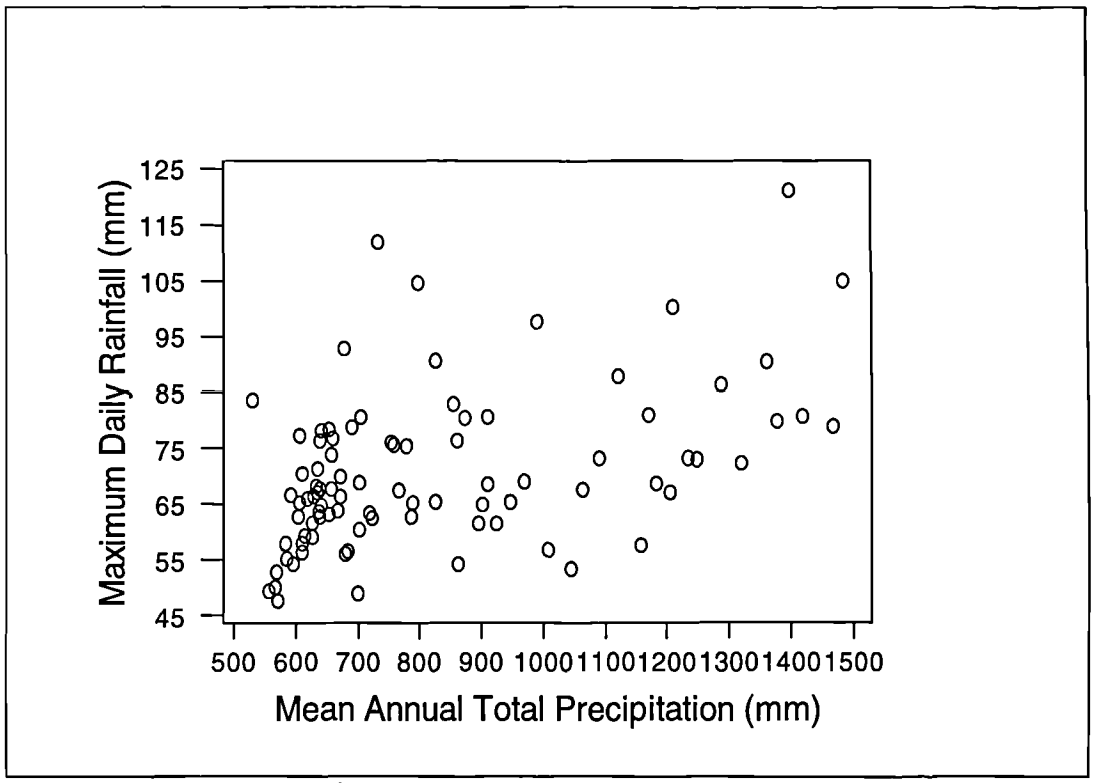

Figure 3-36: Relationship between mean annual precipitation (mm) and maximum daily precipitation (mm) using the time period from 1970-1990.

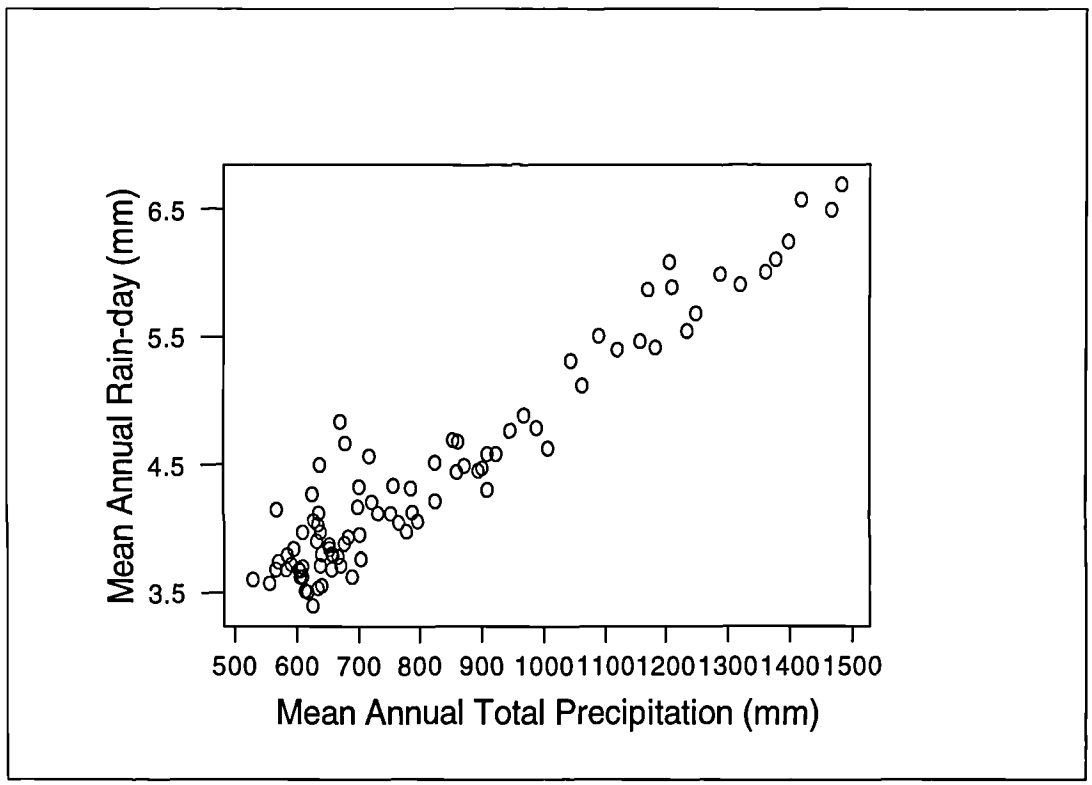

Figure 3-37: Relationship between mean annual rainday (mm) and mean annual precipitation (mm) using the time period from 1970-1990.

An analysis was made of the spatial variability in yield of objective Lamb weather types across Yorkshire. Box-plots of the annual variability in mean daily precipitation and proportion dry days can be found in Figures 3-38 and 3-39 respectively. It can be observed that there is significant spatial variability in both precipitation yield and probability of precipitation for a particular weather type. Westerly and northerly types in particular show large spatial variability. This is due to the precipitation receipt of a northerly or westerly type. A westerly type will bring precipitation to the west but the east will remain dry. The northerly type shows the opposite trend. This was repeated using monthly data (appendix 1, Figures A1-1 to A1-4). It can be seen that the months from June to September show the greatest spatial variability in precipitation receipt for a particular weather type.

Figures 3-40 to 3-42 illustrate the spatial variability in precipitation receipt across Yorkshire associated with the 27 subjective Lamb weather types. Figures 3-43 to 3-45 then show the precipitation receipts associated with the objective weather types. If the two schemes are compared, it can be observed that the anticyclonic and anticyclonic-directional weather types are classified as drier in the subjective scheme than the objective scheme. The opposite is true for the cyclonic and cyclonic-directional weather types. These are wetter in the subjective scheme than the objective scheme. It seems that the objective scheme is a less polarised classification than the subjective Lamb scheme. However, in a spatial sense, the two schemes produce almost identical precipitation maps for a given weather type and the precipitation maps appear physically realistic. Thus, the objective scheme can be used with confidence for precipitation modelling within Yorkshire.

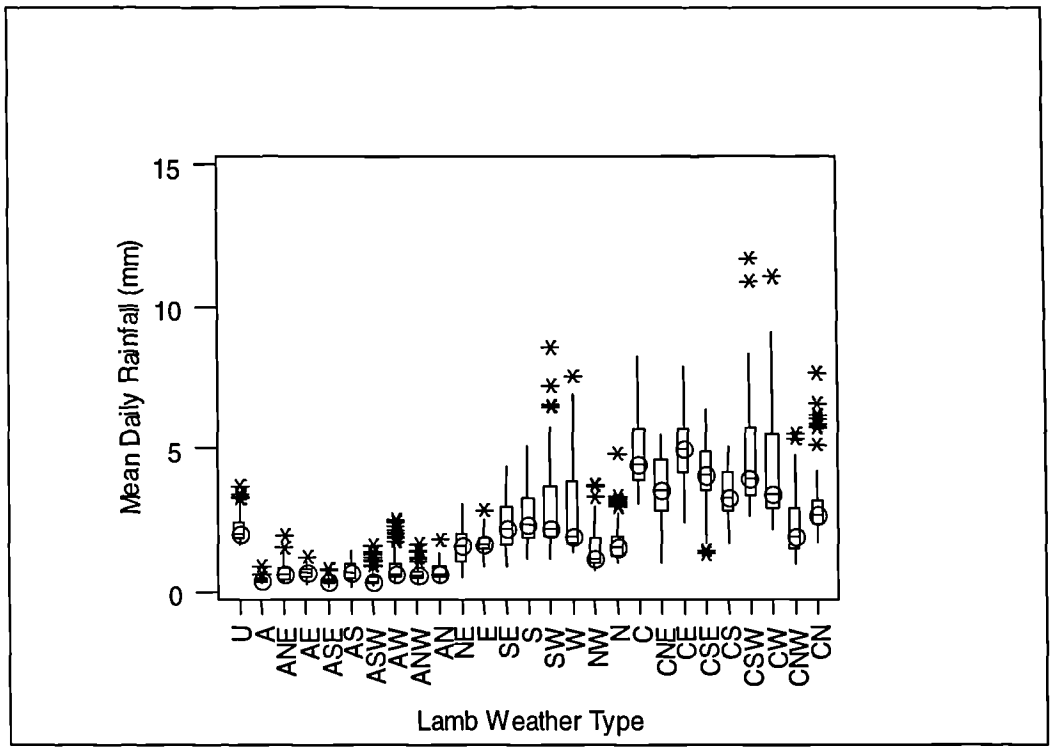

Figure 3-38: Box-plot of variability in annual mean daily precipitation yields for the 27 objective Lamb weather types at sites in Yorkshire from 1961-1990.

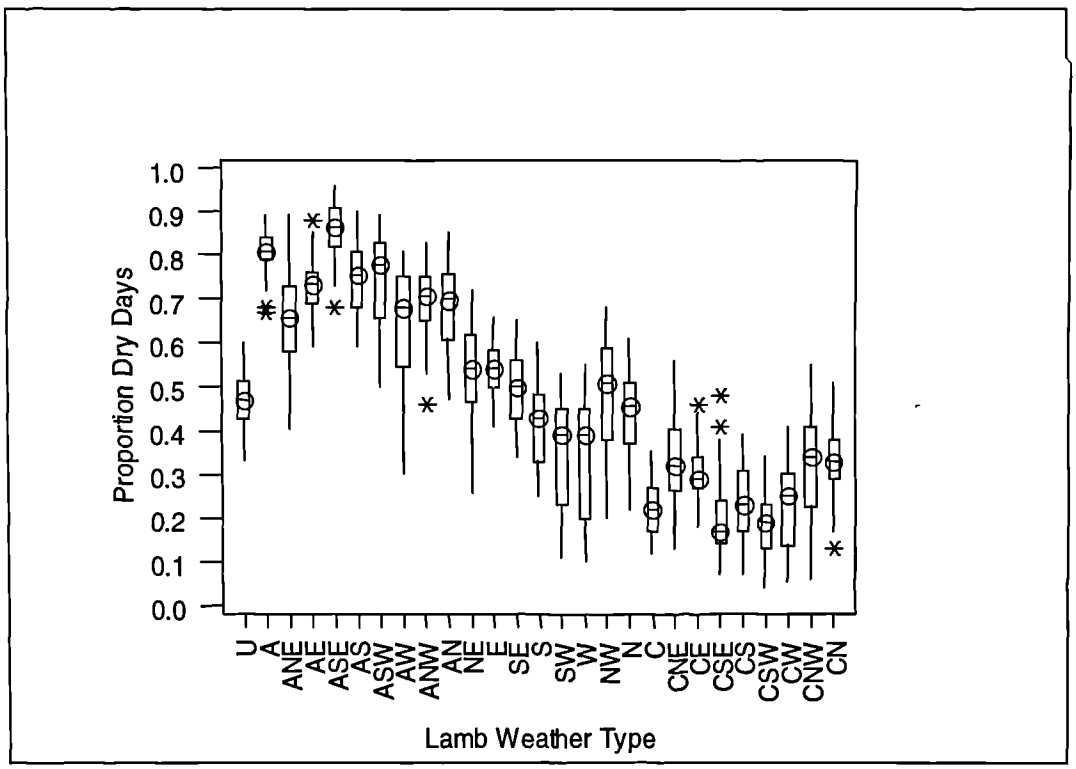

Figure 3-39: Box-plot of variability in annual mean proportion dry days for the 27 objective Lamb weather types at sites in Yorkshire from 1961-1990.

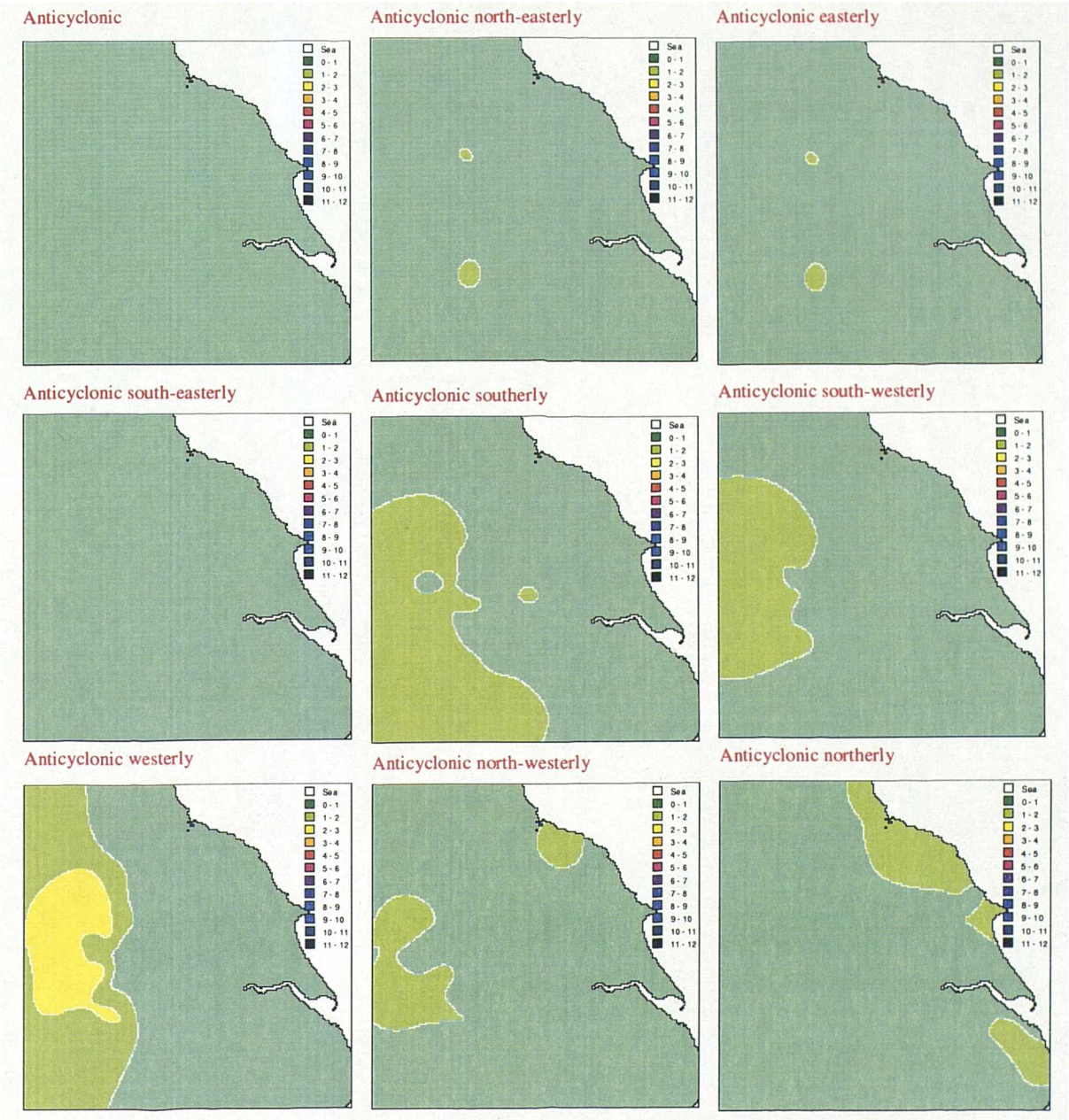

Figure 3-40: Raster maps of spatial patterns of mean annual daily precipitation for Yorkshire (in mm) for the anticyclonic weather types using the Lamb weather types.

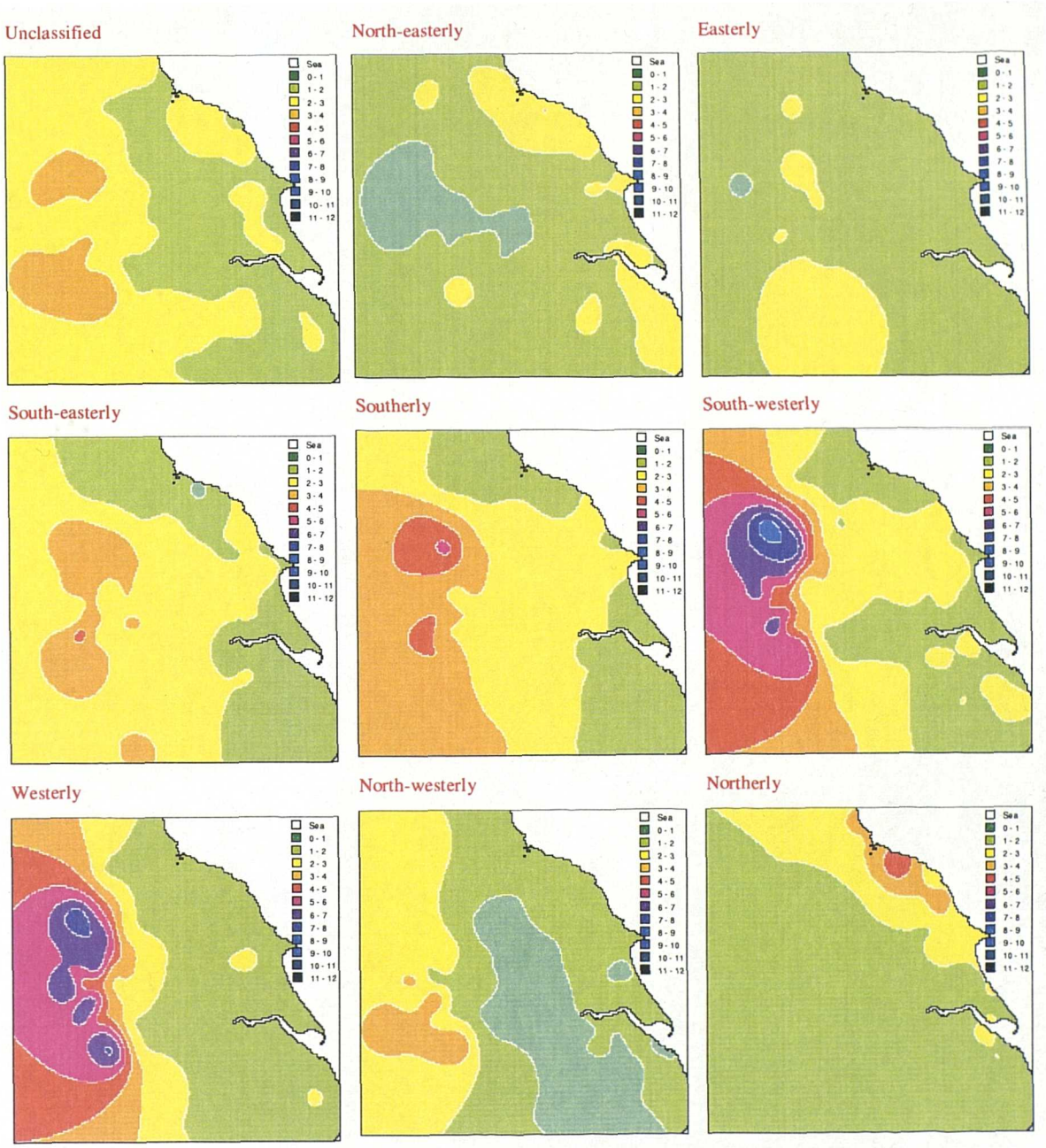

Figure 3-41: Raster maps of spatial patterns of mean annual daily precipitation for Yorkshire (in mm) for the directional weather types and unclassified using the Lamb weather types.

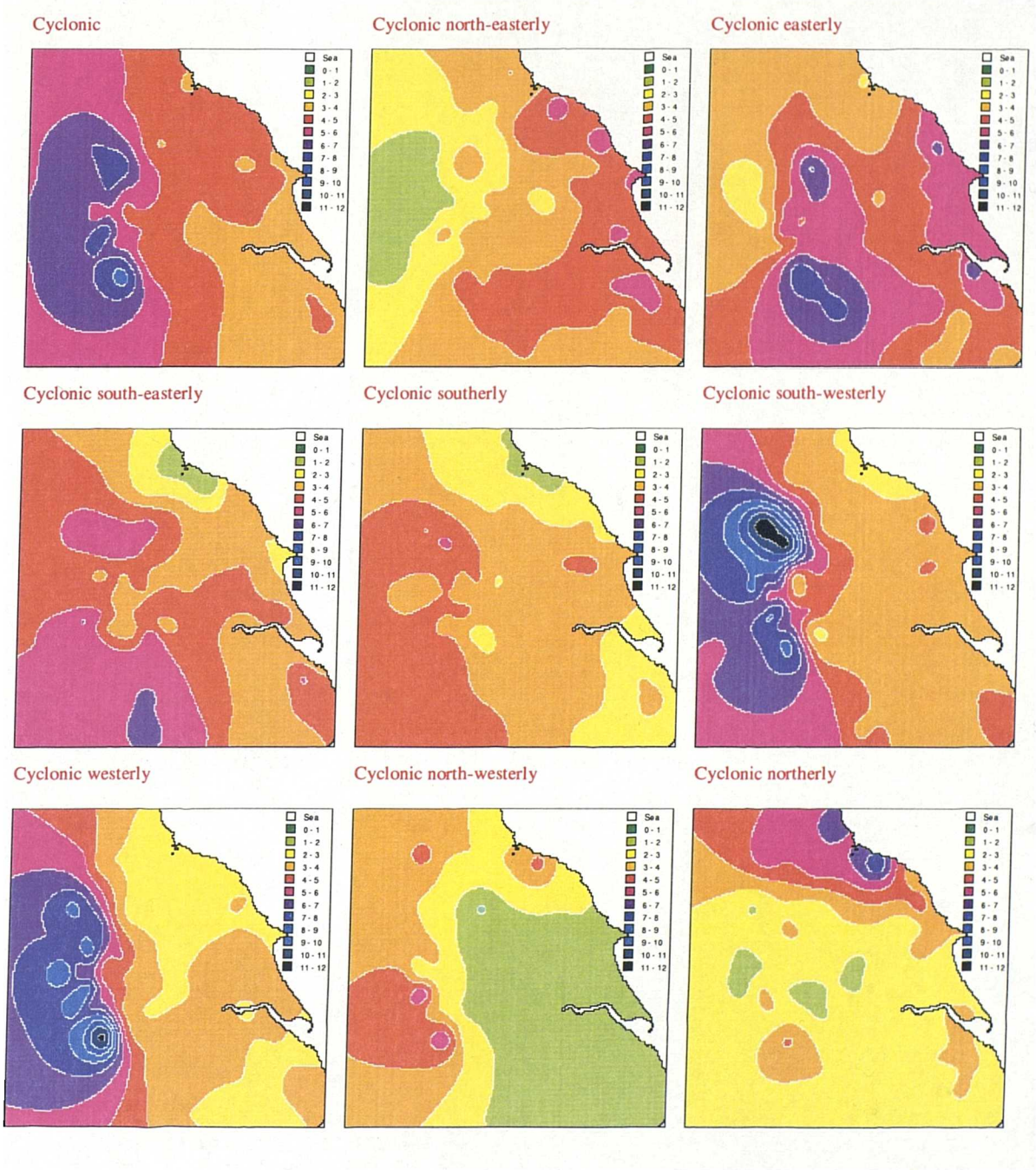

Figure 3-42: Raster maps of spatial patterns of mean annual daily precipitation for Yorkshire (in mm) for the cyclonic weather types using the Lamb weather types.

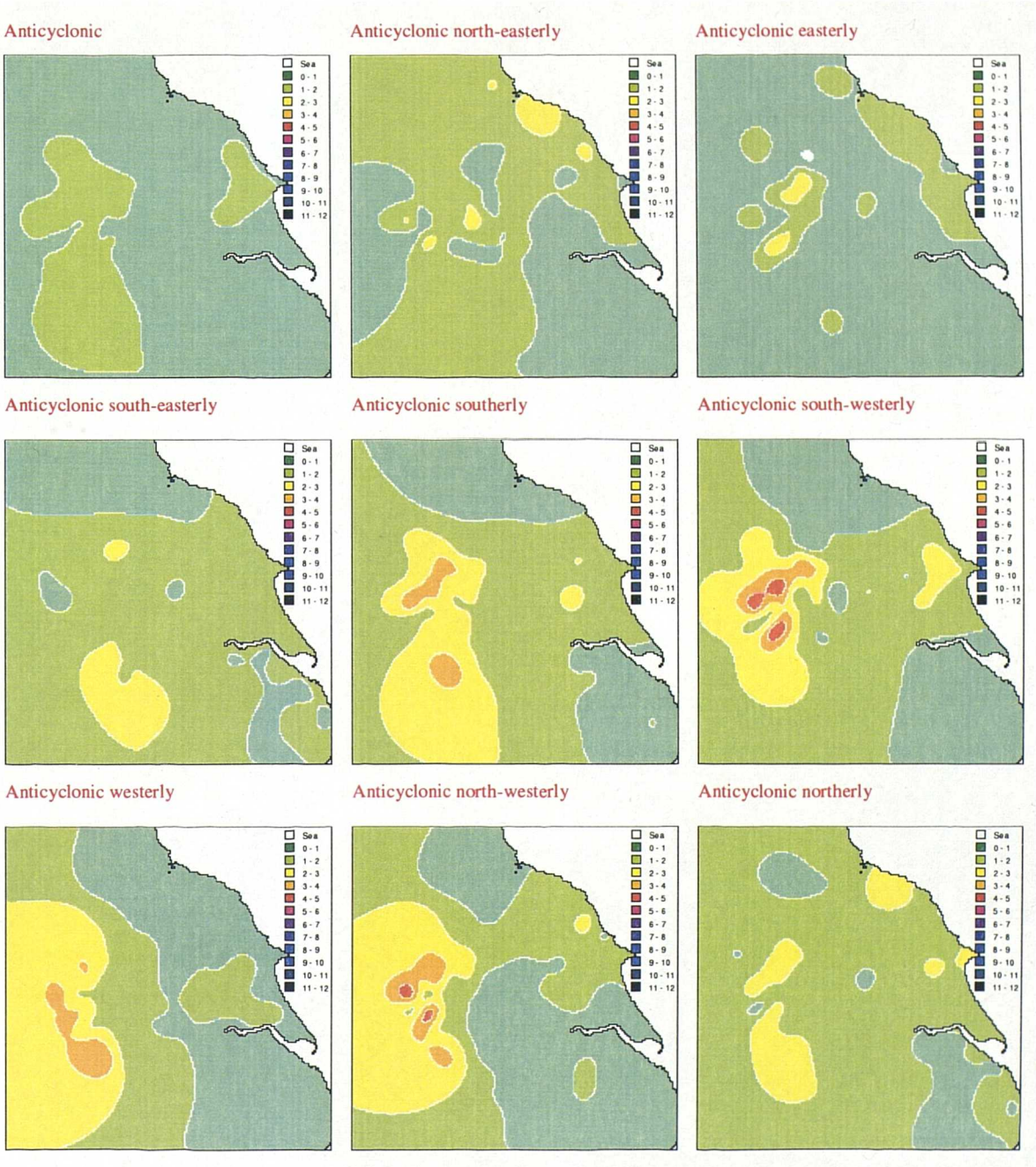

Figure 3-43: Raster maps of spatial patterns of mean annual daily precipitation for Yorkshire (in mm) for the anticyclonic weather types using the objective weather types.

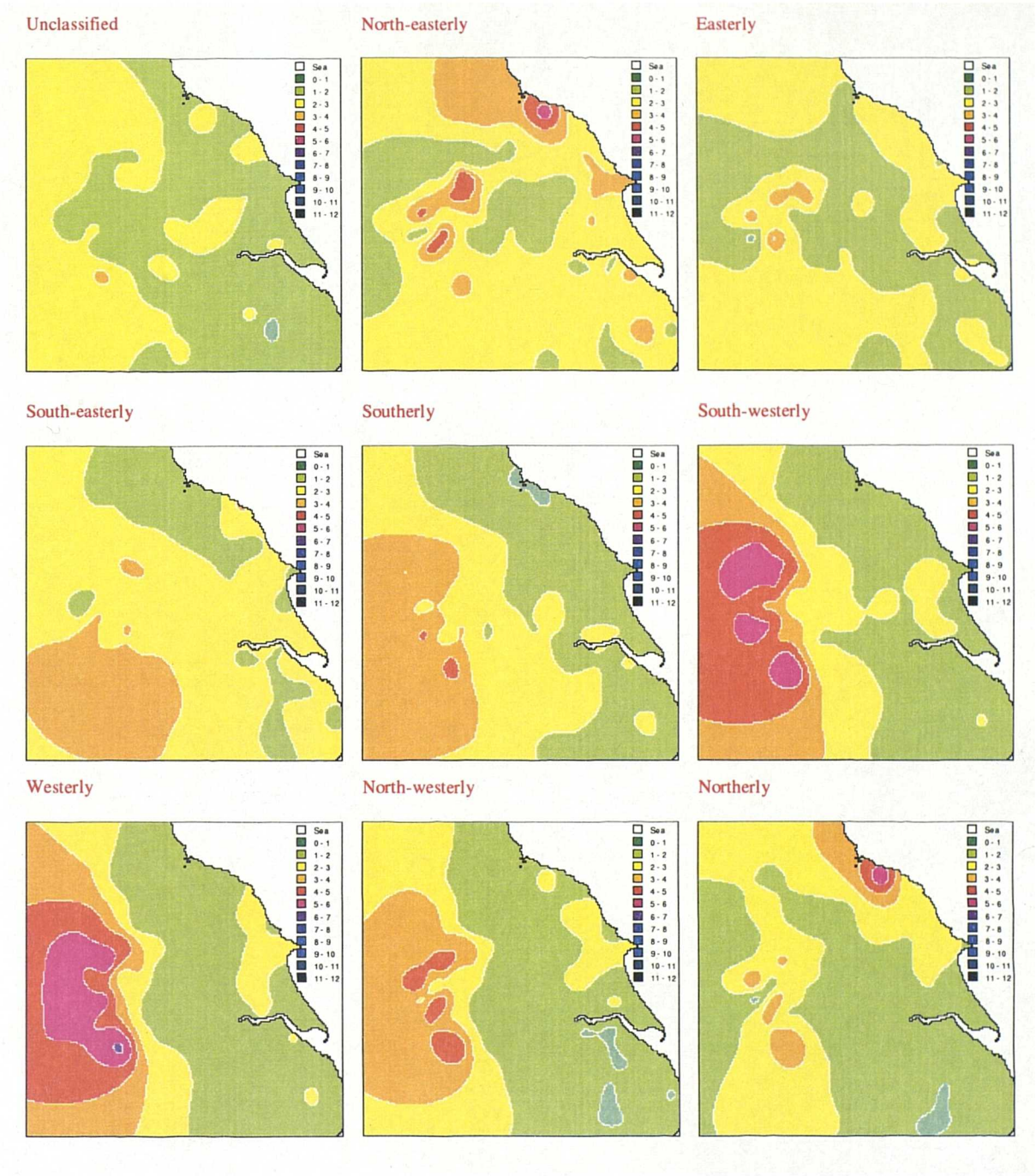

Figure 3-44: Raster maps of spatial patterns of mean annual daily precipitation for Yorkshire (in mm) for the directional weather types and unclassified using the objective weather types.

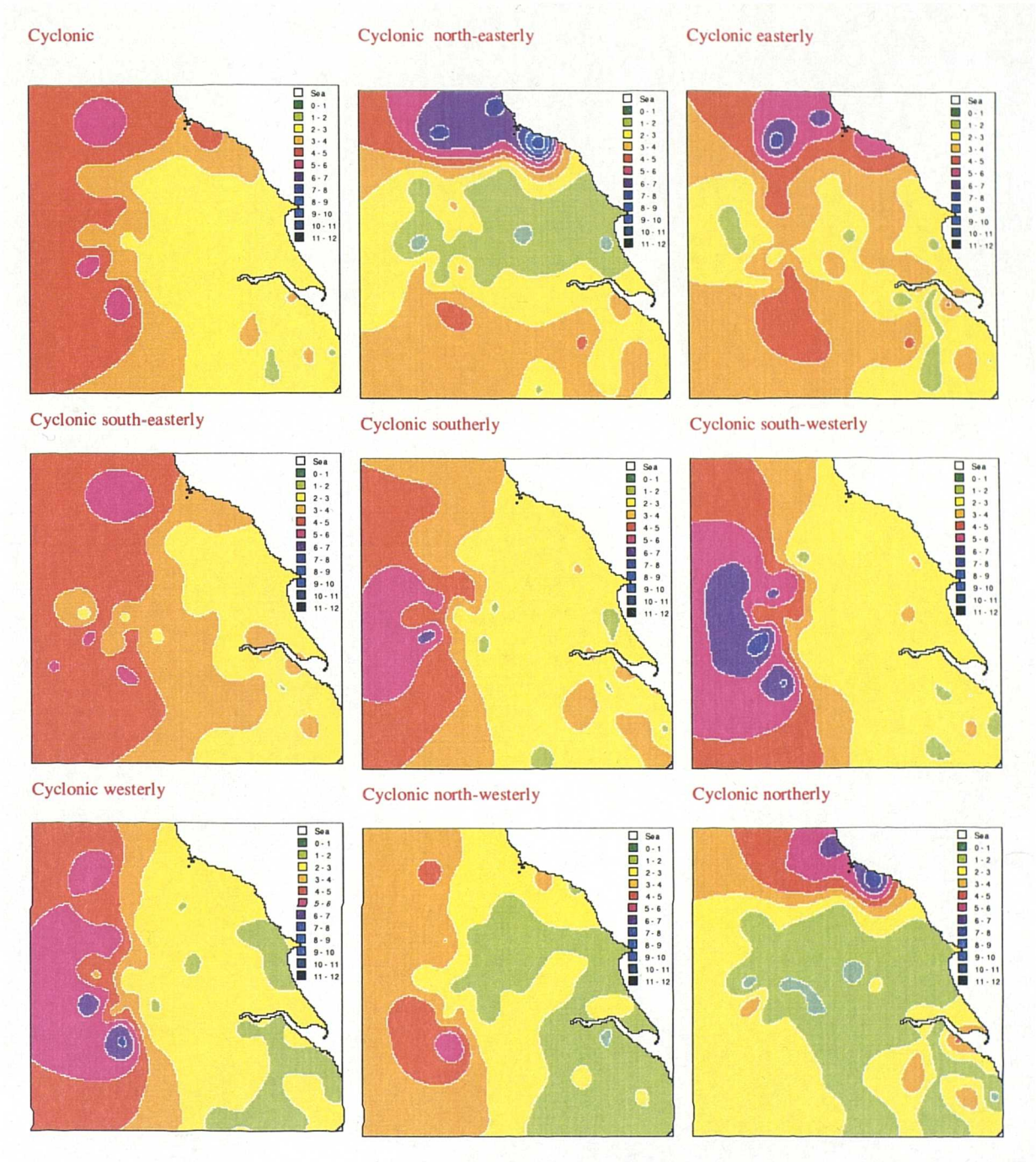

Figure 3-45: Raster maps of spatial patterns of mean annual daily precipitation for Yorkshire (in mm) for the cyclonic weather types using the objective weather types.

Chapter 4: Incidence of drought in Yorkshire

"Individually, the various resources of an undertaking may have a variety of critical drought durations to which they are most susceptible. Thus when one resource fails, another will still have something in hand and if the sources are linked in a system this reserve can be turned into effective yield."

Twort *et al.* (1994)

4.1 Background

The 1990s up to 1996 have been exceptionally dry. This has been noted by Burt *et al.* (1998) and Burt (1999), for Moorhouse (north Pennines) and Blackmoorfoot Reservoir (near Huddersfield, north Yorkshire) respectively. Only the 1880s and the 1930s have recorded more periods of severe drought at Blackmoorfoot. The last 25 years have seen a number of extended droughts in the southern Pennines, many which have encompassed two summers and a dry winter. However, with the recent tendency towards a greater contrast between winter and summer precipitation, with very wet winters and very dry summers, none of the recent Pennine droughts has involved a particularly dry winter. This may imply that severe drought in the Pennines is as much a function of very dry spring and summer weather as of a dry winter (Burt, 1999).

Jones and Lister (1998) used riverflow reconstruction to assess the incidence of hydrologic drought at 15 catchments across England and Wales since 1865. The Wharfe catchment to Addingham was assessed as part of this exercise. This catchment gives a good indication of hydrologic drought in the Yorkshire Pennines. Two consistent drought measures are considered: 6- and 18-month average riverflows ending in September. These measures reflect the short duration droughts experienced by surface reservoirs in the Pennines and Wales and the longer groundwater droughts experienced in the southern half of England respectively. Low flow events are evident on the River Wharfe in 1887/88, 1900/01, 1933/34, 1937/38, and 1975/76. These concur with drought years highlighted by Yorkshire Water, with additionally the years of 1928/29, 1948/49 and 1995/96. Although trends are negligible, there is some decadal scale variability, with drier periods occurring in the 1890s, 1940s and 1990s (Jones and Lister, 1998). These periods may correlate with high phases of the NAO.

Jones *et al.* (1997*a*) calculated the length of dry spells in the British Isles and found that regional differences are less pronounced than for wet spells. Longer dry spells occur in spring than other seasons. It is suggested that the six most extreme short-duration droughts that primarily affect the north of the country have occurred in 1887, 1921, 1929, 1959, 1984 and 1995. Additionally, longer duration droughts occurred from 1854/55, 1869/70, 1933/34,

1975/76 and 1989/90. The droughts that most affected central and northern England were those in 1929, 1959 and 1995.

Goldsmith *et al.* (1997) suggest, in an analysis of northeast England which encompasses some of the Yorkshire region, that in the context of the past century recent drought episodes have been severe locally but not extraordinary. Although the period from 1987-1996 included a large number of severe droughts, so did 1967-1976 and 1947-1956. Events of similar or worse severity, duration and spatial extent occurred in 1905, 1921, 1944, 1973 and 1976. The period from 1977 to 1989 was found to be one of the most drought free this century. The 1984 water supply drought is something of a mystery however, as it does not show up either in duration or severity terms.

However, water resources droughts appear to be occurring more frequently, especially over the last 20 years. These highlight the need for continual reassessment of resources and return period estimates, particularly as demand for water has also increased during this period.

4.2 Using a Drought Severity Index (DSI) to assess drought risk in Yorkshire

4.2.1 Methodology

Several drought severity indices have been developed to assess drought risk but these are not necessarily consistent and reliable. Indices have been based upon precipitation, temperature, evapotranspiration, groundwater levels, river flows. The index used in this study was developed from the accumulated monthly-precipitation deficit concept of Bryant *et al.* (1992), and is similar to that used by Phillips and McGregor (1998) in an analysis of drought risk in southwest England. Mawdsley *et al.* (1994) recommend the use of this type of index as, unlike the Palmer index, it requires little data and can be easily interpreted by users.

The monthly precipitation anomaly, defined in terms of the 1961-1990 mean, provides the only input to the drought severity indices, of which there are two: DSI_3 and DSI_6. DSI_3 uses a three-monthly initiation and termination sequence, after Bryant *et al.* (1992; 1994) and Mawdsley *et al.* (1994). DSI_6 uses a six-monthly rule (after Marsh *et al.*, 1994) and can be thought of as more of a measure of hydrological drought than DSI_3 as precipitation totals over the preceding six months are considered. Drought termination rules can be adapted to suit the dominant water resource of an area by varying the critical duration for which precipitation is aggregated. It is suggested (Goldsmith *et al.*, 1997) that for the northeast region a 3-month termination rule is

appropriate for surface water resource areas, with a 6-month rule for groundwater resource areas.

The formulae used to calculate DSI_3 are given as an example. Those used for DSI_6 are the same only using a six-month period. The precipitation anomaly in month t is denoted Xt. If X_t is negative and precipitation in the preceding three-month period, i.e. Xt, X_{t-1}, X_{t-2}, is also lower than its mean, then a drought sequence is initiated. DSI_3 is assigned a positive value proportional to the precipitation deficit in month t. If the month $t+1$ is then considered and the precipitation deficits in months t and $t+1$ are $-X$ mm and $-Y$ mm respectively, then DSI_3 for month $t+1$ will be $X+Y$ if the mean monthly precipitation total for the preceding three months has not been exceeded. If the precipitation anomaly is positive in month t+1 then the drought can continue only if the three-monthly mean total has not been exceeded, with $DSI_3 = X - Y$. Termination of a drought occurs immediately as the three-monthly mean total has been exceeded, and DSI_3 is assigned a value of zero. DSI_3 and DSI_6 are standardised by dividing the absolute deficit (mm) by the site mean-annual precipitation, and then multiplying by 100 to enable inter-station comparisons. The final index value expresses the accumulated deficit as a percentage of mean annual precipitation.

4.2.2 Comparison of drought severity indices

The drought severity indices, DSI_3 and DSI_6, were used to assess drought risk at the seven stations where long precipitation records are available: Hury Reservoir, Barnard Castle, Raby Castle, Lockwood Reservoir, Scarborough, Moorland Cottage and Kirk Bramwith (details given in Table 3-1, locations in Figure 3-1). These sites should show the intra-regional variability in drought risk that can be seen within a single drought event.

The drought severity indices were compared using the Spearman rank-order correlation coefficient (after Phillips and McGregor 1998) as about one half of the DSI values are zero (Figures 4-1 and 4-2). Coefficients were calculated using the 718 months common to all seven sites and can be found in Table 4-1. All coefficients shown are statistically significant at the 95 percent level.

When a comparison is made of the DSI_3 time series, the largest correlation in drought behaviour is found between Barnard Castle and Hury Reservoir (both located in the northern Pennines), Scarborough and Lockwood Reservoir (both located in east Yorkshire), Moorland Cottage and Hury Reservoir (both in the Pennines), and Raby Castle and Barnard Castle (both in the

northern Pennines). The lowest associations are found between Moorland Cottage and the sites of Lockwood Reservoir, Kirk Bramwith and Raby Castle. Lockwood Reservoir and Kirk Bramwith are both found in the east of the region and Raby Castle is thought to be affected by the Pennine rain-shadow, whereas Moorland Cottage is located in the Pennine west.

	DSI_3						DSI_6						
	47060	29156	28408	28106	37225	87024	34458	47060	29156	28408	28106	37225	87024
DSI_3													
34458	0.22	0.44	0.45	0.37	0.61	0.43	0.16	0.07	0.14	0.16	0.13	0.18	0.16
47060		0.25	0.35	0.53	0.22	0.27		0.19		0.10	0.13		
29156			0.56	0.43	0.39	0.35	0.07	0.10	0.16	0.12	0.14	0.11	0.13
28408				0.62	0.51	0.37	0.14		0.13	0.26	0.16	0.23	0.18
28106					0.44	0.38			0.11	0.19	0.15	0.14	0.11
37225						0.47	0.16	0.08	0.14	0.19	0.14	0.27	0.19
87024							0.17	0.12	0.19	0.22	0.19	0.21	0.35
DSI_6													
34458								0.10	0.38	0.28	0.24	0.50	0.35
47060									0.21	0.31	0.47	0.19	0.19
29156										0.49	0.47	0.38	0.35
28408											0.61	0.38	0.40
28106												0.32	0.32
37225													0.42

Table 4-1: Cross-correlation between the drought severity indices DSI_3 and DSI_6 at the seven sites, using the 718 month period common to all locations (October 1936-December 1996). All coefficients shown are significant at the 95 percent confidence level.

For the DSI_6 index, the strongest associations are again between Barnard Castle and Hury Reservoir, Scarborough and Lockwood Reservoir, Moorland Cottage and Hury Reservoir, Raby Castle and Hury Reservoir, and Raby Castle and Barnard Castle. This suggests both a consistency in drought behaviour, and that the sites can be split into two major groups; a Pennine group and those found to the east of the Pennines. The low correlation found between eastern sites and the Pennine site of Moorland cottage also reinforces this conclusion.

Correlations between the two indices are weaker, especially when indices from two different sites are compared. This concurs with Phillips and McGregor (1998). The correlations between sites in Yorkshire are nowhere near as high as those determined for locations in Cornwall however, and this suggests that the climatology of Yorkshire is more spatially variable.

Of the seven sites shown in Figures 4-1 and 4-2, precipitation deficits are least likely to occur at Lockwood Reservoir (see Table 4-2). Over 46 percent of months at Lockwood Reservoir were assigned a DSI of zero.

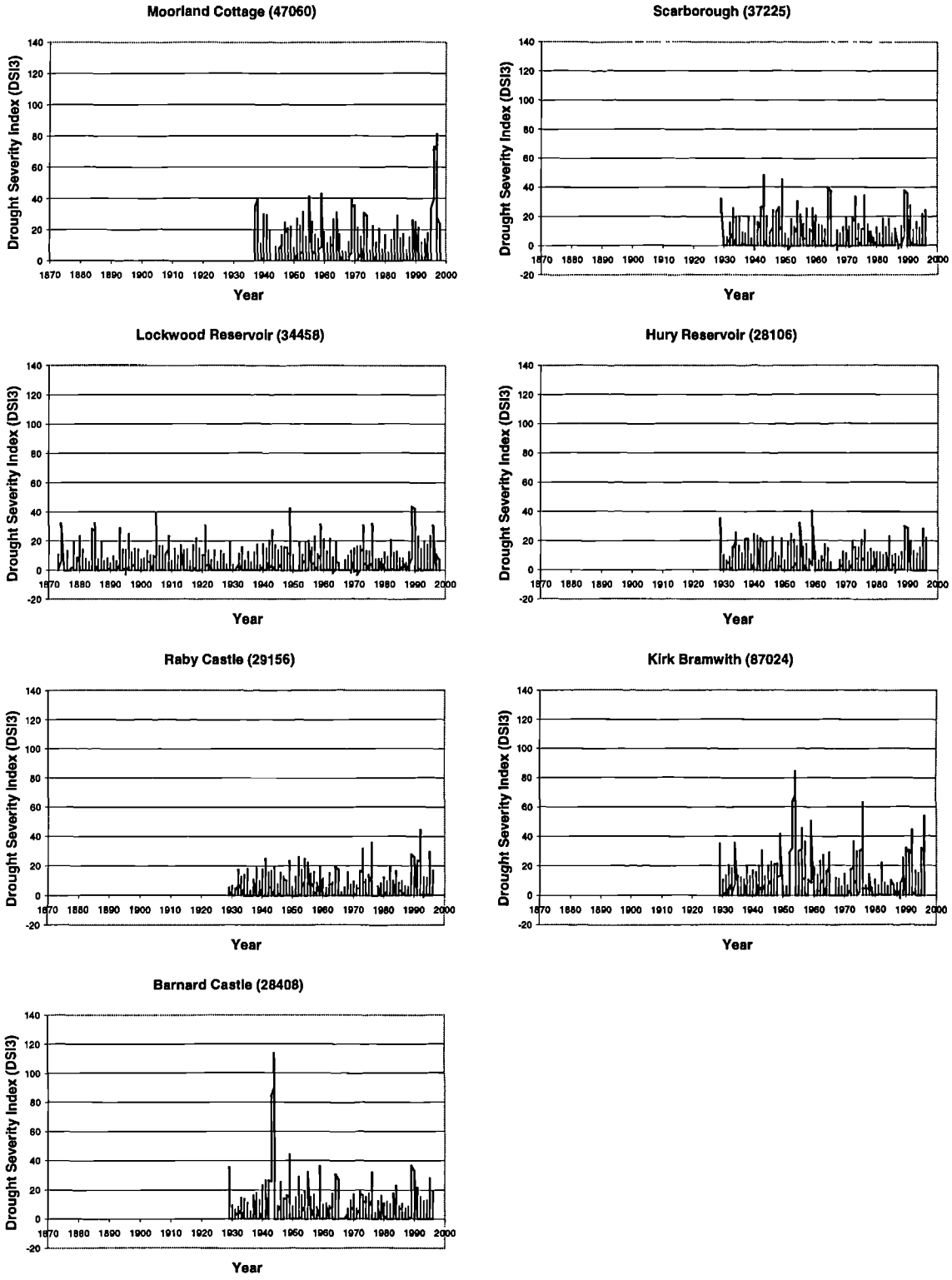

Figure 4-1: Comparison of drought behaviour at the seven long record sites using DSI_3.

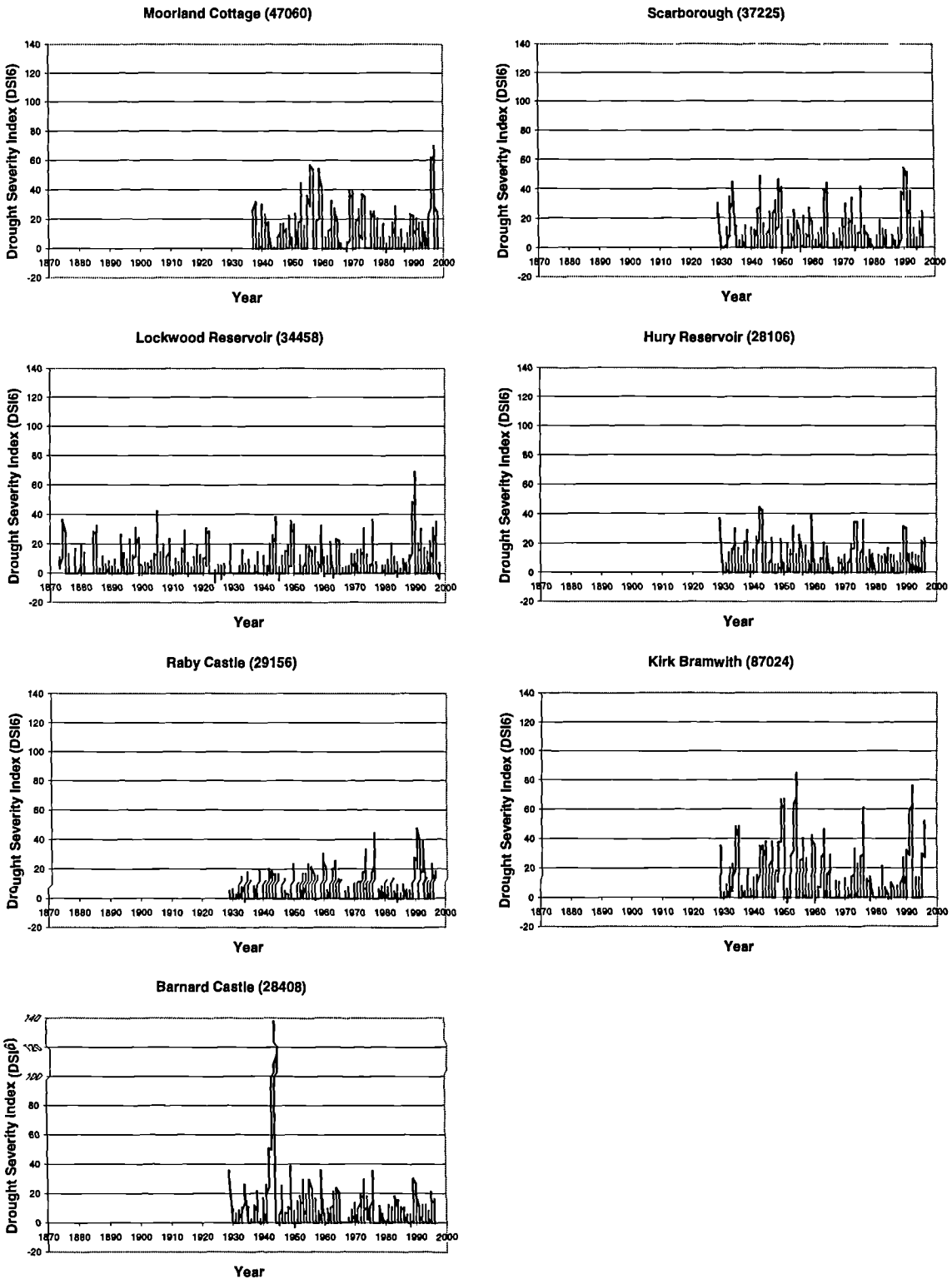

Figure 4-2: Comparison of drought behaviour at the seven long record sites using DSI_6.

	47060		29156		34458		28408		28106		37225		87024	
	DSI_3	DSI_6	DSI_3	DSI_6	DSI_3	DSI_6	DSI_3	DSI_6	DSI_3	DSI_6	DSI_3	DSI_6	DSI_3	DSI_6
<0	0.0	0.8	0.4	1.1	0.2	0.5	0.1	0.8	0.2	0.8	1.0	0.6	0.3	0.7
=0	39.4	39.1	45.1	50.6	46.6	48.2	43.4	43.9	43.9	43.7	43.1	45.0	43.6	44.7
>0	60.6	60.1	54.5	48.3	53.2	51.3	56.5	55.3	55.8	55.5	55.9	54.5	56.1	54.6

Table 4-2: Comparison of drought sequence initiation, in terms of the number of months in which the DSI values were positive, negative or equal to zero. Figures shown are the percentage of total months at a site that satisfied the criterion (after Phillips and McGregor 1998).

Negative values occur when a surplus develops in a shorter time frame than that considered by the index. Interestingly, of the seven sites, the site where a precipitation deficit is most likely to occur is Moorland Cottage, which is located in the Pennines and gives an indication of precipitation supply to the Pennine reservoirs. Lowland sites in the east of the region are also likely to suffer precipitation deficits.

4.2.3 Identifying significant drought events in Yorkshire

Phillips and McGregor (1998) used the number of indices simultaneously exceeding an arbitrary value of ten to determine drought severity and spatial extent. To be classed as a Class I drought, both indices at all four locations must exceed ten, and these months are then termed the 'core' months of the drought.

If the same methodology is applied to the seven sites in Yorkshire, assuming that the indices from sites where data is available for that period all exceed ten simultaneously, many Class I droughts can be observed. These occur in 1893, 1896, 1898, 1905/06, 1909, 1913/14, 1921/22, 1929, 1940, 1942, 1949, 1952, 1955, 1957, 1959, 1962, 1964, 1972, 1975/76, 1989/92 and 1995/96. An in-depth study will be made of the Class I droughts occurring since 1900 (see Table 4-3).

An analysis was also made of the circulation anomalies associated with each of the 14 major Class I droughts identified in Yorkshire during the last century (Table 4-3). The objective Lamb weather types (Jones *et al.,* 1993) were aggregated into eight groups using the classification method of Phillips and McGregor (1998), but omitting the unclassified group. This classification is considered ideal for distinguishing drought patterns in areas of Yorkshire as northerly and easterly winds will generally bring rain only to the north-eastern part of the region, whereas westerly and southerly winds will precipitate mostly in the west.

Drought	Duration	A	C	N&E	S&W	A N&E	A S&W	C N&E	C S&W
1905/6	Jan 1905 – Dec 1906	0.4	-19.3	2.1	8.3	-36.2	21.5	11.8	-22.1
1913/4	Jun 1913 – Dec 1914	-3.5	-21.0	-19.0	13.4	-6.4	15.9	-32.3	-5.4
1933/5	Apr 1933 – Apr 1935	-0.1	4.4	-6.0	-2.3	-14.0	5.4	-14.4	15.3
1941/4	Jul 1941 – Oct 1944	31.6	-7.8	2.3	1.5	-7.8	3.2	-37.6	2.9
1948/9	Jul 1948 – Apr 1950	14.0	-39.0	-38.9	17.9	-19.8	2.1	-23.1	19.7
1952/4	May 1952 – Oct 1954	-10.2	-6.4	-7.3	9.0	6.6	22.5	-31.7	-1.7
1955/7	Apr 1955 – Feb 1957	2.0	-26.1	-11.9	3.6	52.3	25.3	-9.9	-17.0
1959/60	Jan 1959 – Feb 1960	15.3	11.4	-8.2	-8.7	-23.6	8.9	-9.7	-9.0
1962/3	Oct 1962 – Dec 1963	-35.1	9.4	32.8	-5.2	67.7	-15.2	54.3	7.1
1963/65	Feb 1964 – Oct 1965	-19.6	-24.1	5.7	20.7	-7.2	8.9	-13.9	13.4
1972/4	Sep 1972 – Feb 1974	15.1	-19.5	-38.4	12.8	-33.3	17.6	-28.0	-14.7
1975/6	Apr 1975 – Dec 1976	15.4	-21.6	0.1	4.0	-0.4	2.4	-7.5	-16.7
1988/92	Dec 1988 – Dec 1992	4.8	-23.1	-15.4	15.3	-10.7	-7.7	-19.4	7.5
1995/6	May 1995 – Feb 1997	9.8	-6.5	39.7	-14.1	35.2	1.6	5.1	-30.0

Table 4-3: Percentage anomalies for each of the aggregated objective Lamb weather types for Class I droughts occurring this century in Yorkshire when compared to the average for the period from 1861-1990.

4.2.3.1 The 1905/06 drought

Using the drought indices of Phillips and McGregor (1998), the first notable drought of this century occurred in 1905/06 (Figure 4-3). Lockwood Reservoir and Kirk Bramwith are the only sites with long enough records to record this event. The drought contains two peaks: August 1905 and November 1906. If the index DSI_6 is used then the degree of severity is increased. This is particularly true at Kirk Bramwith where the two-peaked drought event becomes a more severe continuous drought event throughout 1905 and 1906.

Large percentage anomalies are apparent in several of the aggregated objective weather types in 1905-06 (Table 4-3). The most prominent change is a reduction in the anticyclonic N&E clustered type of 36.2 percent. A large reduction is also noted in both the cyclonic (19.3 percent) and the cyclonic S&W (21.5 percent) clusters. The easterly types (N&E and C N&E), conversely, show an increase of about 10 percent. A decline in the cyclonic type would be expected to produce lower precipitation totals in the eastern region of Yorkshire. However, the concurrent decline in the cyclonic westerlies suggests that the drought of 1905/06 may have been a region-wide event.

4.2.3.2 The 1913/14 drought

The 1913/14 drought is recorded at the sites of Lockwood Reservoir, Kirk Bramwith and Scarborough (see Figure 4-4). The drought initialises in June 1913 and is terminated at all sites by December 1914. Using DSI_3 the highest severity is recorded in July 1914 at Scarborough. However, hydrologically, the drought was more severe at Kirk Bramwith which records a continuous 19-month $DSI_6 > 10$ sequence and the highest severity, 50.5, in August 1914. At Scarborough, using DSI_6, the drought is as severe as at Kirk Bramwith but is terminated three months earlier in September 1914. The 1913/14 drought is, however, not as severe at Lockwood Reservoir.

During this drought event, a large decline is recorded in easterly types. The two rain-bearing types for the eastern region, C N&E and N&E, record decreases of 32.3 and 19 percent respectively. An increase is noted in westerly occurrence. A large decrease of 21 percent is also recorded in the cyclonic type. These patterns are consistent with an 'eastern' drought that only mildly affected the Pennines.

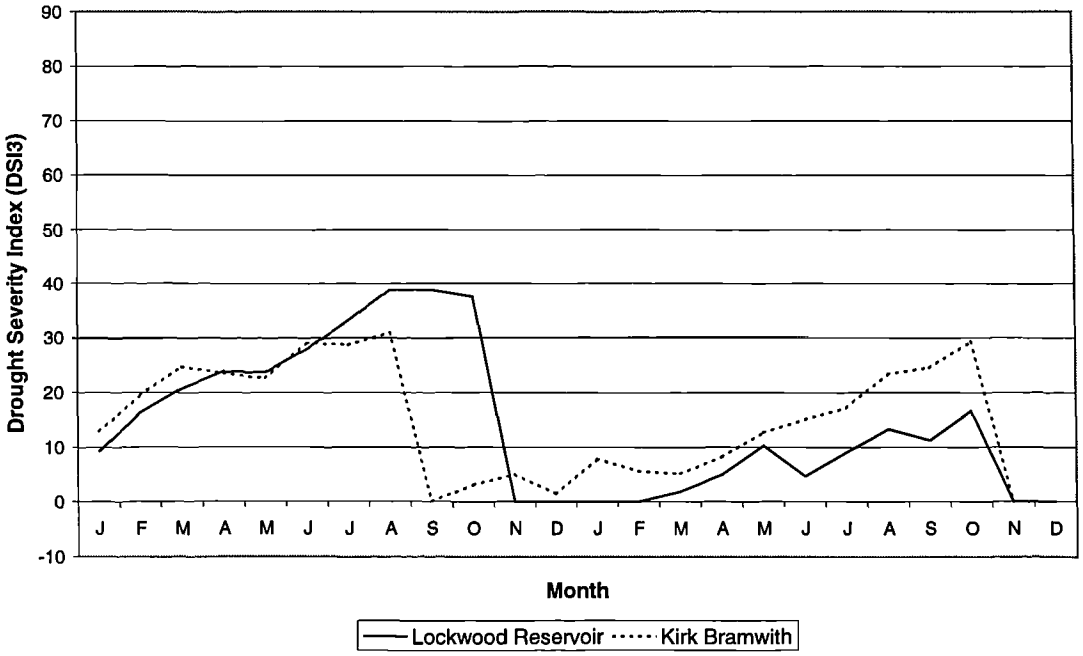

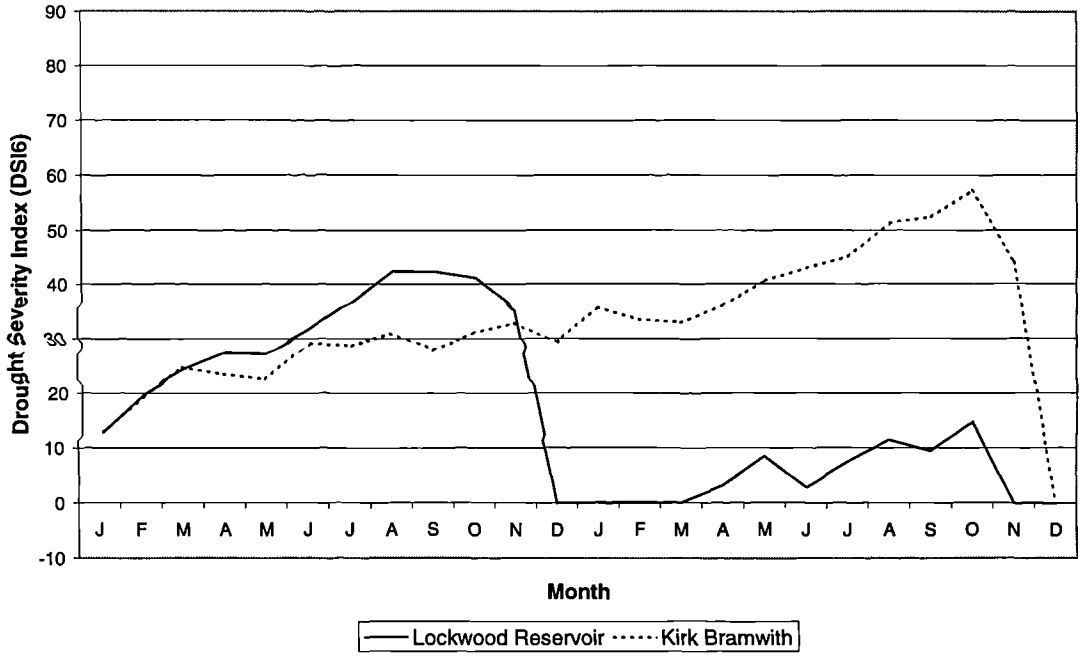

Figure 4-3: DSI_3 and DSI_6 for the 1905/06 drought. Time series start in January 1905 and finish in December 1906.

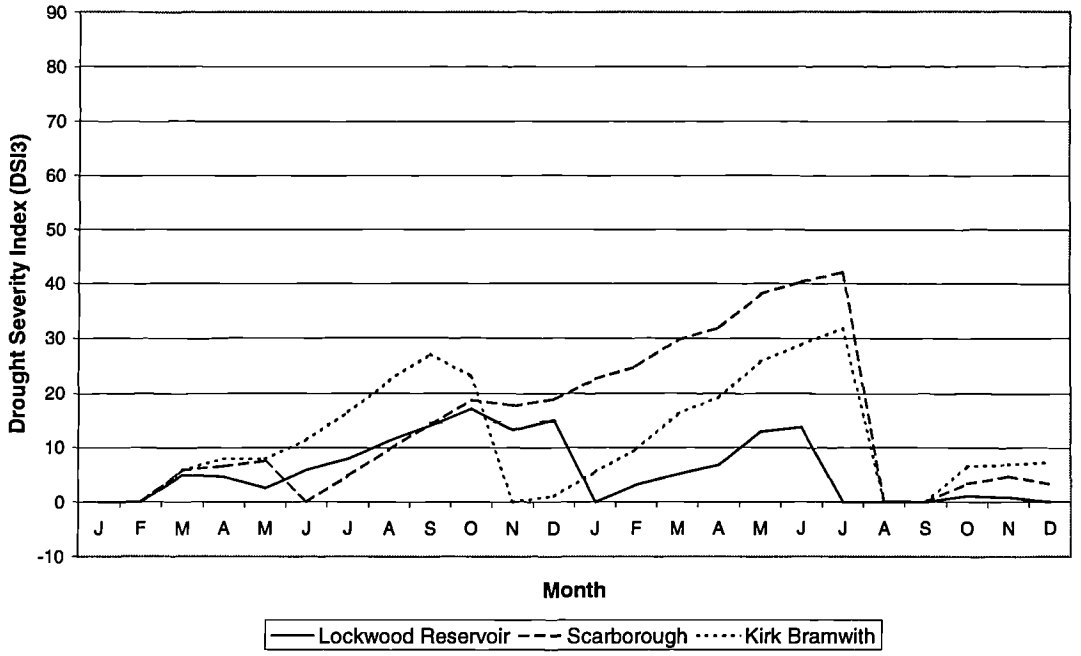

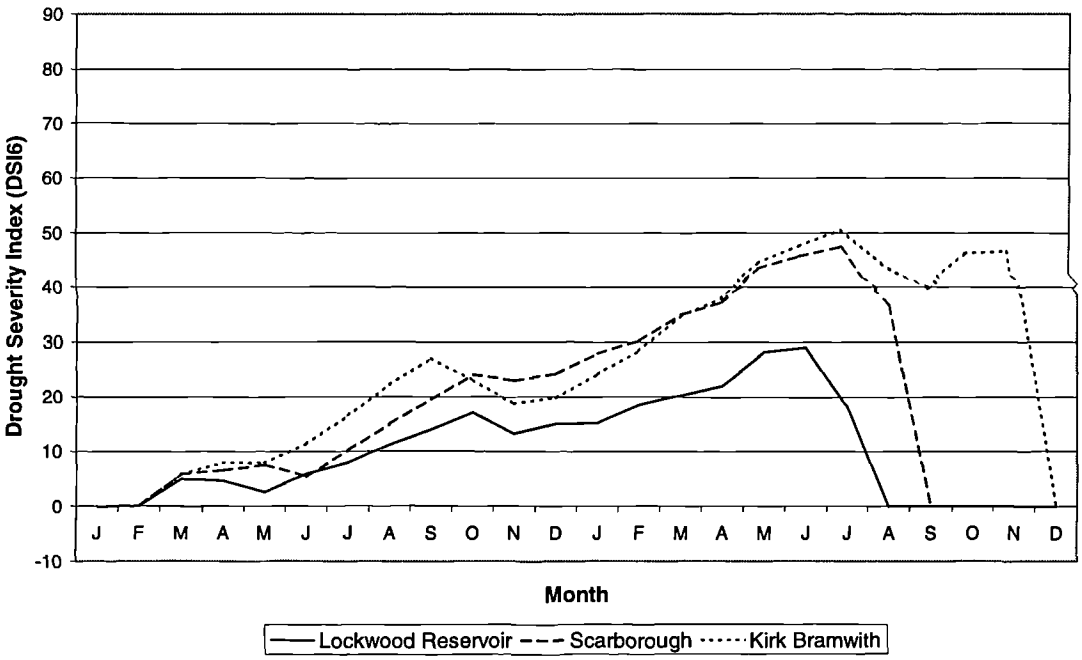

Figure 4-4: DSI_3 and DSI_6 for the 1913/14 drought. Time series start in January 1913 and finish in December 1914.

4.2.3.3 The 1933/35 drought

During the 1933/34 period, data is available from all long record sites except for Moorland Cottage (see Figure 4-5). The drought starts in April 1933 and terminates at most sites by January 1935, the exception being Kirk Bramwith where the drought sequence terminates four months later. The drought is more severe at the eastern sites of Kirk Bramwith and Scarborough than the more western sites. Interestingly though, the site of Lockwood Reservoir in the North York Moors documents very low precipitation deficits during this time-period. The maximum severity of the drought was felt in November and December 1934.

The major characteristic of the 1933-35 drought was a decline in frequency of the easterly types (N&E, A N&E and C N&E) (Table 4-3). This decrease was over 12 percent for both cyclonic easterly and anticyclonic easterly types. This was countered by an increase in the occurrence of cyclonic westerly types. However, the decline in cyclonic easterly types caused a drought in the eastern region of Yorkshire. The drought was less severe in western areas as the westerly weather types were the main bearers of precipitation during this period.

4.2.3.4 The 1941/44 drought

The 1941/44 period provides a 40-month continuous sequence of drought at Barnard Castle, terminating in October 1944 and reaching a highest severity of 137.0 (see Figure 4-6). Other sites show much smaller drought severities during this period. During the latter half of the time-period a drought can be observed at the eastern sites of Lockwood Reservoir and Kirk Bramwith, and during the first half of the period a drought can be seen in all areas. A question mark must be thrown at the data from Barnard Castle during the period from 1941 to 1944, given its proximity to Hury Reservoir and the fact that this site does not show the same severity of drought.

During the period from July 1941 to October 1944 there was a strong decline in cyclonic and cyclonic easterly weather types (i.e. C and C N&E) (Table 4-3) of 7.8 and 37.6 percent respectively. This was accompanied by a large increase in anticyclonic types of 31.6 percent. There was no real change in westerly type occurrence. This explains the drought in the east of the region but lesser effects in the west. However, it does not validate the drought indices determined for Barnard Castle.

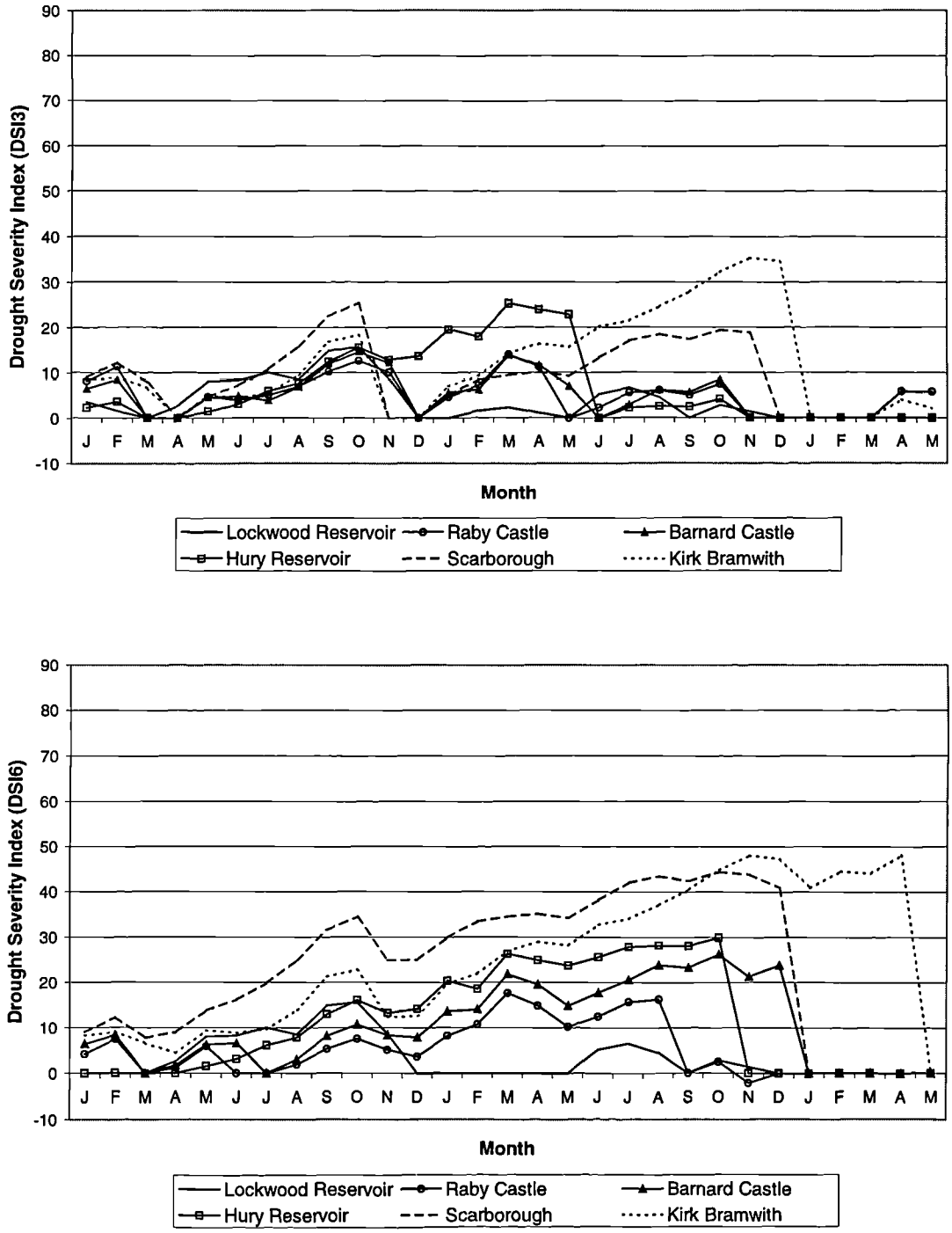

Figure 4-5: DSI_3 and DSI_6 for the 1933/35 drought. Time series start in January 1933 and finish in May 1935.

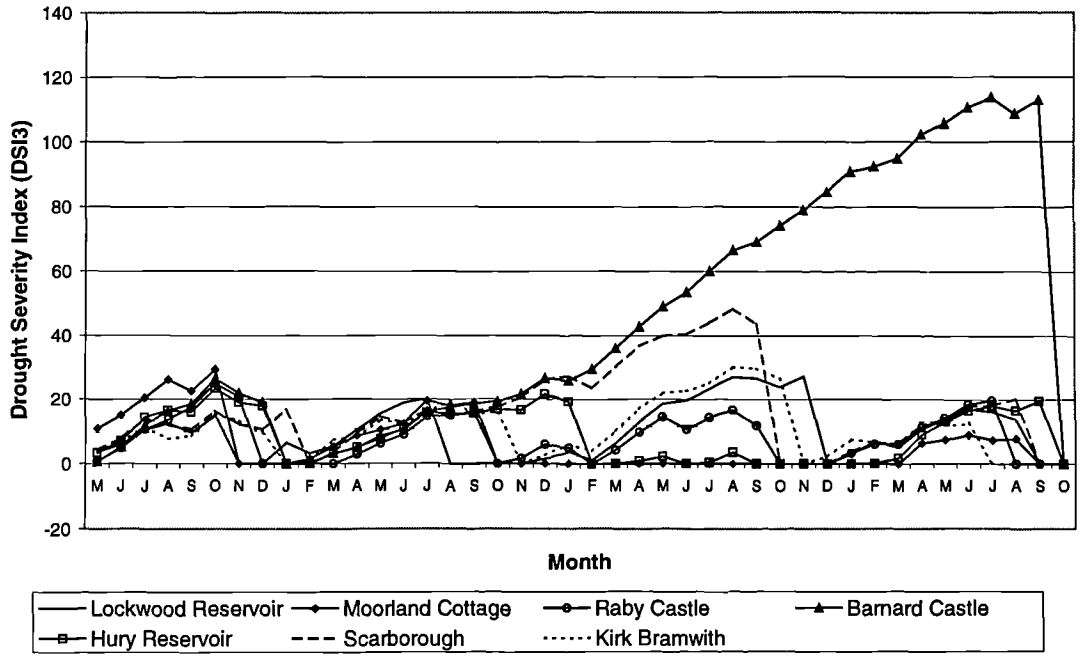

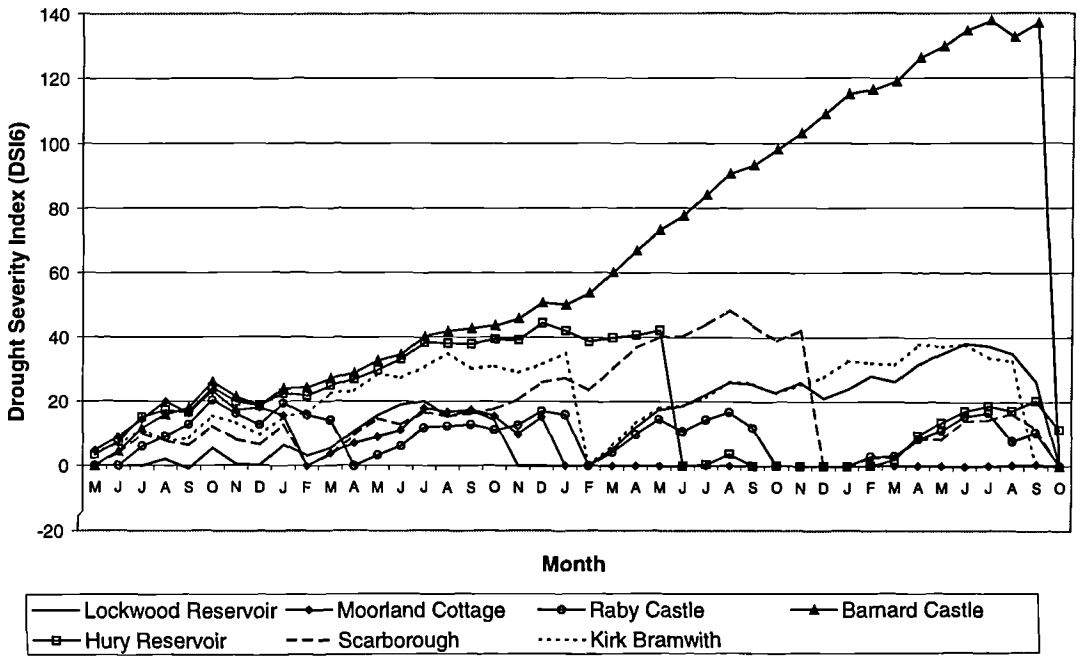

Figure 4-6: DSI_3 and DSI_6 for the 1941/44 drought. Time series start in May 1941 and finish in October 1944.

4.2.3.5 The 1948/50 drought

The 1948/50 drought affected the east of the region far more severely than the west (see Figure 4-7). It is evident that the drought is longer and more severe if the DSI_6 index is used. However, there is spatial variation in intensity and duration. The drought is initialised at Kirk Bramwith prior to April 1948 but starts at other locations within Yorkshire around January 1949, and terminates by the beginning of 1950.

The aggregated Lamb weather types show strong changes in their normal frequencies during this period (Table 4-3). In a similar pattern to other recorded 'eastern' droughts, the easterly types show a decline. This is especially severe from 1948 to 1949 and amounts to some 38.9 percent of the average occurrence. Cyclonic and cyclonic easterly types also show a decrease in frequency of 39 and 23.1 percent respectively. Conversely, westerly types show an increase of nearly 20 percent and the anticyclonic type shows an increase of 14 percent. Therefore, it would be expected that the western half of the Yorkshire region would be well supplied with precipitation but the eastern half would experience drought conditions.

4.2.3.6 The 1952/54 drought

The 1952/54 drought can be split into two halves: the drought in 1953 severely affecting the west of Yorkshire, and in 1954 the east was more affected (see Figure 4-8). The exception to this is Kirk Bramwith that, although located in the east of the catchment, recorded a high drought severity throughout the time-period. It is likely that the record at Kirk Bramwith is erroneous during this period given that other eastern sites do not show the same severity of drought. The drought shows a similar pattern at all western sites, initiating in May 1952 and terminating by December 1953. At eastern sites two short-term, low-severity droughts are recorded: from July to October 1952 and from April to October 1954. Kirk Bramwith again records the longest continuous drought sequence and highest severity, peaking in May 1954.

During this period, the aggregated Lamb weather types show changes that would correlate with a regional drought (Table 4-3). There are small decreases in all weather types, excepting the very large decrease of 31.7 percent in the cyclonic easterly type. The anticyclonic westerly and easterly types show increases however.

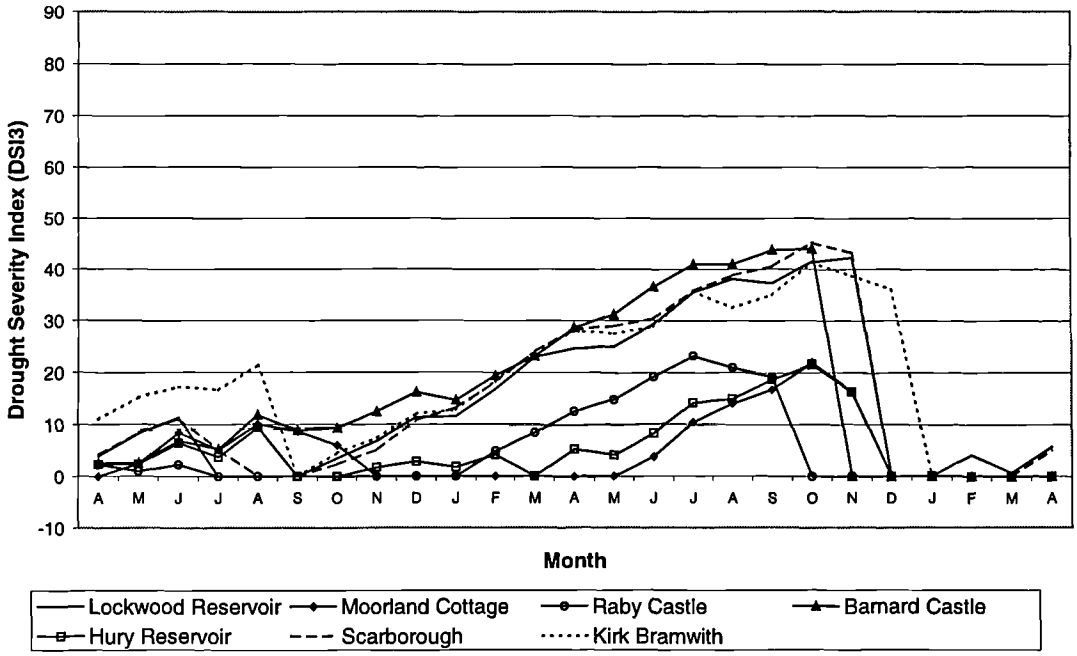

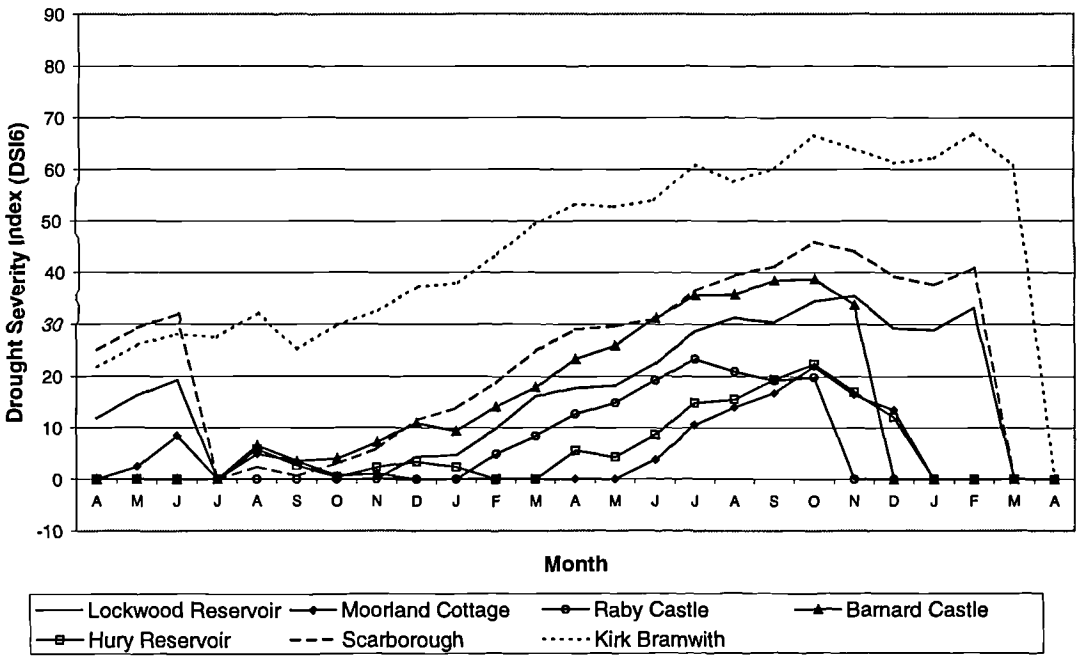

Figure 4-7: DSI_3 and DSI_6 for the 1948/49 drought. Time series start in April 1948 and finish in April 1950.

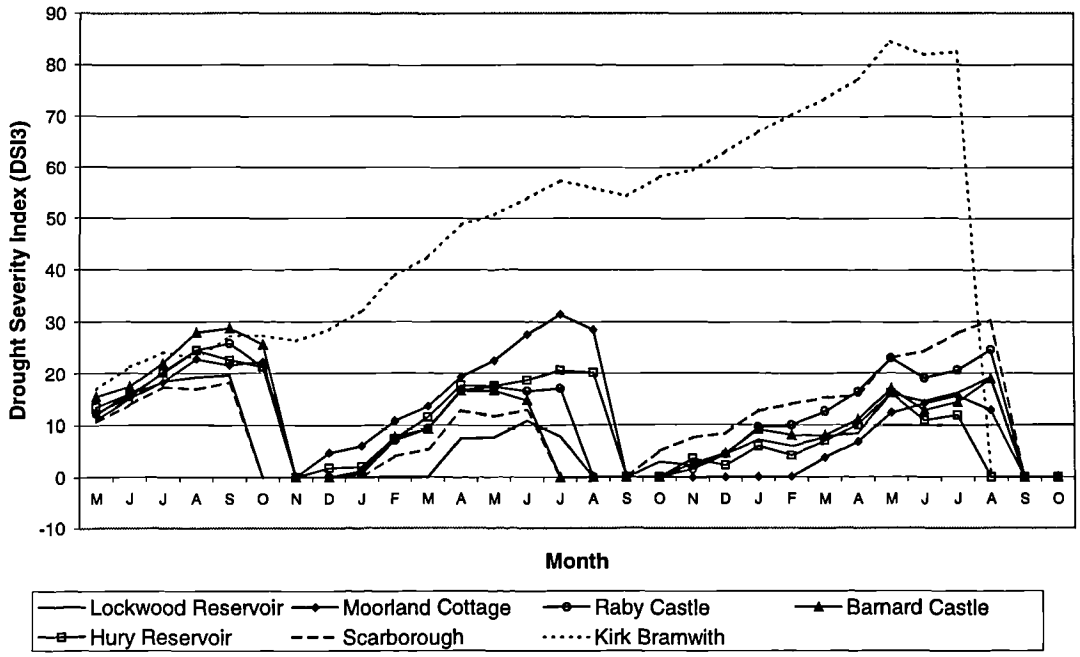

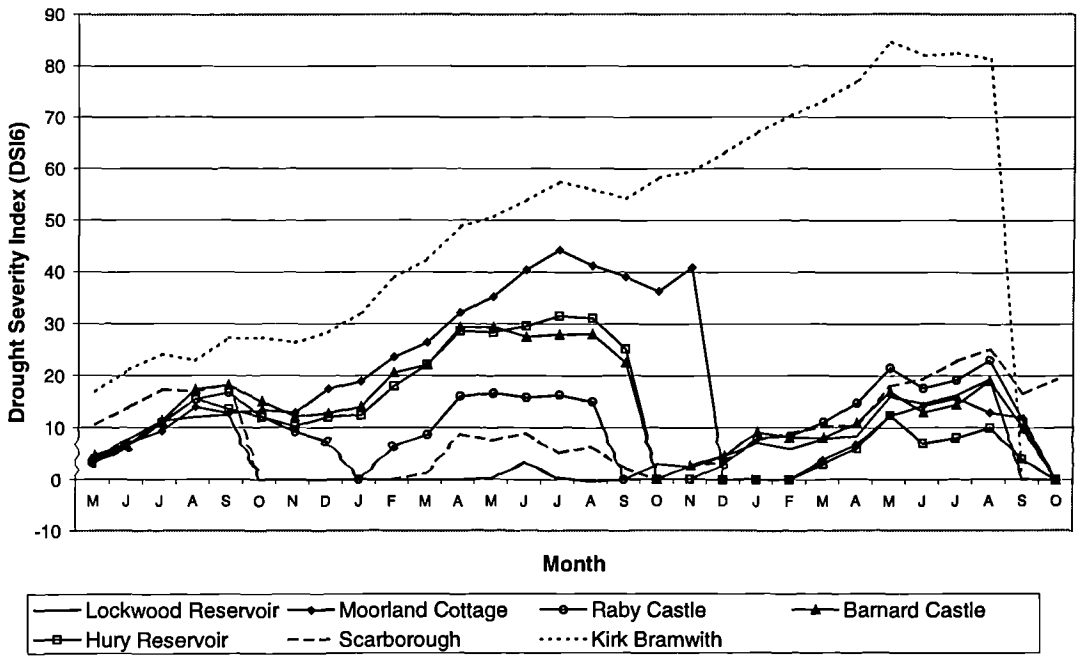

Figure 4-8: DSI_3 and DSI_6 for the 1952/54 drought. Time series start in May 1952 and finish in October 1954.

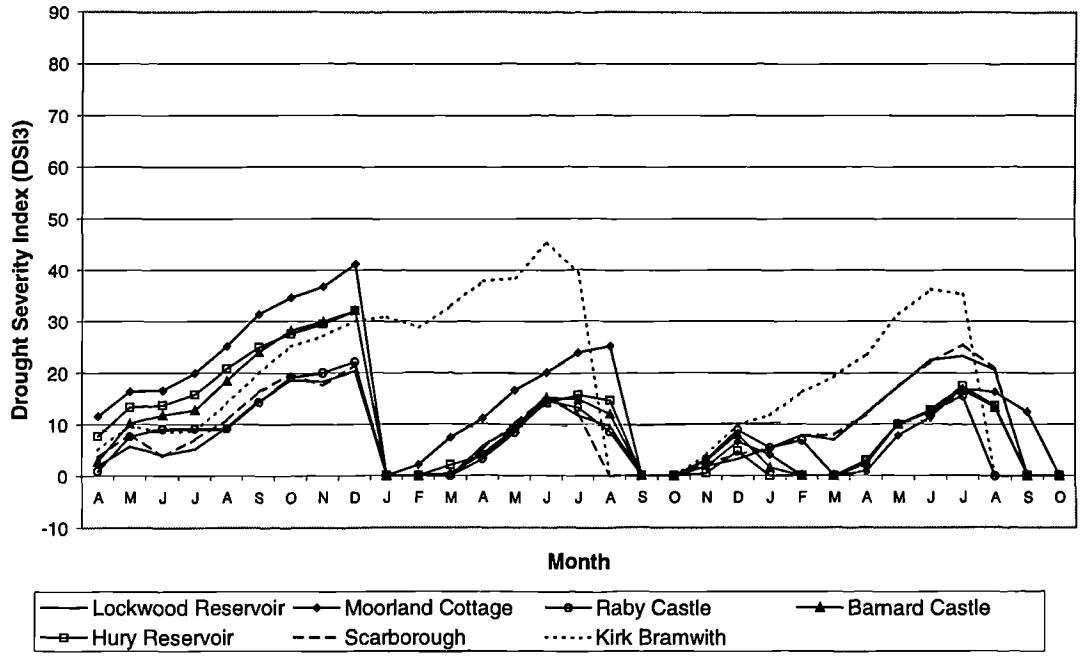

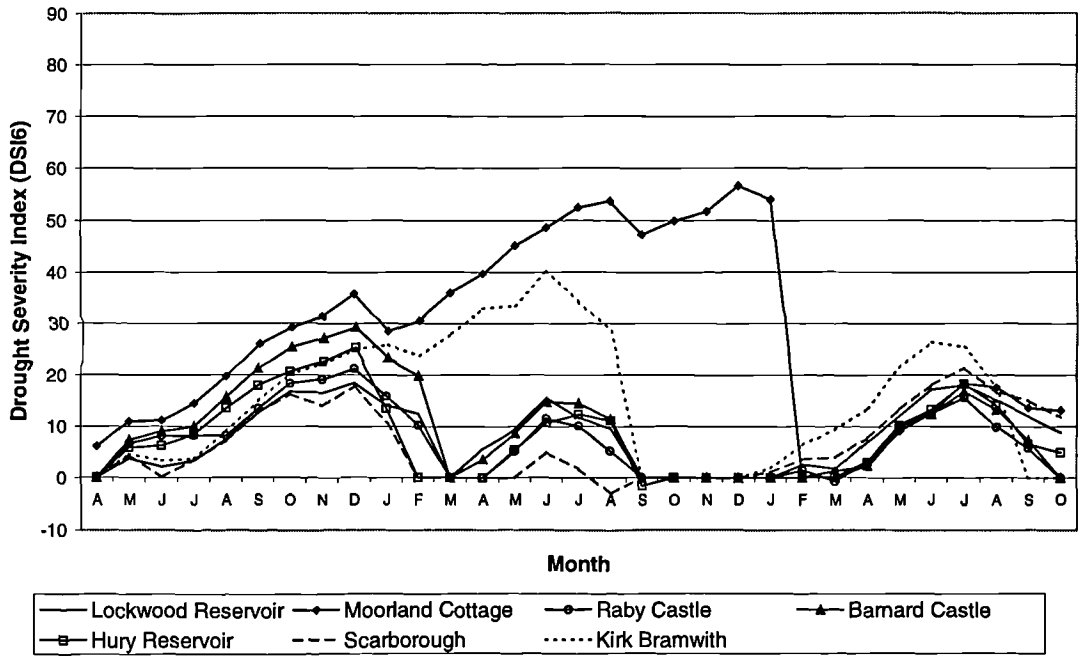

Figure 4-9: DSI_3 and DSI_6 for the 1955/57 drought. Time series start in April 1955 and finish in October 1957.

4.2.3.7 The 1955/57 drought

The 1955/57 drought can be classified as a 'western' drought (see Figure 4-9). Although all areas of Yorkshire were affected, Moorland Cottage provided the longest continuous sequence of drought, 22-months from May 1955 to February 1957, and the greatest severity, 56.6 in December 1956. Other sites show two distinct peaks in precipitation deficit: from July 1955 to February 1956, and from April to October 1957. It is notable that if DSI_3 is used in preference to DSI_6 then the drought severity is reduced at Moorland Cottage and instead two peaks are observed.

From April 1955 to February 1957 there were huge decreases in all rain-bearing Lamb weather types (Table 4-3). These include the cyclonic type, the cyclonic easterlies, the cyclonic westerlies, and the easterlies. The only exception to this rule was the westerlies with a very small increase in frequency of 3.6 percent. The major feature of the 1955/57 drought is the increasing frequency of anticyclonic weather types (A, A S&W and A N&E) which replace the cyclonic types. These show an average rise of over 20 percent, with the anticyclonic easterlies recording an individual increase of 52.3 percent.

4.2.3.8 The 1959/60 drought

The 1959/60 drought exhibits a high degree of spatial coherence in terms of both its duration and its severity, although it shows a higher severity in the west (see Figure 4-10). All areas show an initialisation of drought in January 1959 and a termination in either January or February 1960. Using DSI_3, Kirk Bramwith shows the highest drought severity, in November 1959. However, the hydrological drought, shown by DSI_6, is more acute at Moorland Cottage, peaking in October 1959 at 54.4.

The synoptic circulation shows decreased incidence of easterly and westerly types and their cyclonic hybrids during this time-period (Table 4-3) combined with increased incidence of anticyclonic (15.3 percent) and anticyclonic westerlies (8.9 percent). Cyclonic weather types record an increase of 11.4 percent, but much of this rain falls on eastern Yorkshire, particularly in summer months.

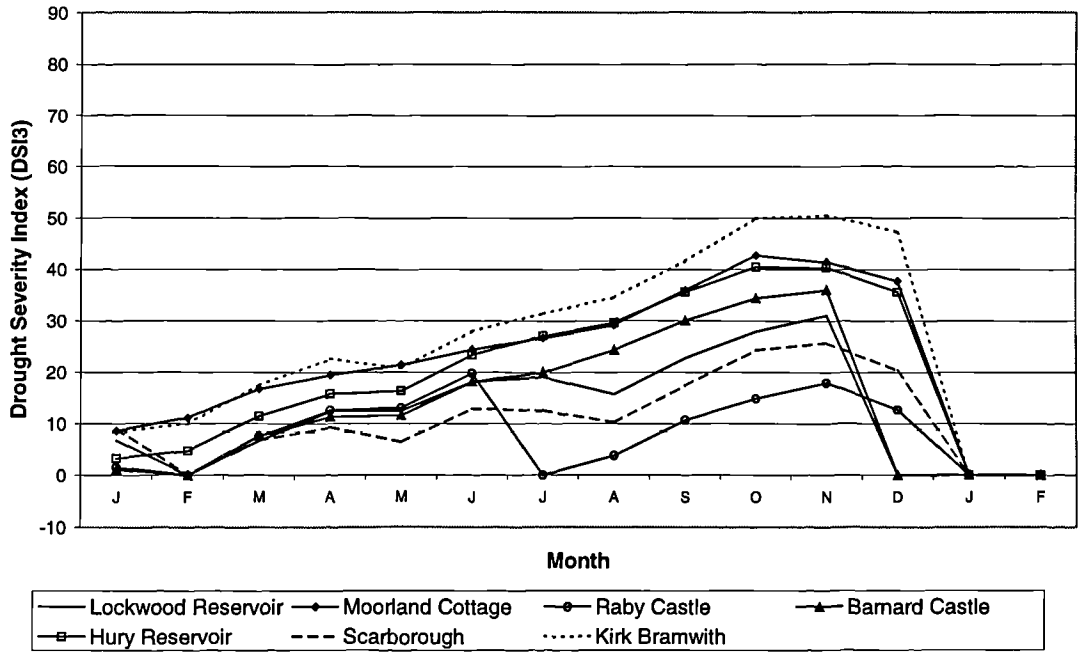

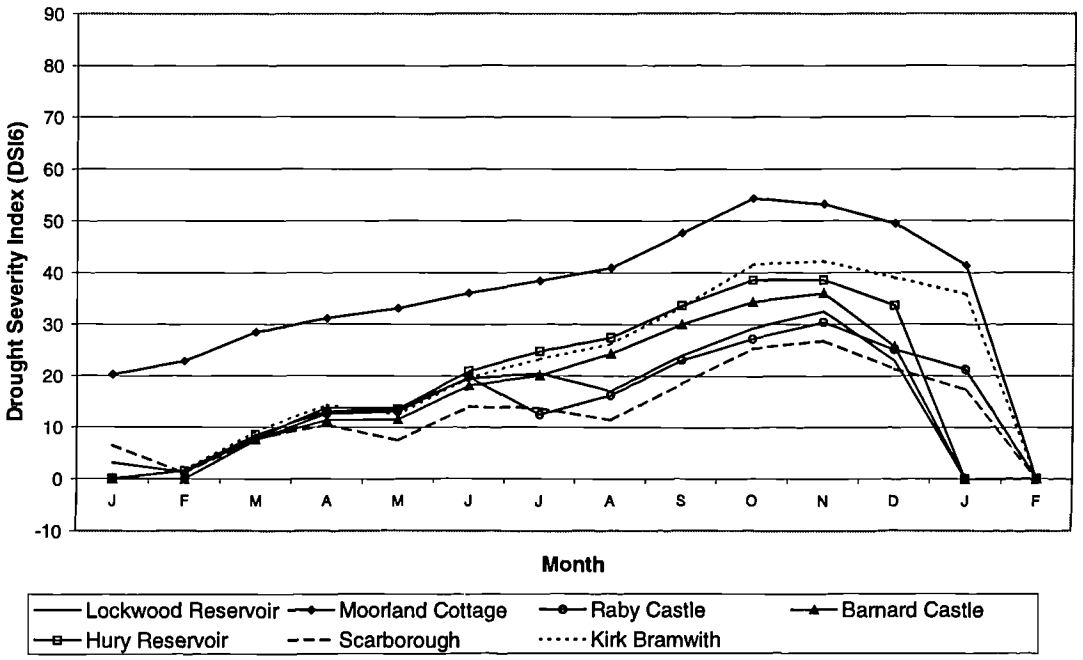

Figure 4-10: DSI_3 and DSI_6 for the 1959 drought. Time series start in January 1959 and finish in February 1960.

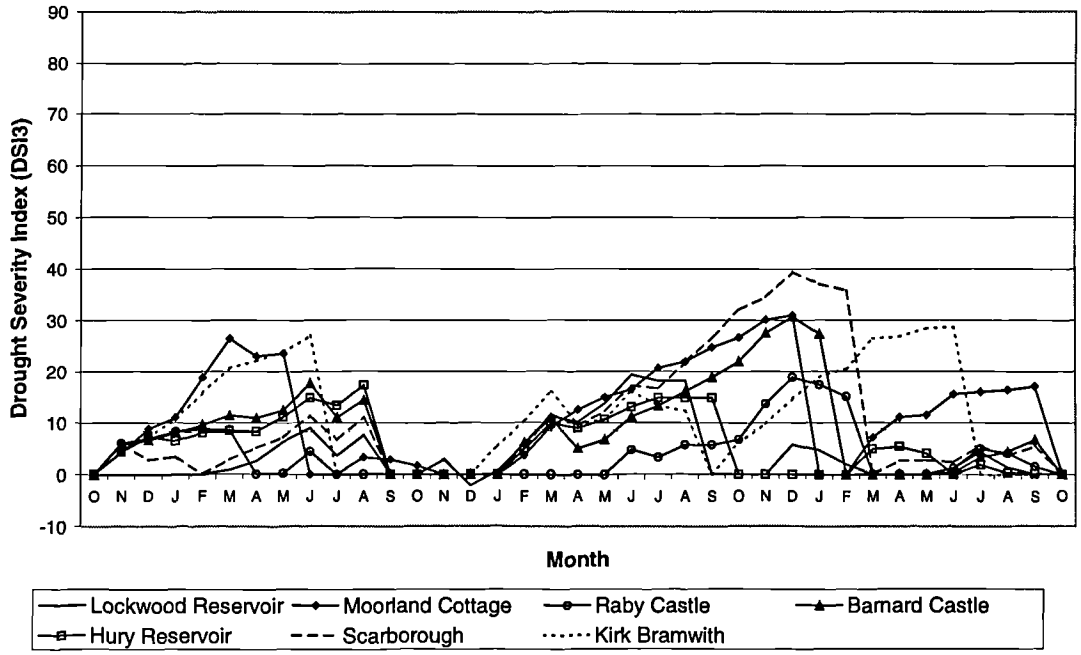

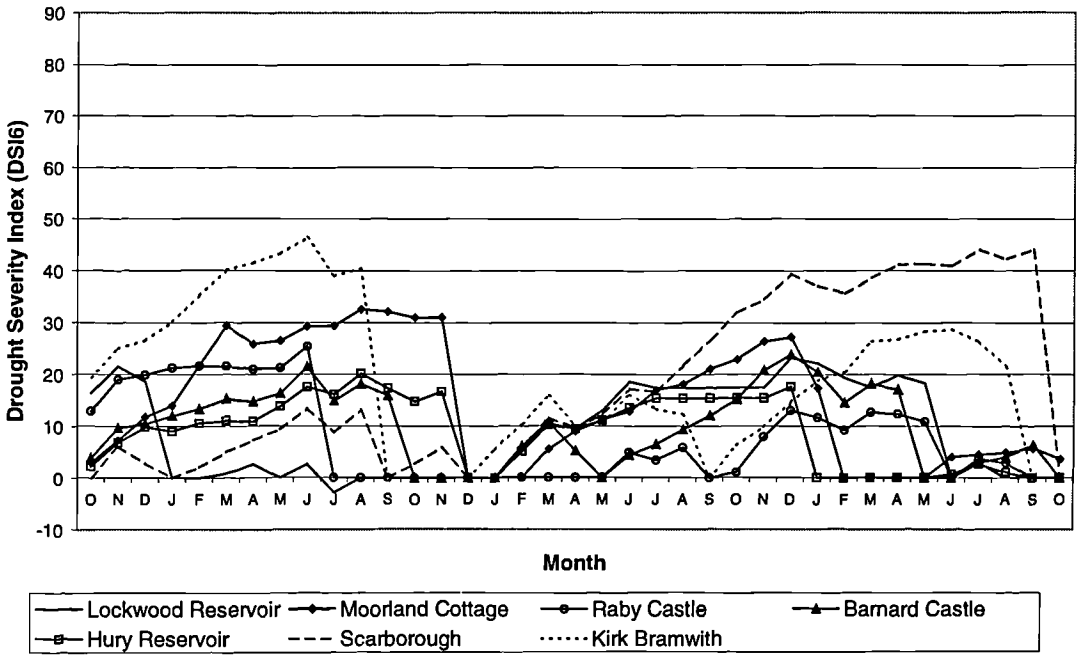

Figure 4-11: DSI_3 and DSI_6 for the 1963/65 drought. Time series start in October 1962 and finish in October 1965.

4.2.3.9 The 1962/65 drought

The 1962/65 drought is really an amalgamation of two droughts: one running from October 1962 to December 1963 and the other from February 1964 to October 1965 (see Figure 4-11). The two droughts show contrasting effects. The first drought affects mainly western sites and peaks in June 1963. However, the second drought produces large precipitation deficits at eastern and coastal sites, peaking in September 1965. A high degree of variability exists between different locations.

The 1962/63 'western' drought records large increases in all easterly types (Table 4-3) of over 30 percent. Westerly types however, show a concurrent decrease. Interestingly, a large decrease in the occurrence of the anticyclonic weather type is also recorded.

In the 1964/65 drought large decreases are recorded in both cyclonic and anticyclonic types. In general, westerly types show increased frequency; for example, the S&W and C S&W showing increases of 20.7 and 13.4 percent respectively, with a concurrent reduction in the occurrence of easterly weather types.

Phillips and McGregor (1998) note the winter 1962/63 drought and the 1964/65 drought within their Class I drought events in Cornwall. It is suggested that during the 1962/63 drought the three easterly types (N&E, A N&E and C N&E) were 22.5 percent more frequent than usual. Westerly groups recorded a deficit of 22.7 percent during the same time-period. These factors account for the drought conditions noted at westerly sites during the winter of 1962/63. During the 1964/65 drought event, anticyclonic, anticyclonic easterly and easterly types were more frequent.

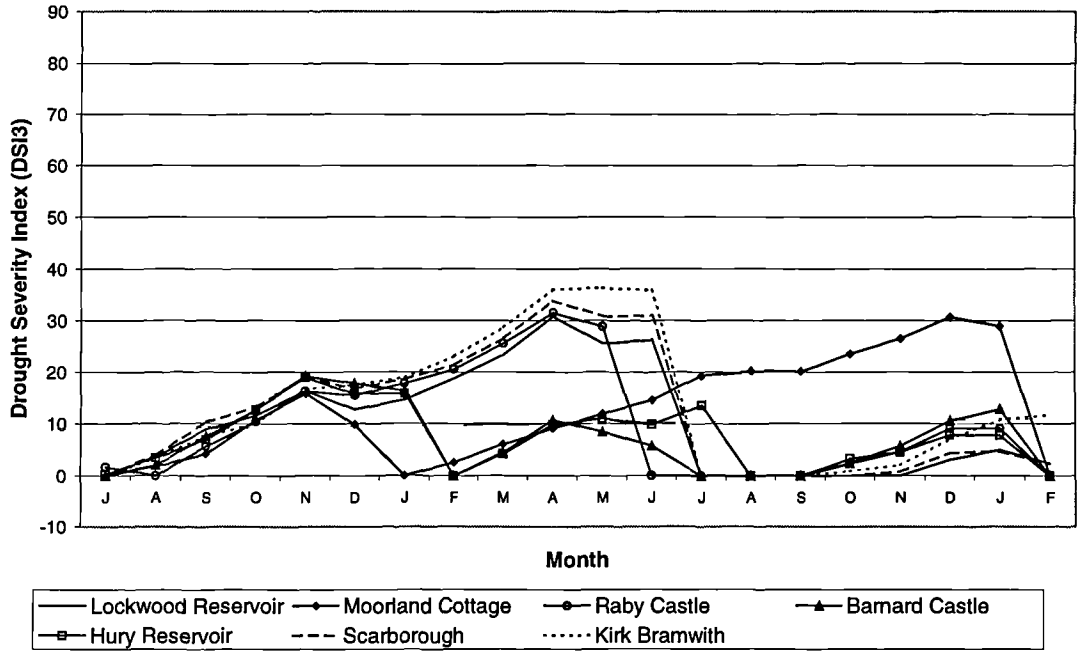

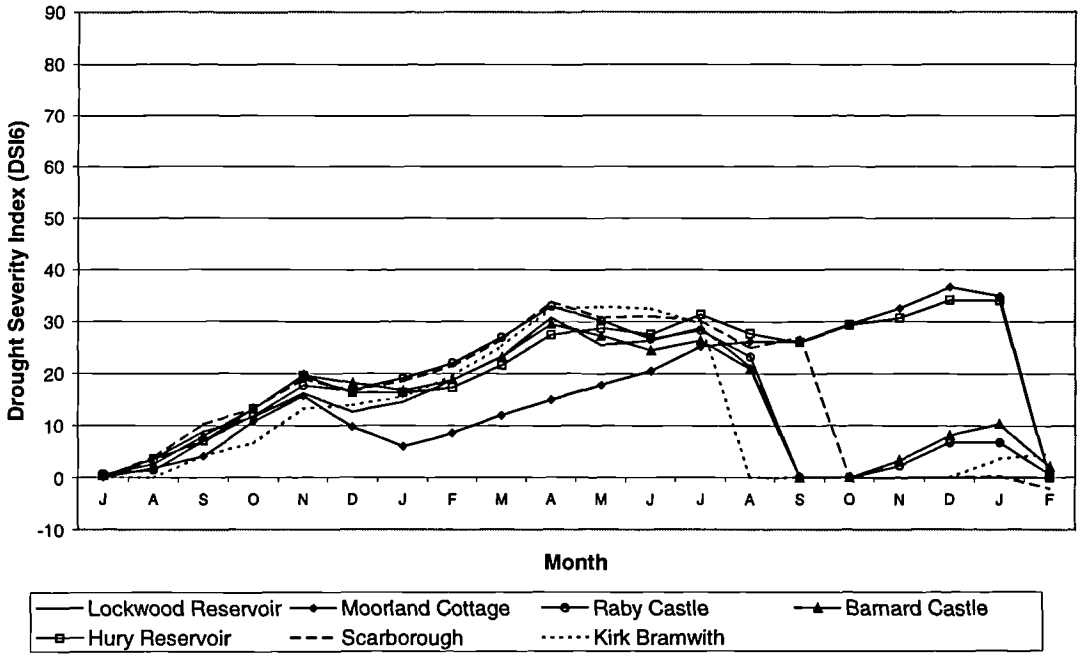

Figure 4-12: DSI_3 and DSI_6 for the 1972/74 drought. Time series start in July 1972 and finish in February 1974.

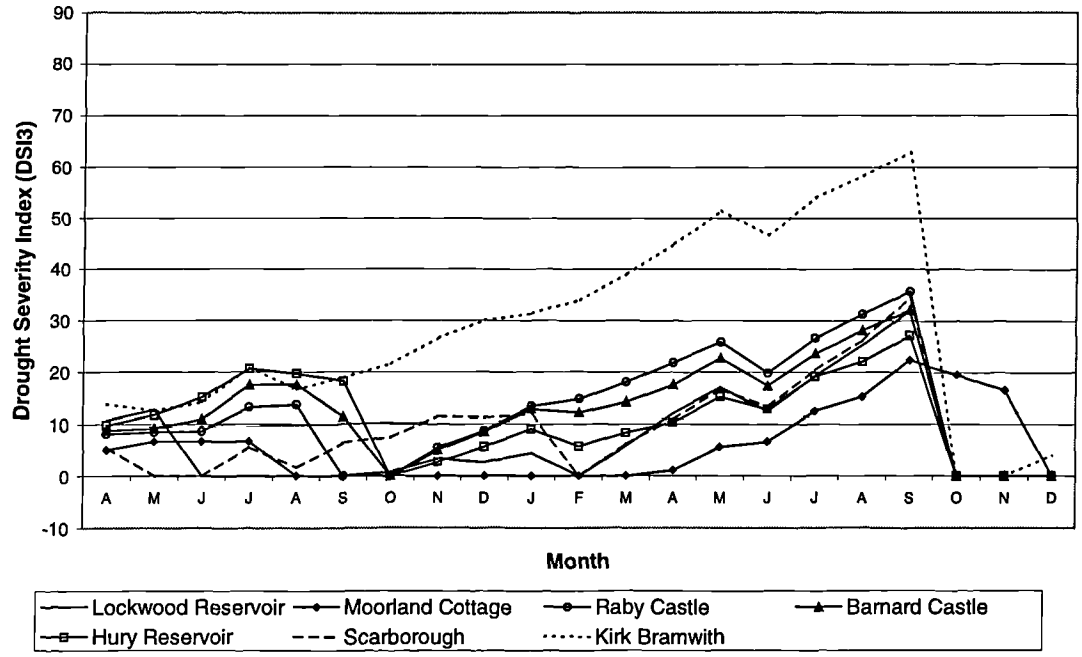

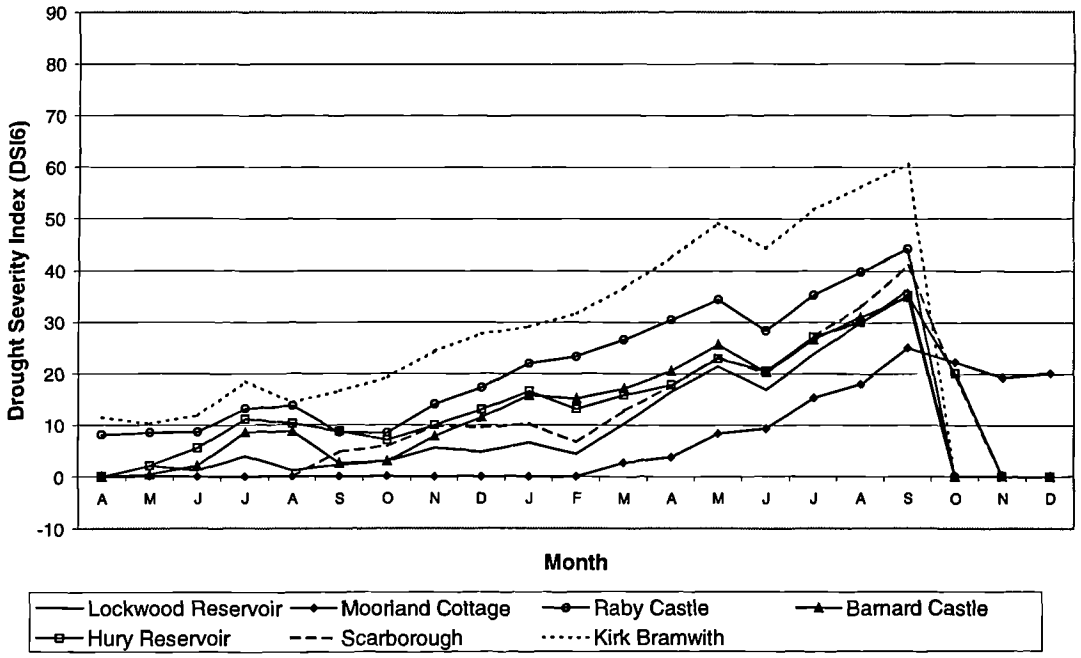

Figure 4-13: DSI_3 and DSI_6 for the 1975/76 drought. Time series start in April 1975 and finish in December 1976.

4.2.3.10 The 1972/74 drought

This drought is less acute than many of the previously recorded drought events (see Figure 4-12). Nevertheless, the drought shows a similar pattern in all areas of Yorkshire, terminating 6-months later in the west than the east of the region. The 1972 drought initiates in September 1972 and terminates in the east between August and October 1973. However, the drought is ongoing at Moorland Cottage and Hury Reservoir in the western Pennines until February 1974. The highest severities are felt in May 1973 in the east and December 1973 in the west.

The main feature of this drought is the decreased incidence of all cyclonic and easterly types. There is also a rise of 15.1 percent in the occurrence of the anticyclonic weather type during this period.

4.2.3.11 The 1975/76 drought

The 1975/76 drought was felt most strongly in the north and east of Yorkshire, having a delayed initiation in the Pennines at Moorland Cottage and reaching only half the severity of other regions (see Figure 4-13). The drought shows the same pattern at all sites, excepting that of Moorland Cottage, an initiation in April 1975 and termination by October 1976. At Moorland Cottage major precipitation deficits are not apparent until June 1976 and a termination of the drought occurs some time after December 1976. The drought shows a steady increase in severity, peaking in September 1976 and recording the most acute effects at Kirk Bramwith.

The 1975/76 drought shows a similar pattern to the 1972/74 event (Table 4-3). An increase in frequency of the anticyclonic weather type is recorded, with decreases in all cyclonic types. This is particularly prominent in the cyclonic and cyclonic westerly types that show decreases of 21.6 and 16.7 percent respectively.

4.2.3.12 The 1988/92 drought

The 1988/92 drought started in December 1988 at eastern sites and showed two or three peaks depending upon which index is used (see Figure 4-14), terminating in September 1992. The drought affected severely only eastern areas, although both indices record in excess of ten at western sites on a number of occasions. DSI_6 records a two-peaked event. Drought severity peaks are recorded in October 1990 and July 1992, most prominently at the eastern sites of Lockwood Reservoir and Scarborough for the first event and at Kirk Bramwith for the second.

The 1988/1992 'European' drought (Marsh and Monkhouse, 1993) was notable mainly for its lack of aquifer recharge. Precipitation for the UK during the 4-year period was very close to the long-term average. However, rain-bearing weather systems tended to follow a more northerly track, greatly accentuating the normal north-west to south-east precipitation gradient and causing southern and eastern England to be exceptionally dry. During this time an increase in anticyclonic conditions was coupled with a decline in the frequency of easterly types (N&E, A N&E and C N&E) of 15.4, 10.7 and 19.4 respectively (Table 4-3). A large decrease in the cyclonic weather type was offset by an increase of 7.5 percent in cyclonic westerlies and 15.3 percent in westerlies, in the western region. This caused the widespread drought in the east of Yorkshire but relatively little precipitation deficit in the west. Phillips and McGregor (1998) note that during the core months of the 1992 drought event a positive anomaly of 19.3 percent of anticyclonic days was recorded. All other weather types, excepting the westerly type, show a negative anomaly during the same period.

4.2.3.13 The 1995/96 drought

The 1995/96 drought provided the most severe drought on record in Yorkshire in terms of water supplies and especially affected the west of the region where most reservoirs are located (see Figure 4-15). Both drought severity indices record the peak severity at Moorland Cottage during January 1997. The drought initiates in May 1995 but heavy precipitation in October 1995 in eastern regions terminates the drought. However, in the Pennines the drought increases in severity to 81.3 before terminating in February 1997. A further precipitation deficit can be seen in the Pennines during the summer of 1997 and continuing through the dry winter.

The aggregated Lamb weather types show an expected pattern during the 1995/96 drought (Table 4-3). The anticyclonic type shows an increased frequency. The cyclonic and cyclonic westerly types show a decrease. However, the largest decline is in the occurrence of westerly types (S&W and C S&W) which show decreases of 14.1 and 30 percent respectively. Easterly types (N&E and A N&E) show an unprecedented rise of 39.7 and 35.2 percent respectively in occurrence, compensating for the decline in cyclonic and westerly types. This explains the acute drought in western Yorkshire but relatively small precipitation deficits in the east.

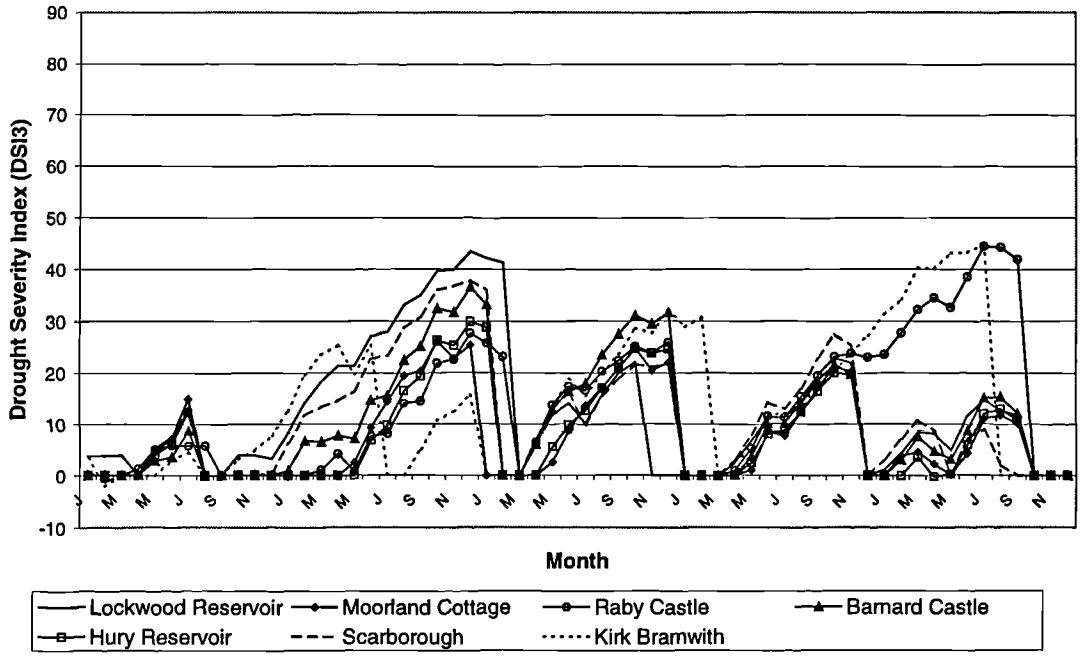

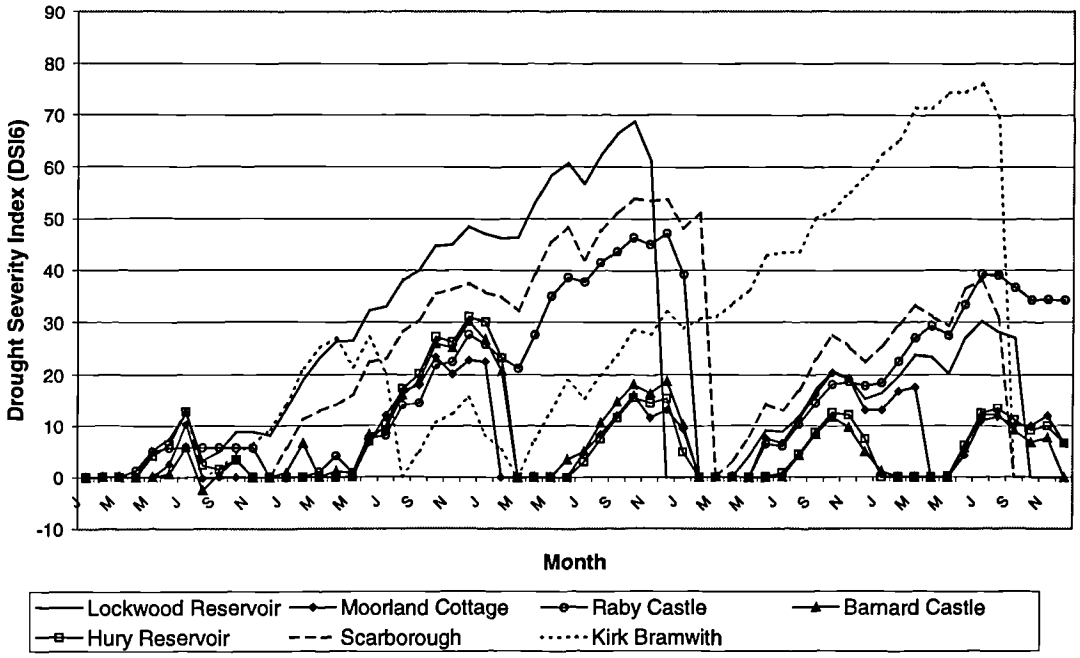

Figure 4-14: DSI_3 and DSI_6 for the 1988/92 drought. Time series start in January 1988 and finish in December 1992.

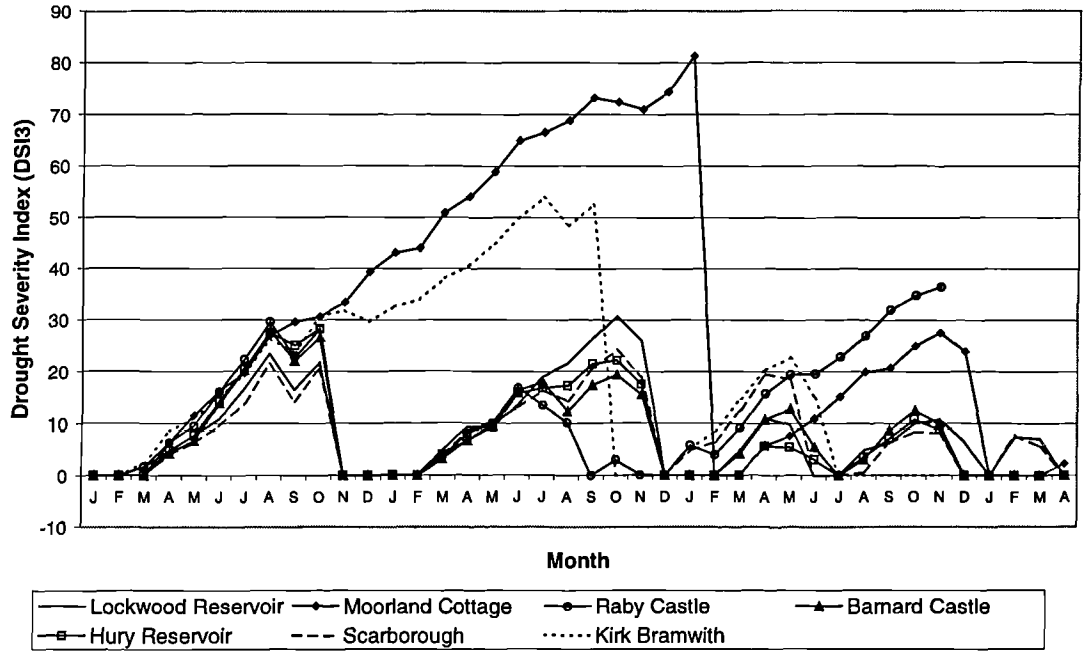

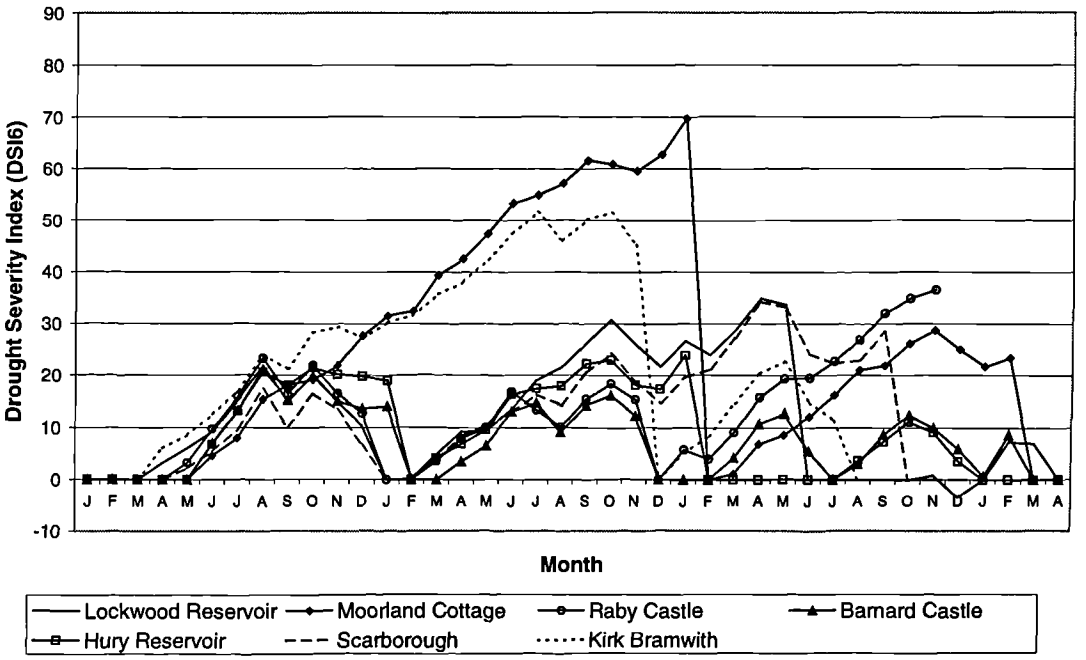

Figure 4-15: DSI_3 and DSI_6 for the 1995/96 drought. Time series start in January 1995 and finish in April 1998.

4.2.4 Classification of major water resource droughts

The north of England is very reliant on surface water resources. Much of Yorkshire, in particular, is dependent upon a large number of single-season upland reservoirs in the Pennine hills. These fill during the winter months and are drawn-down during the summer months, with relatively little carry-over from one year to the next. If low precipitation totals persist into autumn and winter these resources become increasingly vulnerable. Single-season reservoirs are especially sensitive to droughts lasting through one summer season, i.e. six to nine months. Most of the major water-resource droughts in Yorkshire during the last century have involved a very dry spring and summer, with the preceding winter precipitation attaining lesser importance. This can be seen in the drought of 1995. The 32-month period up to the later winter of 1994-95 constituted the wettest on record. Reservoirs were at capacity and groundwater levels were close to seasonal maxima. However, by mid-July there was a notable decline in reservoir levels in the Pennines, to below 20 percent of capacity. The dry winter of 1995-96 only served to exacerbate an existing problem. This implies that severe drought in the Pennines is as much a function of very dry spring and summer weather as a dry winter, due to the reliance upon single season reservoir resources. As most of Yorkshire's water resources are located in the Pennines then 'western' droughts will be the most important in water resource terms and must be examined further.

Mawdsley *et al.* (1994) suggest that weather patterns could theoretically be a good indication of drought severity, and provide an explanatory measure. Therefore, the 14 Class I droughts previously identified were looked at in more detail using two weather type cluster classification systems based on precipitation amount and direction of source. In both cases, the objective Lamb weather types were aggregated to give three distinct clusters. The 'precipitation amount' classification was based on a *k*-means clustering analysis at two Pennine sites. K-means clustering is explained in more detail in Section 2B.1. The objective Lamb weather types were clustered using seasonal statistics of mean daily precipitation and PD at both Moorland Cottage and Great Walden Edge. Both sites have an altitude in excess of 300m and are located in a region known to have been affected by the 1995 drought. Three clusters were found to adequately describe the precipitation regime at the Pennine sites (Figure 4-16).

In the 'directional' classification, weather types were clustered according to direction of source (for more details see Section 5.2). In Yorkshire, the major sources can be split into two: northerly and westerly weather states, with an additional weather state that is dry across the region and encompasses the majority of the anticyclonic types (Figure 4-17). The weather types within the 'westerly' state supply the Pennines with precipitation, whereas the 'northerly' types provide precipitation in the north and east. Therefore, in the Pennines both the 'northerly' and 'anticyclonic' states will produce little precipitation, and a prolonged increase in incidence of

these types would be expected to produce a water resource drought in the single-season Pennine reservoirs.

Weather state	Characteristics	Objective Lamb weather types
Dry/Light	MDR=0.7-1.7mm; PD=0.7-0.8	A, ANE, AE, ASE
Medium	MDR=1.9-4.3mm; PD=0.4-0.7	U, AS, ASW, ANW, AN, NE, E, SE, N, CNE, CN, AW
Heavy	MDR=3.0-9.1mm; PD=0.2-0.5	S, SW, W, NW, C, CE, CSE, CS, CSW, CW, CNW

Table 4-4: Cluster definitions for the Pennine region in summer – 'precipitation classification'.

Weather state	Objective Lamb weather types
Anticyclonic (A)	A, AE, ASE, AS, ASW
Northerly (N)	AN, ANE, N, NE, CN, CNE, E, SE, CE, CSE
Westerly (W)	AW, ANW, S, SW, W, NW, C, CS, CSW, CW, CNW

Table 4-5: Cluster definitions for the 'directional classification'.

The 14 major drought events were examined using these measures, to enable the delineation of 'western' or 'Pennine' droughts that cause water resource deficits in Yorkshire. The characteristics of 'regional' and 'western' droughts were also determined. Droughts highlighted in bold in Table 4-6 refer to 'western' or 'regional' droughts.

It can be observed that 'western' droughts are characterised by a significant increase in the northerly weather state. This may, or may not, be accompanied by an increase in the occurrence of the anticyclonic weather state. The severity of drought depends upon the magnitude of increase of the two weather states. Most 'western' droughts also show a decrease in the number of 'westerly' days, although this may not be severe. The extreme drought of 1995 is highlighted by this analysis. An increase in 'northerly' and 'anticyclonic' occurrence of 28.4 and 17.7 percent respectively, was accompanied by a large decrease of 15.3 percent in 'westerly' weather state frequency. The drought of 1959/60 also shows the same pattern of change, although nowhere near as severe. The 1962/63 'western' drought records a large increase in 'northerly' weather state occurrence of 30.6 percent accompanied by declines in both the 'westerly' and 'anticyclonic' states. This explains the drought to the west of the region, but normal precipitation totals to the east.

Drought	Duration	Precipitation Classification			Directional Classification		
		Dry	Medium	Heavy	A	N	W
1905/6	Jan 1905 – Dec 1906	-5.6	12.2	-3.1	-1.9	3.1	-0.5
1913/4	Jun 1913 – Dec 1914	-4.0	-4.5	1.3	-1.3	-19.9	3.2
1933/5	Apr 1933 – Apr 1935	-2.4	-1.3	1.7	-1.7	0.2	1.1
1941/4	**Jul 1941 – Oct 1944**	**25.3**	**-1.1**	**-1.4**	**19.2**	**-3.0**	**1.5**
1948/9	**Jul 1948 – Apr 1950**	**8.7**	**-17.6**	**3.3**	**18.0**	**-33.6**	**0.7**
1952/4	May 1952 – Oct 1954	-7.5	5.9	1.8	-6.8	-11.6	6.8
1955/7	**Apr 1955 – Feb 1957**	**10.1**	**4.1**	**-6.6**	**-0.2**	**3.2**	**-0.6**
1959/60	**Jan 1959 – Feb 1960**	**8.9**	**-0.2**	**-4.0**	**11.2**	**7.5**	**-7.2**
1962/3	**Oct 1962 – Dec 1963**	**-18.6**	**12.0**	**1.7**	**-11.0**	**30.6**	**-4.4**
1963/65	Feb 1964 – Oct 1965	-17.6	10.5	5.5	-12.7	12.6	3.9
1972/4	**Sep 1972 – Feb 1974**	**7.5**	**-12.2**	**0.7**	**14.2**	**-31.7**	**0.8**
1975/6	**Apr 1975 – Dec 1976**	**12.8**	**-0.2**	**-5.6**	**10.8**	**-4.5**	**-3.4**
1988/92	Dec 1988 – Dec 1992	2.3	-11.4	3.6	-0.8	-13.4	4.1
1995/6	**May 1995 – Feb 1997**	**13.8**	**15.8**	**-13.0**	**17.7**	**28.4**	**-15.3**

Table 4-6: Percentage anomalies for each of the precipitation and directional classifications for Class I droughts occurring this century in Yorkshire when compared to the average for the period from 1861-1990. Those droughts highlighted in bold refer to 'western' or 'regional' droughts.

It appears that using a directional classification, 'western' droughts are characterised by a decrease in frequency of 'westerly' types accompanied by an increased occurrence of 'northerly' types. This may also be supplemented by an increased frequency of 'anticyclonic' types. This will define the extent and severity of the drought. 'Regional' droughts, on the other hand, are generally characterised by an increased frequency of 'anticyclonic' weather types. This can be seen clearly in the droughts of 1941/44, 1949, 1972/74 and 1975/76. 'Eastern' droughts are characterised by a decreased occurrence of 'northerly' types, as in the drought of 1988-1992. These may also be increased in severity by an increased frequency of 'anticyclonic' types.

If the 'precipitation classification' system is used then other features of drought within Yorkshire become apparent. Western droughts are characterised by an increased number of days classified as 'dry' at western sites. A decrease in the occurrence of 'heavy' precipitation days is also apparent for the more severe droughts. The 1995 drought shows a decrease of 13 percent in the occurrence of 'heavy' weather types, coupled with a 13.8 percent increase in the frequency of 'dry' types. This is perhaps unsurprising however. A strong feature of the 1995 drought was a large increase in the occurrence of 'medium' weather types. In summer months, when evapotranspiration demands are high, these weather types may produce no effective precipitation. This may have contributed to the severity of drought felt in 1995 in many upland areas of the Pennines.

Drought	Duration	Precipitation Classification			Directional Classification		
		Dry	Medium	Heavy	A	N	W
1928/29	Summer 1928	-23.4	-22.5	20.2	-25.9	-40.6	20.7
1937/38	Summer 1937	12.9	32.9	-15.6	17.1	1.9	-5.7
1948/9	Summer 1949	113.7	-50.2	-36.7	91.2	-23.6	-35.9
1959/60	Summer 1959	69.3	-16.9	-32.5	79.5	-66.0	-26.5
1962/3	Summer 1963	-51.6	29.3	4.1	-52.1	83.0	-2.9
1975/6	Summer 1975	65.3	5.2	-34.6	60.0	27.4	-34.0
1995/6	Summer 1995	57.2	16.3	-36.7	52.2	35.8	-34.0

Table 4-7: Percentage anomalies for each of the 'precipitation' and 'directional' classifications for 'western' water resource droughts occurring this century in Yorkshire when compared to the average for the period from 1861-1990.

There are two types of 'western' drought. The first type is caused by a dry winter followed by an average or dry summer. This type of drought occurs due to a lack of winter replenishment of water resources. The second type occurs due to the drawdown of resources during a very dry summer. In the summer of 1995, many reservoirs in the Pennines were drawn down to 20 percent of capacity from a full status in April 1995. An analysis was made of summer (JJA) weather during recent water resource droughts ('western' droughts) using the droughts previously identified and those identified by Yorkshire Water. This can be found in Table 4-7. It can be seen that drought in western Yorkshire is, in general, as much the function of a dry summer as a dry winter. Most water resource droughts involve an increased incidence of anticyclonic and northerly weather types during summer months, coupled with a decreased frequency of westerly types. Percentage changes can be very large and reach over 90 percent for anticyclonic types in 1949. The summer of 1928 was very wet in the west, although a drought occurred from 1928/29. An analysis of weather types shows that this was due to the dry winter of 1928/29. The summer of 1963 is also unusual as there was no increase in the anticyclonic type but instead a huge increase in the occurrence of northerly weather types. It can be noted, however, that the 1995 drought was no more severe than any other drought, and particularly similar to the 1976 drought, in terms of the 'precipitation' or 'directional' classification systems.

Therefore, the occurrence of weather type clusters during the summers of 1976 and 1995 were compared. The results can be found in Table 4-7. It can be seen that there is little difference between the two years in terms of the number of days of a particular weather cluster. Dry day sequences were also examined and 1976 was found to contain longer sequences. The longest dry day sequences (by weather cluster) in 1976 were pinpointed as 12 days, from June to July, and 19 days from July to August. In 1995, there was a 14-day dry sequence from June to July, a 10-day sequence in August, another 8-day sequence in August and a 9-day sequence in June. However, in summer months the 'medium' weather type cluster may also be dry, as

evapotranspiration demands are so high. A 34-day 'dry and medium' sequence can be found in 1976 from the 20th July to the 23rd August. This suggests that the summer months of the 1976 drought were as severe as the 1995 drought, although water demand may have been less.

Another measure of drought in Yorkshire, given the incidence of drought is related to hot, dry summers, is the frequency of weather types during the period from April to September. Water years run from October to October each year. The half-year from October to March is considered the recharge period, whereas from April through to September is the drawdown period. A severe drought would be expected to show marked change from normal conditions during the drawdown period. The results from this analysis can be found in Table 4-8.

Drought	Duration	Precipitation Classification			Directional Classification		
		Dry	Medium	Heavy	A	N	W
1928/29	Apr-Sep 1928	-10.6	26.1	-6.4	-21.6	60.6	-7.8
1937/38	Apr-Sep 1937	-2.7	-7.4	5.8	-4.3	-12.7	6.2
1948/9	Apr-Sep 1948	54.9	-43.4	-9.7	49.2	-40.6	-12.9
1959/60	Apr-Sep 1959	43.0	13.2	-28.4	53.0	-12.7	-23.9
1962/3	Apr-Sep 1963	-52.3	13.2	21.2	-48.3	18.7	17.2
1975/6	Apr-Sep 1975	33.0	-7.4	-15.2	33.9	4.7	-19.9
1995/6	Apr-Sep 1995	13.2	36.4	-24.0	9.0	39.7	-17.9

Table 4-8: Percentage anomalies for each of the precipitation and directional classifications for 'western' water resource droughts occurring this century in Yorkshire when compared to the average for the period from 1861-1990.

It can be seen in Table 4-8 that severe droughts can be characterised by an analysis of weather type frequency. The summer droughts of 1948/49, 1959/60, and 1975/76 were characterised by a large increase in the incidence of anticyclonic or 'dry' weather types. In contrast, the 1995 drought exhibited a large increase in the occurrence of northerly types.

A classification system was developed to assess water-resource drought severity in Yorkshire based upon weather typing. For each water year (i.e. October to October), the number of anticyclonic, northerly and westerly weather types in the summer and winter half-years were determined. For each summer and winter, the frequency of anticyclonic days was added to half of the northerly days (as approximately half can be expected to be dry), and this total was divided by the incidence of westerly types. Therefore, an index greater than one implies a high incidence of anticyclonic and northerly types and provides an indication of drought. Water half-years from 1881-1996 were ranked according to the above index and the top 30 summer, winter, summer-winter, winter-summer, and summer-winter-summer droughts can be found in Table 4-9. This kind of index is very useful as it allows the identification of probable drought events where precipitation records are scarce or lacking in either temporal or spatial extent.

Ranking	Summer	Winter	W+S	S+W	S+W+S
1	*1887*	1963	*1886/87*	*1887/88*	*1887/88*
2	1921	*1891*	*1887/88*	1968/69	*1894/95*
3	1984	1969	1946/47	1955/56	**1995/96**
4	*1893*	1944	1958/59	*1894/95*	1968/69
5	*1884*	1938	*1894/95*	**1995/96**	*1886/87*
6	1968	1996	**1995/96**	1941/42	*1884/85*
7	1955	*1895*	1943/44	*1885/86*	*1895/96*
8	1976	*1888*	*1895/96*	*1896/97*	*1885/86*
9	1959	1934	1910/11	1921/22	*1893/94*
10	*1896*	1956	1940/41	1947/48	1983/84
11	*1894*	1940	1948/49	1939/40	1941/42
12	1977	1953	1968/69	*1884/85*	1940/41
13	1949	*1886*	1983/84	1996/97	*1888/89*
14	1947	*1898*	1939/40	1984/85	*1896/97*
15	1982	1942	*1885/86*	1945/46	1939/40
16	1941	1965	*1892/93*	*1895/96*	1975/76
17	1906	1992	*1898/99*	*1886/87*	1976/77
18	1995	*1887*	*1884/85*	*1888/89*	1905/06
19	1911	1947	1905/06	*1897/98*	1910/11
20	*1885*	1932	1941/42	*1889/90*	1944/45
21	1975	1986	*1888/89*	*1890/91*	*1892/93*
22	1989	1946	*1890/91*	1991/92	1958/59
23	1973	1923	1954/55	*1893/94*	1971/72
24	1901	1959	*1883/84*	1933/34	1955/56
25	*1888*	1964	*1893/94*	*1881/82*	1947/48
26	1957	1911	1944/45	1959/60	1982/83
27	1983	1929	1970/71	1944/45	1908/09
28	1915	*1882*	1920/21	1915/16	1972/73
29	*1895*	1941	1937/38	1937/38	1915/16
30	1971	*1899*	1908/09	1940/41	**1948/49**

Table 4-9: Ranked severity of drought events occurring from 1881-1996 using the directional classification for 'western' water resource droughts (all years signify the start of the time-period of drought – i.e. for winter (W) = October, and for summer (S) = April).

This analysis clearly shows a clustering of probable drought events during the 1880s and 1890s. These are italicised in Table 4-9. The period from 1885 through to about 1891 contains a number of severe drought events if the 'directional' classification is used. The period 1886 to 1888 ranks as the most severe drought on record in all categories, excepting winter. The drought of 1995/96 ranks as the fifth most severe summer-winter drought in the period from 1881 to 1996. This is raised to the third most severe drought if an analysis is made of summer-winter-summer weather types, starting in April 1995 and ending in September 1996. This severity, and the unusual nature of the drought; being driven by increased occurrence of northerly weather types rather than anticyclonic types, may have led to the water supply crisis in western Yorkshire during 1995/96. The 1984 water supply problems are also highlighted by this analysis. Previous analyses (e.g. Goldsmith *et al.*, 1997) and this research failed to find a reason for the water resource shortages of 1984. An analysis of weather types has however pinpointed the cause as increased anticyclonic and northerly conditions that led to decreased precipitation in western Yorkshire. The period from April 1983 to September 1984 ranks as the 10th most

severe drought period on record, in terms of weather types. Therefore, the 1984 drought can be defined as an amalgamation of two dry summers with an intervening dry winter. However, this analysis shows that the recent clustering of drought events during the late 1980s and 1990s is within historical variability. Indeed, evidence suggests that the 1880s and 1890s may have had more severe drought events than during recent years. In the context of the historical past, the 1995/96 drought is not a rare event. However, the drought events of ther 1880s and 1890s have generally not been taken into account when return periods for recent drought events have been calculated.

4.2.5 Discussion

Fourteen Class I droughts have occurred in Yorkshire since 1900. In the earlier period, the droughts appear to have been concentrated in the east of the region. However, this is due to the eastern bias in precipitation data available until about 1930. Since this time there has been no evidence of bias towards one of the seven locations. Droughts appear to be highly spatially variable in impact, in both severity and duration.

The aggregated objective Lamb weather type patterns associated with the 14 drought events suggest that there are three main types of drought in Yorkshire; the 'eastern' drought, the 'Pennine' or 'western' drought, and one where the whole region is similarly affected to a lesser or greater degree. A subjective classification of the 14 Class I droughts can be found in Table 4-10.

Drought Classification	Drought Years
Eastern	1905/06, 1913/14, 1941/44, 1964/65, 1988/92
Western/Pennine	1952/54, 1955/57, 1962/63, 1995/96
Regional	1933/35, 1959/60, 1972/74, 1975/76, 1948/50

Table 4-10: Classification of the 14 Class I droughts in Yorkshire occurring since 1900.

Characteristics of the three drought 'types' can be examined. All drought types show an increase in the anticyclonic weather type, although this may be small. Another common feature is a decrease in the occurrence of cyclonic types. However, there is likely to be a larger decrease in cyclonic types during 'eastern' droughts than 'western' droughts. The eastern drought is generally classified by a decrease in the occurrence of easterly and cyclonic easterly weather types. This may also be accompanied by a decline in the frequency of anticyclonic easterlies. Most commonly, these decreases are countered by an increase in frequency of the westerly

types (S&W, A S&W and C S&W). This accounts for the focus of the drought on the east of Yorkshire, while the west enjoys average precipitation conditions.

A 'Pennine' or 'western' drought generally exhibits opposing trends to that of an 'eastern' drought. The drought is characterised by large decreases in the westerly and cyclonic westerly aggregated weather types. The easterly and northerly weather types generally increase in incidence during these events, although cyclonic types also show a rapid decline in frequency. A good example would be the drought of 1995.

A 'regional' drought can be characterised by many different factors. The main feature is a large decrease in rain bearing weather types across the region, usually cyclonic types (C, C S&W and C N&E). This is accompanied by an increase in anticyclonic types; sometimes just the anticyclonic type itself (as in 1975/76) but often in the form of the hybrids (A S&W and A N&E). The directionals (S&W and N&E) also exhibit large decreases during 'regional' droughts, although the magnitude of the decrease will depend upon the drought being examined.

However, it must be remembered that it is not necessarily the number of days of occurrence of a particular weather type that may be important for drought initiation, but instead the sequencing and persistence of a weather type may play an equally prominent role. Although recent droughts have not been unusual occurrences in a historical sense, their rapid onset has also been noted by other researchers (e.g. Phillips and McGregor, 1998). There has been a very quick build up of precipitation deficits in recent drought events. This is in contrast to earlier droughts where large water deficiencies took much longer to develop. In this sense, recent droughts have followed a difference pattern to that of previous historical drought events, both the 1992 and 1995 sequences taking only three months to develop. This may be a result of the enhanced hydrological cycle cited by many researchers. The 1995 drought was unusual, as the controlling factor was a large increase in the incidence of northerly and easterly weather types, whereas normally a larger increase in anticyclonic conditions would be expected.

Phillips and McGregor (1998) also note that regions affected by drought may be highly related to the positioning of the controlling anticyclones. It is suggested that in the 1995 drought the anticyclone had a tendency to be positioned to the north and east of the UK. In other recent droughts, for example 1992 and 1975/76 however, the anticyclone has taken a more southerly and westerly location. This positioning is consistent with the increasing strength of the NAO. If the recent decline in the NAO during the last few years continues then there may be a return to region-wide drought events, as opposed to the clearly defined 'western' and 'eastern' droughts that have been seen in recent years.

Chapter 5: Development of a stochastic rainfall model based on clustered weather types

"The most urgent requirement in making the "downward" linkage from atmosphere to ecosystem is the development of models that can translate the large scale predictions of GCMs into spatially much finer-scale inputs for ecosystem and hydrological models"

International Geosphere-Biosphere Program (1990)

5.1 Division of Yorkshire into coherent precipitation sub-regions

To allow the spatial modelling of precipitation within a water resource area that contains climatologically dissimilar sub-regions, the region must be split into coherent precipitation zones. Wigley *et al.* (1984) used principal components analysis at 55 sites to examine the spatial patterns of precipitation variability across England and Wales for the period 1861-1970. Analyses were performed using monthly, seasonal and annual data and the temporal stability was examined by dividing the data into two time-periods, 1861-1915 and 1916-1970 and repeating the analysis. The same component patterns appeared in each period for the main components and allowed the division of the UK into five coherent precipitation regions. To check the coherence of precipitation variations within each region, a long station record from each region was cross-correlated with the remaining sites using annual, summer and winter seasons. It was found that regional biases are more apparent at higher correlation levels and a critical level of $r = 0.7$ was suggested for the Pennine delineation of northern England into 'western' and 'eastern' regions.

Areas of coherent precipitation within Yorkshire were determined using 150 sites, shown in Figure 5-1, each with at least 10-years precipitation data available during the period 1961-1990. Ideally, weather typing would be used to delineate coherent precipitation sub-regions. A k-means clustering analysis using the mean precipitation and proportion dry days from 1961 to 1990 for each of the 27 LWTs at each site was used to group the 150 sites. This methodology was found to produce the best results when $k = 4$ (see Figure 5-2).

It can be observed in Figure 5-2 that three regional clusters are discernible. Cluster 3 accurately delineates the Pennine region. Cluster 4 is less obvious but shows a clustering of sites in the northeast of Yorkshire. Clusters 1 and 2 can be lumped into one group that describes the southeastern sub-region.

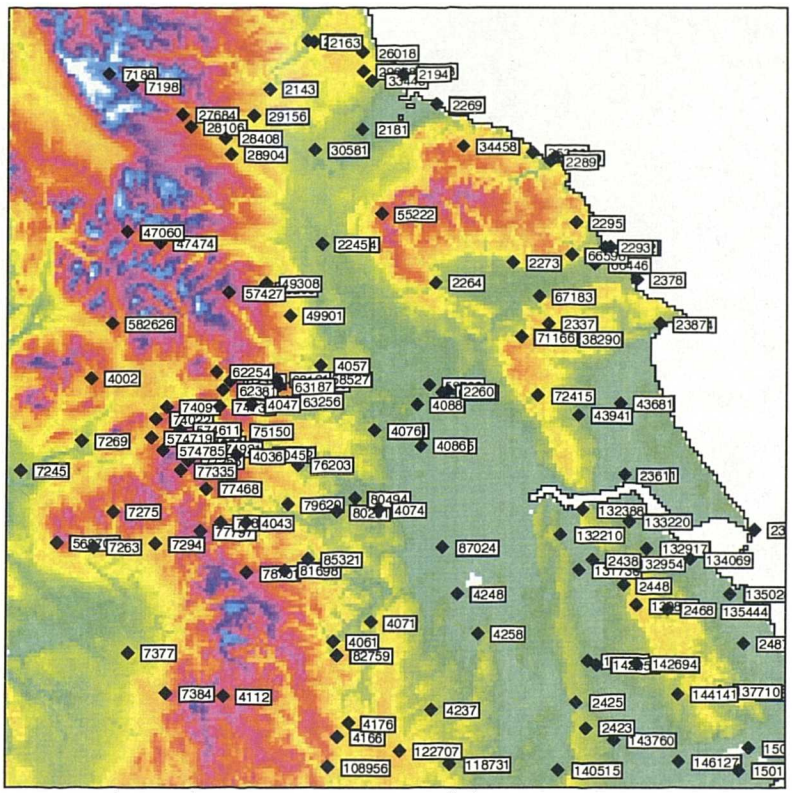

Figure 5-1: The locations of the 150 Yorkshire precipitation gauges used in regional division.

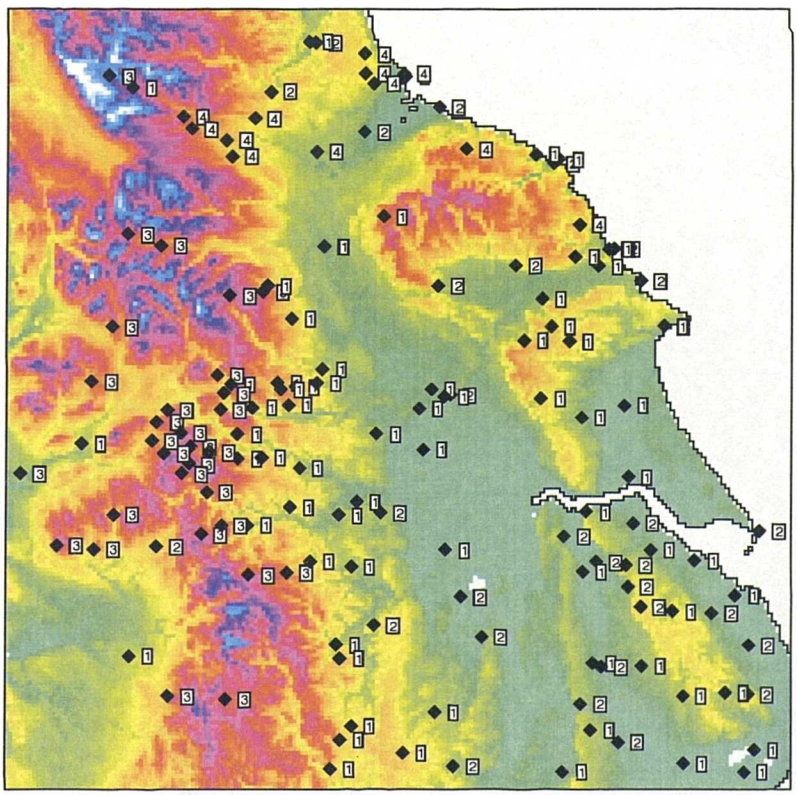

Figure 5-2: Site clustering using 54 variables, k=4.

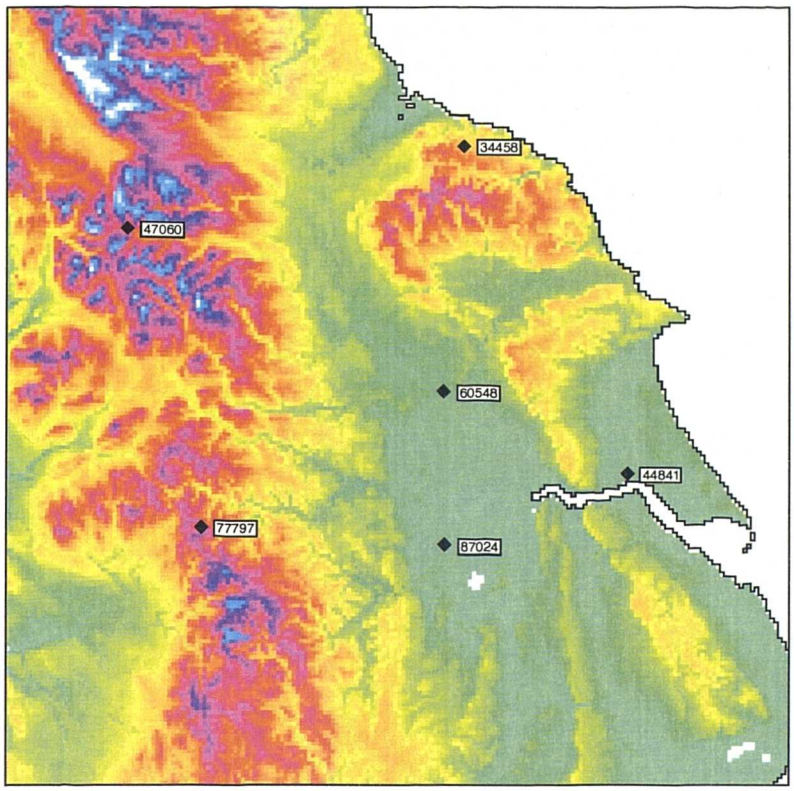

Figure 5-3: Locations of six sites used in cross-correlation analysis.

A more accurate picture may be gained by a similar analysis to that of Wigley *et al.* (1984) however. Monthly totals at the 150 sites were cross-correlated with each of six sites that are evenly distributed across the Yorkshire region and provide a complete record for the 1961-1990 period (Figure 5-3; details in Table 5-1): Moorland Cottage (site 47060), Great Walden Edge (site 77797), Hull (site 44841), York (site 60548), Kirk Bramwith (site 87024) and Lockwood Reservoir (site 34458). Spline interpolation was used to produce a cross-correlation contour map for each of the six sites (see Figure 5-4).

A level of correlation that is considered 'significant' must be selected. Wigley *et al.* (1984) suggested 0.7, approximating fifty percent of the variance, as a critical correlation level, in the case of their work allowing the delineation of eastern- and western-sides of the Pennine range of northern England. Areas exceeding this critical correlation for each of the six sites were used to demarcate Yorkshire into three sub-regions. The west of Yorkshire was shown as distinct from the eastern sub-regions, and bounded by the eastern edge of the Pennines. The area encompassing the North York Moors and Teesside was also shown as distinct from the southeastern sub-region.

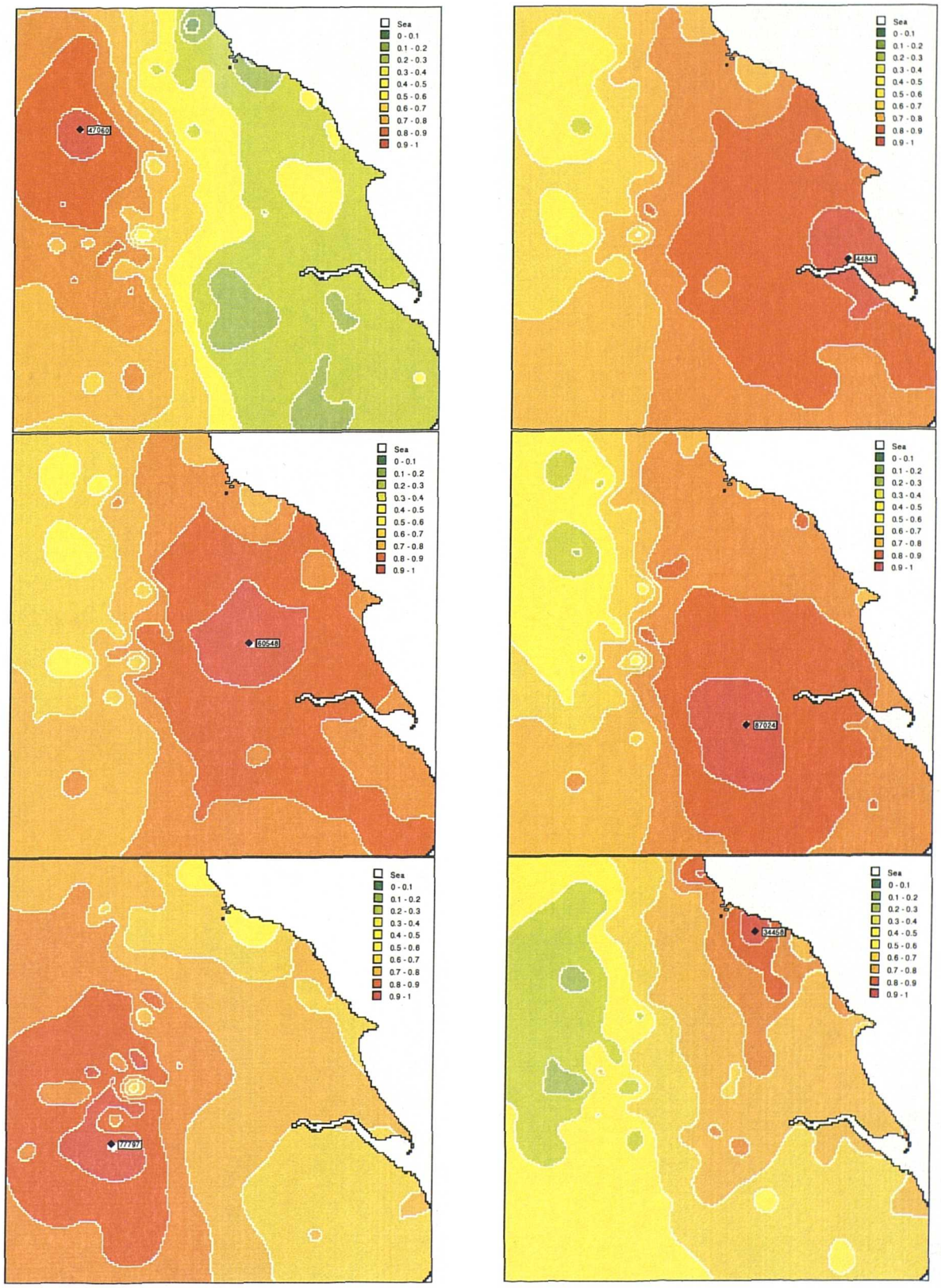

Figure 5-4: Spline interpolation of cross-correlations between the six sites and the other 150 sites in Yorkshire.

Site	Location	Altitude (m)	Missing and Suspect (%)	Mean Annual Precipitation (mm)	Mean Annual PD	Max Daily Precipitation (mm)
34458	Lockwood Reservoir (North York Moors)	193	1.70	803	0.45	104.6 Sep.
44841	Hull, Pearson Park (Humberside)	2	0.29	658	0.51	70.4 Sep.
47060	Moorland Cottage (Southern Pennines)	343	2.49	1939	0.41	102.6 Apr.
60548	The Retreat, York (Vale of York)	18	0.56	640	0.54	67.9 Jul.
77797	Great Walden Edge (Southern Pennines)	346	1.52	1342	0.37	74.7 Jul.
87024	Kirk Bramwith (Vale of York)	7	4.18	593	0.58	74.9 Jul.

Table 5-1: Statistics for the six sites used in weather type k-means clustering. Precipitation statistics are for the period 1961-1990.

It can be observed in Figure 5-6 that the northern Pennine site of Moorland Cottage delineates the Pennine region significantly from the rest of Yorkshire. However, the southern Pennines, at Great Walden Edge, show a high cross-correlation with areas that are more southeasterly. This was thought unusual and so an additional cross-correlation analysis was performed at the neighbouring sites of Ringstone Reservoir (site 77835) and Ramsden Reservoir (site 78701) (Figure 5-5). The same pattern of cross-correlation was found at both sites and it must therefore be assumed that the southern Pennines are less distinct from the eastern region of Yorkshire in terms of precipitation than the northern Pennines. Lockwood Reservoir shows high cross-correlation with other sites in the North York Moors and most of the northeastern seaboard. However, the scarcity of precipitation data from remote areas of the North York Moors precludes a significant correlation being produced across the whole of the North York Moors when using a spline interpolation technique.

To allow an analysis of cross-correlations exceeding 0.7 from each of the six sites, a new raster map was produced for each site. Areas where the cross-correlation was less than 0.7 were masked and labelled area 0, whereas areas where the cross-correlation exceeded 0.7 were labelled as Table 5-2.

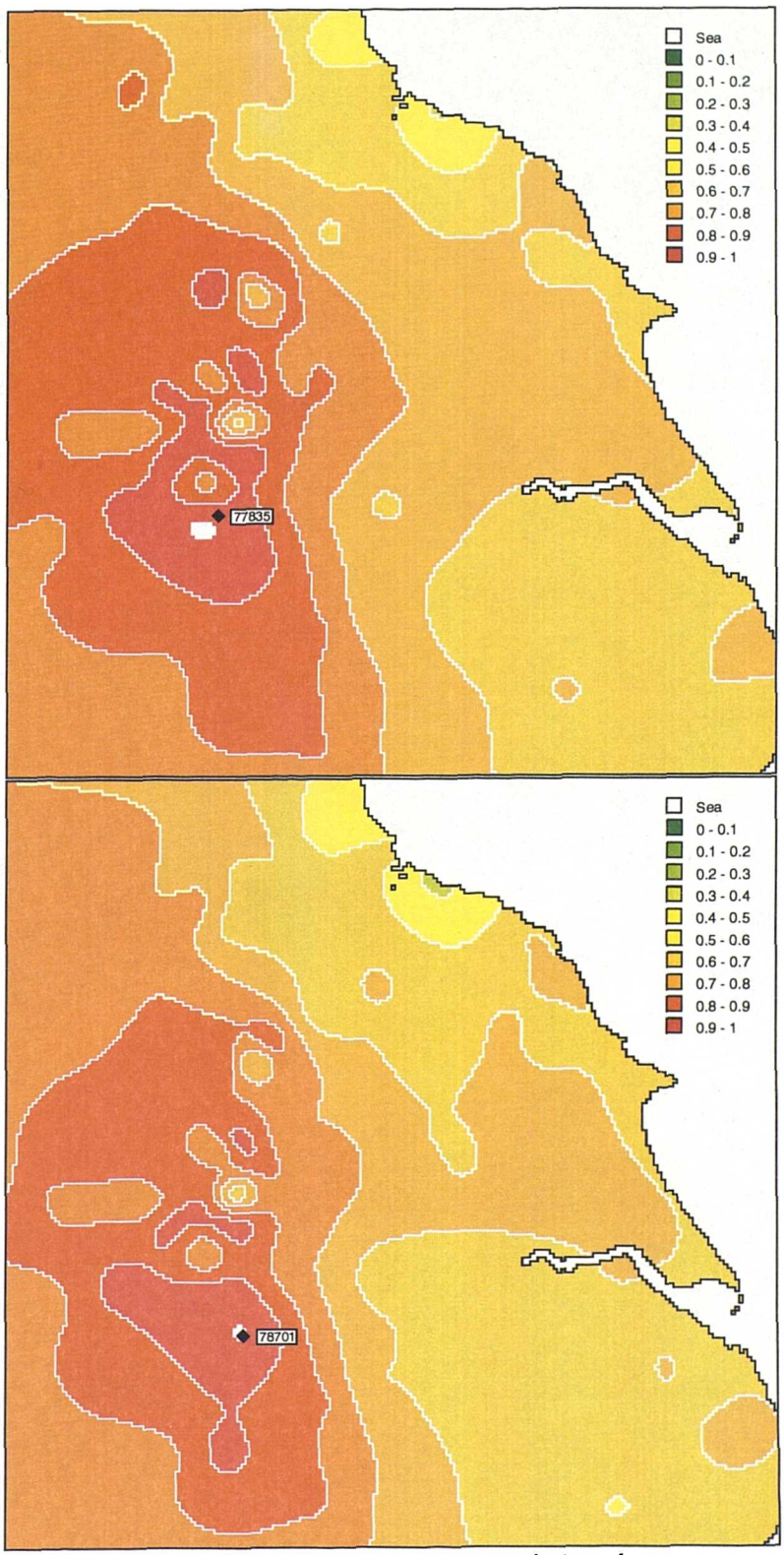

Figure 5-5: Spline interpolation of cross-correlations between two neighbouring sites to Great Walden Edge and the other 150 sites in Yorkshire.

Site	Location	Label
34458	Lockwood Reservoir (North York Moors)	1
44841	Hull, Pearson Park (Humberside)	2
47060	Moorland Cottage (Southern Pennines)	10
60548	The Retreat, York (Vale of York)	20
77797	Great Walden Edge No. 1 (Southern Pennines)	100
87024	Kirk Bramwith (Vale of York)	200

Table 5-2: Labels used in raster map layers for each of the six sites.

The six raster maps were added together, giving 63 possible area codes. For example, site 44841 plus site 47060 would be area code 12. However, in practice, most areas were labelled by one of about eight different codes. Using this approach, the Yorkshire region was objectively split into three sub-regions, as previously suggested by the separate investigation into the climatology of the region (see Chapter 3).

Areas where the cross-correlation was more than 0.7 for the two sites considered within the Pennine sub-region, Moorland Cottage and Great Walden Edge, were plotted on a GIS as a raster layer and labelled area 1. A similar raster layer was produced for the southeastern sites of Kirk Bramwith, York and Hull and labelled area 2. The raster layers were then added together to give areas 1, 2, and 3 (where the areas cross one another). The cross-over area was split subjectively, using altitudinal information from a 1 km^2 Digital Elevation Map (DEM), approximately along the line of the Pennines to produce a new raster map containing two areas; a Pennine sub-region (area 1) and an eastern sub-region (area 2). A raster layer was then produced for areas where the cross-correlation for Lockwood Reservoir was more than 0.7 and labelled area 3. The new raster map showing areas 1 and 2 was then added to the raster layer containing area 3, giving areas 1, 2, 4 (where areas 1 and 3 cross-over), and 5 (where areas 2 and 3 cross-over). Area 4 was very marginal and limited to one anomalous site in the northern Pennines. Thus, area 4 was subsequently ignored. Area 5 contained Teeside, most of the North York Moors and some of the eastern seaboard. It is suggested that all of the North York moors should actually be in area 5 but as a consequence of data scarcity coupled with the averaging imposed by spline interpolation this is not the case. Therefore, a subjective delineation of area 5 was made, including the northeast of Yorkshire up to the Pennine boundary and stretching as far south as the southern North York Moors, and as far east as the seaboard. The final sub-regions

can be seen in Figure 5-6 and are labelled 1, 2, and 3 for the Pennine, northeastern and southeastern sub-regions respectively.

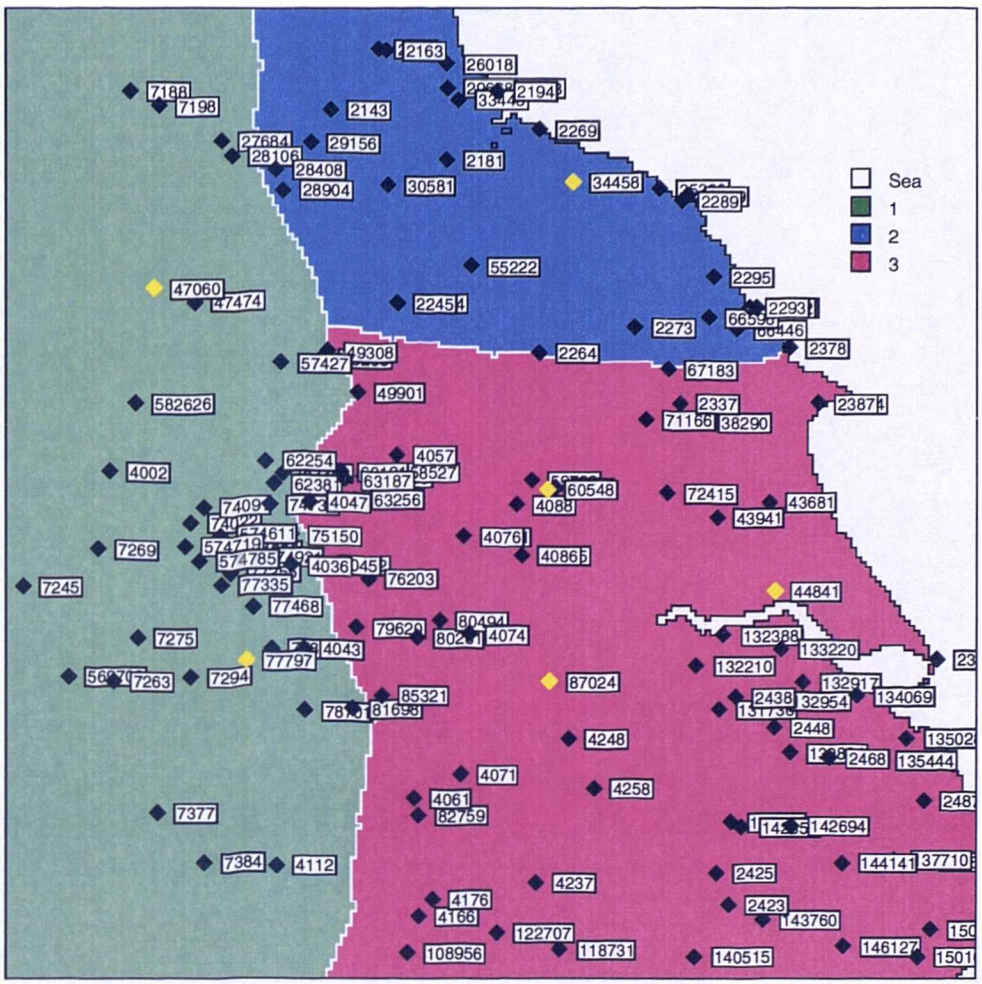

Figure 5-6: The Yorkshire precipitation sub-regions generated by the cross-correlation analysis.

5.2 Weather type clustering

5.2.1 K-means clustering

The grouping of weather types is necessary to reduce model complexity and the effects of over-parameterization of the precipitation process within the less frequently occurring weather types. Within Yorkshire, the overriding spatial precipitation feature is the high precipitation amounts provided by westerly weather types to the western, Pennine sub-region. However, northerly and easterly weather types are the main precipitation-bearers for eastern sub-regions.

To enable spatial cross-correlation within a rainfall generator it is necessary to have the same weather-type groupings for each sub-region. Wilby (1997) investigated the effect of sample size on the estimated mean wet-day amounts for anticyclonic and cyclonic Lamb weather types at Durham. He found that a record of at least 30 years in length must be used to capture the variability of annual precipitation statistics within individual weather types. Precipitation records containing 30-years of data can be found at 33 sites in Yorkshire and the surrounding region (Figure 5-7). However, to formulate physically realistic groups, k-means clustering was applied separately to each of the three sub-regions using weather-type specific seasonal statistics from 1961-1990 for mean daily precipitation and proportion dry days at each of the six sites. These provide good spatial and altitudinal coverage of Yorkshire. This gave two, one and three sites in the Pennine, northeastern and southeastern sub-regions respectively (details in Table 5-3; Figure 5-3).

Region	Sites
Pennines	47060; 77797
North East Yorkshire	37225
South East Yorkshire	87024; 60548; 44841

Table 5-3: Rain gauges used for each regional k-means clustering analysis.

Two of the approaches used by Wilson *et al.* (1992) were adopted for weather-type grouping: k-means clustering and principal components coupled with k-means clustering. In the first instance, PCA was used to condense information in the objective weather types and reduce the number of variables during *k*-means clustering. The first eight principal components were found to explain 99.6 percent of the total annual variance. The principal component scores were then used as input into the k-means algorithm. This method has been suggested as a method for dealing with cases where the input variables into a clustering algorithm are highly correlated (Kendall 1980).

However, using principal components coupled with *k*-means clustering produced highly suspect results. In winter, for example, if all 27 LWTs are used for clustering then using k=2 to k=6 will simply give each hybrid anticyclonic-directional its own weather cluster but cluster all rain-bearing weather types together. Hence, using principal components analysis is not considered appropriate for the OWTs.

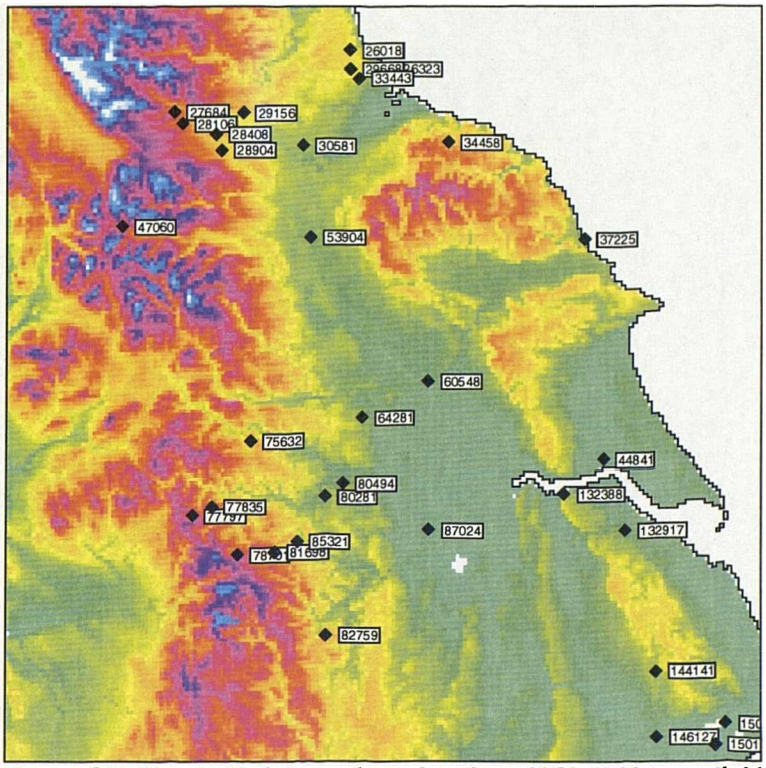

Figure 5-7: Sites in Yorkshire where data from 1961-1990 is available.

k	2	3	4	5	6	7	8	47060		77797	
LWT								MDR	PD	MDR	PD
U	2	3	3	2	3	3	1	4	0.5	3.6	0.6
A	2	2	2	5	2	2	2	2.7	0.7	1.8	0.7
ANE	2	2	2	2	2	2	3	3.6	0.5	2.1	0.7
AE	2	2	4	4	4	4	4	0.6	0.8	0.9	0.8
ASE	2	2	2	5	5	5	5	2	0.6	2	0.7
AS	2	3	3	3	1	1	6	4.3	0.6	5.1	0.7
ASW	2	3	3	2	3	3	1	4.4	0.5	2.9	0.6
AW	2	3	3	3	1	1	7	6	0.4	3.1	0.6
ANW	1	1	1	1	6	7	7	7.8	0.4	4.8	0.5
AN	2	2	2	2	3	3	3	3.1	0.6	2.9	0.7
NE	2	2	2	5	5	5	5	1.9	0.6	2.3	0.6
E	2	2	2	5	5	5	5	2	0.7	3.8	0.6
SE	2	3	3	2	3	3	1	3.7	0.6	3.4	0.5
S	2	3	3	3	1	1	7	5.5	0.4	3.9	0.5
SW	1	1	1	1	6	7	8	8.5	0.3	5.1	0.4
W	1	1	1	1	6	7	8	9.5	0.3	6.1	0.3
NW	1	3	3	3	1	7	7	6.9	0.4	4.4	0.4
N	2	3	3	3	1	1	1	4.7	0.6	4	0.6
C	1	1	1	1	6	7	8	7.9	0.4	5.6	0.3
CNE	2	3	3	3	1	1	1	4.4	0.2	3.9	0.3
CE	2	2	2	5	5	5	5	2.5	0.4	2.7	0.2
CSE	2	3	3	3	1	1	7	5.2	0.3	3.6	0.4
CS	1	1	1	1	6	7	8	9.2	0.2	5.5	0.3
CSW	1	1	1	1	6	6	8	12.1	0.2	8.1	0.2
CW	1	1	1	1	6	6	8	11.8	0.2	8	0.2
CNW	2	3	3	3	1	1	6	4.9	0.4	4.7	0.4
CN	2	2	2	2	3	3	1	3	0.5	3.8	0.4

Table 5-4: k-means clustering for the Pennine region in winter using objective weather types and k=2 to k=8 for sites 77797 and 47060. Site statistics average over 1961-1990.

Using k-means clustering alone, the optimal number of weather clusters for each sub-region and season was set between k=2 and k=8. An arbitrary value of k=8 is suggested as a point where the rainfall generator will become too complicated.

Table 5-4 gives an example of the results from the k-means clustering exercise, for the Pennine region in winter. The cluster memberships are shown clearly for each weather type. Table 5-5 gives an example of the results of the weather clustering exercise with k=3. It is suggested that this is the optimal number of clusters necessary to accurately describe the precipitation regime of Yorkshire. Results for other regions and seasons can be found in Appendix 2.

	Pennines				Northeast				Southeast			
	W	Sp	Su	A	W	Sp	Su	A	W	Sp	Su	A
LWT												
U	2	2	2	2	3	3	3	2	2	3	2	1
A	3	2	3	3	3	3	3	3	3	3	3	3
ANE	3	3	3	3	2	1	3	2	2	3	3	2
AE	3	3	3	3	2	3	3	3	3	3	3	3
ASE	3	3	3	2	3	3	3	3	3	3	3	1
AS	2	2	2	2	3	3	3	3	1	3	3	2
ASW	2	2	2	2	3	3	3	3	3	3	3	2
AW	2	2	1	1	3	3	3	3	2	3	3	3
ANW	1	2	2	2	3	3	3	3	3	3	3	3
AN	3	2	2	2	2	2	3	2	2	3	2	1
NE	3	3	2	2	2	2	1	1	2	3	1	1
E	3	3	2	2	2	2	2	2	1	3	2	2
SE	2	2	2	2	3	3	3	3	1	1	1	2
S	2	1	1	1	3	3	3	3	1	1	2	2
SW	1	1	1	1	3	3	3	3	2	1	2	1
W	1	1	1	1	3	3	3	3	2	1	2	2
NW	2	1	1	2	3	3	2	2	2	3	2	2
N	2	2	2	2	1	2	2	1	2	3	2	2
C	1	1	1	1	2	2	2	1	1	1	1	1
CNE	2	1	2	2	1	1	1	1	2	2	2	1
CE	3	2	1	2	1	1	2	2	2	2	1	1
CSE	2	1	1	1	2	2	2	2	1	2	1	1
CS	1	1	1	2	3	2	3	1	1	2	2	2
CSW	1	1	1	1	2	2	2	2	1	2	2	1
CW	1	1	1	1	2	2	2	2	1	1	2	2
CNW	2	2	1	1	2	2	2	2	2	3	1	1
CN	3	2	2	2	1	2	1	1	1	2	2	2

Table 5-5: Cluster memberships (3=dry/light, 2=medium, 1=heavy) for each sub-region of Yorkshire by season (W = winter, Sp = spring, S = summer, A = autumn)

5.2.2 Clustering using a minimisation of variance routine

Little overall difference was found in weather grouping between the seasons of winter and spring, or those of summer and autumn and three groups adequately describe the spatial precipitation pattern in Yorkshire. Therefore, the weather-type groupings were determined using a variance minimisation algorithm. The year was split into two arbitrary six-month periods and daily precipitation variance within the weather group or 'state' was minimised to ensure the coherency of the groupings. All tested grouping combinations have a substantive physical basis from information obtained from the k-means clustering analysis and the unclassified weather type was omitted from testing.

Analysis of various different clustering combinations suggested that variance is minimised and persistence maximised by the clustering arrangement detailed in Table 5-6. It is suggested that years are split into a 'summer' period from April to September and a 'winter' period from October to March. Three weather state groupings are defined for each season, giving winter-anticyclonic (WA), winter-northerly (WN), winter-westerly (WW), summer-anticyclonic (SA), summer-northerly (SN) and summer-westerly (SW) weather states. It may be noted that in meteorological terms these may be roughly defined as blocking (anticyclonic), zonal (westerly) and meridional (northerly), and that the northerly weather state contains both northerly and easterly Lamb weather types.

Weather state	Objective Lamb weather types
Anticyclonic (A)	A, AE, ASE, AS, ASW
Northerly (N)	AN, ANE, N, NE, CN, CNE, E, SE, CE, CSE
Westerly (W)	AW, ANW, S, SW, W, NW, C, CS, CSW, CW, CNW

Table 5-6: Weather type cluster definitions for the three weather states in both 'summer' and 'winter'.

5.3 Generation of weather type series

5.3.1 Model development

Many researchers have used Markov chain models to generate series of daily weather or atmospheric circulation types (e.g. Gregory *et al.*, 1992; Hughes and Guttorp, 1994), the simplest of which is the Richardson (1981) WGEN model. The approach taken here is similar to

that of Hay *et al.* (1991). A discrete-time semi-Markov process is used to describe the occurrence of daily weather types. Transitions between states are modelled using the theory of Markov chains. However, additionally the duration, in days, of a weather state is modelled by sampling from a distribution fitted to observed persistence or "sojourn time" (Hay *et al.*, 1991) properties. This is an extension to an alternating renewal process that generates sequences of wet then dry periods.

A finite set of weather-type 'states' (**W**) has been defined in the previous section. At an initial time, state i_0 is entered. An equal chance is given to the initial state being any one of the defined weather states for that season. After a random duration within this state, defined by a distribution fitted to the observed persistence probability distribution, the model enters state i_1. The process continues with a randomly defined duration within this state and then a transition to the next state, i_2.

The one-day transition probabilities are defined in two matrices A and B, where A denotes the 'summer' period and B the 'winter' period. These matrices consist of transition probabilities A_{ij} and B_{ij} respectively, where i and j are in the set of **W**. The transition probabilities have values such that $0 \leq A_{ij}, B_{ij} \leq 1$ for all i and j and (5-1):

$$\sum_{i=1}^{n} A_{ij} = 1 \qquad \text{and} \qquad \sum_{i=1}^{n} B_{ij} = 1, \tag{5-1}$$

where n is the number of states and $j = 1, n$. The alternating renewal process, by definition, defines within state transitions as zero, such that (5-2):

$$A_{ii}, B_{ii} = 0, \tag{5-2}$$

for i in the set of **W** (Mode 1985). On a daily level, these are modelled using the persistence probability distribution for a weather state.

Transition probabilities were calculated using LWT data from 1881-1996. These are shown in Tables 5-7 and 5-8. Hay *et al.* (1991) also calculated the mean persistence time for each weather state and determined the distribution of 'sojourn times' using the Kolmogorov-Smirnov goodness of fit test. The geometric and negative binomial probabilities were tested and the geometric probability distribution was chosen, as it could not be rejected at the 99 percent level.

Weather Type	Anticyclonics	Northerlies	Westerlies
Anticyclonics	0	0.273	0.727
Northerlies	0.461	0	0.539
Westerlies	0.573	0.427	0

Table 5-7: One-step observed historical transition probabilities for 'summer' using data from 1881-1996.

Weather Type	Anticyclonics	Northerlies	Westerlies
Anticyclonics	0	0.183	0.817
Northerlies	0.486	0	0.514
Westerlies	0.573	0.427	0

Table 5-8: One-step observed historical transition probabilities for 'winter' using data from 1881-1996.

However, in the case of the LWTs, transition probabilities for one-day transitions were temporally variable, depending upon the duration of the weather state (Figures 5-8 and 5-9). For all weather states, within-state transition probability is significantly lower until the duration reaches at least three days.

A significant difference was found between the observed and fitted geometric distribution using the chi-square goodness-of-fit test. These differences were particularly prominent at the extremes, the geometric distribution underestimating the frequency of occurrence of both short and very long durations of some weather sequences, while overestimating the medium values. Extreme value distributions such as the exponential or gamma distribution were therefore considered, and it was found that the gamma distribution provided the best fit to the persistence probability distribution for each weather state. Although this is a continuous distribution, it can be used as a discrete distribution as described in equation 5-3.

The gamma distribution is given by (5-3):

$$f(x,\alpha,\beta) = \frac{1}{\beta^{\alpha}\Gamma(\alpha)} x^{\alpha-1} e^{-\frac{x}{\beta}} \qquad (5\text{-}3)$$

When $\alpha = 1$, the exponential distribution results. Using integers for x-values cannot provide the required persistence probability distribution for the occurrence of one-day persistence. Therefore, x is replaced in the equation by $n - k$, where n is the number of days that a weather type state persists, and k is a positive non-integer ($k < 1$).

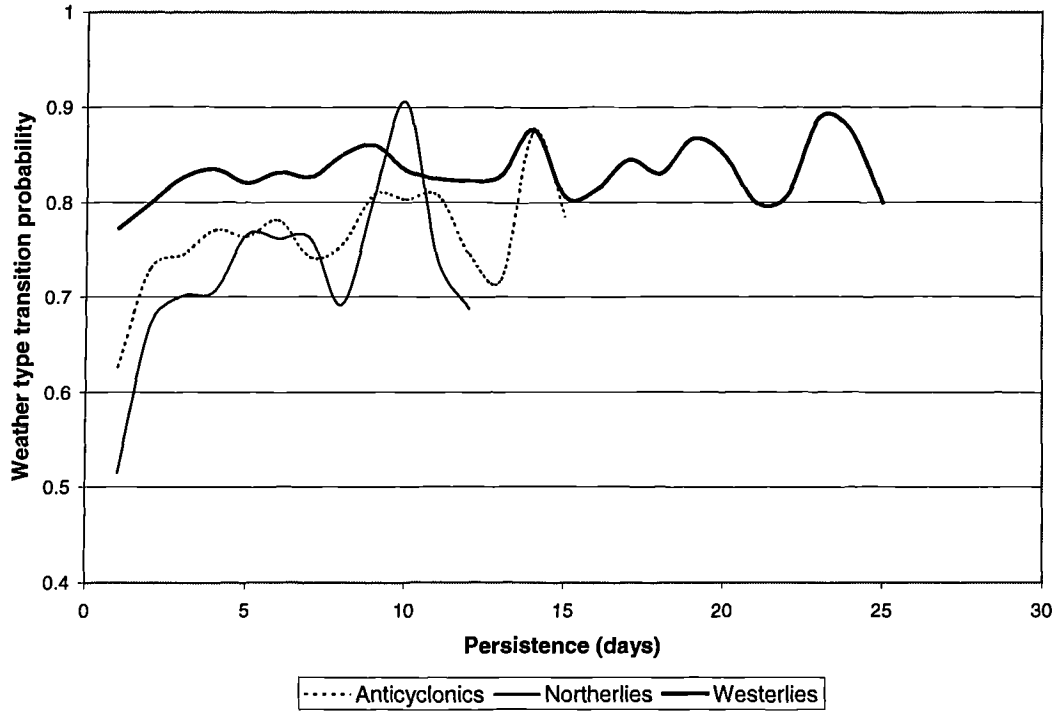

Figure 5-8: Weather state transition probabilities from a state to itself after different persistence durations for the 'winter' period.

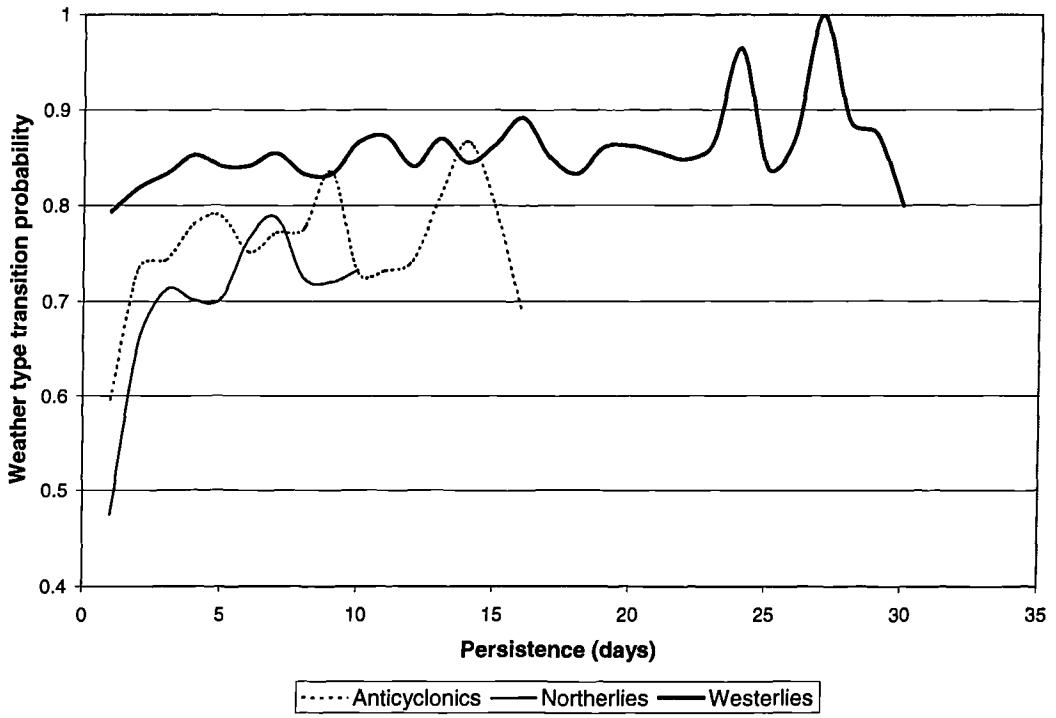

Figure 5-9: Weather state transition probabilities from a state to itself after different persistence durations for the 'summer' period.

A gamma distribution was fitted to the persistence probability distribution of each of the six weather states using L-moments to fit the gamma distribution parameters (see Hosking 1997) with values of k conditioned by the starting value of the distribution. The parameter values in Table 5-9 were obtained.

	'Summer'			'Winter'		
Parameter	A	N	W	A	N	W
k	0.349	0.330	0.400	0.280	0.300	0.411
alpha	0.591	0.549	0.727	0.461	0.480	0.691
beta	3.379	2.500	5.256	3.771	2.430	6.124
MSE	0.368	1.830	0.524	0.604	0.365	0.350

Table 5-9: Calibrated gamma distribution parameters for the six weather states and MSE.

The MSE between the natural logs of the simulated and observed distributions for each weather state is less than 0.7, excepting 'summer' northerlies. The anomalies causing the larger MSE for this weather state can be seen in Figure 5-10. The winter fits are shown in Figure 5-11. The gamma distributions were generated up to an arbitrary value of 65 that is 20 days longer than any persistence noted in the period from 1881-1996.

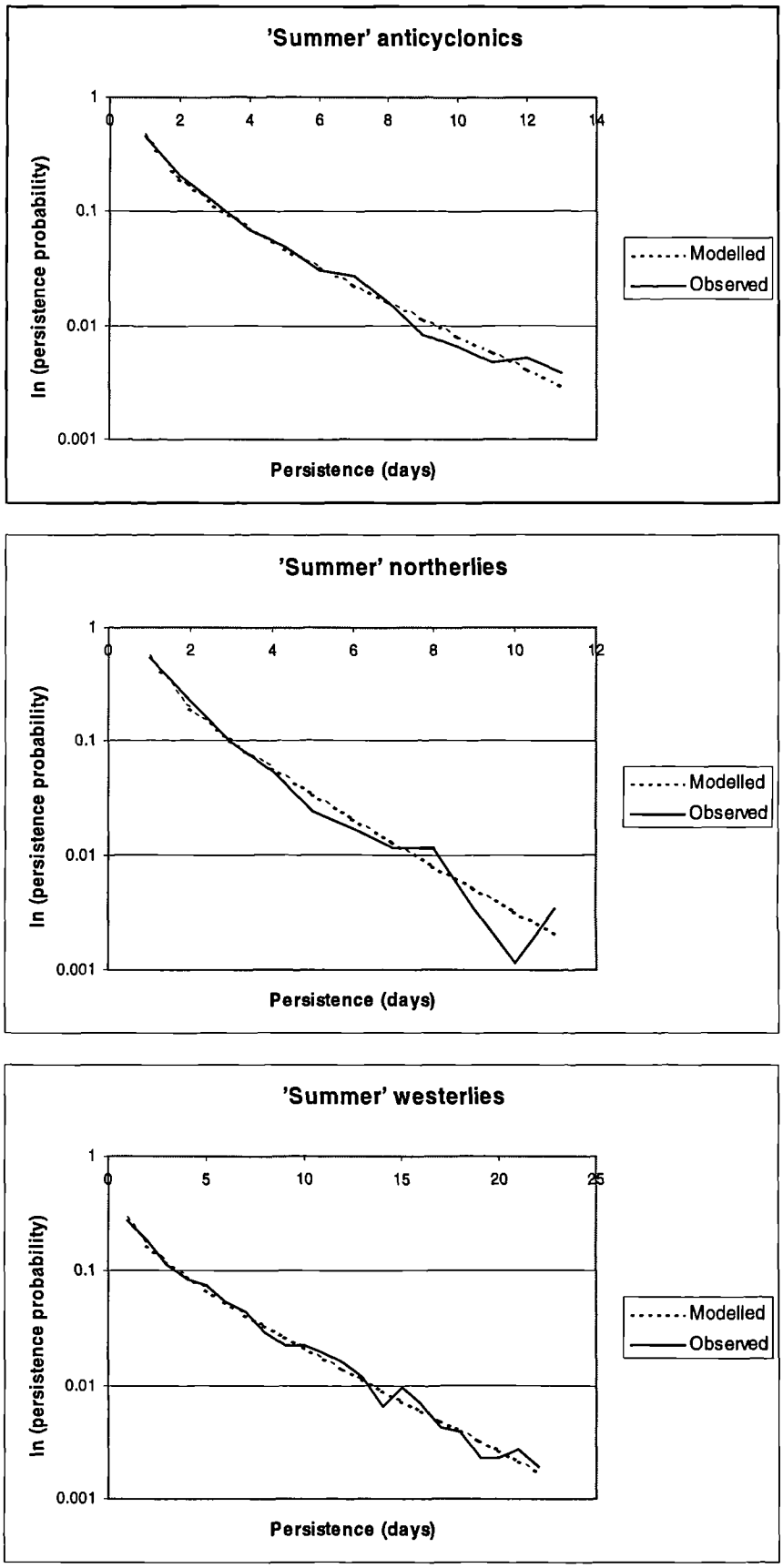

Figure 5-10: Comparison of the 99.5 percentile of observed persistence probability distribution against the fitted gamma distribution for the 'summer' period.

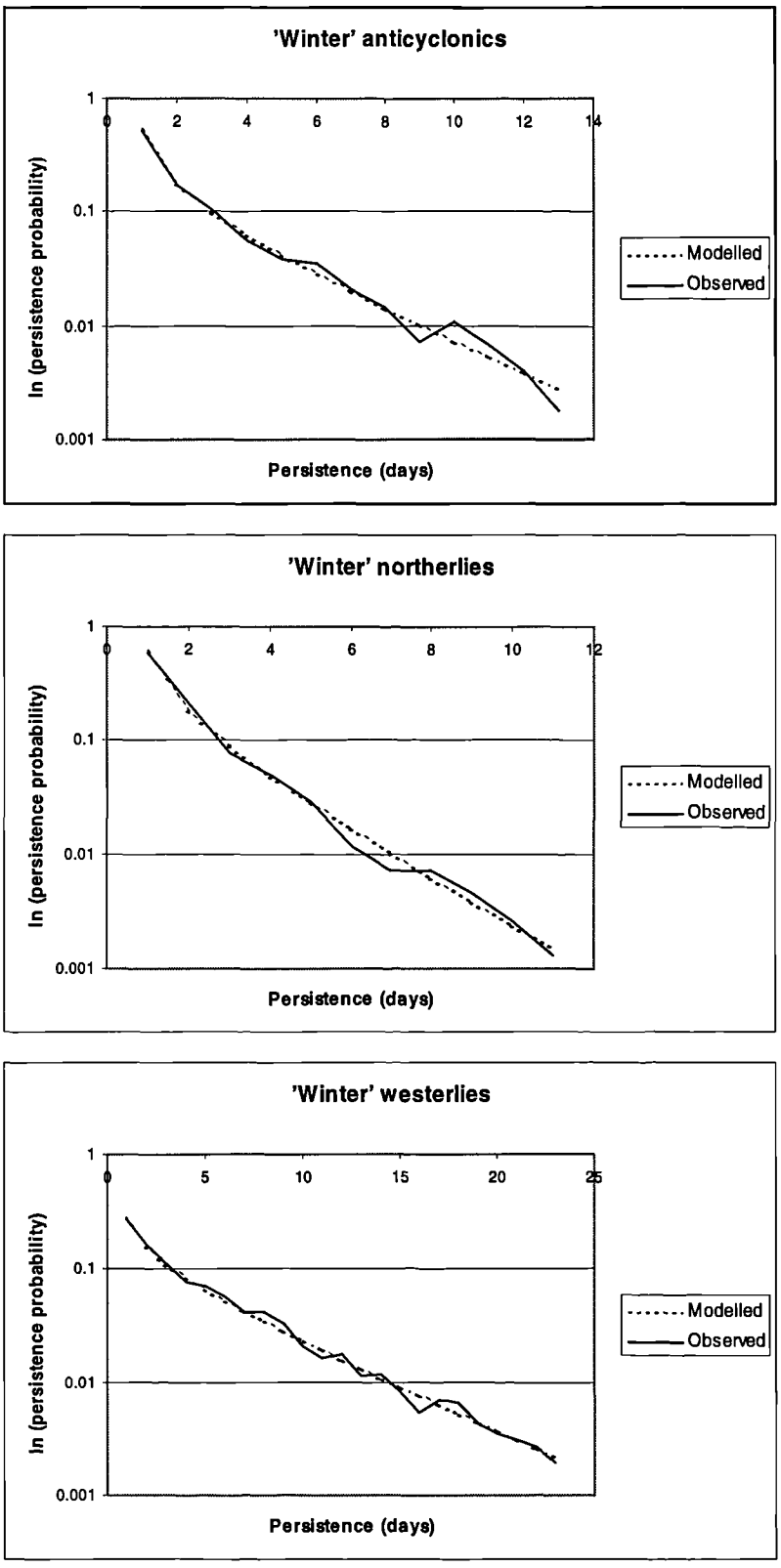

Figure 5-11: Comparison of the 99.5 percentile of observed persistence probability distribution against the fitted gamma distribution for the 'winter' period.

5.3.2 Model validation

A Monte-Carlo experiment consisting of fifty 116-year simulated weather state series was used to evaluate the capability of the model to generate synthetic series with statistics similar to those of the observed OWT 116-year series (1881-1996). Comparisons were made of modelled and observed transition and persistence probability distributions. The overall number of days of each weather state in the 116-year record and the simulated mean-, minimum-, maximum-occurrence, and variance were determined. Finally, a comparison was made of the observed and simulated distribution of annual daily occurrence of a weather state, ordered over the 116-year period.

	'Summer'			'Winter'		
Statistic	A	N	W	A	N	W
Observed A	0.627	0.102	0.272	0.596	0.074	0.331
Modelled A						
Average	0.630	0.100	0.269	0.598	0.074	0.328
Maximum	0.651	0.11	0.29	0.618	0.083	0.34
Minimum	0.614	0.091	0.254	0.583	0.067	0.31
σ	0.009	0.005	0.007	0.008	0.004	0.007
Error	-0.003	0.002	0.003	-0.002	0.000	0.003
Observed N	0.224	0.515	0.261	0.255	0.474	0.271
Modelled N						
Average	0.219	0.526	0.255	0.250	0.484	0.266
Maximum	0.232	0.546	0.277	0.273	0.511	0.286
Minimum	0.205	0.495	0.234	0.235	0.46	0.244
σ	0.006	0.009	0.008	0.009	0.013	0.009
Error	0.005	-0.011	0.006	0.005	-0.010	0.005
Observed W	0.13	0.097	0.773	0.118	0.088	0.794
Modelled W						
Average	0.128	0.095	0.777	0.117	0.088	0.795
Maximum	0.135	0.101	0.784	0.126	0.094	0.808
Minimum	0.121	0.087	0.765	0.112	0.079	0.784
σ	0.003	0.003	0.004	0.003	0.003	0.005
Error	0.002	0.002	-0.004	0.001	0.000	-0.001

Table 5-10: Observed and modelled transition-probability statistics, including within state probabilities, for the fifty Monte-Carlo 116-year series. Error refers to the observed transition probability minus the mean of the 50 simulated transition probabilities.

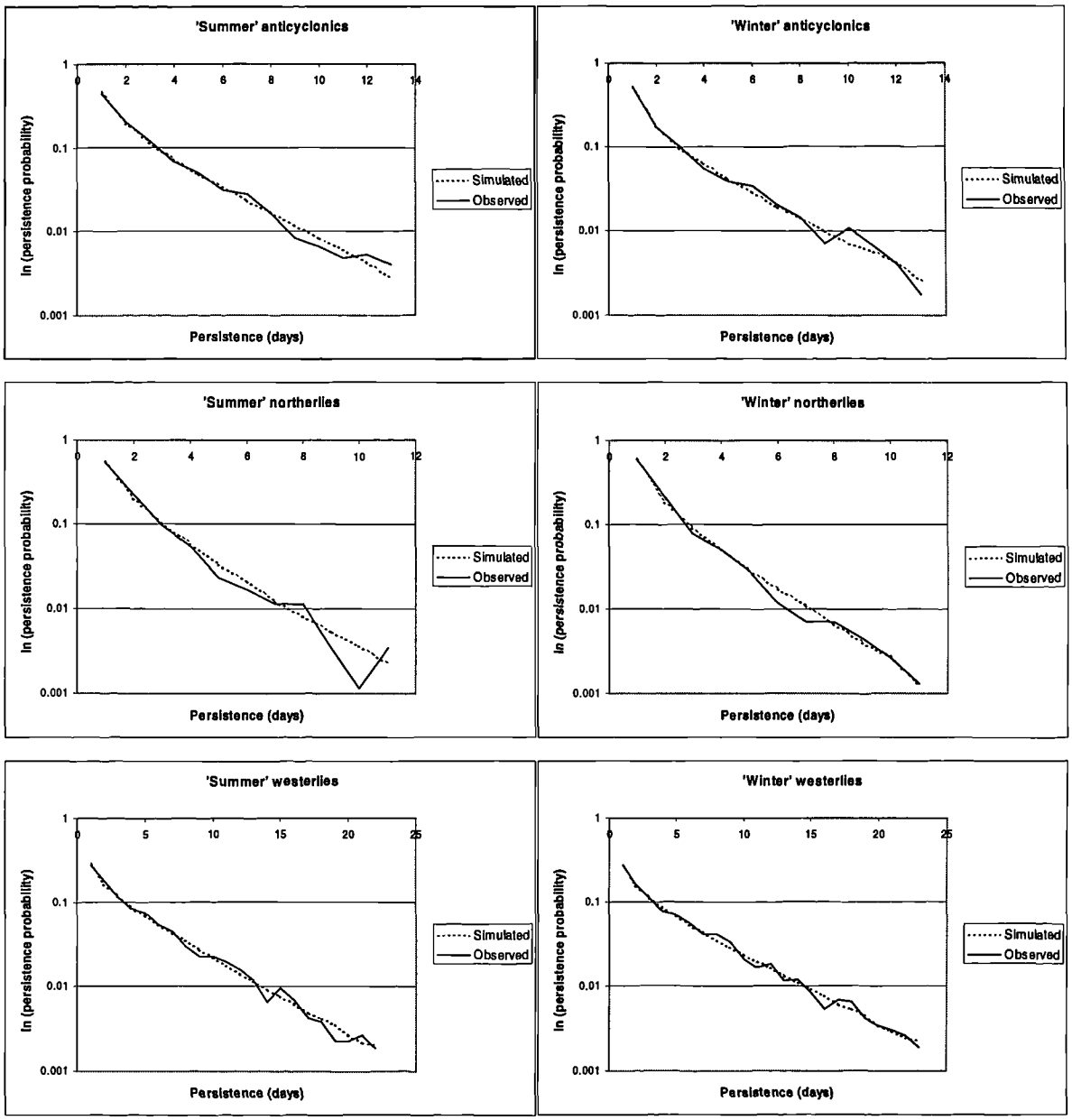

Figure 5-12: Comparison of the lower 99.5 percentile of mean simulated persistence probability distributions against observed persistence probability distributions.

	'Summer'			'Winter'		
WT	A	N	W	A	N	W
Fitted MSE	0.368	1.830	0.524	0.604	0.365	0.350
Simulated MSE	0.441	2.075	0.594	0.504	0.409	0.382

Table 5-11: Comparison of fitted persistence probability gamma distribution MSE and mean simulated MSE for fifty 116-year weather type series. MSE denotes the sum of the squared differences between the natural logs of the observed persistence probability distribution and that simulated or fitted.

It can be observed in Table 5-10, and visually in Figure 5-12, that the transition probabilities are fitted well by the semi-Markov chain model. The largest errors between the observed one-step transition probabilities and those simulated are –0.011 for the transition from the 'summer' northerly type to itself, and –0.010 for the transition from the 'winter' northerly type to itself. This error is about two percent of the total in both cases. All errors are within two standard deviations from the observed value. It can be additionally observed in Table 5-11 that the MSE between the observed persistence and the simulated persistence probability distributions is low and similar to the MSE between the observed and fitted distributions. The model is therefore capable of reproducing both observed transition and persistence probability distributions.

As a more rigorous check of model performance the mean, maximum and minimum total number of days of each of the six weather states simulated by the model in the fifty 116-year simulated series, and the variance within the fifty series were compared against observed statistics. For these purposes the first and last year of each generated series were omitted as the 'winter' and 'summer' seasons overlap calendar years, leaving 144 years of data for comparison.

	'Summer'			'Winter'		
Statistics	A	N	W	A	N	W
Observed	6032	3505	11325	5442	2813	12494
Simulated						
average	6015	3545	11302	5428	2892	12428
maximum	6362	3718	11686	5662	3086	12797
minimum	5759	3281	10896	5200	2710	12142
difference	-17	40	-23	-14	80	-66
σ	126.80	93.51	163.10	104.26	94.97	137.97
2σ	253.60	187.02	326.18	208.51	189.94	275.94
anomaly yr^{-1}	-0.15	0.35	-0.20	-0.12	0.70	-0.58

Table 5-12: Observed and simulated total number of days in 114 years of each weather type. Difference refers to the difference between average simulated and observed values (i.e. average – observed). Anomaly yr^{-1} refers to the number of days per year of each weather type that are over or under-estimated by the model (i.e. difference/114).

Table 5-12 gives the mean simulated statistics for total number of days of each weather type occurring in a 114 year period, and compares this to the historical record. The observed totals, in all cases, lie within one standard deviation of the mean of the fifty simulated series, and annual errors are small. The annual model error in prediction is less than a day for all six weather types, the most anomalous being the 'winter' northerly type with an over-prediction of 0.7 days yr^{-1}.

An analysis was also made of the annual statistics of maximum, minimum, mean daily occurrence and variance for each weather state (Table 5-13) using the fifty simulations. The mean annual occurrence of each weather state is well simulated by the model, with discrepancies of less than a day between observed and simulated statistics. Additionally, the means of the maximum and minimum simulated annual occurrence over the fifty simulations fit the observed maximum and minimum annual occurrence well. The ensemble minimum and ensemble maximum annual totals generated in the fifty simulated 114-year series are lower and higher, respectively, than the observed maxima and minima. Variance is generally under-estimated by the model.

Statistic	Ensemble Maximum	Maximum	Mean	Minimum	Ensemble Minimum	Mean Variance
'Summer'						
Observed A		85	52.9	27		153.8
Simulated A	93	83.3	52.8	25.9	15	133.2
Observed N		53	30.7	14		66.7
Simulated N	67	56.6	31.1	11.2	7	81.1
Observed W		129	99.3	69		166.6
Simulated W	145	132.4	99.1	65.0	49	177.0
'Winter'						
Observed A		78	47.7	25		133.5
Simulated A	93	78.8	47.6	21.7	11	125.3
Observed N		49	24.7	8		92.8
Simulated N	61	50.1	25.4	8.6	4	63.5
Observed W		136	109.6	75		181.3
Simulated W	157	140.8	109.0	73.1	58	170.6

Table 5-13: Comparison of annual statistics for the observed and mean of the simulated fifty 114-year series. Ensemble maximum and minimum indicate the maximum or minimum total days in a year of that weather type within the fifty simulated 114-year series.

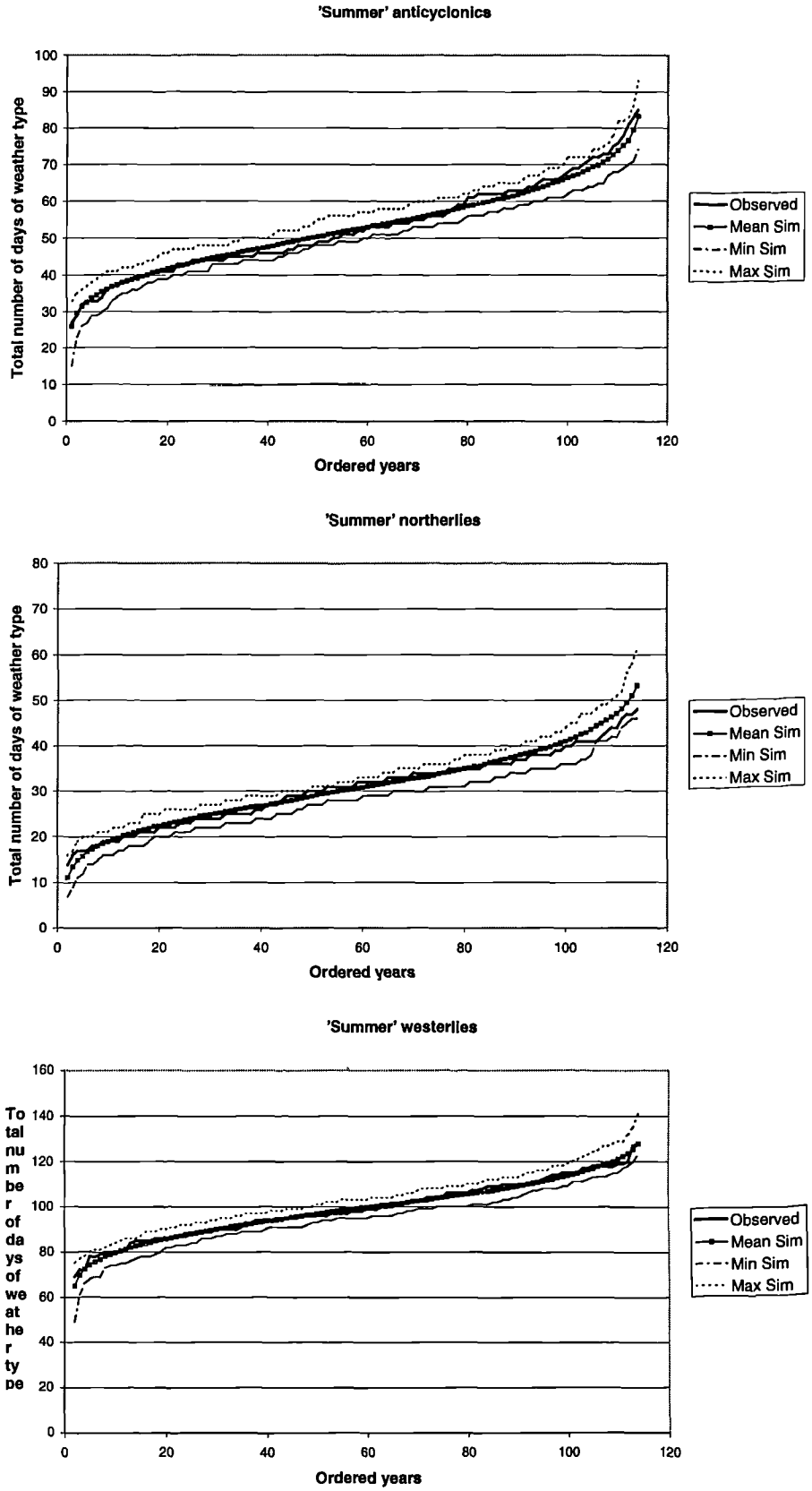

Figure 5-13: Total number of days occurrence of 'summer' weather types for 114 years shown in an ordered sequence with minimum and maximum limits.

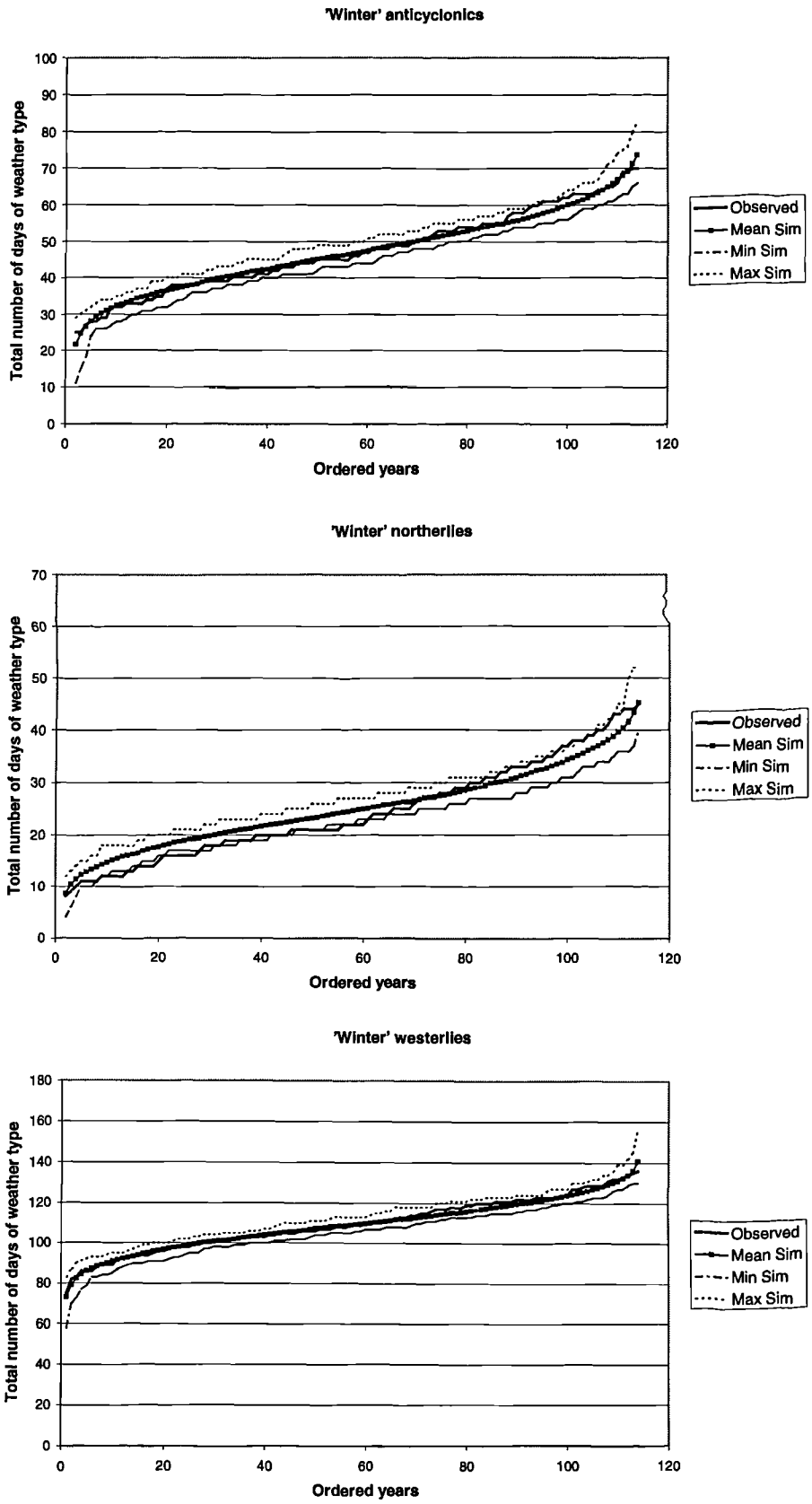

Figure 5-14: Total number of days occurrence of 'winter' weather types for 114 years shown in an ordered sequence with minimum and maximum limits.

The effect of errors in simulated variance and ensemble maxima and minima upon model performance was further investigated. The annual occurrence of each weather state was calculated for each year of the fifty 114-year simulations. These 114 annual totals were then ranked in ascending order for each of the fifty simulations, giving fifty ordered sequences for each weather state. For each rank, the mean of the fifty ordered sequences was calculated. This gave an expected distribution of annual totals for each weather type over a 114-year period. A similar procedure provided maximum and minimum error or uncertainty bounds about this distribution. The observed 114-year series was treated similarly and annual totals were ordered for each weather state. It can be seen in Figures 5-13 and 5-14 that the simulated series follow the observed distribution of annual totals of each weather type very closely. In all cases, the error bands are small. The MSE between observed and mean-simulated ordered sequences can be found in Table 5-14.

	MSE
Winter W	250.9
Winter N	557.6
Winter A	184.6
Summer W	198.3
Summer N	215.1
Summer A	236.9
Total MSE	**1643.4**

Table 5-14: MSE between observed and the mean simulated ordered sequence for each weather type.

The MSE between observed and mean simulated ordered sequences is low for all weather types, excepting that of 'winter' northerlies (WN) (Figure 5-15). The model slightly overestimates the frequency of low annual occurrences of WN, and similarly underestimates the frequency of high occurrence, with a maximum of four days error for any one ranking. However, errors are in the order of one to two days annually, and model simulations are considered satisfactory.

5.4 Development of a rainfall model (WeatherSim)

5.4.1 Expected regional parameters

The Neyman-Scott Rectangular Pulses (NSRP) model, detailed in sections 2B.2.3 and 2B.2.4, is a clustered point-process stochastic rainfall model, and is fully described by Cowpertwait (1991; 1994; 1995) and Cowpertwait *et al.* (1996*a*,*b*). The single-cell model has five parameters when fitted to a single site (Table 5-15). An analysis was made of the fitted model parameters that could be expected within the Yorkshire region. Parameters were fitted to daily precipitation data from 1961-1990 for each of the six sites detailed in Table 5-1 using a one-cell, single-site

model. The model fits were achieved on a monthly basis using the following sample moments: $\mu(1)$, $\phi(24)$, $\gamma(1)$, $\gamma(6)$, $\gamma(12)$, $\gamma(24)$ and $\gamma(48)$, $\rho(1)$, $\rho(6)$, $\rho(12)$, $\rho(24)$, $\rho(48)$, where μ is mean precipitation, ϕ is proportion dry, γ is variance, ρ is auto-covariance and the number in brackets corresponds to the time period in hours (same terminology as Cowpertwait *et al.*, 1996*a*). Hourly variance statistics were derived from the daily variance using regression equations for the UK produced by Cowpertwait *et al.* (1996*a*) (see Section 2B.2.4).

Parameter	Explanation
λ^{-1} (lambda)	the mean waiting time between adjacent storm origins (h^{-1})
β^{-1} (beta)	the mean waiting time for cell origins after the storm origin (h^{-1})
ν (nu)	the mean number of rain cells associated with a storm origin. (-)
η^{-1} (eta)	the mean duration of a cell (h^{-1})
ξ^{-1} (xi)	the mean cell intensity (mm h^{-1})

Table 5-15: The parameters of a one-cell NSRP model.

The fitted λ^{-1} values provided a range for rate of storm arrivals of between two and six days. The highest rate occurs in autumn at Moorland Cottage (Pennines) with a storm origin every 1.8 days. The lowest rate occurs in May at Lockwood Reservoir (northeast region), with a storm origin every six days. Maxima are found in both the southeastern and northeastern sub-regions in autumn, with a minimum in the Pennines during this time. This may be due to an increase in northerly weather types during the months of September and October.

The mean waiting time for rain cell origins after the storm origin, β^{-1}, was between 24- and 48-hours in general. However, the minimum is under 10 hours at Hull (southeastern region) during November. Shorter mean waiting times are found in the winter than the summer, except at Pennine sites where mean waiting times are short throughout the year. The mean number of rain cells per storm, ν, show an approximately sinusoidal relationship with maxima in winter and minima in summer at all sites. The mean number of raincells per storm is four to seven in winter and two to five in summer months, although more raincells are generated per storm at Pennine sites than elsewhere.

The fitted mean cell duration, η^{-1}, is always less than 12 hours. The southeastern sites and the Pennine site of Great Walden Edge have very low mean rain cell duration, especially in winter months. Higher altitude sites, e.g. Lockwood Reservoir and Moorland Cottage, have a high fitted mean cell duration throughout the year. The mean cell intensity, ξ^{-1}, has a maximum of 7 mm hr^{-1} at the high Pennine site of Moorland Cottage in winter months. In general, Pennine sites show a maximum in winter months and minima in summer months. At eastern sites, and

especially prominent at Lockwood Reservoir, the maximum intensity occurs during the months of September and October. This may be related to the marginal difference between the land and the North Sea surface temperature during these months, coupled with an increase in northerly weather types, bringing increased convective precipitation to the east of the region, which would be felt most at higher altitude sites.

5.4.2 Fitting of weather 'state' parameters (model calibration)

5.4.2.1 Investigation into site seasonality

Site seasonality was investigated prior to the NSRP fitting by analysing monthly mean daily precipitation for anticyclonic, westerly and northerly weather states at each of the three sites. These are plotted in Figure 5-16. At Moorland Cottage, the mean daily precipitation distribution of the westerly weather state closely matches the distribution of observed mean daily precipitation. The mean daily precipitation totals for the westerly weather state in August and September are much higher than those of April, May, June and July, and in fact more akin to the winter totals. This reinforces the climatological fact that Pennine summers are very short. The year is split into two periods: April to August (season 1) and September to March (season 2).

At Lockwood Reservoir, a relationship was found between the northerly weather state and observed mean daily precipitation totals. The northerly weather state provides the highest precipitation totals to the northeastern region (Figure 5-15) and splits the climatological year into two approximate intervals, January to June (season 1) and July to December (season 2). At Kirk Bramwith, the year can be split into two intervals, April to September (season 1) and October to March (season 2), based upon the northerly weather state precipitation distribution. Season 1 and season 2 are arbitrarily titled 'summer' and 'winter' in each case.

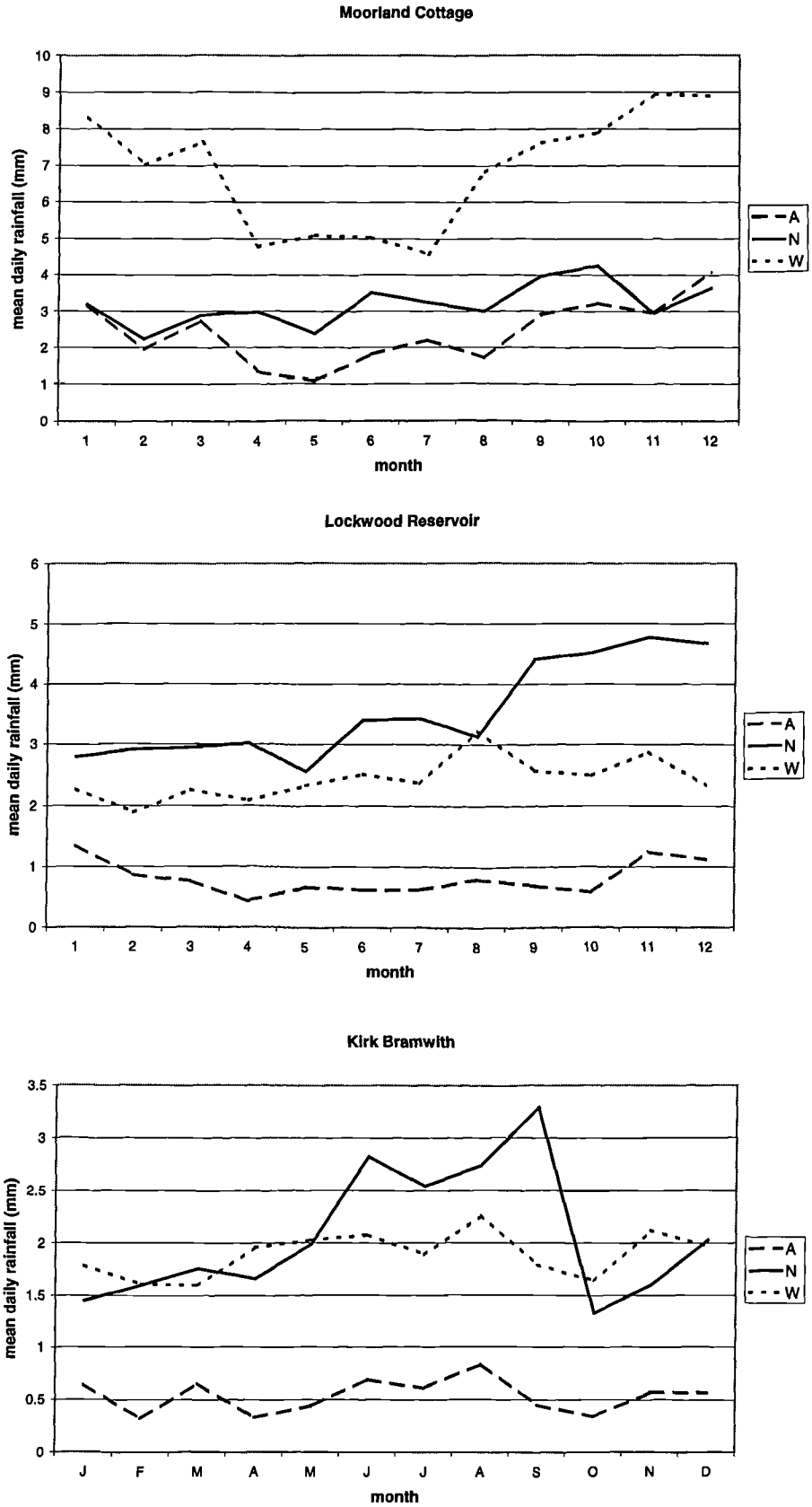

Figure 5-15: Monthly mean daily precipitation plotted for each weather state; anticyclonic, westerly and northerly, at Moorland Cottage, Lockwood Reservoir and Kirk Bramwith.

5.4.2.2 Parameter calibration

The NSRP parameter fitting of the six weather states was achieved using a representative site for each sub-region: Moorland Cottage for the Pennines, Lockwood Reservoir for northeastern, and Kirk Bramwith for southeastern. Daily precipitation data for the 30-year period from 1961 to 1990 were split into the six weather states for each of the three sites using the groups in Table 5-11 (see Table 5-16). 'Unclassified' days were omitted from the analysis. A one-cell model fit was achieved for each of the six weather states for each site using the fitting procedure detailed previously. Simulated series using these parameters provide a close match to observed statistics.

	Weather State					
	SA	SN	SW	WA	WN	WW
Months of data	46.7	29.2	91.3	41.8	22.6	103.5

Table 5-16: Amount of data (in months) used for model fitting of each weather state.

Parameter Weather State	Site	λ^{-1} (h^{-1})	β^{-1} (h^{-1})	ν (-)	η (h^{-1})	ξ ($mm\ h^{-1}$)
SA	MC	0.0094	0.115	1.765	0.621	0.5241
	LR	0.0140	0.063	1.000	0.570	0.8692
	KB	0.0055	0.020	1.524	1.548	0.2162
SN	MC	0.0322	0.403	1.485	0.375	1.0583
	LR	0.0480	0.031	1.058	0.218	1.8642
	KB	0.0099	0.023	4.510	1.061	0.4147
SW	MC	0.0383	0.086	2.346	12.000	0.0308
	LR	0.0338	0.029	1.326	0.327	1.2471
	KB	0.0333	0.347	1.278	0.353	1.3951
WA	MC	0.0076	0.024	3.582	0.385	0.9094
	LR	0.0075	0.043	6.544	12.000	0.1007
	KB	0.0068	0.180	4.637	12.000	0.1180
WN	MC	0.0389	0.184	1.000	0.526	0.7598
	LR	0.0471	0.055	1.285	0.376	0.9351
	KB	0.0100	0.059	11.874	12.000	0.1404
WW	MC	0.0288	0.025	2.770	0.501	0.4293
	LR	0.0206	0.038	3.115	0.765	0.843
	KB	0.0159	0.086	5.545	12.000	0.0943

Table 5-17: Fitted parameters for a one-cell model.

The parameter values produced for the one-cell model can be found in Table 5-17, with a comparison of observed, fitted and simulated 24-hr statistics in Table 5-18. The characteristics of the different weather states at the three sites can be seen from the fitted parameter values (Table 5-17). For example, both the SA and WA states have slow storm arrival rates coupled with a long mean waiting time for raincells after the storm origin. These characteristics are especially prominent in the Pennine and southeastern regions, and produce a very dry weather type. The characteristics of SW and WW in the Pennines are also interesting. In the summer, the westerly weather-state produces short-lived cells with high intensities, suggesting convective precipitation. However, in the winter the rain-cells are of longer duration with much lower intensities, consistent with frontal precipitation. These properties can be represented in the Generalised NSRP by using two distinct cell types ('light' and 'heavy'), but at the expense of parsimony (Cowpertwait, 1995).

Parameter		$\mu(24)$ obs	$\mu(24)$ fitted	$\mu(24)$ sim	$\gamma(24)$ obs	$\gamma(24)$ fitted	$\gamma(24)$ sim	$\phi(24)$ obs	$\phi(24)$ fitted	$\phi(24)$ sim
Weather State	Site									
SA	MC	1.22	1.22	1.32	18.08	18.32	22.71	0.78	0.78	0.79
	LR	0.68	0.68	0.67	6.54	5.72	11.91	0.75	0.75	0.79
	KB	0.60	0.60	0.70	7.12	6.95	9.08	0.85	0.85	0.84
SN	MC	2.90	2.90	3.22	33.43	34.38	37.94	0.49	0.49	0.48
	LR	2.99	2.99	2.57	28.56	26.03	20.36	0.30	0.30	0.36
	KB	2.45	2.45	2.52	27.26	27.58	26.10	0.52	0.52	0.49
SW	MC	5.84	5.84	5.57	80.75	84.29	82.39	0.29	0.29	0.33
	LR	2.64	2.64	2.48	28.38	24.94	22.90	0.38	0.38	0.44
	KB	2.06	2.06	2.06	19.18	18.65	20.76	0.50	0.50	0.54
WA	MC	1.87	1.87	1.78	28.54	23.54	20.92	0.63	0.63	0.63
	LR	0.98	0.98	0.95	4.96	5.19	4.96	0.61	0.61	0.64
	KB	0.53	0.53	0.50	2.99	2.82	2.70	0.80	0.80	0.84
WN	MC	2.34	2.34	2.06	27.29	25.95	19.93	0.49	0.49	0.53
	LR	4.13	4.13	3.98	48.16	48.36	46.47	0.30	0.30	0.35
	KB	1.68	1.68	1.70	9.64	9.51	8.97	0.50	0.50	0.51
WW	MC	8.91	8.90	8.27	182.11	180.03	169.27	0.24	0.24	0.27
	LR	2.39	2.39	2.39	18.07	17.93	17.57	0.36	0.36	0.38
	KB	1.87	1.87	1.92	11.54	11.67	11.95	0.48	0.48	0.49

Table 5-18: Observed, fitted and simulated 24-hour statistics for each of the six weather states at each of the three sites.

5.4.3 Model validation

Model validation was carried out in three stages. Firstly, an analysis was made of the effects of lag within the model upon the accuracy of simulated monthly statistics. Secondly, a Monte-Carlo experiment with fifty 30-yr simulations was undertaken using the historical OWT series to determine whether the correct monthly statistics were generated. Model error within the fifty synthetic series was also quantified. Finally, an examination was made of the ordered sequence of distributions of both modelled and observed daily precipitation for each of the six weather states.

5.4.3.1 The effects of lag

Model performance may be adversely affected by the lag between weather state initiation, and generation of rain-cells associated with that weather state. It has already been shown that a lag of up to a day can be expected before rain cells are produced following the initiation of the wettest weather state, that of WW in the Pennine sub-region. The lag between initiation of a weather-state and the generation of rain cells, however, can be as high as almost 10 days on average (for the SA weather state at Kirk Bramwith).

To demonstrate the lag effects of a 'wet' weather state upon a 'dry' weather state, and vice versa, the year was split into four 3-month periods; Jan-Mar, Apr-Jun, Jul-Sep, and Oct-Nov The periods from January to March and from July to September were assigned a 'dry' weather state and the other two periods were assigned a 'wet' weather state, SA and SW from Moorland Cottage. This gave two crossover periods for a 'wet' to a 'dry' weather state (in January and July) and two for 'dry' to 'wet' (in April and October).

It can be observed in Figures 5-16 and 5-17 that a lag effect is discernible in the crossover months. This translates to an increase in mean precipitation in a 'dry' month preceded by a 'wet' month, and vice versa. However, the effect is short-lived, affecting only the first month of the 3-month period. There is an increase in the proportion of dry days (PD) in April and October, but no significant reduction for the crossover months of January and July. As the SA type is extremely dry and has a very high PD it is likely that the SW weather type provides the major effect on both types of crossover period. The lag causes a reduction in precipitation in a 'wet' month preceded by a 'dry' month.

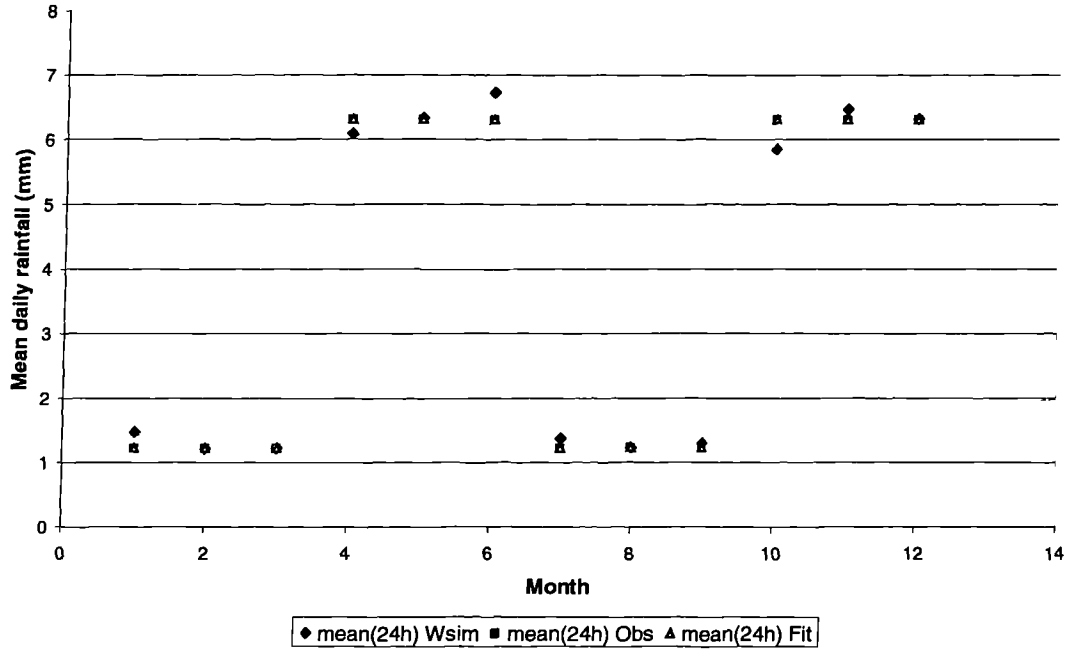

Figure 5-16: The effects of lag on the mean daily precipitation statistic within the 1-cell model, demonstrated by using the SW and SA weather states for Moorland Cottage.

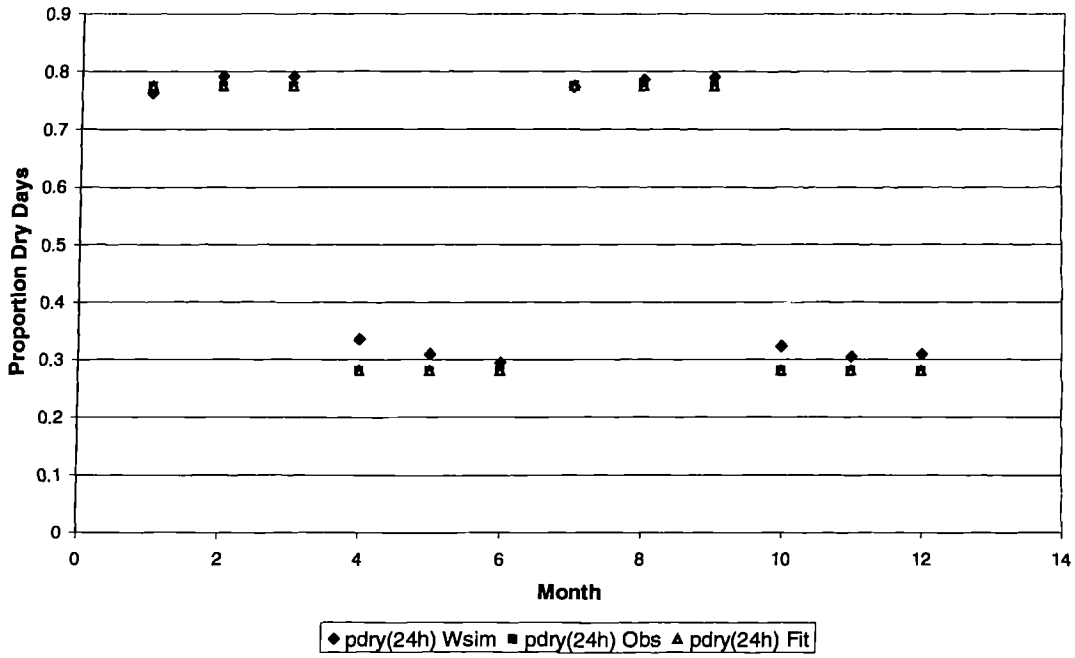

Figure 5-17: The effects of lag on the 24-hr PD statistic within the 1-cell model, demonstrated by using the SW and SA weather states for Moorland Cottage.

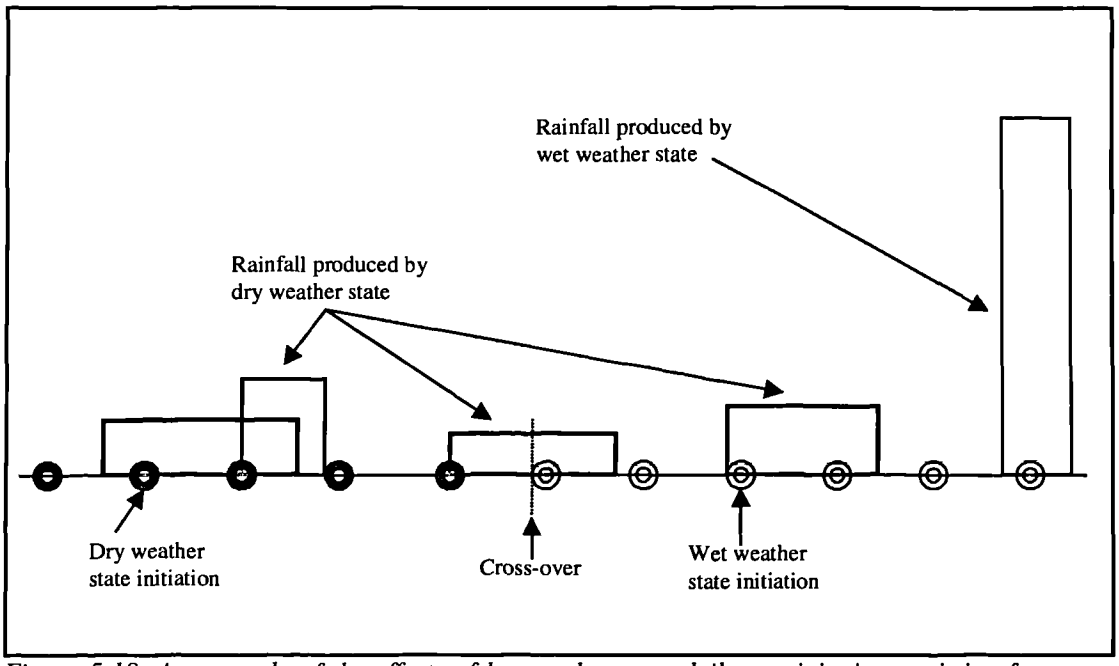

Figure 5-18: An example of the effects of lag on the mean daily precipitation statistic of a wet month given a preceding dry month. The marked cross-over is the cross-over between the two months.

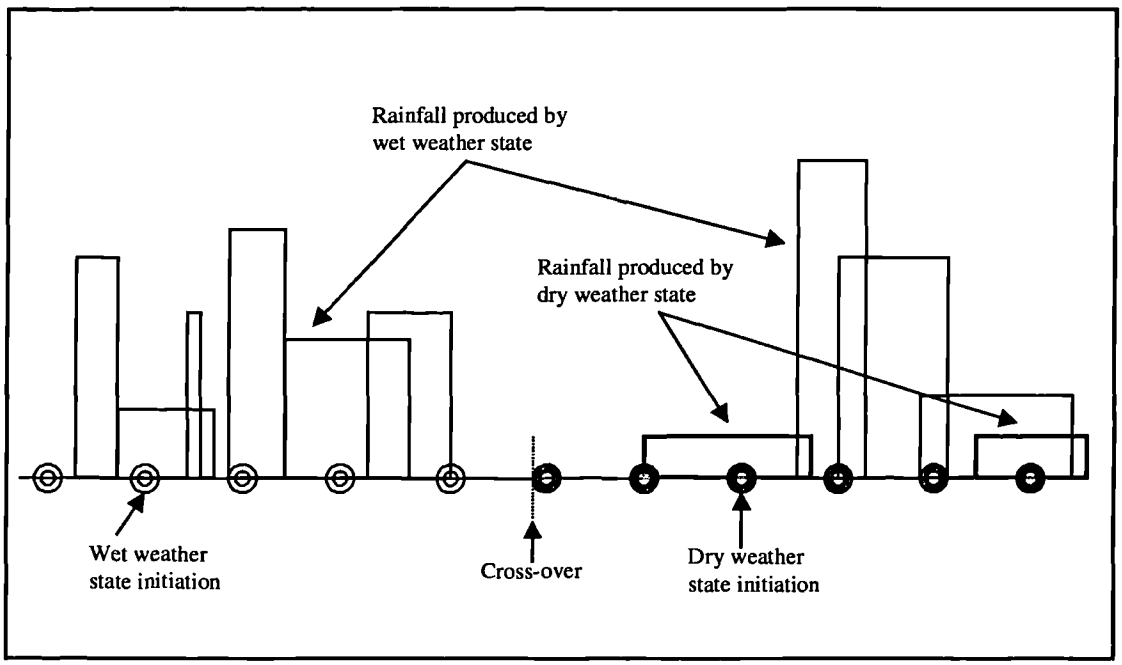

Figure 5-19: An example of the effects of lag on the mean daily precipitation statistic of a dry month given a preceding wet month. The marked cross-over is the cross-over between the two months.

The lag-effect of the previous 'dry' month brings little additional precipitation to the 'wet' month. When coupled with the lag between the initiation of a 'wet' weather state and rain-cell generation this causes a decrease in mean daily precipitation at the beginning of the monthly period. An example of this is given in Figure 5-18. Note the 5-day lag that is apparent between weather state initiation and rain cell generation for the wet weather-state. However, other 'wet' months preceded by a wet month are supplied with rain-cells from initiated wet weather states of the previous month. Similarly, a 'dry' month that incurs rain-cells from a prior 'wet' month will have an increased mean precipitation statistic, but the PD statistic may not be severely affected (see Figure 5-19 for example).

5.4.3.3 Monte-Carlo analysis

A Monte-Carlo analysis consisting of fifty 30-year simulations was used to evaluate the model's ability in reproducing the observed mean precipitation statistics from 1961-1990 at Moorland Cottage, Lockwood Reservoir and Kirk Bramwith. The historical OWT series translated into the appropriate weather states was used as input to the NSRP model. Monthly statistics for mean daily precipitation, proportion dry days (PD) and 24-hr variance were derived from the analysis and plotted against observed statistics. These included an average monthly statistic taken from all fifty 30-year simulations, and 5 and 95 percentiles of the fifty simulations.

The observed and simulated monthly mean daily precipitation statistics for each site can be observed in Figure 5-20. At Kirk Bramwith, all measured statistics are well simulated by the model (see Figures 5-20, 5-21 and 5-22). The historical variability is captured, with a low day-to-day winter variance and large increases in summer months. The PD statistic is stable at approximately 0.6 for the entire year.

At Lockwood Reservoir, the mean daily precipitation statistic is well simulated (Figure 5-20), observed statistics lying within the extremes of the simulated statistics. The PD statistic is well fitted (Figure 5-21), and an especially good match is obtained between May and August. The increased variability in precipitation during autumn months is also captured (Figure 5-22). 'Summer' variance is slightly underpredicted but the observed statistics, in the main, lie within the range of the simulated series.

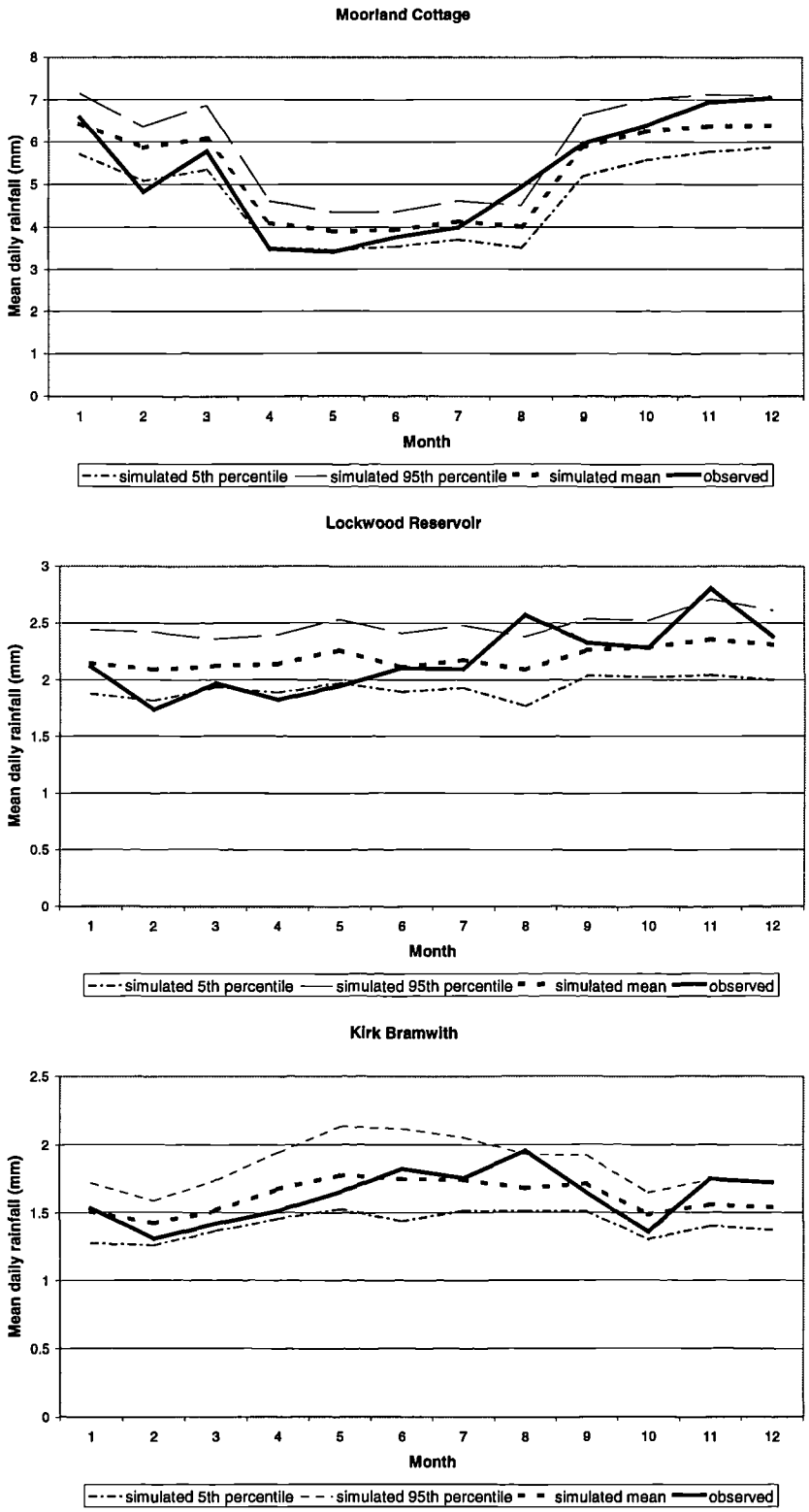

Figure 5-20: The mean daily precipitation statistic; observed, simulated mean, 5 and 95 percentiles for each calendar month using fitted parameters.

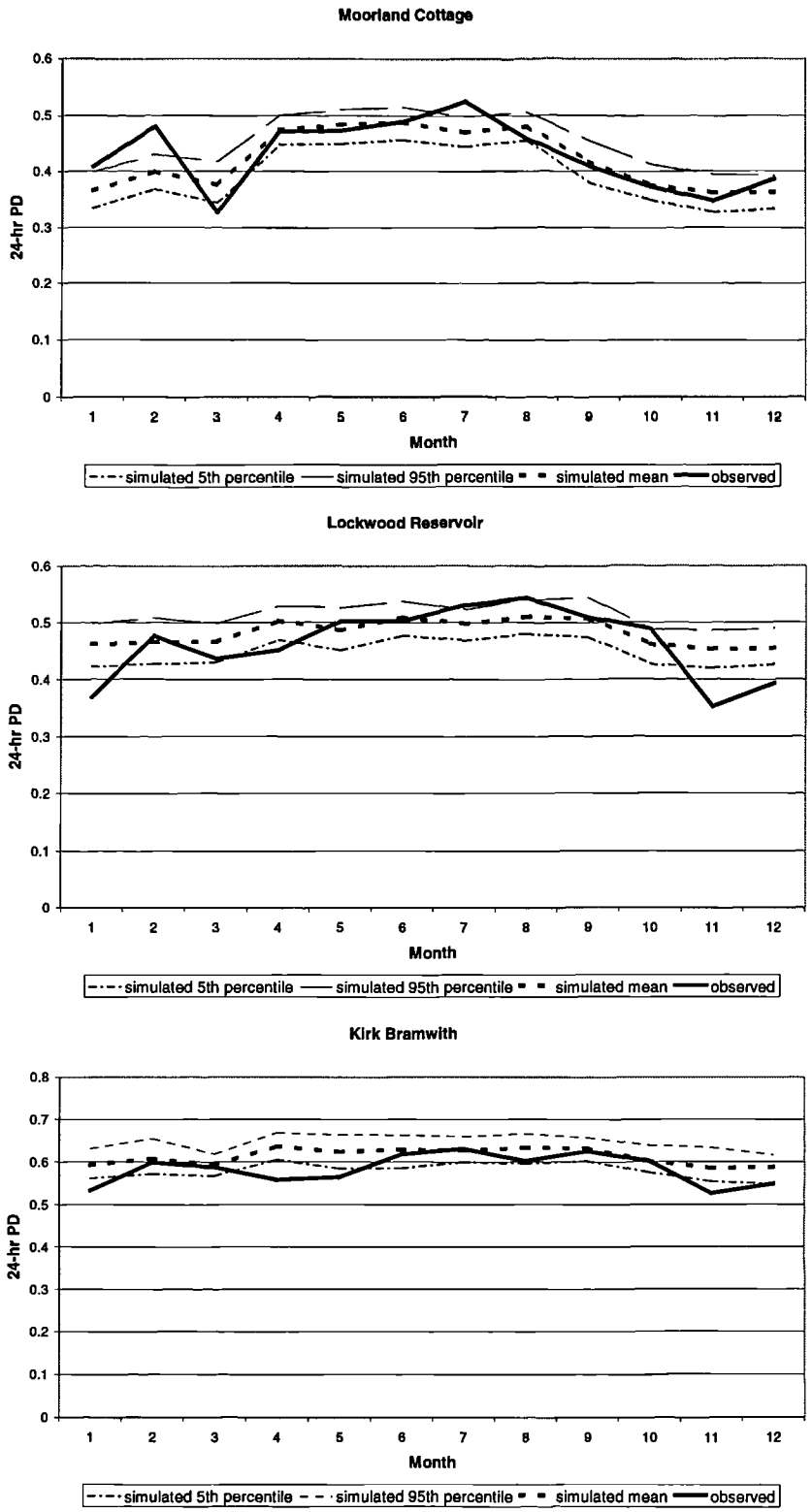

Figure 5-21: The 24-hr PD statistic; observed, simulated mean, 5 and 95 percentiles for each calendar month using fitted parameters.

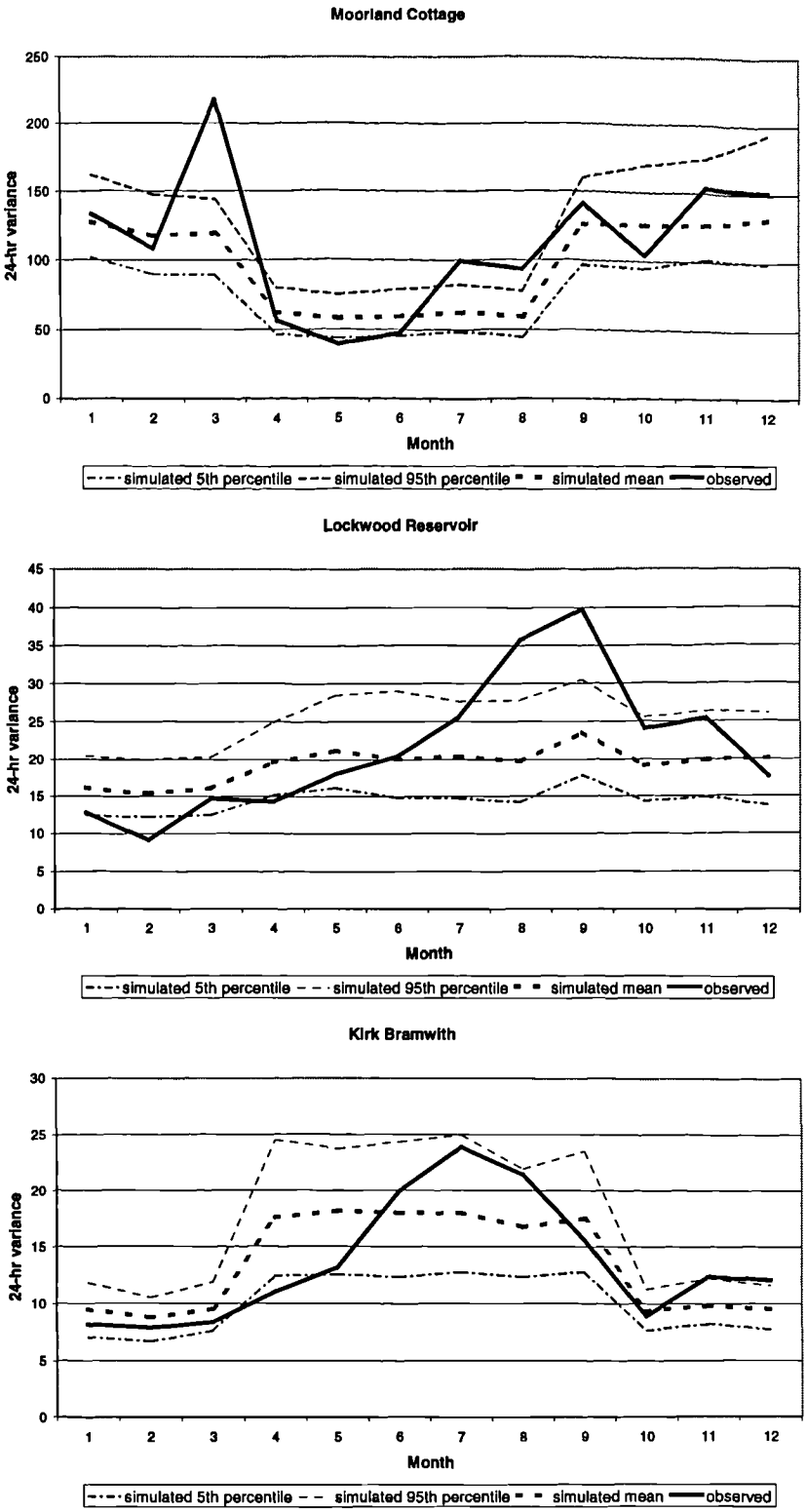

Figure 5-22: The 24-hr variance statistic; observed, simulated mean, 5 and 95 percentiles for each calendar month using fitted parameters.

At Moorland Cottage the mean daily precipitation and PD statistics are well matched (Figures 5-20 and 5-21), apart from the months of February and March which show highly unusual variation in the observed record. The observed variance is adequately reproduced (Figure 5-22), apart from the month of March itself which has very high variability. The model captures this variability to a certain extent but cannot be expected to produce such high values due to the averaging effect imposed by additionally using six other months in the model 'winter' fitting.

5.4.3.4 Expected precipitation estimation

As an additional check upon model performance, a more sophisticated measure was derived for model validation. An estimate was made of the expected precipitation in each month using the 30-year OWT series, again translated to the appropriate weather states. The value for expected mean daily precipitation for each weather state is shown in Table 5-18.

Expected monthly totals were derived for the 360 months from 1961-1990, using the OWT series as input. Mean daily precipitation totals from the fifty simulated series were added to give 360 mean monthly totals for the simulated series. These were then compared to the expected monthly totals using the following formula (5-4) for each month:

$$\%Error = \left(1 - \left(\frac{\hat{x}}{x_{sim}}\right)\right) * 100 \qquad (5\text{-}4)$$

where $\hat{x}$ = expected monthly total

x_{sim} = mean simulated monthly total

The results for Moorland Cottage can be found in Table 5-19. The percentage errors have been ordered per month according to magnitude. The average monthly error is also shown. It can be seen that the largest monthly errors occur in April and October, the crossover months between 'summer' and 'winter' weather-states. April is, on average, wetter than would be expected, and October is drier. These anomalies can be explained by the lag effects referred to in the previous section. This is also true of the other two sites.

Year	J	F	M	A	M	J	J	A	S	O	N	D
1	-22.3	-14.5	-21.7	-5.5	-12	-12.3	-10.8	-14.4	-13.8	-21.7	-16.9	-12.3
2	-18.5	-14.3	-9.6	-4.7	-8.5	-9	-9	-13.8	-13.5	-18.7	-10.2	-11
3	-13.9	-8.9	-6.3	-4.1	-8.4	-8.7	-8.6	-9.8	-4.5	-16.9	-6.2	-9.9
4	-12.6	-8.5	-5.3	-4.1	-7.2	-8.6	-8.1	-8.7	-3.7	-12.3	-4.6	-9.7
5	-9.7	-7.8	-5.1	-4	-6.8	-8.3	-8	-7.6	-3.5	-12.1	-4.2	-8.5
6	-8.5	-7.1	-4.5	-2.8	-5.6	-6.7	-5.6	-7.5	-3.2	-11.5	-3.2	-8.5
7	-7.7	-6.1	-4.5	-1.1	-4.8	-6.3	-5.2	-6.2	-3.1	-11.1	-3.1	-6.9
8	-7.2	-5.8	-4.1	-0.4	-4.2	-6.1	-5.1	-6.2	-1.8	-10.6	-2.6	-6.5
9	-7.1	-3.2	-3	4.3	-3.5	-5.8	-3.1	-4.8	-1.6	-8.9	-1.6	-5.5
10	-6.7	-3	-2.5	4.8	-3.2	-5.7	-1.5	-3.9	-1.6	-8.5	-0.9	-5
11	-3.7	-1.3	-2.5	6	-3.1	-5.4	-1.2	-2.3	-1.4	-8.3	1.3	-4.4
12	-3.1	0.8	-1.2	6.6	-1.5	-5.2	-0.8	-2.3	-1.4	-8.2	1.4	-3.9
13	-2.7	1.1	-0.9	6.7	0	-3.8	-0.4	-0.4	-1.3	-8.2	2	-2.4
14	-2.3	2.2	0.1	6.8	0	-3.6	-0.3	0.3	-1.1	-7.8	2.3	-0.9
15	-0.6	3	0.1	7.9	0.5	-3	0.4	1.3	-0.9	-7.4	2.9	0.2
16	-0.4	3.1	1.3	8.2	1.8	-2.1	1.2	2	-0.7	-7	3.4	0.9
17	-0.3	3.5	2	9.2	1.9	-0.2	1.4	2	-0.4	-5.2	4.1	1.2
18	0.2	3.8	2.3	9.4	2.3	-0.1	3.2	2.3	0.5	-5	4.3	1.2
19	0.8	4.1	2.7	9.6	2.4	0.7	3.3	2.4	0.8	-2.8	5.1	2
20	0.8	5.1	3.7	9.7	2.9	1	3.7	2.6	1.5	-2.8	5.5	2.2
21	2.2	5.8	6.4	10.8	3.1	5	4.3	2.7	2.6	-2.2	5.6	2.2
22	2.3	5.9	6.9	10.8	3.7	5.8	4.5	3.6	3.5	-2.2	6	2.8
23	2.7	6.9	7.2	11	5.7	7.3	5.1	3.6	4.2	-2.2	6.3	4.1
24	2.9	7.3	7.2	11.8	6.1	7.6	5.7	3.7	4.3	-1.7	6.4	4.1
25	3.2	8.5	7.3	13.4	6.3	9	5.9	4.2	4.3	-1.4	7.1	4.7
26	4	8.6	8.1	14	7.1	9.5	6.4	5	6	-0.9	9.3	5
27	7	8.9	10.3	14.7	7.2	10	6.6	6	6.7	0	9.6	5.7
28	9.3	10.4	10.5	15	7.7	10.9	6.9	8.4	7.5	0.9	12	5.8
29	9.9	12.4	13	16	8.3	11.5	7.2	9.7	10.9	1.1	13.2	7.7
30	11	12.9	15	17.5	8.9	11.9	16.3	10.6	14.9	1.4	13.4	8
Av	**-2.4**	**1.1**	**1.1**	**6.6**	**0.2**	**-0.4**	**0.5**	**-0.6**	**0.3**	**-6.7**	**2.3**	**-1.3**

Table 5-19: Ordered sequence of percentage errors between expected and mean simulated monthly totals at Moorland Cottage for the 30-years from 1961-1990.

5.4.3.5 Investigation of the benefit of conditioning by weather-state

Weather-state conditioning introduces a significant extra degree of complexity in the model. A purely stochastic approach is also possible, where an ensemble of possible precipitation series is generated, regardless of weather states. These series will contain sequences similar to observed precipitation and, by definition, contain statistically representative numbers of dry, wet and extreme months and years (e. g. Cowpertwait *et al.*, 1996*a*,*b*). Such a series is certainly of utility for reliability testing of water resource systems, but will not necessarily allow a meaningful re-parameterisation for future climates or the production of correlated regional models for large spatial domains. However, for a conditioned model (i.e. with weather states) to be preferred it is first necessary to demonstrate the improved performance of such a model over the basic stochastic model.

An investigation was therefore made of the benefit of introducing weather type conditioning over the use of an NSRP model unconditioned by weather type information. The NSRP model was fitted to observed precipitation statistics at Moorland Cottage, on a calendar month basis, as described previously. Fifty simulations of 60-yrs duration at hourly resolution were produced and aggregated to annual totals. Mean, 5 and 95 percentile statistics were determined for each calendar year and are shown in Figure 5-23, together with the equivalent statistics derived from the conditioned model. The conditioning of precipitation on synoptic weather types can be seen to significantly reduce uncertainty and increase explained variance. This is quantified by the increase in average correlation between observed annual totals and each of the fifty simulations using weather-type conditioning shown in Table 5-20. This is desirable, as it identifies the effect of weather state conditioning in both controlling the mean and reducing the spread of the precipitation amount distribution for each day and weather-state.

Model	Mean correlation	Maximum correlation	Minimum correlation	Standard Deviation
NSRP	0.01	0.26	-0.18	275
NSRP + weather type conditioning	0.24	0.48	0.08	225

Table 5-20. Simulated mean, minimum and maximum correlation statistics between observed annual totals and each of 50 simulations of the 1937-1996 period at Moorland Cottage using the NSRP model and WeatherSim. Standard deviation refers to the mean standard deviation of the 50 simulations.

The reduction in the conditioned 95th percentile is particularly apparent, and is due to the stipulation of a fixed (observed) proportion of dry weather-states in the conditioned model. This will result in an upper limit on annual precipitation, as opposed to the case of the unconditioned model, which allows years to be simulated containing high totals generated with equal probability in all months or days regardless of weather-state. The same limitation acts in reverse on the fifth percentile to a lesser degree, with a fixed proportion of wet weather-states in the conditioned model.

The introduction of conditioning by weather type is justified by the improvement in explained variance as well as by two additional factors. The first of these is the ability to modify the model for future climate cases by changing proportions of weather-states. The second is the capability to generate correlated series at two or more widely separated sites, conditioned by the same weather-state. These capabilities are discussed in more detail in the next section.

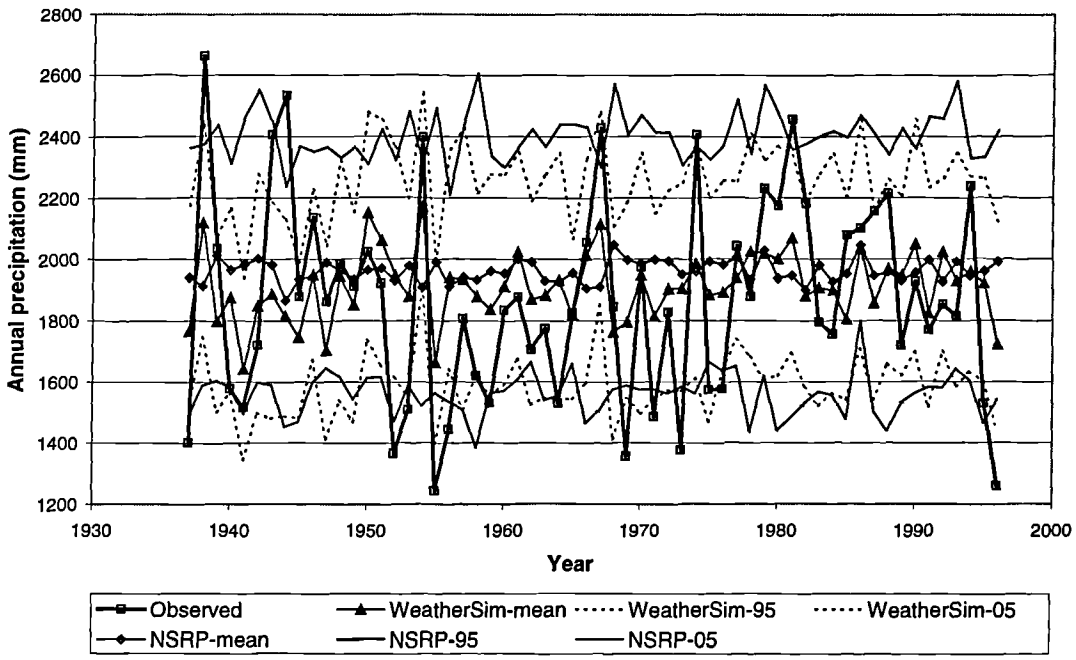

Figure 5-23: Comparison of simulated annual precipitation totals at Moorland Cottage for 1937-1996 using the NSRP model and WeatherSim (NSRP model using weather-type conditioning), showing 5 and 95 percentiles.

5.4.3.6 Reproduction of inter-annual variability and important drought events

It is necessary to validate the model's capability of reproducing inter-annual variability of precipitation and droughts of various return periods, concentrating on those events of crucial importance to water resource reliability. A characteristic or limitation of the method is imposed by the 'non-unique' nature of downscaling. By this it is meant that a wide range of possible precipitation values may be equally likely associated with a single weather type or cluster. This means that the model series cannot be explicitly used in reproducing one-to-one correspondence of precipitation amounts to observed weather types. Rather, the averaged statistical properties of the weather types will be reproduced. This may also be viewed as a low explained variance at the daily and monthly scale.

Figure 5-24 gives an example of this behaviour. Fifty simulations were performed to provide mean, 5th and 95th percentile statistics of annual-precipitation totals for the 1961-1960 period, using the OWT record as input. The model does not reproduce exactly the historical annual precipitation totals due to its stochastic nature. However, it is able to simulate annual precipitation totals within historical limits.

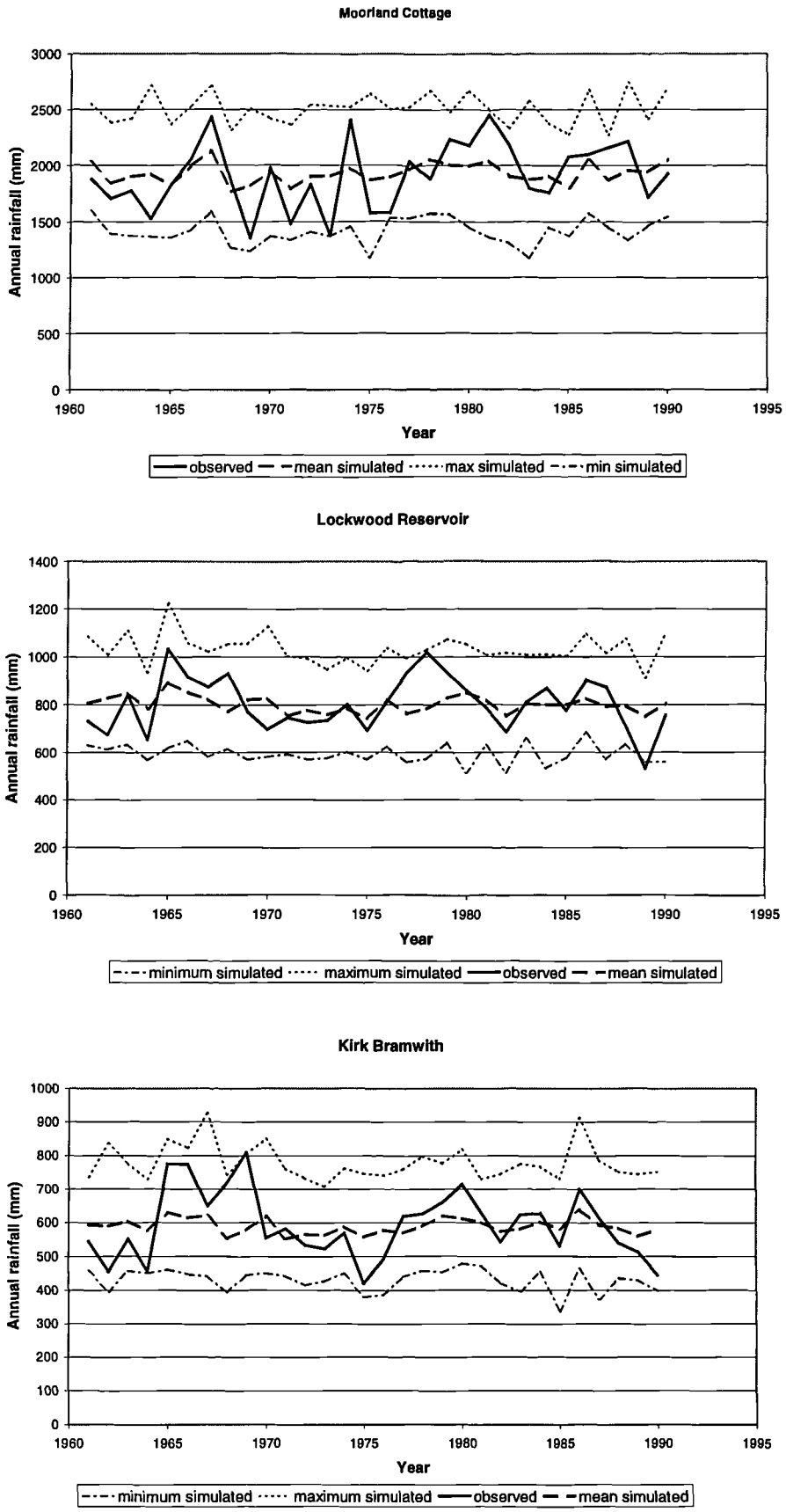

Figure 5-24: Observed and simulated mean, 5th and 95th percentiles of annual precipitation totals for the 1961-1990 period.

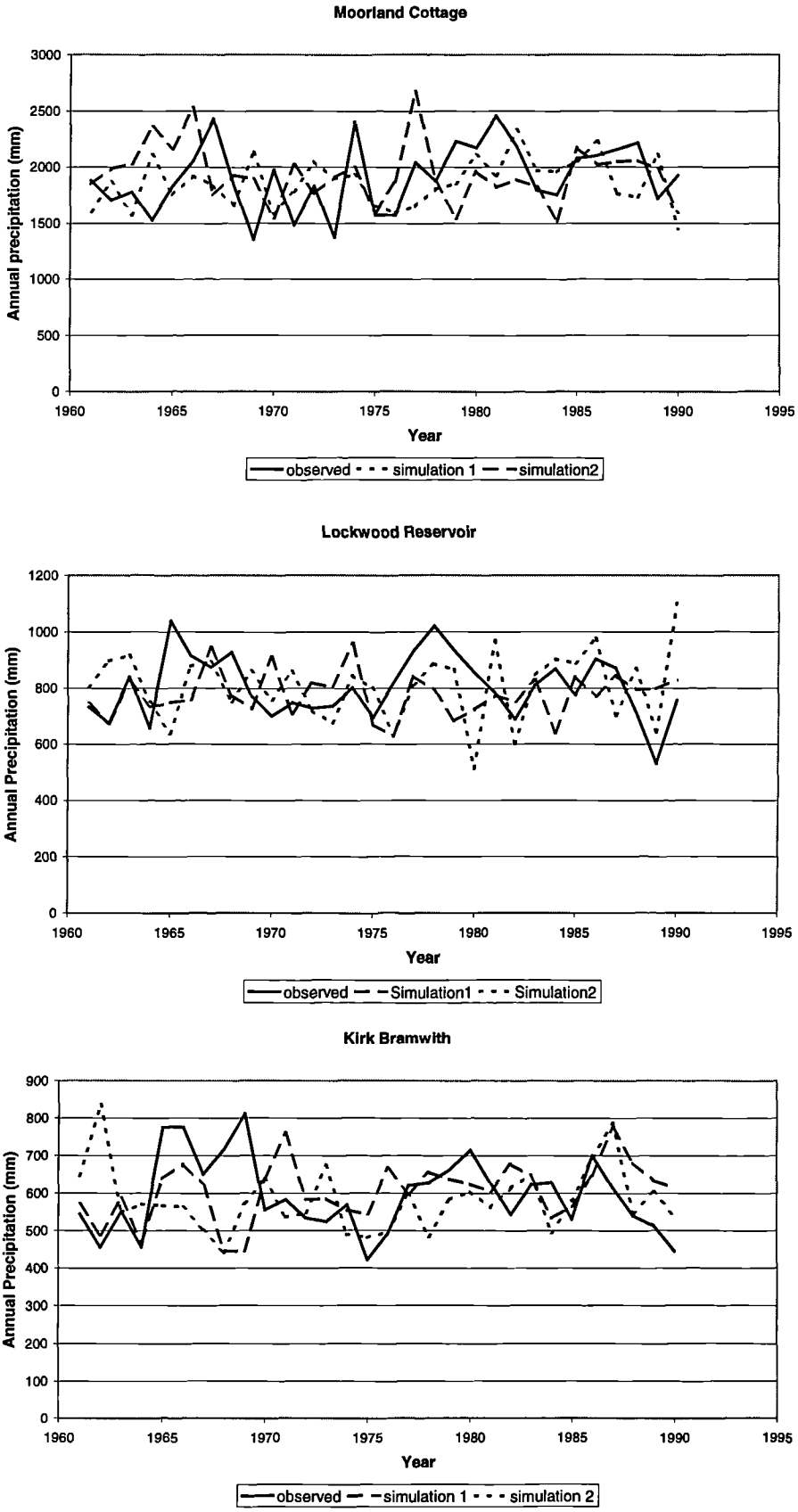

Figure 5-25: Levels of inter-annual variability of precipitation attained by model simulations and observed values for the 1961-1990 period.

Site	Series	Correlation	Mean Annual Precipitation (mm)	Standard Deviation
Moorland Cottage	Observed		1911	300
	Simulated	0.58	1930	225
Lockwood Reservoir	Observed		803	113
	Simulated	0.52	796	109
Kirk Bramwith	Observed		594	101
	Simulated	0.51	589	80

Table 5-21. Observed and simulated mean statistics for 50 simulations of the 1961-1990 period. Correlation refers to the correlation between the annual precipitation totals of the observed and mean simulated series. Standard deviation of the simulated series refers to the mean standard deviation of the simulations.

Table 5-21 gives the correlation between the observed annual precipitation total and the mean annual total of the simulated series. The standard deviation of the observed and simulated series is also shown. All simulated series have reduced standard deviations. However, single simulations for all three sites produce levels of variability akin to observed levels (see Figure 5-25). This behaviour is only a limitation if one-to-one correspondence with an observed series or a meteorological forecast is required. For most purposes, the reproduction of mean statistics is sufficient, and as the model is required for the simulation of long synthetic time-series, the ability to simulate within historical limits is considered a sufficient test.

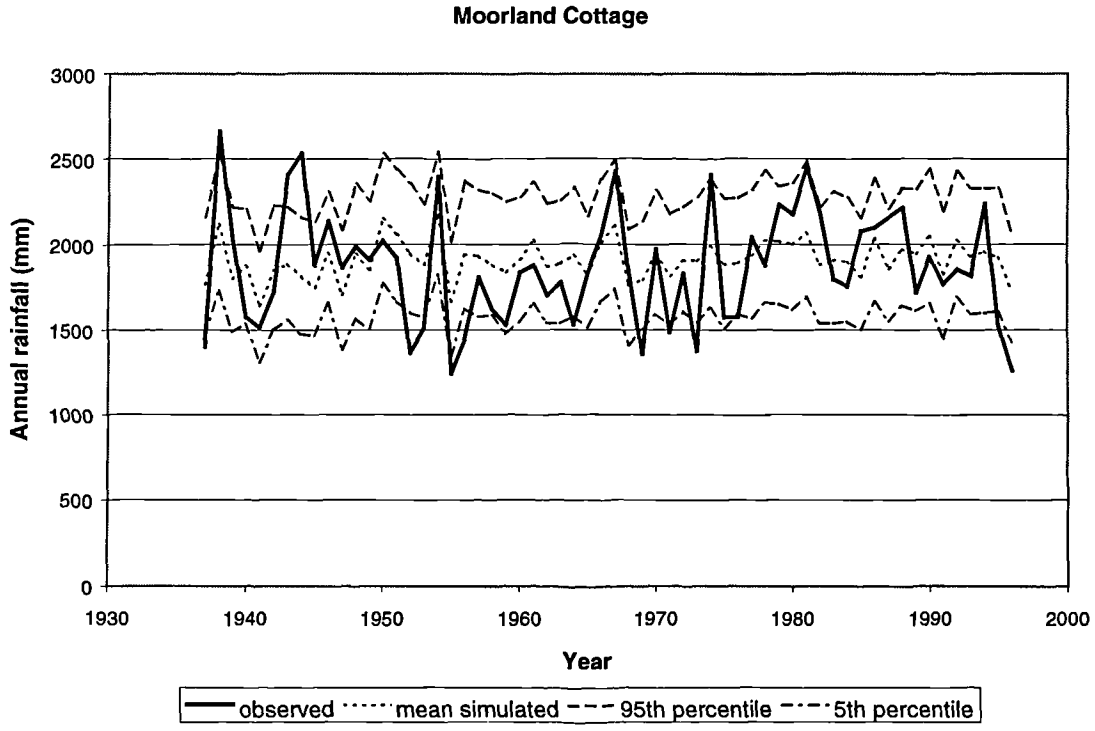

Figure 5-26: Observed and simulated annual precipitation totals at Moorland Cottage for 1937-1996, showing 5 and 95 percentiles.

For a successful analysis of risk within a water resources system, extreme drought events must be reproduced by the model. A report prepared by Mott MacDonald (1996) for Yorkshire Water Services suggests that at some Pennine sites the rainfall return period for the time-period from May 1995 to April 1996 was of the order of one in 1000 years. Therefore, an ensemble of two hundred simulations were produced for the 1937-1996 period at Moorland Cottage, to enable the reproduction of the 1995 drought, which provided the most severe precipitation deficit recorded in the Pennine region. This gave mean, 95 and 5 percentile annual-precipitation totals for the 1937-1996 period, using the OWT record as input, and can be seen in Figure 5-26. It can be observed that the model reproduces the 1995 drought event as a minimum in the simulated series. It would therefore be expected that longer simulated time-series would produce more severe droughts, with appropriate return periods.

5.4.3.7 Testing spatial correlation between sub-regions

To allow the testing of a water resource model of Yorkshire it is important to reproduce historical cross-correlations between sub-regions. Tables 5-22 and 5-23 show the historical cross-correlations for the 1961-1990 period at the three sites for annual and monthly precipitation totals respectively.

Annual	Moorland Cottage	Kirk Bramwith
Lockwood Reservoir	0.24	0.69
Kirk Bramwith	0.21	

Table 5-22: Annual cross-correlations for precipitation totals during the 1961-1990 period.

Monthly	Moorland Cottage	Kirk Bramwith
Lockwood Reservoir	0.21	0.68
Kirk Bramwith	0.20	

Table 5-23: Monthly cross-correlations for precipitation totals during the 1961-1990 period.

Again, the wide range of possible precipitation values that may be associated with a single weather-state imposes a limitation. This means that although the historical cross-correlation can be reproduced, a single realization for each site of the same weather-state time-series will not reproduce one-to-one correspondence of precipitation amounts to observed weather types. This means that the historical cross-correlation may not be produced.

A Monte-Carlo simulation was used to produce an ensemble of fifty realizations of the 1961-1990 period for each site. The cross-correlation of monthly and annual synthetic series was investigated. It was found that the reproduction of the historical cross-correlation between Moorland Cottage and Lockwood Reservoir was viable, at between 0.15 and 0.25. However, care must be taken in the choice of simulated series with the correct cross-correlation at both the monthly and annual levels. The cross-correlation between Lockwood Reservoir and Kirk Bramwith is high and cannot be reproduced synthetically. Therefore, it is proposed that the rainfall model already fitted to Lockwood Reservoir is also used for Kirk Bramwith (by the fitting of a Generalised NSRP model), using additional scale-factors (explained in Section 2B.2.3). This is viable as weather states in southeastern and northeastern sub-regions share similar PD values. This will allow the modelling of the North York Moors water resource region with some accuracy and will be sufficient for the modelling of the River Hull in the southeast sub-region which is known to be dominated by groundwater and of lesser importance for water supplies within the Yorkshire Grid.

The cross-correlation between Lockwood Reservoir and Moorland Cottage will be conserved by the production of many realizations of the same weather-state sequence. A precipitation time-series for each site will be chosen from this ensemble to reproduce the annual and monthly cross-correlation as closely as possible.

5.5 Extension to a spatial NSRP model for eastern and western sub-regions

5.5.1 Data requirements

A spatial NSRP model was fitted to data from the western and eastern (encompassing both the southeastern and northeastern) sub-regions using sites where data from 1961-1990 was available. Precipitation data fitting was required at 19 sites within the western region and 9 sites within the eastern region to fulfill the requirements of the rainfall-runoff models in Chapter 6. Site details can be found in Tables 5-24 and 5-25 for the western and eastern regions respectively. Concatenated series were produced for each 'summer' and 'winter' weather state for each site in the eastern and western model respectively (details in Table 5-26). Weather states in the eastern model derive their seasonality from the model previously fitted to Lockwood Reservoir in Section 5.4. In the western model, the weather state seasonality is taken from the Moorland Cottage model detailed in Section 5.4.

Rain Gauge Identifier	Name	National Grid Reference	Altitude (m)
47060	Moorland Cottage	SD 34 807923	343
2245	Leeming	SE 44 306890	32
28904	Brignall	NZ 45 071122	201
4057	Harrogate	SE 44 303578	66
4061	Sheffield	SK 43 339873	131
57427	Scar House Resr.	SE 44 065766	331
62254	Lower Barden Resr.	SE 44 035563	227
77335	Gorple Resr.	SD 34 945312	313
77797	Great Walden Edge	SD 34 996156	346
78701	Ramsden	SE 44 115051	262
47474	Burtersett	SD 34 891893	297
49308	Leighton Resr.	SE 44 162791	193
49901	Lumley Moor Resr.	SE 44 224706	172
62381	Chelker Resr.	SE 44 052517	223
63121	Fewston Resr.	SE 44 188544	160
74852	Watersheddles Resr.	SD 34 968380	340
77468	Mytholmroyd, Redacre	SE 44 010264	96
77835	Ringstone Resr.	SE 44 048178	293
81698	Ingbirchworth Resr.	SE 44 213056	260

Table 5-24: Precipitation gauges modelled in western region spatial NSRP model.

Rain Gauge Identifier	Name	National Grid Reference	Altitude (m)
55222	Osmotherly Filters	SE 44 458967	147
38290	Sledmere House	SE 44 933648	121
39164	Bridlington	TA 54 173687	48
43681	Tophill Low	TA 54 072483	2
34458	Lockwood Reservoir	NZ 45 668141	193
59792	York, Acomb Landing	SE 44 581527	9
66598	Wykeham Nursery	SE 44 947863	152
67183	Scampston Hall	SE 44 864756	31
71166	Birdsall House	SE 44 818651	94

Table 5-25: Precipitation gauges modelled in eastern region spatial NSRP model.

	Weather State					
Data (months)	SA	SN	SW	WA	WN	WW
Eastern model	54	31	94	43	22	116
Western model	54	31	76	43	22	134

Table 5-26: Amount of data (in months) used for model fitting of each weather state.

5.5.2 Model calibration

A spatial model was fitted for each weather state using the following sample moments, where *i* denotes the index site and *m* denotes a spatial average: $\mu_i(24)$, $\phi_m(24)$, $\gamma_i(24)$, $\gamma_i(48)$ (same terminology as Cowpertwait *et al.*, 1996*a*) and all 24-hr cross-correlations. Auto-correlation was not used in fitting. This is reproduced in the weather state generator by the conservation of historical weather state persistence probabilities. The PD statistic used is a spatial average across the catchment, as the NSRP model is unable to produce spatially varying PD. For the western model, the index site of Moorland Cottage was used and in the eastern model, Osmotherly Filters. Different weights were assigned to sample moments during the fitting procedure based on an investigation into the best weightings to improve the model parameter fitting procedure. $\mu_i(24)$ was given a weighting of 10, $\phi_m(24)$ a weighting of 3, $\gamma_i(24)$ and $\gamma_i(48)$ were unweighted (i.e. scale of 1), and 24-hr cross-correlations were given a weighting of 6 if they contained the index site, or 5 otherwise.

After fitting, the parameters were validated using a Monte Carlo process. An ensemble of 50 simulations of the concatenated series was generated for each weather state. This gave uncertainty bounds about the daily cross-correlation simulations, the most important aspect of a spatial precipitation model, and a measure of fit of the other simulated statistics. The results for the western model are given first, and then those for the eastern model. Adjustments for the difference between the observed and fitted $\mu_i(24)$ were incorporated into the model as a percentage error adjustment to the scale factors. This allows the model to simulate, with accuracy, the precipitation occurring from a mixture of different weather states.

5.5.2.1 Western spatial NSRP model

In Table 5-27, the observed, fitted and simulated statistics used in fitting at the index site, Moorland Cottage are given. It can be observed that the model fitted values and simulated values provide a good match to observed statistics, although variance is generally slightly underestimated.

Tables 5-28 to 5-33 give the observed and simulated mean daily precipitation, PD and variance at all 19 sites within the western model, for each of the SA, SN, SW, WA, WN and WW weather states respectively. The adjusted scale factors at each site for each weather state are also shown.

Parameter Weather State	μ(24) obs	μ(24) fitted	μ(24) sim	ϕ(24) obs	ϕ(24) fitted	ϕ(24) sim	γ(24) obs	γ(24) fitted	γ(24) sim	γ(48) obs	γ(48) fitted	γ(48) sim
SA	1.29	1.33	1.34	0.77	0.73	0.81	20.20	13.48	15.91	43.79	43.30	35.23
SN	2.76	2.80	2.81	0.44	0.38	0.41	33.70	21.17	20.04	77.41	60.08	56.65
SW	5.74	5.73	5.92	0.31	0.31	0.26	80.60	76.70	65.47	169.96	177.14	165.46
WA	2.43	2.52	2.62	0.57	0.58	0.56	39.20	29.54	24.70	91.15	88.81	56.97
WN	2.64	2.83	2.88	0.36	0.32	0.33	30.40	18.17	15.81	64.68	52.99	40.52
WW	8.79	9.08	9.34	0.23	0.21	0.16	152.70	124.10	106.05	362.06	355.51	314.82

Table 5-27: Observed, fitted and simulated statistics for the index site Moorland Cottage, western model.

Site	Scale Factor	Historical			Simulated		
		μ(24)	ϕ(24)	γ(24)	μ(24)	ϕ(24)	γ(24)
47060	0.964	1.29	0.78	20.20	1.30	0.81	14.81
2245	0.407	0.55	0.79	4.80	0.55	0.82	2.65
28904	0.510	0.68	0.77	10.70	0.68	0.81	4.13
4057	0.447	0.60	0.82	7.70	0.60	0.82	3.18
4061	0.491	0.66	0.81	9.80	0.66	0.82	3.85
57427	0.688	0.92	0.73	14.40	0.92	0.81	7.48
62254	0.635	0.85	0.73	12.10	0.85	0.81	6.38
77335	0.720	0.97	0.76	15.80	0.96	0.81	8.27
77797	0.629	0.84	0.76	11.40	0.85	0.81	6.34
78701	0.688	0.92	0.74	16.30	0.92	0.81	7.50
47474	0.631	0.85	0.76	11.50	0.85	0.81	6.28
49308	0.527	0.71	0.75	8.10	0.71	0.81	4.41
49901	0.515	0.69	0.78	8.50	0.69	0.81	4.22
62381	0.538	0.72	0.73	8.50	0.72	0.81	4.59
63121	0.542	0.73	0.78	10.40	0.73	0.81	4.68
74852	0.693	0.93	0.75	16.60	0.93	0.81	7.64
77468	0.533	0.72	0.83	12.00	0.71	0.81	4.52
77835	0.609	0.82	0.77	14.70	0.82	0.81	5.95
81698	0.521	0.70	0.78	12.00	0.70	0.81	4.30

Table 5-28: Observed, fitted and simulated 24-hour statistics for the western model SA weather state.

Site	Scale Factor	Historical			Simulated		
		μ(24)	ϕ(24)	γ(24)	μ(24)	ϕ(24)	γ(24)
47060	0.982	2.76	0.52	33.70	2.76	0.43	19.25
2245	0.686	1.93	0.52	23.80	1.93	0.43	9.41
28904	0.841	2.37	0.43	32.40	2.37	0.43	14.20
4057	0.763	2.15	0.50	31.50	2.15	0.43	11.67
4061	0.980	2.76	0.47	40.60	2.75	0.43	19.28
57427	0.956	2.69	0.36	33.30	2.69	0.43	18.33
62254	0.749	2.11	0.40	24.90	2.11	0.43	11.27
77335	0.980	2.76	0.45	31.80	2.75	0.43	19.21
77797	1.003	2.82	0.43	34.50	2.82	0.41	20.09
78701	1.177	3.31	0.35	42.50	3.31	0.41	27.79
47474	0.683	1.92	0.45	17.30	1.92	0.43	9.30
49308	0.884	2.49	0.41	31.60	2.49	0.43	15.65
49901	0.885	2.49	0.45	34.40	2.49	0.43	15.68
62381	0.755	2.12	0.43	21.80	2.13	0.43	11.44
63121	0.814	2.29	0.44	28.00	2.29	0.43	13.31
74852	0.963	2.71	0.44	28.20	2.71	0.43	18.57
77468	0.789	2.22	0.54	23.10	2.22	0.43	12.44
77835	0.958	2.69	0.44	32.90	2.69	0.43	18.42
81698	1.017	2.86	0.40	36.80	2.86	0.41	20.77

Table 5-29: Observed, fitted and simulated 24-hour statistics for the western model SN weather state.

Site	Scale Factor	Historical			Simulated		
		μ(24)	ϕ(24)	γ(24)	μ(24)	ϕ(24)	γ(24)
47060	0.969	5.74	0.32	80.60	5.74	0.28	61.86
2245	0.367	2.17	0.42	20.80	2.17	0.32	8.79
28904	0.427	2.53	0.36	27.50	2.52	0.31	11.96
4057	0.402	2.38	0.41	24.10	2.38	0.31	10.52
4061	0.400	2.37	0.41	31.20	2.36	0.31	10.45
57427	0.667	3.95	0.24	43.40	3.94	0.29	28.99
62254	0.652	3.86	0.22	34.60	3.86	0.29	27.76
77335	0.541	3.20	0.35	28.10	3.21	0.29	19.32
77797	0.655	3.88	0.28	40.00	3.88	0.29	28.09
78701	0.724	4.29	0.26	53.20	4.27	0.28	34.11
47474	0.676	4.00	0.26	44.20	4.01	0.28	30.09
49308	0.484	2.86	0.35	31.60	2.87	0.31	15.33
49901	0.466	2.76	0.37	28.50	2.76	0.31	14.13
62381	0.568	3.36	0.25	29.10	3.36	0.29	21.18
63121	0.467	2.76	0.34	25.60	2.76	0.31	14.16
74852	0.748	4.42	0.25	41.40	4.43	0.28	36.89
77468	0.701	4.15	0.26	38.00	4.16	0.28	32.41
77835	0.724	4.29	0.26	53.20	4.29	0.28	34.44
81698	0.469	2.77	0.33	31.60	2.77	0.31	14.30

Table 5-30: Observed, fitted and simulated 24-hour statistics for the western model SW weather state.

Site	Scale Factor	Historical			Simulated		
		μ(24)	ϕ(24)	γ(24)	μ(24)	ϕ(24)	γ(24)
47060	0.925	2.43	0.61	39.20	2.43	0.58	21.10
2245	0.258	0.68	0.68	3.50	0.68	0.62	1.65
28904	0.328	0.86	0.59	5.50	0.86	0.61	2.67
4057	0.293	0.77	0.65	4.40	0.77	0.61	2.12
4061	0.326	0.85	0.65	7.70	0.85	0.61	2.61
57427	0.615	1.61	0.48	16.00	1.61	0.59	9.30
62254	0.448	1.18	0.50	9.30	1.18	0.60	4.98
77335	0.608	1.59	0.56	16.10	1.59	0.59	9.13
77797	0.543	1.42	0.55	12.90	1.42	0.59	7.26
78701	0.581	1.52	0.54	14.60	1.52	0.59	8.31
47474	0.618	1.62	0.54	17.40	1.62	0.59	9.43
49308	0.394	1.03	0.58	7.10	1.03	0.60	3.83
49901	0.364	0.96	0.58	5.60	0.95	0.60	3.27
62381	0.386	1.01	0.50	6.70	1.01	0.60	3.69
63121	0.346	0.91	0.57	5.80	0.91	0.60	2.95
74852	0.561	1.47	0.49	12.30	1.47	0.59	7.79
77468	0.396	1.04	0.69	8.70	1.04	0.60	3.88
77835	0.507	1.33	0.58	12.50	1.33	0.59	6.37
81698	0.354	0.93	0.59	6.80	0.93	0.60	3.10

Table 5-31: Observed, fitted and simulated 24-hour statistics for the western model WA weather state.

Site	Scale Factor	Historical			Simulated		
		μ(24)	ϕ(24)	γ(24)	μ(24)	ϕ(24)	γ(24)
47060	0.915	2.64	0.50	30.40	2.64	0.35	13.28
2245	0.664	1.92	0.40	13.80	1.92	0.37	6.99
28904	0.933	2.69	0.34	24.30	2.70	0.35	13.85
4057	0.765	2.21	0.39	22.40	2.21	0.35	9.27
4061	0.879	2.53	0.37	25.80	2.53	0.35	12.12
57427	1.177	3.40	0.25	48.90	3.40	0.33	22.03
62254	0.733	2.11	0.29	20.60	2.11	0.35	8.50
77335	0.922	2.66	0.36	24.70	2.66	0.35	13.48
77797	0.884	2.55	0.36	27.70	2.55	0.35	12.34
78701	1.094	3.16	0.27	37.50	3.15	0.33	18.82
47474	0.783	2.26	0.36	19.10	2.26	0.35	9.75
49308	1.048	3.02	0.31	34.80	3.02	0.33	17.33
49901	0.980	2.83	0.34	33.90	2.82	0.35	15.10
62381	0.726	2.09	0.33	20.50	2.09	0.35	8.35
63121	0.918	2.65	0.35	28.70	2.64	0.35	13.27
74852	0.904	2.61	0.36	22.40	2.61	0.35	12.99
77468	0.766	2.21	0.47	23.00	2.21	0.35	9.27
77835	0.886	2.55	0.36	28.00	2.55	0.35	12.36
81698	0.884	2.55	0.35	25.10	2.54	0.35	12.25

Table 5-32: Observed, fitted and simulated 24-hour statistics for the western model WN weather state.

Site	Scale Factor	Historical			Simulated		
		μ(24)	ϕ(24)	γ(24)	μ(24)	ϕ(24)	γ(24)
47060	0.942	8.79	0.26	152.70	8.80	0.17	94.24
2245	0.213	1.99	0.41	14.70	1.99	0.23	4.80
28904	0.314	2.93	0.29	23.00	2.93	0.21	10.40
4057	0.276	2.58	0.32	19.70	2.57	0.21	8.05
4061	0.326	3.05	0.29	24.00	3.05	0.20	11.31
57427	0.638	5.96	0.16	69.20	5.96	0.18	43.28
62254	0.537	5.01	0.13	42.40	5.02	0.18	30.54
77335	0.509	4.75	0.26	42.50	4.75	0.18	27.51
77797	0.592	5.53	0.19	57.60	5.52	0.18	37.26
78701	0.681	6.36	0.16	73.20	6.36	0.17	49.17
47474	0.708	6.61	0.17	85.20	6.61	0.17	53.18
49308	0.407	3.80	0.25	34.70	3.80	0.19	17.60
49901	0.371	3.46	0.27	29.90	3.46	0.20	14.58
62381	0.443	4.13	0.14	29.50	4.14	0.19	20.85
63121	0.368	3.43	0.22	25.80	3.43	0.20	14.31
74852	0.679	6.34	0.17	62.80	6.34	0.17	49.09
77468	0.591	5.52	0.18	52.10	5.52	0.18	37.14
77835	0.681	6.36	0.16	73.20	6.35	0.17	49.34
81698	0.436	4.07	0.25	37.60	4.07	0.19	20.18

Table 5-33: Observed, fitted and simulated 24-hour statistics for the western model WW weather state.

In the main, site statistics are reproduced for each of the six weather states within the western model. The μ(24) statistic is accurately simulated using the adjusted scale factors. The ϕ(24) statistic is also well simulated, for most weather states within two percent of the areal average historical ϕ(24) (shown in Table 5-27). However, the daily variance is underestimated by the model for all weather states. Daily cross-correlations are well preserved by the western NSRP model. These are shown in Figures 5-27 and 5-28 for the summer and winter western model weather states respectively. It can be observed that many of the observed daily cross-correlations for the winter weather states, particularly the westerly state, lie outside the 5 and 95 percentiles of the simulated series. This can be explained by the high variability in precipitation receipt for the winter westerly weather state, dependent upon altitude and westerliness in the Pennines.

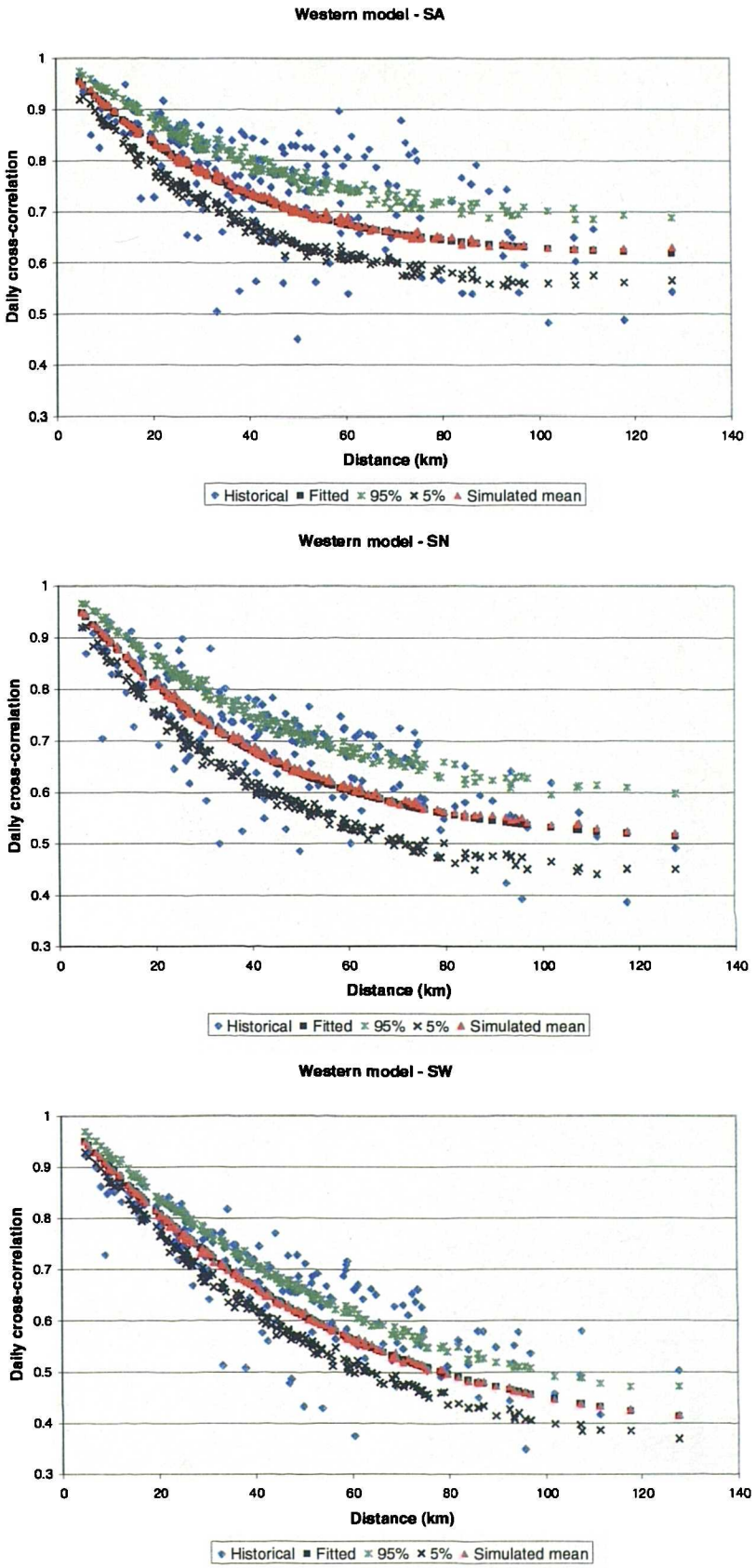

Figure 5-27: Spatial cross-correlations: observed, fitted, simulated with 95 and 5 percentiles from 50 simulations for the western model SA, SN and SW weather states.

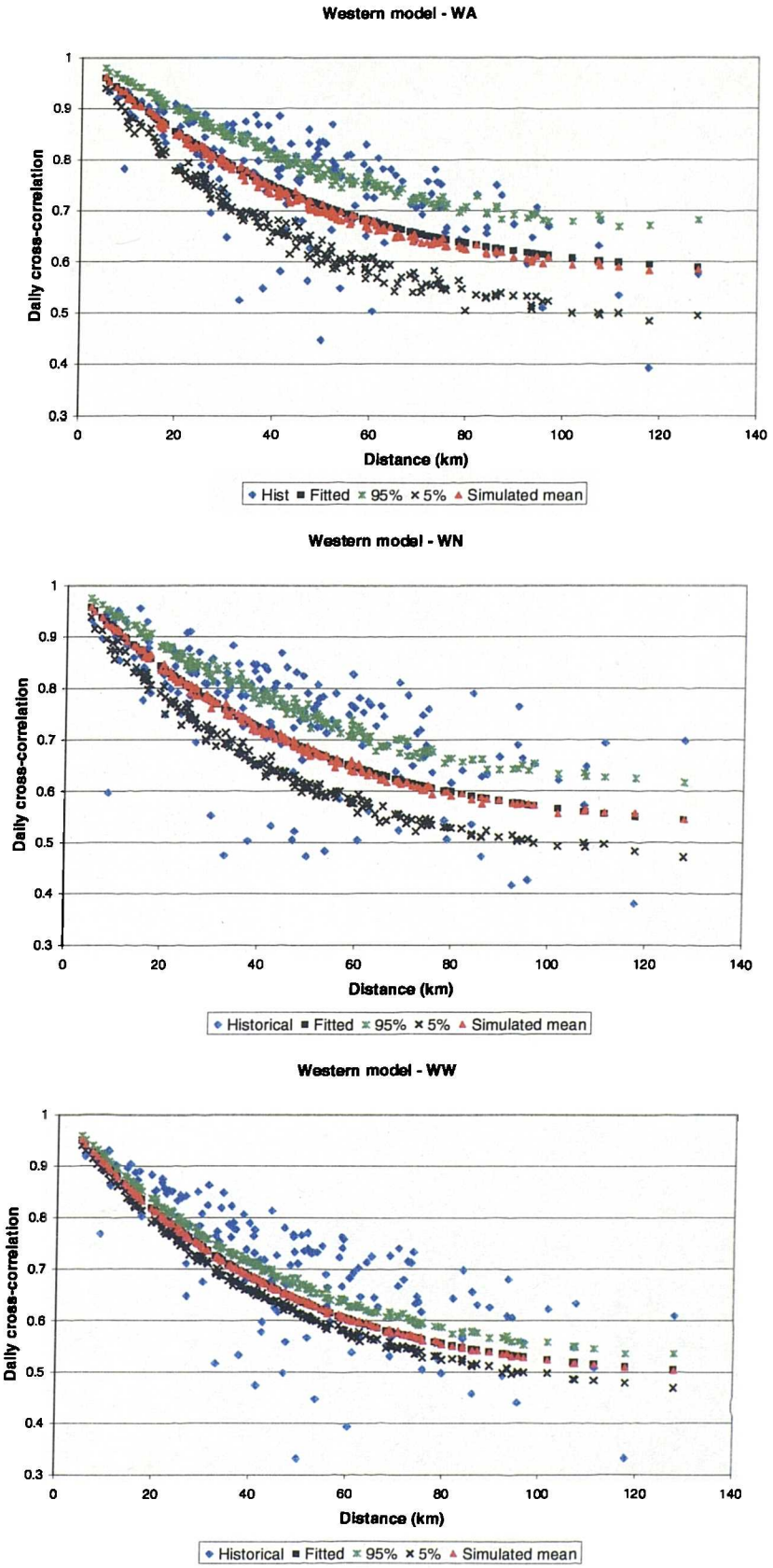

Figure 5-28: Spatial cross-correlations: observed, fitted, simulated with 95 and 5 percentiles from 50 simulations for the western model WA, WN and WW weather states.

5.5.2.2 Eastern spatial NSRP model

The observed, fitted and simulated statistics for the eastern model index site at Osmotherly Filters can be found in Table 5-34. The simulated statistics are very similar to the observed statistics, excepting a slight reduction in variance and increase in PD within the simulated series. An adjustment is made to the scale factors within the model based on the percentage error between observed and fitted μ(24) at the index site.

Parameter	μ(24)	μ(24)	μ(24)	ϕ(24)	ϕ(24)	ϕ(24)	γ(24)	γ(24)	γ(24)	γ(48)	γ(48)	γ(28)
Weather State	obs	fitted	sim	obs	fitted	sim	obs	fitted	sim	obs	fitted	sim
SA	0.62	0.64	0.64	0.81	0.80	0.82	5.70	4.34	4.37	13.19	14.08	14.10
SN	2.39	2.54	2.55	0.42	0.39	0.44	25.60	19.93	20.01	63.46	49.07	49.19
SW	2.61	2.73	2.72	0.44	0.41	0.46	29.10	22.74	22.85	62.36	57.88	57.77
WA	0.92	0.93	0.93	0.63	0.60	0.66	4.90	4.10	4.10	10.76	11.85	11.92
WN	2.73	2.86	2.83	0.41	0.39	0.44	22.80	21.34	21.23	93.16	67.20	66.94
WW	2.36	2.38	2.37	0.38	0.36	0.41	18.10	15.31	15.24	39.85	42.44	42.34

Table 5-34: Observed, fitted and simulated statistics for the index site Osmotherly Filters, eastern model.

Tables 5-35 to 5-40 give the observed and simulated mean daily precipitation, PD and variance at all nine sites within the eastern model, for each of the SA, SN, SW, WA, WN and WW weather states respectively, as well as the adjusted scale factors used within the model.

Site	Scale Factor	Historical			Simulated		
		μ(24)	ϕ(24)	γ(24)	μ(24)	ϕ(24)	γ(24)
55222	0.974	0.62	0.80	5.70	0.62	0.83	4.08
38290	1.006	0.64	0.79	7.90	0.64	0.82	4.39
39164	0.787	0.50	0.80	4.00	0.50	0.83	2.70
43681	0.804	0.52	0.80	4.90	0.51	0.83	2.82
34458	1.029	0.66	0.75	5.80	0.65	0.82	4.57
59792	0.867	0.56	0.85	8.20	0.55	0.83	3.25
66598	0.985	0.63	0.77	6.20	0.62	0.83	4.17
67183	0.893	0.57	0.84	6.40	0.57	0.83	3.45
71166	1.040	0.67	0.86	10.30	0.66	0.82	4.69

Table 5-35: Observed, fitted and simulated 24-hour statistics for the eastern model SA weather state.

Site	Scale Factor	Historical			Simulated		
		μ(24)	ϕ(24)	γ(24)	μ(24)	ϕ(24)	γ(24)
55222	0.936	2.39	0.41	25.60	2.38	0.46	17.59
38290	1.004	2.56	0.38	22.50	2.57	0.44	20.21
39164	0.921	2.35	0.39	22.90	2.35	0.46	16.95
43681	0.832	2.12	0.42	21.90	2.13	0.46	13.89
34458	1.142	2.91	0.31	30.60	2.91	0.44	26.15
59792	0.714	1.82	0.49	15.40	1.82	0.46	10.22
66598	0.808	2.06	0.49	16.50	2.06	0.46	13.06
67183	0.857	2.18	0.49	16.80	2.19	0.46	14.74
71166	1.051	2.68	0.39	24.40	2.68	0.44	22.09

Table 5-36: Observed, fitted and simulated 24-hour statistics for the eastern model SN weather state.

Site	Scale Factor	Historical			Simulated		
		μ(24)	ϕ(24)	γ(24)	μ(24)	ϕ(24)	γ(24)
55222	0.959	2.61	0.42	29.10	2.59	0.48	20.79
38290	0.927	2.52	0.41	26.80	2.52	0.48	19.67
39164	0.787	2.14	0.43	21.30	2.15	0.48	14.25
43681	0.756	2.06	0.45	20.30	2.06	0.48	13.15
34458	0.989	2.69	0.38	32.80	2.69	0.48	22.31
59792	0.776	2.11	0.47	19.50	2.11	0.48	13.82
66598	0.913	2.48	0.37	23.70	2.47	0.48	18.88
67183	0.804	2.19	0.50	20.80	2.18	0.48	14.71
71166	0.903	2.46	0.50	25.00	2.46	0.48	18.74

Table 5-37: Observed, fitted and simulated 24-hour statistics for the eastern model SW weather state.

Site	Scale Factor	Historical			Simulated		
		μ(24)	ϕ(24)	γ(24)	μ(24)	ϕ(24)	γ(24)
55222	0.998	0.92	0.65	4.90	0.93	0.68	4.08
38290	1.047	0.97	0.61	5.60	0.97	0.66	4.51
39164	0.985	0.91	0.60	5.30	0.91	0.68	3.96
43681	0.832	0.77	0.59	4.40	0.77	0.68	2.84
34458	1.082	1.00	0.60	5.30	1.00	0.66	4.79
59792	0.669	0.62	0.70	3.40	0.62	0.68	1.83
66598	1.104	1.02	0.55	4.90	1.02	0.66	4.99
67183	0.837	0.78	0.69	3.70	0.78	0.68	2.88
71166	0.904	0.84	0.72	4.80	0.84	0.68	3.37

Table 5-38: Observed, fitted and simulated 24-hour statistics for the eastern model WA weather state.

Site	Scale Factor	Historical			Simulated		
		μ(24)	ϕ(24)	γ(24)	μ(24)	ϕ(24)	γ(24)
55222	0.962	2.73	0.40	22.80	2.73	0.46	19.67
38290	1.038	2.94	0.39	31.00	2.94	0.44	22.84
39164	0.972	2.75	0.37	27.50	2.75	0.46	20.00
43681	0.855	2.42	0.38	24.60	2.42	0.46	15.45
34458	1.347	3.82	0.29	43.50	3.81	0.44	38.55
59792	0.651	1.85	0.51	19.90	1.84	0.48	8.98
66598	0.805	2.28	0.47	20.00	2.28	0.46	13.76
67183	0.850	2.41	0.48	24.90	2.41	0.46	15.38
71166	0.934	2.65	0.42	27.60	2.65	0.46	18.60

Table 5-39: Observed, fitted and simulated 24-hour statistics for the eastern model WN weather state.

Site	Scale Factor	Historical			Simulated		
		μ(24)	ϕ(24)	γ(24)	μ(24)	ϕ(24)	γ(24)
55222	0.992	2.36	0.42	18.10	2.36	0.44	15.05
38290	1.124	2.67	0.33	19.30	2.67	0.42	19.32
39164	0.896	2.13	0.38	14.80	2.13	0.44	12.30
43681	0.866	2.06	0.34	13.50	2.05	0.44	11.39
34458	1.013	2.40	0.36	17.60	2.41	0.41	15.72
59792	0.831	1.97	0.40	12.70	1.97	0.44	10.51
66598	1.078	2.56	0.31	20.40	2.56	0.42	17.78
67183	0.886	2.10	0.45	13.60	2.11	0.44	11.99
71166	1.026	2.43	0.46	17.80	2.44	0.42	16.05

Table 5-40: Observed, fitted and simulated 24-hour statistics for the eastern model WW weather state.

The observed series for all six weather states in the eastern model are well matched by the simulated series. The μ(24) statistic is accurately simulated using the adjusted scale factors. The ϕ(24) statistic is also well simulated, for most weather states within two percent of the areal average historical ϕ(24) (shown in Table 5-34). The daily variance is also well simulated by the model, with only a slight underestimation for all weather states. The daily cross-correlations fitted by the model can be seen in Figures 5-29 and 5-30 respectively for the summer and winter weather states. The mean of the fifty simulated series is also given, as are the 5 and 95 percentiles. The daily cross-correlations between sites are well matched by the model simulations for all six weather states.

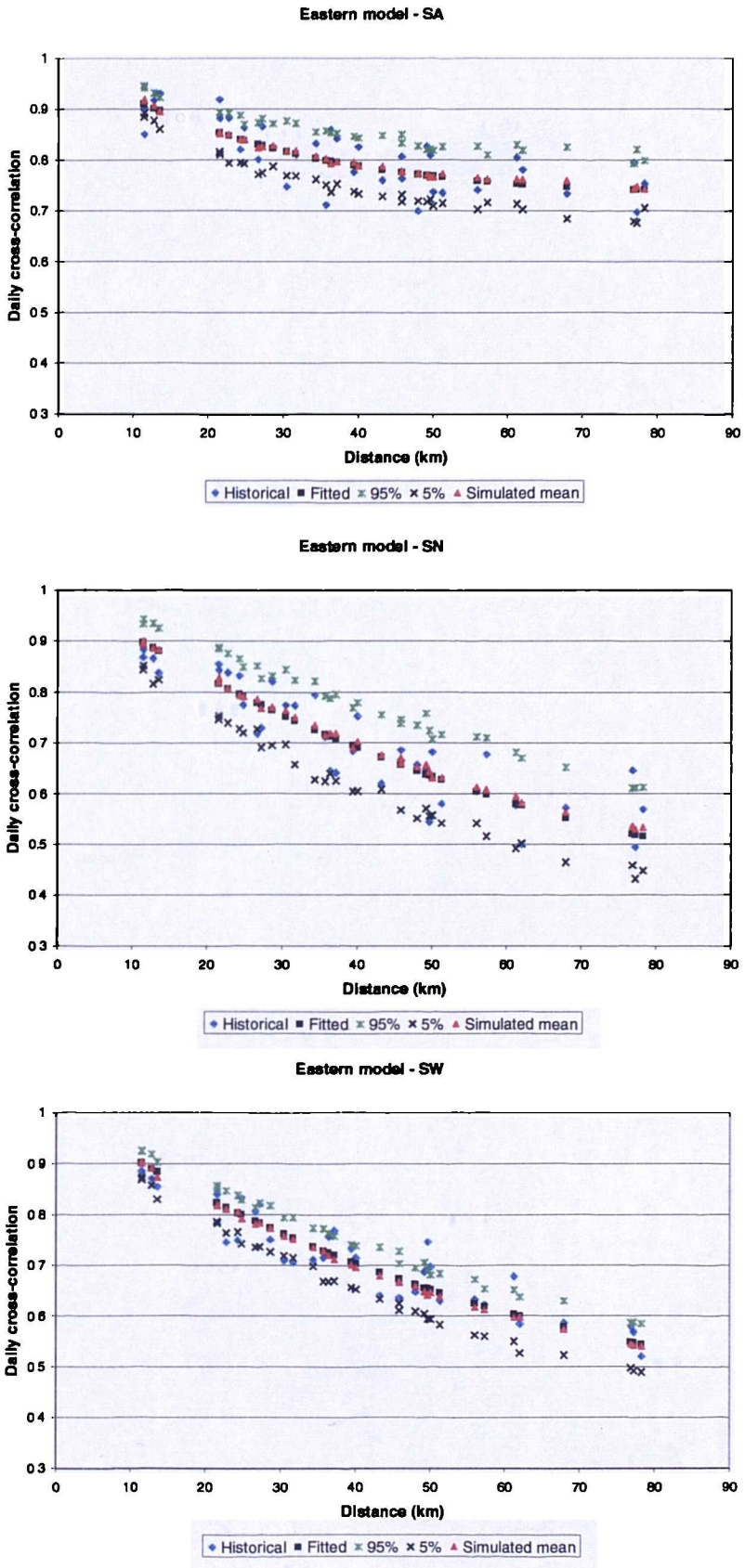

Figure 5-29: Spatial cross-correlations: observed, fitted, simulated with 95 and 5 percentiles from 50 simulations for the eastern model SA, SN and SW weather states.

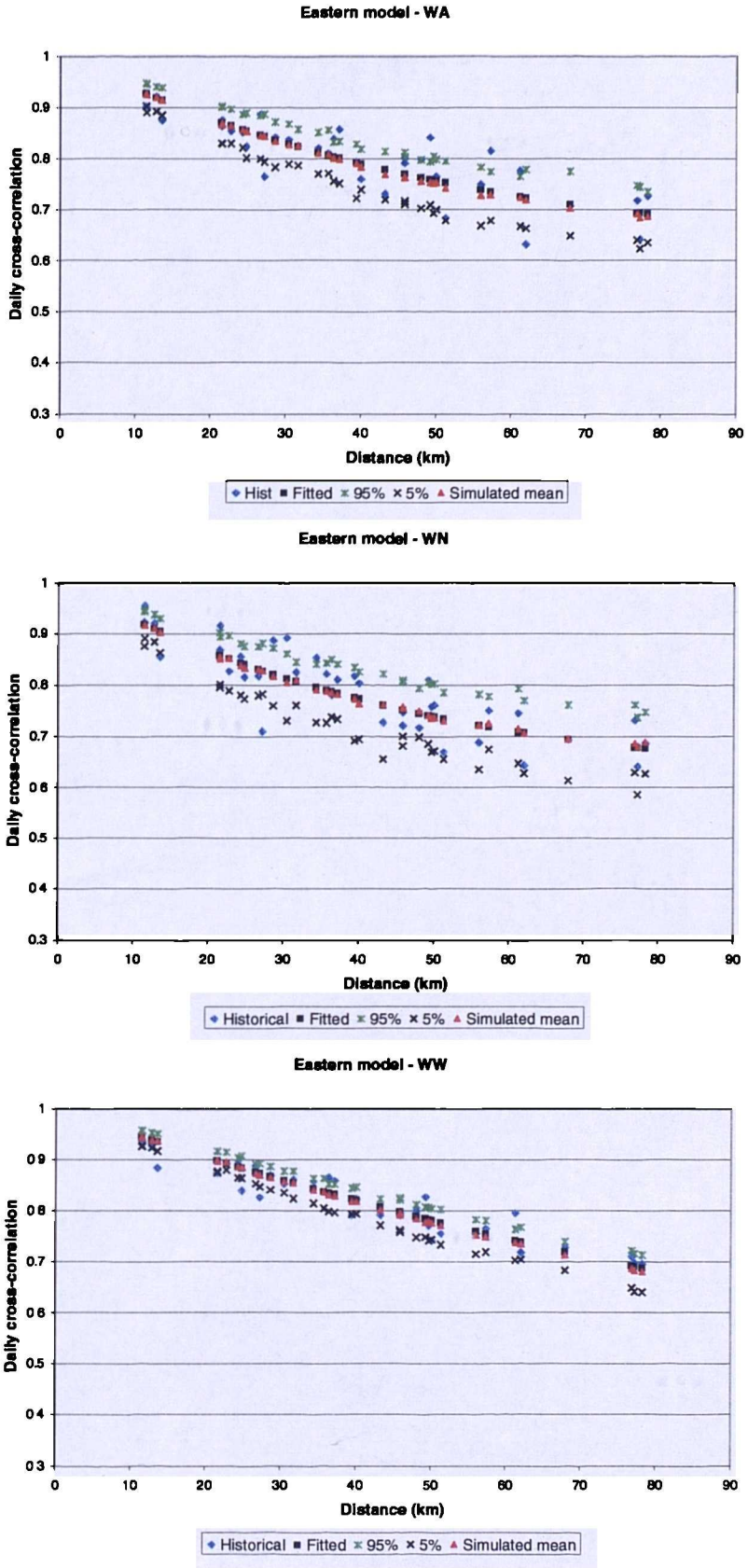

Figure 5-30: Spatial cross-correlations: observed, fitted, simulated with 95 and 5 percentiles from 50 simulations for the eastern model WA, WN and WW weather states.

5.5.2 Fitted parameters

The six parameters of the spatial NSRP model can be found in Table 5-41. These are the same as the single-site model, with the exception that ρ (rho) replaces ν (nu) (as Equation 5-5), and that γ (gamma) is additionally introduced.

$$\nu = \frac{2\pi\rho}{\gamma^2} \tag{5-5}$$

The fitted parameters for the six weather states in the eastern and western model can be found in Table 5-43.

Parameter	Explanation
λ^{-1} (lambda)	the mean waiting time between adjacent storm origins (h^{-1})
β^{-1} (beta)	the mean waiting time for cell origins after the storm origin (h^{-1})
ρ^{-1} (rho)	the mean cell density associated with a storm origin (km^{-2}).
η^{-1} (eta)	the mean duration of a cell (h^{-1})
ξ^{-1} (xi)	the mean cell intensity (mm h^{-1})
γ^{-1} (gamma)	the mean cell radius (km^{-1})

Table 5-42: The parameters of a one-cell NSRP spatial model.

Parameter Weather State	Model	λ^{-1} (h^{-1})	β^{-1} (h^{-1})	ρ (km^{-2})	η (h^{-1})	ξ (mm h^{-1})	γ (km^{-1})
SA	Western	0.0010	0.0101	0.0388	0.1485	4.9862	0.0760
	Eastern	0.0006	0.0100	0.1462	11.9418	0.1814	0.0975
SN	Western	0.0035	0.0100	0.0260	7.9029	0.1369	0.0672
	Eastern	0.0110	0.0276	0.0020	1.0843	0.6754	0.0424
SW	Western	0.0234	0.0630	0.0020	11.9636	0.0395	0.0511
	Eastern	0.0125	0.0420	0.0020	0.2889	2.3424	0.0455
WA	Western	0.0018	0.0101	0.0246	0.6386	1.1660	0.0590
	Eastern	0.0031	0.0216	0.0134	7.2232	0.3266	0.0536
WN	Western	0.0039	0.0100	0.0200	0.9204	1.3531	0.0578
	Eastern	0.0028	0.0101	0.0291	0.2461	4.7707	0.0609
WW	Western	0.0206	0.0534	0.0041	0.1000	3.5412	0.0627
	Eastern	0.0044	0.0100	0.0020	0.3021	2.9205	0.0250

Table 5-43: Fitted parameters for the eastern and western spatial NSRP models.

5.5.3 Spatial NSRP model validation

To ensure that the scale factors were working correctly, and that the two models were producing accurate simulations of precipitation at each site, a 1000-yr weather state series was generated using the Markov chain model described in Section 5.3. This weather state series was then used as input to the eastern and western spatial NSRP models, producing 28 precipitation series. Differences between the two weather state series are that in the eastern model, the SN weather type occurs from January to June, and the WN weather type occurs otherwise. In the western model the summer and winter weather states occur as would be expected, i.e. summer weather states from April to September, and winter weather states otherwise. This is excepting the month of September, which contains the WW weather state rather than the expected SW. These correspond to the seasonality of weather states fitted for the eastern and western spatial NSRP models and are based upon the prior single-site analysis at Lockwood Reservoir and Moorland Cottage respectively. These simulated series were then compared with monthly precipitation values that would be expected, given that particular sequence of weather states.

It can be observed in Figure 5-31, for Lockwood Reservoir, Wykeham Nursery and Birdsall House, that precipitation simulations using the eastern model provide a good match to expected monthly precipitation statistics. A lag effect is seen in April and October due to the weather state model switching from summer to winter weather states and vice versa during these months. However, as the main use of the model will be in the analysis of water resource systems on a monthly time-step and the lag is in the order of days, then this is not considered a problem. The remaining six sites simulated using the eastern model also show a close correspondence to the expected mean daily precipitation. The mean annual expected and simulated precipitation totals are shown in Table 5-44 and are very closely matched.

Site	Expected Total Annual Precipitation	Simulated Total Annual Precipitation
55222	736.5	743.2
38290	776.0	778.2
39164	658.2	662.6
43681	619.9	622.1
34458	801.2	802.0
59792	586.5	588.8
66598	729.5	740.5
67183	642.8	646.8
71166	737.3	733.7

Table 5-44: Expected and simulated total annual precipitation for sites in the eastern spatial NSRP model.

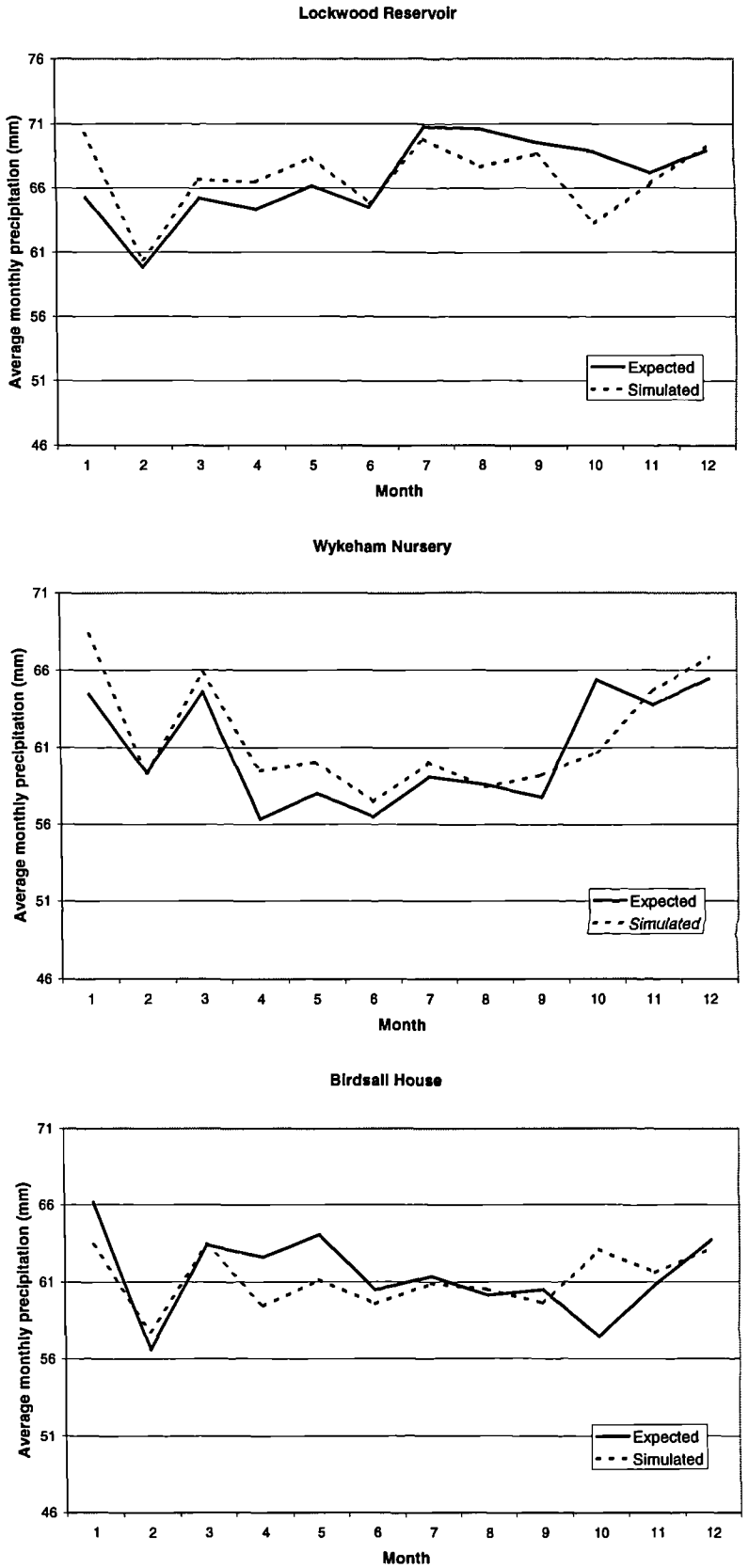

Figure 5-31: Comparison of expected and simulated monthly mean precipitation (mm) at Lockwood Reservoir, Wykeham Nursery and Birdsall House (eastern spatial NSRP model).

Site	Expected	Simulated	Percentage Error
47060	1911.1	1904.5	-0.3
2245	598.3	641.2	7.2
28904	794.6	846.1	6.5
4057	710.5	753.4	6.0
4061	802.8	847.6	5.6
57427	1367.3	1396.3	2.1
62254	1165.9	1168.3	0.2
77335	1140.2	1196.3	4.9
77797	1276.9	1288.5	0.9
78701	1454.4	1468.5	1.0
47474	1396.7	1381.0	-1.1
49308	952.6	995.7	4.5
49901	892.2	936.3	4.9
62381	1000.7	1013.5	1.3
63121	877.9	920.7	4.9
74852	1428.5	1424.3	-0.3
77468	1245.4	1219.0	-2.1
77835	1405.0	1385.1	-1.4
81698	973.9	997.7	2.4

Table 5-45: Expected and simulated total annual precipitation for sites in the western spatial NSRP model.

It can be observed in Table 5-45 that the total annual precipitation is not as accurately simulated in the western spatial NSRP model. This is due to a large disparity in the precipitation receipt of different weather states within the model. In particular, the winter westerly weather state produces twice as much precipitation than any other weather state, at almost every site (see Figure 5-32). This, coupled with the lag effects previously mentioned, can cause increased winter precipitation at sites with a low annual precipitation total. Scale factors are applied on a daily basis, and are dependent upon that day's weather state. However, the Neyman-Scott process may still produce precipitation for that weather state (as rain cells from a storm origin) in the proceeding days. This precipitation may not necessarily occur on a day labelled as 'westerly' and a different scale factor will therefore be applied. This may normally cause small anomalies in the precipitation rescaling process.

However, in the case of the western NSRP model, due to the very wet nature of the winter westerly weather state when compared to other weather states, a significant discrepancy occurs. The only way to rectify this type of error is to determine the origin of rain cells in the Neyman-Scott process. The correct scale factor can then be applied at source. However, this is considered overcomplicated for the current investigation. It can be observed that the excess precipitation occurs in winter months. Therefore, winter precipitation will be scaled appropriately to produce an accurate annual precipitation total at each site.

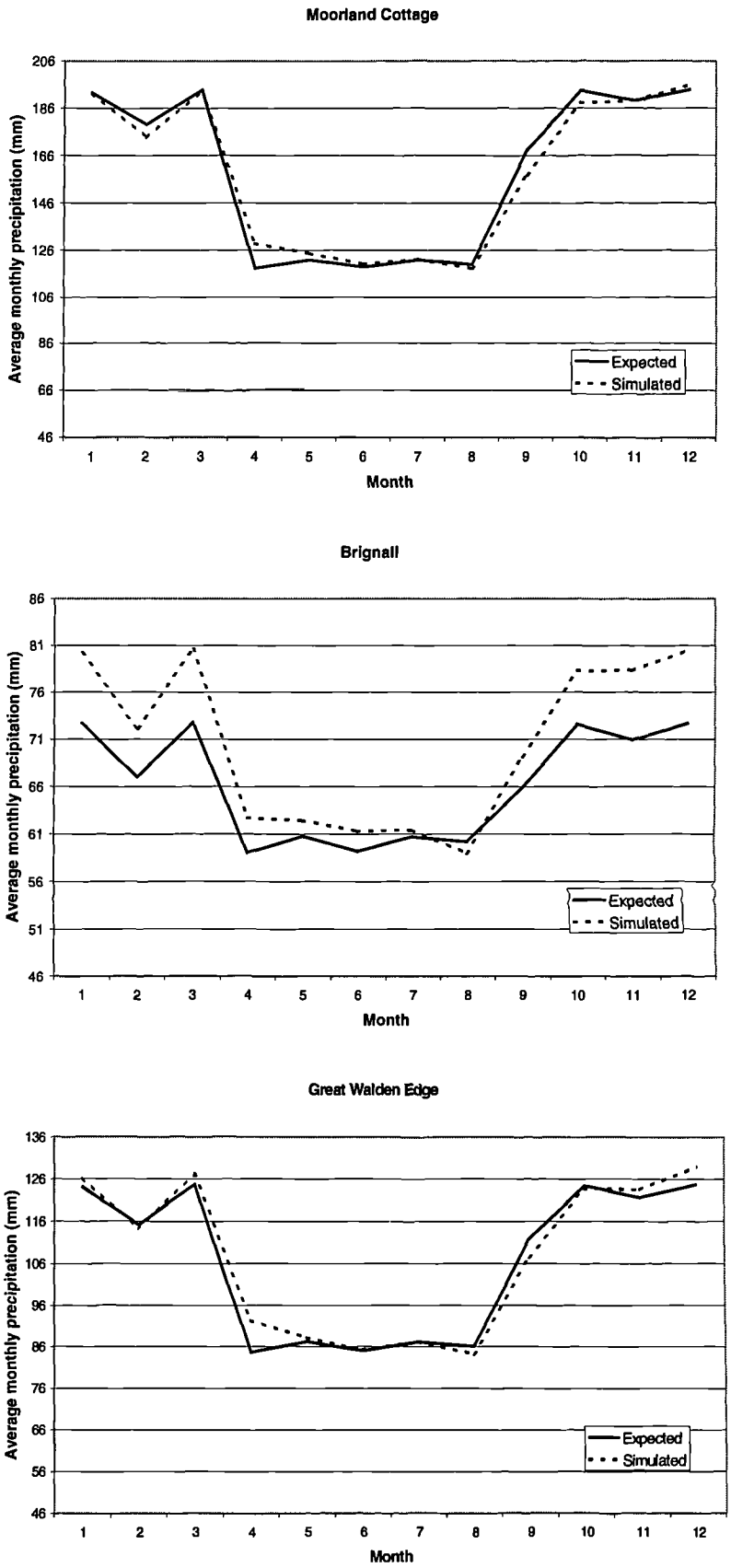

Figure 5-32: Comparison of expected and simulated monthly mean precipitation (mm) at Moorland Cottage, Brignall and Great Walden Edge (western spatial NSRP model).

5.6 Discussion

5.6.1 Limitations and benefits of the downscaling approach

The main strength of this weather type stochastic rainfall model is the provision of a *transferable common methodology* for classification, weather-state simulation and subsequent precipitation modelling, thus overcoming a limitation previously identified by Wilby (1994). The OWTs provide a classification system that is easy to understand, simple to use and has a substantial physical basis in climatology. The OWT system has also been applied, with some success, to regions of both northern and southern Europe (e.g. Brandsma and Buishand, 1997*b*; Goodess and Palutikof, 1998). Weather clusters are delineated using the climatology of the water resource area being studied and weather types are clustered based on a simple variance minimization routine. The over-parameterization of the precipitation process within the less frequently occurring weather types noted by many researchers (e.g. Hay *et al.*, 1991; Wilby, 1994) is also avoided by the production of weather-state clusters.

The flexibility of the approach is also important, with limited parameter re-calibration required for the immediate application to another area. The use of a semi-Markov chain model as a weather-state generator requires the calibration of only three parameters for each weather-state in an automatic routine. Transition probabilities can be taken directly from the observed record. The model provides accurate simulation of OWT clusters and is applicable to other areas using National Centers for Environmental Prediction (NCEP) reanalysis data, although the quality of the NCEP data must be checked. The NSRP model has been applied to many climate regions of Europe and worldwide, its flexible structure allowing a good fit to observed statistics. Although the main aim of the current application is in water resource management where aggregated daily and monthly flows are required, the NSRP methodology provides reproduction of the precipitation statistics at the hourly level, facilitating more detailed impact studies e.g. variations in river flows, flood risk estimation etc.

The weather type approach is appealing as it is founded on physical linkages between climate at the large scale and weather on a local scale. However, there are many limitations. Wilby (1997) suggests some fundamental problems pertaining to issues of classification, scale and stability.

Firstly, downscaling approaches seldom capture spatial and temporal climatic variability at all scales, and there can be interdependence between variables. This is potentially the greatest problem for flood or drought analysis as it influences extremes. For example, Conway *et al.* (1996) compared two downscaling approaches and found that daily characteristics were generally well preserved but inter-annual variability was poorly reproduced.

Secondly, as atmospheric circulation is essentially dynamic then the identification of distinct 24-hr 'weather' types is arbitrary, even when very clearly defined criteria are applied. Even objective classification techniques contain a degree of subjectivity as the results are sensitive to internal parameters such as grid-size or number of different classes used (Yarnal *et al.,* 1988). Additionally, regional airflows may be apparent so that for example, it is often impossible to allocate a single weather type that is spatially representative of the whole UK.

Finally, and perhaps the most serious hindrance to reliable future downscaling approaches (Wilby, 1997), is that in many cases the relationship between weather type and its associated meteorological properties is constantly changing. Wilby (1994) found inter-decadal variability in both mean wet day precipitation amount and probability of precipitation associated with the three dominant Lamb weather type classes of A, C and W. Even assuming stability, the simulated precipitation regime may still be dependent upon the period chosen for model calibration.

A further characteristic or limitation of the method is imposed by the 'non-unique' nature of downscaling. By this it is meant that a wide range of possible precipitation values may be equally likely associated with a single weather type or cluster. This means that the model series cannot be expected to reproduce one-to-one correspondence of precipitation amounts to observed weather types. Rather, the averaged statistical properties of the weather types will be reproduced. This is further discussed in Section 5.4.3.6.

5.6.2 Suitability for climate change impact applications

This weather type precipitation model was developed for use as a tool in climate change research, and particularly for the estimation of reliability of regional water resource systems. The weather type approach improves upon the 'factor' approach adopted by many researchers (e.g. Arnell and Reynard, 1996) and used by UK water companies in recent climate change assessments. That approach simply modified observed precipitation records by a factor change to the mean derived from GCM simulations, resulting in no changes to the temporal and spatial structure of the precipitation fields. The approach described here uses series of weather types to provide the temporal sequence and high time-aggregation behaviour, and the NSRP model to reproduce hourly and daily statistics of precipitation. The methodology allows the results of GCMs to be used directly, via analyzed GCM OWTs, or indirectly, as trends in both weather-state and precipitation characteristics can be extracted and interpreted within the model.

However, the use of model derived estimates of change must be very carefully justified as there are huge differences between models on a regional scale (McGuffie *et al.*, 1999).

The coupling of weather-states to local precipitation characteristics also contains a spatial element that has often been lacking in previous studies. The multiple site generation of precipitation has been previously demonstrated by Wilks (1998) using the Richardson (1981) weather generator, WGEN, but with no use of weather type information. This model allows the concurrent analysis of different water resource areas within a region that may have very different climatological patterns. Yorkshire is split into two zones that receive precipitation from diverse sources. Spatial variation is provided by the separate fitting of each weather state for a region.

Finally, the obstacle to downscaling arising from the internal instability of a weather type itself (Wilby, 1997) may have been avoided to some extent. The methodology provides the opportunity to examine the effects of internal instability of a weather state upon precipitation statistics within a water resource region. Parameters within the NSRP model that have been fitted on precipitation information from 1961-1990, forming a baseline period, can be adjusted to quantify the effect upon spatial precipitation. In this way, recent concerns about change to precipitation intensities, mean characteristics or increased variability can be evaluated. This is in addition to the frequency and persistence characteristics of the weather states that can be investigated by adjusting probability distributions within the weather state generator.

Chapter 6: Development of rainfall-runoff models

"One of the most important – and yet least well-understood – consequences of future changes in climate may be alterations in regional hydrologic cycles and subsequent changes in the quantity and quality of regional water resources."

Gleick (1987*b*)

6.1 Precipitation data requirements

The ADM model requires daily series of precipitation and potential evapotranspiration (PE) for each catchment. Inflow series for ten reservoired catchments and four river catchments are available from 1934 to 1996. However, digitised precipitation data availability is poor prior to 1970. Hence, daily data series from 1970 to 1996 will be produced for the calibration and validation of the ADM model. This will allow more accurate modelling of the Yorkshire water supply system as data quantity and quality both improve after this date.

All daily precipitation series available for the 1970 to 1996 period were identified. The locations are shown in Figure 5-1.

6.1.1 Reservoir catchment precipitation series

The Water Resources Planning Model (WRPM) requires the input of ten reservoired catchment inflow series. These are detailed in Table 6-1, and Figures 6-1 to 6-10.

The allocation of precipitation gauges was performed subjectively, taking into account river patterns and the very small areas of most catchments. The gauge allocations can be found in Table 6-3, with the precipitation gauge details given in Table 6-2.

It can be observed in Figure 6-1 that all reservoirs in the Washburn group are clustered around the rain gauge at Fewston Reservoir (63121), excepting an eastern outlier. The reservoir at Eccup is used for pump-storage only and has no catchment area. Therefore, precipitation data for Washburn should be derived from the rain gauge 63121.

WRPM Reservoir Group	Yorkshire Water Service Reservoirs	Grid Reference	Usable Capacity 1996 T. C. M.	Catchment Area Km^2	Group Catchment Area Km^2
Washburn	Thruscross	SE152578	7894	28.87	
	Fewston	SE187541	3814	23.91	
	Swinsty	SE196528	4655	16.28	
	Eccup	SE309417	7010		69.06
Winscar	Broadstone		360	1.00	
	Snailsden	SE136040	165	0.84	
	Harden	SE153037	335	1.20	
	Winscar	SE153026	7590	7.10	
	Windleden Upper	SE153013	597	2.00	
	Windleden Lower	SE158019	343	0.78	12.92
Pennine	Ingbirchworth	SE215060	1229	7.73	
	Royd Moor	SE222048	851	4.53	
	Scout Dyke	SE235047	694	2.92	
	Langsett	SE214002	5492	21.06	
	Midhope	SK223994	1877	5.53	
	Underbank	SK253992	2867	12.15	
	Broomhead	SK269958	4937	21.97	
	Morehall	SK287958	2173	4.33	
	Strines	SK232905	1923	11.70	
	Dale Dyke	SK243917	2049	4.41	
	Agden	SK261923	2902	12.14	
	Damflask	SK284907	5106	15.17	
	Rivelin Upper	SK271868	200	11.59	
	Rivelin Lower	SK277867	616	18.05	
	Redmires Upper	SK259855	1382	8.86	
	Redmires Middle	SK264855	769	0.98	
	Redmires Lower	SK268855	628	0.57	163.69
Nidd/Barden	Angram	SE040760	4639	14.65	
	Scar House	SE058769	9414	30.31	
	Barden Upper	SE012578	1943	6.35	
	Barden Lower	SE035567	2200	7.81	
	Chelker	SE055515	982	5.22	64.34
Grimwith	Grimwith	SE060645	21764	28.33	28.33
Worth Valley	Keighley Moor	SD989394	246	1.57	
	Watersheddles	SD969380	839	6.48	
	Ponden	SD995372	891	3.49	
	Lower Laithe	SE013368	1235	4.37	
	Eldwick	SE122413	103	0.75	16.66
Calderdale	Gorpley	SD910230	556	2.83	
	Gorple Upper	SD920314	1716	3.81	
	Gorple Lower	SD940314	1214	4.21	
	Widdop	SD930330	2771	9.00	

WRPM Reservoir Group	Yorkshire Water Service Reservoirs	Grid Reference	Usable Capacity 1996 T. C. M.	Catchment Area Km^2	Group Catchment Area Km^2
	Walshaw Dean Upper	SD968345	862	4.69	
	Walshaw Dean Middle	SD966335	1063	3.01	
	Walshaw Dean Lower	SD960330	658	1.70	
	Warley Moor	SE030317	913	3.72	
	Dean Head Upper	SE022308	240	1.52	
	Dean Head Lower	SE022305	276	0.17	
	Castle Carr	SE023301		1.05	
	Ogden	SE063309	974	4.61	
	Mixenden	SE060290	451	0.77	41.09
Boothwood	Withens Clough	SD984230	1467	4.95	
	Baitings	SE010189	3307	13.37	
	Ryburn	SE023187	995	4.76	
	Green Withens	SD990163	1365	4.59	
	Booth Dean Upper	SE011160			
	Booth Dean Lower	SE014160			
	Boothwood	SE030163	3374	2.74	
	Ringstone	SE050180	991	5.77	
	Ardsley		1671	0.28	36.46
Huddersfield	Deanhead	SE038152	438	2.02	
	Scammonden	SE053167	7420	20.90	
	Wessenden Head	SE068076	359	3.26	
	Wessenden Old	SE058087	324	3.30	
	Blakeley	SE054096	137	3.92	
	Butterley	SE047105	1725	2.37	
	Deerhill	SE070117	752	3.84	
	Blackmoorfoot	SE099130	2968	8.12	47.73
Brownhill	Digley	SE110070	3443	1.46	
	Yateholme	SE112047	416	1.19	
	Riding Wood	SE116052	190	2.32	
	Ramsden	SE114056	324	3.07	
	Brownhill	SE117064	1243	3.02	
	Holmestyes	SE140056	312	2.19	13.25

Table 6-1: Details of ten reservoired catchment inflow series required for WRPM model, where T.C.M. is thousand cubic metres.

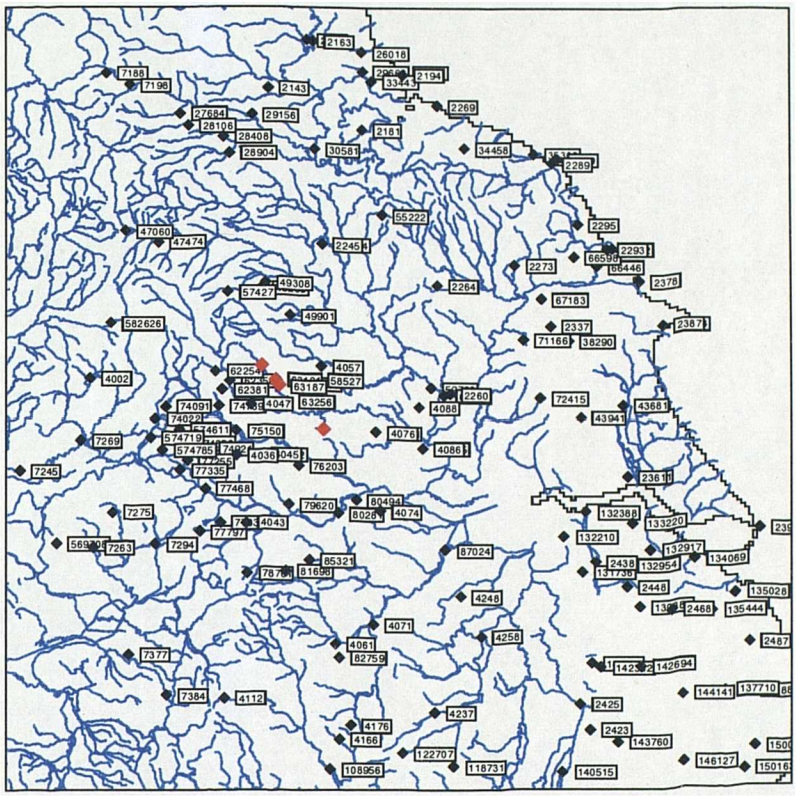

Figure 6-1: Location of reservoirs in the Washburn group.

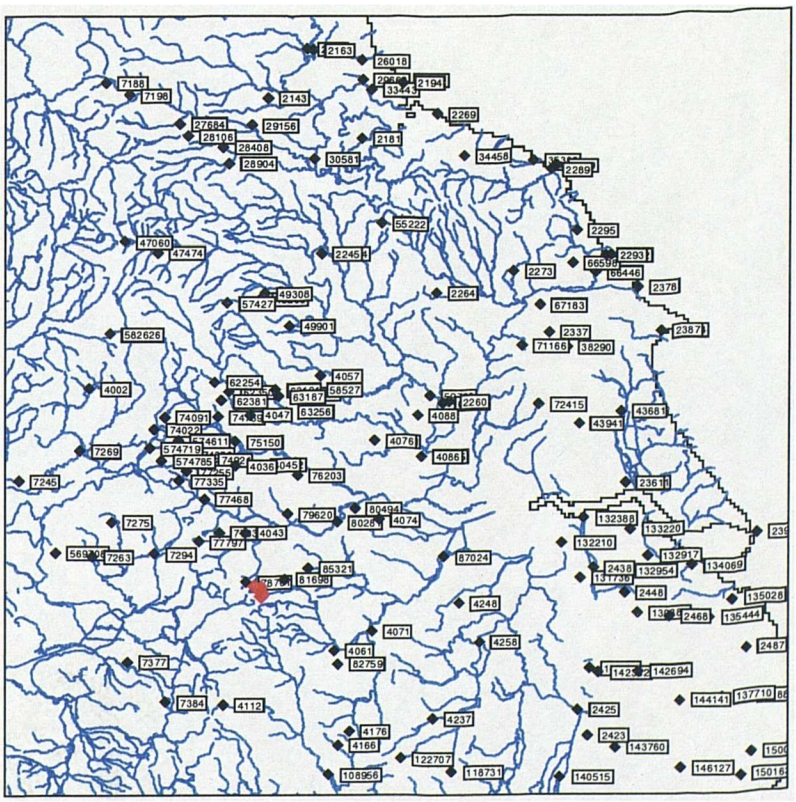

Figure 6-2: Location of reservoirs in the Winscar group.

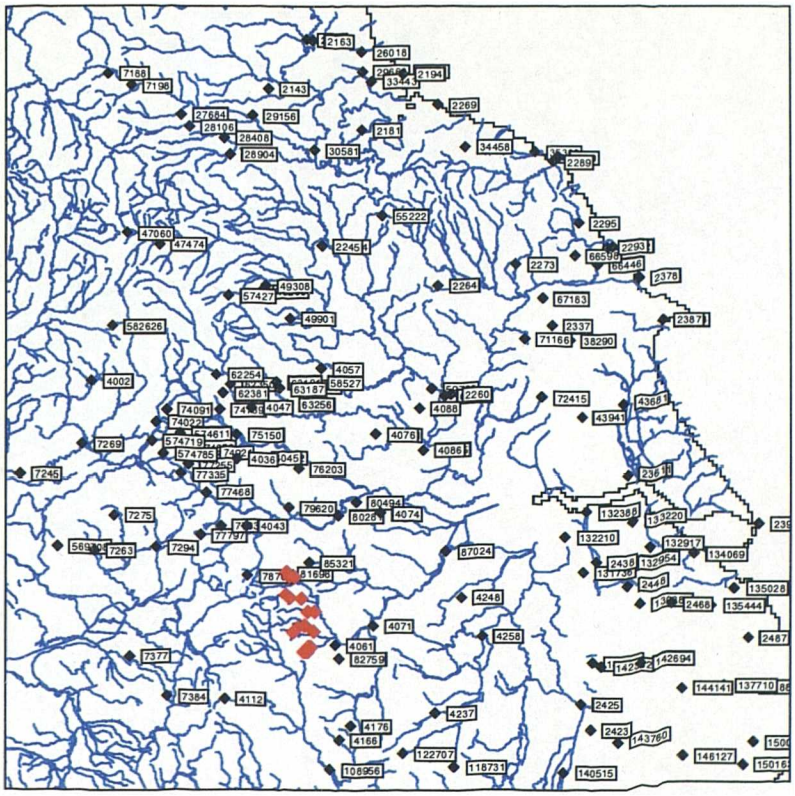

Figure 6-3: Location of reservoirs in the Pennine group.

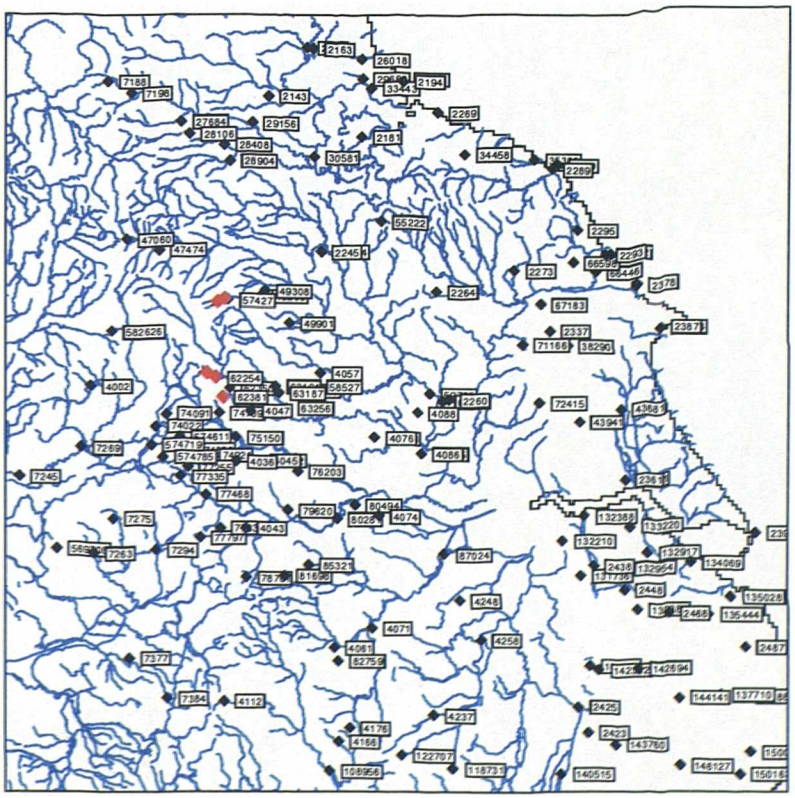

Figure 6-4: Location of reservoirs in the Nidd/Barden group.

Figure 6-2 shows the Winscar reservoir group, which is clustered about the rain gauge at Ramsden (78701). Precipitation time-series for Winscar should be derived from this gauge. Figure 6-3 shows the location of the Pennine group reservoirs. These can be split into two groups. The precipitation for the northern group, with a total catchment area of 80.22 km^2, is best approximated using the precipitation gauge at Ingbirchworth Reservoir (81698). The precipitation gauge at Sheffield (4061) best describes the southern group, encompassing an area of 83.47 km2.

The location of the Nidd/Barden group reservoirs is shown by Figure 6-4. This group shows a three-way partitioning. The northernmost two reservoirs are best described by the precipitation gauge at Scar House Reservoir (57427) and have a catchment area of 44.96 km^2, the majority of the group catchment area. A middle group can be delineated and the precipitation gauge at Lower Barden Reservoir (62254) is used. The southernmost reservoir has a catchment area of only 5.22 km^2 and precipitation data from Chelker Reservoir (62381) is the most appropriate.

Figure 6-5 shows the location of Grimwith Reservoir. As Lower Barden Reservoir (62254) provides the nearest gauge, this will be used to generate a precipitation series for Grimwith. Figure 6-6 shows the location of reservoirs within the Worth Valley group. All reservoirs are clustered about the precipitation gauge of Watersheddles Reservoir (74852), excepting that of Eldwick Reservoir, which has a very small catchment area of 0.75 km^2.

The Calderdale reservoir group is shown by Figure 6-7. The reservoirs can be split into three groups; northeastern, northwestern and a southwestern outlier. The precipitation gauge at Gorple Reservoir (77335) best describes the northwestern group, with a catchment area of 26.42 km2. The northeastern group takes its precipitation data from Mytholmroyd, Redacre (77468), and also provides precipitation data to the southern outlier at Gorpley, giving a catchment area of 14.67 km^2.

The locations of the Boothwood reservoir group are shown by Figure 6-8. Precipitation data for the northernmost outlier at Withens Clough, with a catchment area of 4.95 km^2, is taken from the precipitation gauge at Mytholmroyd, Redacre (77468). The clustered group is split into two along an east-west line and the northernmost three reservoirs, with a catchment area of 23.90 km^2, take precipitation data from the gauge at Ringstone Reservoir (77835). The southern three reservoirs use precipitation data from Great Walden Edge (77797), with a catchment area of 7.33 km^2.

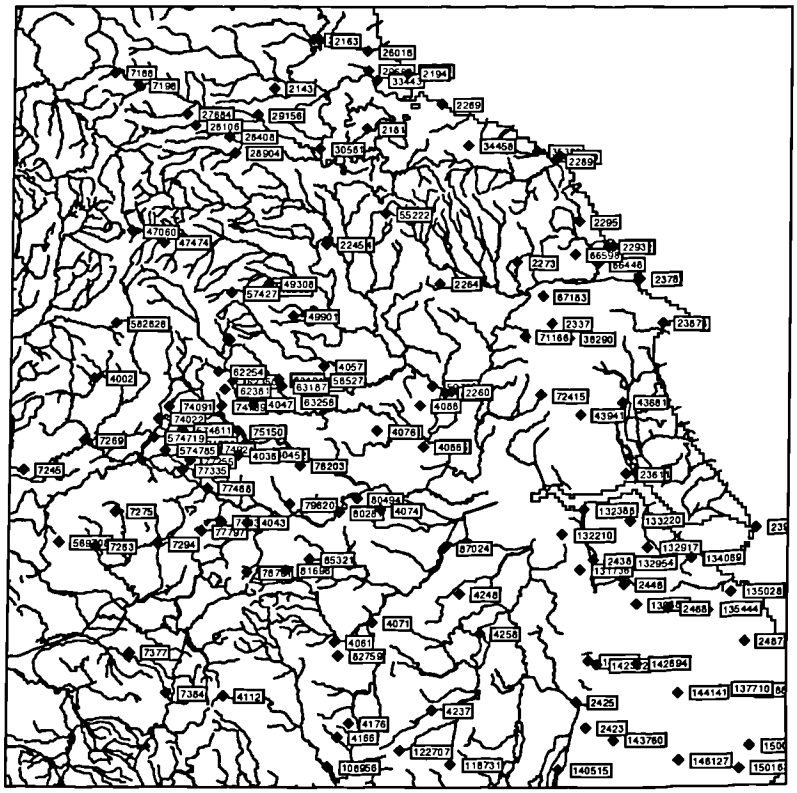

Figure 6-5: Location of reservoirs in the Grimwith group.

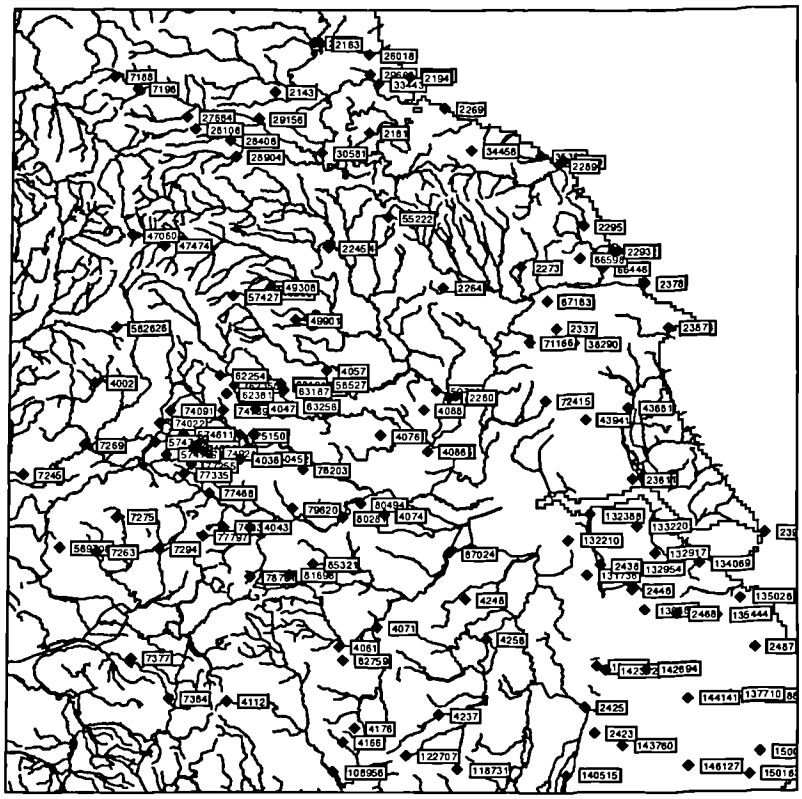

Figure 6-6: Location of reservoirs in the Worth Valley group.

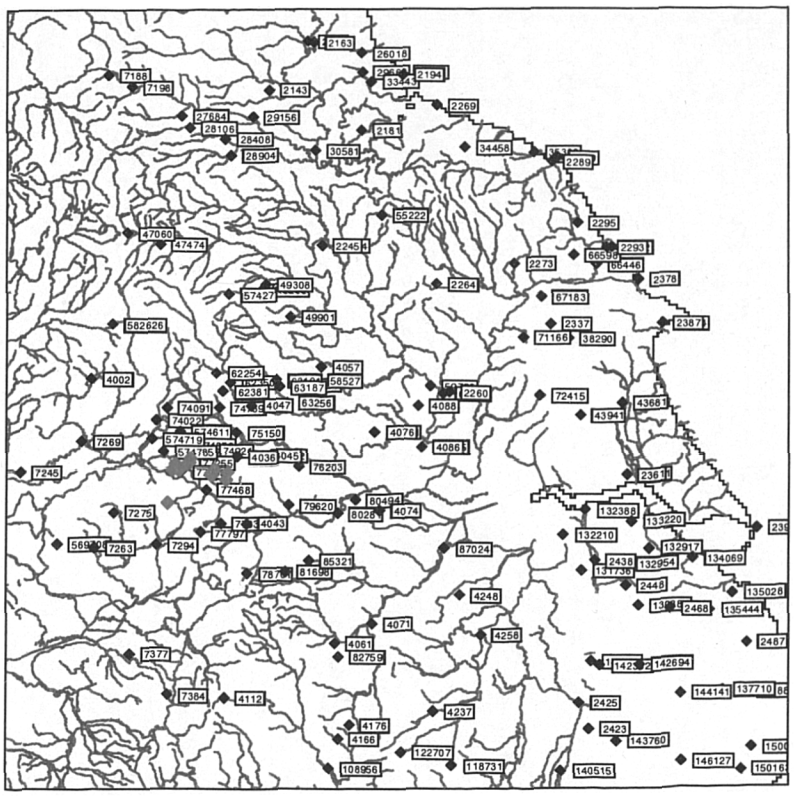

Figure 6-7: Location of reservoirs in the Calderdale group.

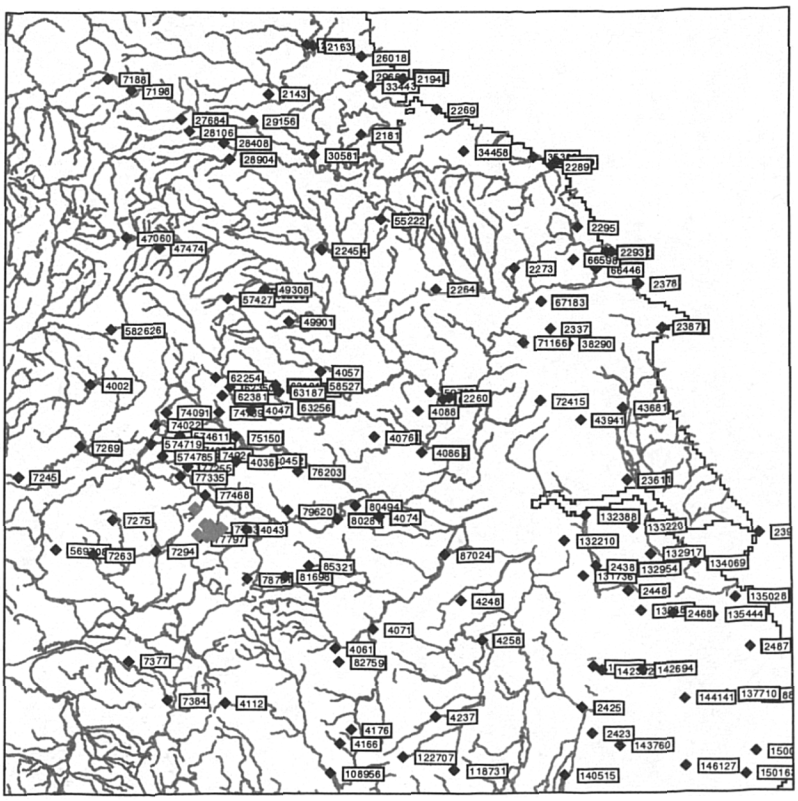

Figure 6-8: Location of reservoirs in the Boothwood group.

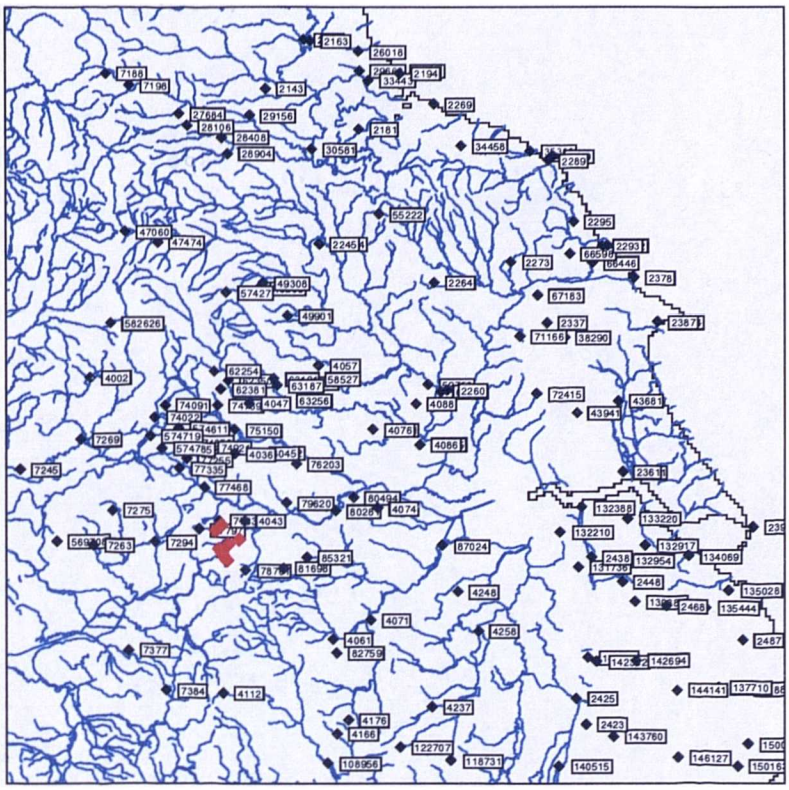

Figure 6-9: Location of reservoirs in the Huddersfield group.

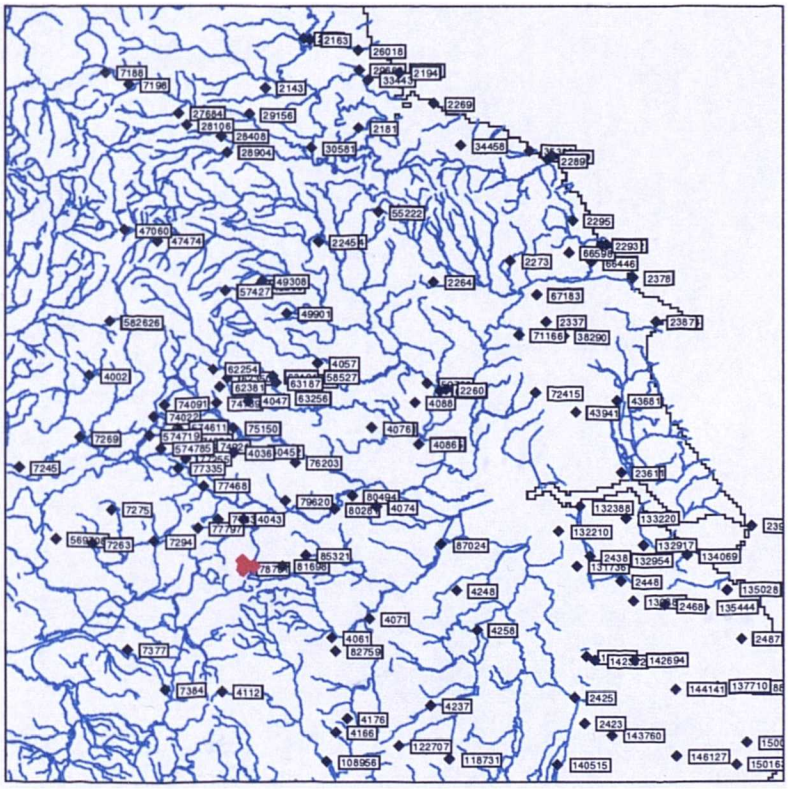

Figure 6-10: Location of reservoirs in the Brownhill group.

Figure 6-9 shows the locations of reservoirs within the Huddersfield group. This is split into two; the precipitation gauge at Ringstone reservoir (77835) best describing the northern 22.92 km^2 of the catchment. The southern 24.81 km^2 uses precipitation data from the gauge at Ramsden (78701).

Figure 6-10 shows the location of Brownhill group reservoirs. These are clustered around the precipitation gauge at Ramsden (78701) and have a catchment area of 13.25 km^2.

Rain Gauge Identifier	Name	Grid Reference	Altitude (m)	Missing data (% of 1970-96)	Suspect data (% of 1970-96)
4061	Sheffield	SK 43 339873	131	1.9	0.0
57427	Scar House Resr.	SE 44 065766	331	0.0	1.0
62254	Lower Barden Resr.	SE 44 035563	227	0.3	0.0
62381	Chelker Resr.	SE 44 052517	223	0.3	0.3
63121	Fewston Resr.	SE 44 188544	160	0.0	1.0
74852	Watersheddles Resr.	SD 34 968380	340	0.0	0.0
77335	Gorple Resr.	SD 34 945312	313	0.0	0.0
77468	Mytholmroyd, Redacre	SE 44 010264	96	0.0	2.2
77797	Great Walden Edge	SD 34 996156	346	0.6	0.0
77835	Ringstone Resr.	SE 44 048178	293	0.3	0.3
78701	Ramsden	SE 44 115051	262	0.0	0.0
81698	Ingbirchworth Resr.	SE 44 213056	260	0.0	0.6

Table 6-2:Precipitation records used for generation of reservoir group precipitation series.

Daily precipitation data from the gauges in Table 6-2 was checked for missing and suspect data. Precipitation data files from the Environment Agency do not specifically indicate the occurrence of monthly data. Data was therefore analysed for the occurrence of just one non-zero value in a month. Where this occurred on the last day of the month, it was clear that the value was a monthly total. In these cases, the monthly total was retained but the daily values set to missing. It is assumed that all other data is true daily data. It is possible, however, that some series have periods of data at less frequent intervals. For example, precipitation gauges may only record data on weekdays and have an accumulated 3-day total every Monday. However, it would be very difficult to find such discrepancies within a data series. Moreover, it would make little difference to the eventual precipitation series, as it will be a disaggregated monthly total.

WRPM Reservoir Group	Group Catchment Area Km^2	Rain Gauge Catchment Area	Rain Gauge Identifier	Proportion
Washburn	69.06	69.09	63121	1.00
Winscar	12.92	12.92	78701	1.00
Pennine	163.69	80.22	81698	0.49
		83.47	4061	0.51
Nidd/Barden	64.34	5.22	62381	0.08
		14.16	62254	0.22
		44.96	57427	0.70
Grimwith	28.33	28.33	62254	1.00
Worth Valley	16.66	16.66	74852	1.00
Calderdale	41.09	26.42	77335	0.64
		14.67	77468	0.36
Boothwood	36.46	4.95	77468	0.14
		7.33	77797	0.20
		23.90	77835	0.66
Huddersfield	47.73	22.92	77835	0.48
		24.81	78701	0.52
Brownhill	13.25	13.25	78701	1.00

Table 6-3:Rain gauge proportions used for generation of reservoired catchment precipitation series.

For the purposes of catchment modelling, it is necessary to have complete catchment precipitation series. Missing daily values were infilled using the record from the nearest neighbouring station with a complete record for the missing time-period. The infilled values were factored using the mean daily precipitation from 1970-1995. All infilling was carried out using original data. See Table 6-4 for details of precipitation gauges used for infilling.

The mean historical precipitation for each reservoir group was then established by taking the weighted proportion of precipitation from each of the sites for a particular day and totalling them. This gave the total areal average daily precipitation for that day for a particular reservoir group. This was repeated for all other days of the record to give a 26-year record of total daily areal average rainfalls for each reservoired catchment group.

Rain Gauge Identifier	Name	Infilling Station	Name	NGR	Factor
4061	Sheffield	82759	Norton Lees	SK 43 348838	1.02
57427	Scar House Resr.	49308	Leighton Resr.	SE 44 162791	1.43
62254	Lower Barden Resr.	62350	Bolton Abbey	SE 44 071539	1.26
62381	Chelker Resr.	62350	Bolton Abbey	SE 44 071540	1.08
63121	Fewston Resr.	62350	Bolton Abbey	SE 44 071541	0.99
74852	Watersheddles Resr.	N/A	N/A	N/A	N/A
77335	Gorple Resr.	77255	Walshaw Dean Lodge	SD 34 964336	1.04
77468	Mytholmroyd, Redacre	77335	Gorple Resr.	SD 34 945312	0.75
77797	Great Walden Edge	77835	Ringstone Resr.	SE 44 048178	1.03
77835	Ringstone Resr.	77797	Great Walden Edge	SD 34 996156	0.98
78701	Ramsden	N/A	N/A	N/A	N/A
81698	Ingbirchworth Resr.	78701	Ramsden	SE 44 115051	0.67

Table 6-4:Precipitation gauges used for infilling (reservoired catchments).

6.1.2 River catchment precipitation series

Four major river abstractions are modelled within the WRPM model, requiring four daily inflow series. These are detailed in Table 6-5 and river catchments can be seen in Figure 6-11.

WRPM River Source	Abstraction Point	Grid Reference	Catchment Area (km^2)	Altitude (mOD)	Mean Flow ($m^3 s^{-1}$)	Q95 ($m^3 s^{-1}$)	Q10 ($m^3 s^{-1}$)	61-90 Average Precipitation (mm)
Wharfe	Addingham	SE 092 494	427	79.7	13.89	1.611	35.3	1383
Ouse	Skelton	SE 568 554	3315	4.6	48.92	7.304	122.3	900
Derwent	Buttercrambe	SE 731 587	1586	9.5	15.83	3.827	32.3	765
Hull	Hempholme	TA 080 498	378.1	2.8	3.41	0.486	7.3	701

Table 6-5: Details of the four river catchment inflow series required for WRPM model.

The River Wharfe rises in the Northern Pennines (Yorkshire Dales) close to Ribblehead, and is formed at the confluence of Oughtershaw and Langstrothdale becks at Beckermonds, moving through the Vale of York and becoming tidal before entering the River Ouse to the east of Ryther. It rises surrounded by hills that are often above 600 m AOD in height. Great Whernside, the highest point in the catchment is 704 m AOD.

The Wharfe at Addingham has a Crump profile weir that overestimates high flows. A flashy flow regime is substantially influenced by reservoir operation, with Grimwith regulation

releases since June 1984, and many other public water supply reservoirs. There has also been significant public water supply abstraction upstream at Lobwood since 1980. Upper Wharfedale comprises a sequence of limestones and shales (Carboniferous Limestone). The rocks become progressively newer as the river flows downstream to the Dales, changing to Carboniferous Millstone Grit and finally to Magnesian Limestone and Sherwood Sandstone before the confluence with the River Ouse.

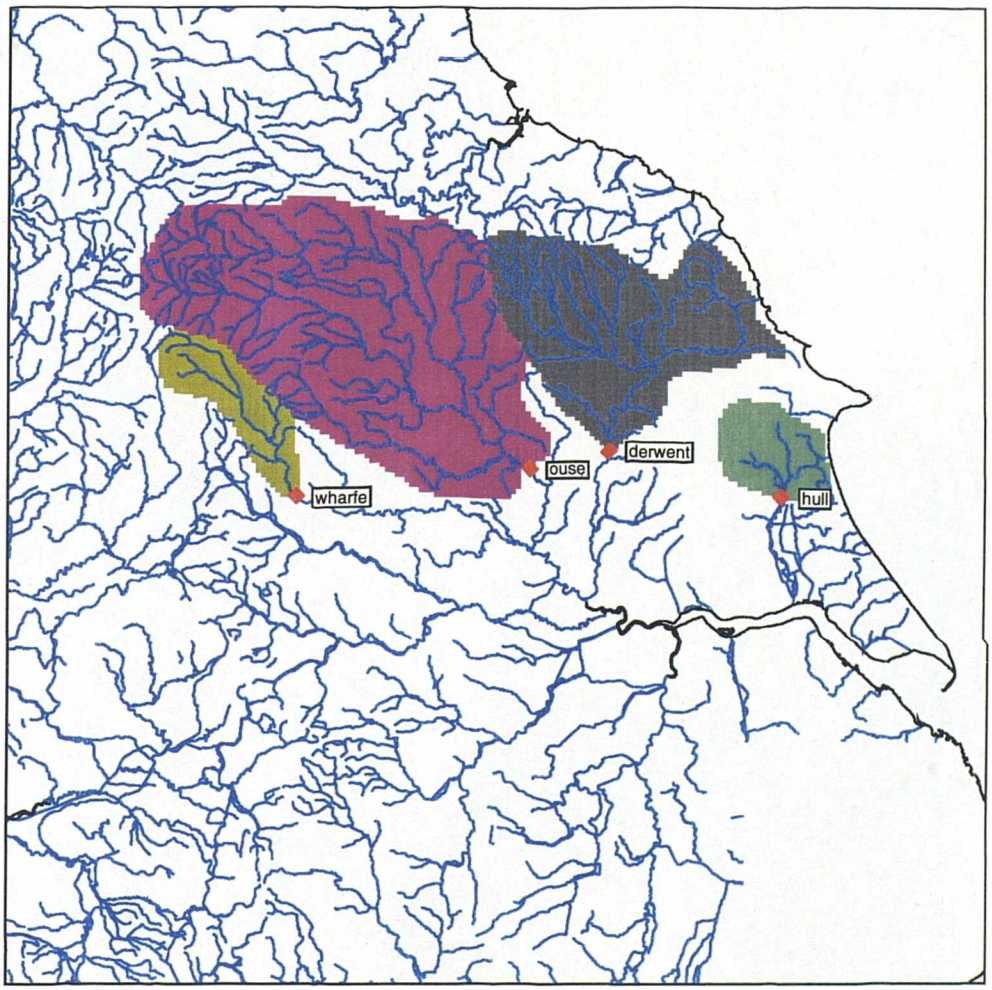

Figure 6-11: Location of river catchments in Yorkshire.

Groundwater is an important component of the hydrology of the Wharfe catchment, although only marginally used in the upper stretches, it is extensively abstracted in the lower reaches of the Dales; major aquifers existing in the Magnesium Limestone and the Sherwood Sandstone.

The Derwent catchment is principally rural and drains one-tenth of Yorkshire. It rises on Fylingdales Moor in the North York Moors National Park and joins the Ouse at Barmby-on-the-Marsh. Its principal tributaries drain the North York Moors and springs from the chalk aquifer contribute to a significant part of the flow. The catchment also includes the Sea Cut, a man-

made channel connecting the River Derwent with the North Sea near Scarborough. Peak flows from the headwaters upstream of Forge Valley (eight percent of the catchment) are diverted down the Sea Cut. At Buttercrambe, a crump weir is used to record flows, with a high flow rating derived from a limited number of gaugings. This structure was drowned and bypassed in the March 1999 flood event.

The Derwent catchment possesses major aquifers of Chalk, Corallian limestone and Sherwood sandstone. The Corallian series outcrops on hills surrounding the Vale of Pickering in the north of the catchment and is very important in determining catchment response as the northern hills receive the vast majority of the catchment's precipitation input. The Corallian outcrop consists of a sequence of limestones and sandstones; total thickness up to 100 metres. These are extensively faulted and dissected by the rivers flowing south from the North York Moors, effectively dividing the aquifer into a series of semi-independent blocks. This well-developed fissure system within the Corallian Limestone permits a rapid response to precipitation (often within one day). Additionally, the river Rye and the river Derwent at West Ayton have swallow holes in the riverbed where a considerable amount of water is lost to the aquifer. The ingress of river water on the north side of the limestone outcrop and its discharge a few kilometres downstream, often at very large springs, is common.

The River Hull is a predominantly rural catchment draining the chalk outcrop of the Yorkshire Wolds. There is significant groundwater abstraction from the chalk aquifer. Monthly abstraction data from 1983-1995 shows little variation in abstraction over the period, with a monthly abstraction rate of approximately 450 Ml. Flows at Hempholme are recorded using two tilting-gate weirs. The very flat gradient causes occasional drowning and it is possible that low flows are underestimated. There are appreciable public water supply abstractions upstream at Tophill Low, which are thought to reduce the flow by approximately 0.6 $m^3 s^{-1}$.

The River Ouse is a predominantly rural catchment draining northern parts of the Vale of York and the Yorkshire Dales. It has a mixed geology with a similar progression downstream to that of the Wharfe catchment. Flows are measured at Skelton using a multi-path ultra-sound. Public water supply abstractions upstream are having an increasing impact upon very low flows, although some artificial groundwater augmentation now has a counterbalancing influence. The many public water supply reservoirs within the catchment also affect runoff. Naturalised flows were found to be generally higher than recorded flows by 2.3 $m^3 s^{-1}$ from 1982 to 1991, but lower during the drought years of 1984 and 1990 (Mott MacDonald, 1996).

Rain Gauge Identifier	Name	Grid Reference	Altitude (m)	Missing data (%)	Suspect data (%)
2245	Leeming	SE 44 306890	32	5.7	0.0
2387	Bridlington	TA 54 173687	48	3.8	0.0
4057	Harrogate	SE 44 303 578	66	1.9	0.0
28904	Brignall	NZ 45 071 122	201	0.3	7.7
34458	Lockwood Resr.	NZ 45 668141	193	0.1	0.3
38290	Sledmere House	SE 44 933648	121	0.0	0.0
43681	Tophill Low	TA 54 072483	2	0.3	0.6
47060	Moorland Cottage	SD 34 807923	343	0.0	1.0
47474	Burtersett	SD 34 891893	297	0.0	1.3
49308	Leighton Resr.	SE 44 162791	193	0.3	0.6
49901	Lumley Moor Resr.	SE 44 224706	172	0.0	2.6
55222	Osmotherly Filters	SE 44 458967	147	0.0	2.2
57427	Scar House Resr.	SE 44 065766	331	0.0	1.0
59792	York, Acomb Landing	SE 44 581527	9	0.0	0.0
62254	Lower Barden Resr.	SE 44 035563	227	0.3	0.0
66598	Wykeham Nursery	SE 44 947863	152	0.0	3.2
67183	Scampston Hall	SE 44 864756	31	1.3	1.9
71166	Birdsall House	SE 44 818651	94	0.0	0.6

Table 6-6:Precipitation records used for generation of river precipitation series.

Using digital elevation (at one km^2 resolution) and river location information the four catchments were digitised upstream of their abstraction point using an automatic procedure of catchment definition. The catchments were then adjusted so that the catchment area equalled that suggested by the Agency for that catchment. Thiessen Polygons were then used to divide the total area of the catchment into polygons whose sides are the perpendicular bisectors of the line joining adjacent rain gauges. In this way, each rain gauge in Table 6-6 was assigned a proportional area of the catchment (see Table 6-7, and Figures 6-12 to 6-15).

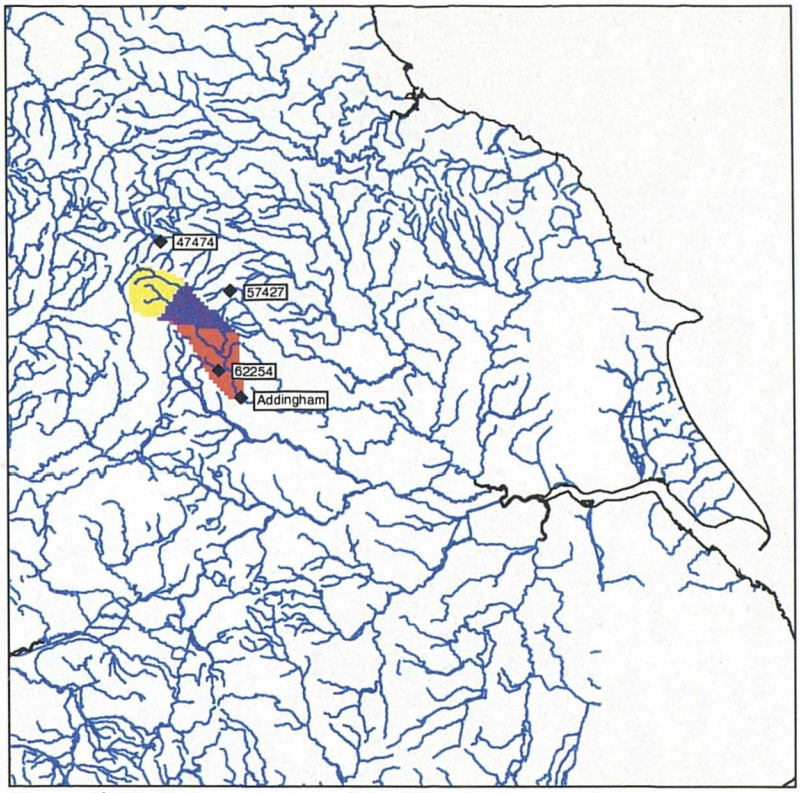

Figure 6-12: Polygonisation of the Wharfe river catchment.

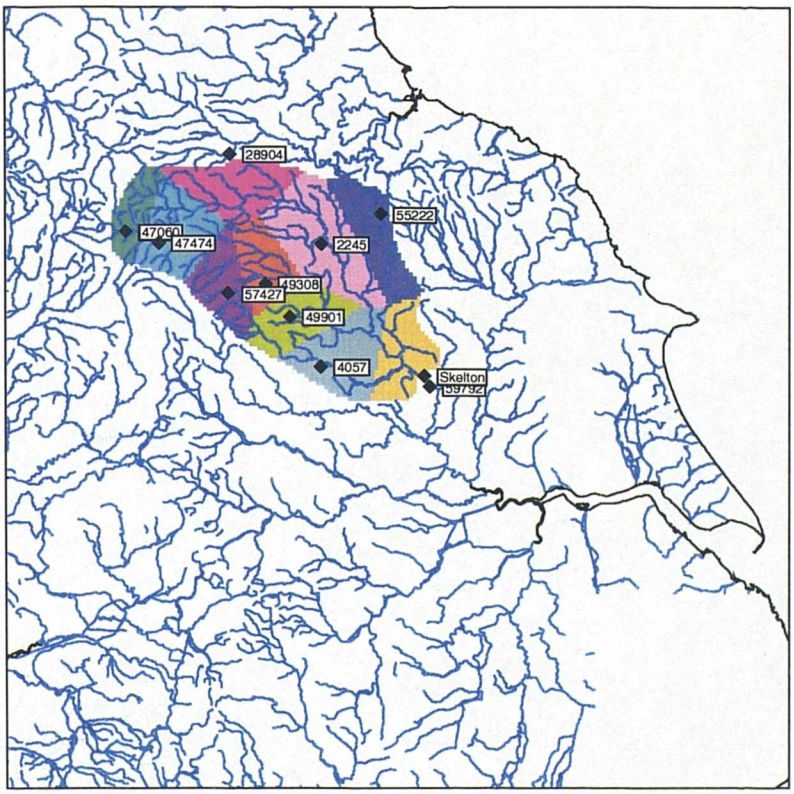

Figure 6-13: Polygonisation of the Ouse river catchment.

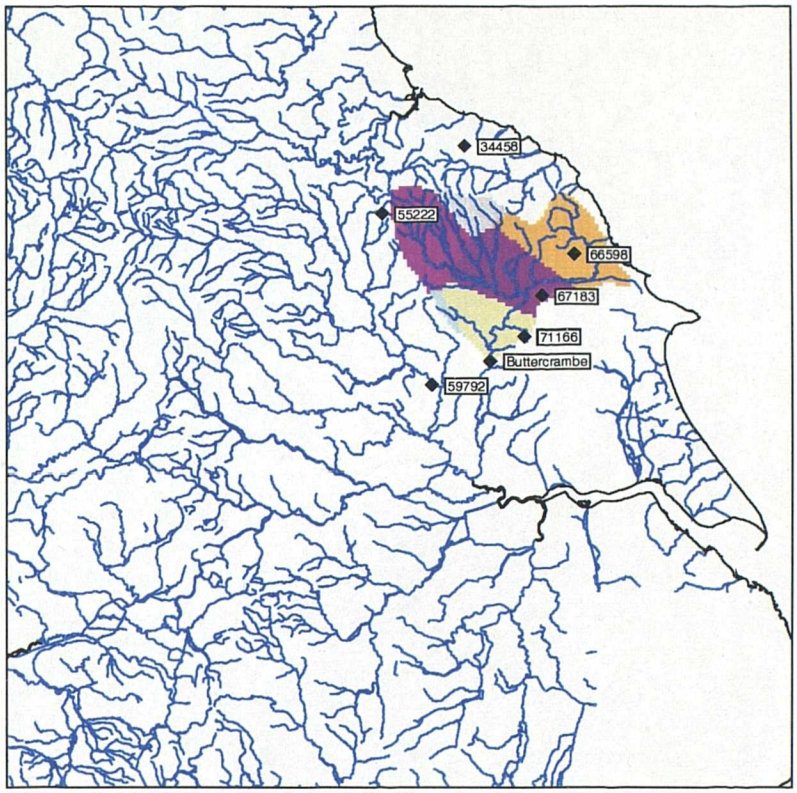

Figure 6-14: Polygonisation of the Derwent river catchment.

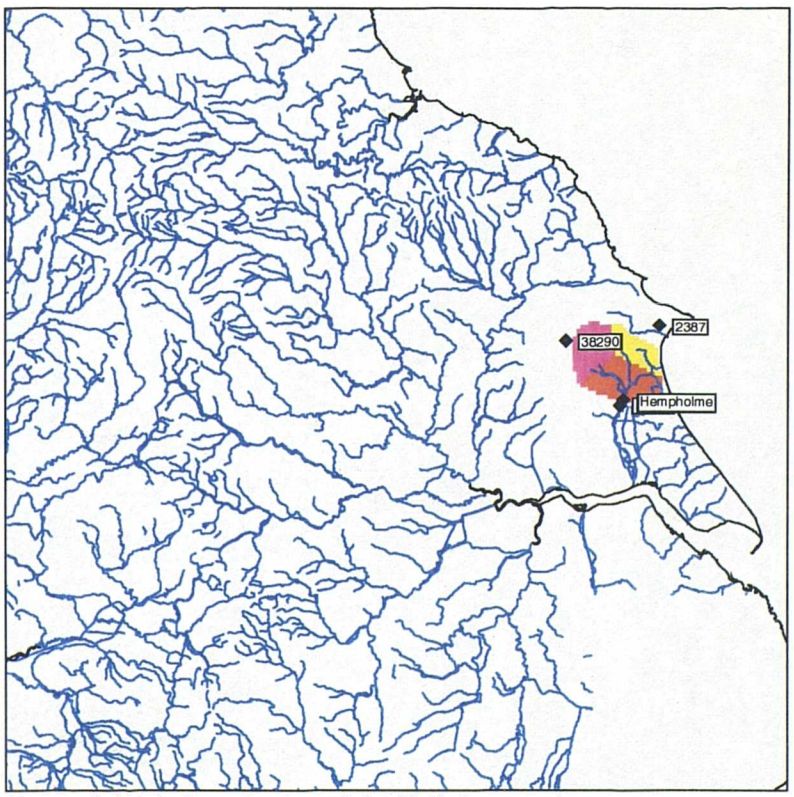

Figure 6-15: Polygonisation of the Hull river catchment.

WRPM River Source	Catchment Area Km^2	Rain Gauge Catchment Area	Rain Gauge Identifier	Proportion
Wharfe	427	131	47474	0.31
		112	57427	0.26
		184	62254	0.43
Ouse	3315	555	2245	0.17
		392	4057	0.12
		354	28904	0.11
		195	47060	0.06
		345	47474	0.10
		259	49308	0.08
		304	49901	0.09
		340	55222	0.10
		271	57427	0.08
		300	59792	0.09
Derwent	1586	119	34458	0.08
		360	55222	0.23
		431	66598	0.27
		386	67183	0.24
		259	71166	0.16
		31	59792	0.02
Hull	378	85	39164	0.22
		125	38290	0.33
		168	43681	0.45

Table 6-7:Rain gauge proportions used for generation of river catchment precipitation series.

Missing and suspect data values were treated in the same way as the reservoired catchment data series, and infilled using neighbouring precipitation gauge measurements. Details are given in Table 6-8.

The mean historical precipitation for each river catchment was then established by taking the weighted proportion of precipitation from each of the sites for a particular day and totalling them. This gave the total areal average daily precipitation for that day. This was repeated for all other days of the record to give a 26-year record of total daily areal average rainfalls for each river catchment.

Rain Gauge Identifier	Name	Infilling Station	Name	NGR	Factor
2245	Leeming	55222	Osmotherly Filters	SE 44 458967	1.13
2387	Bridlington	2378	Filey	TA 54 113801	1.03
4057	Harrogate	58527	Harlow Hill Resr.	SE 44 289543	0.98
28904	Brignall	28408	Barnard Castle, Bowe	NZ 45 056164	1.06
34458	Lockwood Resr.	35300	Mulgrave Castle	NZ 45 845126	1.18
38290	Sledmere House	N/A	N/A	N/A	N/A
43681	Tophill Low	43941	South Dalton	SE 44 965452	0.92
47060	Moorland Cottage	47474	Burtersett	SD 34 891893	1.37
47474	Burtersett	47060	Moorland Cottage	SD 34 807923	0.73
49308	Leighton Resr.	57427	Scar House Resr.	SE 44 065766	0.70
49901	Lumley Moor Resr.	49308	Leighton Resr.	SE 44 162791	0.93
		57427	Scar House Resr.	SE 44 065766	0.65
55222	Osmotherly Filters	2245	Leeming	SE 44 306890	1.21
57427	Scar House Resr.	49308	Leighton Resr.	SE 44 162791	1.43
59792	York, Acomb Landing	N/A	N/A	N/A	N/A
62254	Lower Barden Resr.	62350	Bolton Abbey	SE 44 071539	1.26
66598	Wykeham Nursery	66446	Irton P. Sta.	TA 54 004840	1.21
67183	Scampston Hall	2337	High Mowthorpe	SE 44 888685	0.87
71166	Birdsall House	2337	High Mowthorpe	SE 44 888686	0.98

Table 6-8:Precipitation gauges used for infilling (river catchments).

6.2 Potential Evapotranspiration (PE) data

6.2.1 Data comparison

PE data was derived for the ten reservoired and four river catchments using 0.5° lat x 0.5° long gridded average PE for Europe developed at the Climatic Research Unit (CRU), University of East Anglia, UK for the WRINCLE project (Water Resources: the INfluence of CLimate change in Europe). This is based upon the 1961 to 1990 mean monthly terrestrial climatology of New *et al.* (1999) produced for a suite of climate variables: precipitation, wet-day frequency, mean temperature, diurnal temperature range, vapour pressure, cloud cover, sunshine duration, ground frost frequency and wind speed. This uses the FAO (UN Food and Agriculture Organization) recommended combination formula for Reference Evapotranspiration. The combination formula is (6-1):

$$ET_o = \frac{0.408\,\Delta(R_n - G) + \gamma \frac{900}{T+273} U_2 (e_a - e_d)}{\Delta + \gamma(1 + 0.34 U_2)} \qquad (6\text{-}1)$$

where: ET_o = reference crop evapotranspiration [mm d^{-1}]

R_n	=	net radiation at crop surface [MJ m^{-2} d^{-1}]
G	=	soil heat flux [MJ m^{-2} d^{-1}]
T	=	average temperature [°C]
U_2	=	windspeed measured at 2m height [m s^{-1}]
(e_a-e_d)	=	vapour pressure deficit [kPa]
Δ	=	slope vapour pressure curve [kPa $°C^{-1}$]
γ	=	psychrometric constant [kPa $°C^{-1}$]
900	=	conversion factor

Monthly anomaly grids were constructed and merged with the baseline climatology to produce 1901-1996 monthly time-step climate fields (New *et al.*, 2000). This baseline climatology was also directly compared with the output from the HadCM2 CONTROL experiment for the period 1961-1990. The monthly fields of temperature, total short-wave radiation, windspeed and vapour pressure were used to construct PE fields from regridded 0.5° resolution data. Annual and seasonal total PE for the control period from the GCM showed good agreement with observations. PE data for the time-period from 1970 to 1995 was therefore extracted and used in calibration and validation.

A comparison was made of the standard MORECS (Meteorological Office Rainfall and Evaporation Calculation System) PE dataset (Thompson *et al.*, 1981) and the PE derived by New *et al.* (2000). MORECS has been in operation since 1961 and provides estimates of monthly evaporation in the form of 40x40 km grid-cell averages for Great Britain using daily observations of sunshine, temperature, vapour pressure, wind speed and precipitation from approximately 131 stations. These point measurements are then interpolated to obtain grid-cell averages for each variable. MORECS is the standard scheme used for evapotranspiration in the UK, and gives a 30-yr climatological normal for the 1961-90 time-period.

Figure 6-16 shows a comparison of the MORECS and New *et al.* (2000) datasets for PE estimation in Yorkshire during the period from 1970-1990 (1995 in the case of the WRINCLE data). The England and Wales series is an average PE over England and Wales taken from the MORECS data. The numbers correspond to the grid-squares in the MORECS scheme and the nearest square from the New *et al.* (2000) scheme has been chosen for comparison and similarly numbered. For example, the MORECS and WRINCLE-98 and -92 squares are representative of the majority of the WRPM reservoir groups. It can be observed that the MORECS-98 and WRINCLE-98 series match very well, but for MORECS-92 there is an underestimation of PE when compared to WRINCLE-92. Since neighbouring MORECS squares show much higher PE values, this is taken to be an anomaly in the MORECS dataset. The MORECS-99 grid-square

also shows a large underestimation of PE when compared to the WRINCLE-99 record. However, in this case the WRINCLE-99 grid-square is assumed an overestimation, as no other record shows as high values. This record is relevant for the Pennine WRPM group but the neighbouring record of WRINCLE-98 will instead be used in calibration. MORECS-94 corresponds to the Derwent grid-cell and shows good agreement. In general, there is a good agreement between the MORECS and WRINCLE PE records for Yorkshire, although it is appreciated that in general the WRINCLE record shows an overestimation of PE when compared to MORECS for most of England. A further improvement may have been obtained by rescaling the WRINCLE data to average catchment height. Therefore, the WRINCLE record will be used in calibration and validation of the rainfall-runoff models, as future PE estimations are also available in the same format.

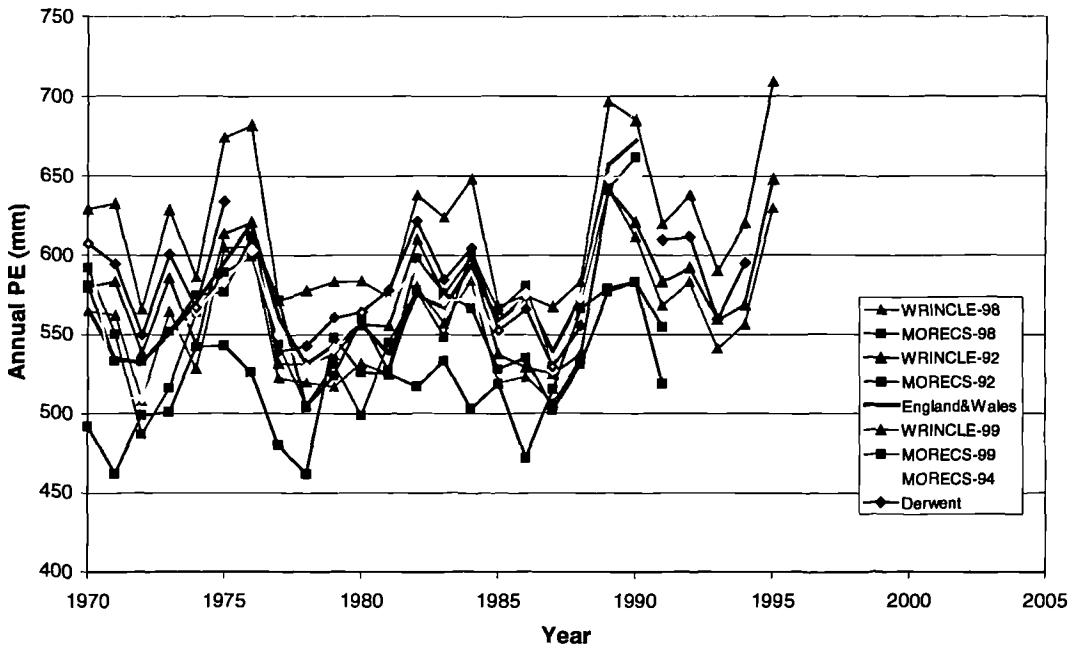

Figure 6-16: Comparison of MORECS and New et al. (2000) estimation of PE in Yorkshire. The numbers correspond to the MORECS grid-square scheme.

6.2.2 Data collection methodology

For the reservoired catchments, the majority of reservoirs within a WRPM group lay within a single grid-square. For the river catchments, the proportional area of the catchment contained within each grid-square was added to give an average PE across the catchment. Details of the grid squares used can be found in Table 6-9.

WRPM Group	Catchment Area Km^2	Grid-Square Catchment Area	Grid-Square Identifier (row, column)	Corresponding MORECS grid-square	Proportion
Washburn	69.06	69.09	383 (39, 21)	98	1.00
Winscar	12.92	12.92	383 (39, 21)	98	1.00
Pennine	163.69	163.69	383 (39, 21)	98	1.00
Nidd/Barden	64.34	64.34	357 (40, 21)	92	1.00
Grimwith	28.33	28.33	357 (40, 21)	92	1.00
Worth Valley	16.66	16.66	383 (39, 21)	98	1.00
Calderdale	41.09	41.09	383 (39, 21)	98	1.00
Boothwood	36.46	36.46	383 (39, 21)	98	1.00
Huddersfield	47.73	47.73	383 (39, 21)	98	1.00
Brownhill	13.25	13.25	383 (39, 21)	98	1.00
Wharfe	427.00	205.00	356 (40, 20)	92	0.48
		153.00	357 (40, 21)	92	0.36
		69.00	383 (39, 21)	98	0.16
Ouse	3315.00	485.00	356 (40, 20)	92	0.15
		1495.00	357 (40, 21)	92	0.45
		1097.00	358 (40, 22)	93	0.33
		217.00	384 (39, 22)	99	0.07
Derwent	1586.00	358.00	358 (40, 22)	93	0.23
		1093.00	359 (40, 23)	94	0.69
		135.00	360 (40, 24)	95	0.08
Hull	378.00	18.00	359 (40, 23)	94	0.05
		190.00	360 (40, 24)	95	0.50
		5.00	385 (39, 23)	99	0.01
		165.00	386 (39, 24)	100	0.44

Table 6-9: PE grid-square data used for ADM model calibration and validation.

6.3 River flow and reservoir inflow data

6.3.1 Reservoir inflows

Mott MacDonald has undertaken many studies for Yorkshire Water Services (YWS) concerning reservoir inflow series for particular groups of reservoirs (Mott MacDonald, 1996; 1997). Data series were produced for weekly and monthly inflows for the period 1934 to 1996 for individual reservoirs within the ten main reservoir groups detailed in Table 6-1. Where adequate data was available, reservoir inflows were derived from reservoir operation data, and catchment models were calibrated so that values could be generated for a period when operation data was unavailable.

Reservoir inflows were derived using a standard water balance approach, taking account of change in reservoir storage, spill, compensation or other releases, abstractions for supply, and transfers to/from other reservoir groups. However, for most reservoirs, there was insufficient data available and thus flows were generated for the whole period using a catchment model whose main parameters were based on those of a nearby catchment.

The inflow series for the ten reservoir groups were obtained from the Agency. Due to a lack of information on reservoir operation data, these previously derived monthly inflow series will be used for model calibration and validation, using a monthly time-step.

6.3.2 River flows

Previous work on generating river flows for the period from 1920 to 1996 has been performed by Mott MacDonald (1996). The HYSIM model (Manley, 1993) was used to model the catchments using naturalised flow series, where available. It was assumed that all flow series already take account of upstream abstractions and discharges. High R^2 values were obtained for all four catchments. Therefore, these modelled flows will be used for model calibration and validation.

6.4 ADM model calibration and validation

A full description of the ADM model can be found in section 2B.3. Since 26 years of precipitation, evapotranspiration and flow data were available from 1970 to 1995, a split-sample approach was taken. The 13 years of data from 1970 to 1982 being used for model calibration and the remaining data used for model validation.

6.4.1 Calibration methodology

In recent years, many automated approaches to calibration have been developed. However, many difficulties in the application of such methods have been reported (e.g. Johnston and Pilgrim 1976) and is summarised as follows by Moore and Clarke (1981):

- *the parameters of the model may be interdependent, so the same values of the objective function correspond to a wide range of parameter values.*
- *the objective function may be indifferent to the values of the parameters, so that little or no change in the objective function occurs in response to appreciable changes in the value of a parameter.*
- *discontinuities may exist in the parameter space for which the objective function is non-differentiable.*
- *local optima may exist for which the search for a minima through an optimisation algorithm may terminate at a point on the surface of the objective function lower than those surrounding it, but higher than other points situated in another region of parameter space. The global optimum may not be found.*

To these purely technical considerations can be added a more general one (Todini, 1988). An automatic calibration technique requires the adoption of some statistical measure, or index of agreement, between observed and simulated flows (i.e. least-squares, regression, maximum likelihood, etc.). These are based on an analysis of the residuals and neglect the physical characteristics of the model. As a procedure of automatic calibration does not capitalise on *a priori* knowledge, the effectiveness of any particular model may thus be reduced (Franchini and Pacciani, 1991).

The genetic algorithm is a search procedure based upon the mechanics of natural selection and natural genetics, and is often associated with local search optimisation techniques in the calibration of conceptual rainfall-runoff models (e.g. Wang, 1991; Franchini, 1996; Franchini

and Galaeti, 1997). Problems often occur when genetic algorithms fail to find global optima. However, a powerful new global optimisation procedure has been developed and tested using the SIXPAR conceptual rainfall-runoff model. The shuffled complex evolution method for global optimisation (SCE-UA) developed at the University of Arizona (Duan *et al.*, 1992) was consistently able to locate the global optimum of the SIXPAR model and appears capable of solving the conceptual rainfall-runoff model optimisation problem. The SCE-UA combines the strengths of the simplex procedure (Nelder and Mead, 1965) with the concept of controlled random search (Price, 1987), competitive evolution (Holland, 1975) and complex shuffling.

The SCE-UA approach treats the global search as a process of natural evolution. A number of points are sampled and these constitute a population. This population is then partitioned into several communities (complexes), each of which evolves independently and hence searches the optimisation space in different directions. After a number of generations, the communities are mixed through a procedure of random shuffling. This helps to share information gathered by the various communities about the search space. To ensure that the evolution process is 'competitive' the 'parents' with the better objective function value will have a greater chance of reproducing than others. This directs evolution in an improvement direction using a triangular probability distribution. In addition, offspring are introduced randomly in space (mutations) to ensure that the process of evolution is not trapped in less than optimal regions.

Parameter	Minimum Limit	Maximum Limit	Starting Value
W_m	250.0	600.0	50.0
B	0.0	10.0	0.1
D_1	0.1	10.0	3.0
D_2	2.0	20.0	5.0
Conv	1.0	4.0	1.5
Diff	1000.0	10000.0	5000.0

Table 6-10: Parameter starting values and lower and upper constraints used in calibration (after Franchini 1996)

To fix the optimisation space, certain physically feasible parameter limits were imposed upon the calibration. These can be found in Table 6-10.

The Nash and Sutcliffe 'efficiency' measure developed in 1970 (Nash and Sutcliffe, 1970) has been adopted as a standard estimate of model accuracy and was used as the optimisation criterion for model calibration. They started with a sum of the squares criterion such as (6-2):

$$F^2 = \sum \left(Qr_i - Qs_i \right)^2 \qquad (6\text{-}2)$$

where F^2 is the index of disagreement and Qr and Qs are the observed and simulated discharges at a particular time. The sum may be taken over all Q's at regular intervals, or at preselected times such as peaks or troughs in the hydrograph. F^2 is analogous to the residual variance of a regression analysis. .

They then defined the initial variance, F_0^2 , as (Equation 6-3):

$$F_0^2 = \sum (Qr_i - \mu_r)^2 \qquad (6\text{-}3)$$

where; μ_r is the mean of the Qr's (recorded discharges).

This then enabled them to define the 'efficiency of a model', CE, as the proportion of the initial variance accounted for by that model (Equation 6-4):

$$CE = 1 - \frac{F^2}{F_0^2} \qquad (6\text{-}4)$$

6.4.2 Calibration and validation results

The results of the calibration and validation (CE) values and water-balance statistics can be found in Table 6-11. It can be observed that the majority of calibration and validation CE values are in excess of 0.7. One reservoir catchment however, appears to show a change in regime halfway through testing. This causes a reduction in CE from 0.59 to 0.48 for the Winscar WRPM group. The River Derwent also has a low CE statistic in both calibration and validation stages. This is due to the complex underlying geology of the catchment. Both the River Derwent and River Hull incorporate a large proportion of groundwater flow, the River Hull being almost entirely groundwater flow driven (see Figure 6-17 for example). The catchment geology means that a better calibration will not be achieved for either river catchment with the ADM. The River Hull inflow will therefore be treated as constant. The River Ouse also has a low CE statistic due to the lumped model approach taken. However, this model will be used to reduce complexity within the model inputs for the WRPM.

WRPM Group	Calibration CE	Calibration Water-balance	Validation CE	Validation Water-balance
Washburn	0.79	1.01	0.72	0.93
Winscar	0.59	1.10	0.48	0.98
Pennine	0.83	1.00	0.81	1.09
Nidd/Barden	0.62	0.91	0.76	0.98
Grimwith	0.79	0.98	0.87	1.01
Worth Valley	0.86	1.07	0.83	1.13
Calderdale	0.93	1.00	0.93	0.96
Boothwood	0.88	0.94	0.88	0.95
Huddersfield	0.92	0.95	0.90	0.97
Brownhill	0.84	0.87	0.83	0.90
Wharfe	0.69	1.07	0.66	1.10
Ouse	0.60	1.15	0.61	1.16
Derwent	0.61	1.06	0.59	1.08
Hull	< 0	–	< 0	–

Table 6-11: Calibration and validation statistics for the 14 WRPM catchment inflows. CE refers to the Nash and Sutcliffe 'efficiency' measure. The water-balance statistic refers to the simulated total inflow/observed total inflow.

It can be observed in Table 6-11 that for the majority of the WRPM groups a satisfactory water-balance statistic is achieved when simulated and observed total flows are compared for both the calibration and validation periods. A satisfactory water-balance statistic is defined as between 0.95 and 1.05; i.e. a margin of error of five percent in each direction is given for measurement errors. The Brownhill WRPM group shows up strongly as under-simulating the total inflow statistic, in both the calibration and validation stages. A multiplicative factor of 1.14 should be applied to any inflow simulations for this group. The Worth Valley WRPM group and the rivers Wharfe, Derwent and Ouse show an overestimation of flow. Multiplicative factors of 0.91, 0.93, 0.93 and 0.87 respectively should be applied. Other WRPM groups show under or overestimation in either the validation or the calibration stages. As these are less than 10 percent, they will be ignored.

An improvement in calibration was attempted for the Winscar reservoir inflows by using the whole 26-yr period for model calibration. However, this did not improve the CE statistic and since the validation water balance is almost exact, the previously fitted model will be used. The calibrated parameter values for the fourteen WRPM inflows can be found in Table 6-12. The calibration and validation of the river catchments of the Wharfe, Ouse and Derwent are shown in Figures 6-18, 6-19 and 6-20 respectively. It can be observed that all show an underestimation of high flows. An example of the monthly calibration and validation of a reservoired catchment is shown in Figure 6-21 using the Washburn group.

WRPM Group	W_m	b	D_1	D_2	Conv	Diff
Washburn	229.17	0.94	0.37	5.42	2.40	6315.22
Winscar	799.74	0.76	0.02	2.00	2.61	5186.26
Pennine	216.35	1.86	0.16	3.80	2.78	4115.47
Nidd/Barden	599.95	3.83	0.10	19.99	1.00	2665.79
Grimwith	174.29	2.42	0.10	8.02	3.21	7726.29
Worth Valley	298.98	1.02	0.10	5.64	3.45	4735.69
Calderdale	193.85	1.60	0.10	5.42	3.75	8196.14
Boothwood	256.89	1.20	0.10	10.27	3.82	3724.52
Huddersfield	153.65	1.19	0.10	19.99	3.74	4673.10
Brownhill	50.14	0.70	9.92	4.29	3.81	6039.45
Wharfe	119.13	0.01	1.10	3.90	1.00	3158.27
Ouse	337.45	0.00	0.74	7.91	1.04	7147.12
Derwent	302.12	0.00	0.17	4.50	3.29	5059.54
Hull	–	–	–	–	–	–

Table 6-12: Calibrated ADM model parameter values for the 14 WRPM model inflows.

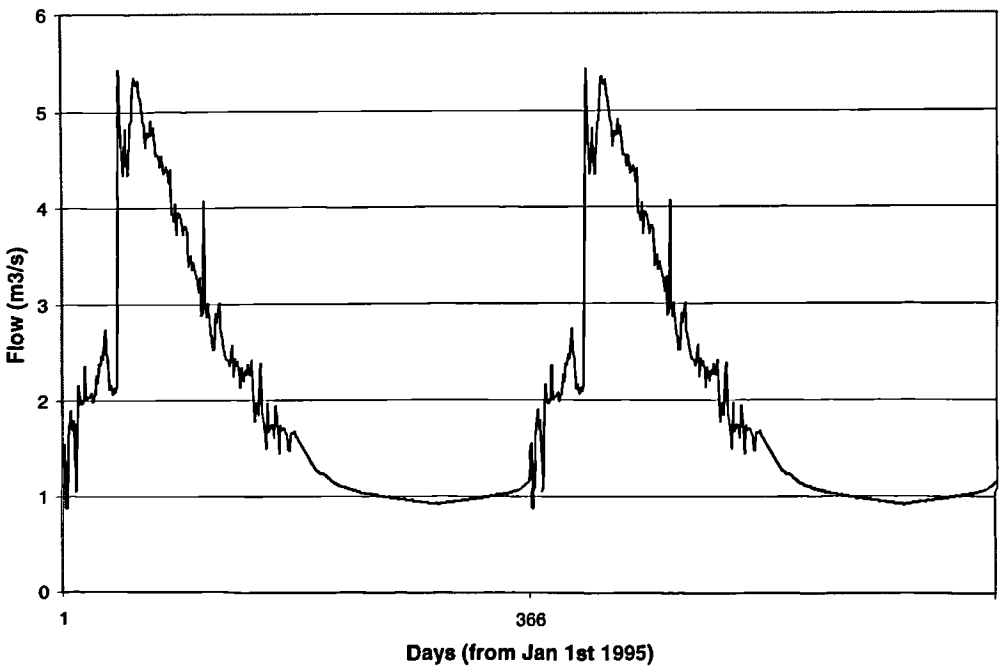

Figure 6-17: Daily flow measurements at Hempholme, River Hull for January 1st 1995 to December 31st 1996.

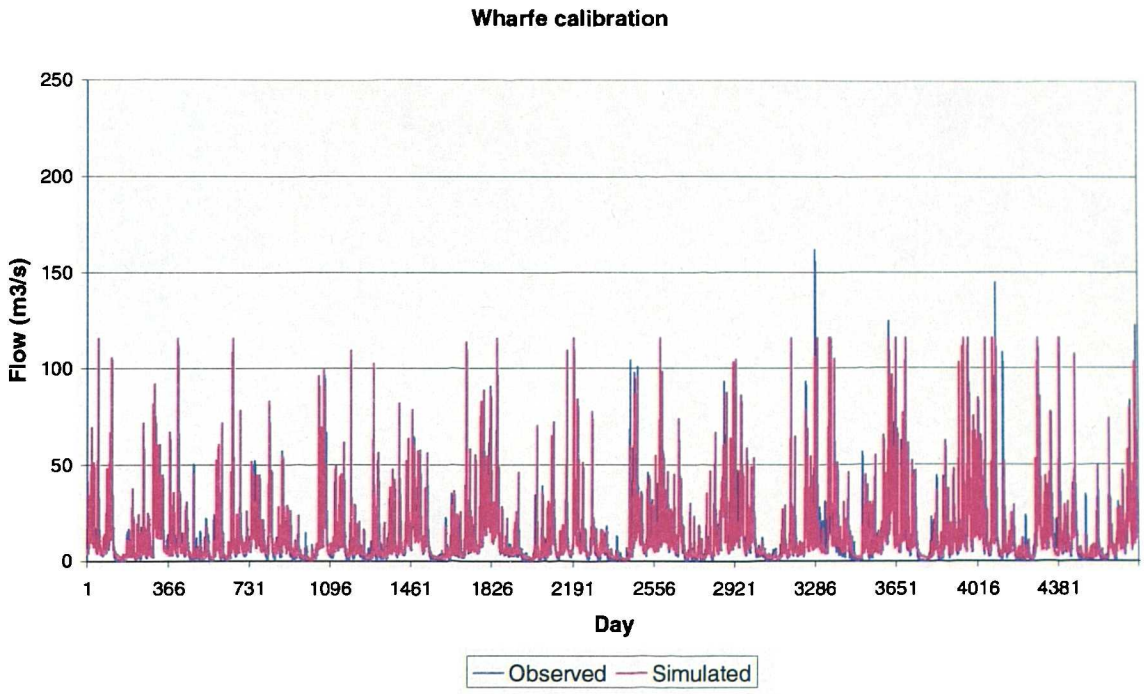

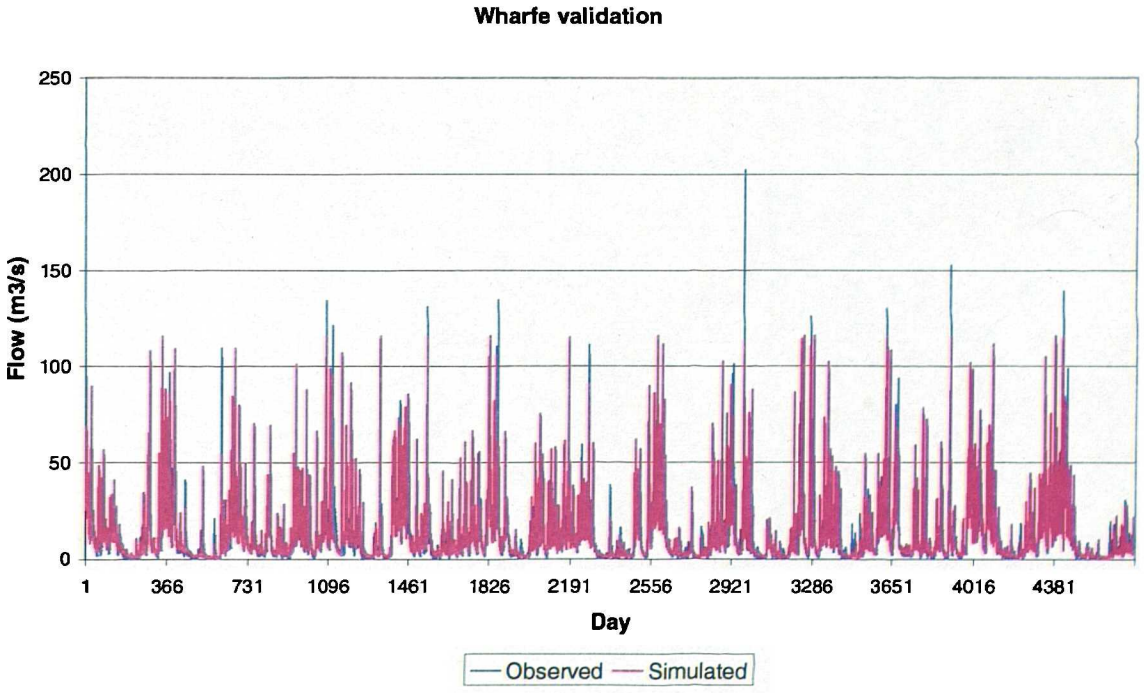

Figure 6-18: The River Wharfe calibration and validation sequences showing observed and simulated daily flows.

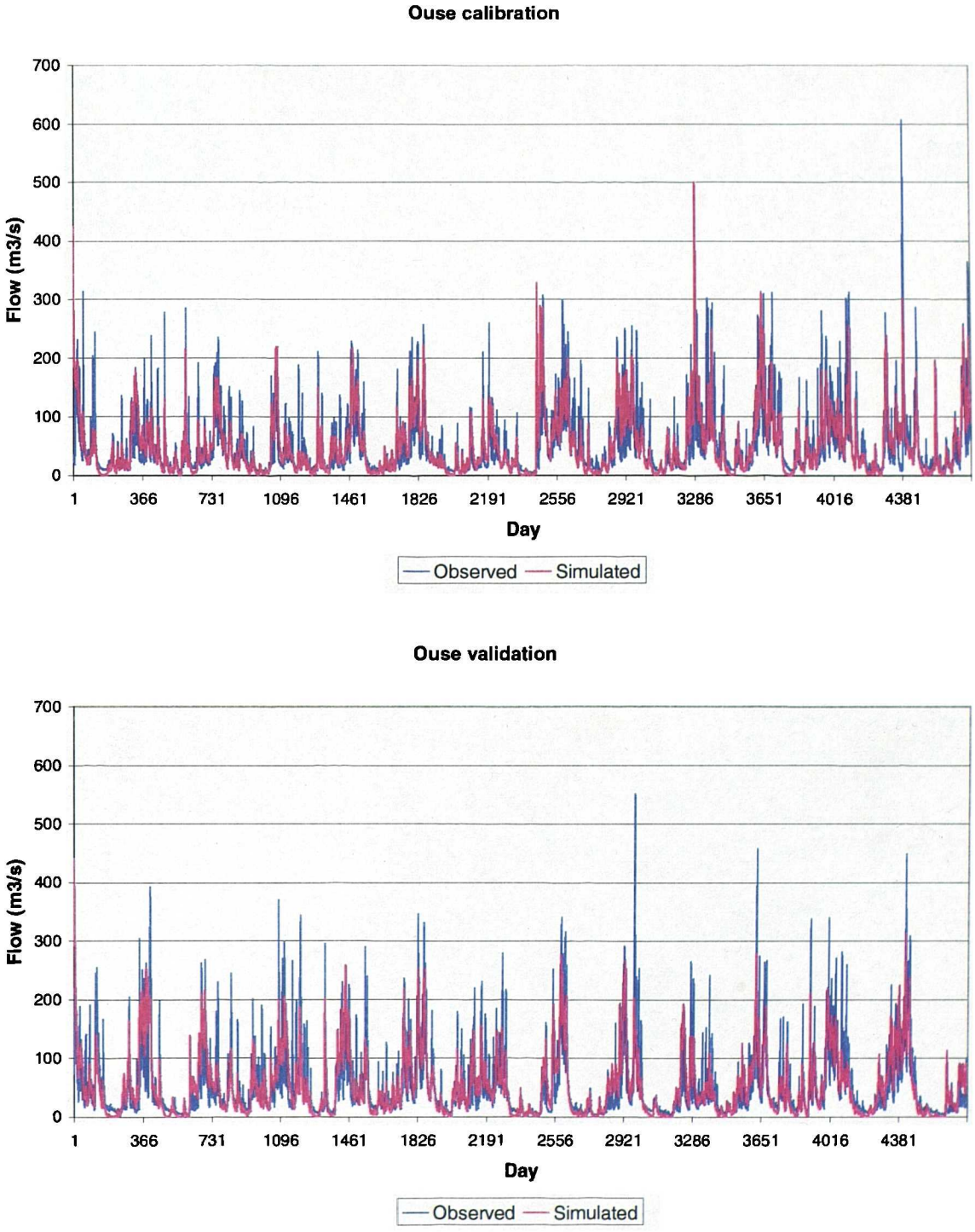

Figure 6-19: The River Ouse calibration and validation sequences showing observed and simulated daily flows.

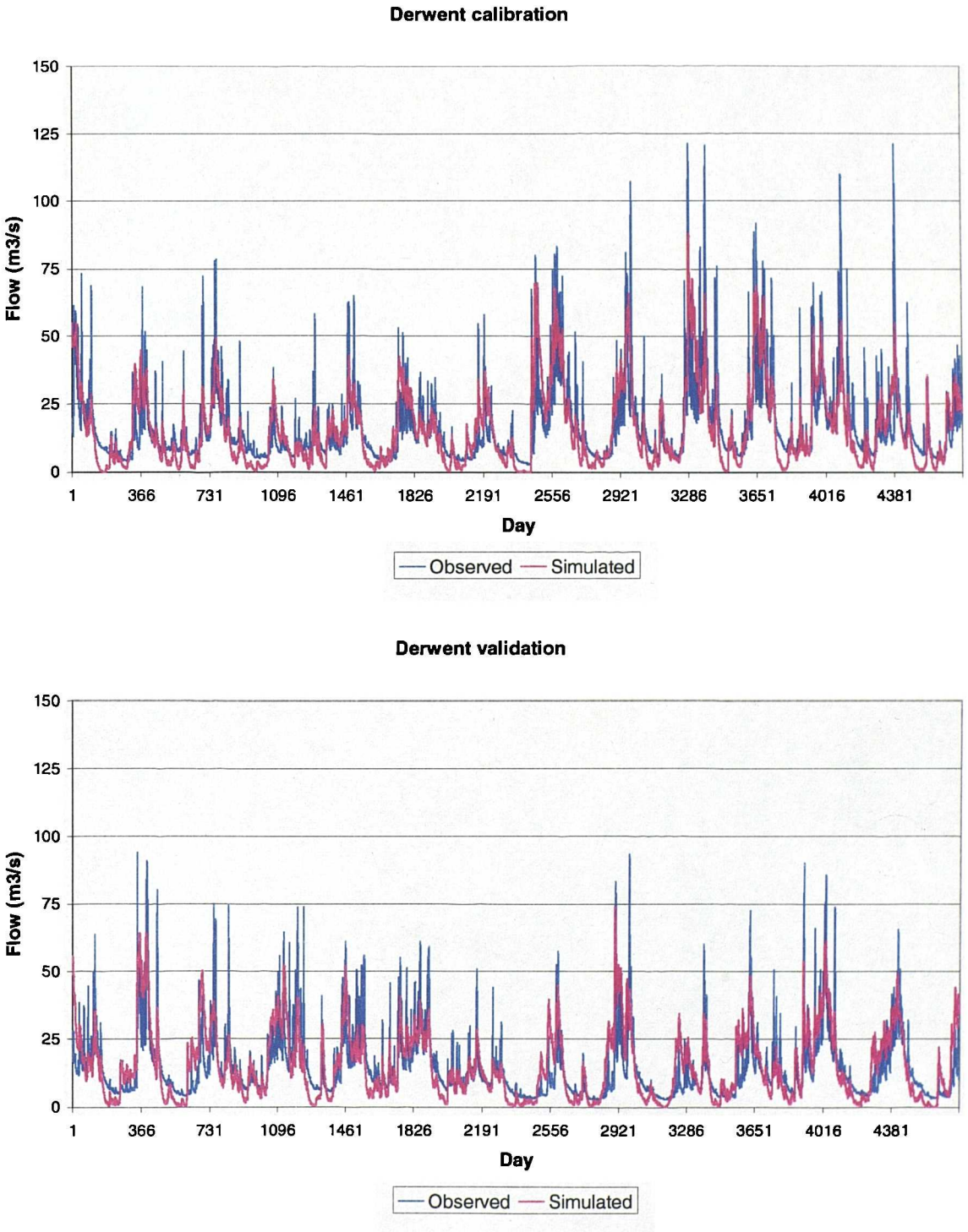

Figure 6-20: The River Derwent calibration and validation sequences showing observed and simulated daily flows.

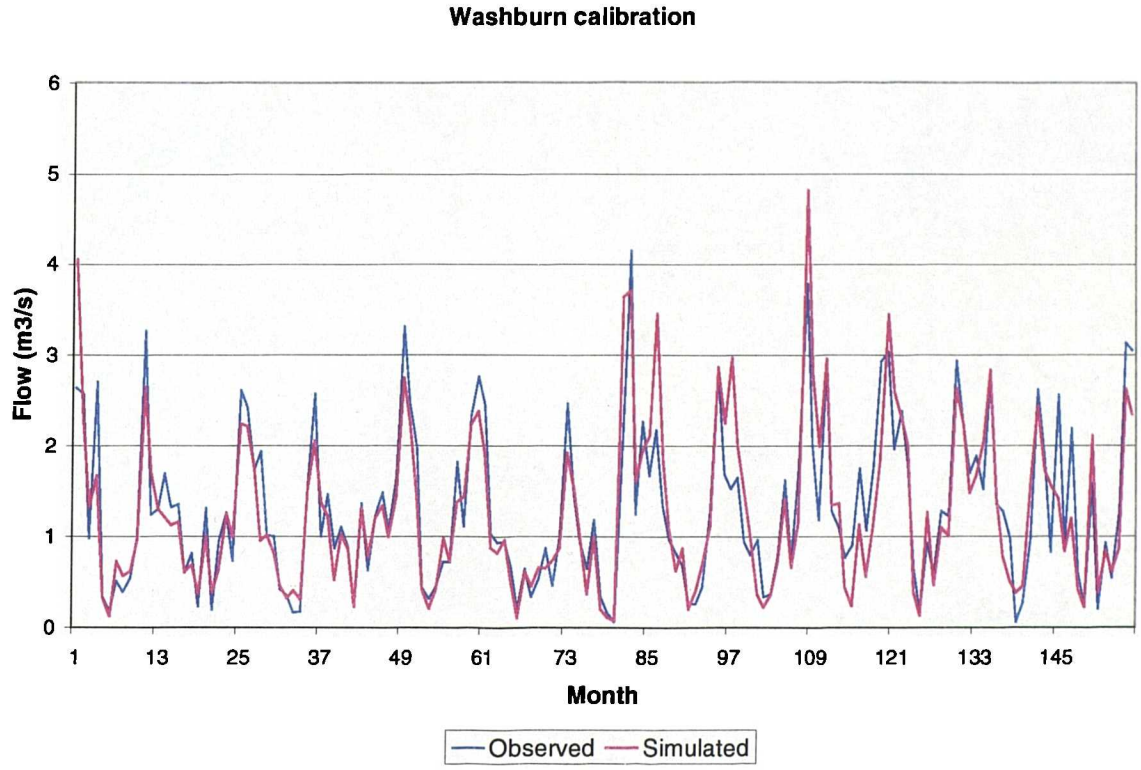

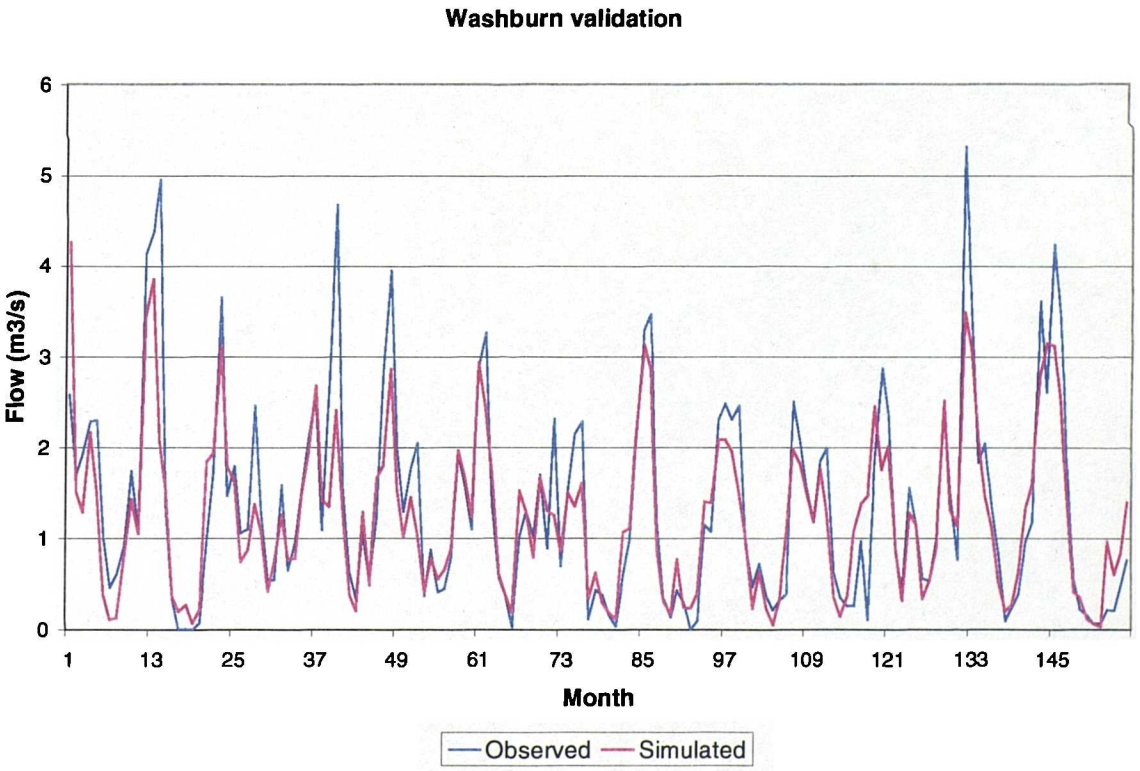

Figure 6-21: The Washburn reservoir group calibration and validation sequences showing observed and simulated monthly flows.

Chapter 7: Risk analysis of the Yorkshire Grid: natural climatic variability and future climatic change

"The question that appears important in this context...is whether the sensitivity of the water resource system to such climate variations is so small that it can be included in the modelling error, and the water system so robust that it will not even feel it, or is it large enough to be taken into account?"

(Nemec and Schaake 1982)

This chapter details the construction of a baseline 1961-1990 and various future climate change scenarios. The UKCIP98 Medium-High climate change scenario is used for the construction of scenarios for 2021-2050 and 2051-2080. The impacts of natural climatic variability are also considered using the example of the NAO. The scenarios do not consider changes to demand.

7.1 Methodology

7.1.1 Production of synthetic weather state and precipitation series

For each of the defined baseline and climate change scenarios, a 1000-yr weather state series was generated using the semi-Markov chain model detailed in Section 5.3. The parameters used for series generation depend upon the scenario adopted. Each weather state series was then adjusted by the site seasonalities required for the eastern and western NSRP models. Hence, for the western model the SW weather states in the month of September were replaced by WW weather states. In the eastern model, the northerly weather types were adjusted so that the SN weather state occurs from January to June, and thereafter the WN weather state.

Fifty 1000-yr daily simulations of precipitation were then generated using the eastern and western spatial NSRP models, using the same weather state series as input for each. These were totalled to give monthly precipitation series. The correlation between the eastern and western monthly precipitation series was then determined for each of the fifty series, giving 2500 possible cross-correlations between Moorland Cottage and Lockwood Reservoir. In Section 5.4.3.7 the historical monthly and annual cross-correlation for precipitation totals at Moorland Cottage (western model) and Lockwood Reservoir (eastern model) were determined as 0.21 and 0.24 respectively. To preserve this historical cross-correlation it was necessary to divide the precipitation series into shorter sections.

In this procedure, there is a trade-off between maximisation of the cross-correlation statistic, and reproduction of the correct precipitation statistics over the 1000-yr series. This is shown by Figure 7-1. A 10-yr section enables the reproduction of a higher cross-correlation statistic than a 50-yr section. To ensure coherence with historical records however, a section length must be chosen that does not compromise the model reproduction of average observed statistics. It is useful therefore, to maximise the length of section while still producing an accurate monthly cross-correlation between Moorland Cottage and Lockwood Reservoir. A 50-year section was found to give monthly cross-correlation statistics between 0.1 and 0.2 for Moorland Cottage and Lockwood Reservoir and this is the maximum section length that could reproduce the correct cross-correlation. The use of shorter time-periods may compromise the model, as years with a greater proportion of dry days may show a higher cross-correlation. This will bias any precipitation series thus produced. The current methodology does not produce a bias and this was checked by the production of mean statistics for the two sites.

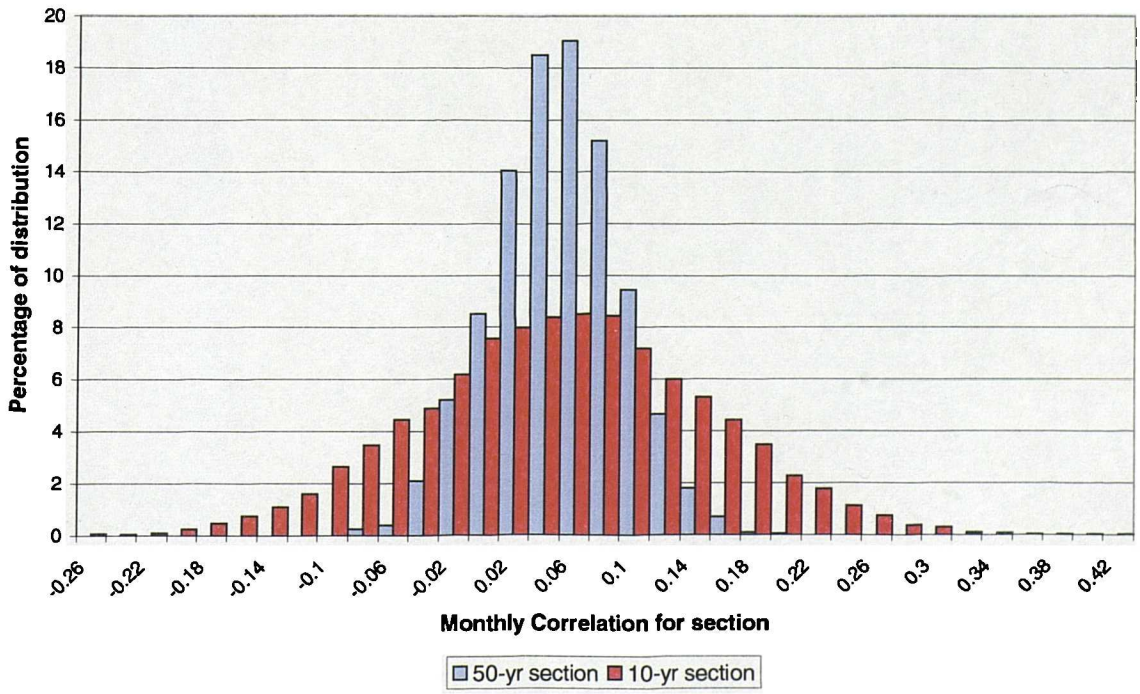

Figure 7-1: Comparison of distribution of the monthly correlations for 10-yr and 50-yr sections.

Therefore, for each 50-yr section, *k*, the model simulation was chosen that maximised the monthly cross-correlation between the two sites, generally between 0.1 and 0.2. This produced two 20-value time-series that define which of the fifty daily precipitation simulations should be used for each 50-year section of the 1000-yr series for the eastern and western model respectively. This is shown in Figure 7-2. The fifty precipitation time series for Lockwood Reservoir are denoted by *i*, and the fifty precipitation time series for Moorland Cottage are

denoted by *j*. Each 50-yr section is denoted by *k*. The box in Figure 7-2 gives an example of the precipitation series *i* and *j* that define the highest cross-correlation for each 50-yr section, *k*. For each *k*, thus, an *i* and *j* are defined.

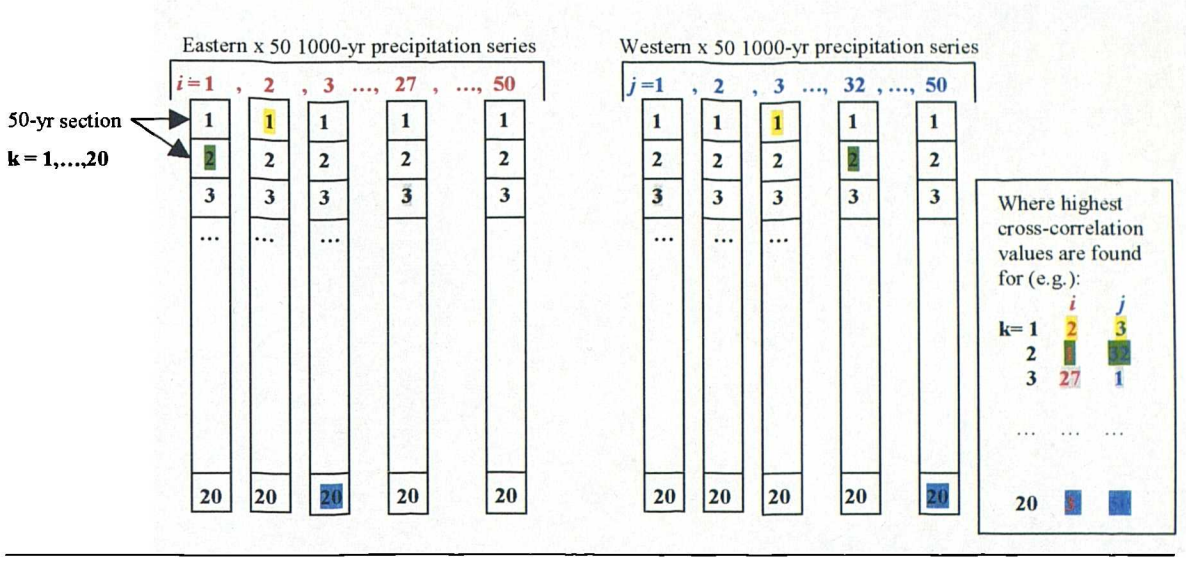

Figure 7-2: Methodology of precipitation series production.

The defined sections were then used to produce a single 1000-yr daily precipitation series for each of the 19 sites in the western model and the 9 sites in the eastern model site. This procedure retains accurate cross-correlation properties between the two models. These daily precipitation series were then rescaled using the scale factors detailed in Section 5.5 for each site, based on the daily weather state series. Finally, the mean annual expected and simulated totals were compared for sites in the eastern and western NSRP models. Winter precipitation at sites where this difference was found to be in excess of one percent were adjusted using the methodology detailed in Section 5.5.3.

7.1.2 Production of daily PE time-series

An analysis was made of the relationship between PE and precipitation in Yorkshire to allow a synthetic 1000-yr daily PE series to be generated. Rather than using the 1961-1990 long-term average for the 1000-yr PE series, it is intended that the PE will be based upon the synthetic precipitation series. The Yorkshire drought of 1995 was caused by a summer precipitation deficit, but also high PE. There is of course a natural correlation between high PE and rainfall deficit. It is likely therefore, that a strong relationship exists between summer precipitation totals and PE.

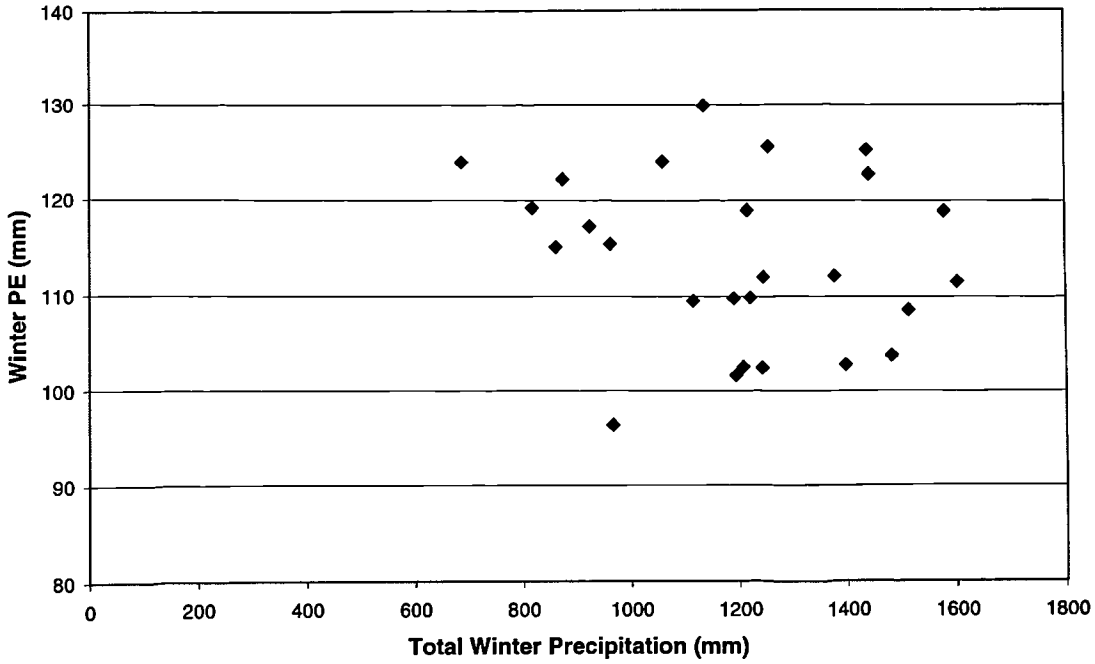

Figure 7-3: The relationship between winter precipitation and winter PE for the western spatial NSRP model.

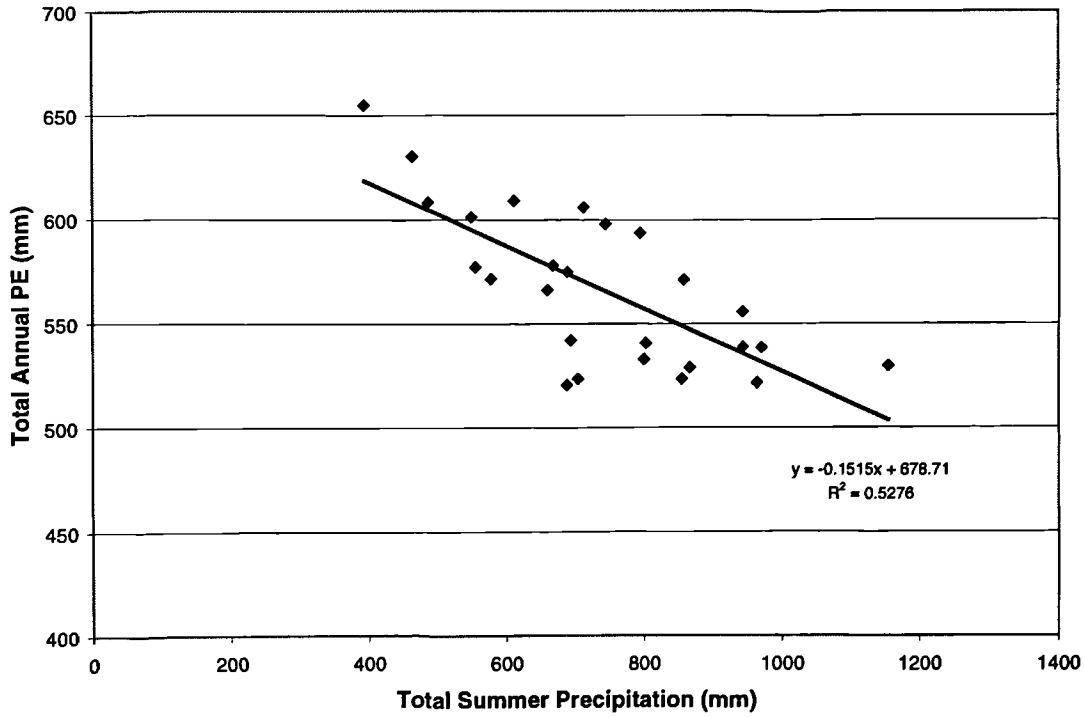

Figure 7-4: The relationship between summer precipitation and annual PE for the Wharfe PE series in the western spatial NSRP model.

Regressions relationships were determined between winter and summer PE and precipitation totals over the period 1961-1990, using the sites of Moorland Cottage and Lockwood Reservoir

that were also used in the cross-correlation analysis. The previously derived Derwent PE series was compared with precipitation data from Lockwood Reservoir for the eastern model. The WRINCLE PE series that correspond to MORECS grid squares 92 and 98, and the Wharfe and Ouse PE series were compared with precipitation data from Moorland Cottage for the western model. For the following analysis, summer is defined as April to September, and winter as October to March.

It can be observed in Figure 7-3 that winter PE in the western model has a small range, from 100 to 140 mm per year, and is not dependent upon winter precipitation totals. However, if an analysis is made of annual PE and summer precipitation at Moorland Cottage, a strong relationship is found for all PE grid squares in the western region. Figure 7-4 shows this relationship for the Wharfe PE series.

The other PE grid squares used by the western model also show strong relationships with precipitation at Moorland Cottage. These are given in the regression relationships (Equations 7-1 to 7-4) for the WRINCLE grid squares that correspond to MORECS 92 and 98, and the Wharfe and Ouse PE series. These relate summer precipitation totals to annual PE. It can be observed that all four equations are very similar, showing the coherency of the region.

WRINCLE92	$PE = -0.147\,ppt + 681.68$	$R^2 = 0.54$	(7-1)
WRINCLE98	$PE = -0.158\,ppt + 673.72$	$R^2 = 0.52$	(7-2)
Wharfe	$PE = -0.152\,ppt + 678.71$	$R^2 = 0.52$	(7-3)
Ouse	$PE = -0.152\,ppt + 680.56$	$R^2 = 0.53$	(7-4)

These equations will be applied to the synthetically generated precipitation series to produce annual PE series. These will then be disaggregated into monthly proportions using a sinusoidal relationship based on average historical proportions from 1961-90. Figure 7-5 gives an example of the monthly PE totals for the Wharfe PE series from 1970-1975.

For the eastern model, a comparison was made of the Derwent PE series and precipitation at Lockwood Reservoir. It can be observed in Figure 7-6 that a much stronger relationship is apparent between winter precipitation and winter PE for the Derwent PE series than for any of the western model PE series. However, in summer the relationship is reduced (see Figure 7-7).

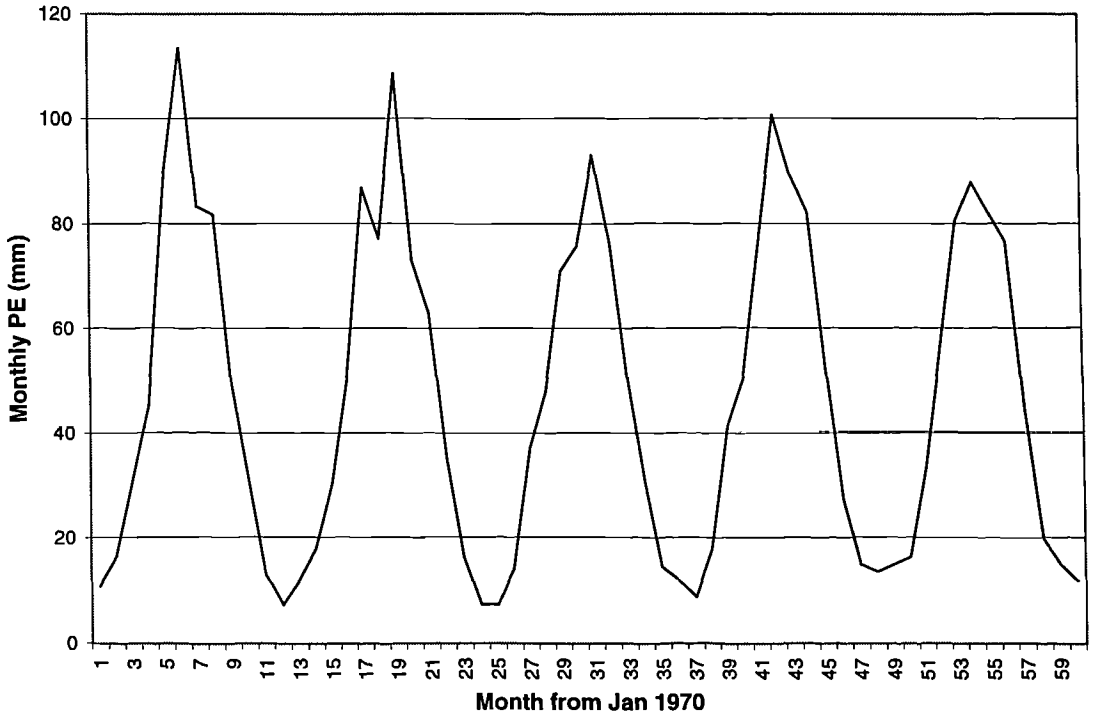

Figure 7-5: Monthly PE for the Wharfe series from 1970-1975.

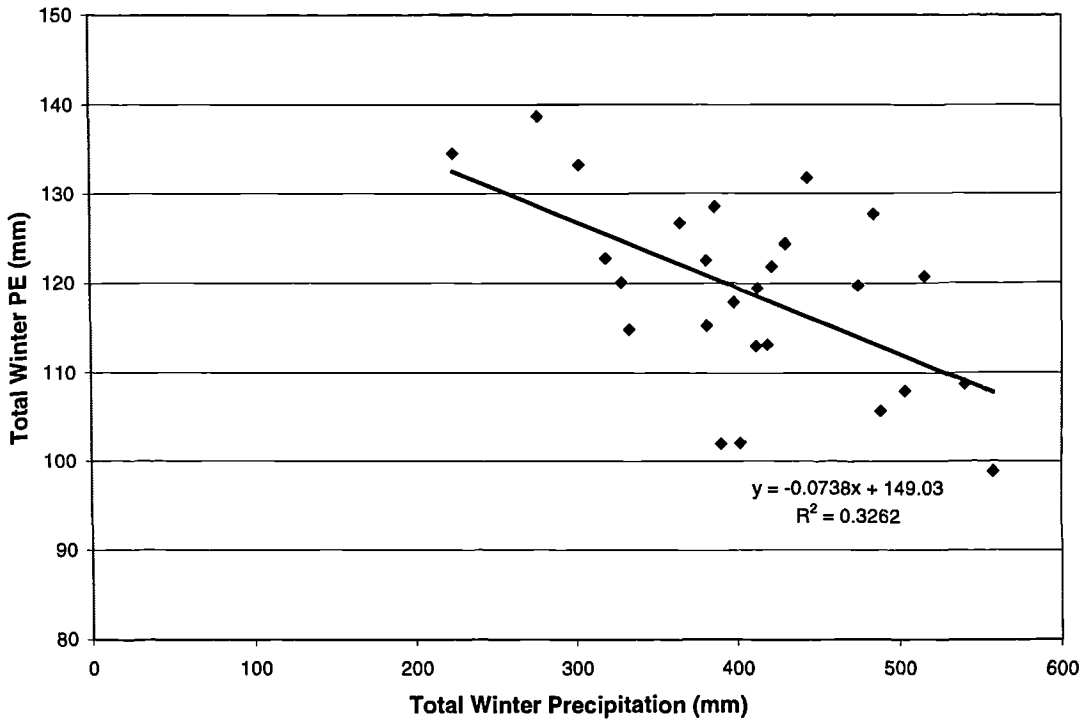

Figure 7-6: The relationship between winter precipitation and winter PE for the eastern spatial NSRP model.

The regression relationships for both winter and summer PE prediction from precipitation have very low R^2 values and are fairly insignificant. However, a rough approximation to annual PE can be made by using the following equation relating summer precipitation and annual PE totals (Equation 7-5) and then using a sinusoidal relationship to disaggregate monthly totals:

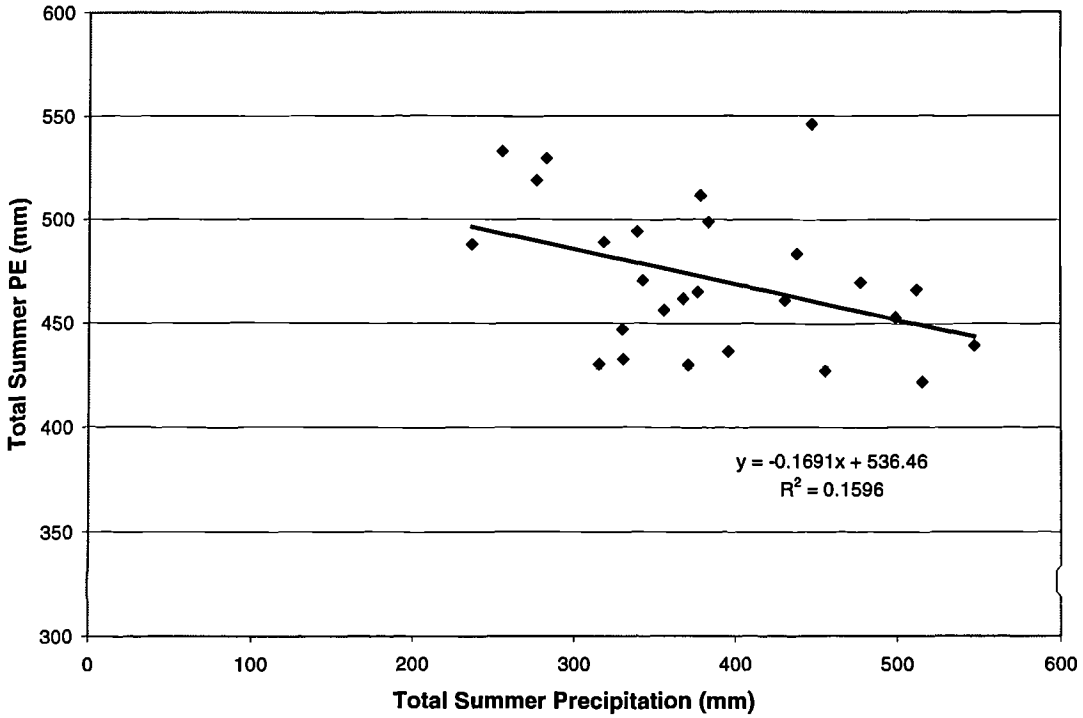

Figure 7-7: The relationship between summer precipitation and summer PE for the eastern spatial NSRP model.

Derwent $PET = -0.197\,ppt + 666.21$ $R^2 = 0.21$ (7-5)

The sinusoidal relationship used to disaggregate monthly totals from annual PE was based upon the 1961-1990 mean percentage of annual PE found in each month. The monthly factors used can be found in Table 7-1.

Month	Percentage of annual total PE
J	2.0
F	2.9
M	6.1
A	9.4
M	14.4
J	15.9
J	17.0
A	14.3
S	8.9
O	4.9
N	2.5
D	1.7

Table 7-1: Monthly disaggregation factors applied to annual PE.

7.1.3 Production of inflow time-series

The precipitation series generated by the methodology detailed in Section 7.1.1 were then used as input to the rainfall-runoff models previously calibrated in Chapter 6. The appropriate PE time-series for each climate change scenario were also used as input. This generated 13 1000-yr inflow series for each scenario. These series were then rescaled using the scale factors detailed in Section 6.4 if appropriate. Therefore, rescaling was applied to the series for the rivers Wharfe, Ouse and Derwent, and the reservoir groups at Worth Valley and Brownhill. These inflows were then used as input to the YGrid2000 model.

7.1.4 Measuring system sustainability (RRV)

Sustainability indices are defined as system performance criteria. These are summarised as statistical measures of *reliability*, *resilience* and *vulnerability* (RRV) (Hashimoto *et al.*, 1982*a*,*b*). The relative sustainability of the system can be measured as a weighted combination of these values. The higher the system sustainability, the greater the reliability and resilience, and lower the vulnerability criteria.

For a water resource system, a criterion, C, must be defined using reservoir storage or river flow for example, where water supplies from that source may be restricted (ASCE, 1998). These are defined in the form of reservoir control curves for reservoir sources, or abstraction limits for river sources. A time series of values, X_t, from a simulation study can be evaluated, where the simulated time periods, t, extend to some future time, T. The range of values that are considered satisfactory must be defined. Values below this critical value are considered unsatisfactory. Each water supply source will have own range of satisfactory, S, and unsatisfactory, U, values defined by the criterion, C (Equation 7-6):

$$\begin{array}{llllll} \text{If} & X_t \geq C & \text{then} & X_t \in S & \text{and} & Z_t = 1 \\ & & \text{Else} & X_t \in U & \text{and} & Z_t = 0 \end{array} \qquad (7\text{-}6)$$

If another indicator is defined, W_t, that indicates a transition from a unsatisfactory to an satisfactory state, then (7-7):

$$W_t = \begin{cases} 1, & \text{if } X_t \in U \text{ and } X_{t+1} \in S \\ 0, & \text{otherwise} \end{cases} \qquad (7\text{-}7)$$

If the periods of unsatisfactory X_t are then defined as $J_1, J_2, \ldots, J_N$ then *reliability*, *resilience* and *vulnerability* can thus be defined (Equations 7-8 to 7-10):

Reliability: $$C_R = \frac{\sum_{t=1}^{T} Z_t}{T} \quad (7\text{-}8)$$

Resilience: $$C_{RS} = \frac{\sum_{t=1}^{T} W_t}{T - \sum_{t=1}^{T} Z_t} \quad (7\text{-}9)$$

Vulnerability: $$C_V = max\left\{\sum_{t \in J_i} C - X_t, \quad i = 1,\ldots,N\right\} \quad (7\text{-}10)$$

Reliability, C_R, is defined as the number of satisfactory, $X_t \in S$, values divided by the total number of simulated periods, T. It is the probability that any X_t value will be within the range of the values considered satisfactory. *Resilience*, C_{RS}, is the number of times that a satisfactory value ($X_{t+1} \in S$) follows an unsatisfactory value ($X_t \in U$), divided by the total number of unsatisfactory values. It is an indication of the speed of recovery of the system from a failure or unsatisfactory condition. *Vulnerability*, C_V, is a statistical measure of the extent of failure and is the maximum cumulative amount of a failure, $X_t \in U$, in the case of either reservoir control curves or river abstraction limits.

The extent of failure of any criterion can be defined in a number of ways. In the case of a water resource system, it is useful to define a conjunctive use element (Wood *et al.*, 1997; Lettenmaier *et al.*, 1999). The *reliability*, *resilience* and *vulnerability* of water sources within a system can be determined on an individual basis, but shortages in supply may only occur when concurrent shortfalls occur at more than one source. Therefore, concurrent failure at more than one source must be considered.

For the baseline and future climate change scenarios, the *reliability*, *resilience* and *vulnerability* of sources and demands will be examined. For demands, the *vulnerability* will be quantified as both the maximum duration of failure in days, and the cumulative maximum extent of failure in Ml. The maximum cumulative duration and extent of failure of the grid will also be considered. Failure is defined as the failure of any one demand to be adequately supplied. For sources,

vulnerability is defined as the minimum storage of the reservoir. For river sources, only the *reliability* of the source will be assessed. The conjunctive failure of demands within the system will also be assessed.

In addition, the likelihood of occurrence of a drought as severe in extent as the 1995-96 Yorkshire drought will be examined. If an assessment is made of the duration of failure of water supplies during the 1995-96 drought using historical inflows generated by Mott MacDonald (1996; 1997), a failure of some 148 days is observed. A return period for this severity of drought will be produced for each climate change scenario, assuming a severity exceeding 147 days.

7.1.5 The YGrid2000 model

The complex and awkward style of the YG97 model precludes its use for the study of long inflow data series. The current EA model produces an output data file for each year of analysis, and is set up for analysis of only 49 years of data. Therefore, a simpler version of the YG97 model was written in Fortran.

This contains the same reservoir control rules (Table 7-2) and river abstraction limits (Table 7-3) as the YG97 model. It also contains constraints based on pipe-link sizes between sources (see Figure 2-9 for a full explanation). The main differences between this model YGrid2000 and the YG97 model are:

- The omission of the Hull demand; Hull is assumed to be solely supplied by the River Hull and the Hull and Wolds boreholes.
- The exclusion of the Selby demand; Selby is assumed to be solely supplied by the Selby boreholes, with an excess outflow of 5 Ml d^{-1} to the grid.
- The Ouse source is split into low and high priority. High priority is given to the demand zones of Sheffield, Doncaster and Wakefield. Any excess flow can then be used by the rest of the grid.

Reservoir	Max Capacity Ml d^{-1}	J Ml d^{-1}	F Ml d^{-1}	M Ml d^{-1}	A Ml d^{-1}	M Ml d^{-1}	J Ml d^{-1}	J Ml d^{-1}	A Ml d^{-1}	S Ml d^{-1}	O Ml d^{-1}	N Ml d^{-1}	D Ml d^{-1}	Allowable abstraction Ml d^{-1}	Compensation Ml d^{-1}
Washburn	23373	5750	9410	12940	14260	13220	10580	9210	7970	6420	5090	5090	5530	195.0	0.00
		2540	2540	2540	2540	2540	2540	2540	2540	2540	2540	2540	2540	175.0	0.00
Winscar	9390	2880	3940	3920	3910	3900	3440	3240	2700	2000	1900	2350	2540	15.3	12.00
		650	650	650	650	650	650	650	650	650	650	650	650	13.8	8.00
Pennine	35695	11988	21356	24032	24398	24587	24164	21318	17365	13655	10757	9546	9955	169.0	76.00
		4447	4447	4447	4447	4447	4447	4447	4447	4447	4447	4447	4447	152.1	50.90
Nidd/Barden	19178	8330	9170	12930	13110	11160	10480	8380	7690	6670	4440	4410	5020	107.1	0.00
		2200	2200	2200	2200	2200	2200	2200	2200	2200	2200	2200	2200	96.4	0.00
Grimwith	21764	8380	12140	16190	18070	16150	13100	10810	10060	8740	5580	5210	8370	113.6	0.00
		2000	2000	2000	2000	2000	2000	2000	2000	2000	2000	2000	2000	100.0	0.00
Worth Valley	3312	1180	2160	2230	2310	2400	2240	1960	1740	1310	980	950	950	20.6	0.88
		430	430	430	430	430	430	430	430	430	430	430	430	18.5	0.60
Calderdale	11694	3335	4332	4481	4933	5326	5398	5334	4607	4116	3675	3425	2705	40.7	25.27
		1400	1400	1400	1400	1400	1400	1400	1400	1400	1400	1400	1400	36.6	16.90
Boothwood	11499	5430	7940	8070	8200	8330	6890	6310	5400	5050	4700	4350	3930	27.7	27.46
		1228	1228	1228	1228	1228	1228	1228	1228	1228	1228	1228	1228	24.9	18.40
Huddersfield	14123	3680	6110	6270	6430	8390	7490	7000	6110	4430	3500	3500	3500	45.9	28.35
		1748	1748	1748	1748	1748	1748	1748	1748	1748	1748	1748	1748	41.3	19.00
Brownhill	5928	1460	1860	2370	2530	3120	3320	3130	2690	2040	1460	1460	1460	17.6	14.27
		726	726	726	726	726	726	726	726	726	726	726	726	15.8	9.60

Table 7-2: Reservoir control rules; allowable abstraction rate above given level for given month.

River	Control Rule A			Control Rule B			Control Rule C		
	Flow	Supply	Compen-sation	Flow	Supply	Compen-sation	Flow	Supply	Compen-sation
	Ml d^{-1}	Ml d^{-1}	Ml d^{-1}	Ml d^{-1}	Ml d^{-1}	Ml d^{-1}	Ml d^{-1}	Ml d^{-1}	Ml d^{-1}
Wharfe	469.0	127.2	0.0	379.0	113.6	0.0	242.0	31.8	0.0
Ouse	1120.0	294.0	0.0	726.0	144.0	0.0	68.0	68.0	0.0
Derwent	10.0	305.0	0.0						

Table 7-3: River abstraction rates; allowable abstraction rate above given level, and compensation flows.

	Skipton Ml d^{-1}	Bradford Ml d^{-1}	Calder Ml d^{-1}	Harrogate Ml d^{-1}	Malton Ml d^{-1}	Leeds Ml d^{-1}	Wakefield Ml d^{-1}	Selby Ml d^{-1}	Doncaster Ml d^{-1}	Sheffield Ml d^{-1}
J	16.0	175.0	189.0	36.0	8.0	210.0	87.0	44.0	94.0	313.0
F	16.2	176.8	190.9	36.4	8.1	212.1	87.9	44.4	94.9	316.1
M	16.3	178.5	192.8	36.7	8.2	214.2	88.7	44.9	95.9	319.3
A	15.8	173.3	187.1	35.6	7.9	207.9	86.1	43.6	93.1	309.9
M	15.9	174.1	188.1	35.8	8.0	209.0	86.6	43.8	93.5	311.4
J	16.2	176.8	190.9	36.4	8.1	212.1	87.9	44.4	94.9	316.1
J	16.9	184.6	199.4	38.0	8.4	221.6	91.8	46.4	99.2	330.2
A	15.8	172.4	186.2	35.5	7.9	206.9	85.7	43.3	92.6	308.3
S	15.6	170.6	184.3	35.1	7.8	204.8	84.8	42.9	91.7	305.2
O	15.7	171.5	185.2	35.3	7.8	205.8	85.3	43.1	92.1	306.7
N	15.8	173.3	187.1	35.6	7.9	207.9	86.1	43.6	93.1	309.9
D	15.8	173.3	187.1	35.6	7.9	207.9	86.1	43.6	93.1	309.9

Table 7-4: Daily demands for urban centres within the Yorkshire water supply grid.

	Skipton Ml d^{-1}	Bradford Ml d^{-1}	Calder Ml d^{-1}	Harrogate Ml d^{-1}	Malton Ml d^{-1}	Leeds Ml d^{-1}	Wakefield Ml d^{-1}	Doncaster Ml d^{-1}	Sheffield Ml d^{-1}	Total Ml d^{-1}
J	16.0	175.0	189.0	1.0	8.0	203.0	87.0	4.0	273.0	956
F	16.2	176.8	190.9	1.4	8.1	205.1	87.9	4.9	276.1	967.4
M	16.3	178.5	192.8	1.7	8.2	207.2	88.7	5.9	279.3	978.6
A	15.8	173.3	187.1	0.6	7.9	200.9	86.1	3.1	269.9	944.7
M	15.9	174.1	188.1	0.8	8.0	202.0	86.6	3.5	271.4	950.4
J	16.2	176.8	190.9	1.4	8.1	205.1	87.9	4.9	276.1	967.4
J	16.9	184.6	199.4	3.0	8.4	214.6	91.8	9.2	290.2	1018.1
A	15.8	172.4	186.2	0.5	7.9	199.9	85.7	2.6	268.3	939.3
S	15.6	170.6	184.3	0.1	7.8	197.8	84.8	1.7	265.2	927.9
O	15.7	171.5	185.2	0.3	7.8	198.8	85.3	2.1	266.7	933.4
N	15.8	173.3	187.1	0.6	7.9	200.9	86.1	3.1	269.9	944.7
D	15.8	173.3	187.1	0.6	7.9	200.9	86.1	3.1	269.9	944.7

Table 7-5: Adjusted daily demands for urban centres within the Yorkshire water supply grid used within the YGrid2000 model.

The water supply demand in Ml d^{-1} for the nine urban areas is shown in Table 7-4. For Sheffield, the demand has been reduced by 40 Ml d^{-1} due to the constant source from Ladybower reservoir. The Doncaster demand has similarly been reduced by 45 Ml d^{-1} and 40 Ml d^{-1} for the supplies from the Doncaster and Nutwell boreholes respectively. An additional 5 Ml

d^{-1} is assumed to be supplied by the Selby boreholes. The Harrogate reservoir supply is treated as a constant supply to Harrogate of 35 Ml d^{-1}, as no data on this source is available. The Leeds demand is reduced by 7 Ml d^{-1} from the Angram borehole source. These sources can be seen in Figure 2-9. The adjusted demands used in the model are therefore shown in Table 7-5. It can be seen that the total demand is at a minimum in October at 927.9 Ml d^{-1}, and at a maximum in July, at 1018 Ml d^{-1}.

Source	Demand priorities
Wharfe	Bradford, Leeds, Calder, Wakefield
Ouse	Malton, Sheffield, Doncaster, Wakefield, Leeds, Bradford, Calder
Derwent	Sheffield, Doncaster, Wakefield
Grimwith	Bradford, Calder, Wakefield
Nidd/Barden	Skipton, Bradford, Calder, Wakefield
Calderdale	Calder, Wakefield
Winscar	Wakefield, Calder
Pennine	Sheffield
Washburn	Harrogate, Leeds, Bradford, Calder, Wakefield
Boothwood	Wakefield, Calder
Worth Valley	Bradford, Calder, Wakefield
Huddersfield	Calder
Brownhill	Calder

Table 7-6: Source priorities used within the YGrid2000 model, based upon those of Ribas (1994).

The same priorities for water supply are used as in the YG97 model. These are detailed by Ribas (1994) and the Environment Agency priorities are used, as they provide a more robust operating system than those used by Yorkshire Water prior to the 1995 drought. These are detailed in Table 7-6 and Table 7-7.

Demands	Source priority
Bradford	Wharfe, Worth Valley, Nidd/Barden, Grimwith
Leeds	Ouse, Washburn, Harrogate, Wharfe, Derwent
Harrogate	Harrogate, Washburn
Malton	Ouse
Doncaster	Doncaster boreholes, Selby boreholes, Derwent
Calder	Calderdale, Wharfe, Nidd/Barden, Grimwith, Ouse, Washburn, Brownhill, Huddersfield, Winscar, Boothwood
Sheffield	Ladybower transfer, Pennine, Derwent, Ouse
Wakefield	Derwent, Ouse, Boothwood, Winscar, Wharfe, Grimwith, Nidd/Barden
Skipton	Nidd/Barden

Table 7-7: Demand priorities used within the YGrid2000 model, based upon those of Ribas (1994).

The model was validated internally using 1 year of data, checking demand shortfalls and inflow residuals at each step. A comparison was also made of output from the YGrid2000 and YG97 models using the historical inflows generated by Mott MacDonald (1996; 1997). The results were comparable in both duration of failure of supplies and magnitude of failure. The YGrid2000 model outputs reliability statistics for the 13 sources and 9 demand centres and, additionally, resilience and vulnerability statistics for the demands. Conjunctive failure of water supply at more than one demand centre is also considered. Reliability statistics for sources are based on three levels of failure for rivers, and two for reservoirs. These relate to control rules A, B and C in Table 7-2 for river abstractions, and control levels in Table 7-3 for reservoir levels.

7.2 1961-1990 baseline scenario

Prior to any climate change scenario analysis, it is important to set a baseline, or standard, that the future risk of failure can be set against. The period from 1961-90 is the current standard baseline in climatological study. In this study, the 1961-90 period will be used as a baseline.

7.2.1 Baseline scenario production

For the baseline scenario, the parameters detailed in Section 5.3 were used in the Markov process for the generation of a 1000-yr weather state series. The fitted parameters detailed in Section 5.5 were then used for the generation of a 1000-yr daily precipitation series for each of the 19 sites in the western spatial NSRP model and the 9 sites in the eastern spatial NSRP model, using the methodology detailed in Section 7.1.1. This produced monthly and annual correlation statistics of 0.15 and 0.20 respectively between the sites of Moorland Cottage and Lockwood Reservoir. These precipitation series were used as input to the rainfall-runoff models for the 13 required inflows. Additionally, the baseline PE series produced using Equations 7-1 to 7-5 were used as input to the appropriate models. The 13 1000-yr daily inflow series were generated and used as input to the YGrid2000 model.

Table 7-8 shows the capability of the grid to supply the nine demand centres of Skipton, Bradford, Calder, Harrogate, Malton, Leeds, Wakefield, Doncaster and Sheffield. This capability is measured in terms of the reliability, resilience and vulnerability of a meeting the water supply for a demand. The vulnerability is defined as a maximum duration of time in days that a demand cannot be met, and the maximum cumulative supply shortfall in Ml. Statistics are also given for total demand shortfalls.

Demand	Reliability	Resilience	Vulnerability	
			Duration (days)	Extent (Ml)
Skipton	1.0000	–	–	–
Bradford	0.9185	0.428	25	681.0
Calder	0.8456	0.244	97	5395.0
Harrogate	0.9390	0.701	13	44.2
Malton	0.9999	0.086	22	352.0
Leeds	0.9029	0.262	79	20930.0
Wakefield	0.8990	0.062	157	16288.4
Doncaster	0.9999	0.086	22	176.0
Sheffield	0.8906	0.047	158	17429.0
Total	0.7341	0.169	165	74562.4

Table 7-8: Baseline scenario: reliability, resilience and vulnerability statistics for demands. Total refers to failure to supply at least one demand centre.

It can be observed that only one demand does not fail at all during the 1000-yr period. Skipton is well supplied by the Nidd/Barden reservoir group. Other demands with high reliability are Malton and Doncaster. These have return periods of failure in excess of 1 in 10,000 years under present climate conditions. The resilience of the Doncaster and Malton demands is very low however. Doncaster and Malton will both suffer supply shortfalls when the flow in the Ouse is less than 68 Ml d^{-1}, and no abstractions are allowed. The low resilience is caused as low flows will tend to persist for short periods, in this case 22 days, with no recovery during this time.

Other demands fail on a more regular basis. There appear two types of failure. Some supplies fail for short periods but have a relatively high resilience and so produce smaller water supply deficits. Both the Bradford and Harrogate demand centres fit into this category. Other supplies fail for long time-periods, and have a lower resilience but larger vulnerability, particularly in terms of the extent of cumulative failure. The Sheffield, Leeds, Wakefield and Calder demand centres fit into this category.

The lowest supply reliability is to the Calder demand, supplies failing 16 percent of the time. This is closely followed by the Wakefield, Leeds and Sheffield supplies, all of which fail approximately 10 percent of the time. If the whole grid is analysed then there is a failure in supply somewhere just over 25 percent of the time. This can be as extensive as 165 consecutive days and reach a cumulative deficit of 74,562 Ml. Wakefield and Sheffield seem particularly vulnerable to long shortages. In the case of Sheffield, this is due to the reliance upon a single source, the Pennine reservoir group, to supply most of the demand. If this fails then constrictions in the system mean that even if enough water is available to meet the demand from the Rivers Derwent and Ouse, the demand would not be fully met. The supply to Wakefield is similarly affected by a pipe capacity constraint. Supplies from the Ouse and Derwent are

prioritised by Sheffield and Doncaster. If these are low then Wakefield can only be supplied via a 30 Ml d^{-1} link to the Calder supply system. If there is an excess of water in this system then it cannot be used to supply Wakefield.

The likelihood of conjunctive failure of demands is assessed in Table 7-9. The system appears to be very reliant upon supplies from the River Ouse. The highest concurrent failures all pinpoint the Ouse, and possibly the Washburn, as the cause. If the flow in the Ouse is too low to supply Malton then the supply to Wakefield, Sheffield and Doncaster will also be affected. Bradford, however, is affected by flows from the River Wharfe, and concurrent failures are likely to occur with the Calder demand centre.

	Skipton	Bradford	Calder	Harrogate	Malton	Leeds	Wakefield	Doncaster	Sheffield
Skipton	–	0.00	0.00	0.00	0.00	0.00	0.00	0.00	0.00
Bradford		–	4.01	1.14	0.00	0.00	0.00	0.00	0.39
Calder			–	5.16	0.00	9.39	8.61	0.00	6.03
Harrogate				–	0.00	4.10	2.13	0.00	2.30
Malton					–	0.00	0.01	0.01	0.01
Leeds						–	7.69	0.00	5.18
Wakefield							–	0.01	4.93
Doncaster								–	0.01
Sheffield									–

Table 7-9: Baseline scenario: likelihood of conjunctive failure of supply to demand centres, expressed as percentage of total simulation time.

	Reliability			Minimum Storage	
	1st level	2nd level	3rd level	Ml	% Maximum
Washburn	0.559	0.939	–	2365.0	10.1
Winscar	1.000	1.000	–	7133.0	76.0
Pennine	0.847	0.997	–	4295.5	12.0
Nidd/Barden	0.999	1.000	–	8401.1	43.8
Grimwith	0.985	1.000	–	5003.4	23.0
Worth Valley	0.998	1.000	–	1545.8	46.7
Calderdale	0.999	1.000	–	3926.7	33.6
Boothwood	1.000	1.000	–	6987.6	60.8
Huddersfield	1.000	1.000	–	6705.1	47.5
Brownhill	1.000	1.000	–	2723.7	45.9
Wharfe	0.929	0.903	0.924	–	–
Ouse	0.942	0.957	1.000	–	–
Derwent	1.000	–	–	–	–

Table 7-10: Baseline scenario: reliability of sources.

Table 7-10 shows source reliability, and minimum levels of reservoirs. The most vulnerable source is the Washburn reservoir group. During low flows on the rivers Ouse and Wharfe the

Leeds demands is supplied entirely using this source. It is therefore drawn down rapidly during drought events, as the Leeds demand is large. Similarly, the Pennine reservoir group is also vulnerable to drought events. During low flow events on the rivers Ouse and Derwent, the Sheffield demand is supplied using the Pennine reservoir group.

During the baseline simulation, the river Ouse never fails on the third level of reliability. Therefore, it always supplies some water to the grid. However, the Wharfe is unable to supply any water to the grid approximately 8 percent of the time. This accounts for the water shortages at the Bradford and Calder demand centres. The flow in the river Derwent never falls below the level at which any abstraction is ceased.

In terms of severity of drought, the baseline scenario suggests that the a drought as severe as the 1995-96 drought can be expected to occur 6 times in 1000 years, a 1 in 166-yr event. However, the duration of the most severe drought is 11 percent longer than any historical drought event during the period from 1948 to 1996. The Sheffield and Wakefield demand centres seem the most vulnerable to long-term drought.

7.2.2 Comparison with historical inflows

Historical daily inflows were available for the YG97 model from 1948-1996 (Mott MacDonald 1996; 1997). These were input to the YGrid2000 model and a comparison made with the 1961-1990 baseline scenario.

Demand	Reliability	Resilience	Vulnerability	
			Duration (days)	Extent (Ml)
Skipton	1.000	–	–	–
Bradford	0.877	0.364	19	1385.6
Calder	0.710	0.120	99	13167.2
Harrogate	0.928	0.403	47	60.0
Malton	1.000	–	–	–
Leeds	0.792	0.131	91	24007.4
Wakefield	0.795	0.095	100	10397.6
Doncaster	1.000	–	–	–
Sheffield	0.879	0.085	102	18312.2
Total	0.607	0.118	148	105253.0

Table 7-11: Historical inflows: reliability, resilience and vulnerability statistics for demands. Total refers to failure to supply at least one demand centre.

It is noticeable in Tables 7-11 and 7-12 that the overall reliability of water supply from the Yorkshire Grid is substantially reduced during the 1948 to 1996 period when compared to the modelled baseline scenario for 1961-1990. This is partially due to the cluster of dry summers during the late 1980s and early 1990s. This is particularly shown in the reliability statistics for the rivers Wharfe and Ouse in Table 7-13. These are much lower than those of the baseline scenario for all levels of failure in the river Wharfe. If the years from 1988-1996 are omitted from the analysis then similar reliability statistics to those of the baseline scenario emerge. However, the modelled baseline scenario inflow for the River Wharfe contains less low flow events than its historical counterpart. This error is produced by the ADM model calibrated in Section 6.4. Unfortunately, the simple conceptual model chosen for modelling is unable to reproduce both very high flow events and periods of low baseflow. This is a shortcoming of most hydrological models. To rectify this problem a more sophisticated model must be used. However, as reliability of the river Wharfe source is within five percent of the baseline scenario with the omission of the years from 1988-1996, then this will be sufficient for modelling purposes.

	Skipton	Bradford	Calder	Harrogate	Malton	Leeds	Wakefield	Doncaster	Sheffield
Skipton	–	0.00	0.00	0.00	0.00	0.00	0.00	0.00	0.00
Bradford		–	6.10	1.25	0.00	0.46	0.31	0.00	0.97
Calder			–	6.46	0.00	20.46	19.59	0.00	9.89
Harrogate				–	0.00	5.74	4.14	0.00	3.28
Malton					–	0.00	0.00	0.00	0.00
Leeds						–	19.15	0.00	8.74
Wakefield							–	0.00	8.49
Doncaster								–	0.00
Sheffield									–

Table 7-12: Historical inflows: likelihood of conjunctive failure of supply to demand centres, expressed as percentage of total simulation time.

The conjunctive failure statistics in Table 7-12 are also higher than the baseline scenario. The error is as large as ten percent for some demands. The baseline scenario shows the correct pattern of conjunctive failure for the grid, but at a lower magnitude. The majority of the increased percentage of conjunctive failure for the Leeds, Calder and Wakefield demand centres is a result of the years from 1990 to 1996, and in particular the 1995-96 drought. If these are omitted then the conjunctive failure rates are within a few percent of the baseline scenario.

The source reliability detailed in Table 7-13 is of similar magnitude to the baseline scenario, apart from the river Wharfe that has previously been discussed. The very low storages achieved by the reservoir sources occurred during the 1995-96 drought event. If this is omitted then

minimum levels are comparable to those seen in the baseline scenario. It can be observed that the only reservoirs that fail on the second reliability level are those at Washburn, Pennine and Grimwith. This is comparable to the baseline scenario where only the Washburn and Pennine reservoirs fail on the second reliability level. The levels of failure are also very similar for the two groups. The failure of Grimwith reservoir to supply at the drought control level (the second reliability level) is observed only during the 1995-96 drought. Therefore, a model based on the period 1961-90 would not necessarily be expected to reproduce this failure.

	Reliability			Minimum Storage	
	1st level	2nd level	3rd level	Ml	% Maximum
Washburn	0.730	0.928	–	2365.0	10.1
Winscar	1.000	1.000	–	4946.2	52.7
Pennine	0.823	0.990	–	4295.0	12.0
Nidd/Barden	0.983	1.000	–	4326.1	22.6
Grimwith	0.937	0.994	–	1900.1	8.7
Worth Valley	0.979	1.000	–	805.9	24.3
Calderdale	0.986	1.000	–	2409.5	20.6
Boothwood	0.990	1.000	–	4223.3	36.7
Huddersfield	0.986	1.000	–	3175.0	22.5
Brownhill	0.988	1.000	–	1395.2	23.5
Wharfe	0.924	0.855	0.789	–	–
Ouse	0.861	0.933	1.000	–	–
Derwent	1.000	–	–	–	–

Table 7-13: Historical inflows: reliability of sources.

Results from the baseline scenario appear to comply with failure rates suggested using historical data if the years during the 1990s are ignored. Therefore, the baseline scenario is seen as representative of expected supply failure rates during the 1961-90 time-period.

7.2.3 Investigating natural climatic variability

It has been shown in Chapter 3, that precipitation receipts are affected by the phase of the North Atlantic Oscillation (NAO), whether negative or positive. This is a result of both changes in weather state frequencies and the internal properties of a weather state (see Section 3.3). Figure 7-8 shows the 11-yr centred moving average of the summer- and winter-NAO and fitted weather states for the period 1882-1996. A clear correlation can be observed between the NAO indices and the frequency of weather states, especially the anticyclonic and westerly states. Large anticorrelation is observed between the SW and SA, and WW and WA weather states respectively.

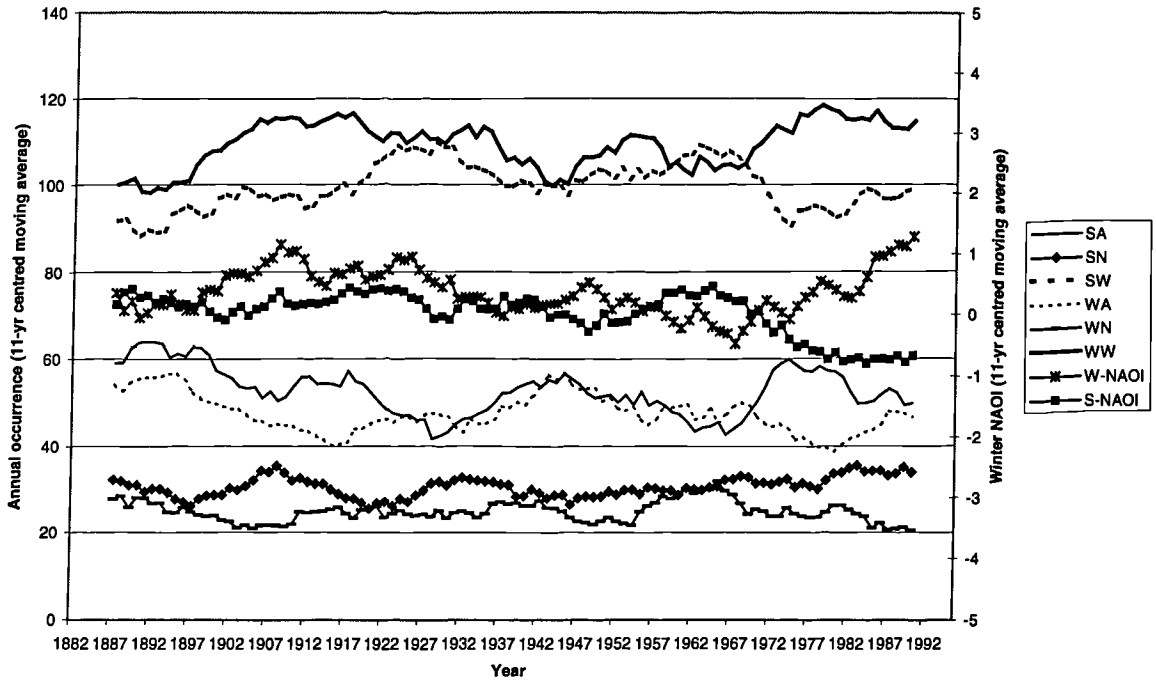

Figure 7-8: 11-year centred moving averages of the winter and summer NAO (W-NAO and S-NAO) and the 6 weather states.

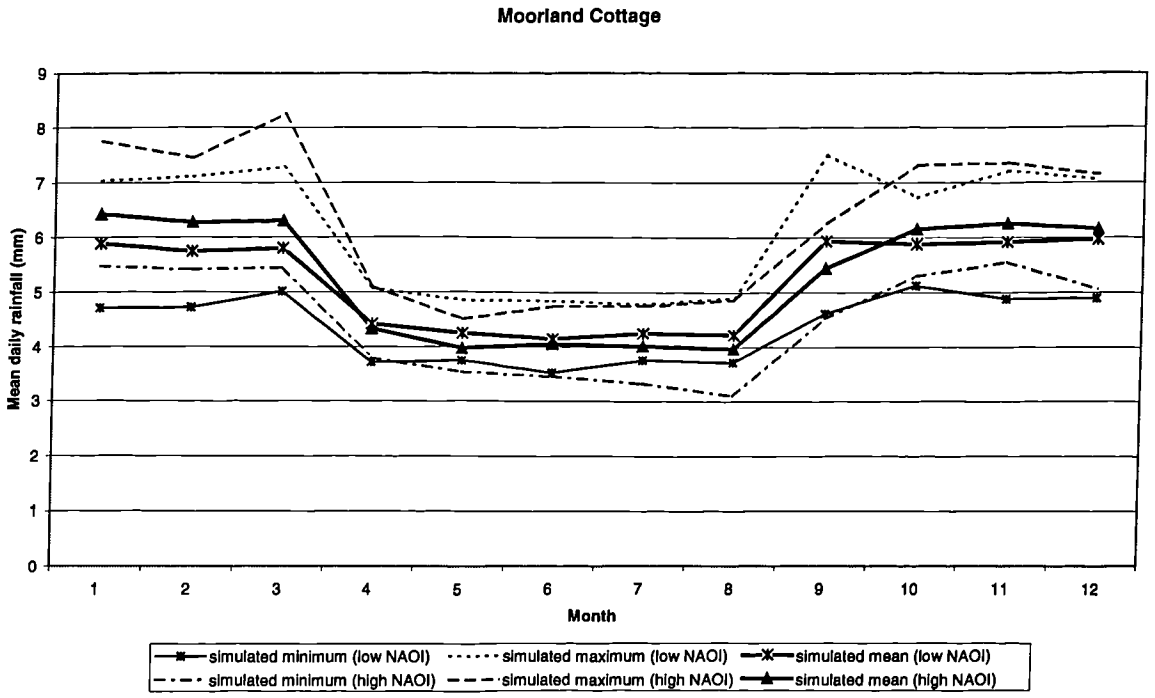

Figure 7-9: Mean daily precipitation for a high- and low-NAO scenario, with limits obtained from 50 simulations.

During a high winter-NAO period, such as from 1980-1990, there is an increased frequency of the WW and SA weather states, to the detriment of the SW and WA weather states. In a low winter-NAO period, such as 1960-1970, the reverse situation occurs. For this investigation a high-phase NAO is defined as a positive winter-NAO and a low-phase NAO is defined as a negative winter-NAO.

To illustrate the use of NAO, the semi-Markov chain model parameters were re-fitted on the period from 1980-1990 and the period from 1960-1970 to simulate high and low instances of the NAO respectively. Fifty 30-year synthetic series of weather states were produced and precipitation simulated for Moorland Cottage using the NSRP model. The high-NAO simulation would be expected to show the enhanced seasonality that was observed in the 1980s and early 1990s. The low-NAO simulation would conversely show reduced seasonality. This can be observed in Figure 7-9. This approach provides a method of simulating the changes in the frequency of occurrence of weather states without the additional adjustment of internal precipitation model parameters.

This approach was used to investigate the change in water resource reliability during low- and high-NAO phases. A 1000-yr daily weather state series was produced using the parameters fitted on the period from 1980-1990 and 1960-1970, simulating high and low instances of the NAO respectively. A 1000-yr daily precipitation series was then produced for every site for each of the high- and low-NAO simulations using the methodology in Section 7.1.1. This produced monthly and annual cross-correlations of 0.15 and 0.20 for the low-NAO scenario, and monthly and annual cross-correlations of 0.12 and 0.16 for the high-NAO scenario. The effects of the phase of the NAO upon water resources in Yorkshire was then examined by the production of inflow sequences for the two scenarios.

		High-phase NAO % change from Baseline	Low-phase NAO % change from Baseline
East	Summer	+0.0	+5.0
	Winter	+1.0	–2.0
West	Summer	–1.0	+6.0
	Winter	+2.0	–4.0

Table 7-14: Changes in winter and summer precipitation receipts resulting from a high- or low-phase NAO when compared to the baseline 1961-90.

The difference in summer and winter precipitation receipts at Moorland Cottage and Lockwood Reservoir during high- and low-phase NAO periods is compared to the baseline scenario of

1961-1990 in Table 7-14. During a high-phase NAO there is an increase in winter precipitation receipt of two percent in the west and one percent in the east. This is offset by a slight reduction of one percent in summer precipitation receipts in the west, but no change is observed in the east. During a low-phase NAO the opposite effect occurs, raising summer precipitation receipts by 5-6 percent and lowering winter receipts by 2-4 percent.

7.2.3.1 High-phase NAO

During a high-phase NAO, such as from 1980-1990, the model simulation would suggest that reliability is slightly decreased at all major demand centres (Table 7-15). This is excepting the Skipton demand, which is supplied 100 percent of the time. The Malton and Doncaster demand centres only suffer a shortfall 0.01 percent of the time; the same percentage failure as the baseline scenario. However, the likelihood of conjunctive failure of demands is very similar to the baseline scenario (Table 7-16). The major difference in supply reliability between the baseline scenario and the high-phase NAO is that when supplies fail they fail more severely. This can be seen in the vulnerability statistics for all the major demand centres. The longest duration of failure is 189 days rather than the 165 days maximum of the baseline scenario. The total shortfall in Ml is also greater. The Calder, Wakefield and Leeds supplies seem increasingly vulnerable under a positive winter-NAO. The duration of supply failure and extent of failure in Ml both increase for these demand centres. The Sheffield demand shows an increase in the extent of failure but with slightly shorter duration failures.

Demand	Reliability	Resilience	Vulnerability	
			Duration (days)	Extent (Ml)
Skipton	1.0000	–	–	–
Bradford	0.9105	0.421	22	615.6
Calder	0.8462	0.235	121	8049.4
Harrogate	0.9406	0.728	21	30.0
Malton	0.9999	0.118	19	304.0
Leeds	0.9018	0.248	106	26888.2
Wakefield	0.8944	0.060	178	19432.6
Doncaster	0.9999	0.118	19	152.0
Sheffield	0.8921	0.047	144	20262.0
Total	0.7331	0.167	189	84115.5

Table 7-15: High-phase NAO: reliability, resilience and vulnerability statistics for demands. Total refers to failure to supply at least one demand centre.

	Skipton	Bradford	Calder	Harrogate	Malton	Leeds	Wakefield	Doncaster	Sheffield
Skipton	–	0.00	0.00	0.00	0.00	0.00	0.00	0.00	0.00
Bradford		–	3.93	1.07	0.00	0.00	0.00	0.00	0.35
Calder			–	5.23	0.00	9.46	8.52	0.00	5.69
Harrogate				–	0.00	3.24	1.75	0.00	1.85
Malton					–	0.00	0.01	0.01	0.01
Leeds						–	7.58	0.00	4.88
Wakefield							–	0.01	5.01
Doncaster								–	0.01
Sheffield									–

Table 7-16: High-phase NAO: likelihood of conjunctive failure of supply to demand centres, expressed as percentage of total simulation time.

This increased vulnerability is also reflected in the likelihood of occurrence of a drought event as severe as that of 1995-96. Under a high-phase NAO this is reduced to a one in 100-yr event, occurring 10 times in the 1000-yr simulation period.

	Reliability			Minimum Storage	
	1st level	2nd level	3rd level	Ml	% Maximum
Washburn	0.6099	0.9506	–	2365.0	10.1
Winscar	1.0000	1.0000	–	6942.3	73.9
Pennine	0.8723	0.9997	–	4295.1	12.0
Nidd/Barden	0.9983	1.0000	–	9270.4	48.3
Grimwith	0.9886	1.0000	–	5000.5	23.0
Worth Valley	0.9984	1.0000	–	1741.1	52.6
Calderdale	0.9987	1.0000	–	3414.3	29.2
Boothwood	0.9998	1.0000	–	6691.4	58.2
Huddersfield	0.9998	1.0000	–	6173.1	43.7
Brownhill	1.0000	1.0000	–	3318.2	56.0
Wharfe	0.9310	0.9060	0.9260	–	–
Ouse	0.9470	0.9580	1.0000	–	–
Derwent	1.0000	–	–	–	–

Table 7-17: High-phase NAO: reliability of sources.

During a high-phase NAO, reliability of sources is generally improved (Table 7-17). This is due to the increased winter precipitation that allows increased replenishment of resources. However, due to decreased summer precipitation, some supplies are more likely to fail and minimum storage levels are reduced. Therefore, when failure does occur it is generally more severe. This accounts for the increased vulnerability of supplies to failure, but no apparent change in reliability.

7.2.3.2 Low-phase NAO

The opposite effect is observed in the low-phase NAO simulation. Supply reliability is significantly improved when compared to the baseline scenario (Table 7-18). Supply vulnerability is decreased in general, with the longest failure duration being 150 days compared to 165 for the baseline scenario. At Leeds and Calder, the vulnerability duration statistic is increased, but at all other sites it is reduced. The extent of the total grid shortfall is reduced by approximately 1000 Ml.

This increased reliability in supply is also reflected in the drought severity statistic. A drought as severe as the 1995-96 drought would only be expected to occur once every 1000-yrs under a low-phase NAO. This constitutes a huge reduction upon the baseline scenario. Conjunctive failures are also significantly reduced (Table 7-19).

Demand	Reliability	Resilience	Vulnerability	
			Duration (days)	Extent (Ml)
Skipton	1.000	–	–	–
Bradford	0.9209	0.409	23	935.2
Calder	0.8688	0.227	105	5624.2
Harrogate	0.9603	0.725	14	48.0
Malton	0.9999	0.083	16	256.0
Leeds	0.9234	0.233	98	22934.4
Wakefield	0.9140	0.065	146	16255.0
Doncaster	0.9999	0.083	16	128.0
Sheffield	0.9148	0.049	126	15854.4
Total	0.7730	0.170	150	73955.6

Table 7-18: Low-phase NAO: reliability, resilience and vulnerability statistics for demands. Total refers to failure to supply at least one demand centre.

	Skipton	Bradford	Calder	Harrogate	Malton	Leeds	Wakefield	Doncaster	Sheffield
Skipton	–	0.00	0.00	0.00	0.00	0.00	0.00	0.00	0.00
Bradford		–	3.69	0.87	0.00	0.00	0.00	0.00	0.33
Calder			–	3.42	0.00	7.44	7.30	0.00	4.76
Harrogate				–	0.00	2.61	1.42	0.00	1.50
Malton					–	0.00	0.01	0.01	0.01
Leeds						–	6.45	0.00	4.02
Wakefield							–	0.01	4.11
Doncaster								–	0.01
Sheffield									–

Table 7-19: Low-phase NAO: likelihood of conjunctive failure of supply to demand centres, expressed as percentage of total simulation time.

	Reliability			Minimum Storage	
	1st level	2nd level	3rd level	Ml	% Maximum
Washburn	0.6692	0.9603	–	2365.0	10.1
Winscar	1.0000	1.0000	–	6798.4	72.4
Pennine	0.8860	0.9999	–	4295.3	12.0
Nidd/Barden	0.9997	1.0000	–	10134.7	52.8
Grimwith	0.9923	1.0000	–	7631.5	35.1
Worth Valley	0.9993	1.0000	–	1484.9	44.8
Calderdale	0.9993	1.0000	–	3072.2	26.3
Boothwood	0.9998	1.0000	–	6941.4	60.4
Huddersfield	0.9999	1.0000	–	6876.7	48.7
Brownhill	1.0000	1.0000	–	2871.0	48.4
Wharfe	0.9300	0.9070	0.9320	–	–
Ouse	0.9510	0.9630	1.0000	–	–
Derwent	1.0000	–	–	–	–

Table 7-20: Low-phase NAO: reliability of sources.

The likelihood of source failure is also significantly improved when compared to the baseline scenario. This is due to increased summer precipitation but similar winter precipitation to the baseline scenario. The increased summer precipitation during a low-phase NAO event is seen to significantly reduce the risk of severe drought in Yorkshire.

7.3 Using the UKCIP98 climate change scenarios

The UKCIP98 climate change scenarios (Hulme and Jenkins, 1998) were constructed using the HadCM2 GCM outputs. These scenarios are based upon the HadCM2 experiments that use a one percent rise per annum in greenhouse gas concentrations over the next century; similar to the IS92a emissions scenario (Leggett *et al.*, 1992). Four scenarios are presented (as explained in Section 2A.3): Low, Medium-Low, Medium-High and High for 30-yr periods centred on 2020, 2050 and 2080. Climate change scenarios are not definitive predictions of the future but, instead, informed sensitivity analyses of climate change impacts. It is important to remember that future climate in the UK will be different from that of 1961-90 even without climate change due to natural variability. This has been considered previously, in the investigation into the impacts of high- and low-phase NAO. A separation of the effects of natural variability from those of climate change was considered as part of the UKCIP98 scenarios. For certain seasons and periods, precipitation changes in the intra-ensemble range are larger than the ensemble mean change. This suggests that a high proportion of the seasonal-mean precipitation changes in the Medium-High scenario are due to natural climate variability rather than anthropogenically induced climate change (Hulme and Jenkins, 1998). This natural variability can be seen in the analysis of long precipitation records in Chapter 3.

The Medium-High scenario provides more detail than the other three scenarios, and for this reason has generally been used for climate change impact assessments. Seasonal and annual changes in a range of variables are considered for 30-yr periods centred on 2020, 2050 and 2080: diurnal temperature range, vapour pressure, relative humidity, incident short-wave radiation, total cloud cover, mean 10m wind speed, potential evaporation and precipitation. In this analysis, two climate change scenarios will be considered: 2021-2050 and 2051-2080. The impacts of changes in precipitation and potential evaporation on reservoir inflows and river flows, and the translation to impacts on water supply will be examined. It is therefore assumed that the parameters of the ADM rainfall-runoff models, calibrated on present conditions, will not change under a future climate.

The UKCIP98 scenarios are based upon 30-yr periods centred on the years 2020, 2050 and 2080. The 2021-2050 scenario is thus analogous to a middle-ground between the UKCIP98 Medium-High scenarios for 2020 and 2050. Similarly, the 2051-2080 scenario lies between the UKCIP98 Medium-High scenarios for 2050 and 2080. Four grid-cells cover the UK. Unfortunately, the Yorkshire region is not properly covered by the UKCIP98 grid-cells. Those parts that are covered lie equally in the northern England grid-square and the southeastern England grid-square. It is assumed, therefore, that precipitation and PE change in Yorkshire will be the mean of the two grid-squares for each scenario.

The likely changes in precipitation amount, precipitation variability and PE for summer and winter, defined as April to September and October to March respectively, for the two climate change scenarios are shown in Table 7-21.

Season	2021-2050			2051-2080		
	Precipitation Change (%)	Precipitation Variability Change (%)	PE Change (%)	Precipitation Change (%)	Precipitation Variability Change (%)	PE Change (%)
Summer	–5	+10	+6	–9	+10	+8
Winter	+9	+5	0	+16	+15	+10
Annual	+3 to +5	–	+6	+4 to +10	–	+10

Table 7-21: Climate change scenarios for 2021-50 and 2051-80: precipitation and PE changes.

The likely changes in airflow characteristics over the British Isles under the UKCIP98 Medium-High scenario are also assessed by Hulme and Jenkins (1998). The analysis suggests a reduction of northerly and easterly flow in autumn. Summer may become slightly more anticyclonic with increased westerly and northwesterly flows. Winter and spring become less anticyclonic. This suggests that any increase in winter precipitation will come from an increase in westerly flows

combined with an increase in mean daily precipitation on a westerly day. In summer months, there is a reduction in precipitation. This is an outcome of an increase in anticyclonic conditions and a reduction in westerly mean daily precipitation.

		2021-2050		2051-2080	
		$\mu(24)$	$\gamma(24)$	$\mu(24)$	$\gamma(24)$
Eastern	SW	2.40	32.0	2.24	32.0
	WW	2.68	19.0	2.93	20.8
Western	SW	5.37	88.7	5.14	88.7
	WW	9.52	160.3	10.25	175.6

Table 7-22: Climate change scenarios for 2021-50 and 2051-80: precipitation amount and variability changes.

These changes in airflow characteristics are similar to those of the high-phase NAO. During a positive winter-NAO period, such as from 1980-1990, there is an increased frequency of the WW and SA weather states, to the detriment of the SW and WA weather states. Therefore, to simulate precipitation changes for the climate change scenarios, the high-phase NAO weather state series will be used. Further change in mean precipitation amount and variability was applied by the refitting of the SW and WW weather states for the eastern and western NSRP model, taking into account the changes to mean precipitation already achieved by the use of the high-phase NAO scenario rather than the baseline (see Table 7-14). The new statistics for $\mu(24)$ and $\gamma(24)$ for the SW and WW weather states can be found in Table 7-22. The new fitted parameters can be found in Table 7-23 and Table 7-24 for the 2021-50 and 2051-80 climate change scenarios respectively. These provide accurate statistics, as Table 7-22, in simulation if the scale factor adjustments are applied as detailed in Section 5.5, multiplied by the additional factor given in Tables 7-23 and 7-24.

Parameter Weather State	Model	λ^{-1} (h^{-1})	β^{-1} (h^{-1})	ρ (km^{-2})	η (h^{-1})	ξ ($mm\ h^{-1}$)	γ (km^{-1})	Scale Adj.
SW	Western	0.005	0.010	0.007	0.131	2.682	0.052	0.998
	Eastern	0.002	0.011	0.028	2.171	0.418	0.067	0.966
WW	Western	0.031	0.245	0.002	0.100	3.146	0.062	0.995
	Eastern	0.017	0.079	0.003	6.227	0.240	0.041	0.993

Table 7-23: Fitted parameters for 2021-50 climate change scenario.

Parameter Weather State	Model	λ^{-1} (h^{-1})	β^{-1} (h^{-1})	ρ (km^{-2})	η (h^{-1})	ξ ($mm\ h^{-1}$)	γ (km^{-1})	Scale Adj.
SW	Western	0.006	0.012	0.005	0.100	3.205	0.051	0.991
	Eastern	0.003	0.012	0.024	0.696	1.491	0.069	0.935
WW	Western	0.024	0.062	0.004	0.106	3.237	0.062	1.006
	Eastern	0.023	0.130	0.002	2.271	0.635	0.040	0.998

Table 7-24: Fitted parameters for the 2051-80 climate change scenario.

For the climate change scenarios, firstly the effect of change in PE is assessed alone. Then the additional impact of change in precipitation is assessed. For the PE-only climate change scenarios, the baseline precipitation series previously generated are used. It should be noted that these are not likely future climate change scenarios but rather, give an indication of the impact of changes in PE upon water resources. For the precipitation and PE climate change scenarios, new series are generated using the new fitted parameters in Tables 7-23 and Table 7-24. These examine the impacts of realistic future climate change scenarios using output from the HadCM2 GCM.

7.3.1 Potential evapotranspiration (PE) change

7.3.1.1 Applying a PE scenario for 2021-2050

Scenarios of future PE for Europe have been derived using output from the HadCM2 Greenhouse Gas only experiment ensemble mean (Jones *et al.*, 1999*b*). Considerable differences were found in the percent changes in PE with the same climate scenarios according to the method of PE estimation used. The FAO recommends the use of the Penman-Monteith method however, as it has been found to out-perform other methods over a wide range of climatic conditions. This was used to produce a scenario of future PE for 2021-2050. This PE change is analogous to a middle-ground between the UKCIP98 Medium-High scenarios for 2020 and 2050.

Series	Annual PE 2021-2050	Annual PE 1961-1990	% change
WRINCLE92	586	557	+5.2
WRINCLE98	610	573	+6.4
Wharfe	606	567	+6.9
Ouse	596	568	+5.0
Derwent	598	575	+3.9

Table 7-25: Comparison of baseline and future PE, 2021-2050.

An estimate can be made of the expected change in PE from 2021-2050 using the UKCIP98 scenarios. Annually, PE would be expected to change by approximately 4 to 7 percent between 2021 and 2050 across the Yorkshire region. There is no increase in winter months (DJF), but a slight increase in spring (MAM) of approximately 4 percent. The largest increases are seen in autumn months (SON), approximating 15 percent, and summer (JJA), approximating 6 percent.

Table 7-25 details the annual PE produced by New *et al.* (2000) for the baseline scenario of 1961-1990. The future PE for 2021-2050 shows, on average, between five to six percent increase on the baseline. This is in the same approximate range as the UKCIP98 Medium-High scenario (see Table 7-21) (Hulme and Jenkins, 1998). A more interesting change, however, may be the distribution of PE throughout the year. The average monthly PE distribution across Yorkshire, as a percentage of annual PE, suggested by Jones *et al.* (1999*b*) is shown in Table 7-26. The largest increases occur in late summer and early autumn, although there is also a relative decrease in spring PE. The percentages shown in Table 7-26 are relative changes from 1961-90 and are similar to those suggested by UKCIP98.

Month	Percentage of annual total PE 1961-1990	Percentage of annual total PE 2021-2050	Percentage Change
J	2.0	1.9	−5.0
F	2.9	2.6	−10.3
M	6.1	4.9	−19.7
A	9.4	7.4	−21.3
M	14.4	10.7	−25.7
J	15.9	14.1	−11.3
J	17.0	17.4	+2.4
A	14.3	17.7	+23.8
S	8.9	13.1	+47.2
O	4.9	5.9	+20.4
N	2.5	2.6	+4.0
D	1.7	1.7	0.0

Table 7-26: Monthly disaggregation factors applied to future annual PE, 2021-2050, and comparison with baseline PE monthly disaggregation factors.

If the estimated future increases (Table 7-25) are applied to the previously derived equations (7-1 to 7-5) then this produces an estimate for future PE, assuming no change in future precipitation levels. This is obtained by multiplying the whole of the right-hand side of the equation by the appropriate percentage increase (Equations 7-11 to 7-15):

WRINCLE92(2050)	$PE = -0.155\,ppt + 716.90$	(7-11)
WRINCLE98(2050)	$PE = -0.168\,ppt + 717.08$	(7-12)
Wharfe(2050)	$PE = -0.163\,ppt + 725.59$	(7-13)
Ouse(2050)	$PE = -0.160\,ppt + 714.34$	(7-14)
Derwent(2050)	$PE = -0.205\,ppt + 692.49$	(7-15)

A future scenario for 2021-2050 for an increase in PE was thus produced. An annual PE series was generated based on the precipitation totals of the baseline synthetic series using Equations 7-11 to 7-15 and disaggregated monthly using the percentages in Table 7-26. Inflows were then produced using the synthetic 1000-yr daily precipitation series generated for the baseline scenario and the disaggregated PE series. These inflow series were used as input to the YGrid2000 model to determine how future changes in PE, both annual magnitude and monthly distribution, may affect water supplies.

Demand	Reliability	Resilience	Vulnerability	
			Duration (days)	Extent (Ml)
Skipton	1.0000	–	–	–
Bradford	0.9183	0.449	25	681.0
Calder	0.8201	0.247	124	11580.4
Harrogate	0.9183	0.686	17	57.8
Malton	0.9999	0.140	22	352.0
Leeds	0.8816	0.267	94	29375.4
Wakefield	0.8755	0.052	159	17788.4
Doncaster	0.9999	0.140	22	176.0
Sheffield	0.8663	0.046	150	19404.8
Total	0.7012	0.162	200	86938.5

Table 7-27: PE only 2021-2050 scenario: reliability, resilience and vulnerability statistics for demands. Total refers to failure to supply at least one demand centre.

	Skipton	Bradford	Calder	Harrogate	Malton	Leeds	Wakefield	Doncaster	Sheffield
Skipton	–	0.00	0.00	0.00	0.00	0.00	0.00	0.00	0.00
Bradford		–	4.23	1.40	0.00	0.00	0.00	0.00	0.40
Calder			–	7.03	0.01	11.45	10.52	0.01	8.05
Harrogate				–	0.00	5.71	3.30	0.00	3.45
Malton					–	0.01	0.01	0.01	0.01
Leeds						–	9.38	0.01	7.01
Wakefield							–	0.01	6.89
Doncaster								–	0.01
Sheffield									–

Table 7-28: PE only 2021-2050 scenario: likelihood of conjunctive failure of supply to demand centres, expressed as percentage of total simulation time.

	Reliability			Minimum Storage	
	1st level	2nd level	3rd level	Ml	% Maximum
Washburn	0.513	0.918	–	2365.0	10.1
Winscar	1.000	1.000	–	6920.2	73.7
Pennine	0.822	0.999	–	4295.0	12.0
Nidd/Barden	0.999	1.000	–	8012.3	41.8
Grimwith	0.978	1.000	–	1906.6	8.8
Worth Valley	0.997	1.000	–	1358.6	41.0
Calderdale	0.998	1.000	–	3670.2	31.4
Boothwood	1.000	1.000	–	7110.6	61.8
Huddersfield	1.000	1.000	–	6674.8	47.3
Brownhill	1.000	1.000	–	2847.6	48.0
Wharfe	0.928	0.901	0.916	–	–
Ouse	0.938	0.938	1.000	–	–
Derwent	1.000	–	–	–	–

Table 7-29: PE only 2021-2050 scenario: reliability of sources.

As would be expected, given the increased PE and the subsequent reduction of runoff, the reliability of water supplies in Yorkshire is reduced (Table 7-27). This constitutes only a three percent reduction in reliability on average across the grid, but the maximum extent of supply vulnerability is increased by almost 15 percent. The maximum duration of failure is also significantly increased, from 165 days in the baseline scenario to 200 days in the PE-only 2021-2050 scenario. Individually, the only supply that shows a significant increased vulnerability in terms of failure duration is that of Calder demand. The Calder, Leeds, Wakefield and Sheffield supplies all show decreased reliability and increased vulnerability in terms of failure extent.

The likelihood of conjunctive failure is also increased for the Calder, Leeds, Wakefield and Sheffield demands when compared to the baseline scenario (Table 7-28). The Calder, Leeds and Wakefield supplies generally fail at the same time and this is approximately ten percent of the simulation time of 1000-yrs. These supplies fail when flows on the river Ouse are low. This decreased reliability is also reflected in the increased occurrence of severe droughts. The likelihood of a drought as severe as the 1995-96 drought occurring is increased to nine times in 1000 years; a one in 111 year event.

Interestingly, in general, source reliability is not significantly reduced (Table 7-29). However, certain sources show a large reduction. The rivers Wharfe and Ouse show a reduction in reliability at all levels, but especially at the lower levels of failure. This failure in supply is taken up by the reservoirs, which are less reliable. Grimwith reservoir in particular exhibits a reduction in reliability and the minimum storage is reduced to 8.8 percent when compared to 23 percent for the baseline scenario due to the reductions in supply from the Wharfe. The Washburn and Pennine reservoir groups also show a reduction in reliability.

7.3.1.2 Applying a PE scenario for 2051-2080

A similar PE scenario was produced for the period from 2051-2080. PE change during this period lies somewhere between the UKCIP98 scenarios centred on 2050 and 2080. The annual PE change in Yorkshire would be between a 9 and 12 percent increase (Hulme and Jenkins, 1998). For this climate change scenario, a 10 percent annual PE increase was applied to all five PE series (see Table 7-21). This gave the equations (7-16 to 7-20):

WRINCLE92(2080)	$PE = -0.162\,ppt + 749.85$	(7-16)
WRINCLE98(2080)	$PE = -0.174\,ppt + 741.09$	(7-17)
Wharfe(2080)	$PE = -0.167\,ppt + 746.58$	(7-18)
Ouse(2080)	$PE = -0.167\,ppt + 748.62$	(7-19)
Derwent(2080)	$PE = -0.217\,ppt + 732.83$	(7-20)

An annual PE series was generated based on the precipitation totals of the baseline synthetic series using Equations 7-16 to 7-20 and disaggregated monthly using the percentages in Table 7-26, as no other data on likely future monthly distribution was available. Inflows were then produced using the synthetic 1000-yr daily precipitation series generated for the baseline scenario and the disaggregated PE series. These inflow series were used as input to the YGrid2000 model to determine how future changes in PE, both annual magnitude and monthly distribution, may affect water supplies.

Demand	Reliability	Resilience	Vulnerability	
			Duration (days)	Extent (Ml)
Skipton	1.0000	–	–	–
Bradford	0.9186	0.472	19	675.4
Calder	0.7972	0.254	112	10532.6
Harrogate	0.8960	0.668	17	57.8
Malton	0.9998	0.139	22	352.0
Leeds	0.8621	0.274	102	31046.0
Wakefield	0.8555	0.049	161	18067.4
Doncaster	0.9998	0.139	22	176.0
Sheffield	0.8407	0.044	182	27165.0
Total	0.6681	0.159	201	95504.2

Table 7-30: PE only 2051-2080 scenario: reliability, resilience and vulnerability statistics for demands. Total refers to failure to supply at least one demand centre.

It is noticeable that some demand centres show significantly reduced reliability and resilience, and increased vulnerability under a PE-only 2051-2080 climate change scenario (Table 7-30). Others, however, do not exhibit much change when compared to the baseline scenario. The Skipton demand centre is still well supplied by the Nidd/Barden reservoir and no failure in supply is recorded. Similarly, the Bradford, Doncaster and Malton demands show only a slight reduction in reliability and a slight increase in vulnerability. The major changes in reliability under a PE-only climate change scenario for 2051-2080 are seen at the Calder, Wakefield, Leeds and Sheffield demand centres, with a reduction of 4 to 5 percent on the baseline scenario. The total grid reliability is reduced by seven percent. The duration of failure of the grid increases by only one day when compared to the 2021-2050 PE-only climate change scenario. However, the extent of vulnerability is increased dramatically, now some 22 percent higher than the baseline scenario.

	Skipton	Bradford	Calder	Harrogate	Malton	Leeds	Wakefield	Doncaster	Sheffield
Skipton	–	0.00	0.00	0.00	0.00	0.00	0.00	0.00	0.00
Bradford		–	4.51	1.73	0.00	0.01	0.01	0.00	0.44
Calder			–	8.97	0.02	13.34	12.14	0.02	9.83
Harrogate				–	0.01	7.35	4.48	0.01	4.61
Malton					–	0.02	0.02	0.02	0.02
Leeds						–	10.86	0.02	8.60
Wakefield							–	0.02	8.57
Doncaster								–	0.02
Sheffield									–

Table 7-31: PE only 2051-2080 scenario: likelihood of conjunctive failure of supply to demand centres, expressed as percentage of total simulation time.

The conjunctive failure of supplies is also increased by the increase in summer PE (Table 7-31). The Calder, Wakefield and Leeds supplies are now likely to fail some 12 percent of the total simulation period. Other demand centres also show similar increases in conjunctive failure. This is reflected in the increased frequency of severe drought predicted under this scenario. The return period of a drought as severe as that of 1995-96 is decreased to one in every 91 years. Therefore, under this scenario the likelihood of severe drought is almost doubled when a comparison is made to the baseline scenario.

The reliability of sources is similarly affected by the PE-only 2051-2080 climate change scenario (Table 7-32). Only the Winscar and Brownhill reservoir groups do not fail during the 1000-yr simulation period. All sources have decreased reliability. However, the rivers Wharfe and Ouse do not show significantly reduced reliability except at the third level of failure. This means that any increase in failure rates will have a severe effect upon water supplies as this level of failure allows no abstraction of water for the grid.

	Reliability			Minimum Storage	
	1st level	2nd level	3rd level	Ml	% Maximum
Washburn	0.4691	0.8960	–	2365.0	10.1
Winscar	1.0000	1.0000	–	6702.0	71.4
Pennine	0.7884	0.9987	–	4294.9	12.0
Nidd/Barden	0.9984	1.0000	–	7803.9	40.7
Grimwith	0.9678	0.9999	–	1904.0	8.7
Worth Valley	0.9964	1.0000	–	1281.2	38.7
Calderdale	0.9975	1.0000	–	3219.6	27.5
Boothwood	0.9997	1.0000	–	6888.8	59.9
Huddersfield	0.9997	1.0000	–	6677.3	47.3
Brownhill	1.0000	1.0000	–	2814.5	47.5
Wharfe	0.9280	0.9000	0.9120	–	–
Ouse	0.9330	0.9220	1.0000	–	–
Derwent	1.0000	–	–	–	–

Table 7-32: PE only 2051-2080 scenario: reliability of sources.

7.3.2 Change in precipitation and potential evapotranspiration

7.3.2.1 Climate change scenario: 2021-2050

For the climate change scenario 2021-2050, both precipitation and PE changes were considered. Fifty 1000-yr synthetic daily precipitation series were produced using a weather-state series generated using the high-phase NAO scenario. This used the new parameters for the SW and WW weather states given in Table 7-23, and old parameters for the other weather states (Table 5-43). This provides the summer precipitation decrease and winter precipitation increase detailed in Table 7-21. The methodology detailed in Section 7.1.1 was then applied to the precipitation series for the eastern and western NSRP spatial models to produce a 1000-yr precipitation series for each of the 28 sites, giving monthly and annual cross-correlations of 0.15 and 0.18 respectively.

The same PE scenarios as detailed previously in Table 7-25 were used, with the monthly disaggregation factors as Table 7-26. However, as the equation for PE is dependent upon summer precipitation an adjustment must be made for the decrease in summer precipitation under this scenario. The reduction in summer precipitation is some five percent for the 2021-2050 climate change scenario (see Table 7-21). The equations 7-21 to 7-25 simulate an instance of summer precipitation decrease of five percent coupled to increases of PE as detailed in Table 7-25.

WRINCLE92(CC2050) $$PE = -0.163\,ppt + 717.13 \qquad (7\text{-}21)$$

WRINCLE98(CC2050)	$PE = -0.177\,ppt + 716.84$	(7-22)
Wharfe(CC2050)	$PE = -0.171\,ppt + 725.54$	(7-23)
Ouse(CC2050)	$PE = -0.168\,ppt + 714.59$	(7-24)
Derwent(CC2050)	$PE = -0.215\,ppt + 692.19$	(7-25)

An annual PE series was generated based on the summer totals of the synthetic precipitation series using Equations 7-21 to 7-25 and disaggregated monthly using the percentages in Table 7-26. Inflows were then produced using the synthetic 1000-yr daily precipitation series generated for this scenario and the disaggregated PE series. These inflow series were used as input to the YGrid2000 model to determine how future changes in PE, both annual magnitude and monthly distribution, may affect water supplies.

Demand	Reliability	Resilience	Vulnerability	
			Duration (days)	Extent (Ml)
Skipton	1.0000	–	–	–
Bradford	0.9227	0.418	17	618.8
Calder	0.8435	0.208	112	8856.8
Harrogate	0.9515	0.699	14	37.0
Malton	0.9997	0.119	39	640.2
Leeds	0.9020	0.219	104	31510.0
Wakefield	0.8864	0.052	176	19007.2
Doncaster	0.9997	0.119	39	519.6
Sheffield	0.8881	0.046	145	20812.2
Total	0.7405	0.151	196	81138.5

Table 7-33: 2021-2050 scenario: reliability, resilience and vulnerability statistics for demands. Total refers to failure to supply at least one demand centre.

The differences between the PE-only climate change scenario for 2021-50, and that which also considers precipitation change is immediately apparent (Table 7-33). The reliability of supply to most demand centres is very similar to that of the baseline scenario. In some cases, the overall reliability is actually increased by the 2021-50 climate change scenario. This is true for the Bradford and Harrogate demand centres. The reliability of the grid is also improved in general, as can be seen by the increase in the total reliability statistic when compared to the baseline scenario. However, interestingly, the resilience of supplies to all major demand centres, excluding Malton and Doncaster, is reduced. The increased vulnerability of the system to severe drought is also shown by the increase in the duration of drought and its extent. Every demand centre, excepting Bradford, is more vulnerable to severe drought under the 2021-2050 climate

change scenario. The extent of supply deficits has increased at most demand centres, some doubling the extent of vulnerability when compared to the baseline scenario. The total duration of the most severe drought is also increased, from 165 days in the baseline scenario, to 196 days in this scenario. The total grid deficit is increased by nine percent to 81138.5 Ml.

The conjunctive failure of supplies to major demand centres is also slightly increased by the 2021-2050 climate change scenario (Table 7-34). However, this is not especially significant. The occurrence of severe droughts in Yorkshire is not particularly changed from the baseline scenario by 2021-2050. The return period for a drought as severe as the 1995-96 drought is one in every 143 years. However, as can be seen in the increased vulnerability statistics, these droughts will be more extensive in both magnitude and duration than severe historical droughts.

	Skipton	Bradford	Calder	Harrogate	Malton	Leeds	Wakefield	Doncaster	Sheffield
Skipton	–	0.00	0.00	0.00	0.00	0.00	0.00	0.00	0.00
Bradford		–	3.82	0.97	0.00	0.00	0.00	0.00	0.34
Calder			–	4.24	0.02	9.59	9.54	0.02	6.82
Harrogate				–	0.01	3.32	1.99	0.01	2.08
Malton					–	0.02	0.03	0.03	0.03
Leeds						–	8.44	0.02	5.88
Wakefield							–	0.03	6.29
Doncaster								–	0.03
Sheffield									–

Table 7-34: 2021-2050 scenario: likelihood of conjunctive failure of supply to demand centres as percentage of total simulation time.

	Reliability			Minimum Storage	
	1st level	2nd level	3rd level	Ml	% Maximum
Washburn	0.6195	0.9515	–	2365.0	10.1
Winscar	1.0000	1.0000	–	7003.8	74.6
Pennine	0.8748	0.9998	–	4295.1	12.0
Nidd/Barden	0.9982	1.0000	–	8628.1	45.0
Grimwith	0.9879	1.0000	–	5125.0	23.5
Worth Valley	0.9975	1.0000	–	1604.4	48.4
Calderdale	0.9986	1.0000	–	3657.0	31.3
Boothwood	0.9996	1.0000	–	6650.8	57.8
Huddersfield	0.9998	1.0000	–	5813.4	41.2
Brownhill	1.0000	1.0000	–	3125.0	52.7
Wharfe	0.9320	0.9050	0.9170	–	–
Ouse	0.9450	0.9410	1.0000	–	–
Derwent	1.0000	–	–	–	–

Table 7-35: 2021-2050 scenario: reliability of sources.

Source reliability is on the whole, improved by 2021-2050 (Table 7-35). Reservoir sources exhibit increased reliability and many show an improvement in minimum levels. However, the

reliability of river sources is substantially reduced, particularly at the third fail level where no abstraction is allowed. Low-flows are therefore more prevalent during 2021-2050. As the abstraction from river sources exerts such a strong control on the successful supply of water to the Yorkshire grid then this provides a significant effect and is a cause of the increased vulnerability of demand centres. The increased severity of drought events is also due to the increase of low-flow events, and a possible increase in the persistence of low-flow events on the rivers Wharfe and Ouse.

7.3.2.2 Climate change scenario: 2051-2080

For the climate change scenario 2051-2080 considering both precipitation and PE changes, a similar construction methodology to that of the scenario for 2021-2050 was used. Fifty 1000-yr synthetic daily precipitation series were produced using a weather-state series generated using the high-phase NAO scenario. This used the new parameters for the SW and WW weather states given in Table 7-24, and old parameters for the other weather states (Table 5-43). This provides the summer precipitation decrease and winter precipitation increase detailed in Table 7-21. The methodology detailed in Section 7.1.1 was then applied to the precipitation series for the eastern and western NSRP spatial models to produce a 1000-yr precipitation series for each of the 28 sites, giving monthly and annual cross-correlations of 0.14 and 0.20 respectively.

The same PE increase of ten percent was then applied. An adjustment was also made for change in summer precipitation of –9 percent (see Table 7-21). Therefore, the same equations as Section 7.3.1.2 were used, only the precipitation gradient was divided by 0.91. This simulates an instance of summer precipitation decrease of nine percent coupled to a 10 percent increase in PE. This gave Equations 7-26 to 7-30:

WRINCLE92(CC2080)	$PE = -0.178\,ppt + 749.85$	(7-26)
WRINCLE98(CC2080)	$PE = -0.191\,ppt + 741.09$	(7-27)
Wharfe(CC2080)	$PE = -0.184\,ppt + 746.58$	(7-28)
Ouse(CC2080)	$PE = -0.184\,ppt + 748.62$	(7-29)
Derwent(CC2080)	$PE = -0.238\,ppt + 732.83$	(7-30)

An annual PE series was generated based on the summer totals of the synthetic precipitation series using Equations 7-26 to 7-30 and disaggregated monthly using the percentages in Table 7-26. Inflows were then produced using the synthetic 1000-yr daily precipitation series

generated for this scenario and the disaggregated PE series. These inflow series were used as input to the YGrid2000 model to determine how future changes in PE, both annual magnitude and monthly distribution, may affect water supplies.

It can be observed in Table 7-36 that the reliability of water supplies to many of the demand centres is similar or improved when compared to that of the baseline scenario. In fact, the only likely reductions in reliability during the 2051-2080 time-period are at Calder, Leeds, Sheffield and Wakefield, and these are small. Overall, the total reliability of water supplies in the grid is slightly improved during 2051 to 2080. The resilience of water supplies is in all cases reduced by 2080 however. The vulnerability of water supplies is markedly increased at almost all demand centres, excepting Bradford and Harrogate. The failure duration reaches a total duration of 222 days for the whole grid, which can be compared to 165 days during the period 1961 to 1990. The magnitudes of failure are also substantially greater than that of the baseline scenario. The total grid deficit is increased to 10 percent larger than the baseline scenario, but only two percent greater than the period from 2021-2050.

Demand	Reliability	Resilience	Vulnerability	
			Duration (days)	Extent (Ml)
Skipton	1.000	–	–	–
Bradford	0.926	0.411	17	592.2
Calder	0.840	0.190	112	8962.6
Harrogate	0.957	0.695	16	37.0
Malton	0.999	0.092	41	673.8
Leeds	0.898	0.199	104	28649.4
Wakefield	0.874	0.049	180	19720.8
Doncaster	0.999	0.092	41	556.4
Sheffield	0.881	0.045	148	22271.4
Total	0.736	0.139	222	81955.8

Table 7-36: 2051-2080 scenario: reliability, resilience and vulnerability statistics for demands. Total refers to failure to supply at least one demand centre.

The likelihood of conjunctive failure of water supplies is also increased during the period from 2051 to 2080. These increases are not particularly large. However, an interesting development is that those demand centres reliant upon reservoir resources seem to be failing less than those reliant upon at least a minimum abstraction from river sources. Hence, the Bradford demand centre shows a reduction in conjunctive failure with all other demand centres. However, the Sheffield, Wakefield and Leeds demand centres exhibit an increase in conjunctive supply failure. The likelihood of occurrence of severe droughts is not increased markedly during the period from 2051 to 2080. The return period for a 1995-96 drought event is one in 125 years.

However, when such events occur they are likely to be more severe than the 1995-96 drought, in terms of both duration and magnitude.

	Skipton	Bradford	Calder	Harrogate	Malton	Leeds	Wakefield	Doncaster	Sheffield
Skipton	–	0.00	0.00	0.00	0.00	0.00	0.00	0.00	0.00
Bradford		–	3.62	0.85	0.00	0.00	0.00	0.00	0.33
Calder			–	3.79	0.05	10.05	10.38	0.05	7.49
Harrogate				–	0.01	2.98	1.88	0.01	1.95
Malton					–	0.05	0.05	0.05	0.05
Leeds						–	9.08	0.05	6.45
Wakefield							–	0.05	7.31
Doncaster								–	0.05
Sheffield									–

Table 7-37: 2051-2080 scenario: likelihood of conjunctive failure of supply to demand centres as percentage of total simulation time.

	Reliability			Minimum Storage	
	1st level	2nd level	3rd level	Ml	% Maximum
Washburn	0.6495	0.9569	–	2365.0	10.1
Winscar	1.0000	1.0000	–	7057.0	75.2
Pennine	0.8817	0.9998	–	4296.0	12.0
Nidd/Barden	0.9982	1.0000	–	8606.0	44.9
Grimwith	0.9897	1.0000	–	4741.0	21.8
Worth Valley	0.9967	1.0000	–	1552.5	46.9
Calderdale	0.9986	1.0000	–	3894.6	33.3
Boothwood	0.9995	1.0000	–	6419.3	55.8
Huddersfield	0.9997	1.0000	–	5662.9	40.1
Brownhill	1.0000	1.0000	–	3062.4	51.7
Wharfe	0.9330	0.9050	0.9140	–	–
Ouse	0.9440	0.9310	0.9990	–	–
Derwent	1.0000	–	–	–	–

Table 7-38: 2051-2080 scenario: reliability of sources.

Source reliability is again likely to improve on average during the period from 2051 to 2080. However, the drawdown of certain reservoir sources will reach lower minimum levels. The major effect upon the Yorkshire water supply grid will again come from increased low flow in rivers during summer drought events. The grid is particularly vulnerable to low flow in the rivers Ouse and Wharfe. Although the likelihood of failure at level one is reduced, the likelihood of no water abstractions is increased to some nine and one percent of the simulation time for the rivers Wharfe and Ouse respectively. The increased severity of drought events may be a result of the increased persistence and frequency of low-flow events.

7.4 Discussion

The impacts of natural climatic variability were examined as well as the impacts of potential future climate change. A summary of results is given in Table 7-39. Natural climatic variability may play a large role in the frequency of occurrence of drought events and their magnitude within Yorkshire and elsewhere in the UK. The impacts of natural climate variability were examined using the NAO. An assessment was made of the changing risk of drought events and the effect upon water resource reliability, resilience and vulnerability of low- and high-phase NAO events. During a low-phase NAO summer precipitation across the UK is increased and there is reduced seasonality. During a high-phase NAO, however, enhanced seasonality causes a reduction in summer precipitation and increases in winter precipitation across much of the UK.

Scenario	Change in annual PE (% from baseline)	Change in precipitation amount and (variability) (% from baseline)		Change in average water supply reliability (% from baseline)	Change in total grid resilience (% from baseline)	Change in total grid vulnerablity (% from baseline)		Return period of 1995 drought event (years)
		Winter	Summer			Duration (Days)	Extent (Ml)	
Baseline (1961-90)	–	–	–	–	–	–	–	166
High-NAO	–	+2	–1	-0.1	-1.2	+14.5	+12.8	100
Low-NAO	–	–3	+5	+1.3	+0.6	-9.1	-0.8	1000
2021-2050 PE Only	+6	–	–	-1.4	-4.1	+21.2	+16.6	111
2051-2080 PE Only	+10	–	–	-2.7	-5.9	+21.8	+28.1	91
2021-2050 PE + PPT	+6	+9 (+5)	–5 (+10)	0.0	-10.7	+18.8	+8.8	143
2051-2080 PE + PPT	+10	+16 (+15)	–9 (+10)	-0.3	-17.8	+34.5	+9.9	125

Table 7-39: Summary of results.

During a high-phase NAO, water supply reliability is slightly decreased at all major demand centres within Yorkshire. However, vulnerability is significantly increased, showing that when supplies fail they fail more severely. This is true both of duration of failure, and shortfall in Ml (see Table 7-39). The Calder, Leeds and Wakefield demands are increasingly vulnerable under a high-phase NAO. This increased vulnerability is also reflected in the likelihood of occurrence of a drought event as severe as that of 1995-96. Under a high-phase NAO this is reduced to a one in 100-yr event, occurring 10 times in 1000 years of simulation compared to six times under the baseline scenario from 1961 to 1990. Reliability of sources is generally improved due to increases in winter precipitation. However, reduced summer precipitation lowers the minimum reservoir storage level and increases the severity of failure when it occurs.

Under a low-phase NAO, the opposite effect is observed. Supply reliability is significantly improved when compared to the baseline scenario and supply vulnerability is decreased. The extent of the total grid shortfall is reduced by approximately 1000 Ml. This increased reliability in supply is also reflected in the drought severity statistic. A drought as severe as the 1995-96 drought would only be expected once every 1000-yrs under a low-phase NAO. This constitutes a huge reduction in frequency upon the baseline scenario. Conjunctive failures are also significantly reduced. The likelihood of source failure is also significantly improved when compared to the baseline scenario. This is due to increased summer precipitation and similar winter precipitation to the baseline scenario. The increased summer precipitation during a low-phase NAO event is seen to significantly reduce the risk of severe drought in Yorkshire.

The impact of future climate change upon water resources in Yorkshire was assessed using a two-tiered approach. Firstly, the effects of change in potential evaporation (PE) were assessed, and then the combined effects of change in precipitation and PE. Two scenarios were examined: 2021-50 and 2051-80.

Water resources in Yorkshire are likely to become increasingly vulnerable to severe drought events under future climate change. Both PE-only scenarios suggest a large increase in water supply vulnerability and the incidence of severe drought. This is due to an overall reduction in source reliability. In the 2021-2050 PE-only scenario, the maximum extent of supply vulnerability is increased by almost 15 percent when compared to the baseline. This is increased further to 22 percent if the 2051-2080 PE-only scenario is considered. The grid reliability shows a reduction of three and seven percent respectively for the two scenarios. The likelihood of conjunctive failure is also increased in both scenarios.

The likelihood of a drought as severe as the 1995-96 drought event is also increased. For the 2021-2050 PE-only scenario, this is now a one in 111 year event, and by 2051-80 it has become even more frequent, a one in 91 year event. Therefore, under the 2051-80 PE-only scenario the likelihood of severe drought is almost doubled when compared to the baseline scenario. In general, source reliability is not significantly reduced in either PE-only scenario. However, the rivers Wharfe and Ouse show a reduction in reliability at all levels, but especially at the lower levels of failure.

These results are interesting but must be combined with likely precipitation changes for the potential impacts of future climate change upon water resources in Yorkshire to be accurately assessed. Precipitation changes were assessed using the UKCIP98 climate change scenarios, and

adjusting the parameters of the SW and WW weather states within the spatial NSRP models. The combined impact of precipitation and PE changes upon water resources was then examined.

The 2021-50 and 2051-80 climate change scenarios produced water supply reliability results very similar to that of the baseline scenario. Indeed, in some cases the overall reliability of water supply to a demand centre is actually improved. However, the resilience of water supplies is reduced for all demand centres. The increased vulnerability of the system to severe drought events is also shown by the increase in cumulative supply deficits and duration of failure. The total duration of the most severe drought is increased from 165 days in the baseline scenario, to 196 days by 2050. This increases to 222 days by 2080. The total cumulative grid supply deficit is also increased by nine percent and ten percent respectively for the two scenarios. Interestingly, the occurrence of severe droughts is only slightly raised. The return period for a drought as severe as the 1995-96 drought is once in 143 years by 2050 and once in 125 years by 2080. However, as can be seen in the increased vulnerability statistics, the important fact is that these droughts will be more extensive in both magnitude and duration than severe historical droughts.

Source reliability is on the whole, improved by 2050. Reservoir sources exhibit increased reliability and many show an improvement in minimum levels. By 2080, however, minimum levels may again fall. The major impact on the Yorkshire water supply grid comes from increased low flow in rivers during summer drought events, as the grid is particularly vulnerable to low flow in the rivers Ouse and Wharfe. The reliability of river sources is substantially reduced, particularly at the third fail level where no abstraction is allowed for both climate change scenarios, and particularly by 2080. The increased severity of drought events is due to the increase of low-flow events, and a possible increase in the persistence of low-flow events on the rivers Wharfe and Ouse.

Chapter 8: Conclusions

"I think the world, for far too long, has simply treated this issue of climate change as not sufficiently important - well that's no longer an option."

UK Prime Minister, Tony Blair, 3rd November 2000

The importance of taking climate change issues seriously has recently been raised by the Prime Minister, Tony Blair, following the devastating floods of autumn 2000. Planning for future climatic variability and change is now high on the political agenda. It is essential to remember, however, that this 'climate change' may simply be part of the natural variability of the climate system. Future climate in the UK will be different from that of 1961-90, even without any human influence on the climate system. The magnitude of changes due to natural climate variability may be as great as those felt from anthropogenic effects. It is therefore essential to examine historical variability of the climate system, placing current and future climate change and variability into context. Likely future climate change impacts can then be assessed.

In Yorkshire, the impacts of future climatic change and variability may be widespread. The worst floods on record in York have recently caused the evacuation of 3000 homes, and brought flood defences to within inches of being overrun. Other areas have suffered two 100-year flood events in three weeks. These events have occurred only four years after the worst drought on record. The 1995-96 drought capped a run of very dry summers from 1988 and produced a huge deficit in water supplies, especially in the Bradford and Calder areas.

This study has investigated the impacts of climate change and variability on the normal spatial precipitation pattern and the impact of this on water supply in Yorkshire. In the 1995-96 drought, unusual precipitation variability resulted in severe stress to the Yorkshire water supply, necessitating the emergency measure of tanking in water from outside the region. An examination of natural climate variability in Yorkshire using long-term records was presented in Chapter 3. This was followed by an assessment of the incidence of historical drought in Chapter 4. This led to the development of two stochastic spatial precipitation models in Chapter 5 that are capable of preserving historical precipitation statistics at 28 sites within the region. These are conditioned using weather type information, linking precipitation to large-scale atmospheric circulation. The sensitivity of the region to natural climatic variability was examined in Chapter 7 using the example of low- and high-phase NAO, and rainfall-runoff models calibrated in Chapter 6. Finally, the impacts of climate change scenarios for 2021-50 and 2051-80 on water resource reliability, resilience and vulnerability were quantified in Chapter 7. It is likely that

water resources in Yorkshire will become increasingly vulnerable to severe drought events in the future.

8.1 Summary

An investigation has been made into variations in the normal precipitation pattern in Yorkshire and how these may translate into impacts on the water supply system. Historical precipitation variability has been examined, to provide a context of natural climatic variability in which to view future climate change. Long-term daily precipitation records show a declining trend of summer precipitation throughout the region starting in the 1960s, coupled with an increase in winter precipitation at western sites since the 1970s. These changes can be linked to the large-scale atmospheric circulation. A high winter-NAO since the mid-1970s is likely to have caused the increase in winter precipitation at western sites. The opposite effect is observed for summer-NAO, which has been mainly negative since the 1960s and has contributed to declining summer precipitation totals. The NAO and precipitation can be correlated at temporal aggregations down to the monthly level, and show highly significant relations, particularly at western sites. Precipitation variability is also linked to synoptic weather type occurrence. The frequency of the major Lamb weather types is intimately linked to both the NAO and precipitation receipt.

Drought in Yorkshire was found to be as much a function of a dry spring and summer, as of a dry winter. Major drought events over the past 100 years have been primarily caused by a dry summer and shortfalls can be large due to the reliance upon single-season reservoir resources and river abstractions. It is important to realise that the occurrence of drought is intimately linked to the frequency of synoptic weather types. These control precipitation receipt within the Yorkshire region and are strongly related to the phase of the NAO. Drought in Yorkshire is characterised by changes to the normal synoptic weather patterns. An increase in anticyclonic and northerly weather types is generally accompanied by a decrease in westerly and cyclonic occurrence. Percentage changes can be very large and these determine drought severity. An analysis of historical drought suggests that the severe drought of 1995 lies within historical variability. However, it is notable that recent drought events have had a very rapid onset compared to earlier droughts. This may be a result of the enhanced hydrological cycle under global warming cited by many researchers or the very strongly positive NAO during 1995-96, or both.

The high correlation between synoptic weather types and precipitation also allowed the development of a spatial stochastic rainfall model conditioned using weather types. Daily

precipitation statistics were used to split Yorkshire into three distinct precipitation sub-regions. The objective Lamb weather types were then clustered into sub-groups based on precipitation receipt in the three sub-regions. This demarcation was performed using experience gained from the assessment of historical climate variability and drought within the Yorkshire region. A semi-Markov chain model was developed to reproduce observed weather state persistence and transition probabilities and allow the synthesis of long daily weather state series. A Neyman-Scott Rectangular Pulses model was then parameterised using historical data from the 1961-90 period for two spatial models of the east and west of Yorkshire. These models were found to reproduce observed precipitation statistics and accurately preserve daily cross-correlations between sites.

This enabled the examination of both natural climatic variability and the impacts of future climate change upon precipitation receipts. The structure of the stochastic rainfall model allows both variations in weather state persistence and frequency, and changes to internal weather state properties to be investigated. The impacts of natural climatic variability and future climate change were assessed using rainfall-runoff models calibrated for 13 inflows required for a model of the Yorkshire water supply grid. These were calibrated for the baseline period 1961-1990, with parameters assumed to stay constant under a future climate.

The YGrid2000 model was developed to simulate the Yorkshire water supply grid, due to the inadequacies of the YG97 model for the analysis of long data sequences. A synthetic baseline scenario was produced for 1961-90 and the reliability, resilience and vulnerability of water supplies in Yorkshire were compared to those generated using historical data from 1948-96. It was observed that low flows are not generated by the rainfall-runoff models with high enough frequency when the baseline is compared to historical flows. An improvement would therefore be to increase the fitting of low flow events by the rainfall-runoff model, possibly at the expense of accurately simulating high flow events. Other statistics were well simulated by the baseline scenario.

Natural climatic variability was examined using the example of high- and low-phase NAO. The reliability of water supplies was found to vary by only a few percent. However, the frequency of severe drought events was found to be highly dependent upon the phase of the NAO. During a high-phase NAO, a drought of the same magnitude as that of 1995-96 can be expected once every 100 years. This reduces to once every 1000 years during a low-NAO. This natural variability causes large difference in water supply vulnerability between the two scenarios.

The impacts of future climatic changes were also assessed using the UKCIP98 climate change scenarios for 2021-50 and 2051-80. Results suggest that the overall reliability of water supplies

will remain constant or improve when compared to the baseline scenario. However, water supply resilience, the ability of a water supply to rebound after failure, is reduced at all demand centres. The water supply system in Yorkshire becomes increasingly vulnerable to drought under the examined climate change scenarios, although severe drought events comparable to that of 1995 show only a slight increase in frequency by 2080. However, there will be a significant increase in both magnitude and duration of severe drought. This is indicated by the increases in both the magnitude and duration of water supply failure.

The results of this investigation into the effects of natural climatic variability and future climate change on water resources in Yorkshire suggest that:

1. Current natural climatic variability may produce more frequent severe drought events than is estimated for the examined future climate change scenarios.
2. In the future, there will be an exacerbation of severe drought, with increases in both magnitude and duration. This is due to a combination of increases in summer PE and declining summer precipitation that will increase the likelihood of summer water shortages.
3. Although an increase in winter precipitation will improve water resource reliability on average, increased variability coupled with decreased summer precipitation may mean that in the future a dry winter will produce a more severe drought in single-season reliant regions than under current climatic conditions.
4. There will be an improvement in water supply reliability but declines in resilience and vulnerability statistics under the examined future climate change scenarios.

Linking the prevalence of synoptic weather patterns and precipitation receipts to the NAO may yet provide an important predictor of future hydrological drought in Yorkshire however. Strong connections have been found between winter precipitation totals and the winter-NAO, particularly in western Yorkshire, where most surface water supplies are located. If winter NAO can be predicted in advance then it may be possible to forecast the winter replenishment of water resources in western Yorkshire. Water managers in Yorkshire may be able to use this and possible future climate scenario information to alleviate some of the problems that have been associated with severe droughts of the past and allow the forward planning and prioritisation of water supplies in the future.

8.2 Discussion and conclusions

8.2.1 Examination of historical climate records

Precipitation data from seven long-term daily records around Yorkshire, UK, were examined for evidence of climate change. At all stations, there is evidence of a decline in summer (JJA) precipitation of 20 percent on average since the 1960s. This is most marked at western sites, which also exhibit a concurrent and similar magnitude increase in winter (DJF) precipitation totals. However, there is no significant change in annual precipitation, even at western sites. Since 1975, increased winter precipitation at western sites has occurred mainly during March, approximating a 30 percent increase. There is also a slight increase in March precipitation at eastern sites in the post-1975 period, with a lowering of both July and February totals.

An analysis of inter-annual and inter-seasonal variability in precipitation receipt has highlighted the recent partitioning of summer and winter precipitation regimes. The winter/summer precipitation ratio was high during the early 1990s, with six from seven years (1990-1996) ranking in the top 13 places of a 123-yr record. Over the entire region, six of seven years from 1990-1996 are found in the 23 driest summers, from a 123-yr record. Annually, however, the 1990s are not particularly dry due to wetter than average winters. An analysis of PD shows similar trends, with increases in summer and decreases in winter months. During the winters of 1992 and 1993, however, a high PD is linked to high precipitation totals. This may be related to increased convective activity in the winter that has been suggested by both Gregory and Mitchell (1995) and Osborn *et al.* (1999).

Although there appears to have been a shift towards longer dry spells in western Yorkshire, and longer wet spells in eastern Yorkshire since the early 1970s this is not reflected in an extreme value analysis. In the west of the region, the frequency of 24-hr extreme precipitation occurrence is similar in the pre- and post-1975 periods. In eastern Yorkshire, there has been a slight decrease in 24-hr extreme events since 1975.

Linkages between the NAO and precipitation showed that a high-phase winter-NAO is related to higher winter precipitation totals at western sites and lower totals at eastern sites. At western sites, annual totals also exhibit a significantly positive relationship with the NAO. Significant correlations were also found between winter PD and the NAO. These are positive at eastern sites and negative in the west, suggesting change in winter precipitation receipt is mainly due to increased wet day frequency rather than wet day amount. For low NAO winters, conversely, positive anomalies were found at eastern sites and large negative anomalies at western sites. In summer, no significant relationships were found.

The NAO and precipitation were also linked on a monthly time-scale. High correlations were obtained between monthly-NAO and winter precipitation at western sites, with low correlations in summer. At eastern sites, high correlations are obtained only in July (positive) and October (negative), the declining NAO in July contributing to reduced July precipitation totals. The monthly-NAO index has increased dramatically in recent years during January, February and March. This has increased precipitation during these months at western sites, such as Moorland Cottage. However, a declining monthly-NAO since the mid-1980s has caused a decrease in precipitation receipt at western sites during autumn months.

The NAO controls the frequency of occurrence of different weather types across the UK. Therefore, weather states defined in Chapter 5 were linked to the NAO. A positive relationship was found between the monthly-NAO and occurrence of the westerly-weather state for all months. The correlation is particularly strong in the month of March, at 0.932, and may account for the increased precipitation totals during March in Yorkshire. Importantly, all three weather states display a close link to monthly-NAO. This has large implications for the prediction of monthly precipitation totals in regard to water resources and the prediction of droughts.

The effect of low and high winter-NAO phases upon precipitation totals, PD and variability at a western site was examined. Mean daily precipitation for 'winter' weather states is increased during a high phase winter-NAO and is, conversely, decreased during a low phase. For summer weather states there is little change. The 24-hr PD is, in general, reduced during a low phase winter-NAO and increased during a high phase. Variability of summer and winter westerly weather state precipitation is noticeably enhanced during a low phase, but northerly and anticyclonic weather states show reduced variability. These relationships are reversed during a high phase.

The main conclusions of this investigation of natural climatic variability are that:

1. There has been declining summer precipitation since the 1960s in Yorkshire.
2. At western sites, there has been increasing winter precipitation since the 1970s.
3. Extreme daily events show no increase from 1873 to present.
4. Precipitation receipt is intimately linked to both the NAO and frequency of weather type occurrence on monthly, seasonal and annual levels.
5. Strong connections between winter precipitation totals and the winter-NAO, particularly in western Yorkshire, where most surface water supplies are located, may be very important in the prediction of precipitation. Recent research (Sutton and Allen 1997; Rodwell *et al.*

1999) suggests that the winter-NAO may be predicted in advance using sea surface temperature. It may therefore be possible to estimate the winter replenishment of many Pennine reservoirs a few months, or possibly a year, in advance.

6. This may provide an important predictor of future hydrological drought episodes and allow the forward planning and management of many water resource systems located in western regions.

8.2.2 Examination of historical drought events

Much of Yorkshire is dependent upon a large number of single-season upland reservoirs in the Pennine hills to provide water supplies. Single-season reservoirs are especially sensitive to droughts lasting through one summer season, i.e. six to nine months. Most of the major water-resource droughts in Yorkshire during the last century have involved a very dry spring and summer, although a dry winter will also cause water shortages.

Fourteen Class I droughts have occurred in Yorkshire since 1900 and appear to be highly spatially variable in impact, in both severity and duration. Aggregated OWT patterns (see Chapter 5) associated with these drought events suggest three main types of drought in Yorkshire: the 'eastern' drought, the 'Pennine' or 'western' drought, and the 'regional' drought. However, as most of Yorkshire's water resources are located in the Pennines then 'western' droughts will be the most important in water resource terms.

Regional droughts are generally characterised by an increased frequency of anticyclonic weather types and a concurrent decrease in rain-bearing weather types, particularly the cyclonic types. The directionals (S&W and N&E) may also exhibit large decreases. Eastern droughts are characterised by a decreased occurrence of easterlies and cyclonic easterlies. Most commonly, these decreases are countered by an increase in frequency of the westerly weather type. The drought may also be increased in severity by an increased frequency of anticyclonic types.

Western droughts are generally characterised by a significant increase in northerly weather types. This may also be supplemented by an increased frequency of anticyclonic types that will define the severity of the drought. Most western droughts also show a decrease in the number of westerly days, although this may not be severe. A decrease in the occurrence of heavy precipitation days is also apparent for the more severe droughts.

Two types of western drought are distinguishable. The first type is caused by a dry winter followed by an average or dry summer. This type of drought occurs due to a lack of winter replenishment of water resources. The second type occurs due to the drawdown of resources during a very dry summer. Recent drought events in western Yorkshire, including the 1995 drought, have been as much the function of a dry summer as a dry winter. Most water resource droughts in Yorkshire involve the increased incidence of anticyclonic and northerly weather types during summer months, coupled with a decreased frequency of westerly types. The summer droughts of 1948/49, 1959/60, and 1975/76 were characterised by a large increase in the incidence of anticyclonic weather types. In contrast, the 1995 drought exhibited a large increase in the occurrence of northerly types. Percentage changes can be very large and reach over 90 percent for anticyclonic types in 1949. It can be noted, however, that the 1995 drought was no more severe than any other drought, and particularly similar to the 1976 drought, in terms of a weather type classification.

An analysis of the historical weather type record, using weather type information for drought delineation, clearly shows a clustering of probable drought events during the 1880s and 1890s that are generally forgotten now. The period from 1886-88 is the most severe drought on record in all categories, excepting winter. The drought of 1995/96 is the fifth most severe summer-winter drought in the period from 1881 to 1996. This is raised to the third most severe drought if the summer of 1996 is also included, starting in April 1995 and ending in September 1996. This severity, and the unusual nature of the drought; being driven by increased occurrence of northerly weather types rather than anticyclonic types, led to the water supply crisis in western Yorkshire during 1995/96.

This analysis shows that:

- The recent clustering of drought events during the late 1980s and 1990s is within historical variability. Indeed, evidence suggests that the 1880s and 1890s may have had more severe drought events than during recent years.
- Recent drought events in western Yorkshire, including the 1995 drought, have been as much the function of a dry summer as a dry winter.
- Most water resource droughts in Yorkshire involve the increased incidence of anticyclonic and northerly weather types during summer months, coupled with a decreased frequency of westerly types.
- In the context of the historical past, the 1995/96 drought is not a rare event. However, it must be remembered that it is not necessarily the number of days of occurrence of a

particular weather type that may be important for drought initiation. The sequencing and persistence of a weather type may play an equally prominent role.

- Although recent droughts have not been unusual occurrences in a historical sense, they have had a rapid onset. This is in contrast to earlier droughts where large water deficiencies took much longer to develop. In this sense, recent droughts have followed a different pattern to that of previous historical drought events, both the 1992 and 1995 sequences taking only three months to develop. This may be a result of the enhanced hydrological cycle cited by many researchers, as associated with global warming.
- The 1995 drought was also unusual, as the controlling factor was a large increase in the incidence of northerly and easterly weather types, whereas normally a larger increase in anticyclonic conditions would be expected.

8.2.3 Development of a spatial-temporal stochastic precipitation model for Yorkshire

A regional stochastic rainfall model was developed conditioned on weather types. The spatial dimension of the model allows the concurrent simulation of precipitation series for very different climatological sub-regions within the same water resource area. The separate fitting of each weather state provides this spatial variation for a region. In Yorkshire, this split is between the east and west of the region, as the dominant westerlies bring much precipitation to the high ground of the Pennines in the west, with lower precipitation in the lee to the east. Conversely, in easterly airflows, most precipitation falls in the east, with little reaching the Pennines. The normal precipitation pattern has resulted in the installation of supply reservoirs, predominantly in the Pennines to the west of the region.

Daily precipitation statistics at multiple sites within the region of Yorkshire were linked to the OWTs and used to split the region into three distinct precipitation sub-regions. Using a variance minimisation criterion, the 27 OWTs were then clustered into three physically realistic groups or 'states'. A semi-Markov chain model was then used to synthesise long sequences of weather states, maintaining the observed persistence and transition probabilities. The Neyman-Scott Rectangular Pulses (NSRP) model was then fitted for each weather state, using a defined summer and winter period. A spatial model was then developed for an eastern and western sub-region. The combined model reproduces key aspects of the historic precipitation regime at temporal resolutions down to the hourly level.

The coupling of a semi-Markov based weather generator parameterised on historical data, with a stochastic rainfall model, such as the NSRP model, is extremely powerful. It permits investigation into not only the impacts of variations in weather type persistence or frequency, but also the alteration of rainfall model statistics to simulate instances of increased intensity or proportion of dry days for example, for an *individual* weather class. A *transferable common methodology* is provided for classification, weather-state simulation and subsequent precipitation modelling. The OWTs provide a classification system that is easy to understand, simple to use and has a substantial physical basis in climatology. Weather clusters are delineated using the climatology of the water resource area being studied and weather types are clustered based on a simple variance minimization routine.

The weather type approach improves upon the 'factor' approach adopted by many researchers (e.g. Arnell and Reynard, 1996) and used by UK water companies in recent climate change assessments. That approach simply modified observed precipitation records by a factor change to the mean derived from GCM simulations, resulting in no changes to the temporal and spatial structure of the precipitation fields. The approach described here uses series of weather types to provide the temporal sequence and high time-aggregation behaviour, and the NSRP model to reproduce hourly and daily statistics of precipitation. The methodology allows the results of GCMs to be used directly, via analyzed GCM OWTs, or indirectly, as trends in both weather-state and precipitation characteristics can be extracted and interpreted within the model.

The approach is very flexible, with limited parameter re-calibration required for the immediate application to another area. The use of a semi-Markov chain model as a weather-state generator requires the calibration of only three parameters for each weather-state in an automatic routine. Transition probabilities can be taken directly from the observed record. The model provides accurate simulation of OWT clusters and is applicable to other areas using the National Centers for Environmental Prediction (NCEP) reanalysis data. Although the main aim of the current application is in water resource management where aggregated daily and monthly flows are required, the NSRP methodology provides reproduction of the precipitation statistics at the hourly level, facilitating more detailed hydrological impact studies e.g. variations in river flows, flood risk estimation etc.

8.2.4 Risk analysis of the Yorkshire water supply grid

The impacts of natural climatic variability on water resources in Yorkshire were examined as well as the impacts of potential future climate change. Rainfall-runoff models were calibrated for flow input to the Yorkshire water supply grid model, using the ADM model. The stochastic

rainfall model conditioned on weather types was used to generate precipitation data series. Relationships between historical precipitation and PE data were derived and used to produce synthetic PE series. These data sources were then combined and used as input to these rainfall-runoff models to simulate natural climatic variability and future climate change scenarios.

The impacts of natural climate variability were examined using the NAO. An assessment was made of the changing risk of drought events and the effect upon water resource reliability, resilience and vulnerability of low- and high-phase NAO events. Under natural climatic variability the occurrence of a drought as severe as the 1995-96 drought was found to vary from a one in 100-yr event to a one in 1000-yr event. Likewise, water supply reliability was found to vary by only a few percent, decreasing during a high-phase NAO and increasing during a low-phase NAO. Water supply vulnerability however, shows significant natural variability, increasing significantly during a high-phase NAO, and decreasing during a low-phase NAO. Reliability of sources is also dependent upon natural climatic variability. Increases in winter precipitation improve overall reliability. However, reduced summer precipitation increases the severity of failure when it occurs.

The impact of future climate change upon water resources in Yorkshire was assessed using the UKCIP98 climate change scenarios for 2021-50 and 2051-80 (Hulme and Jenkins, 1998). Perturbations in both precipitation and potential evapotranspiration were examined. Precipitation changes were modelled by refitting the parameters of the SW and WW weather states with adjusted daily mean and variance statistics. The combined impact of precipitation and PE changes upon water resources was then examined. Water resources in Yorkshire are likely to become increasingly vulnerable to severe drought events under future climate change. The projected changes to water supplies in Yorkshire under the UKCIP98 Medium-High scenarios for 2021-50 and 2051-80 are:

- Water supply reliability is very similar to that of the baseline scenario. Indeed, in some cases the overall reliability of water supply to a demand centre is improved by 2080.

- The resilience of water supplies is reduced for all demand centres.

- The water supply system is increasingly vulnerable to severe drought events. This is shown by the increase in cumulative supply deficits and duration of failure.

- Source reliability is on the whole, improved by 2050. Reservoir sources exhibit increased reliability and many show an improvement in minimum levels. By 2080, however, minimum levels may again fall.

- The major impact on the Yorkshire water supply grid comes from increased low flow in rivers during summer drought events. The reliability of river sources is substantially reduced for both climate change scenarios, particularly in terms of increases in low flows where no abstraction is allowed.

- The increased severity of drought events is due to the increase of low-flow events, and a possible increase in the persistence of low-flow events on the rivers Wharfe and Ouse.

- The occurrence of severe drought is only slightly raised. The return period for a drought as severe as the 1995-96 drought is once every 143 years by 2050 and once in 125 years by 2080. However, the important fact is that these droughts will be more extensive in both magnitude and duration than severe historical droughts, and may occur more rapidly.

8.3 Recommendations for further research

This thesis has opened many avenues for further research. A few are briefly listed.

- The development of a semi-Markov chain model conditioned monthly, instead of seasonally, for different weather state transition and persistence probabilities would allow current monthly trends in weather type occurrence to be examined more accurately. However, this would be very complex and may be too difficult to calibrate successfully.

- To explore the non-stationary nature of weather pattern versus rainfall conditioning using long precipitation records to assess the stability and transferability of model parameters to future climate change scenarios. Presently, a constant baseline of 1961-1990 is assumed.

- To develop a stochastic spatial-temporal rainfall model conditioned on continuous atmospheric variables rather than the discrete Lamb weather types. This may improve the model's ability to simulate climatic extremes and allow some of the problems associated with the use of discrete weather types that are representative of the whole of the UK to be overcome.

- To reparameterise the stochastic rainfall model for Yorkshire with skewness fitting and additionally derived variance statistics included. This will significantly improve the

reproduction of extreme precipitation at the hourly level and enable the model to be used for the analysis of extreme events such as flooding.

- To apply the model to another water resource region within the UK. The use of the Lamb weather types should make the model easily applicable to other areas. This will prove the transferability and versatility of model design.

Many of these research proposals will be carried out under the auspices of the European SWURVE (Sustainable Water: Uncertainty, Risk and Vulnerability in Europe) project due to start in January 2001.

APPENDIX 1: Relationship between precipitation and Lamb Weather Types in Yorkshire

A1.1 Site details

Site	Mean Annual Precipitation (mm)	Proportion in winter half-year	Annual PD	Average annual rainday (mm)	Maximum summer half-year daily precipitation (mm)	Maximum winter half-year daily precipitation (mm)
35300	672	0.516	0.50	3.70	66.0	41.6
37225	660	0.524	0.52	3.78	76.6	66.3
38290	778	0.539	0.46	3.97	75.2	69.8
39164	657	0.535	0.52	3.79	73.6	55.0
43681	618	0.520	0.52	3.50	65.7	52.3
43941	667	0.514	0.51	3.77	63.6	40.7
44841	657	0.510	0.51	3.67	67.4	40.7
49268	1063	0.570	0.43	5.12	67.3	60.4
49308	969	0.567	0.46	4.88	68.9	58.0
49901	909	0.561	0.46	4.58	59.2	68.3
53904	605	0.502	0.55	3.66	64.9	52.1
55222	734	0.514	0.51	4.11	52.5	112.0
57427	1378	0.594	0.38	6.11	79.6	63.0
58460	872	0.548	0.47	4.49	69.8	80.1
58527	786	0.544	0.50	4.31	62.4	61.1
59792	595	0.496	0.57	3.83	54.0	48.5
60548	633	0.494	0.55	3.89	67.9	45.9
62254	1182	0.573	0.40	5.41	68.3	53.6
62350	924	0.556	0.45	4.58	61.4	50.9
62381	1009	0.563	0.40	4.62	56.6	54.2
63121	895	0.553	0.45	4.45	57.5	61.4
63187	902	0.551	0.45	4.47	64.7	58.7
63256	825	0.549	0.46	4.21	65.1	51.0
64281	654	0.514	0.54	3.86	63.0	50.6
64425	591	0.488	0.56	3.71	66.4	40.0
66446	654	0.542	0.53	3.83	78.2	43.1
66598	788	0.538	0.48	4.12	64.9	58.6
67183	635	0.522	0.57	4.02	50.7	71.1
71166	718	0.525	0.57	4.56	57.3	63.2
72415	703	0.511	0.55	4.32	58.4	68.7
74022	1205	0.583	0.46	6.09	66.7	57.8
74091	1046	0.580	0.46	5.31	53.1	44.6
74739	947	0.561	0.46	4.76	65.2	48.2
74852	1362	0.580	0.38	6.01	90.2	55.6
74921	1209	0.587	0.44	5.89	100.0	63.6
75150	860	0.572	0.47	4.44	76.0	44.2
75632	855	0.555	0.50	4.69	82.8	43.9
76203	753	0.532	0.50	4.11	75.8	46.2
77255	1398	0.575	0.39	6.25	121.1	57.4
77335	1469	0.585	0.38	6.50	75.5	78.7
77468	1091	0.586	0.46	5.51	73.0	51.6

Site	Mean Annual Precipitation (mm)	Proportion in winter half-year	Annual PD	Average annual rainday (mm)	Maximum summer half-year daily precipitation (mm)	Maximum winter half-year daily precipitation (mm)
77797	1321	0.570	0.39	5.91	67.6	72.1
77835	1288	0.586	0.41	5.99	86.2	63.5
78701	1484	0.584	0.39	6.69	104.9	73.9
79620	702	0.523	0.51	3.94	60.2	42.7
80281	637	0.504	0.58	4.11	63.3	40.5
80494	610	0.499	0.58	3.96	70.2	48.0
81698	990	0.567	0.43	4.78	97.5	57.6
82759	826	0.539	0.50	4.51	90.4	41.3
85321	757	0.526	0.52	4.33	75.4	52.0
47474	1419	0.622	0.41	6.57	80.4	61.8
62254	1182	0.573	0.40	5.41	68.3	53.6
26018	704	0.510	0.49	3.75	72.1	80.4
26323	626	0.500	0.49	3.39	52.3	61.4
28106	909	0.568	0.42	4.30	80.5	80.1
28408	765	0.543	0.48	4.04	64.9	67.3
29668	690	0.502	0.48	3.61	68.6	78.7
30581	640	0.495	0.54	3.79	48.8	78.0
33443	635	0.499	0.51	3.53	58.7	66.7
34458	797	0.513	0.46	4.05	56.4	104.6
108956	862	0.555	0.50	4.68	54.0	42.2
118731	680	0.501	0.60	4.66	55.8	50.0
122707	723	0.512	0.53	4.20	62.1	46.2
569708	1159	0.566	0.42	5.46	57.3	48.6
574611	1121	0.574	0.43	5.40	87.8	50.4
574719	1171	0.581	0.45	5.87	80.7	62.2
574785	1249	0.571	0.40	5.68	72.6	52.8
582626	1234	0.591	0.39	5.54	73.0	52.4
130884	638	0.496	0.61	4.49	67.4	41.2
131736	641	0.499	0.51	3.55	64.4	59.4
132210	628	0.495	0.58	4.05	66.1	35.7
132388	627	0.501	0.60	4.26	58.7	38.0
132917	677	0.509	0.52	3.87	92.8	46.0
132954	638	0.490	0.56	3.96	76.0	46.4
133220	638	0.510	0.53	3.70	62.4	50.9
134069	605	0.514	0.54	3.61	77.0	44.7
135028	584	0.523	0.56	3.67	57.6	37.7
135444	671	0.518	0.62	4.83	69.8	51.3
135886	683	0.511	0.52	3.92	56.3	42.5
137661	585	0.521	0.58	3.78	55.0	37.0
137710	700	0.509	0.54	4.16	48.8	46.5
140515	530	0.471	0.60	3.59	83.5	41.9
142001	609	0.481	0.54	3.61	56.0	45.0
142352	609	0.489	0.55	3.69	57.6	44.4
142694	569	0.514	0.62	4.14	52.6	38.6
143760	557	0.495	0.57	3.57	49.3	38.8
144141	614	0.502	0.52	3.51	59.1	38.3
146127	566	0.482	0.58	3.67	49.9	43.9
150032	604	0.499	0.55	3.67	62.4	38.6
150163	571	0.500	0.58	3.73	47.5	32.2

Table A1-1: Site statistics for 90 sites used in the OWT analysis. Data shown is for 1970-1990.

A1.2 Spatial variability in monthly yield of objective Lamb Weather Types

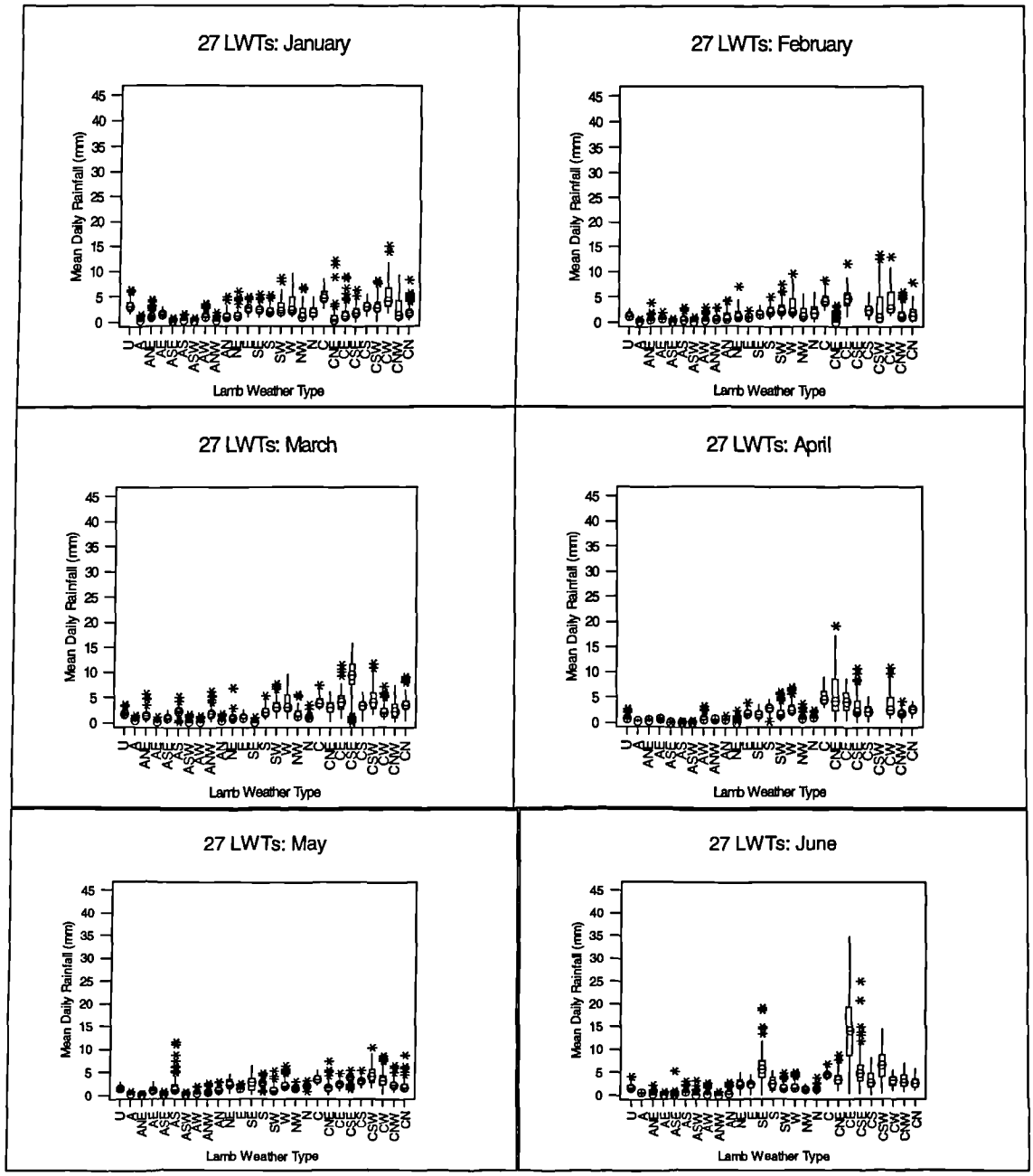

Figure A1-1: Box-plot of variability in monthly mean daily precipitation yields for the 27 objective weather types at sites in Yorkshire from 1961-1990 (January to June).

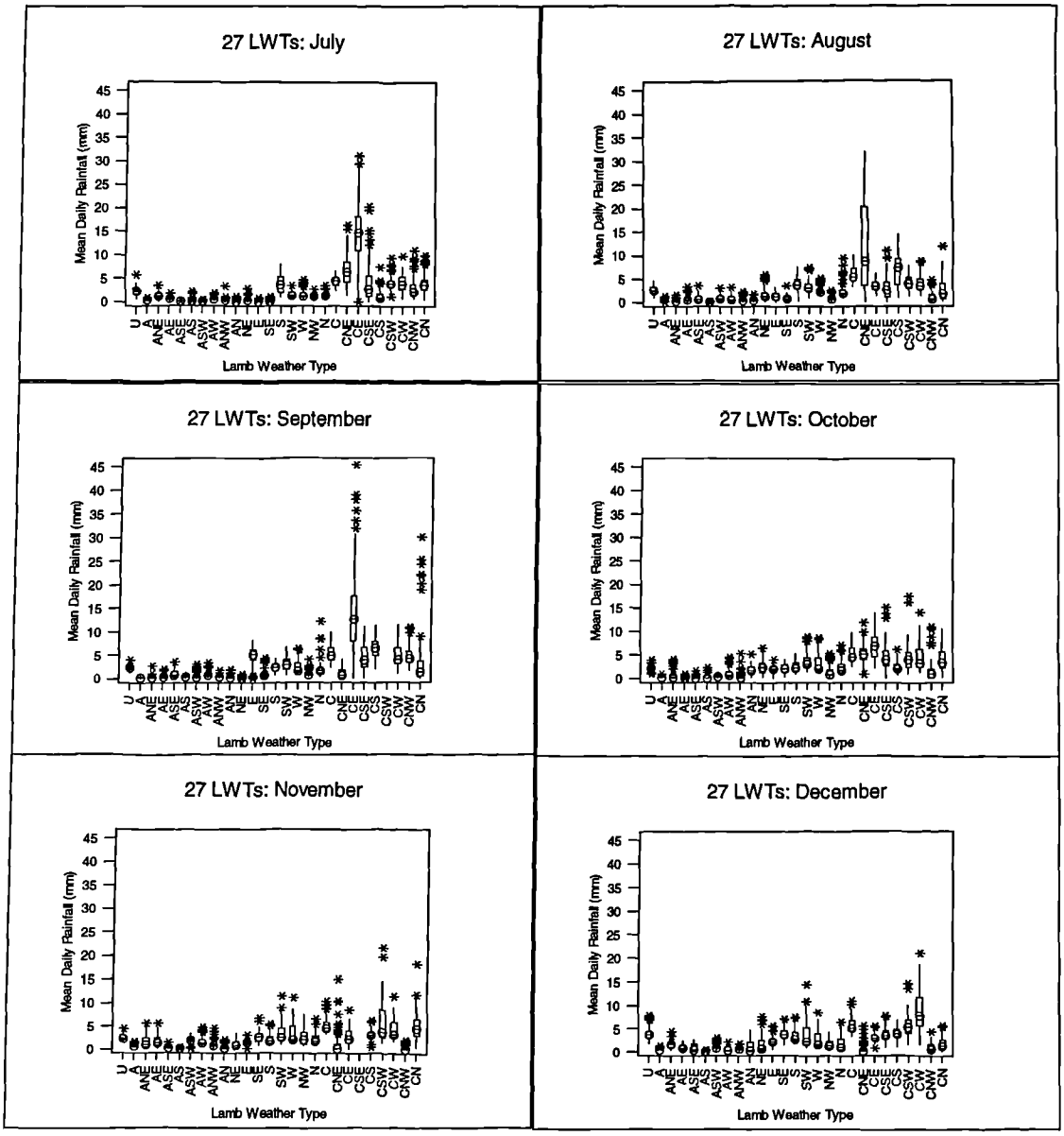

Figure A1-2: Box-plot of variability in monthly mean daily precipitation yields for the 27 objective weather types at sites in Yorkshire from 1961-1990 (July to December).

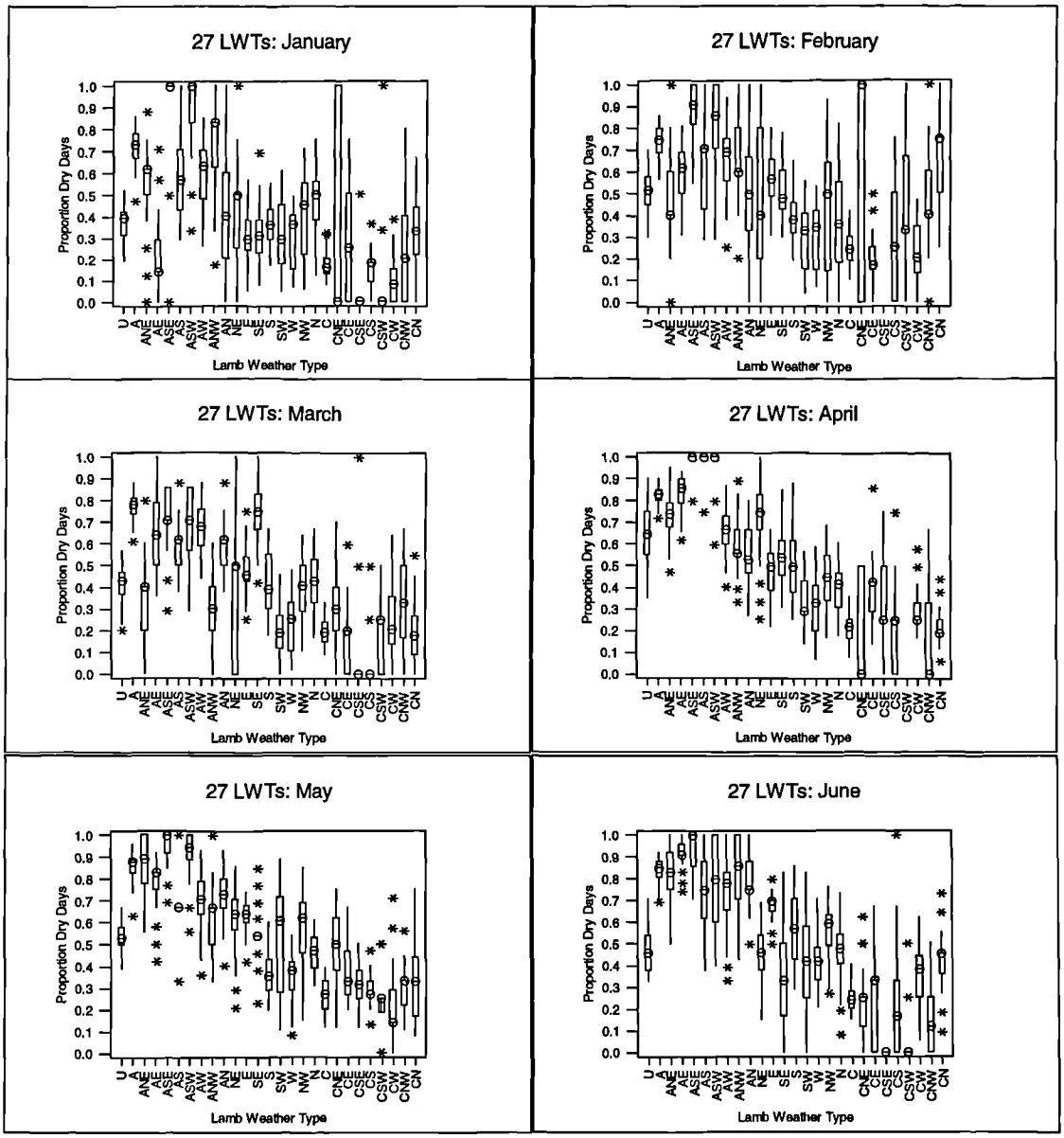

Figure A1-3: Box-plot of variability in monthly mean proportion dry days for the 27 objective weather types at sites in Yorkshire from 1961-1990 (January to June).

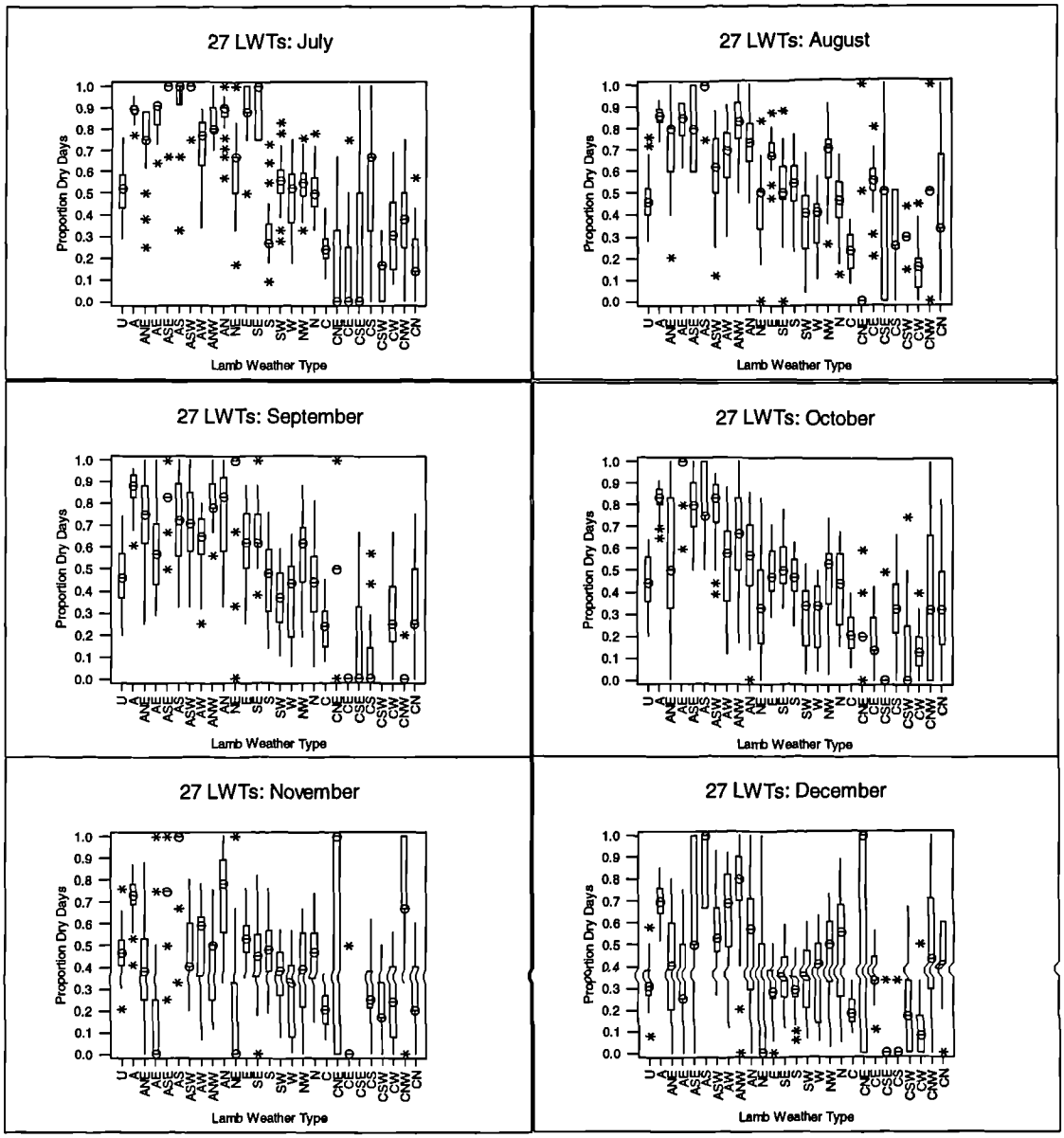

Figure A1-4: Box-plot of variability in monthly mean proportion dry days for the 27 objective weather types at sites in Yorkshire from 1961-1990 (July to December).

APPENDIX 2: Weather clustering analysis

A2.1. Site Cross-correlations

A2.1.1 Winter

	44841-P	60548-P	77797-P	87024-P	34458-P
44841-P					
60548-P	0.892				
77797-P	0.623	0.674			
87024-P	0.715	0.716	0.567		
34458-P				0.429	
47060-P	0.404	0.478	0.908	0.396	

Table A2-1: Site cross-correlations in winter using the mean daily precipitation statistic (1961-1990) for the 27 objective weather types. Correlations shown are statistically significant at the 95 percent level.

	44841-pd	60548-pd	77797-pd	87024-pd	34458-pd
44841-pd					
60548-pd	0.514				
77797-pd	0.381	0.717			
87024-pd	0.752	0.685	0.655		
34458-pd	0.597	0.466	0.374	0.598	
47060-pd	0.286	0.473	0.847	0.556	

Table A2-2: Site cross-correlations in winter using the mean proportion dry days (1961-1990) for the 27 objective weather types. Correlations shown are statistically significant at the 95 percent level.

A2.1.2 Spring

	44841-P	60548-P	77797-P	87024-P	34458-P
44841-P					
60548-P	0.812				
77797-P	0.376	0.73			
87024-P	0.724	0.914	0.666		
34458-P					
47060-P		0.497	0.893	0.447	

Table A2-3: Site cross-correlations in spring using the mean daily precipitation statistic (1961-1990) for the 27 objective weather types. Correlations shown are statistically significant at the 95 percent level.

	44841-pd	60548-pd	77797-pd	87024-pd	34458-pd
44841-pd					
60548-pd	0.666				
77797-pd	0.448	0.72			
87024-pd	0.528	0.645	0.615		
34458-pd					
47060-pd		0.405	0.776	0.461	

Table A2-4: Site cross-correlations in spring using the mean proportion dry days (1961-1990) for the 27 objective weather types. Correlations shown are statistically significant at the 95 percent level.

A.2.1.3 Summer

	44841-P	60548-P	77797-P	87024-P	34458-P
44841-P					
60548-P	0.885				
77797-P	0.788	0.829			
87024-P	0.929	0.921	0.766		
34458-P	0.396				
47060-P	0.389	0.429	0.749		

Table A2-5: Site cross-correlations in summer using the mean daily precipitation statistic (1961-1990) for the 27 objective weather types. Correlations shown are statistically significant at the 95 percent level.

	44841-pd	60548-pd	77797-pd	87024-pd	34458-pd
44841-pd					
60548-pd	0.894				
77797-pd	0.872	0.865			
87024-pd	0.876	0.794	0.764		
34458-pd	0.503	0.368	0.383	0.585	
47060-pd	0.678	0.663	0.847	0.537	0.466

Table A2-6: Site cross-correlations in summer using the mean proportion dry days (1961-1990) for the 27 objective weather types. Correlations shown are statistically significant at the 95 percent level.

A.2.1.4 Autumn

	44841-P	60548-P	77797-P	87024-P	34458-P
44841-P					
60548-P	0.729				
77797-P	0.549	0.621			
87024-P	0.654	0.69	0.56		
34458-P					
47060-P	0.426	0.56	0.816		

Table A2-7: Site cross-correlations in autumn using the mean daily precipitation statistic (1961-1990) for the 27 objective weather types. Correlations shown are statistically significant at the 95 percent level.

	44841-pd	60548-pd	77797-pd	87024-pd	34458-pd
44841-pd					
60548-pd	0.739				
77797-pd	0.813	0.837			
87024-pd	0.646	0.845	0.715		
34458-pd	0.599	0.596	0.632	0.516	
47060-pd	0.729	0.85	0.906	0.678	0.534

Table A2-8: Site cross-correlations in autumn using the mean proportion dry days (1961-1990) for the 27 objective weather types. Correlations shown are statistically significant at the 95 percent level.

A2.2 Cluster details

A2.2.1 Winter

k	2	3	4	5	6	7	8	47060		77797	
LWT								MDR	PD	MDR	PD
U	2	3	3	2	3	3	1	4	0.5	3.6	0.6
A	2	2	2	5	2	2	2	2.7	0.7	1.8	0.7
ANE	2	2	2	2	2	2	3	3.6	0.5	2.1	0.7
AE	2	2	4	4	4	4	4	0.6	0.8	0.9	0.8
ASE	2	2	2	5	5	5	5	2	0.6	2	0.7
AS	2	3	3	3	1	1	6	4.3	0.6	5.1	0.7
ASW	2	3	3	2	3	3	1	4.4	0.5	2.9	0.6
AW	2	3	3	3	1	1	7	6	0.4	3.1	0.6
ANW	1	1	1	1	6	7	7	7.8	0.4	4.8	0.5
AN	2	2	2	2	3	3	3	3.1	0.6	2.9	0.7
NE	2	2	2	5	5	5	5	1.9	0.6	2.3	0.6
E	2	2	2	5	5	5	5	2	0.7	3.8	0.6
SE	2	3	3	2	3	3	1	3.7	0.6	3.4	0.5
S	2	3	3	3	1	1	7	5.5	0.4	3.9	0.5
SW	1	1	1	1	6	7	8	8.5	0.3	5.1	0.4
W	1	1	1	1	6	7	8	9.5	0.3	6.1	0.3
NW	1	3	3	3	1	7	7	6.9	0.4	4.4	0.4
N	2	3	3	3	1	1	1	4.7	0.6	4	0.6
C	1	1	1	1	6	7	8	7.9	0.4	5.6	0.3
CNE	2	3	3	3	1	1	1	4.4	0.2	3.9	0.3
CE	2	2	2	5	5	5	5	2.5	0.4	2.7	0.2
CSE	2	3	3	3	1	1	7	5.2	0.3	3.6	0.4
CS	1	1	1	1	6	7	8	9.2	0.2	5.5	0.3
CSW	1	1	1	1	6	6	8	12.1	0.2	8.1	0.2
CW	1	1	1	1	6	6	8	11.8	0.2	8	0.2
CNW	2	3	3	3	1	1	6	4.9	0.4	4.7	0.4
CN	2	2	2	2	3	3	1	3	0.5	3.8	0.4

Dry/Light	(MDR=0.6-3.8mm; PD=0.5-0.8)	A, ANE, AE, ASE, AN, NE, E, CE, CN
Medium	(MDR=2.9-6.0mm; PD=0.2-0.7)	U, AS, ASW, AW, SE, S, NW, N, CSE, CNE, CNW
Heavy	(MDR=4.8-12.1mm; PD=0.2-0.5)	ANW, SW, W, C, CS, CSW, CW

Table A2-9: k-means clustering for the Pennine region in winter using objective weather types and k=2 to k=8 for sites 77797 and 47060. Site statistics average over 1961-1990. Cluster definitions shown for Pennines-obj-winter.

k	2	3	4	5	6	7	8	34458	
LWT								MDR	PD
U	2	2	1	1	1	1	1	2.3	0.6
A	2	2	2	2	2	2	2	0.8	0.8
ANE	1	1	3	3	3	3	3	4.2	0.3
AE	1	1	3	3	3	3	3	6	0.5
ASE	2	2	2	5	5	5	5	0.2	0.9
AS	2	2	2	5	6	6	6	0.4	0.9
ASW	2	2	2	2	2	2	2	0.6	0.8
AW	2	2	2	2	2	2	2	0.6	0.8
ANW	2	2	2	2	6	7	8	1.5	0.6
AN	1	1	3	3	3	3	3	4.8	0.3
NE	1	1	3	3	3	3	3	6.4	0.3
E	1	1	3	3	3	3	3	4.1	0.4
SE	2	2	2	2	6	7	7	1.3	0.7
S	2	2	2	5	6	6	6	1	0.7
SW	2	2	2	2	6	7	7	1	0.7
W	2	2	2	2	6	7	8	1.4	0.6
NW	2	2	1	1	6	7	8	1.7	0.7
N	1	3	4	4	4	4	4	8.4	0.2
C	1	1	3	3	3	3	3	5	0.3
CNE	1	3	4	4	4	4	4	15.5	0.2
CE	1	3	4	4	4	4	4	10.1	0.2
CSE	1	1	3	3	3	3	3	4.8	0.5
CS	2	2	1	1	1	1	1	2.3	0.6
CSW	2	1	1	1	1	1	1	3.1	0.3
CW	2	1	3	3	3	3	3	3.8	0.4
CNW	1	1	3	3	3	3	3	4.3	0.3
CN	1	3	4	4	4	4	4	8.1	0.2

Dry/Light	(MDR=0.2-3.7mm; PD=0.6-0.9)	U, A, ASE, AS, ASW, AW, ANW, SE, S, SW, W, NW CS
Medium	(MDR=0.5-6.4mm; PD=0.3-0.8)	ANE, AE, AN, NE, E, C, CSE, CSW, CW, CNW
Heavy	(MDR=1.7-15.5mm; PD=0.2-0.6)	N, CNE, CE, CN

Table A2-10: k-means clustering for the northeast Yorkshire region in winter using objective weather types and k=2 to k=8 for site 34458. Site statistics average over 1961-1990. Cluster definitions shown for NE-obj-winter.

k	2	3	4	5	6	7	8	44841		60548		87024	
LWT								MDR	PD	MDR	PD	MDR	PD
U	2	1	2	5	1	1	1	1.6	0.9	1.3	0.7	0.9	0.8
A	2	2	2	2	2	2	2	0.8	0.8	0.9	0.8	0.6	0.8
ANE	2	1	1	1	3	3	3	1.7	0.6	1.4	0.7	1.7	0.7
AE	2	2	4	4	4	4	4	0.3	0.9	0.5	0.8	0.2	0.9
ASE	2	2	2	2	5	5	5	1	0.8	1.2	0.7	0.7	0.8
AS	1	3	3	3	6	6	6	2.4	0.8	2.4	0.8	1.6	0.8
ASW	2	2	2	2	5	7	7	1	0.8	1.1	0.7	1	0.7
AW	2	1	2	5	1	1	8	1.4	0.8	1.3	0.8	1.2	0.8
ANW	2	2	2	5	5	7	7	1.2	0.7	1.2	0.7	0.9	0.8
AN	2	1	1	1	3	3	3	1.7	0.6	1	0.8	1.8	0.7
NE	2	1	2	5	1	1	1	1.7	0.5	1	0.7	1	0.6
E	1	3	3	3	6	6	6	4	0.3	2.8	0.6	1.9	0.5
SE	1	3	3	3	6	6	6	2.1	0.7	2.2	0.6	2.1	0.7
S	1	3	3	3	6	6	6	2.6	0.6	2.1	0.7	1.8	0.6
SW	2	1	1	1	3	3	3	2	0.7	1.9	0.7	1.6	0.7
W	2	1	1	1	3	3	3	1.9	0.7	1.7	0.6	1.4	0.7
NW	2	1	1	1	3	3	3	2	0.7	1.6	0.7	1.3	0.7
N	1	1	1	1	3	3	3	2.2	0.6	1.9	0.6	1.6	0.6
C	1	3	3	3	6	6	6	2.8	0.6	3	0.6	2.6	0.6
CNE	2	1	1	1	3	3	3	1.6	0.5	1	0.7	2.9	0.3
CE	2	1	1	1	3	3	3	1.5	0.8	1.6	0.4	1.4	0.5
CSE	1	3	3	3	6	6	6	3	0.4	2.8	0.4	2	0.4
CS	1	3	3	3	6	6	6	2.2	0.6	2.3	0.5	1.8	0.5
CSW	1	3	3	3	6	6	6	2.9	0.4	2.9	0.5	2.3	0.5
CW	1	3	3	3	6	6	6	3.2	0.6	2.8	0.6	2.6	0.6
CNW	2	1	1	1	3	3	3	1.8	0.5	1.9	0.6	1.5	0.6
CN	1	3	3	3	6	6	6	2.4	0.4	2.9	0.5	2.8	0.6

Dry/Light	(MDR=0.2-1.2mm; PD=0.7-0.9)	A, AE, ASE, ASW, ANW
Medium	(MDR=0.9-2.9mm; PD=0.3-0.9)	U, ANE, AW, AN, NE, SW, W, NW, N, CNE, CE, CNW
Heavy	(MDR=1.6-4.0mm; PD=0.3-0.8)	AS, E, SE, S, C, CSE, CS, CSW, CW, CN

Table A2-11: k-means clustering for the southeast Yorkshire region in winter using objective weather types and k=2 to k=8 for sites 44841, 60548 and 87024. Site statistics average over 1961-1990. Cluster definitions shown for SE-obj-winter

A2.2.2 Spring

k	2	3	4	5	6	7	8	47060		77797	
LWT								MDR	PD	MDR	PD
U	2	3	3	2	3	3	1	4	0.5	3.6	0.6
A	2	2	2	5	2	2	2	2.7	0.7	1.8	0.7
ANE	2	2	2	2	2	2	3	3.6	0.5	2.1	0.7
AE	2	2	4	4	4	4	4	0.6	0.8	0.9	0.8
ASE	2	2	2	5	5	5	5	2	0.6	2	0.7
AS	2	3	3	3	1	1	6	4.3	0.6	5.1	0.7
ASW	2	3	3	2	3	3	1	4.4	0.5	2.9	0.6
AW	2	3	3	3	1	1	7	6	0.4	3.1	0.6
ANW	1	1	1	1	6	7	7	7.8	0.4	4.8	0.5
AN	2	2	2	2	3	3	3	3.1	0.6	2.9	0.7
NE	2	2	2	5	5	5	5	1.9	0.6	2.3	0.6
E	2	2	2	5	5	5	5	2	0.7	3.8	0.6
SE	2	3	3	2	3	3	1	3.7	0.6	3.4	0.5
S	2	3	3	3	1	1	7	5.5	0.4	3.9	0.5
SW	1	1	1	1	6	7	8	8.5	0.3	5.1	0.4
W	1	1	1	1	6	7	8	9.5	0.3	6.1	0.3
NW	1	3	3	3	1	7	7	6.9	0.4	4.4	0.4
N	2	3	3	3	1	1	1	4.7	0.6	4	0.6
C	1	1	1	1	6	7	8	7.9	0.4	5.6	0.3
CNE	2	3	3	3	1	1	1	4.4	0.2	3.9	0.3
CE	2	2	2	5	5	5	5	2.5	0.4	2.7	0.2
CSE	2	3	3	3	1	1	7	5.2	0.3	3.6	0.4
CS	1	1	1	1	6	7	8	9.2	0.2	5.5	0.3
CSW	1	1	1	1	6	6	8	12.1	0.2	8.1	0.2
CW	1	1	1	1	6	6	8	11.8	0.2	8	0.2
CNW	2	3	3	3	1	1	6	4.9	0.4	4.7	0.4
CN	2	2	2	2	3	3	1	3	0.5	3.8	0.4

Dry/Light	(MDR=0.6-3.8mm; PD=0.5-0.8)	A, ANE, AE, ASE, AN, NE, E, CE, CN
Medium	(MDR=2.9-6.0mm; PD=0.2-0.7)	U, AS, ASW, AW, SE, S, NW, N, CSE, CNE, CNW
Heavy	(MDR=4.8-12.1mm; PD=0.2-0.5)	ANW, SW, W, C, CS, CSW, CW

Table A2-12: k-means clustering for the Pennine region in spring using objective weather types and k=2 to k=8 for sites 77797 and 47060. Site statistics average over 1961-1990. Cluster definitions shown for Pennines-obj-spring.

k	2	3	4	5	6	7	8	34458	
LWT								MDR	PD
U	2	2	1	1	1	1	1	2.3	0.6
A	2	2	2	2	2	2	2	0.8	0.8
ANE	1	1	3	3	3	3	3	4.2	0.3
AE	1	1	3	3	3	3	3	6	0.5
ASE	2	2	2	5	5	5	5	0.2	0.9
AS	2	2	2	5	6	6	6	0.4	0.9
ASW	2	2	2	2	2	2	2	0.6	0.8
AW	2	2	2	2	2	2	2	0.6	0.8
ANW	2	2	2	2	6	7	8	1.5	0.6
AN	1	1	3	3	3	3	3	4.8	0.3
NE	1	1	3	3	3	3	3	6.4	0.3
E	1	1	3	3	3	3	3	4.1	0.4
SE	2	2	2	2	6	7	7	1.3	0.7
S	2	2	2	5	6	6	6	1	0.7
SW	2	2	2	2	6	7	7	1	0.7
W	2	2	2	2	6	7	8	1.4	0.6
NW	2	2	1	1	6	7	8	1.7	0.7
N	1	3	4	4	4	4	4	8.4	0.2
C	1	1	3	3	3	3	3	5	0.3
CNE	1	3	4	4	4	4	4	15.5	0.2
CE	1	3	4	4	4	4	4	10.1	0.2
CSE	1	1	3	3	3	3	3	4.8	0.5
CS	2	2	1	1	1	1	1	2.3	0.6
CSW	2	1	1	1	1	1	1	3.1	0.3
CW	2	1	3	3	3	3	3	3.8	0.4
CNW	1	1	3	3	3	3	3	4.3	0.3
CN	1	3	4	4	4	4	4	8.1	0.2

Dry/Light	(MDR=0.2-3.7mm; PD=0.6-0.9)	U, A, ASE, AS, ASW, AW, ANW, SE, S, SW, W, NW CS
Medium	(MDR=0.5-6.4mm; PD=0.3-0.8)	ANE, AE, AN, NE, E, C, CSE, CSW, CW, CNW
Heavy	(MDR=1.7-15.5mm; PD=0.2-0.6)	N, CNE, CE, CN

Table A2-13: k-means clustering for the northeast Yorkshire region in spring using objective weather types and k=2 to k=8 for site 34458. Site statistics average over 1961-1990. Cluster definitions shown for NE-obj-spring.

k	2	3	4	5	6	7	8	44841		60548		87024	
LWT								MDR	PD	MDR	PD	MDR	PD
U	2	1	2	5	1	1	1	1.6	0.9	1.3	0.7	0.9	0.8
A	2	2	2	2	2	2	2	0.8	0.8	0.9	0.8	0.6	0.8
ANE	2	1	1	1	3	3	3	1.7	0.6	1.4	0.7	1.7	0.7
AE	2	2	4	4	4	4	4	0.3	0.9	0.5	0.8	0.2	0.9
ASE	2	2	2	2	5	5	5	1	0.8	1.2	0.7	0.7	0.8
AS	1	3	3	3	6	6	6	2.4	0.8	2.4	0.8	1.6	0.8
ASW	2	2	2	2	5	7	7	1	0.8	1.1	0.7	1	0.7
AW	2	1	2	5	1	1	8	1.4	0.8	1.3	0.8	1.2	0.8
ANW	2	2	2	5	5	7	7	1.2	0.7	1.2	0.7	0.9	0.8
AN	2	1	1	1	3	3	3	1.7	0.6	1	0.8	1.8	0.7
NE	2	1	2	5	1	1	1	1.7	0.5	1	0.7	1	0.6
E	1	3	3	3	6	6	6	4	0.3	2.8	0.6	1.9	0.5
SE	1	3	3	3	6	6	6	2.1	0.7	2.2	0.6	2.1	0.7
S	1	3	3	3	6	6	6	2.6	0.6	2.1	0.7	1.8	0.6
SW	2	1	1	1	3	3	3	2	0.7	1.9	0.7	1.6	0.7
W	2	1	1	1	3	3	3	1.9	0.7	1.7	0.6	1.4	0.7
NW	2	1	1	1	3	3	3	2	0.7	1.6	0.7	1.3	0.7
N	1	1	1	1	3	3	3	2.2	0.6	1.9	0.6	1.6	0.6
C	1	3	3	3	6	6	6	2.8	0.6	3	0.6	2.6	0.6
CNE	2	1	1	1	3	3	3	1.6	0.5	1	0.7	2.9	0.3
CE	2	1	1	1	3	3	3	1.5	0.8	1.6	0.4	1.4	0.5
CSE	1	3	3	3	6	6	6	3	0.4	2.8	0.4	2	0.4
CS	1	3	3	3	6	6	6	2.2	0.6	2.3	0.5	1.8	0.5
CSW	1	3	3	3	6	6	6	2.9	0.4	2.9	0.5	2.3	0.5
CW	1	3	3	3	6	6	6	3.2	0.6	2.8	0.6	2.6	0.6
CNW	2	1	1	1	3	3	3	1.8	0.5	1.9	0.6	1.5	0.6
CN	1	3	3	3	6	6	6	2.4	0.4	2.9	0.5	2.8	0.6

Dry/Light	(MDR=0.2-1.2mm; PD=0.7-0.9)	A, AE, ASE, ASW, ANW
Medium	(MDR=0.9-2.9mm; PD=0.3-0.9)	U, ANE, AW, AN, NE, SW, W, NW, N, CNE, CE, CNW
Heavy	(MDR=1.6-4.0mm; PD=0.3-0.8)	AS, E, SE, S, C, CSE, CS, CSW, CW, CN

Table A2-14: k-means clustering for the southeast Yorkshire region in spring using objective weather types and k=2 to k=8 for sites 44841, 60548 and 87024. Site statistics average over 1961-1990. Cluster definitions shown for SE-obj-spring.

A2.2.3 Summer

k	2	3	4	5	6	7	8	47060		77797	
LWT								MDR	PD	MDR	PD
U	2	2	2	2	6	7	1	3.5	0.6	2.9	0.6
A	2	3	3	5	5	2	2	1.7	0.8	1.3	0.8
ANE	2	3	4	3	3	3	3	0.7	0.7	1.1	0.8
AE	2	3	4	4	4	4	4	0.8	0.7	0.8	0.7
ASE	2	3	3	5	5	5	5	1.4	0.8	1.6	0.8
AS	2	2	3	5	2	6	6	2.5	0.7	1.5	0.7
ASW	2	2	3	5	2	6	7	2.6	0.5	2.2	0.6
AW	1	1	2	2	6	7	1	4.5	0.5	3.3	0.5
ANW	2	2	2	2	6	7	1	3.4	0.6	2.1	0.7
AN	2	2	3	5	2	6	7	2.5	0.7	2	0.6
NE	2	2	2	2	6	7	1	3.4	0.6	2.8	0.6
E	2	2	3	5	2	6	6	2.1	0.7	1.9	0.6
SE	2	2	2	2	6	7	1	2.6	0.5	4.3	0.4
S	1	1	2	2	6	7	1	4.6	0.5	3	0.5
SW	1	1	1	1	1	1	8	7.1	0.3	4.3	0.4
W	1	1	1	1	1	1	8	6.2	0.4	4.3	0.4
NW	1	1	1	1	1	1	8	7.5	0.5	4	0.5
N	2	2	2	2	2	6	7	2.7	0.6	2.6	0.6
C	1	1	1	1	1	1	8	5.6	0.4	4.3	0.4
CNE	2	2	3	5	2	6	7	2.2	0.5	2	0.6
CE	1	1	1	1	1	1	8	3.6	0.4	6.3	0.2
CSE	1	1	1	1	1	1	8	4.6	0.4	4.3	0.3
CS	1	1	1	1	1	1	8	5.1	0.5	3.5	0.5
CSW	1	1	1	1	1	1	8	5.5	0.4	4.3	0.4
CW	1	1	1	1	1	1	8	9.1	0.3	4.5	0.4
CNW	1	1	1	1	1	1	8	6.9	0.4	6.4	0.3
CN	2	2	2	2	6	7	1	3.5	0.4	2.3	0.6

Dry/Light	(MDR=0.7-1.7mm; PD=0.7-0.8)	A, ANE, AE, ASE
Medium	(MDR=1.9-4.3mm; PD=0.4-0.7)	U, AS, ASW, ANW, AN, NE, E, SE, N, CNE, CN
Heavy	(MDR=3.0-9.1mm; PD=0.2-0.5)	AW, S, SW, W, NW, C, CE, CSE, CS, CSW, CW, CNW

Table A2-15: k-means clustering for the Pennine region in summer using objective weather types and k=2 to k=8 for sites 77797 and 47060. Site statistics average over 1961-1990. Cluster definitions shown for Pennines-obj-summer.

k	2	3	4	5	6	7	8	34458	
LWT								MDR	PD
U	2	3	4	4	4	4	4	1.7	0.7
A	2	2	2	2	2	2	2	0.5	0.9
ANE	2	3	4	4	4	4	4	1.4	0.6
AE	2	2	2	5	6	6	6	1.2	0.8
ASE	2	2	2	2	5	5	5	0.4	0.9
AS	2	2	2	2	5	5	2	0.6	0.9
ASW	2	2	2	2	2	7	7	0.2	0.9
AW	2	2	2	2	2	2	8	0.4	0.9
ANW	2	2	2	5	6	6	6	1.2	0.8
AN	2	3	4	4	4	4	4	1.5	0.6
NE	1	1	1	1	1	1	1	5.1	0.4
E	2	3	4	4	4	4	4	2.2	0.6
SE	2	3	4	4	4	4	4	1.4	0.7
S	2	3	4	4	4	4	4	1	0.8
SW	2	3	4	4	4	4	4	1.1	0.8
W	2	3	4	4	4	4	4	1.1	0.7
NW	2	3	4	4	4	4	4	2.3	0.6
N	1	1	3	3	3	3	3	3.5	0.4
C	1	1	3	3	3	3	3	3.6	0.4
CNE	1	1	1	1	1	1	1	8.8	0.3
CE	1	3	3	3	3	3	3	2.3	0.6
CSE	1	1	3	3	3	3	3	3.7	0.4
CS	2	3	4	4	4	4	4	1.7	0.6
CSW	1	3	3	3	3	3	3	2.9	0.4
CW	1	3	3	3	3	3	3	3.2	0.3
CNW	1	3	3	3	3	3	3	2.5	0.5
CN	1	1	1	1	1	1	1	5.2	0.3

Dry/Light	(MDR=0.2-1.2mm; PD=0.8-0.9)	A, AE, ASE, AS, ASW, AW, ANW
Medium	(MDR=1.1-3.5mm; PD=0.3-0.8)	U, ANE, AN, E, SE, S, SW, W, NW, CE, CS, CSW, CW, CNW
Heavy	(MDR=1.7-5.2mm; PD=0.3-0.8)	NE, N, C, CNE, CSE, CN

Table A2-16: k-means clustering for the northeast Yorkshire region in summer using objective weather types and k=2 to k=8 for site 34458. Site statistics average over 1961-1990. Cluster definitions shown for NE-obj-summer.

k	2	3	4	5	6	7	8	44841		60548		87024	
LWT								MDR	PD	MDR	PD	MDR	PD
U	2	2	4	5	5	5	8	2.2	0.7	1.6	0.7	1.3	0.6
A	2	3	3	3	3	4	6	0.8	0.8	0.7	0.8	0.7	0.8
ANE	2	3	3	3	3	3	3	0.9	0.9	0.4	0.9	0.7	0.8
AE	2	3	3	3	3	4	4	0.9	0.9	0.6	0.8	0.8	0.9
ASE	2	3	3	3	4	4	6	1	0.8	0.9	0.8	0.9	0.8
AS	2	3	3	3	4	4	6	0.8	0.8	0.8	0.9	0.8	0.8
ASW	2	3	3	3	4	7	7	0.8	0.8	1.4	0.7	0.6	0.8
AW	2	3	2	4	6	6	5	1.3	0.8	0.9	0.8	1.1	0.8
ANW	2	3	3	2	2	2	2	0.5	0.8	0.6	0.8	0.4	0.8
AN	2	2	2	4	6	6	5	1.5	0.7	0.9	0.8	1.2	0.6
NE	1	1	1	1	1	1	1	3	0.6	2.3	0.6	2.5	0.5
E	2	2	4	5	5	5	8	1.8	0.7	1.8	0.7	1.3	0.7
SE	1	1	4	5	5	5	8	2.2	0.6	2.5	0.5	2.6	0.4
S	1	2	4	5	5	5	8	2.1	0.6	2.1	0.6	1.9	0.6
SW	2	2	4	5	5	5	8	1.8	0.6	1.9	0.6	1.5	0.7
W	2	2	2	4	6	6	5	1.5	0.7	1.2	0.7	1.1	0.7
NW	1	2	4	5	5	5	8	2.1	0.6	1.7	0.7	1.8	0.6
N	2	2	2	4	6	6	5	1.6	0.7	1.4	0.7	1.4	0.7
C	1	1	4	5	5	5	8	2.5	0.5	2.4	0.6	2.1	0.5
CNE	2	2	2	4	6	6	5	2	0.7	0.6	0.8	1.5	0.5
CE	1	1	1	1	1	1	1	4.1	0.4	4.7	0.2	3.7	0.3
CSE	1	1	1	1	1	1	1	2.8	0.5	3.2	0.5	3.5	0.4
CS	1	2	4	5	5	5	8	1.7	0.6	2	0.6	1.7	0.6
CSW	1	2	4	5	5	5	8	1.9	0.6	2	0.6	1.7	0.5
CW	1	2	4	5	5	5	8	1.7	0.6	2.1	0.5	1.6	0.6
CNW	1	1	1	1	1	1	1	3.6	0.4	2.9	0.4	2.7	0.5
CN	2	2	2	4	6	6	5	1.4	0.7	1.4	0.7	1.3	0.7

Dry/Light	(MDR=0.4-1.3mm; PD=0.7-0.9)	A, ANE, AE, AS, ASE, ASW, AW, ANW
Medium	(MDR=0.9-2.2mm; PD=0.5-0.8)	U, AN, E, S, SW, W, NW, N, CNE, CS, CSW,CW, CN
Heavy	(MDR=2.1-4.7mm; PD=0.3-0.6)	NE, SE, C, CE, CSE, CNW

Table A2-17: k-means clustering for the southeast Yorkshire region in summer using objective weather types and k=2 to k=8 for sites 44841, 60548 and 87024. Site statistics average over 1961-1990. Cluster definitions shown for SE-obj-summer.

A2.2.4 Autumn

k	2	3	4	5	6	7	8	47060		77797	
LWT								MDR	PD	MDR	PD
U	2	2	2	5	6	6	6	4.3	0.6	2.6	0.6
A	2	3	3	3	2	2	2	1.7	0.8	1.4	0.7
ANE	2	3	3	3	3	3	3	0.9	0.8	1.2	0.8
AE	2	3	4	4	4	4	4	0.1	1	0.3	1
ASE	2	2	2	2	5	5	5	2.7	0.7	2.3	0.7
AS	2	2	2	2	5	5	6	3.3	0.6	2.7	0.7
ASW	2	2	2	5	6	7	6	3.6	0.5	3	0.6
AW	1	1	1	1	1	6	1	5.5	0.6	2.8	0.6
ANW	2	2	2	2	5	5	5	3.2	0.6	1.9	0.7
AN	2	2	2	5	6	7	7	3.5	0.6	3.7	0.6
NE	2	2	2	5	6	7	7	3.2	0.6	3.5	0.5
E	2	2	2	5	6	7	7	2.7	0.6	4.5	0.6
SE	2	2	2	2	5	5	5	2.7	0.6	2.3	0.7
S	1	1	1	1	1	6	1	5.3	0.4	3.5	0.5
SW	1	1	1	1	1	1	8	6.6	0.4	4.3	0.4
W	1	1	1	1	1	6	1	5.4	0.5	3.5	0.5
NW	1	2	2	5	6	6	1	4.6	0.5	3.8	0.5
N	2	2	2	5	6	7	6	3.9	0.6	3.3	0.6
C	1	1	1	1	1	6	1	5.3	0.4	4.5	0.4
CNE	2	2	2	5	6	7	7	3.1	0.4	4.7	0.3
CE	2	2	2	2	5	5	5	2.6	0.6	2.5	0.4
CSE	1	1	1	1	1	1	8	8.6	0.2	7.7	0.3
CS	2	2	2	5	6	7	6	3.3	0.4	3.2	0.5
CSW	1	1	1	1	1	1	8	7.5	0.3	5.8	0.3
CW	1	1	1	1	1	1	8	7	0.3	3.6	0.3
CNW	1	1	1	1	1	1	8	6.1	0.5	5.3	0.5
CN	2	2	3	2	5	5	5	2.5	0.5	1.9	0.5

Dry/Light	(MDR=0.1-1.7mm; PD=0.7-1.0)	A, ANE, AE
Medium	(MDR=1.9-4.6mm; PD=0.4-0.7)	U, ASE, AS, ASW, ANW, AN, NE, E, SE, NW, N, CNE, CE, CS, CN
Heavy	(MDR=2.8-8.6mm; PD=0.2-0.6)	AW, S, SW, W, C, CSE, CSW, CW, CNW

Table A2-18: k-means clustering for the Pennine region in autumn using objective weather types and k=2 to k=8 for sites 77797 and 47060. Site statistics average over 1961-1990. Cluster definitions shown for Pennines-obj-autumn.

k	2	3	4	5	6	7	8	34458	
LWT								MDR	PD
U	2	3	3	3	6	7	7	2.6	0.6
A	2	2	4	4	4	2	2	0.5	0.9
ANE	2	3	4	4	3	3	3	2	0.7
AE	2	2	4	4	4	4	4	0.2	0.9
ASE	2	2	2	5	5	5	5	0.5	0.9
AS	2	2	2	2	2	6	6	0.1	1
ASW	2	2	2	2	2	6	6	0.7	0.8
AW	2	2	4	4	4	2	2	0.6	0.7
ANW	2	2	4	2	2	2	8	1.2	0.8
AN	2	3	2	2	6	7	7	1.6	0.6
NE	1	1	1	1	1	1	1	5.9	0.4
E	2	3	2	2	6	7	7	1.6	0.7
SE	2	2	4	2	2	6	6	0.4	0.8
S	2	2	2	2	2	6	6	0.5	0.8
SW	2	2	2	2	2	6	6	0.7	0.7
W	2	2	2	2	2	6	6	1.3	0.6
NW	2	3	3	3	3	3	3	2.9	0.5
N	1	1	1	1	1	1	1	6.2	0.4
C	1	1	1	1	1	1	1	5.2	0.3
CNE	1	1	1	1	1	1	1	7.1	0.2
CE	2	3	3	3	6	7	7	2.4	0.8
CSE	2	3	3	3	3	7	7	1.9	0.5
CS	1	1	1	1	1	1	1	4.9	0.5
CSW	2	3	3	3	6	7	7	2	0.5
CW	2	3	3	3	6	7	7	2.2	0.5
CNW	2	3	3	3	3	7	7	3.6	0.3
CN	1	1	1	1	1	1	1	10.8	0.3

Dry/Light ANW	(MDR=0.2-1.2mm; PD=0.8-0.9)	A, AE, ASE, AS, ASW, AW,
Medium	(MDR=1.1-3.5mm; PD=0.3-0.8)	U, ANE, AN, E, SE, S, SW, W, NW, CE, CS, CSW, CW, CNW
Heavy	(MDR=1.7-5.2mm; PD=0.3-0.8)	NE, N, C, CNE, CSE, CN

Table A2-19: k-means clustering for the northeast Yorkshire region in autumn using objective weather types and k=2 to k=8 for site 34458. Site statistics average over 1961-1990. Cluster definitions shown for NE-obj-autumn.

k	2	3	4	5	6	7	8	44841		60548		87024	
LWT								MDR	PD	MDR	PD	MDR	PD
U	1	1	1	1	1	1	1	2.5	0.7	3.4	0.6	3.5	0.6
A	2	2	2	2	2	2	2	0.9	0.9	0.8	0.8	0.8	0.8
ANE	2	3	2	2	3	3	3	0.3	0.9	1.2	0.9	2.2	0.8
AE	2	2	4	4	4	4	4	0.1	1	0.1	0.9	0.2	0.9
ASE	1	1	1	5	5	5	5	4.6	0.8	2.8	0.8	2.4	0.8
AS	2	3	3	3	6	7	7	1.4	0.8	2.2	0.7	1.9	0.7
ASW	2	3	3	3	6	7	7	1.7	0.8	1.9	0.8	1.8	0.7
AW	2	2	2	2	2	2	8	0.8	0.8	1.1	0.7	0.6	0.8
ANW	2	2	2	2	2	2	8	0.9	0.8	1	0.8	0.7	0.8
AN	1	1	1	1	1	6	6	3.1	0.7	2.6	0.7	2.6	0.6
NE	1	1	1	1	6	6	6	2.2	0.6	1.9	0.6	3	0.5
E	1	3	3	3	6	7	7	2	0.7	2.1	0.7	2.3	0.7
SE	2	3	3	3	6	7	7	1.8	0.7	2.2	0.7	2.2	0.7
S	2	3	3	3	6	7	7	1.4	0.7	1.8	0.6	1.9	0.7
SW	1	1	1	1	1	6	6	2.8	0.6	2.7	0.6	2.5	0.6
W	2	3	3	3	6	7	7	2	0.7	1.7	0.7	1.3	0.7
NW	2	3	3	3	6	7	7	1.9	0.7	1.7	0.7	1.6	0.7
N	2	3	3	3	6	7	7	2	0.7	2.2	0.7	1.8	0.7
C	1	1	1	1	1	6	6	2.5	0.6	3	0.5	2.6	0.6
CNE	1	1	1	1	1	1	1	2.2	0.7	2	0.5	4.5	0.5
CE	1	1	1	1	1	1	1	3.5	0.6	2.3	0.7	4.4	0.6
CSE	1	1	1	1	1	1	1	4	0.6	2.9	0.3	3.9	0.2
CS	1	3	3	3	6	6	6	1.5	0.8	3.1	0.6	2.4	0.7
CSW	1	1	1	1	1	1	1	2.4	0.7	2.9	0.6	3.5	0.6
CW	1	3	3	3	6	6	6	2.2	0.5	2.6	0.5	2.4	0.7
CNW	1	1	3	3	6	6	6	2.7	0.6	2.8	0.6	2.1	0.6
CN	2	3	3	3	6	7	7	2.5	0.6	1.7	0.7	1.8	0.7

Dry/Light	(MDR=0.1-1.1mm; PD=0.7-1.0)	A, AE, AW, ANW
Medium	(MDR=0.3-3.1mm; PD=0.5-0.9)	ANE, AS, ASW, E, SE, S, W, NW, N, CS, CW, CN
Heavy	(MDR=1.9-4.6mm; PD=0.2-0.8)	U, ASE, AN, NE, SW, C, CNE, CE, CSE, CSW, CNW

Table A2-20: k-means clustering for the southeast Yorkshire region in autumn using objective weather types and k=2 to k=8 for sites 44841, 60548 and 87024. Site statistics average over 1961-1990. Cluster definitions shown for SE-obj-autumn

REFERENCES

Airey, M. and Hulme, M. 1995. *Evaluating climate model simulations of precipitation: methods, problems and performance.* Prog. Phys. Geog., **19**: 427-448.

Al-Awadhi, S. and, Jolliffe, I. 1998. *Time series modelling of surface pressure data.* Int. J. Climatol., **18**: 443-455.

Arkin, P.A. and Xie, P. 1994. *The Global Precipitation Climatology Project: first algorithm intercomparison project.* Bull. Am. Meteorol. Soc., **75**: 401-419.

Arnell, N.W. 1992*a*. *Impacts of climate change on river flow regimes in the UK.* J. Inst. Wat. Env. Manag., **6**: 432-442.

Arnell, N.W. 1992*b*. *Factors controlling the effects of climate change on river flow regimes in a humid temperate environment.* J. Hydrol., **132**: 321-342.

Arnell, N.W. 1996. Global warming, river flows and water resources. Wiley, Chichester.

Arnell, N.W. and Reynard, N.S. 1989. *Estimating the impacts of climate change on river flows; some examples from Britain.* Paper presented at the Conference on Climate and Water. Helsinki, 1984.

Arnell, N.W. and Reynard, N.S. 1993. *Impact of climate changes on river flow regimes in the United Kingdom.* Report to the Department of the Environment, London, UK.

Arnell, N.W. and Reynard, N.S. 1996. *The effects of climate change due to global warming on river flows in Great Britain.* J. Hydrol., **183**: 397-424.

Arnell, N.W., Brown, R.P.C. and Reynard, N.S. 1990. *Impact of climate variability and change on river flow regimes in the UK.* Institute of Hydrology Report 107. Wallingford, UK Institute of Hydrology.

Arnell, N.W., Jenkins, A. and George, D.G. 1994. *The implications of climate change for the National Rivers Authority.* National Rivers Authority R & D Report 12. HMSO, London.

ASCE, 1998, Sustainability Criteria for Water Resource Systems, Task Committee on Sustainability Criteria, Water Resources Planning and Management Division, ASCE and Working Group of UNESCO/IHP IV Project M-4.3, ASCE, Reston, Va, USA, ISBN 0-7844-0331-7

Aston, A.R. 1984. *The effect of doubling atmospheric CO2 on streamflow: A simulation.* J. Hydrol., **67**: 273-280.

Ayers, M.A., Wolock, D.M., McCabe, G.J. and Hay, L.E. 1990. *Hydrologic effects of climatic change in the Delaware River Basin.* USGS Yearbook, Fiscal year 1989, 31-33.

Bardossy, A. and Caspary, H. 1990. *Detection of climate change in Europe by analyzing European circulation patterns from 1881 to 1989.* Theor. Appl. Climatol., **42**: 155-167.

Bardossy, A. and Plate, E.J. 1991. *Modeling daily rainfall using a semi-Markov representation of circulation pattern occurrence.* J. Hydrol., **122**: 33-47.

Bardossy, A. and Plate, E.J. 1992. *Space-time model for daily rainfall using atmospheric circulation patterns.* Water Resour. Res., **28**: 1247-1259.

Bardossy, A., Duckstein, L. and Bogardi, I. 1995. *Fuzzy rule-based classification of atmospheric circulation patterns.* Int. J. Climatol., **15**, 1087-1097.

Bardossy, A., Muster, H., Duckstein, L. and Bogardi, I. 1994. *Knowledge based classification of circulation patterns for stochastic precipitation modelling.* In: Hipel, K.W., McLeod, A.W., Panu, U.S., and Sing, V.P. (eds.) Stochastic and statistical methods in hydrology and environmental engineering. Volume 3, Dordrecht: Kluwer.

Barros, A.P. and Lettenmaier, D.P. 1993. *Dynamic modeling of the spatial distribution of precipitation in remote mountainous areas.* Monthly Weather Review, **121**: 1195-1214.

Barrow, E., Hulme, M., and Jiang, T. 1993. A 1961-1990 baseline climatology and future climate change scenarios for Great Britain and Europe, Part 1: 1961-1990 Great Britain Baseline Climatology. Climatic Research Unit, University of East Anglia.

Barry, R.G. 1967. *The prospect for synoptic climatology: a case study.* In: R.W. Steel and R. Lawton (eds.) Liverpool Essays in Geography. Longmans, London, 85-106.

Bates, B.C., Charles, S.P. and Hughes, J.P. 1998. *Stochastic downscaling of numerical climate model simulations.* Environ. Modell. Softw., **13**: 325-331.

Bellone, E., Hughes, J.P. and Guttorp, P. 2000. *A hidden Markov model for downscaling synoptic atmospheric patterns to precipitation amounts.* Climate Res., **15**: 1-12.

Beven, K. 1993. *Prophecy, reality and uncertainty in distributed hydrological modeling.* Adv. Water Resour., **16**: 41-51.

Black, A.R. and Bennet, A.M. 1995. *Regional flooding in Strathclyde, December 1994.* 1994 Yearbook, Hydrological Data UK Series, Institute of Hydrology, 29-34.

Blackwell, S. 1988. Dwr Cymru – Conjunctive Use Model. Unpublished M.Sc. Thesis, Lancaster University.

Boorman, D.B. and Sefton, C.E.M. 1997. *Recognising the uncertainty in the quantification of the effects of climate change on hydrological response.* Climatic Change., **35**: 415-434.

Bradley, R.S., Diaz, H.F., Eischeid, J.K., Jones, P.D., Kelly, P.M. and Goodess, C.M. 1987. *Precipitation fluctuations over Northern Hemisphere land areas since the mid-19th century.* Science, **237**: 171-275.

Brandsma, T. and Buishand, T.A. 1997*a*. *Statistical linkage of daily precipitation in Switzerland to atmospheric circulation and temperature.* J. Hydrol., **198**: 98-123.

Brandsma, T. and Buishand, T.A. 1997*b*. *Rainfall Generator for the Rhine Basin: single-site generation of weather variables by nearest-neighbour resampling.* KNMI-publication 186-I, KNMI, De Bilt.

Brandsma, T. and Buishand, T.A. 1998. *Simulation of extreme precipitation in the Rhine Basin by nearest-neighbour resampling.* Hydrol. Earth Syst. Sci., **2**: 195-209.

Brandsma, T. and Buishand, T.A. 1999. *Rainfall Generator for the Rhine Basin: Multi-site generation of weather variables by nearest-neighbour resampling.* KNMI-publication 186-II, KNMI, De Bilt.

Briffa, K.R., Jones, P.D. and Kelly, P.M. 1990. *Principal component analysis of the Lamb Classification of daily weather types: Part 2, seasonal frequencies and update to 1987.* Int. J. Climatol., **10**: 549-563.

Briffa, K.R., Jones, P.D. and Hulme, M. 1994. *Summer moisture variability across Europe 1892-1991: an analysis based on the Palmer drought severity index.* J. Climatol., **14**: 475-506.

Brunetti, M., Buffoni, L., Maugeri, M. and Nanni, T. 2000. *Precipitation intensity trends in northern Italy.* Int. J. Climatol., **20**: 1017-1031.

Brugge, R. 1992. *Three years of warm weather over the British Isles.* Weather, **47**: 230-236.

Bryant, S.J., Arnell, N.W. and Law, F.M. 1992. *The long-term context for the current hydrological drought.* In: Proc. IWEM Conf. on the Management of Scarce Water Resources.

Bryant, S.J., Arnell, N.W. and Law, F.M. 1994. *The 1988-92 drought in its historical perspective.* J. IWEM., **8**, 39-51.

Buishand, T.A. and Beersma, J.J. 1996. *Statistical tests for comparison of daily variability in observed and simulated climates.* J. Climate, **9**: 2538-2550.

Buishand, T.A. and Brandsma, T. 1997. *Comparison of circulation classification schemes for predicting temperature and precipitation in the Netherlands.* Int. J. Climatol., **17**: 875-889.

Bultot, F., Coppens, A., Dupriez, G.L., Gellens, D. and Meulenberghs, F. 1988. *Repercussions of a CO_2 doubling on the water cycle and on the water balance - a case study for Belgium.* J. Hydrol., **99**, 319-347.

Burlando, P. and Rosso, R. 1991. *Extreme storm rainfall and climate change.* Atmos. Res., **27**: 169-189.

Burn, D.H. 1994. *Hydrologic effects of climatic change in west-central Canada.* J. Hydrol., **137**: 199-208.

Burt, S. 1992. *Weather and streamflow in central southern England during water year 1989/90.* Weather, **47**: 2-10.

Burt, T.P. 1999. *A note on the long rainfall record for Blackmoorfoot Reservoir, near Huddersfield.* Submitted to Meteorol. Mag.

Burt, T.P., Adamson, J.K. and Lane, A.M. J. 1998. *Long-term rainfall and streamflow records for north central England: putting the Environmental Change Network site at Moor House, Upper Teesdale, in context.* Hydrol. Sci. J., **43**: 775-787.

Calenda, G. and Napolitano, F. 1999. *Parameter estimation of Neyman-Scott processes for temporal point rainfall simulation.* J. Hydrol., **225**: 45-66.

Carter, T.R., Parry, M. L., Harasawa, H., and Nishioka, S. 1994. IPCC Technical Guidelines for Assessing Climate Change Impacts and Adaptations. Intergovernmental Panel on Climate Change, Special Report to Working Group II of IPCC, 59pp.

Cess, R.D., Potter, G.L., Blanchet, J.P., Boer, G.J., Delgenio, A.D., Deque, M., Dymnikov, V., Galin, V., Gates, W.L., Ghan, S.J., Kiehl, J.T., Lacis, A.A., Letreut, H., Li, Z.X., Liang, X.Z., McAvaney, B.J., Meleshko, V.P., Mitchell, J.F.B., Morcrette, J.J., Randall, D.A., Rikus, L., Roeckner, E., Royer, J.F., Schlese, U., Sheinin, D.A., Slingo, A., Sokolov, A.P., Taylor, K.E., Washington, W.M., Wetherald, R.T., Yagai, I., Zhang, M.H. 1990. *Intercomparison and*

interpretation of climate feedback processes in 19 atmospheric General-Circulation Models. J. Geophys. Res. – Atmos., **95**: 16601-16615.

Chiew, F.H.S. and McMahon, T.A. 1993. *Detection of trend or change in annual flow of Australian rivers.* Int. J. Climatol., **13**: 643-653.

Chiew, F.H.S., Whetton, P.H., McMahon, T.A. and Pittock, A.B. 1995. *Simulation of the impacts of climate change on runoff and soil moisture in Australian catchments.* J. Hydrol., **167**: 121-147.

CCIRG. 1991. The potential effects of climate change in the United Kingdom: first report. United Kingdom Climate Change Impacts Review Group, HMSO: London.

CCIRG. 1996. Review of the potential effects of climate change in the United Kingdom: second report. United Kingdom Climate Change Impacts Review Group, HMSO: London.

Cohen, S.J. 1986. *Impacts of CO_2-induced climate change on water resources in the Great Lake Basin.* Climatic Change, **8**, 135-153.

Cole, J.A., Slade, S. and Jones, P.D. 1991. *Reliable yield of reservoirs and possible effects of climatic change.* Hydrol. Sci. J., **36**: 579-598.

Conway, D. and Jones, P.D. 1996. POPSICLE - Production of Precipitation Scenarios for CLimate Impacts in Europe. European Community Environment Research Programme, Climatic Research Unit: Final Report (Contract: EV5V-CT-94-0510), 50pp.

Conway, D. and Jones, P.D. 1998. *The use of weather types and air flow indices for GCM downscaling.* J. Hydrol., **213**: 348-361.

Conway, D., Wilby, R.L. and Jones, P.D. 1996. *Precipitation and air flow indices over the British Isles.* Climate Res., **7**, 169-183.

Cooper, D.M., Wilkinson, W.B. and Arnell, N.W. 1995. *The effects of climate change on aquifer storage and river baseflow.* Hydrol. Sci., **10**: 615-632.

Corte-Real, J., Qian, B.D. and Xu, H. 1998. *Regional climate change in Portugal: Precipitation variability associated with large-scale atmospheric circulation.* Int. J. Climatol., **18**: 619-635.

Cowpertwait, P.S.P. 1991*a*. *Further developments of the Neyman-Scott clustered point process for modelling rainfall.* Water Resour. Res., **27**: 1431-1438.

Cowpertwait, P.S.P. 1991*b*. The stochastic generation of rainfall time series. Ph.D. Thesis, University of Newcastle upon Tyne.

Cowpertwait, P.S.P. 1994. *A generalized point process model for rainfall.* Proc. R. Soc. Lond. A, **447**: 23-37.

Cowpertwait, P.S.P. 1995. *A generalized spatial-temporal model of rainfall based on a clustered point process.* Proc. R. Soc. Lond. A., **450**: 163-175.

Cowpertwait, P.S.P and Cox, T.F. 1992. *Clustering population means under heterogeneity of variance with an application to a rainfall time series problem.* Statistician, **41**: 113-121.

Cowpertwait, P.S.P. and O'Connell, P.E. 1997. *A Regionalised Neyman-Scott Model of Rainfall with Convective and Stratiform Cells.* Hydrol. Earth Sys. Sci., **1**: 71-80.

Cowpertwait, P.S.P., O'Connell, P.E., Metcalfe, A.V. and Mawdsley, J.A. 1996*a*. *Stochastic point process modelling of rainfall. I. Single-site fitting and validation.* J. Hydrol, **175**: 17-46.

Cowpertwait, P.S.P., O'Connell, P.E., Metcalfe, A.V. and Mawdsley, J.A. 1996*b*. *Stochastic point process modelling of rainfall. II. Regionalisation and disaggregation.* J. Hydrol., **175**: 47-65.

Cowpertwait, P.S.P. 1998. *A Poisson-cluster model of rainfall: high-order moments and extreme values.* Proc. Roy. Soc. Lond. A Mat., **454**: 885-898.

Crane, R.G. and Barry, R.G. 1988. *Comparison of the MSL synoptic pressure patterns of the arctic as observed and simulated by the GISS general-circulation model.* Meteorol. Atmos. Phys., **39**: 169-183.

Cubasch, U., Voss, R., and Mikolajewicz, U. 2000. *Precipitation: A parameter changing climate and modified by climate change.* Climatic Change, **46**: 257-276.

Daly, C., Neilson, R.P. and Phillips, D.L. 1994. *A statistical-topographic model for mapping climatological precipitation over mountainous terrain.* J. Appl. Meteorol., **33**: 140-158.

Delworth, T.L. and Mann, M.E. 2000. *Observed and simulated mutidecadal variability in the Northern Hemisphere.* Climate Dynamics, **16**: 661-676.

Deser, C. and Blackmon, M.L. 1993. *Surface climate variations over the north-Atlantic ocean during winter - 1900-1989.* J. Climate, **6**: 1743-1753.

Diaz, H.F., Bradley, R.S. and Eischeid, J.K. 1989. *Precipitation fluctuations over global land areas since the late 1800s.* J. Geophys. Res., **94**: 1195-1240.

DoE. 1996. Water Resources and Supply: Agenda for Action. Department of the Environment and the Welsh Office. The Stationery Office, London.

Doorembos, J., Pruitt, W.O., Aboukhaled, A., Damagnez, J., Dastane, N.G., van de Berg, C., Rijtema, P.E., Ashford, O.M. and Frere, M., 1984. *Guidelines for predicting crop water requirements.* FAO Irrig. Drainage Pap., 24.

Drake, B.G. 1992. *The impact of rising CO_2 on ecosystem production.* Water, Air and Soil Pollution, **64**: 25-44.

Dorman, C.E. and Bourke, R.H. 1981. *Precipitation over the Atlantic Ocean, 30° S to 70° N.* Mon. Wea. Rev., **109**: 554-563.

Duan, Q., Sorooshian, S. and Gupta, V.K. 1992.*Effective and Efficient Global Optimization for Conceptual Rainfall-runoff.* Water Resour.Res., **28**: 1015-1031.

Easterling, D.R., Meehl, G.A., Parmesan, C., Changnon, S.A., Karl, T.R. and Mearns, L.O. 2000. *Climate extremes: Observations, modeling, and impacts.* Science, **289**: 2068-2074.

El-Kadi, A.K.A. and Smithson, P.A. 1992. *Atmospheric classifications and synoptic climatology.* Prog. Phys. Geog., **16**: 432-455.

Elliot, T., Younger, P.L. and Chadha, D.S. 1998. *The future sustainability of groundwater resources in East Yorkshire: past and present perspectives.* In: H. Wheater and C. Kirby (eds.) Hydrology in a Changing Environment. Volume II. Proceedings of the British Hydrological Society International Conference, Exeter, July 1998, 21-31.

Entekhabi, D., Rodriguez-Iturbe, I. and Eagleson, P.S. 1989. *Probabilistic representation of the temporal rainfall process by a modified Neyman-Scott rectangular pulses model: parameter estimation and validation.* Water Resour. Res., **25**: 295-302.

Environment Select Committee. 1996. Water Conservation and Supply. Report of the House of Commons Select Committee on the Environment. The Stationery Office, London.

Essery, C.L. and Wilcock, D.N. 1991. *The variation in rainfall catch from standard UK Meteorological Office rain gauges: a twelve year case study.* Hydrol. Scis. J., **36**: 23-34.

Ewing, R. 1993. Optimisation of Grimwith Reservoir. Unpublished M.Sc. Thesis, Lancaster University.

Fisher, R.A. and Cornish, E.A. 1960. *The percentile points of distributions having known cumulants.* Technometrics, **2**: 209-225.

Folland, C.K. 1988. *Numerical models of the raingauge exposure problem, field experiments and an improved collector design.* Q. J. R. Meteorol. Soc., **114**: 1485-1516.

Folland, C.K., Parker, D.E. and Newman, M. 1984, *Worldwide marine temperature variations on the season to century timescale.* 9th Climate Diagnostics Workshop, Corvallis, USA.

Folland, C.K., Karl, T.R. and Vinnikov, K.Ya. 1990. *Observed climate variations and change.* In: J.T. Houghton, G.J. Jenkins and J.J. Euphraums (eds.) Climate change, the IPCC scientific assessment. Cambridge University Press, Cambridge, 195-238.

Foufoula-Georgiou, E. and Guttorp, P., 1986. *Compatibility of continuous rainfall occurrence models with discrete rainfall observations.* Water Resour. Res,. **22**: 1316-1322.

Foufoula-Georgiou, E. and Guttorp, P., 1987. *Assessment of a class of Neyman-Scott models for temporal rainfall.* J. Geophys. Res., **92**: 9679-9682.

Fox, I.A. and Johnson, R.C. 1997. *The hydrology of the river Tweed.* Sci. Total. Env., **194/195**: 163-172.

Fraedrich, K. and Muller, K. 1992. *Climate anomalies in Europe associated with ENSO extremes.* Int. J. Climatol., **12**: 25-31.

Franchini, M. 1996. *Use of a genetic algorithm combined with a local search method for the automatic calibration of rainfall-runoff models.* Hydrol. Sci. J., **41**: 21-40.

Franchini, M. and Galeati, G. 1997. *Comparing several genetic algorithm schemes for the calibration of conceptual rainfall-runoff models.* Hydrol. Sci. J., **42**: 357-379.

Franchini, M. and Pacciani, M., 1991. *Comparative analysis of several conceptual rainfall runoff models.* J. Hydrol., **122**: 161-219.

Gabriel, K.R. and Neumann, J., 1962. *A Markov chain model for daily rainfall occurrence at Tel Aviv.* Q. J. R. Meteorol. Soc., **88**: 90-95.

Garnett, M.H., Ineson, P., and Adamson, J.K. 1997. *A long-term upland temperature record: no evidence for recent warming.* Weather, **52**: 342-351.

Gates, W.L., Mitchell, J.F.B., Boer, G.J., Cubasch, U. and Meleshiko, U.P. 1992. *Climate modelling, climate prediction and model validation.* In: Houghton, J.T., Callander, B.A., and Varney, S.K. (eds.) Climate Change 1992: The supplementary report to the IPCC scientific assessment. Cambridge University Press, Cambridge, 97-134.

Gellens, D. 1991. *Impact of a CO^2-induced climatic change on river flow variability in three rivers in Belgium.* Earth Surf. Proc. Land., **16**: 619-625.

Gifford, R.M. 1988. *Direct effect of higher carbon dioxide concentrations on vegetation.* In: Pearman, G. L. (ed.) Greenhouse: Planning for Climatic Change. CSIRO, Melbourne, 506-519.

Giorgi, F. 1990. *Simulation of regional climate using a limited area model nested in a general circulation model.* J. Climate, **3**: 941-963.

Giorgi, F., Brodeur, C.S. and Bates, G.T. 1994. *Regional climate change over the United States produced with a nested regional climate model.* J. Climate, **7**: 375-399.

Gleick, P.H. 1986. *Methods for evaluating the regional hydrologic impacts of global climatic changes.* J. Hydrol., **88**, 99-116.

Gleick, P.H. 1987*a*. *The development and testing of a water balance model for climate impact assessment: Modelling the Sacremento basin.* Water Resour. Res., **23**, 1049-1061.

Gleick, P.H. 1987*b*. *Global climate changes and regional hydrology: Impacts and responses.* In: S. I. Solomon, M. Beran and W. Hogg (Eds.), Proceedings of the Vanquover Symposium, 168. IAHS Publication, Vanquover. 389-402.

Goldsmith, H., Mawdsley, J., and Homann, S. 1997. *Drought, climate change and water resources in north east England.* BHS 6th National Hydrology Symposium, Salford, 1997.

Golubev, V.S. 1975. *Results of the intercomparison of precipitation gauges.* Trans. State Hydrol. Instit., **224**: 38-46.

Gong, X. and Richman, M. B. 1992. *An examination on methodological issues in clustering North American precipitation.* Proceedings of the 5th International Meeting on Statistical Climatology, Toronto, 22-26 June 1992.

Goodess, C.M. and Palutikof, J.P. 1998. *Development of daily rainfall scenarios for southeast Spain using a circulation-type approach to downscaling.* Int. J. Climatol., **18**: 1051-1083.

Gordon, H.B., Whetton, P.H., Pittock, A.B., Fowler, A.M. and Haylock, M.R. 1992. *Simulated changes in daily rainfall intensity due to the enhanced greenhouse-effect - implications for extreme rainfall events.* Climate Dynamics, **8**: 83-102.

Gregory, J.M., Jones, P.D. and Wigley, T.M.L. 1991. *Precipitation in Britain: An analysis of area-average data updated to 1989.* Int. J. Climatol., **11**: 331-345.

Gregory, J.M., Wigley, T.M.L. and Jones, P.D. 1992. *Determining and interpreting the order of a 2-state Markov-chain - application to models of daily precipitation.* Water Resour. Res., **28**: 1443-1446

Gregory, J.M., and Mitchell, J.F.B. 1995. *Simulation of daily variability of surface temperatures and precipitation over Europe in the current and 2 x CO_2 climates using the UKMO climate model.* Q. J. R. Meteorol. Soc., **121**: 1451-1476.

Groisman, P.Ya. and Easterling, D.R. 1994. *Variability and trends of precipitation and snowfall over the Unites States and Canada.* J. Climate, **7**: 184-205.

Groisman, P.Ya. and Legates, D.R. 1995. *Documenting and detecting long-term precipitation trends: where we are and what should be done.* Climatic Change., **31**: 601-622.

Groisman, P.Y., Karl, T.R., Easterling, D.R., Knight, R.W., Jamason, P.F., Hennessy, K.J., Suppiah, R., Page, C.M., Wibig, J., Fortuniak, K., Razuvaev, V.N., Douglas, A., Forland, E., and Zhai, P.M. 1999. *Changes in the probability of heavy precipitation: Important indicators of climatic change.* Climatic Change, **42**: 243-283.

Grotch, S.L. and MacCracken, M.C. 1991. *The Use of General Circulation Models to Predict Regional Climatic Change.* J. Climate, **4**: 286-303.

Gupta, V.K. and Waymire, E. 1979. *A stochastic kinematic study of subsynoptic space-time rainfall.* Water Resour. Res., **15**: 637-644.

Hartigan, J.A. and Wong, M.A. 1979. *Algorithm AS 136: A K-means clustering algorithm.* Appl. Stat., **28**: 100-108.

Hashimoto, T., Loucks, D.P., and Stedinger, J.R. 1982*a*. *Robustness of Water Resources Systems.* Water Resour. Res., **18**, 21-26.

Hashimoto, T., Stedinger, J.R. and Loucks, D.P., 1982*b*. *Reliability, Resiliency, and Vulnerability Criteria for Water Resource System Performance Evaluation.* Wat. Resour. Res., **18**,14-20.

Hay, L.E. and McCabe, G.J. 1992. *Use of Weather Types to disaggregate GCM predictions.* J. Geophys.Res., **97**: 2781-2790.

Hay, L.E., McCabe, G.J., Wolock, D.M. and Ayers, M.A. 1991. *Simulation of precipitation by weather type analysis.* Water Resour. Res., **27**: 493-501.

Hendry, G.R., Lewin, K.F. and Nagy, J. 1993. *Free air carbon dioxide enrichment: development, progress, results.* Vegetatio, **104/105**: 17-31.

Hennessey, K.J., Whetton, P.H., Katzfey, J.J., McGregor, J.L., Jones, R.N., Page, C.M. and Nguyen, K.C. 1998. Fine resolution climate change scenarios for New South Wales. Chatswood, Australia: NSW Environmental Protection Agency.

Hess, P., and Brezowsky, H. 1977. *Katalog der Gosswetterlagen Europas (1881-1976).* In: Berichte des Deutschen Wetterdienst Bd 15, Offenbach am Main: Selbstverlag des Deutschen Wetterdienstes.

Hewett, B.A.O., Harries, C.D. and Fenn, C.R. 1993. *Water resources planning in the uncertainty of climate change: a water company perspective.* In White, R. (ed.) Engineering for Climatic Change. Thomas Telford, London, 38-54.

Hewitson, B.C. and Crane, R.G. 1992. *Regional climates in the GISS global circulation model - synoptic-scale circulation.* J. Climate, **5**: 1002-1011.

Hewitson, B.C. and Crane, R.G. 1996. *Climate downscaling: techniques and application.* Climate Res., **7**: 85-95.

Holland, J. H. 1975. Adaptation in Natural and Artificial Systems, University of Michegan Press, Ann Arbor.

Hosking, J. R. M. 1990. *L-moments: analysis and estimation of distributions using linear combinations of order statistics.* J. Roy. Stat. Soc. Ser. B, **52**: 105-124.

Hosking, J.R.M. 1997. *Fortran routines for use with the method of L-moments.* Research Report RC 20525 (90933) Version 3.02, IBM Research Division, New York, 33pp.

Hosking, J.R.M. and Wallis, J.R. 1997. Regional Frequency Analysis: An Approach Based on L-moments. Cambridge University Press.

Hostetler, S.W. 1994. *Hydrological and atmospheric models: the (continuing) problem of discordant scales.* Climatic Change, **27**: 345-350.

Hughes, J.P., and Guttorp, P. 1994. *A class of stochastic models for relating synoptic atmospheric patterns to regional hydrologic phenomena.* Water Resour. Res., **30**: 1535-1546.

Hughes, J.P., and Guttorp, P. 1999. *A non-homogeneous hidden Markov model for precipitation occurrence.* J. Roy. Stat. Soc. C - App., **48**: 15-30.

Hulme, M. 1992. *A 1951-80 global land precipitation climatology for the evaluation of General Circulation Models.* Climate Dynamics, **7**: 57-72.

Hulme, M. 1994. *Validation of large-scale precipitation fields in general circulation models.* In: M. Debois and F. Desalmand (eds.) Global Precipitation and Climate Change. Berlin: Springer-Verlag, 387-405.

Hulme, M. 1995. *Estimating global changes in precipitation.* Weather, **50**: 34-42.

Hulme, M. 1999. *Global warming.* Prog. Phys. Geog., **23**: 283-291.

Hulme, M. and Brown, O. 1998. *Portraying climate scenario uncertainties in relation to tolerable regional climate change.* Climate Res., **10**: 1-14.

Hulme, M., and Jenkins, G.J. 1998. Climate change scenarios for the UK: scientific report. UKCIP Technical Report No. 1, Climatic Research Unit, Norwich, 80pp.

Hulme, M. and Jones, P.D. 1994. *Global climate-change in the instrumental period.* Environ. Pollut., **83**: 23-36.

Hulme, M., Briffa, K.R., Jones, P.D. and Senior, C.A. 1993. *Validation of GCM control simulations using indexes of daily air-flow types over the British-Isles.* Climate Dynamics, **9**: 95-105.

Hulme, M., Mitchell, J., Ingram, W., Lowe, J., Johns, T., New, M. and Viner, D. 1999. *Climate change scenarios for global impact studies.* Global Environ. Change, **9**: S3-S19.

Hurrell, J.W. 1995. *Decadal trends in the North Atlantic Oscillation: regional temperatures and precipitation.* Science, **269**: 676-679.

Hurrell, J.W. 1996. *Influence of variations in extratropical wintertime teleconnections on Northern Hemisphere temperature.* Geophys. Res. Lett., **23**: 665-668.

Hurrell, J.W. and van Loon, H. 1997. *Decadal variations in climate associated with the North Atlantic Oscillation.* Climatic Change, **36**: 301-326.

Hutchinson, M.F. 1990. *A point rainfall model based on a three-state continuous Markov occurrence process.* J. Hydrol., **114**: 125-148.

Hutchinson, M. 1995. *Stochastic space-time weather models from ground-based data.* Agric. For. Meteor., **73**: 237-265.

Idso, S.B. and Brazel, A.J. 1984. *Rising carbon dioxide concentrations may affect streamflow.* Nature, **312**, 51-53.

Islam, S., Entekhabi, D., Bras, R.L. and Rodriguez-Iturbe, I. 1990. *Parameter estimation and sensitivity anaysis for the modified Bartlett-Lewis rectangular pulses model of rainfall.* J. Geophys. Res., **95**: 2093-2100.

IPCC (Intergovernmental Panel on Climate Change). 1990. Climate Change. The IPCC Scientific Assessment. Houghton J.T., Jenkins, A., and Euphrams, J. J. (eds.), Cambridge University Press, Cambridge.

IPCC (Intergovernmental Panel on Climate Change). 1992. Climate change 1992: the supplementary report to the IPCC scientific assessment. Report prepared for IPCC by Working Group 1. Houghton J.T., Callender, B.A. and Varney, SA.L. (eds.), Cambridge University Press.

IPCC (Intergovernmental Panel on Climate Change). 1996. Climate Change 1995. The Science of Climate Change. Contribution of Working Group I to the Second Assessment Report of the Intergovernmental Panel on Climate Change. Houghton, J.T., Meira Filho, L.G., Callendar, B.A., Harris, A., Kattenberg, A., and Maskell, K. (eds.), Cambridge University Press.

Iwashima, T. and Yamamoto, R. 1993. *A statistical analysis of the extreme events: long-term trend of heavy daily precipitation.* J. Meteorol. Soc. Jap., **71**: 637-640.

Jenkins, C. and Tong, K. 1996. Water Resources Planning Model development for the Environment Agency. Unpublished MSc. Thesis, Lancaster University.

Jenkinson, A.F. and Collinson, B.P. 1977. *An initial climatology of gales over the North Sea.* Synoptic Climatology Branch Memorandum No. 62, Bracknell Meteorological Office.

Johns, T.C., Carnell, R.E., Crossley, J.F., Gregory, J.M., Mitchell, J.F.B., Senior, C.A., Tett, S.F.B. and Wood, R.A. 1997. *The second Hadley Centre coupled ocean-atmosphere GCM: model description, spinup and validation.* Climate Dynamics, **13**: 103-134.

Johnston, P.R. and Pilgrim, D.H., 1976. *Parameter optimization for watershed models.* Water Resour. Res., **12**: 477-486.

Jones, P.D., and Conway, D. 1997. *Precipitation in the British Isles: an analysis of area-average data updated to 1995.* Int. J. Climatol. **17**: 427-438.

Jones, P.D., and Kelly, P.M. 1982. *Principal component analysis of the Lamb Classification of daily weather types: Part 1, annual frequencies.* J. Climatol., **2**: 147-157.

Jones, P.D., and Lister, D.H. 1998. *Riverflow reconstructions for 15 catchments over England and Wales and an assessment of hydrologic drought since 1865.* Int. J. Climatol., **18**: 999-1013.

Jones, P.D. and Wigley, T.M.L. 1990. *Global warming trends.* Sci. Am., **263**: 84-91.

Jones, P.D., Hulme, M., and Briffa, K.R. 1993. *A comparison of Lamb circulation types with an objective classification scheme.* Int. J. Climatol., **13**: 655-663.

Jones, P.D., Conway, D., and Briffa, K.R. 1997*a*. *Precipitation variability and drought.* In: Hulme, M., and Barrow, E. (eds.) Climates of the British Isles: Present, Past and Future. Routledge, pp. 197-219.

Jones, P.D., Jónsson, T., and Wheeler, D. 1997*b*. *Extension to the North Atlantic Oscillation using early instrumental pressure observations from Gibraltar and south-west Iceland.* Int. J. Climatol., **17**: 1433-1450.

Jones, P. D., Horton, E.B., Folland, C.K., Hulme, M., Parker, D.E. and Basnett, T.A. 1999*a*. *The use of indices to identify changes in climatic extremes.* Climatic Change, **42**: 131-149.

Jones, P. D., Conway, D. and Reid, P. 1999*b*. WRINCLE: Water Resources: the Impact of Climate Change in Europe. Second Annual Report, Jan 1999 – Dec 1999. Climatic Research Unit, University of East Anglia.

Kalkstein, L.S, Dunne, P. and Vose, R. 1990.*Detection of climatic change in the western North American Arctic using a synoptic climatological approach.* J. Climate, **3**, 1153-1167.

Kalkstein, L.S., Sheridan, S.C. and Graybeal, D.Y. 1998. *A determination of character and frequency changes in air masses using a spatial synoptic classification.* Int. J. Climatol., **18**: 1223-1236.

Karl, T.R. 1994. *Climate-change - Smudging the fingerprints.* Nature, **371**: 380-381.

Karl, T.R. and Knight, R.W. 1998. *Secular trends of precipitation amount, frequency, and intensity in the United States.* Bull. Amer. Meteor. Soc., **79**: 231-241.

Karl, T.R. and Riebsame, W.E. 1989. *The impact of decadal fluctuations in mean precipitation and temperature on runoff: a sensitivity study over the United States.* Climatic Change, **15**: 423-447.

Karl, T.R., Knight, R.W. and Plummer, N. 1995. *Trends in high-frequency climate variability in the twentieth century.* Nature, **377**: 217-220.

Karl, T.R., Quayle, R.G. and Groisman, P.Ya. 1993. *Detecting climate variations and change: new challenges for observing and data management systems.* J. Climate, **6**: 1481-1494.

Karl, T.R., Wang, W-C, Schlesinger, M.E., Knight, R.W. and Portman, D. 1990. *A method of relating GCM simulated climate to the observed local climate. Part I, Seasonal statistics.* J. Climate, **3**: 1053-1079.

Karoly, D.J., Cohen, J.A., Meehl, G.A., Mitchell, J.F.B., Oort, A.H., Stouffer, R.J. and Wetherald, R.T. 1994. *An example of fingerprint detection of greenhouse climate change.* Climate Dynamics, **10**: 97-105.

Kattenberg, A., Giorgi, F., Grassl, H., Meehl, G.A., Mitchell, J.F.B., Stouffer, R.J., Tokioka, T., Weaver, A.J. and Wigley, T.M.L. 1996. *Climate models projections of future climate.* In: Houghton, J.T., Meira Filho, L.G., Callander, B.A., Harris, N., Kattenberg, A. and Maskell, K. (eds.) Climate Change 1995: the science of climate change, contribution of Working Group I to the second assessment report of the Intergovernmental Panel on Climate Change, Cambridge University Press, Cambridge, 285-357.

Katz, R.W. 1996. *Use of conditional stochastic models to generate climate change scenarios.* Climatic Change, **32**, 237-255.

Katz, R.W. and Brown, B.G. 1992. *Extreme events in a changing climate: Variability is more important than averages.* Climatic Change., **1**, 289-302.

Kavvas, M.L. and Delleur, J.W. 1975. *The stochastic and chronologic structure of rainfall sequence: Application to Indiana.* Tech. Rep 57, Water Resour. Res. Cent., Purdue Univ., West Layfayette, Ind.

Kay, P.A. and Kutiel, H. 1994. *Some remarks on climatic maps of precipitation.* Climate Res., **4**: 233-241.

Kelly, P.M., Jones, P.D. and Briffa, K.R. 1997. *Classifying the winds and weather.* In: M. Hulme and E. Barrow (eds.) Climates of the British Isles; present, past and future. Routledge, London, 153-172.

Kendall, M.G. 1980. Multivariate Analysis. MacMillan, New York.

Khaliq, M.N. and Cunnane, C. 1996. *Modelling point rainfall occurrences with the modified Bartlett-Lewis rectangular pulses model.* J. Hydrol., **180**: 395-396.

Kiely, G. 1999. *Climate change in Ireland from precipitation and streamflow observations.* Adv. Water Resour., **23**: 141-151.

Kilsby, C.G., Cowpertwait, P.S.P., O'Connell, P.E., and Jones, P.D. 1998*a*. *Predicting rainfall statistics in England and Wales using atmospheric circulation variables.* Int. J. Climatol., **18**: 523-539.

Kilsby, C.G., Fallows, C.S., and O'Connell, P.E. 1998*b*. *Generating rainfall scenarios for hydrological impact modelling.* In: Wheater, H. and Kirby, C. (eds.) Hydrology in a Changing Environment, Volume 1, British Hydrological Society, Exeter, 7-10 July 1998.

Kimball, B.A., Mauney, J.R., Nakayama, F.S., and Idso, S.B. 1993. *Effects of increasing atmospheric CO_2 on vegetation.* Vegetario, **104/105**: 65-75.

Kite, G.W. 1989. *Use of time series analysis to detect climate change.* J. Hydrol., **111**: 259-279.

Kite, G.W. 1993. *Analysing hydrometeorological time series for evidence of climatic change.* Nordic. Hydrol., **24**: 135-150.

Kite, G.W., Dalton, A., and Dion, K. 1994. *Simulation of streamflow in a macroscale watershed using general circulation model data.* Water Resour. Res., **30**: 1547-1559.

Kozuchowski, K.M. 1993. *Variations of hemispheric zonal index since 1899 and its relationship with air temperature.* Int. J. Climatol., **13**: 853-864.

Krasovskaia, I. and Gottschalk, L. 1992. *Stability of river flow regimes.* Nordic Hydrol., **23**: 137-154.

Krasovskaia, I. and Gottschalk, L. 1993. *Frequency of extremes and its relation to climate fluctuations.* Nordic Hydrol., **24**: 1-12.

Kuchment, L.S., Demidov, V.N., Naden, P.S., Cooper, D.M. and Broadhurst, P., 1996. *Rainfall-runoff modelling of the Ouse basin, North Yorkshire: an application of a physically based distributed model.* J. Hydrol., **181**: 323-342.

Kuhl, S.C., and Miller, J.R. 1992. *Seasonal river runoff calculated from a global atmospheric model.* Water Resour. Res., **28**: 2029-2039.

Kushnir, Y. 1994. *Interdecadal variations in north-Atlantic sea-surface temperature and associated atmospheric conditions.* J. Climate, **7**: 141-157.

Lall, U. and Sharma, A. 1996. *A nearest neighbour bootstrap for resampling hydrologic time series.* Water Resour. Res., **32**: 679-693.

Lamb, H.H. 1972. *British Isles weather types and a register of the daily sequence of circulation patterns, 1861-1971.* Geophysical Memoir 116, London: HMSO, 85 pp.

Law, M., Wass, P., and Grimshaw, D. 1997. *The hydrology of the Humber catchment.* Sci. Tot. Env., **194**: 119-128.

Le Cam, L.M. 1961. *A stochastic description of precipitation.* In: Neyman, J. (ed.) Proceedings of the Fourth Berkeley Symposium on Mathematical Statistics and Probability. University of California, Berkeley, Calif., Vol 3: 165-186.

Legates, D.R. 1987. *A climatology of global precipitation.* Publ. Climatol., **40**: 84 pp.

Legates, D.R., and Willmott, C.J. 1990. *Mean seasonal and spatial variability in gauge-corrected, global precipitation.* Int. J. Climatol., **15**: 237-258.

Leggett, J., Pepper, W., Swart, R.J., Edmonds, J., Meira Filho, L.G., Mintzer, I., Wang, M.X. and Watson, J. 1992. *Emissions scenarios for the IPCC: An update.* In: Houghton, J.T., Callander, B.A., and Varney, S.K. (eds.) Climate Change 1992: The supplementary report to the IPCC scientific assessment. Cambridge University Press, Cambridge, 75-95.

Lettenmaier, D.P. and Gan, T.Y. 1990. *Hydrologic sensitivities of the Sacramento-San Joaquin river basin, California, to global warming.* Water Resour. Res., **26**: 69-86.

Lettenmaier, D.P., Wood, E.F. and Wallis, J.R. 1994. *Hydro-climatological trends in the continental United States 1948-1988.* J. Climate, **7**: 586-607.

Lettenmaier, D.P., Wood, A.W., Palmer, R.N., Wood, E.F. and Stakhiv, E.Z., 1999. *Water resources implications of global warming: A US regional perspective.* Climatic Change, **43**, 537-579.

Lindroth, A. 1996. *Will rising levels of atmospheric CO_2 and temperature lead to enhanced or suppressed rates of evapotranspiration? A comment.* Weather, **51**: 285-286.

Lins, H. and Michaels, P.J. 1994. *Increased US streamflow linked to greenhouse forcing.* Eos, **75**: 281-285.

Lockwood, J.G. 1993. *Impact of global warming on evapotranspiration.* Weather, **48**: 291-299.

Lockwood, J.G. 1994. *Climatic change, grass pasture and potential evapotranspiration.* Weather, **49**: 318-321.

Lockwood, J.G. 1995. *The suppression of evapotranspiration by rising levels of atmospheric CO_2.* Weather, **50**: 304-308.

Maheras, P. 1989. *Delimitation of the summer-dry period in Greece according to the frequency of weather-types.* Theor. Appl. Climatol., **39**: 171-176.

Manabe, S., and Stouffer, R.J. 1995. *Simulation of abrupt climate change induced by freshwater input to the North Atlantic Ocean.* Nature, **378**: 165-167.

Manabe, S., Stouffer, R.J., Spellman, M.J., and Brian, K. 1991. *Transient responses of a coupled ocean-atmosphere model to gradual changes of atmospheric CO_2. Part 1: Annual mean response.* J. Climate, **4**: 785-818.

Manabe, S., Spellman, M.J., and Stouffer, R.J. 1992. *Transient responses of a coupled ocean-atmosphere model to gradual changes of atmospheric CO_2. Part 2: Seasonal response.* J. Climate, **5**: 105-126.

Manley, G. 1974. *Central England Temperatures: monthly means 1659 to 1973.* Quat. J. Roy. Meteorol. Soc., **100**: 389-405

Manley, R.E. 1993. HYSIM reference manual. R. E. Manley Consultancy, Cambridge, 63pp.

Marengo, J.A. 1995. *Variations and change in South American streamflow.* Climatic Change, **31**: 99-117.

Marsh, T.J. 1996. *The 1995 drought - a signal of climatic instability?* Procs. Inst. Civ. Engs. (Wat. Mar. Eng.), **118**: 189-195.

Marsh, T.J., and Bryant, S.J. 1991. *1990 - a year of floods and droughts.* 1990 Yearbook. Hydrological Data UK Series, Institute of Hydrology and British Geological Survey, Wallingford, 25-37.

Marsh, T.J., and Lees, M.L. 1985. *The 1984 Drought.* Hydrological Data UK Series, Institute of Hydrology, Wallingford.

Marsh, T.J., and MacRuairi, R.E. 1993. *1988-1992: a demonstration of the United Kingdom's vulnerability to drought.* Paper presented at the British Hydrological Society national symposium, Cardiff.

Marsh, T.J., and Monkhouse, R.A. 1991. *A year of hydrological extremes - 1990.* Weather, **46**: 366-376.

Marsh, T.J., and Monkhouse, R.A. 1993. *Drought in the United Kingdom, 1988-92.* Weather, **48**: 15-22.

Marsh, T.J., and Sanderson, F.J. 1997. *A review of hydrological conditions throughout the period of the LOIS monitoring programme - considered within the context of the recent UK climatic volatility.* Sci. Tot. Env., **194**: 59-69.

Marsh, T.J., Monkhouse, R.A., Arnell, N.W., Lees, M.L., and Reynard, N.S. 1994. *The 1988-92 Drought.* Institute of Hydrology and British Geological Survey. Wallingford, Oxon. 80pp.

Martin, E., Timbal, B., and Brun, E. 1997. *Downscaling of general circulation model outputs: simulation of the snow climatology of the French Alps and sensitivity to climate change.* Climate Dynamics, **13**: 45-56.

Martin, P., Rosenberg, N.J., and McKenny, M.S. 1989. *Sensitivity of evapotranspiration in a wheat field, a forest, and a grassland to changes in climate and direct effects of carbon dioxide.* Climatic Change, **14**: 117-151.

Matalas, N.C. 1997. *Stochastic hydrology in the context of climate change.* Climatic Change, **37**: 89-101.

Matyasovszky, I., Bogardi, I., Bardossy, A., and Duckstein, L. 1993. *Space-time precipitation reflecting climate change.* Hydrol. Scis. J., **38**: 539-558.

Mawdsley, J., Petts, G., and Walker, S. 1994. *Assessment of drought severity.* British Hydrological Society, Occasional Paper No. 3, British Hydrological Society, UK.

Mayes, J. C. 1991*a*. *Recent trends in summer rainfall in the UK.* Weather, **46**, 190-196.

Mayes, J.C. 1991*b*. *Regional air-flow patterns in the British-Isles.* Int. J. Climatol., **11**: 473-491.

Mayes, J. C. 1994. *Recent changes in the monthly distribution of regional weather types in the British Isles.* Weather, **49**, 156-162.

Mayes, J.C. 1995. *Changes in the distribution of annual rainfall in the British Isles.* J. C.I.W.E.M., **9**: 531-539.

Mayes, J.C. 1996. *Spatial and temporal fluctuations of monthly rainfall in the British Isles and variations in the mid-latitude westerly circulation.* Int. J. Climatol., **16**: 585-596.

Mayes, J.C. 1998. *United Kingdom summer weather over 50 years - continuity or change?* Weather, **53**: 2-11.

McCabe, G. J. 1989. *A conceptual weather-type classification procedure for the Philadelphia, Pennsylvania, area.* U.S. Geol. Surv. Water Resour. Invest. Rep., **89**: 4183.

McCabe, G.J., and Hay, L.E. 1995. *Hydrological effects of hypothetical climate change in the East River Basin, Colorado, USA.* Hydrol. Sci. J., **40**: 303-318.

McGuffie, K., Henderson-Sellers, A., Holbrook, N., Kothavala, Z., Balachova, O., Hoekstra, J. 1999. *Assessing simulations of daily temperature and precipitation variability with global climate models for present and enhanced greenhouse climates.* Int. J. Climatol., **19**: 1-26.

Mearns, L.O., Giorgi, F., McDaniel, L., and Shields, C. 1995*a*. *Analysis of variability and diurnal range of daily temperature in a nested regional climate model: comparison with observations and doubled CO_2 results.* Climate Dynamics, **11**: 193-209.

Mearns, L.O., Giorgi, F., McDaniel, L., and Shields, C. 1995*b*. *Analysis of daily variability of precipitation in a nested regional climate model: comparison with observations and doubled CO_2 results.* Global and Planetary Change, **10**: 55-78.

Mearns, L.O., Rosenzweig, C., and Goldberg, R. 1996. *The effect of changes in daily and interannual climatic variability on ceres-wheat: a sensitivity study.* Climatic Change, **32**: 257-292.

Mellor, D. 1992. The modified turning bands method for space-time precipitation. Ph.D. these, Department of Civil Engineering, University of Newcastle Upon Tyne.

Metcalfe, A.V. 1994. Statistics in Engineering: A Practical Approach. Chapman and Hall, London.

Mitchell, J.F.B. and Hulme, M. 1999. *Predicting regional climate change: living with uncertainty.* Prog. Phys. Geog., **23**: 57-78.

Mitchell, J.F.B. and Johns, T.C. 1997. *On modification of global warming by sulfate aerosols.* J. Climate, **10**: 245-267.

Mitchell, J.F.B., Johns, T.C., Gregory, J.M. and Tett, S.F.B. 1995*a*. *Climate response to increasing levels of greenhouse gases and sulphate aerosols.* Nature, **376**, 501-506.

Mitchell, J.F.B., Davis, R.A., Ingram, W.J., and Senior, C.A. 1995*b*. *On surface temperature, greenhouse gases, and aerosols: models and observations.* J. Climate, **8**: 2364-2386.

Mitchell, J.F.B., Johns, T.C., Eagles, M., Ingram, W.J. and Davis, R.A. 1999. *Towards the construction of climate change scenarios.* Climatic Change, **41**: 547-581.

Mitosek, H.T. 1995. *Climate variability and change within the discharge time series: a statistical approach.* Climatic Change, **29**: 101-116.

Mode, C.J. 1985. Stochastic Processes in Demography and Their Computer Implementation. Springer-Verlag, New York, 389pp.

Moore, R.J. and Clarke, R.T., 1981. *A distribution function approach to rainfall-runoff modelling.* Water Resour. Res., **17**: 1367-1382.

Morris, S.E., and Marsh, T.J. 1985. *United Kingdom rainfall 1975-1984: Evidence of climatic instability?* J. Meteorol., **10**: 324-332.

Moses, T., Kiladis, G.M., Diaz, H.F. and Barry, R.G. 1987. *Characteristics and frequency of reversals in the mean sea level pressure in the North Atlantic sector and their relationship to long-term temperature trends.* J. Climatol., **7**: 13-30.

Mott MacDonald. 1996. Updating of YWS Hydrological Records (Sheffield/Barnsley Reservoirs and Rivers Wharfe, Ouse, Derwent and Hull). Rep. 35894BA01/1/B, Yorkshire Water Services.

Mott MacDonald. 1997. YWS Hydrological Records 1996 (Sheffield, Barnsley, Calder, Worth and Bradford High Level Reservoirs). Rep. 39413BA01/1/B. Yorkshire Water Services.

Murphy, J.M., and Mitchell, J.F.B. 1995. *Transient response of the Hadley Centre coupled ocean-atmosphere model to increasing carbon-dioxide. Part II: Spatial and temporal structure of response.* J. Climate, **8**: 57-80.

Murray, R. 1992. *Some notable features of Manley's central England mean temperatures with special reference to very warm years.* Weather, **47**: 98-103.

Musk, L.F. 1988. *Applied climatology.* Prog. Phys. Geog., **12**: 421-434.

Nash, L.L., and Gleick, P.H. 1991. *Sensitivity of streamflow in the Colorado River Basin to climatic changes.* J. Hydrol., **125**: 221-241.

Nash, J.E. and Sutcliffe, J.V., 1970. *River flow forecasting through conceptual models. Part I - A discussion of principles.* J. Hydrol., **10**: 282-290.

Nelder, J.A. and Mead, R. 1965. *A simplex method for function minimization.* Comput. J., **7**: 308-313.

Nemec, J. and Shaake, J. 1982. *Sensitivity of water resource systems to climate variation.* Hydrol. Scis. J., **27**: 327-343.

New, M. 1999. *Uncertainty in representing observed climate.* ECLAT-2 Commentary for ECLAT Workshop 1 (Red), Helsinki, 14-16 April 1999.

New, M., Hulme, M. and Jones, P. 1999. *Representing twentieth-century climate variability. Part I: Development of a 1961-90 mean monthly terrestrial climatology.* J. Climate, **12**: 829-856.

New, M., Hulme, M. and Jones, P. 2000. *Representing twentieth-century climate variability. Part II: Development of 1901-96 monthly grids of terrestrial surface climate.* J. Climate, **13**: 2217-2238.

Neyman, J. and Scott, E. L., 1958. *Statistical approach to problems of cosmology.* J. R. Stat. Soc., **B 20**: 1-43.

Nicholas, F.J. and Glasspoole, J. 1931. *General monthly rainfall over England and Wales, 1727 to 1931.* British Rainfall, 299-306.

Noda, A. and Tokioka, T. 1989. *The effect of doubling the CO_2 concentration on convective and non-convective precipitation in a General-Circulation Model coupled with a simple mixed layer ocean model.* J. Meteorol. Soc. Jpn., **67**: 1057-1069.

Olaniran, O.J. 1982. *Problems in the measurement of rainfall - an experiment in Ilorin, Nigeria.* Weather, **37**: 201-204.

Onof, C. and Wheater, H.S. 1993. *Modelling of British rainfall using a random parameter Bartlett-Lewis rectangular pulses model.* J. Hydrol., **149**: 67-95.

Osborn, T.J., Briffa, K.R., Tett, S.F.B., Jones, P.D. and Trigo, R.M. 1999. *Evaluation of the North Atlantic Oscillation as simulated by a coupled climate model.* Climate Dynamics, **15**: 685-702.

Osborn, T.J., Hulme, M., Jones, P.D. and Basnett, T.A. 2000. *Observed trends in the daily intensity of United Kingdom precipitation.* Int. J. Climatol., **20**, 347-364.

Palutikof, J.P., Winkler, J.A., Goodess, C.M., Andresen, J.A. 1997. *The simulation of daily temperature time series from GCM output .1. Comparison of model data with observations.* J. Climate, **10**: 2497-2513.

Panagoulia, D. 1992. *Impact of GISS-modelled climate changes on catchment hydrology.* Hydrol. Sci. J., **37**: 141-163.

Parker, D.E., Legg, T.P. and Folland, C.K. 1992. *A new daily central England temperature series, 1772-1991.* Int. J. Climatol., **12**: 317-342.

Parker, D.E., Jones, P.D., Folland, C.K., and Bevan, A. 1994. *Interdecadal changes of surface-temperature since the late-19th-century.* J. Geophys. Res., **99**: 14373-14399.

Phillips, I.D., and McGregor, G.R. 1998. *The utility of a drought index for assessing the drought hazard in Devon and Cornwall, South West England.* Meteorol. Appl., **5**: 359-372.

Pielke, R.A., Daly, G.A., Snook, J.S., Lee, T.J., and Kittel, T.G.E. 1991. *Nonlinear influence of mesoscale land use on weather and climate.* J. Climate, **4**: 1053-1069.

Pilling, C. and Jones, J.A.A. 1999. *High resolution climate change scenarios: implications for British runoff.* Hydrol. Process., **13**: 2877-2895.

Pilling, C., Wilby, R.L., and Jones, J.A.A. 1998. *Downscaling of catchment hydrometeorology from GCM output using airflow indices in upland Wales.* In: Wheater, H. and Kirby, C. (eds.) Hydrology in a Changing Environment, Volume 1, British Hydrological Society, 191-208.

Price, W.L. 1987. *Global optimization algorithms for a CAD workstation.* J. Optim. Theory Appl., **55**: 133-146.

Price, M. 1998. *Water storage and climate change in Great Britain – the role of groundwater.* Proc. Instn. Civ. Engrs. Wat. Marit. &Energy, **130**: 42-50.

Quayle, R.G. 1974. *A climatic comparison of ocean weather stations and transient ship records.* Marine Wea. Log, **18**: 307-311.

Rabbinge, R., Van Latesteijn, H.C., and Goudriaan, J. 1993. *Assessing the greenhouse effect in agriculture.* In: Lake, J.V., Bock, G.R., and Ackrill, K. (eds.) Environmental change and human health. Ciba Foundation Symposium 175. Wiley, Chichester, 62-79.

Racsko, P., Szeidl, L., and Semenov, M. 1991. *A serial approach to local stochastic weather models.* Ecol. Model., **57**: 27-41.

Radziejewski, M., Bardossy, A., and Kundzewicz, Z.W. 1998. *Intercomparison of tests for detection of changes in long time series of river flow.* In: Lemmela, R., and Helenius, N. (eds.) Proceedings of the Second International Conference on Climate and Water, Volume 3, Espoo, Finland, 17-20 August 1998, 1120-1129.

Rahmstorf, S. 1995. *Bifurcations of the Atlantic thermohaline circulation in response to changes in the hydrological cycle.* Nature, **378**: 145-149.

Reed, R.K. 1980. *Comparison of ocean and island rainfall in the tropical North Pacific.* J. Appl. Meteorol., **19**: 877-880.

Ribas, L.M.L. 1994. Optimisation of the Yorkshire Water Supply Grid. Unpublished M.Sc. Thesis, Lancaster University.

Richardson, C.W. 1981. *Stochastic simulation of daily precipitation, temperature and solar radiation.* Water Resour. Res., **17**: 182-190.

Rind, D., Goldberg, R. and Ruedy, R. 1989. *Change in climate variability in the 21st-century.* Climatic Change, **14**: 5-37.

Rind, D., Rosenzweig, C., and Goldberg, R. 1992. *Modelling the hydrological cycle in assessments of climate change.* Nature, **358**: 119-122.

Rodriguez-Iturbe, I., Gupta, V.K., and Waymire, E. 1984. *Scale considerations in the modelling of temporal rainfall.* Water Resour. Res., **20**: 1611-1619.

Rodriguez-Iturbe, I., Cox, D.R. and Isham, V. 1987*a*. *Some models for rainfall based on stochastic point processes.* Proc. R. Soc. London A, **410**: 269-288.

Rodriguez-Iturbe, I., Febres de Power, B. and Valdes, J.B. 1987*b*. *Rectangular pulses point process models for rainfall: analysis of empirical data.* J. Geophys. Res. **92**: 9645-9656.

Rodriguez-Iturbe, I., Cox, D.R., and Isham, V. 1988. *A point process model for rainfall: further developments.* Proc. R. Soc. London Ser. A, **417**: 283-298.

Rodriguez-Iturbe, I., Entekhabi, D., and Bras, R.L. 1991*a*. *Nonlinear dynamics of soil moisture at climate scales, 1, Stochastic analysis.* Water Resour. Res., **27**: 1899-1906.

Rodriguez-Iturbe, I., Lee, Jae-Soo., and Bras, R.L. 1991*b*. *Nonlinear dynamics of soil moisture at climate scales, 2, Chaotic analysis.* Water Resour. Res., **27**: 1907-1915.

Rodwell, M.J., Rowell, D.P., and Folland, C.K. 1999. *Oceanic forcing of the wintertime North Atlantic Oscillation and European climate.* Nature, **398**: 320-323.

Rogers, J.C. 1985. *Atmospheric circulation changes associated with the warming over the northern North-Atlantic in the 1920s.* J. Clim. Appl. Meteorol., **24**: 1303-1310

Rotmans, J., Hulme, M., and Downing, T.E. 1994. *Climate change scenarios for Europe - an application of the ESCAPE model.* Env. Change, **4**: 97-124.

Rowntree, P.R. 1990. *Estimates of future climate change over Britain. Part 2: Results.* Weather, **45**: 38-42.

Rowntree, P.R., Murphy, J.M. and Mitchell, J.F.B. 1993. *Climate change and future rainfall predictions.* J. Inst. Water Env. Manag., **7**: 464-470.

Rumsby, B.T., and Macklin, M.G. 1994. *Channel and floodplain response to recent abrupt climate change: the Tyne basin, northern England.* Earth Surf. Proc. Land., **19**: 499-515.

Santer, B.D. 1996. *A search for human influences on the thermal structure of the atmosphere.* Nature, **384**: 39-46.

Santer, B.D., Bruggemann, W., Cubasch, U., Hasselmann, K., Hock, H., Maier Reimer, E., and Mikolajewicz, U. 1994. *Signal-to-noise analysis of time-dependent greenhouse warming experiments. Part I: Pattern analysis.* Climate Dynamics., **9**: 267-285.

Santer, B.D., Taylor, K.E., Wigley, T.M.L., Penner, J.E., Jones, P.D. and Cubasch, U. 1995. *Towards the detection and attribution of an anthropogenic effect on climate.* Climate Dynamics., **12**: 77-100.

Sauter, M. and Leidl, R. 1998. *The impact of climate change on water resources in a carbonate aquifer.* In: H. Wheater and C. Kirby (eds.) Hydrology in a Changing Environment. Volume II. Proceedings of the British Hydrological Society International Conference, Exeter, July 1998, 21-31.

Schaake, J.C. 1990. *From climate to flow.* In: Waggoner, P.E. (ed.) Climate Change and US Water Resources. Wiley, New York, 177-206.

Schadler, B. 1987. *Long water balance time series of four important rivers in Europe - indicators for climatic changes.* In: The influence of climatic change and climatic variability on the hydrologic regime and water resources. Int. Assoc. Hydrol. Sci. Publ., **168**: 209-219.

Sefton, C.E.M. and Boorman, D.B. 1997. *A regional investigation of climate change impacts on UK streamflows.* J. Hydrol., **195**: 26-44.

Semenov, M.A. and Barrow, E.M. 1997. *Use of a stochastic weather generator in the development of climate change scenarios.* Climatic Change, **35**: 397-414.

Semenov, M.A. and Porter, J.R. 1994. *The implications and importance of non-linear responses in modelling of growth and development of wheat.* In: Grasman, J. and van Straten, G. (eds.) Predictability and non-linear modelling in natural sciences and economics. Wageningen.

Senior, C.A. and Mitchell, J.F.B. 1993. *CO_2 and climate: the impact of cloud parameterizations.* J. Climate, **6**, 393-418.

Sevruk, B. 1982. *Methods of correction for systematic error in point precipitation measurement for operational use.* Operational Hydrology Report 21, **WMO no. 589**, Geneva: World Meteorological Organization.

Sharma, A., Tarboton, D.G. and Lall, U. 1997. *Streamflow simulation: A non-parametric approach.* Water Resour. Res., **33**: 291-308.

Shultz, P., Barron, E.J. and Sloan II, J.L. 1992. *Assessment of NCAR general circulation model precipitation in comparison with observations.* Palaeogeography, Palaeoclimatology, Palaeoecology (Global and Planetary Change Section), **97**: 269-310.

Skiles, J.W. and Hanson, J.D. 1994. *Responses of arid and semiarid watersheds to increasing carbon dioxide and climate change as shown by simulation studies.* Climatic Change, **26**: 377-397.

Smith, K. 1995. *Precipitation over Scotland, 1757-1992; some aspects of temporal variability.* Int. J. Climatol., **15**: 543-556.

Smith, R.N.B. 1990. *A scheme for predicting layer clouds and their water content in a general circulation model.* Q. J. R. Meteorol. Soc., **116**: 435-460.

Sowden, I.P. and Parker, D.E. 1981. *A study of climatic variability of daily Central England Temperatures in relation to the Lamb synoptic types.* J. Climatol., **1**: 3-10.

Stephenson, D.B., Pavan, V. and Bojariu, R. 2000. *Is the North Atlantic Oscillation a random walk?* Int. J. Climatol., **20**: 1-18.

Stouffer, R.J., Manabe, S. and Vinnikov, K.Y. 1994. *Model assessment of the role of natural variability in recent global warming.* Nature, **367**: 634-636.

Suppiah, R. and Hennessey, K. J. 1996. *Trends in the intensity and frequency of heavy rainfall in tropical Australia and links with the Southern Oscillation.* Austr. Meteorol. Mag., **45**: 1-17.

Sutton, R.T. and Allen, M.R. 1997. *Decadal predictability of North Atlantic sea surface temperature and climate.* Nature, **388**: 563-567.

Sweeney, J.C. and O'Hare, G.P. 1992. *Geographical variations in precipitation yields and circulation types in Britain and Ireland.* Trans. Instit. Br. Geogs., **17**: 448-463.

Tabony, R.C. 1981. *A Principal Component and Spectral Analysis of European Rainfall.* J. Climatol., **1**, 283-294.

Taylor, K. and Penner, J.E. 1994. *Climate system response to aerosols and greenhouse gases: A model study.* Nature, **369**: 734-737.

Thompson, N., Barrie, I.A. and Ayles, M. 1981. *The Meteorological Office Rainfall and Evaporation Calculation System: MORECS.* Hydrological Memorandum 45. Meteorological Office, Bracknell, 73pp.

Thomsen, R. 1990. *Effect of climate variability and change in groundwater in Europe - Keynote paper presented at the Conference on Climate and Water, Helsinki, 11-15 September, 1989.* Nord. Hydrol., **21**: 185-194.

Todini, E., 1988. *Rainfall runoff modelling: past, present and future.* J. Hydrol., **100**: 341-352.

Todini, E., 1996. *The ARNO rainfall-runoff model.* J. Hydrol., **175**: 339-382.

Todorovic, P. and Yevjevich, V. 1969. *Stochastic processes of precipitation.* Colorado State Univ., Hydrol. Pap. 35, 1-61.

Trenberth, K.E., Branstator, G.W. and Arkin, P. 1988. *Origins of the 1988 North American drought.* Science, **242**: 1640-1645.

Twort, A.C., Law, F.M., Crowley, F.W. and Ratnayaka, D.D. 1994. Water Supply, 4th edition. Edward Arnold.

Tyree, M.T. and Alexander, J.D. 1993. *Plant water relations and the effects of elevated CO_2: a review and suggestions for future research.* Vegetatio, **104/105**: 47-62.

Uff, J. 1996. Water Supply in Yorkshire. Report of the Independent Commission of Inquiry. Tourcrete Ltd, London.

UKWIR/EA. 1997. Effects of climate change on river flows and ground water recharge: Guidelines for resource assessment. Rep. 97/CL/04/1.

Valdes, J.B., Rodriguez-Iturbe, I. and Gupta, V.K. 1985. *Approximations of temporal rainfall from a multidimensional model.* Water Resour. Res., **21**: 1259-1270.

Valdes, J.B., Seoane, R.S. and North, G.R. 1994. *A methodology for the evaluation of global warming impact on soil moisture and runoff.* J. Hydrol., **161**: 389-413.

Van der Wateren-de-Hoog, B. 1995. *The effect of climate variability on discharge, as dependent on catchment characteristics in the Upper Loire Basin, France.* Hydrol. Sci. J., **40**: 633-646.

Van der Wateren-de-Hoog, B. 1998. *A regional model to assess the hydrological sensitivity of medium sized catchments to climate variability.* Hydrol. Processes, **12**: 43-56.

Velghe, T., Troch, P.A., De Troch, F.P. and Van de Velde, J. 1994. *Evaluation of cluster-based rectangular pulses point process models for rainfall.* Water Resour. Res., **30**: 2847-2857.

Viney, N.R. and Sivapalan, M. 1996. *The hydrological response of catchments to simulated changes in climate.* Ecol. Model., **86**: 189-193.

Von Storch, H., Zorita, E. and Cubasch, U. 1993. *Downscaling of global climate change estimates to regional scales: an application to Iberian rainfall in wintertime.* J. Climate, **6**: 1161-1171.

Walker, S. 1998. *Sustainable water resources management beyond the 1995-96 drought.* Proc. Instn. Civ. Engrs. Wat. Marit. &Energy, **130**: 207-216.

Wallis, J.R. and Guttman, N.B. 1997. The National Electronic Drought Atlas (NEDA). IBM Technical Services, USA.

Walsh, J.E. 1993. *The elusive Arctic warming.* Nature, **361**: 300-301.

Wang, Q.J. 1991. *The genetic algorithm and its application to calibrating conceptual rainfall-runoff models.* Water Resour. Res., **27**: 2467-2471.

Wardlaw, R.B., Hulme, M. and Stuck, Y. 1996. *Modelling the impacts of climate change on water resources.* J. CIWEM, **10**: 355-364.

Watanabe, M., and Nitta, T. 1999. *Decadal changes in the atmospheric circulation and associated surface climate variations in the Northern Hemisphere winter.* J. Climate, **12**: 494-510.

Whetton, P.H., Fowler, A.M., Haycock, M.R., and Pittock, A.B. 1993. *Implications of climate change due to the enhanced greenhouse effect on floods and droughts in Australia.* Climatic Change, **25**: 289-317.

White, D., Richman, M. and Yarnal, B. 1991. *Climate regionalization and rotation of principal components.* Int. J. Climatol., **11**: 1-25.

Wigley, T.M.L. and Jones, P.D. 1985. *Influence of precipitation changes and direct CO_2 effects on streamflow.* Nature, **314**: 149-152.

Wigley, T.M.L. and Jones, P.D. 1987. *Recent changes in precipitation and precipitation variability in England and Wales.* J. Climatol., **7**, 231-246.

Wigley, T.M.L. and Santer, B.D. 1990. *Statistical comparison of spatial fields in model validation, perturbation and predictability experiments.* J. Geophys. Res., **95**: 851-865.

Wigley, T.M.L., Lough, J.M. and Jones, P.D. 1984. *Spatial patterns of precipitation in England and Wales and a revised, homogenous England and Wales precipitation series.* J. Climatol., **4**: 1-25.

Wigley, T.M.L., Jones, P.D., Briffa, K.R. and Smith, G. 1990. *Obtaining sub-grid scale information from coarse-resolution general circulation model output.* J. Geophys. Res., **92**, 1943-1953.

Wilby, R.L. 1993*a*. *The influence of variable weather patterns on river water quantity and quality regimes.* J. Climatol., **13**: 447-459.

Wilby, R.L. 1993*b*. *Evidence of ENSO in the synoptic climate of the British Isles since 1880.* Weather, **48**: 234-239.

Wilby, R.L. 1994. *Stochastic weather type simulation for regional climate change impact assessment.* Water Resour. Res., **30**: 3395-3403.

Wilby, R.L. 1997. *Non-stationarity in daily precipitation series: Implications for GCM down-scaling using atmospheric circulation indices.* Int. J. Climatol., **17**: 439-454.

Wilby, R.L. 1998. *Modelling low-frequency rainfall events using airflow indices, weather patterns and frontal frequencies.* J. Hydrol., **212-213**: 380-392.

Wilby, R.L. and Vitkovic, G. 1993. *Climate, abstraction and land-use changes: impacts on low flows in UK catchments.* Paper presented at the British Hydrological national Symposium, Cardiff.

Wilby, R.L. and Wigley, T.M.L. 1997. *Downscaling general circulation model output: a review of methods and limitations.* Prog. Phys. Geog., **21**: 530-548.

Wilby, R.L., Barnsley, N. and O'Hare, G. 1995. *Rainfall variability associated with Lamb weather types: the case for incorporating weather fronts.* Int. J. Climatol., **15**: 1241-1252.

Wilby, R.L., Greenfield, B. and Glenny, C. 1994. *A coupled synoptic-hydrological model for climate change impact assessment.* J. Hydrol., **153**: 165-190.

Wilby, R.L., Hassan, H. and Hanaki, K. 1998*a*. *Statistical downscaling of hydrometeorological variables using general circulation model output.* J. Hydrol., **205**: 1-19.

Wilby, R.L., O'Hare, G. and Barnsley, N. 1997. *The North Atlantic Oscillation and British Isles climate variability, 1865-1996.* Weather, **52**: 266-276.

Wilby, R.L., Wigley, T.M.L., Wilks, D.S., Hewitson, B.C., Conway, D. and Jones, P.D. 1996*a*. *Statistical downscaling of general circulation model output.* A report prepared by the National Center for Atmospheric Research on behalf of the Electric Power Research Institute, Palo Alto, CA, 730pp.

Wilby, R.L., Conway, D., and Jones, P.D. 1996*b*. *GCM downscaling using airflow indices.* In: Proceedings of the International Conference on Water Resources and Environment Research: Towards the 21st Century, Kyoto, Japan, 29-31 October 1996.

Wilby, R.L., Wigley, T.M.L., Conway, D., Jones, P.D., Hewitson, B.C., Main, J., and Wilks, D.S. 1998*b*. *Statistical downscaling of general circulation model output: a comparison of methods.* Water Resour. Res., **34**: 2995-3008.

Wilkinson, W.B., and Cooper, D.M. 1993. *The response of idealized aquifer/river systems to climate change.* Hydrol. Scis. J., **38**: 379-390.

Wilks, D.S. 1992. *Adapting stochastic weather generation algorithms for climate change studies.* Climatic Change, **22**, 67-84.

Wilks, D.S. 1998. *Multisite generalization of a daily stochastic precipitation generation model.* J. Hydrol., **210**, 178-191

Wilks, D.S. 1999. *Multisite downscaling of daily precipitation with a stochastic weather generator.* Climate Res., **11**: 125-136.

Willmott, M. 1996. *Recent hot summers?* Weather, **51**: 359-360.

Willmott, C.J. and Legates, D.R. 1991. *Rising estimates of terrestrial and global precipitation.* Climate Res., **1**: 179-186.

Wilson, L.L., Lettenmaier, D.P. and Wood, E.F. 1991. *Simulation of daily precipitation in the pacific-northwest using a weather classification scheme.* Surv. Geophys., **12**: 127-142.

Wilson, L.L., Lettenmaier, D.P. and Skyllingstad, E. 1992. *A hierarchical stochastic-model of large-scale atmospheric circulation patterns and multiple station daily precipitation.* J. Geophys. Res. – Atmos., **97**: 2791-2809.

Wilson, C.A. and Mitchell, J.F.B. 1987. *A doubled CO_2 climate sensitivity experiment with a Global Climate Model including a simple ocean.* J. Geophys. Res. – Atmos., **92**: 13315-13343.

Wood, N.H.L. 1989. *Rainfall variability at London and Plymouth, 1921-87.* Weather, **44**: 202-208.

Wood, A.W., Lettenmaier, D.P., Palmer, R.N., 1997, *Assessing Climate Change Implications for Water Resources Planning*, Climatic Change, **37**, 203-228

Yarnal, B., White, D.A. and Leathers, D.J. 1988. *Subjectivity in a computer-assisted synoptic climatology, II, Relationships to surface climate.* J. Climatol., **8**: 227-241.

YWSL. 1998. Draft Water Resources Plan: Executive Summary. Yorkshire Water Services Limited, November 1998.

Zhai, P.M., Sun, A.J., Ren, F.M., Liu, X.N., Gao, B. and Zhang, Q. 1999. *Chances of climate extremes in China.* Climatic Change, **42**: 203-218.

Zhao, R.J., 1977. Flood forecasting methods for humid regions of China. East China College of Hydraulic Engineering, Nanjing.

Zhao, R.J., 1984. Watershed Hydrological Modelling. Water Resources and Electric Power Press, Beijing.

Zorita, E., Kharin, V., and von Storch, H. 1992. *The atmospheric circulation and sea surface temperature in the North Atlantic area in winter: Their interaction and relevance for Iberian precipitation.* J. Climate, **5**: 1097-1108.

Zucchini, W. and Guttorp, P. 1991. *A hidden Markov model for space-time precipitation.* Water Resour. Res., **27**: 1917-1923.